UNIVERSITY OF LONDON THESIS

Degree PhD Year 2006 Name of Author ROBINSON Jamie

THE EVOLUTION OF THE EARLY TETRAPOD MIDDLE EAR AND ASSOCIATED STRUCTURES

JAMIE ROBINSON

April 2006

UNIVERSITY COLLEGE LONDON

A thesis presented to the University of London in partial fulfilment of the requirements for the degree of Doctor of Philosophy, Ph.D.

ProQuest LLC
789 East Eisenhower Parkway
P.O. Box 1346
Ann Arbor, MI 48106-1346

'I, Jamie Robinson, confirm that the work presented in this thesis is my own. Where information has been derived from other sources, I confirm that this has been indicated in the thesis.'

Signed:

ABSTRACT

This thesis utilises modern techniques to investigate the origin and evolution of hearing in tetrapods with particular emphasis on the evolution of the middle ear region of early tetrapods and the proposed relatives of lissamphibians.

Recent advances in computed tomography (CT) scanning and 3D computer reconstruction has allowed the re-examination of many important specimens in the early tetrapod fossil record. The combination of CT scanning and 3D reconstruction has permitted the detailed visualisation of many aspects of these fossil specimens that could not have been easily achieved by traditional means.

These modern techniques have been used to model the middle ear region in a range of early tetrapods. This was undertaken to investigate the form of the middle ear region in stem group tetrapods and temnospondyls, a group frequently cited in the origin of lissamphibians. The high resolution models created by the modern techniques have been utilised to investigate the function of the middle ear region in early tetrapods. Additionally, fossil evidence for the origin of the varied middle ear structures observed in the extant lissamphibians has been elucidated from the new models. Furthermore, these models allow the quantitative measurements of many aspects of the middle ear.

The analysis of the new models has demonstrated that the support function for the stapes in early tetrapods has been overstated. A crude but transitional hearing function for the stapes is proposed for a range of stem group tetrapods. It is shown that temnospondyls, which are thought to possess tympanic membranes also appear to have possessed numerous specialisations of the middle ear present in extant lissamphibians.

CONTENTS

1. INTRODUCTION 13

1.1. OVERVIEW 13

1.1.1. NEONTOLOGICAL SECTION 14

1.1.2. PALAEONTOLOGICAL SECTION 33

1.1.3. AIMS 53

2. METHODS 56

2.1.1. OVERVIEW 56

2.1.2. HIGH RESOLUTION X-RAY COMPUTED TOMOGRAPHY 61

2.1.3. PARTICULAR HRXCT SET-UP UTILISED 64

2.1.4. DATA PROCESSING 66

2.1.5. GLOSSARY OF TERMS 72

2.1.6. LIST OF INSTITUTIONS 73

2.1.7. LIST OF ABBREVIATIONS 74

3. RESULTS 78

3.1. ACANTHOSTEGA 79

3.1.1. BACKGROUND 80

3.1.2. RECONSTRUCTION PARAMETERS 84

3.1.3. DESCRIPTION 85

3.1.4. DISCUSSION 109

3.2. KYRINION 115

3.2.1. BACKGROUND 117

3.2.2. RECONSTRUCTION PARAMETERS 122

3.2.3. DESCRIPTION 126

3.2.4. DISCUSSION 172

3.3. DENDRERPETON ***183***

3.3.1. BACKGROUND 185

3.3.2. RECONSTRUCTION PARAMETERS 192

3.3.3. DESCRIPTION 195

3.3.4. DISCUSSION 244

3.4. LYDEKKERINA ***255***

3.4.1. BACKGROUND 257

3.4.2. RECONSTRUCTION PARAMETERS 261

3.4.3. DESCRIPTION 263

3.4.4. DISCUSSION 324

3.5. MICROPHOLIS ***331***

3.5.1. BACKGROUND 332

3.5.2. RECONSTRUCTION PARAMETERS 336

3.5.3. DESCRIPTION 338

3.5.4. DISCUSSION 384

4. OVERALL DISCUSSION AND CONCLUSIONS 390

4.1.1. NEONTOLOGICAL QUESTIONS: 390

4.1.2. PALAEONTOLOGICAL QUESTIONS: 400

4.1.3. CONCLUSIONS 409

5. ACKNOWLEDGEMENTS 413

6. REFERENCES 414

TABLE OF FIGURES

Figure 1.1.1—1 19

Figure 1.1.1—2 21

Figure 1.1.1—3 22

Figure 1.1.1—4 25

Figure 1.1.1—5 26

Figure 1.1.1—6 29

Figure 1.1.1—7 30

Figure 1.1.2—1 40

Figure 1.1.2—2 41

Figure 1.1.2—3 42

Figure 1.1.2—4 43

Figure 1.1.2—5 46

Figure 1.1.2—6 51

Figure 1.1.3—1 55

Figure 2.1.1—1 59

Figure 2.1.1—2 60

Figure 3.1.1—1 83

Figure 3.1.3—1 86

Figure 3.1.3—2 87

Figure 3.1.3—3 88

Figure 3.1.3—4 89

Figure 3.1.3—5 90

Figure 3.1.3—6 93

Figure 3.1.3—7 100

Figure 3.1.3—8 101

Figure 3.1.3—9 102

Figure 3.1.3—10 103

Figure 3.1.3—11 104

Figure 3.1.3—12 107

Figure 3.1.3—13 108

Figure 3.1.4—1 110

Figure 3.2.1—1 120

Figure 3.2.1—2 121

Figure 3.2.2—1 124

Figure 3.2.2—2 125

Figure 3.2.3—1 128

Figure 3.2.3—2 129

Figure 3.2.3—3 130

Figure 3.2.3—4 134

Figure 3.2.3—5 135

Figure 3.2.3—6 138

Figure 3.2.3—7 139

Figure 3.2.3—8 143

Figure 3.2.3—9 144

Figure 3.2.3—10 145

Figure 3.2.3—11 146

Figure 3.2.3—12 152

Figure 3.2.3—13 153

Figure 3.2.3—14 158

Figure 3.2.3—15 159

Figure 3.2.3—16 160

Figure 3.2.3—17 161

Figure 3.2.3—18 162

Figure 3.2.3—19 163

Figure 3.2.3—20 164

Figure 3.2.3—21 168

Figure 3.2.3—22 169

Figure 3.2.3—23 170

Figure 3.2.3—24 171

Figure 3.2.4—1 173

Figure 3.2.4—2 177

Figure 3.3.1—1 189

Figure 3.3.1—2 190

Figure 3.3.1—3 191

Figure 3.3.3—1 196

Figure 3.3.3—2 198

Figure 3.3.3—3 199

Figure 3.3.3—4 203

Figure 3.3.3—5 204

Figure 3.3.3—6 205

Figure 3.3.3—7 208

Figure 3.3.3—8 209

Figure 3.3.3—9 214

Figure 3.3.3—10 215

Figure 3.3.3—11 216

Figure 3.3.3—12 217

Figure 3.3.3—13 218

Figure 3.3.3—14 221

Figure 3.3.3—15 222

Figure 3.3.3—16 226

Figure 3.3.3—17 227

Figure 3.3.3—18 228

Figure 3.3.3—19 229

Figure 3.3.3—20 230

Figure 3.3.3—21 233

Figure 3.3.3—22 234

Figure 3.3.3—23 235

Figure 3.3.3—24 239

Figure 3.3.3—25 240

Figure 3.3.3—26 241

Figure 3.3.3—27 243

Figure 3.3.4—1 245

Figure 3.4.1—1 260

Figure 3.4.3—1 264

Figure 3.4.3—2 265

Figure 3.4.3—3 266

Figure 3.4.3—4 267

Figure 3.4.3—5 269

Figure 3.4.3—6 273

Figure 3.4.3—7 274

Figure 3.4.3—8 275

Figure 3.4.3—9 280

Figure 3.4.3—10 281

Figure 3.4.3—11 284

Figure 3.4.3—12 285

Figure 3.4.3—13 289

Figure 3.4.3—14 290

Figure 3.4.3—15 291

Figure 3.4.3—16 292

Figure 3.4.3—17 293

Figure 3.4.3—18 294

Figure 3.4.3—19 295

Figure 3.4.3—20 296

Figure 3.4.3—21 299

Figure 3.4.3—22 300

Figure 3.4.3—23 302

Figure 3.4.3—24 303

Figure 3.4.3—25 309

Figure 3.4.3—26 310

Figure 3.4.3—27 311

Figure 3.4.3—28 312

Figure 3.4.3—29 313

Figure 3.4.3—30 314

Figure 3.4.3—31 315

Figure 3.4.3—32 316

Figure 3.4.3—33 319

Figure 3.4.3—34 320

Figure 3.4.3—35 321

Figure 3.4.3—36 322

Figure 3.4.3—37 323

Figure 3.4.4—1 325

Figure 3.5.1—1 335

Figure 3.5.3—1 339

Figure 3.5.3—2 340

Figure 3.5.3—3 341

Figure 3.5.3—4 344

Figure 3.5.3—5 345

Figure 3.5.3—6 346

Figure 3.5.3—7 350

Figure 3.5.3—8 351

Figure 3.5.3—9 352

Figure 3.5.3—10 353

Figure 3.5.3—11 356

Figure 3.5.3—12 357

Figure 3.5.3—13 361

Figure 3.5.3—14 362

Figure 3.5.3—15 365

Figure 3.5.3—16 366

Figure 3.5.3—17 368

Figure 3.5.3—18 372

Figure 3.5.3—19 373

Figure 3.5.3—20 374

Figure 3.5.3—21 375

Figure 3.5.3—22 376

Figure 3.5.3—23 377

Figure 3.5.3—24 378

Figure 3.5.3—25 381

Figure 3.5.3—26 382

Figure 3.5.3—27 383

Figure 3.5.4—1 385

Figure 4.1.1—1 399

Figure 4.1.2—1 408

1. INTRODUCTION

1.1. OVERVIEW

This thesis aims to utilise CT scanning and 3D reconstruction to investigate questions regarding the origin and evolution of the varied hearing morphology observed in extant tetrapods with particular emphasis on the evolution of the hearing systems of extant amphibians. Recent advances in computed tomography (CT) scanning and 3D computer reconstruction allows the re-examination of many crucial and important specimens in the fossil record. The combination of CT scanning and 3D reconstruction permits the detailed visualisation of many aspects of specimens that cannot be easily achieved by traditional means.

1.1.1. NEONTOLOGICAL SECTION

The extant tetrapods have extremely varied ear morphologies which have been studied and described in detail in many prior studies. This section of the introduction will provide a brief review of the hearing morphology of extant amniotes followed by a more in depth analysis of the varied hearing anatomy in extant amphibians. These analyses raise various questions that will be address in this thesis.

The ability of extant tetrapods to perceive airborne sound is accomplished via a specialised hearing system. This system contains three basic parts; the outer, middle and inner ear. The outer ear consists of the external layer of the tympanic membrane and, additionally, in mammalian groups the pinna and ear canal (often called the external auditory meatus). In its basic form the outer ear is the gas-solid interface where the airborne sound waves are collected. For effective perception of the airborne sound the outer ear is coupled to the middle ear which consists of one or more ear ossicles in an air filled space called the middle ear cavity. The ear ossicles channel vibrations from the tympanic membrane (which is a compound outer and middle ear structure) to the fenestra ovalis and the inner ear. The area of the fenestra ovalis is much smaller than the area of the tympanic membrane and thereby accomplishes a pressure amplification of sound waves. Vibrations reaching the fenestra ovalis pass through the perilymphatic fluid and into the endolymphatic fluid. The latter envelops thousands of sensory hair cells attached to one or more membranes which transduce some of the vibratory energy into electrical energy which is passed along auditory (VIII) nerve to the brain. The inner ear is not a closed system, as this would not allow the smooth flow of vibratory waves. Sound vibrations can pass out of the inner ear via numerous passages including the 'round window' (also called 'fenestra rotunda') or via a duct into the other inner ear

space. All extant tetrapods which have the ability to perceive airborne sound do so via the amplification system of the middle ear coupled to a tympanic membrane and inner ear.

The overall interrelationships of the extant tetrapods groups are well established with only a few areas of dispute (Figure 1.1.1—1). One area of recent contention regards the monophyly of the lissamphibians and the interrelationships of the extant amphibian orders. It is now generally accepted from molecular studies using DNA sequences of mitochondrial 12S and 16S ribosomal RNA genes (Hay, Ruvinsky, Hedges & Maxson, 1995; Hedges & Maxson, 1993) or more recently complete mitochondrial genomes (Zardoya & Meyer, 2001) that Lissamphibians form a monophyletic grouping with respect to amniotes. The monophyly of each extant amphibian order is also now well supported by molecular (Hay et al., 1995; Hedges & Maxson, 1993; Zardoya & Meyer, 2001) and morphological studies (see for example analysis II: soft-morphology and osteological characters of Trueb & Cloutier (1991)). However, it is still unclear which two extant amphibian orders together form a monophyletic group to the exclusion of the third extant amphibian order (Meyer & Zardoya, 2003). A monophyletic grouping of urodeles and caecilians with the exclusion of anurans has been suggested by Hedges & Maxson (1993) using DNA sequences of mitochondrial 12S ribosomal RNA genes and by Feller & Hedges (1998) using DNA sequences of mitochondrial 12S and 16S ribosomal RNA genes, an intervening $tRNA^{VAL}$ gene and a portion of the $tRNA^{LEU(UUR)}$ gene. It should be noted that by their own admission the result suggested by Hedges & Maxson (1993) is not statistically significant. The phylogenetic tree produced from the comparison of complete mitochondrial genomes (Zardoya & Meyer, 2001) has a statistically significant monophyletic grouping of anurans and urodeles with the exclusion of caecilians. The analysis using DNA sequences of mitochondrial 12S and

16S ribosomal RNA genes (Hay et al., 1995) was not able to resolve successfully the interrelationships between the extant orders of amphibians.

Among the diverse extant tetrapod groups (Figure 1.1.1—1) at least some members of the anurans, chelonians, squamates, rhynchocephalians, crocodilians, aves, monotremes, marsupials and placental mammals possess a middle ear coupled to a tympanic membrane. Some members of these groups lack a tympanic membrane, such as snakes, whilst others have no members which possess a tympanic membrane, such as urodeles and caecilians. The lack of a tympanic membrane in an extant group can suggest that members of its lineage have never possessed such a transduction apparatus. The alternative to this is that the tympanic membrane was the ancestral condition for the lineage and that it has subsequently been lost. Loss of a tympanic membrane seems to occur when tetrapods are in close contact with the substrate (for example with a burrowing or forest floor lifestyle) or in an aquatic environment; in these cases they receive sound through solid or liquid (rather than air) contact with their bodies.

The extant mammalian groups all possess primitively a tympanic membrane which is coupled to three middle ear bones, the malleus, incus and stapes. It is generally accepted that this particular ear morphology adapted to the perception of airborne sound had evolved in the common ancestor of all three extant groups, although the middle ear might not have been fully developed in their common ancestor (see (Rich, Hopson, Musser, Flannery & Vickers-Rich, 2005). Any members of the groups that do not possess a normal functioning tympanic membrane, such as cetaceans, have done so via adaptation of the ancestral condition caused by close contact with the substrate or an aquatic lifestyle.

The lepidosauromorphs (squamates and rhynchocephalians) are generally thought to have possessed primitively a tympanic membrane coupled to an ossified stapes and a cartilaginous extrastapes. If this is the correct interpretation then it follows that snakes and amphisbaenians have lost the transduction apparatus as neither group possesses any member with a tympanic membrane (Wever, 1978). The extant archosauromorphs (crocodilians and aves) seem likely to have the presence of a tympanic membrane coupled to an ossified stapes and cartilaginous extrastapes as the ancestral condition. Furthermore, chelonians also possess a tympanic membrane coupled to an ossified stapes and cartilaginous extrastapes (Wever, 1978).

There are three orders of extant amphibians; Urodela, Gymnophiona (caecilians) and Anura which are collectively known as the Lissamphibians. Of these by far the most speciose is the Anura with over 4600 species currently recognised, followed by Urodela with over 540 and Gymnophiona with approximately 168 species (Fouquette, 2004). It is not surprising then that extant anurans show the greatest variety of hearing structures and that caecilians show relatively little variation.

Of the extant amphibians only anurans possess a tympanic membrane coupled to a stapes. Urodeles and caecilians do not possess a tympanic membrane or middle ear space, although most do possess a stapes. Uniquely amongst extant tetrapods members of the anurans and urodeles possess an additional element in the fenestra ovalis, the operculum (note, however, that there is some uncertainty as to whether the caecilian *Ichthyophis glutinosus* also processes such a system – see Peter (1898)). This element, which is usually cartilaginous, has muscular connection to the cartilaginous suprascapular or the scapulocoracoid of the shoulder girdle. It should be noted that the operculum seen in the fenestra ovalis of anurans and urodeles is in no way homologous

to the operculum which covers the gill region in bony fish (including *Panderichthys*). The muscle connecting the operculum, of anurans and urodeles, to the shoulder girdle is known as the opercularis muscle and is normally derived from the levator scapulae (Wever, 1985) (although in Plethodontidae urodeles a branch of the cucullaris major forms the opercularis muscle (Monath, 1965)). Its function has been debated ever since Kingsbury & Reed (1909) speculated that vibrations from the substrate would pass up the forelimb via the shoulder girdle and opercularis muscle to the operculum and into the inner ear. Alternatively, it has been suggested that the operculum functioned as a protective mechanism for the inner ear (Wever, 1985). See recent work with *Rana catesbeiana* Shaw, 1802 (Mason & Narins, 2002a; Mason & Narins, 2002b) for a review of the literature and some recent observations regarding opercular function. Mason and Narins (2002b) conclude that the opercularis system is involved with protecting the inner ear from extremely high amplitude movements of the stapedial footplate caused by vocalisation and breathing. Furthermore, there is a muscular connection between the columella and the shoulder girdle in anurans. This muscle has been described as the columellaris muscle (Wever, 1979; Wever, 1985) or simply a branch of the levator scapulae superior (Hetherington, 1987; Hetherington & Lombard, 1983).

A recent synopsis of extant amphibians has been gained from work undertaken by Fouquette (2004), whose taxonomic arrangement is based primarily on Duellman & Trueb (1986) and Frost (1985) and will be used in this thesis as a basis for reviewing the ear anatomy of each of the three orders in more detail. To review the anatomy each order will be taken in turn.

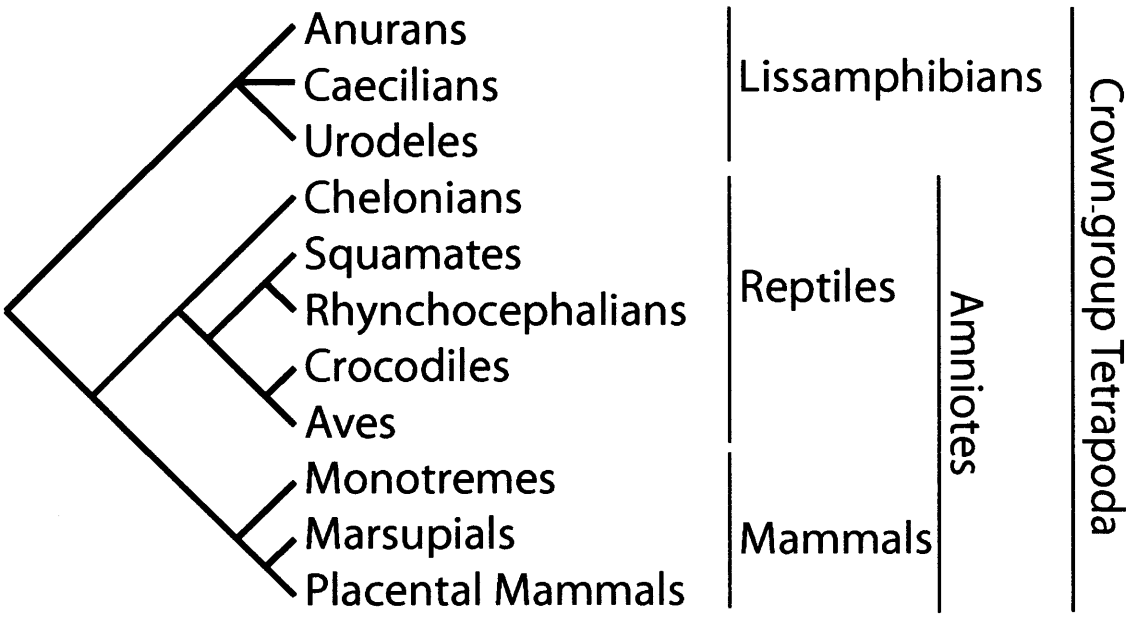

Figure 1.1.1—1 Basic phylogeny of the major extant tetrapods showing the unresolved intrarelationships of the lissamphibians.

Gymnophiona

Of the six families of caecilians recognised by Fouquette ((2004) and references therein) all except, Scolecomorphidae Taylor, possess stapes (Nussbaum & Wilkinson, 1989). Actually, Scolecomorphidae are claimed not to even possess a fenestra ovalis (Figure 1.1.1—2) (Nussbaum & Wilkinson, 1989). In the other five families (Rhinatrematidae Nussbaum, Ichthyophiidae Taylor, Uraeotyphlidae Nussbaum, Caeciliaidae Gray and Typhlonectidae Taylor) the stapes is in contact with the quadrate in most cases (Figure 1.1.1—2 and 3). The two families, Rhinatrematidae and Ichthyophiidae (Figure 1.1.1—2), have a stapedial foramen which may have been lost in, supposedly, more derived families. No member of any caecilian family possesses an operculum in the fenestra ovalis (Nussbaum & Wilkinson, 1989). However Peter (1898) labelled an 'Operculum stapedis' and a 'Columella stapedis' in his description of *Ichthyophis glutinosus* Linnaeus, a feature which is also mentioned by Noble (1931). The presence or absence of an operculum in *Ichthyophis glutinosus* is not to be validated in this thesis. The lack of a shoulder girdle and, hence, possibility of connections between the scapulocoracoid and the otic capsule in caecilians might preclude the presence of an opercular apparatus.

The evolutionary reason behind the ear character states which are observed in extant caecilians remains unclear. Whether the current morphology represents a reduction of a previous airborne sound adapted ear or retention of an ancestral condition is not known.

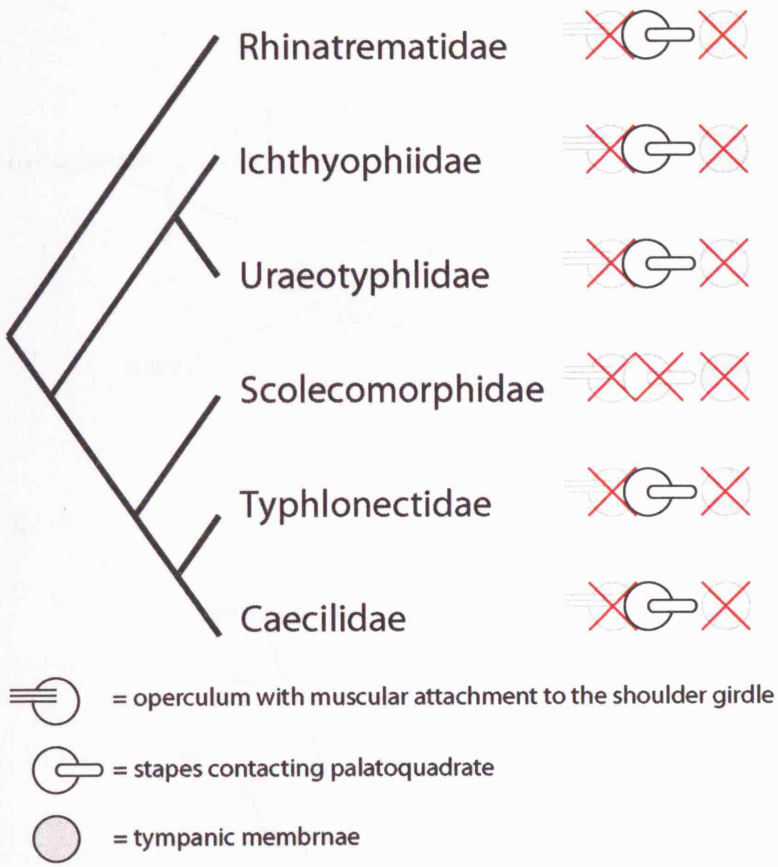

Figure 1.1.1—2 Extant caecilian phylogeny (based on San Mauro, Vences, Alcobendas, Zardoyo & Meyer (2005)) with diagrammatic representations of their middle ear character states. The phylogeny of San Mauro, Vences, Alcobendas, Zardoyo & Meyer (2005) was utilised because it is the most complete analysis of caecilian intrarelationships and is based on the largest data set so far. For morphological references see the neontological section of the introduction.

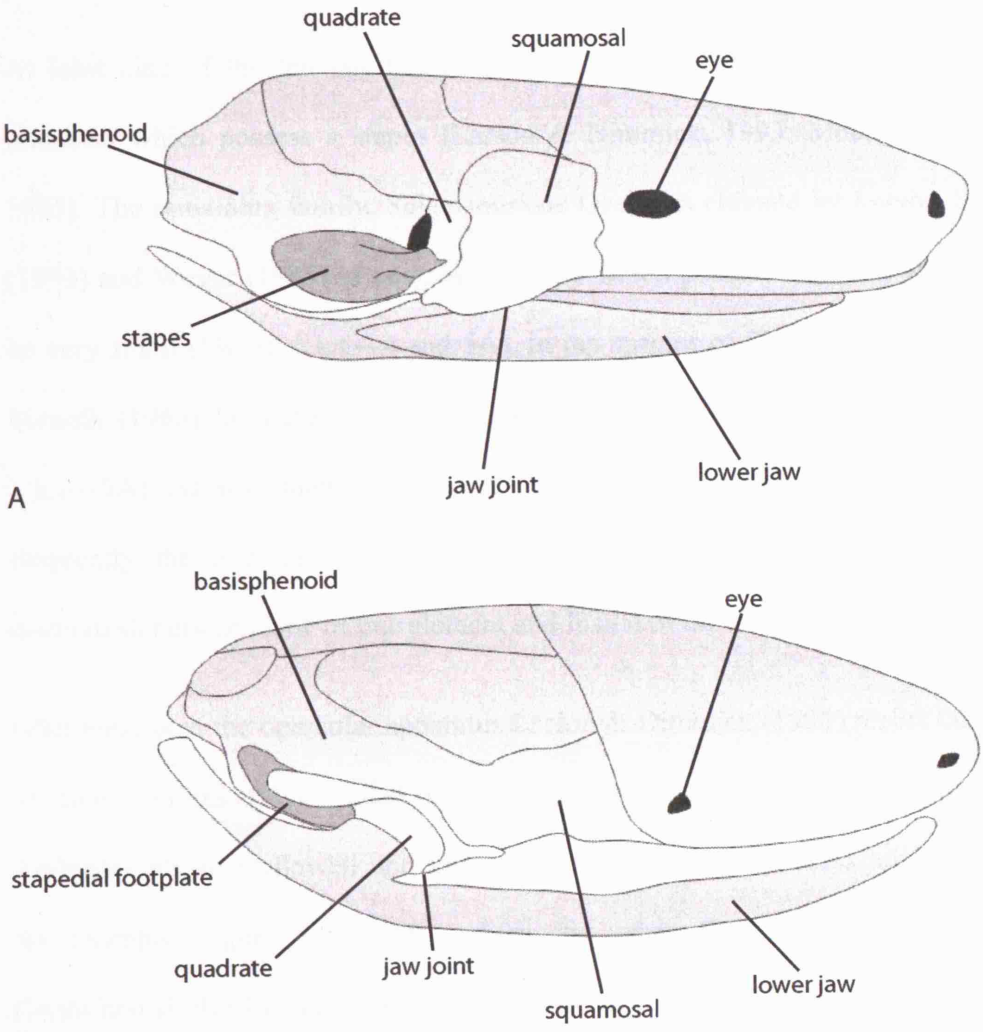

Figure 1.1.1—3 A, diagrammatical representation of the head of *Dermophis mexicanus* showing the middle ear region, anterior to the right (after Wever (1985)). B, diagrammatical representation of the head of *Ichthyophis glutinosus* showing the middle ear region, anterior to the right (after Wever (1985)).

Urodela

At least nine of the ten families (Figure 1.1.1—4) recognised by Fouquette contain members which possess a stapes (Larson & Dimmick, 1993; Monath, 1965; Wever, 1985). The remaining family, Salamandridae Grady, is claimed by Larson & Dimmick (1993) and Wever (1985) to contain members which possess a stapes, although it may be very small (Figure 1.1.1—4 and 5A). In the species of Salamandridae examined by Monath (1965) he states 'no columella or stylus evident' (see for example)Figure 1.1.1—5A). As with many urodeles this situation is made difficult to clarify because frequently the operculum and stapes become fused and it is, therefore, hard to distinguish between lack of one element and fusion of the two.

With regards to the opercular apparatus Larson & Dimmick (1993) report that members of five families (Hynobiidae Cope, Plethodontidae Gray, Salamandridae Grady, Ambystomatidae Hallowell and Dicamptodontidae Tihen) possess an operculum (see for example Figure 1.1.1—5B) whilst the other five families (Sirenidae Gray, Cryptobranchidae Fitzinger, Amphiumidae Cope, Rhyacotritonidae Tihen and Proteidae Tschudi) have no members possessing an operculum (Figure 1.1.1—4). In so far as Monath (1965) covers these families he agrees with Larson & Dimmick's report. By contrast, Wever (1985) states that members of Sirenidae do possess an operculum. In Hynobiidae, Salamandridae and Ambystomatidae the operculum, if present, is connected to the cartilaginous suprascapular via the opercularis muscle which is a branch of the levator scapulae (see for example Figure 1.1.1—5). In Salamandridae the opercularis muscle (composed of levator scapulae inferior and superior) sometimes has additional contact with the bony scapulocoracoid. Additionally, in some Salamandridae and Ambystomatidae species the intertransversarius capitis inferior connects with the

operculum (Monath, 1965). As mentioned previously, in Plethodontidae a branch of the cucullaris muscle rather than the levator scapulae connects the scapulocoracoid to the operculum (Monath, 1965).

Clearly, the ear anatomy of extant urodeles is not fully described and understood. It seems likely that it is most parsimonious to assume that multiple loss of a characteristic is easier than multiple gain of the same character state and therefore it is tentatively conclude that the presence of both an operculum and stapes is the ancestral condition for urodeles. The lack of tympanic annulus, tympanic membrane and middle ear cavity in all extant urodeles also suggests that this is the ancestral condition for urodeles.

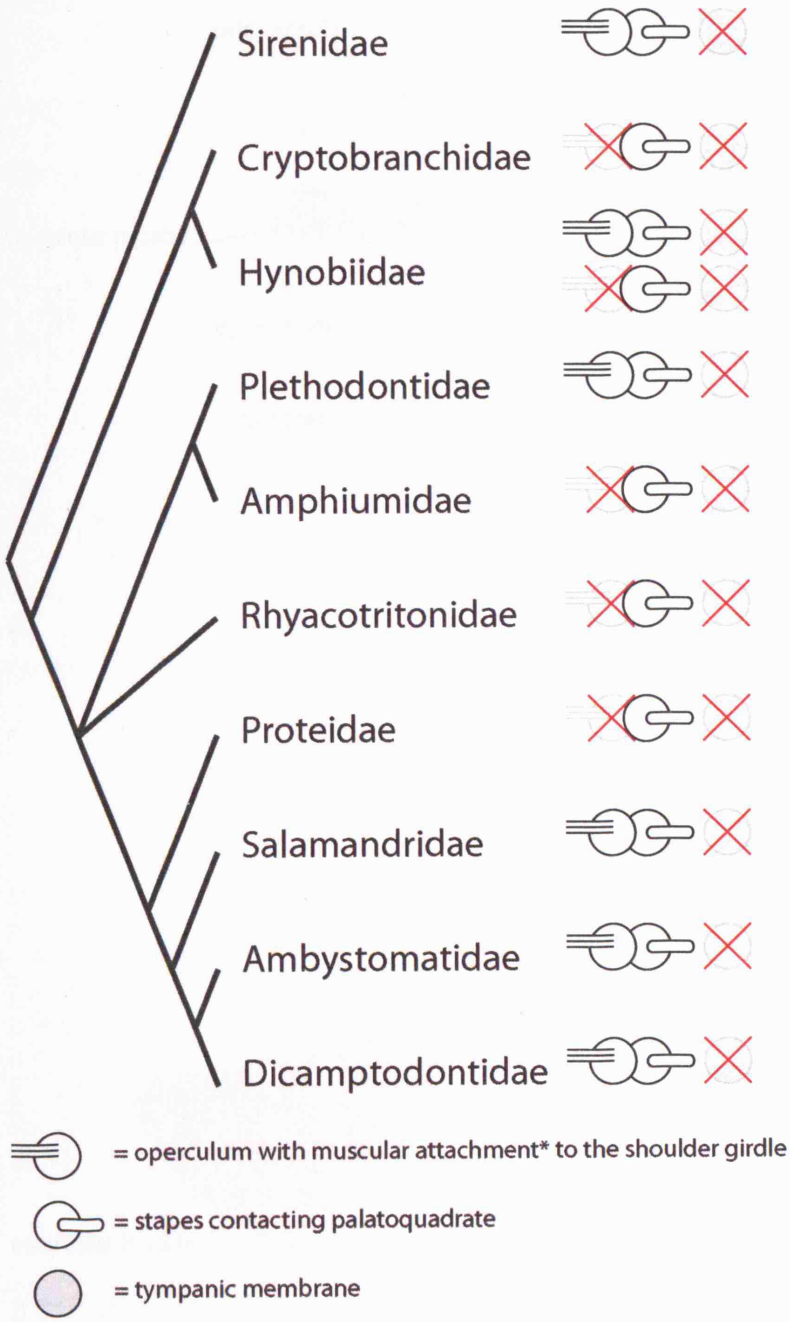

Figure 1.1.1—4 Extant urodele phylogeny (based on Larson & Dimmick's strict consensus of 40 most parsimonious trees (1993)) with diagrammatic representations of their middle ear character states. The phylogeny of Larson & Dimmick (1993) was utilised here because it the most recent urodele phylogeny which includes all ten of the currently recognised urodele families. For morphological references see the neontological section of the introduction. * = in Plethodontidae this connection is with a branch of the cucullaris muscle rather than a branch of the levator scapulae muscle.

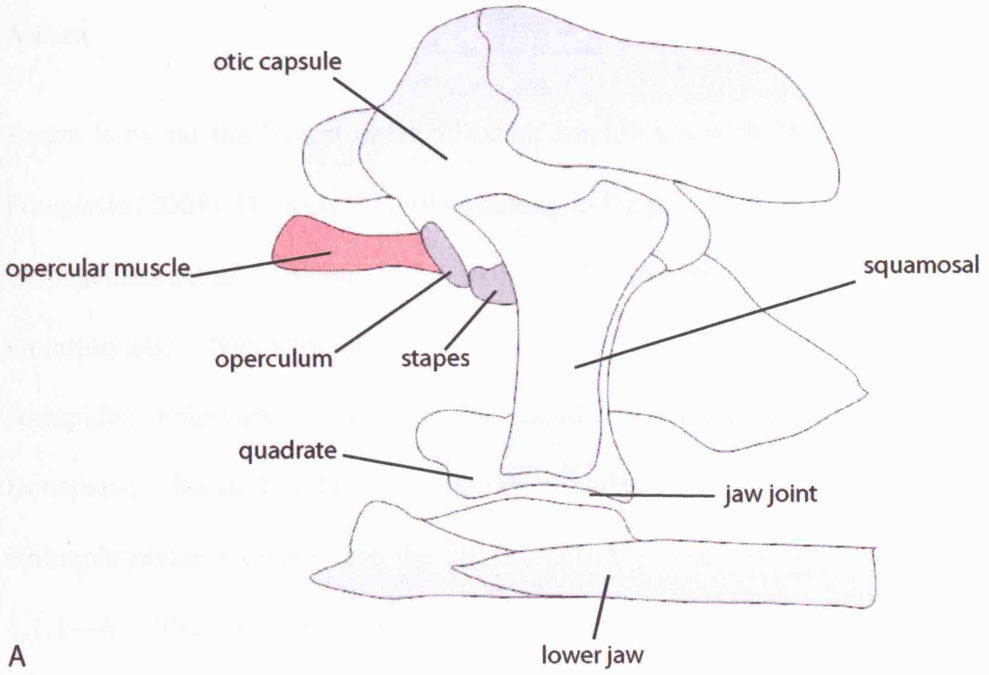

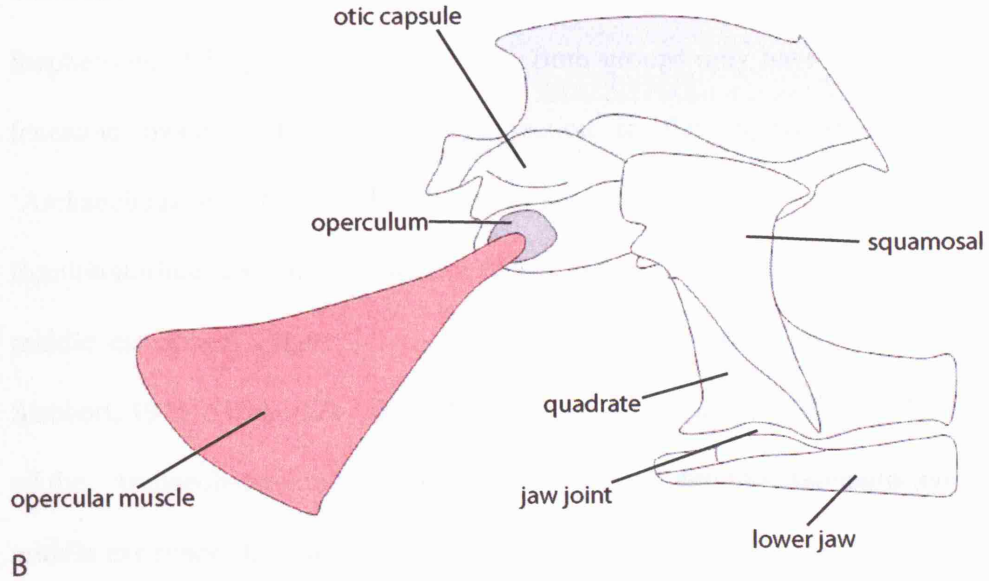

Figure 1.1.1—5 A, Diagrammatic representation of the middle ear region of *Ambystoma tigrinum* with anterior to the right (after Wever (1985)). B, Diagrammatic representation of the middle ear region of *Taricha torosa* with anterior to the right (after Wever (1985)).

Anura

Anura is by far the largest order of extant amphibians with 28 families recognised by Fouquette (2004). Of these 9 families belong to the paraphyletic assemblage of so called 'Archaeobatrachia' (Figure 1.1.1—6) while the remaining 19 belong to the monophyletic Neobatrachia. The 'Archaeobatrachia' (Leiopelmatidae Mivart, Ascapidae Fejervary, Discoglossidae Günther, Bombinatoridae Gray, Pelobatidae Bonaparte, Megophryidae Noble, Pelodytidae Bonaparte, Pipidae Gray and Rhinophrynidae Günther) are the phylogenetically most basal extant anurans (Figure 1.1.1—6). The two most basal families (Leiopelmatidae and Ascapidae), each representing only one genus do not possess stapes, tympanic annulus, tympanic membrane or middle ear space (Figure 1.1.1—6) (DeVilliers, 1934; Pusey, 1943; Stephenson, 1951a; Stephenson, 1951b). Both groups only have an operculum in their fenestrae ovales with muscular connection to the suprascapular. Of the other 'Archaeobatrachia' families Rhinophrynidae and the genus *Bombina* (the 'Unke') with Bombinatoridae also do not possess stapes, tympanic annulus, tympanic membrane or middle ear space (Figure 1.1.1—6) (Cannatella & Trueb, 1988; Ramaswami, 1943; Slabbert, 1945; Slabbert & Maree, 1945; Trueb & Cannatella, 1982). All other members of the 'Archaeobatrachia' possess stapes, tympanic annulus, tympanic membrane and middle ear space (Cannatella & Trueb, 1988; Clarke, 1987; DeVilliers, 1934; Lathrop, 1997; Maglia, 1998; Maree, 1945; Parker, 1881; Ramaswami, 1943; Rocek, 1981; Slabbert, 1945; Slabbert & Maree, 1945; Taylor & Noble, 1924; Trueb & Cannatella, 1982), although, according to Wever (1985) in the genera *Xenopus* and *Pipa* the tympanum is a solid disk below the skin surface rather than a thin membrane at the body surface (Figure 1.1.1—6). All the 'Archaeobatrachia' possess an opercular apparatus with a muscular connection to the suprascapular with the exception of

numerous members of the Pipidae (Figure 1.1.1—6) (such as the genera *Pipa* (DeVilliers, 1934), *Hemipipa* and *Hymenochirus* (Wever, 1985)). Additionally, in the pipid *Xenopus* the operculum is claimed to be part of the stapedial footplate (according to Wever (1985)).

The remaining 19 families of extant anurans belong to the Neobatrachia which contains over 95% of all living anuran species. The vast majority of these families contain members which possess stapes, tympanic annulus, tympanic membrane, middle ear space and opercular system (Figure 1.1.1—6 and 7). Those that are known not to possess this full compliment may be in close association with the substrate (in the case of the burrowing family Hemisotidae) or their ear anatomy may simply be poorly understood.

It seems likely that the ancestral condition for extant anurans is the possession of a full complement of hearing structures as seen in most Neobatrachia. However, due to the lack of many such features in Leiopelmatidae and Ascaphidae this has previously been questioned (Stephenson, 1951b; Tumarkin, 1949). Stephenson (1951b), in fact, concluded that the condition seen in 'primitive frogs...may well represent a primary condition and not a secondary loss'. A similar point of view was put forward by Tumarkin (1949) when he proposed the lack of tympanic membranes observed in caecilians, urodeles and phylogenetically basal anurans, along with many amniotes groups, was not degenerative or secondary. Tumarkin (1949) appears to have believed that an ear adapted to the perception of airborne sounds could have evolved numerous times within amphibians and amniotes.

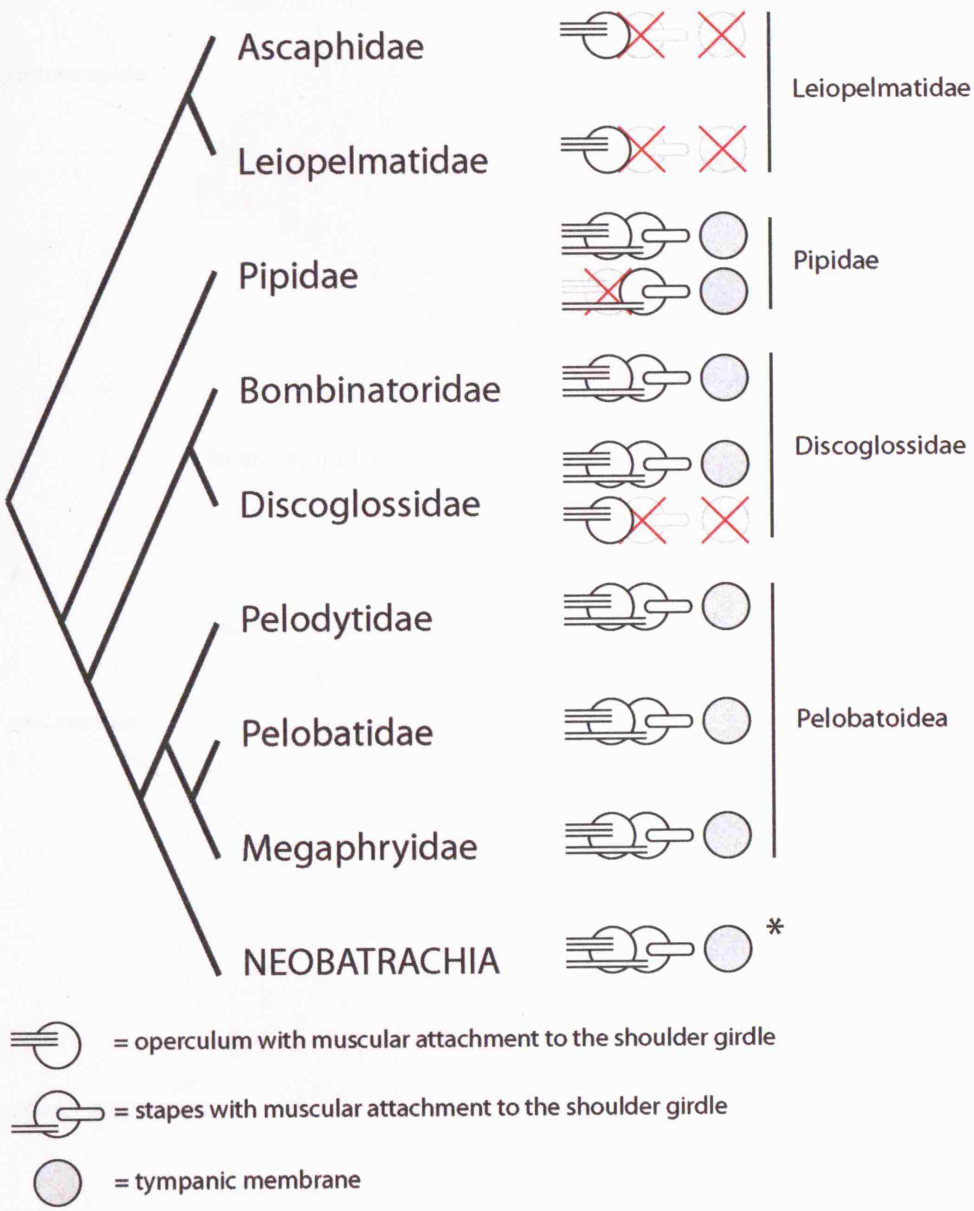

Figure 1.1.1—6 Phylogeny of extant 'Archaeobatrachia' based on San Mauro et al. (2005). The family Rhinophrynidae was not included in this analysis. Names used by San Mauro et al. are shown to the right of the phylogeny. Diagrammatic representations of their middle ear character states are also shown. The phylogeny of San Mauro et al. (2005) was utilised here because it is the most recent analysis available and used the largest data set so far published. For morphological references see the neontological section of the introduction. * = NEOBATRACHIA is a very large phylogenetic grouping with certain members which may not contain the full compliment of middle ear features.

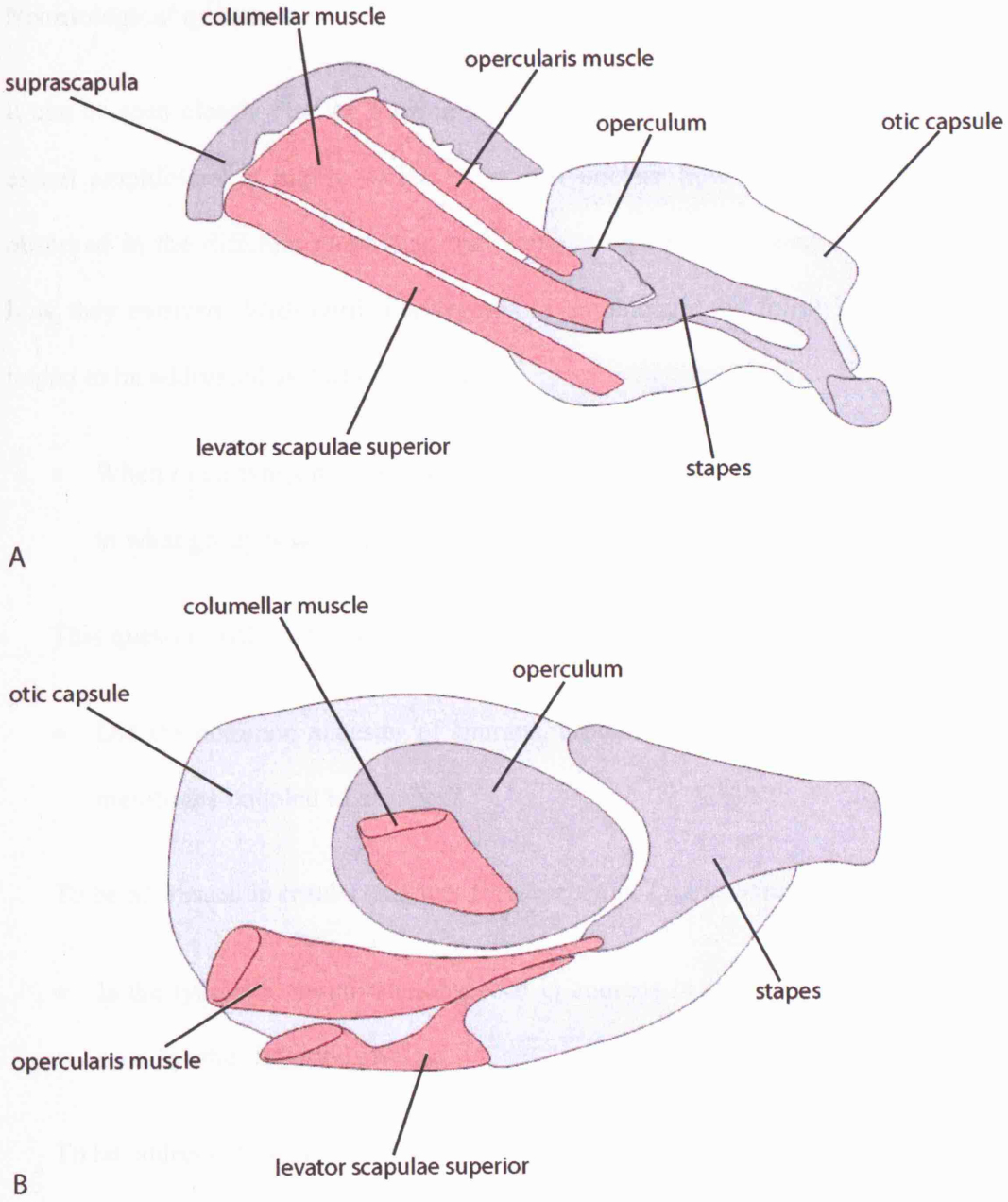

Figure 1.1.1—7 A, Diagrammatic representation of the middle ear region of *Rana pipiens* with anterior to the right (after Wever (1985)). B, Diagrammatic representation of the middle ear region of *Rana catesbeiana* with anterior to the right (after Wever (1985)).

Neontological questions

It can be seen clearly that the hearing anatomy in extant tetrapods and, particularly, in extant amphibians is highly varied. It is still unclear how the extant morphologies observed in the different amphibian and amniote orders are related to each other and how they evolved. With particular regards to amphibians the following questions are hoped to be addressed as part of this thesis:

- When did a tympanic membrane coupled to a stapes first evolve in tetrapods and in what group was this?

This question will be addressed in results chapters *Dendrerpeton* and *Lydekkerina.*

- Did the common ancestor of anurans, urodeles and caecilians have a tympanic membrane coupled to a stapes?

To be addressed in results chapters *Dendrerpeton, Lydekkerina* and *Micropholis.*

- Is the tympanic membrane observed in anurans in any way homologous to that seen in other tetrapod groups?

To be addressed in the overall discussion and conclusions, 4.

- When is the first evidence of a muscle connecting the stapes to the shoulder girdle?

To be addressed in results chapters *Dendrerpeton, Lydekkerina* and *Micropholis* with particular emphasis on chapter *Dendrerpeton.*

- When did the opercular apparatus evolve in tetrapods and in what group was this?

To be addressed in results chapters *Dendrerpeton*, *Lydekkerina* and *Micropholis* with particular emphasis on chapter *Lydekkerina*.

- Did the common ancestor of batrachians, lissamphibians or all tetrapods possess an opercular apparatus?

To be addressed in results chapters *Dendrerpeton*, *Lydekkerina*, *Micropholis* and in the overall discussion and conclusions, 4.

- When is the first evidence of a muscle connecting the opercular apparatus to the shoulder girdle?

To be addressed in results chapters *Dendrerpeton*, *Lydekkerina* and *Micropholis* with particular emphasis on chapter 3.4.

1.1.2. PALAEONTOLOGICAL SECTION

It is important to look at the fossil record of tetrapods in order to investigate the evolutionary sequence of character state acquisitions and loss behind the varied soft-tissue and osteological hearing anatomy observed in extant tetrapods. Of course, the most important fossils are those which can be directly attributed to one of the extant amphibian orders. Unfortunately, the amphibian fossil record is very poor, with a sparse range of specimens currently described. In addition, the specimens which are available are highly dorsoventrally compressed and the detail of the hearing anatomy is poorly known. Following a description of the most important specimens which can be attributed to one of the extant amphibian tetrapod orders a review of the hearing anatomy of early tetrapods will be presented. This section will demonstrate that our knowledge of the hearing anatomy of early tetrapods is in no way complete. It will further show that the application of CT scanning and 3D reconstruction on significant early tetrapod specimens can be used to help address the many remaining questions. CT scanning and 3D reconstruction allows the high resolution visualisation of specimens which can provide evidence of important soft-tissue characteristics which cannot be easily gleaned from traditional preparation.

The earliest known caecilian is *Eocaecilia micropodia* Jenkins & Walsh from the Early Jurassic of Coconino County, Arizona USA which unlike extant caecilians possesses limbs (Jenkins & Walsh, 1993). Similarly to extant caecilians, *Eocaecilia micropodia* does not possess a temporal notch suggesting that it did not have a tympanic membrane. Its stapes is known and consists of a uniquely shaped ossification which contacts the fenestra ovalis, extends forwards and expands distally to contact both the quadrate and

the braincase (Jenkins & Walsh, 1993). Additionally, it is suggested that the stapes had a synovial contact with the retroarticular process (Jenkins & Walsh, 1993).

Two of the earliest urodeles are *Karaurus sharovi* Ivachnenko and *Valdotriton gracilis* Evans & Milner from the Late Jurassic and Early Cretaceous respectively. Both are claimed to have not possessed temporal notches (Estes, 1981; Evans & Milner, 1996; Ivachnenko, 1978) and so are thought not to have had tympanic membranes. The stapes in both species have broad and rounded footplates and short robust styli (Estes, 1981; Evans & Milner, 1996; Ivachnenko, 1978).

The earliest known salientian (anurans plus stem group anurans) specimen is *Triadobatrachus massinota* Piveteau from the Early Triassic of Madagascar which is definitely a stem-group rather than crown-group anuran. Although, there is no tympanic annulus preserved, as would be expected for it is cartilaginous in extant anurans, there is a posterior emargination in the squamosal (Rage & Rocek, 1989). This emargination suggests that a tympanic membrane may well have been present. However, Rage and Rocek (1989) state this is not certain and that the emargination could have served as a muscular attachment point. The stapes has a stout round proximal footplate and a rod which becomes narrow with an unfinished distal end suggesting a cartilaginous component as seen in extant anurans (Wever, 1985). The stapes is unknown or poorly known in two other early salientians, *Vieraella herbstii* Reig and *Notobatrachus degiustoi* Reig (Báez & Basso, 1996). Báez & Basso do, however, suggest that *Notobatrachus degiustoi* could have possessed an operculum.

The early fossil specimens that can be ascribed to the modern amphibian orders provide only limited information regarding the hearing structures of early members of these orders. Therefore in order to understand the evolutionary history of the varied hearing

anatomy of extant tetrapods it is clearly necessary to investigate the phylogenetic context of extant amphibians within Tetrapoda. As mentioned in the previous section the monophyly of extant amphibians (i.e. Lissamphibia) is now well supported by both molecular and morphological means. It is also clear that all other extant tetrapods belong to the Amniota. Both Lissamphibia and Amniota evolved from the paraphyletic assemblage loosely termed 'early tetrapods'. Early tetrapods are a vast array of groups including colosteids, baphetids, temnospondyls, lepospondyls (which contains microsaurs, lysorophids, acherontiscids, adelospondyls, nectrideans and aistopods, but may or may not form a natural group), embolomeres, gephyrostegids, seymouriamorphs, diadectamorphs and unambiguous stem group tetrapods, such as, *Acanthostega* and *Ichthyostega.* Current hypotheses about the interrelationships of these groups are best illustrated by the phylogenies of Ruta, Coates & Quicke (2003a) (Figure 1.1.2—1) and Laurin & Reisz (1997) (Figure 1.1.2—2). It can be seen from these two phylogenies that the interrelationships of the early tetrapods are quite stable (Figure 1.1.2—3). However, it can also be seen from these phylogenies that the exact placement of the lissamphibian orders within the early tetrapods is contentious. The phylogenetic position of the Lissamphibian orders relative to different early tetrapod groups has been recently debated (Anderson, 2001; Anderson, 2002; Laurin, 2002; Laurin & Reisz, 1997; Ruta et al., 2003a; Ruta, Jeffery & Coates, 2003b).

Among the numerous early tetrapod groups, temnospondyls and lepospondyls are most frequently cited in the debate about the origins of the extant amphibian orders. The view obtained from cladistic analyses that the extant amphibians form a monophyletic grouping nested within the temnospondyls has most recently been supported by Ruta et al. (2003a) while a monophyletic grouping nested within the lepospondyls has been suggested by Laurin & Reisz (1997). A phylogenetic origin of caecilians from within

the lepospondyls has been suggested (Anderson, 2001; Carroll & Currie, 1975). As mentioned by Laurin (2002) the monophyly of extant amphibians (the Lissamphibia) relative to amniotes does not preclude the possibility that the different orders of extant amphibians are closely related to different early tetrapod groups as long as the monophyletic grouping formed excludes amniotes. This means that, although, the monophyly of the lissamphibians is well supported by molecular analysis a dual origin of lissamphibians within the early tetrapods cannot be discounted by the molecular evidence alone. Judgement on which group or groups the extant orders are most closely related to depends entirely on morphological data and cladistic analysis. Clearly, the phylogeny produced from cladistic analysis of the morphological character can affect greatly the inferred evolutionary origins of the ear anatomy observed in the extant amphibian orders.

Both the phylogeny produced by Laurin & Reisz (1997) and that of Ruta et al. (2003a) are rooted with osteolepiforms being a sister group to elpistostegids and tetrapods. *Eusthenopteron*, one of the best known osteolepiforms, did not have an ear adapted to the perception of airborne sound, its hyomandibular, the likely homolog to the tetrapod stapes, has a bi-facetted proximal end which articulates with equivalent facets on the braincase (one on the lateral commissure and the other near the vestibular fontanelle) (Jarvik, 1980) (see Figure 1.1.2—4A). The hyomandibular morphology seen in *Eusthenopteron* is general for sarcopterygians, and crown group gnathostomes with the exception of the proximal bi-facetted head. The vestibular fontanelle present in *Eusthenopteron* and other osteolepiforms is more ventral than the fenestra ovalis seen in tetrapods. The hyomandibular runs posteroventrally in close proximity, but without contact, to the palatoquadrate (see Figure 1.1.2—4A). Its distal end reaches for, but does not have an ossified contact with the quadrate. Early published hyomandibular/stapedial

anatomy of *Panderichthys* (Ahlberg, Clack & Lukševičs, 1996; Vorobyeva & Schultze, 1991) showed a high degree of similarity to the condition witnessed in *Eusthenopteron.* However, a recent re-examination of *Panderichthys* (Brazeau & Ahlberg, 2006) describes a slender, rod-like hyomandibula whose distal end contacted the mesial face of the cheek operculum rather than extending further towards the quadrate. The element identified as the hyomandibular by Ahlberg et al. (1996) is in fact a compound structure of several epibranchials (Ahlberg pers.comm.). It seems that the ossified distal end of the hyomandibula of *Panderichthys* may be homologous to the mid-shaft opercular process of *Eusthenopteron* (Brazeau & Ahlberg, 2006). Therefore, by comparison with *Panderichthys*, the tetrapod stapes could correspond to only the proximal half of the hyomandibula of *Eusthenopteron* and osteichthyans in general. *Panderichthys* possesses paired openings or slits in the posterodorsal skull margin which are much larger than those seen in *Eusthenopteron.* These slits are claimed to be spiracular openings for the exit of the spiracular canal (Vorobyeva & Schultze, 1991).

The earliest and phylogenetically most basal tetrapods include *Ventastega*, *Acanthostega*, *Ichthyostega*, and *Tulerpeton.* Very little is known about the ear anatomy of *Ventastega* or *Tulerpeton*, although, it is presumed that they possessed a stapes sitting in a fenestra ovalis in a manner similar to that observed in *Acanthostega*, *Ichthyostega* and all other early tetrapods for which this area of the braincase is known. Although, both *Acanthostega* and *Ichthyostega* possess stapes in a fenestra ovalis their ear anatomy is quite different. While *Ichthyostega* has a unique ear, with a fan shaped stapes (Clack, Ahlberg, Finney, Dominguez Alonso, Robinson & Ketcham, 2003) which may be adapted to underwater hearing, *Acanthostega* has a stapedial morphology with many similarities to those seen in other early tetrapods such as *Greererpeton* (see

Figure 1.1.2—4C) and *Pholiderpeton* (see Figure 1.1.2—4B) and, therefore, may be a more representative ancestral condition.

As with *Panderichthys* many early tetrapods possess paired openings on the posterodorsal margin of the skull roof. These openings, often termed temporal notches, are present in *Acanthostega* (Clack, 2002a; Clack, 2003b), *Ichthyostega* (Jarvik, 1996), *Ventastega* (Ahlberg pers.comm.), *Whatcheeria* (Lombard & Bolt, 1995) and all baphetids (Beaumont, 1977; Beaumont & Smithson, 1998; Clack, 2003a). Other major tetrapod groups which possess these so called temporal notches include embolomeres (Clack, 1987; Holmes, 1984; Holmes, 1989; Panchen, 1977), gephyrostegids (Boy & Bandel, 1973; Carroll, 1970), seymouriamorphs (Berman, Henrici, Sumida & Martens, 2000; Berman, Reisz & Eberth, 1987; Boy & Bandel, 1973; Carroll, 1970; Klembara, 1997; Laurin, 1995; Laurin, 1996) and most temnospondyls. The colosteids (Hook, 1983; Smithson, 1982), lepospondyls (with the exception of *Adelospondylus watsoni* Carroll) (Carroll, Bossy, Milner, Andrews & Wellstead, 1998; Carroll & Gaskill, 1978; Wellstead, 1991), *Limnoscelis* (Berman & Sumida, 1990; Romer, 1946), *Captorhinus* (Fox & Bowman, 1966; Heaton, 1979), *Paleothyris* (Carroll, 1969) (see Figure 1.1.2—4F) and *Petrolacosaurus* (Peabody, 1952; Reisz, 1977) do not possess temporal notches.

It is generally presumed that all early tetrapods possessed a stapes, however, in many groups information is limited or non-existent. No stapes has been identified in any specimen of gephyrostegid, nectridean, adelospondyl, or acherontiscid. In addition, stapedial morphology is poorly known in:

- Aistopods - a single possible disc like stapes has been identified in a specimen of *Phlegethontia linearis* Cope (Carroll et al., 1998).

- Baphetids - a poorly preserved stapes in *Spathicephalus mirus* Watson is known (Beaumont & Smithson, 1998) along with a partial description of the stapes of *Kyrinion martilli* Clack, 2003.

- Embolomeres - the well described stapes of *Pholiderpeton scutigerum* (see Figure 1.1.2—4B) is known (Clack, 1983) along with the stapes of *Palaeoherpeton decorum* (Clack, 1983).

The stapes is relatively well known in temnospondyls, where it can generally be described as rod like and dorsolaterally orientated (see for example *Edops* in Figure 1.1.2—4D), and in seymouriamorphs where it is dorsolaterally orientated and often poorly ossified. In microsaurs the stapes is well known and can be generally described as having a relatively large round footplate with a short button rod which reaches laterally towards and frequently contacts the quadrate (Carroll et al., 1998; Carroll & Gaskill, 1978) (see for example *Cardiocephalus* in Figure 1.1.2—4E). Stapedial morphology is also known in *Greererpeton*, which possesses a large and robust fan shaped stapes.

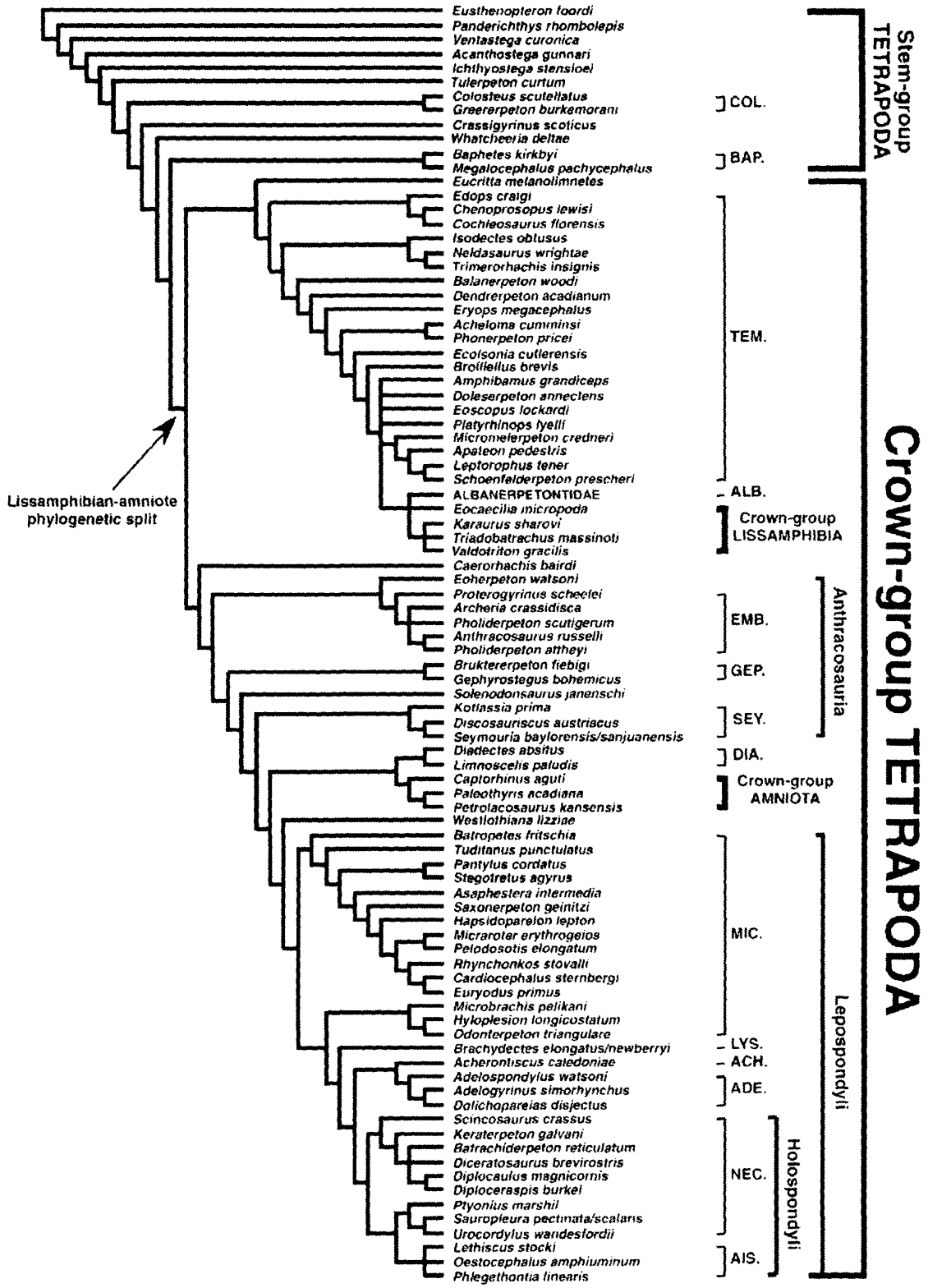

Figure 1.1.2—1 Ruta et al.'s 2003 phylogeny of early tetrapods based on a strict consensus of 64 parsimonious trees. Decay index values have been removed from original figure. Abbreviations used by Ruta et al. in figure: ACH = Acherontiscidae, ADE = Adelospondyli, AIS = Aistopoda, ALB = Albanerpetontidae, BAP = Baphetidae, COL = Colosteidae, DIA = Diadectomorpha, EMB = Embolomeri, GEP = Gephyrostegidae, LYS = Lysorophia, MIC = Microsauria, NEC = Nectridea, SEY = Seymouriamorpha, TEM = Temnospondyli.

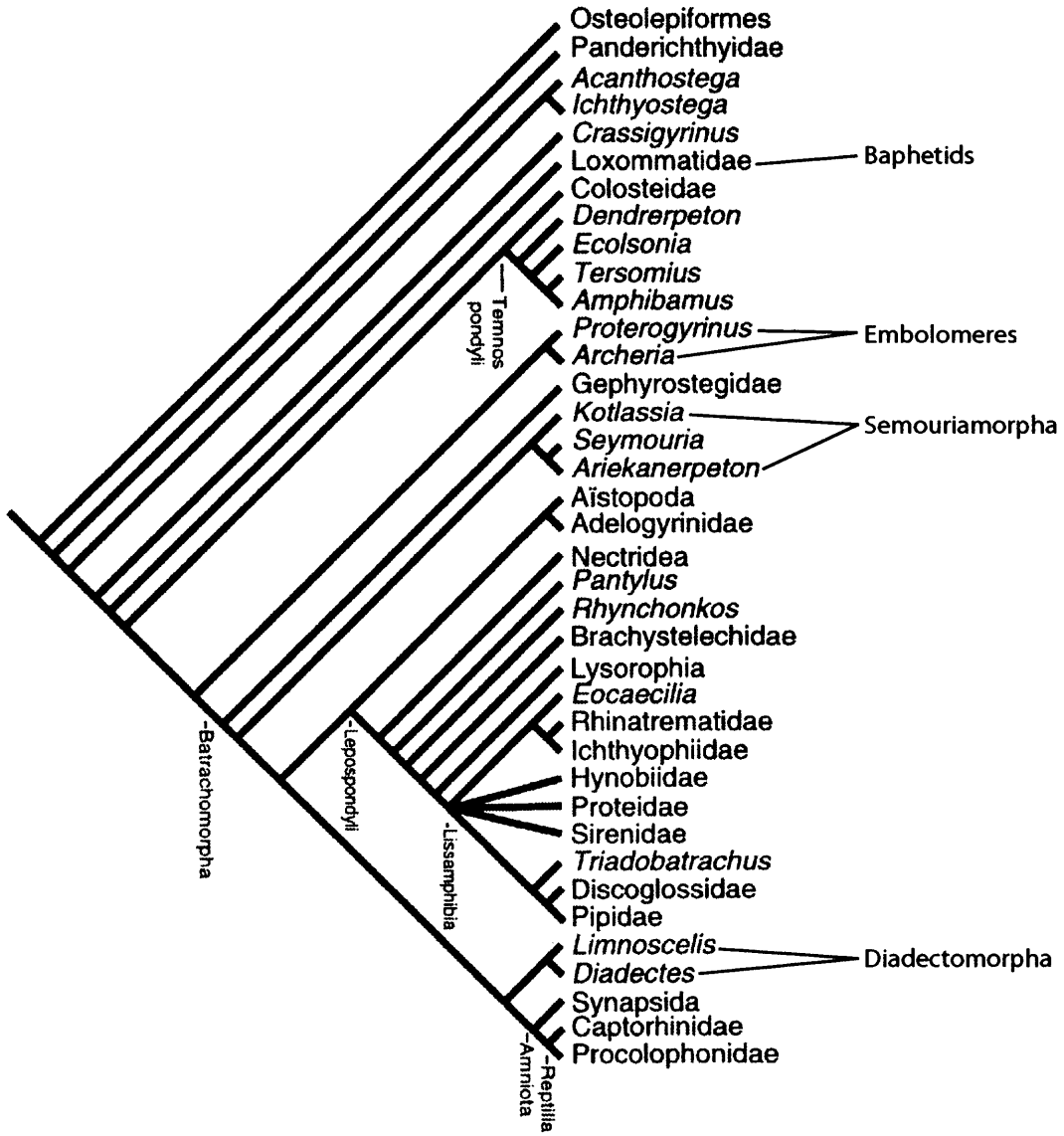

Figure 1.1.2—2 Laurin & Reisz's 1997 phylogeny of early tetrapods based on most parsimonious tree. Letter abbreviations have been removed from original figure. Labelling on the right of the figure has been subsequently added.

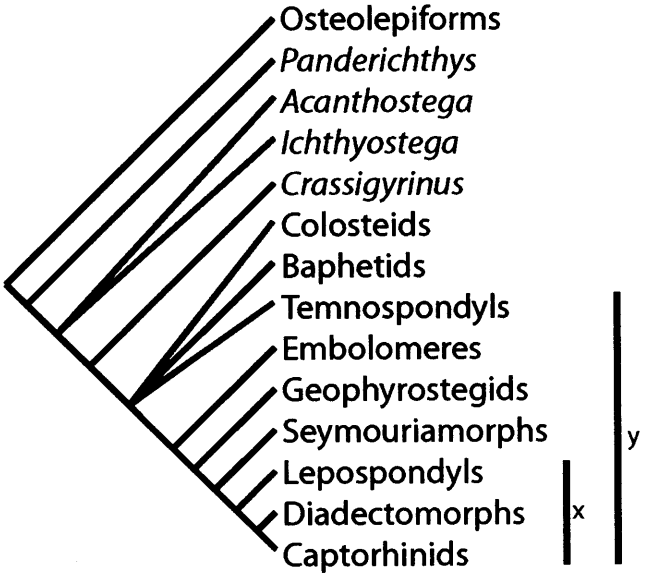

Figure 1.1.2—3 Basic phylogenetic consensus created from the early tetrapod phylogenies of Ruta et al. (2003) and Laurin & Reisz (1997). x = crown-group Tetrapoda of Laurin & Reisz. y = crown-group Tetrapoda of Ruta et al.

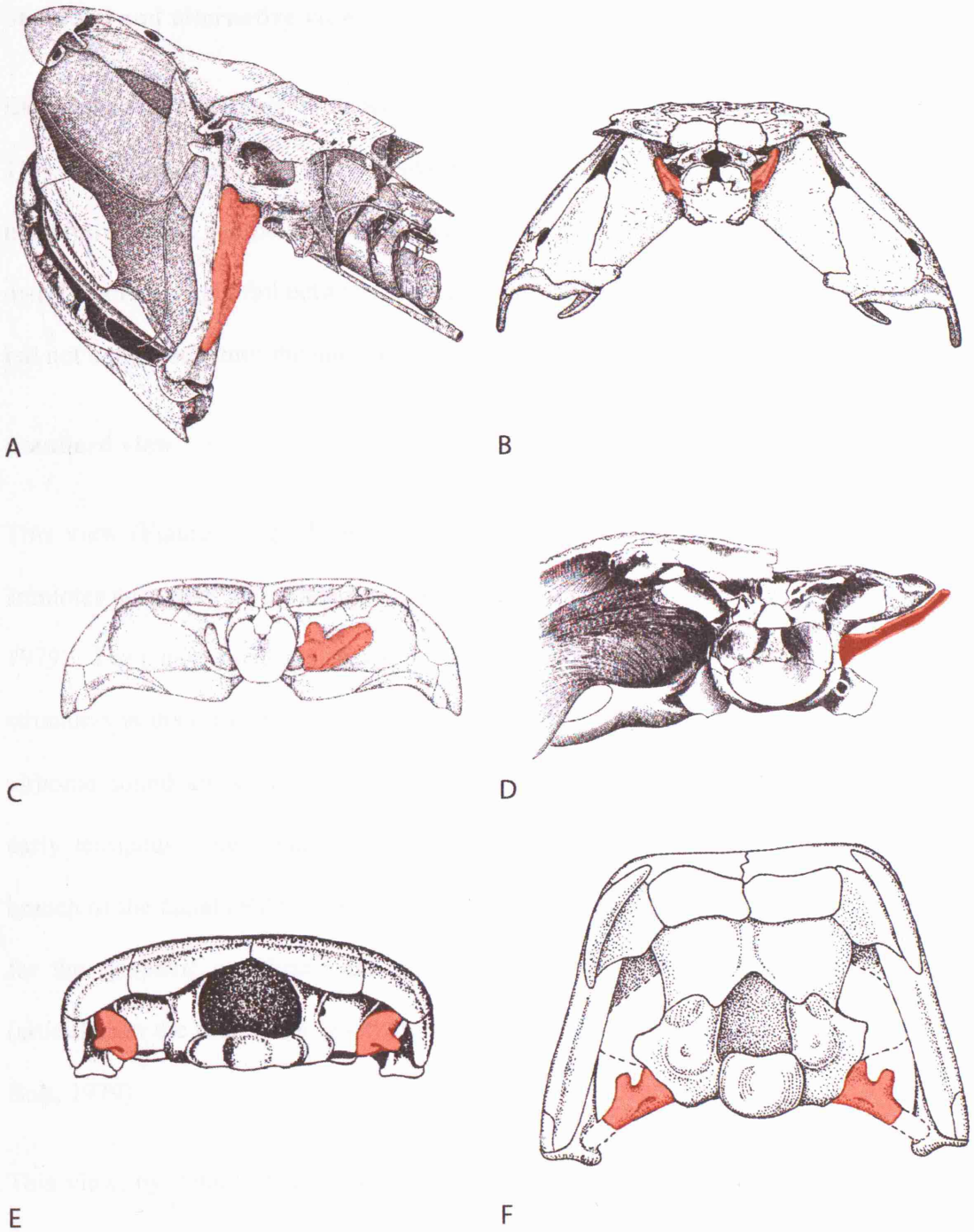

Figure 1.1.2—4 Posterior views of various important specimens otooccipital regions, with the hyomandibula-stapes highlighted in red. Not to comparable scales. A, *Eusthenopteron* (left offset posterior view) adapted from Jarvik (1980). B, *Pholiderpeton* from Clack (1987). C, *Greererpeton* adapted from Smithson (1982). D, *Edops* adapted from Romer & Witter (1942). E, *Cardiocephalus* adapted from Carroll (1998). F, *Palaeothyris* adapted from Carroll (1980).

Standard and alternative views

Early tetrapods are crucial to understanding the evolution of hearing in tetrapods *per se*. This significance has lead to extensive prior study of their 'hearing' structures. These numerous studies can be summarised as being two opposing views, although, there are many theories which fall between these two extremes. The standard view was prevalent but not unopposed until the late 1970s when the alternative view became dominant.

Standard view

This view (Figure 1.1.2—5) proposed that the common ancestor of amphibians and amniotes possessed an ear adapted to the perception of airborne sound (Lombard & Bolt, 1979). Thus any variation which is seen in the hearing apparatus and associated structures in the different extant groups which possess ears adapted to the perception of airborne sound are simply due to specialisations which have occurred since the first early tetrapods. These variations include differing paths of the internal mandibular branch of the facial (VII) nerve, positions of the tympanic membrane, support structures for the tympanic membrane and the addition of an incus (quadrate) and a malleus (articular) to the middle ear ossicular sound conducting chain in mammals (Lombard & Bolt, 1979).

This view, by default, hypothesises that any extant group of tetrapods which does not possess an ear adapted to the perception of airborne sound has secondarily lost this specialisation. Also it has been described as 'the standard view' (Lombard & Bolt, 1979), 'the textbook theory' (Tumarkin, 1949) or 'the orthodox theory' (Tumarkin, 1949). Proponents of this 'standard view' included Parrington (1949; 1958), Westoll (1943), Eaton (1939) and many others. When Parrington was extolling the virtues of a

single origin of a tetrapod ear adapted to the perception of airborne sound there was relatively little information on the middle ear and associated structures in tetrapods from the Carboniferous and the Devonian. The character states for the middle ear anatomy in early tetrapods were gleaned from 'labyrinthodonts', such as *Lydekkerina huxleyi* which possesses rod-like stapes directed towards paired posterior notches. It was, therefore, presumed that early tetrapods which possessed paired posterior notches would have similar stapes and an ear adapted to the perception of airborne sound. This rational interpretation fostered the view that the first tetrapods, such as *Ichthyostega*, had already evolved an ear adapted to the perception of airborne sound. Hence it was assumed that as the first tetrapods possessed such an ear all extant tetrapods have ears which are simply adapted from this original evolution. The lack of paired posterior notches and large stapes which contacted the quadrate in early amniote specimens, such as captorhinids, was not thought as a barrier to this assumption. It was in fact claimed that these specimens had a tympanic membrane and a cartilaginous tympanic process of the stapes even though there was little palaeontological evidence to support this view.

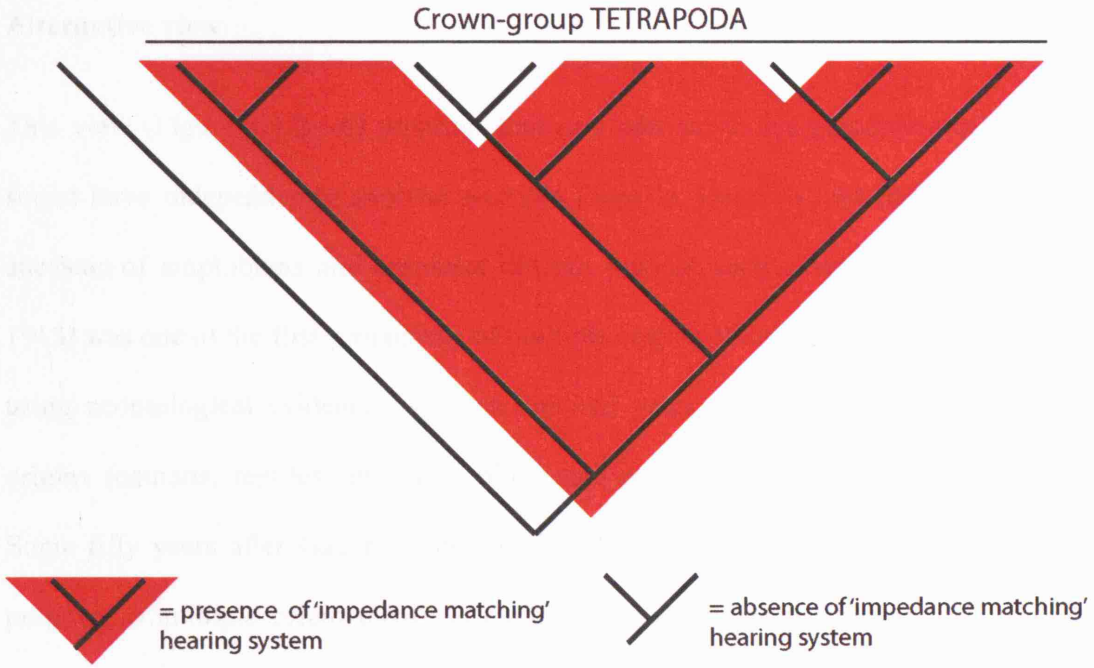

Figure 1.1.2—5 Diagrammatic representation of the 'standard view' of the evolution of an ear adapted to the perception of airborne sound. The common ancestor of crown-group Tetrapoda possessed such a system.

Alternative view

This view (Figure 1.1.2—6) proposes that ears adapted to the perception of airborne sound have independently evolved multiple times in tetrapods and that the common ancestor of amphibians and amniotes did not possess such a system. Gaupp (1898; 1913) was one of the first proponents of multiple origins of airborne sound adapted ears, using neontological evidence over one hundred years ago to propose three separate origins (anurans, reptiles (including birds) and mammals) (Lombard & Bolt, 1979). Some fifty years after Gaupp, Tumarkin (1948; 1949) appears to have independently proposed a multiple origin theory to explain the varied hearing anatomy observed in extant tetrapods. Parrington (1949) dismissed the multiple origins of the airborne sound adapted ears proposed by Tumarkin (1949; 1968) stating that the problems involved in the standard view, involving the varied ear anatomy observed in extant tetrapods, are far smaller than those involved in Tumarkin's hypothesis, involving parallel evolution. Given the palaeontological evidence available to Parrington it is not surprising that he was extremely sceptical of the multiple origin hypothesis proposed by Tumarkin. The robust stapedial morphologies observed in several early tetrapods were not known at that time. In fact, even with the increased palaeontological evidence that is available today in favour of multiple origins of airborne sound adapted ears, few would regard there to be as many origins of stapes coupled to tympanic membranes as was suggested by Tumarkin (for example Tumarkin proposed that secondary loss of an airborne sound adapted ear is rare or non-existent and that lizards evolved such a hearing system separately from rhynchocephalians).

There was renewed interest in multiple origin hypotheses with two papers published by Lombard & Bolt (1979) and Carroll (1980). Lombard and Bolt argued that a multiple

origin hypotheses gave a more satisfying explanation for the many inconsistencies observed in the airborne sound adapted ears in extant tetrapods. Carroll described the stapes (which he termed hyomandibular) of *Greererpeton*, a colosteid from the Lower Carboniferous, which he claimed to have functioned as a supportive element and was in no way functioning in an ear adapted to the perception of airborne sound (*Greererpeton* did not possess paired posterior notches). This two-pronged support for a multiple origin of an ear adapted to the perception of airborne sound was strengthened by the full cranial description of *Greererpeton* (Smithson, 1982) and the discovery of a stapes in a specimen of *Pholiderpeton scutigerum* Huxley, an embolomere from the Upper Carboniferous (Clack, 1983). The stapes of *Pholiderpeton* had morphology comparable to that of *Greererpeton* and was not of a *Lydekkerina* rod-like type as had previously been expected. *Pholiderpeton* was interpreted as not possessing a tympanic membrane yet it did possess paired posterior notches. The discovery of a similar stapes in *Acanthostega* (Clack, 1989) further strengthened the view that early tetrapods did not have ears adapted to the perception of airborne sound.

The alternative view was subsequently considered in greater detail and many aspects of it debated and elaborated on (Clack, 1992; Clack, 1997; Clack, 2002d; Clack & Allin, 2004; Laurin, 1998). Clack especially took into consideration various functional aspects of the early tetrapod head that impacted directly on the stapes and its proposed role (Clack, 1992; Clack, 2002d). In 1992 Clack proposed that the early tetrapod skull was not fully autostylic and that there was no contact between the otic region of the braincase and the palatoquadrates. This meant that the braincase was only in contact with the palate in two places, the basipterygoid articulations and the stapes, both of which were envisaged to allow a degree of movement (Clack, 1992). This of course rested on the assumption that the stapes of early tetrapods such as *Acanthostega* and

Pholiderpeton did indeed contact the palatoquadrate, although Clack (1983) had not initially envisaged this to be the case in *Pholiderpeton* (indeed Clack (1983) suggested a hearing function for the stapes of *Pholiderpeton* which the author believes is not dissimilar to that proposed for *Kyrinion* within this thesis).

Clack (1992) proposed that the stapes of early tetrapods functioned as supporting the palate (a function similar to that outlined above) and also as being involved in operating the ventilation mechanism. This dual function of the stapes was suggested to have constrained the use of the stapes in any advanced hearing system (Clack, 1992). It was further proposed that the adaptation of the stapes to be used in hearing could only take place once the stapes had been freed from these constraining functions. This meant, for example, that temnospondyls could only utilise their stapes for hearing once the braincase had become more fully attached to the skull roof, the basipterygoid articulation had become less mobile and once their proposed buccal breathing system had been developed (Clack, 1992).

It was envisaged that the early amniotes, such as pelycosaurs, utilised the stapes as part of their static pressure feeding system (Clack, 1992). It was suggested that the different functions of the stapes in the groups believed to lead to modern amphibians and amniotes were fundamental to the different middle ear morphologies we see today (Clack, 1992; Clack, 2002c; Clack, 2002d).

Clack (2002d) stated that if anurans had evolved from temnospondyls then there would still have been as many as six separate evolutions of a stapes coupled to a tympanic membrane (temnospondyls/anurans, diapsid reptiles, turtles, mammals, seymouriamorphs and diadectamorphs). Clack (2002d) further stated that if the phylogeny of Laurin & Reisz (1997) was used it would suggest that temnospondyls and anurans had evolved a stapes coupled to a tympanic membrane separately and that it

would suggest seven separate evolutions of such a system. Laurin (1998) suggested that if anurans had evolved from temnospondyls then a tympanic ear had evolved a maximum of five time. If the crown group tetrapods had all evolved from lepospondyls then Laurin (1998) envisaged a maximum of six independent evolutions of such a hearing system.

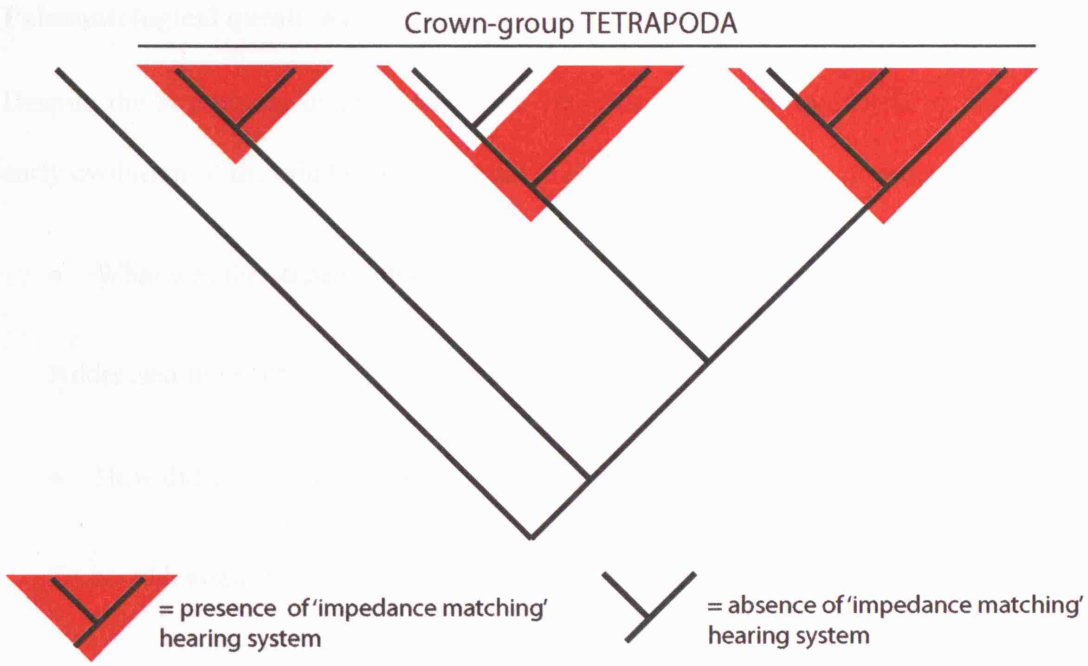

Figure 1.1.2—6 Diagrammatic representation of the 'alternative view' of the evolution of an ear adapted to the perception of airborne sound. The common ancestor of crown-group Tetrapoda did not possess such a system – it evolved numerous times within the crown-group Tetrapoda.

Palaeontological questions

Despite the acceptance of the 'alternative view' there are still questions regarding the early evolution of the middle and outer ear in early tetrapods. These questions include:

- What was the stapedial function before it was coupled to a tympanic membrane?

Addressed in results chapters *Acanthostega*, *Kyrinion* and *Dendrerpeton.*

- How did a stapes coupled to a tympanic membrane evolve?

To be addressed in results chapters *Acanthostega*, *Kyrinion* and *Dendrerpeton.*

- How did the proposed ear, adapted to the perception of airborne sound, change once already evolved? Can an increase in amplification potential be detected in phylogenetically more advanced early tetrapods?

To be addressed in the overall discussion and conclusions, 4.

- Did early tetrapods have a spiracle and did this get transformed into a middle ear space? If not, what was the function of the paired notches in early tetrapods?

To be addressed in results chapters *Acanthostega*, *Kyrinion* and *Dendrerpeton.*

- Is the proposed spiracular opening in early tetrapods in anyway homologous to the tympanic membrane? If so, is this in all tetrapods?

To be addressed in results chapters *Kyrinion* and *Dendrerpeton.*

- How did the tetrapod otic region of the braincase and particularly the fenestra ovalis evolve? To be addressed in results chapter *Acanthostega.*

1.1.3. AIMS

The neontological and palaeontological sections clearly illustrate that many aspects in the evolution of the hearing systems of tetrapods are not fully understood. The questions at the end of each of the previous sections need to be investigated in order to gain a more complete picture. This thesis aims to tackle these questions by using CT scanning and 3D reconstruction to re-examine crucial early tetrapod specimens.

The specimens chosen for CT scanning and 3D reconstruction are:

- *Acanthostega gunnari* – an unambiguous stem group tetrapod which will be used to address questions regarding the evolution of the fenestra ovalis and overall braincase morphology of early tetrapods.

- *Kyrinion martilli* – a baphetid (possible stem group tetrapods) which will be utilised to investigate early stapedial function and the origin of the middle ear space.

- *Dendrerpeton acadianum* – a phylogenetically basal temnospondyl whose previous descriptions (see chapter 3.3 for details) suggest that it may be utilised to investigate early stapedial function and the origin of a stapes coupled to a tympanic membrane.

- *Lydekkerina huxleyi* – a stereospondyl temnospondyl whose middle ear region will be used to investigate osteological character states which provide evidence for middle ear specialisation. It is hoped that it will help investigate the origin of the numerous middle ear specialisations of extant amphibians.

- *Micropholis stowii* – a temnospondyl probably phylogenetically relatively close to the proposed origin of anurans, batrachians or all lissamphibians. It will, therefore, be utilised to investigate the origin of the middle ear character states observed in extant amphibians, especially anurans.

See Figure 1.1.3—1 for the phylogenetic position of each of these species.

Apart from their suitability for investigating the origin and evolution of the middle ear region in early tetrapods the following criteria also had to be considered when choosing specimens for scanning and 3D reconstruction:

- Good preservation; free from extensive crushing and distortion.
- Previous descriptions which have not completely described all details of the hearing structures and associated regions.
- Availability and practicality of scanning – excludes large, fragile and inaccessible specimens.

In addition to the above criteria, the number and variety of specimens chosen is limited by the cost of scanning and the time available to reconstruct them. For this reason it was decided to concentrate on stem group tetrapods and temnospondyls. Future work should concentrate on the specimens on the lineage leading to amniotes and also the other early tetrapod groups which have been implicated in the origin of the extant amphibian orders.

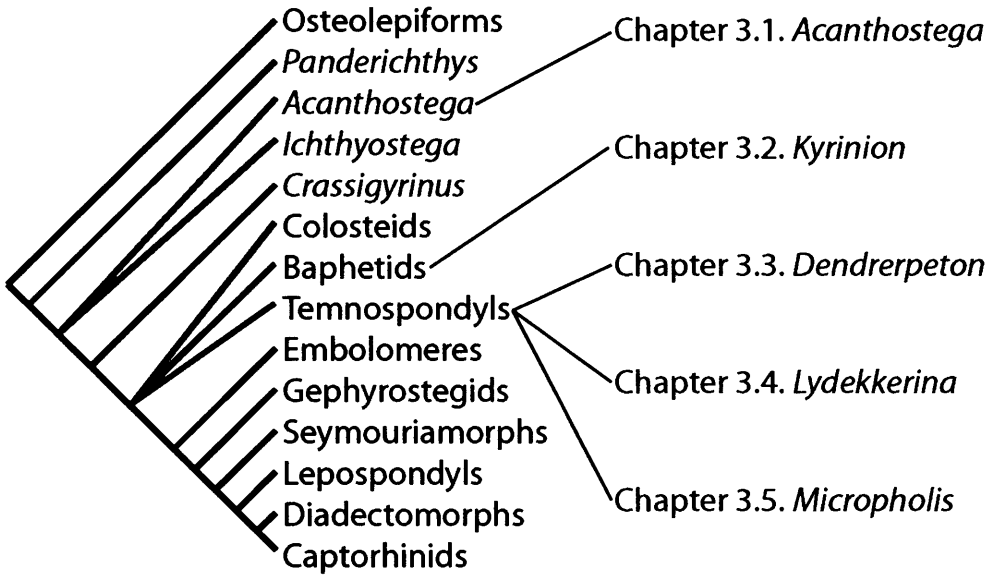

Figure 1.1.3—1 Agreed phylogenetic consensus based on the early tetrapod phylogenies of Ruta et al. (2003) and Laurin & Reisz (1997) with specimen positions indicated. This phylogeny was created by collapsing any disagreements between the two phylogenies to polytomies - this was done by hand, by the author - no computer program was utilised.

2. METHODS

2.1.1. OVERVIEW

The stapes/hyomandibular, braincase and associated elements form part of the internal cranial structures which have by their very nature proved far more difficult to investigate than external cranial structures. Traditional methods of palaeontological investigation involving manual preparation have nevertheless had some success in visualising internal cranial structures of some early tetrapods. For example preparation on *Greererpeton* (Smithson, 1982) and *Kyrinion* (Clack, 2003a) has allowed details of the occipital condyle and posterior views of the stapes to be visualised. The use of manual preparation on these articulated specimens clearly does not give us full information regarding the stapes and how it relates to the fenestra ovalis. Manual preparation on specimens which are disarticulated can allow more detailed information on stapedial and braincase morphology to be observed. Work, for example, with *Pholiderpeton* (Clack, 1983) and *Acanthostega* (Clack, 1989) has allowed near complete visualisation of the stapedial morphology of these early tetrapods. However, the disarticulated nature of the *Pholiderpeton* and *Acanthostega* limits the amount of information regarding how the stapes are orientated and how they would have interacted with braincase and palatoquadrate complex, both of which are crucially important in defining stapedial function.

In addition, to manual preparation serial sectioning has been employed to investigate the internal cranial structures of early tetrapods. Crania of *Acanthostega* (Clack, 1998) and *Tersomius* (Carroll, 1964) have both been investigated in this manner providing information on stapedial morphology and the relationship of the stapes to other internal cranial structures. The damage to the specimen from serial sectioning depends on the

thickness of the wire used and the frequency of the sectioning. More sections per centimetre is preferred for increasing the detail of the model but clearly this increases the damage to the actual specimen and makes it less aesthetically pleasing for future display. Serial sectioning is used as a compromise between leaving the specimen fully intact and producing a grinding series. To gain maximal information from a specimen a grinding series is needed, although, the specimen is entirely destroyed in the process.

Detailed grinding series have been produced from specimens of *Lysorophus* (Sollas, 1920), *Eusthenopteron* (Jarvik, 1980) and *Thrinaxodon* (Fourie, 1974). The production of a grinding series involves grinding away a small amount of the specimen and then recording the exposed surface via camera lucida or photography and then grinding a small fraction more of the specimen and repeating the process until no more of the specimen remains. The camera lucida drawings or photographic prints can then be studied directly or used as the basis for constructing an enlarged 3D model, usually from wax or plaster. Although Jarvik's work (1980 and references therein) with *Eusthenopteron* and many other fish specimens is the most famous use of this technique, it is neither the first such application or the most relevant to this study area. The production of an enlarged 3D model from a grinding series was reported by Sollas at the start of the twentieth century (Sollas, 1901). One of the earliest applications of this method was to investigate the enigmatic specimens of *Palaeospondylus gunni*, Traquair (Sollas & Sollas, 1903). Later Sollas applied a somewhat improved version of the technique to the study of two specimens of *Lysorophus* (which of course no longer exist) (Sollas, 1920). Regarding this technique Sollas states 'there is, I am convinced, a great future for this method, which is bound to add largely to our knowledge of fossils, rendering the study of palaeontology more exact' (Sollas, 1920). The model produced by Sollas (1920) was ground-breaking in its visualisation of an early tetrapod fossil.

However, Sollas could have been somewhat blinded by the beauty of the model when he stated 'The loss of the original specimen is of little account, for all that can be known of its form and structure is preserved on photographic plates' (Sollas, 1920). He was correct in believing that the photographic plates could be 'multiplied at will' but clearly wrong in not realising that early tetrapod specimens are rare and should be preserved for general observation and for more advanced methods of study that may come at some later date. Nevertheless, Sollas set the path for 3D reconstruction of tetrapod crania using serial sections of specimens.

The next major advance in the 3D reconstruction of tetrapod crania came with the application of high resolution X-ray computed tomography to a skull of *Stenopsochoerus* (Figure 2.1.1—2), a Miocene ungulate (Conroy & Vannier, 1984). This revolutionary use of a, then relatively, new medical technique produced an accurate 3D model of the skull with matrix absent from the reconstruction and most importantly no damage caused to the specimen. Moreover, the 3D model could be manipulated on the computer screen allowing both frontal and transverse sections of the model to be visualised. The accuracy and efficacy of high resolution X-ray computed tomography is now so greatly improved that it has recently become a common tool for investigating the internal cranial anatomy of fossils. The first known example of the application of high resolution X-ray computed tomography to the study of early tetrapods is the reconstruction of the middle ear and braincase of *Ichthyostega* (Clack et al., 2003).

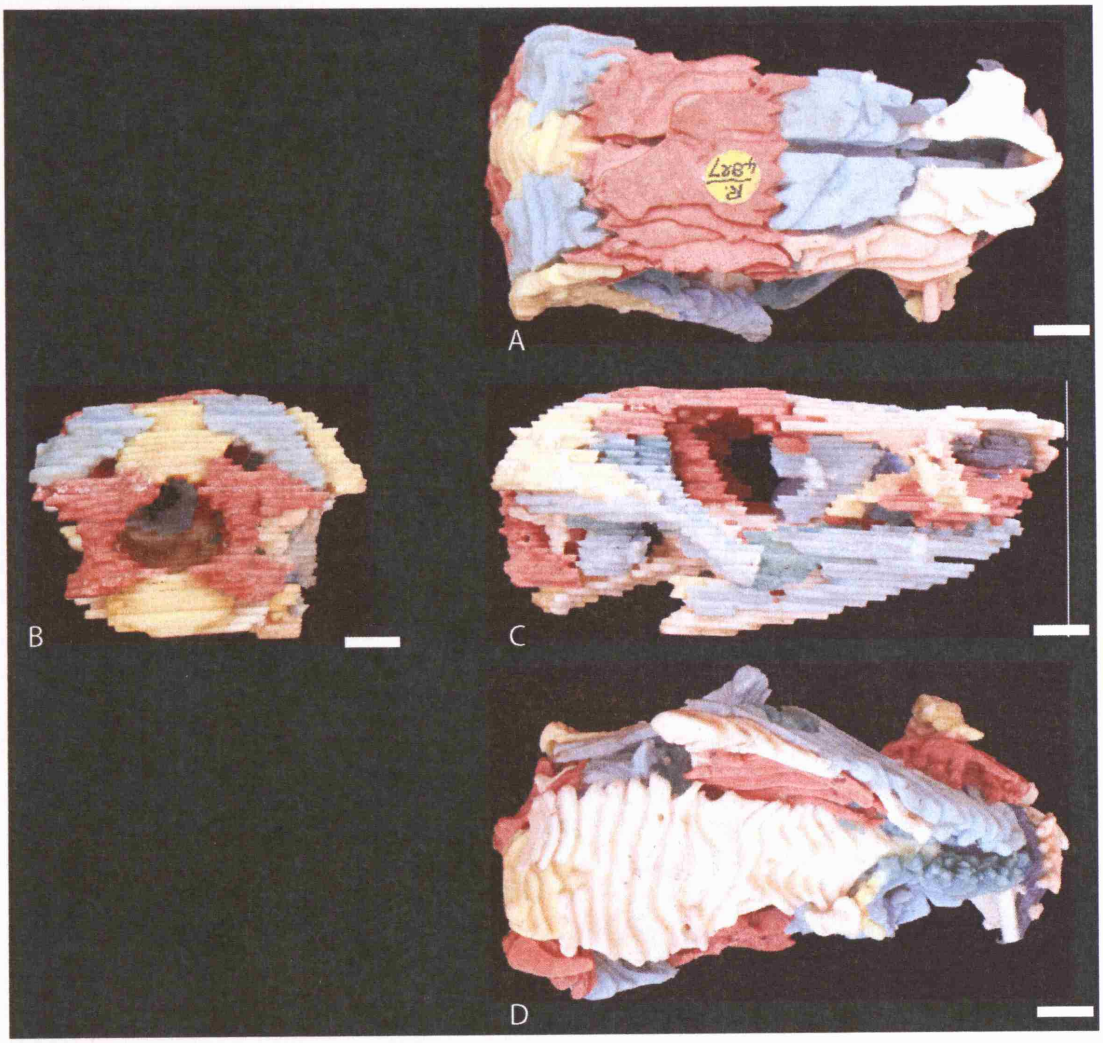

Figure 2.1.1—1 Plaster model of *Lysorophus* created by Sollas now catalogued as BMNH R.4827. A, dorsal view. B, posterior view. C, right lateral view. D, ventral view. Scale bars = 10mm.

2.1.2. HIGH RESOLUTION X-RAY COMPUTED TOMOGRAPHY

High resolution x-ray computed tomography (HRXCT) relies on the fact that x-rays pass through materials, such as matrix containing a fossil, which is fully opaque to light. Of course if the x-rays travelled through the specimen unimpeded without any attenuation then no structural information of the specimen would be gained. Fortunately materials within a specimen, such as matrix versus the fossilised material, attenuate x-rays to differing degrees. Attenuation of the x-rays in specimens is caused by two main processes, scattering and absorption (a third process, pair production of an electron and a positron, is not really a factor in fossil specimens). Scattering of the x-rays occurs when they interact with an electron in an outer shell of an atom. This interaction causes some of the energy from the x-ray to be transferred to the electron, causing it to be ejected from the electron shell, and for the reduced energy x-ray to have changed direction. Absorption of x-rays occurs when interaction is with an electron in an inner shell of an atom. Ejection of an electron from an inner shell needs far more energy than is needed to eject an electron from an outer shell, thus the remnant electromagnetic energy is much smaller. Electromagnetic radiation of lower energy than x-rays has a lower frequency and cannot pass through the specimen. HRXCT utilises the differing attenuation of x-rays to distinguish between materials within the specimen with dissimilar x-ray opacities. Materials which have high x-ray opacity allow fewer x-rays through than materials with lower x-ray opacity. Frequently, but not universally, fossilised material is more x-ray opaque than the surrounding matrix.

There have been numerous developments and specialisations of HRXCT; the following methodological overview concerns the procedures utilised as part of this thesis. All scans were produced with a so-called 'third generation' HRXCT scanner in which the

specimen is rotated within the x-ray field, rather than the source and detector of x-rays rotating around the specimen. In all generalised scanners the source emits x-rays with a range of energies distributed in a negatively skewed bell shaped curve. There is usually a defined maximum to the energy distribution.

Frequently after being emitted the x-rays pass through a filter, such as a thin plate of brass or aluminium, to remove very low energy radiation. After filtration x-rays pass through a collimator, a highly x-ray opaque material with a horizontal slit, which produces a laminar x-ray field. These x-rays pass through the specimen and are attenuated to differing degrees depending on the composition and length of their path through the specimen. X-rays then hit a linear detector array where the variation in intensity across the laminar x-ray field is recorded. This single detection of x-rays is known as a 'view'. The specimen is then rotated within the x-ray field and another view recorded – the angle of rotation between each view varies between specimens and the particular scanner used. The total number of views per rotation varies for each specimen scanned. The complete set of views from a single rotation can be displayed as a sinogram where views are stacked vertically on top of each other. Once a full rotation has been completed the specimen is moved up a set distance and the process of rotation and view capture is repeated. This procedure is repeated until the area of interest, or the whole specimen, has been scanned.

The complete set of sinograms from a specimen can then be converted to a corresponding set of 2D images (one sinogram producing one 2D image known as a 'slice'). This conversion is accomplished with the use of complex computer algorithms (such as the 'convolution method' (Ramachandran & Lakshminarayanan, 1971)).

The above procedure is an overview of HRXCT (refer to Ketchum & Carlson (2001) and references therein for more detailed information). There are numerous specialisations that depend on the specimen scanned and the scanner used which will be described in the following section.

2.1.3. PARTICULAR HRXCT SET-UP UTILISED

Three different HRXCT scanners were utilised; two at the HRXCT facility at the University of Texas at Austin (UTCT) and one at the Center for Quantitative Imaging, The Energy Institute at Pennsylvania State University (Penn State). Information regarding the UTCT systems come mainly from the BIR website (www.bio-imaging.com) and Ketchum and Carlson (2001).

High energy subsystem at UTCT

Manufactured by BIR, this system consists of a Pantak HF420 x-ray source with a maximum energy of 420kV. The detector model is a P250D which is a linear array of 512 discrete transducers. The presence of a set limit of 512 transducer elements limits the resolution of simple rotation scans with this system to 512 x 512. To increase resolution to 1024 x 1024 offset rotation is frequently utilised. Offset rotation places only half the specimen within the x-ray field at any single angle of rotation; this allows the specimen to be placed closer to the x-ray source and artificially creates a 1024 resolution across the specimen (512 + 512).

Ultra-high resolution subsystem at UTCT

As with the high energy subsystem at UTCT the ultra-high resolution subsystem was manufactured by BIR. It consists of a Feinfocus FXE-200.20 x-ray source with a maximum energy of 200kV. The detector is a Toshiba AI-5764-HVP near 23cm intensifier which does not have a discrete number of transducers, unlike the high energy subsystem at UTCT. Instead the intensifier produces a real-time video output which is converted to a 1024 x 1024 digital signal. This signal is then artificially converted to a virtual 1024 detector array. In practice, this means that at a single angle of rotation

views for different slices can be detected and thus in a single rotation sinograms for numerous slices can be produced. Frequently with this particular system the detection of each particular view is repeated producing numerous 'samples'. These samples can then be combined together to produce a single view which has a reduced amount of scan noise.

HRXCT at Penn State

Manufactured by Universal Systems (www.universal-systems.com) this consists of a HD-600 CT system with subsystems from BIR and X-tek. The system has two energy sources, a large and a micro focal source with maximal energies of 320kV and 225kV respectively. The detector works in a similar manner to the high energy subsystem at UTCT – allowing numerous slices to be produced from a single rotation.

With all HRXCT scanning systems utilised, one of the persistent problems is beam hardening. This is an artefact which causes the outside of a specimen to appear lighter than its interior even when comparing areas which have the same inherent x-ray opacity. The effect is caused when x-rays with a spectrum of different energies pass with varying path lengths through the specimen. Lower energy x-rays are attenuated at a greater rate than higher energy x-rays meaning that a path of length Y will attenuate total x-rays more than half a path of length 2Y. Beam hardening can be limited by removing low energy x-rays with a filter, such as brass or aluminium. Additionally, the data contained in a sinogram can be processed, using a computer algorithm, to remove the most pronounced effects of beam hardening. Each sinogram is then converted to 2D slice usually in the Tag(ged) Image File Format (TIFF). A series of slices through a specimen is known as a 'stack'. A stack of slices can then be imported into a suitable 3D reconstruction program.

2.1.4. DATA PROCESSING

3D reconstruction was undertaken with Mimics (versions 7.1, 7.3, 8.0 and 8.1), a medical reconstruction program from Materialise (www.materialise.com). A stack of slices, usually as TIFFs and all of the same file size, can be easily imported into Mimics with the following information:

General

- Slice/Image size – either 1024 x 1024 pixels or 512 x 512 pixels.
- Slice distance/thickness (mm).
- Slice field of view – maximum length of reconstruction (mm).
- Pixel size – calculated from slice field of view (mm) divided by number of pixels in a single row of a slice (1024 or 512).

Specific image/pixel properties

- Type (signed byte, unsigned byte, signed short, unsigned short, signed long or unsigned long) – specifying how the image is encoded.
- Byte swapping (low byte first or high byte first) – further information on image encoding needed with certain images (those coded as signed short, unsigned short, signed long or unsigned long).
- File header size – adjust to centre specimen in centre of image.
- Minimum/Maximum image values – grey scale values which do not code information of interest can be removed at this stage, although this can also be done at a later stage after the importation of the stack is complete.

Successful importation of the stack produces a project folder (PAT) with Mimics versions 7.1 and 7.3 and a project file (MCS) with Mimics versions 8.0 and 8.1. Both

PAT folders and MCS files are known as 'projects' in which the 3D reconstruction is undertaken. Each project contains the stack of slices in which the relative x-ray opacity is represented by grey scale values; darker greys for lower x-ray opacities, lighter greys for higher x-ray opacities. Usually, the fossilised material is more x-ray opaque compared to the matrix, however, in *Kyrinion* the reverse is true. The interpretation of the information held within the project can be improved via contrast adjustment allowing clearer visualisation of the structures of interest. If the slices within the project are relatively free from background noise and shadow artefacts, caused by highly x-ray opaque mineral deposits, a blanket grey scale threshold tool can be used to create a 'mask' of the fossilised material. This mask of all fossilised material can then be distinguished by various degrees into component bones. The ability to dissect the mask into individual ossifications depends on the quality of the scans and the degree of fusion between the bones.

With all scan series utilised (except *Dendrerpeton* (Robinson, Ahlberg & Koentges, 2005)), relatively high levels of noise and/or poor levels of preservation made the application of a blanket grey scale threshold unsuitable. In these cases a local manual threshold technique is used. Manual selection allows different grey scale threshold values to be utilised in different slices and parts of the same slice. As with the blanket approach the mask created from the manual selection can be demarcated into component bones. This splitting involves separating two areas with an erase tool so that there is no pixel contact between the two areas. One of the areas can then be transferred to a new mask and the process repeated with all slices in which the original mask appears. Even with manual selection there is always some noise in the masks which can subsequently be removed by recognising spurious pixels and erasing them.

Internal moulds of fossilised material that are no longer present in the specimen can be modelled in Mimics. By setting the manual grey scale threshold values to those which solely correspond to the values at the margin between the matrix and the air it is possible to model the contours of the mould. It is possible to model airspaces, such as those which have been produced by the 'preparation away' of fossilised material, by setting the grey scale threshold values to that which corresponds to the air around the specimen. In a similar manner spaces within fossilised material (such as inner ear spaces and endocasts) can be modelled by setting the manual grey scale threshold values so that matrix is selected in preference to fossilised material.

Once all masks from a given project have been created and noise removed, Mimics converts the masks, which are a collection of 2D images, into 3D volume meshes. These 3D versions of the masks can be visualised within Mimics, however, it is more convenient and useful to export them into a 3D manipulation program. With all projects, masks are converted and exported in the 'binary STL' file format.

One of the overriding problems with utilising Mimics to interpret a stack of slices from a HRXCT scan series is the limited number of masks that can be produced in a single project (maximum 16 but increased to 32 with Mimics version 9.0). Frequently, this number is too small. A solution to this problem involves creating numerous projects from the same stack of slices. As long as the projects from the same stack of slices are setup with identical parameters the STL files produced from the masks in the different projects will retain their relative positions and orientations in space as those in the original stack and allowing the various STL files from different projects to be easily combined in the 3D manipulation program.

An additional problem with Mimics is the necessity of all imported slices in a stack to be of exactly the same file size. Frequently the TIFF images produced by the scanners used are of differing file size, for example, the first half of the stack slices being slightly larger than the second half. In practice, this means that a stack of TIFF slices has been split into two stacks and imported independently into separate projects. The STL files produced within these projects can then be exported and married together in the 3D manipulation program: this process was undertaken with *Kyrinion* 3.2. In a similar manner, if a specimen has been scanned twice, as was the case with *Dendrerpeton* (Robinson et al., 2005), the STL files produced from different projects, which have in turn been created from stacks of different scan series, can be married together in the 3D manipulation software.

The 3D manipulation software used is called Rhino3D (versions 3.0 and 3.1) from Robert McNeel & Associates (www.rhino3d.com). STL files from a Mimics project can be easily imported into 3DM files created by Rhino3D. If the STL files are from the same project, or from projects created from the same stack of slices using identical parameters, the relative sizes and orientations will be preserved in the 3DM file. If, however, the stack had to be split due to differing TIFF file sizes Rhino3D has to be informed of the correct positions of the STL files from one project relative to the next. This involves importing the STL files from one project as normal and then importing the STL files from subsequent projects with altered X, Y or Z coordinates and a possible scaling factor. When STL files are to be combined from separate scan series, which invariably have different orientations of the slices within their stacks, they have to be imported normally and then aligned manually within Rhino3D.

Rhino 3D allows the following:

- Movement of STL elements relative to one another. This allows correction of translocations that occurred during the preservation process, for example the left stapes of *Dendrerpeton* (for further details see chapter 3.3 and (Robinson et al., 2005)).
- The correction of taphonomic distortion by manipulation of an individual STL element. This, for example, allowed the cracked palatoquadrates to be returned to their original shape in *Lydekkerina* (for more detail see chapter 3.4 and figures therein).
- Smoothing of STL elements to reduce any remaining noise.
- Scaling of STL elements.
- Mirroring of STL elements to correct for distortion and lack of detail on one side of a specimen, such as the lack of the right palatoquadrate complex in *Dendrerpeton* specimen BMNH R.436 (see chapter 3.3 and (Robinson et al., 2005)).
- High quality rendering of individual STL elements or all those within a given 3DM file.
- Stereo pairs to be produced using Rhino3D. The angle of rotation between images for right and left eyes is 3°.
- The visualisation of a structure from any angle required. This means that it is possible to rotate a specimen for optimal observation of a particular character trait. It is even possible to visualise internal structures and magnify areas of interest.
- The alteration of STL element visual properties. This allows certain STL elements to be made transparent to enhance the clarity of a given figure.

Using a plug-in for Rhino3D called Bongo (version 1.0) again from Robert McNeel & Associates (www.rhino3d.com) allows the production of animations of the STL elements. Bongo produces a series of image files, such as jpegs, which are then converted to a movie file, such as an mpeg or avi.

2.1.5. GLOSSARY OF TERMS

3DM	file format created by Rhino3D
HRXCT	High Resolution X-ray Computed Tomography
mask	a series of selected areas on numerous slices with a project
MCS	project file created by Mimics versions 8.0 and 8.1
PAT	project folder created by Mimics versions 7.1 and 7.3
project	a file or folder which contains a stack of slices and up to 16 masks
sample	a single detection of x-ray intensities - often averaged together to produce a single view
sinogram	a diagrammatic representation of all views used to create a single slice
slice	a 2D image produced via computed tomography from a sinogram
stack	a continuous sequence of slices produced from a scan
STL	a file format containing a 3D triangle mesh representation of a mask
view	the x-ray intensities through a specimen at a given level and angle of rotation

2.1.6. LIST OF INSTITUTIONS

BMNH	Natural History Museum, London
MGUH	Museum Geologicum Universitatis Hafniensis (Geological Museum, University of Copenhagen)
NEWHM	Hancock Museum, Newcastle, Tyne & Wear
NSM	Nova Scotia Museum of Natural History
UMZC	University Museum of Zoology Cambridge

2.1.7. LIST OF ABBREVIATIONS

a scc	anterior semicircular canal
a scc amp	ampulla of anterior semicircular canal
ant cham	anterior chamber
arc pla	arcual plate
art	basipterygoid articulation
art at	articulatory surface with atlas
art ax	articulatory surface with axis
art cond	articulatory surface with condyle
art soc	basipterygoid articulation socket
asc pro	ascending process of epipterygoid
av pro	antero-ventral process
bo-eo	basioccipital-exoccipital complex
bs	basisphenoid
bs-ps	basisphenoid-parasphenoid complex
ca gro	groove for carotid artery
cla_l	left clavicle
cla_r	right clavicle
cle_l	left cleithrum
cle_r	right cleithrum
cor for	coracoid foramen
cri obl	crista obliqua
cri sel	crista sellaris
cul pro	cultriform process

den for	dental foramen
dep	dorsal epipterygoid process
dia	diapophysis
dor com	dorsal component of footplate
dor pro	dorsal clavicular process
ep	epipterygoid
ep lip	unfinished lip of epipterygoid
ep mus sca	epipterygoid muscle scar
ep-pt_l	left epipterygoid-pterygoid complex
ep-pt_r	right epipterygoid-pterygoid complex
eq pro	process for extension to quadrate
ex tym	excavatio tympanica
f/o	fenestra ovalis
fm	foramen magnum
fp	footplate of stapes
gle for	glenoid foramen
gle foss	glenoid fossa
h scc amp	ampulla of horizontal semicircular canal
h ssc	horizontal semicircular canal
hum	humerus
ig rec	infraglenoid recess
ig rid	infraglenoid ridge
im foss	inframeckelian fossa
int cen	intercentrum
int cla	interclavicle

jug gro	groove for jugular vein
lat flan	lateral flange of parasphenoid
lsr	laterosphenoid region
mand art	mandibular articulatory surface
mand foss	mandibular fossa
$mand_l$	left mandible
$mand_r$	right mandible
mid pro	mid-line prong of dorsum sellae
neu can	neural canal
not path	notochordal path
not pit	notochordal pit
NVI	foramen for abducens (VI) nerve
NVII	foramen for facial (VII) nerve
NVIII	foramen for auditory (VIII) nerve
NX	foramen for vagus (X) nerve
occ cond	occipital condyle
oc_l	left otic capsule
oc_r	right otic capsule
or_l	left orbit
or_r	right orbit
ot for	otic capsule foramen or post-temporal foramen
p scc amp	ampulla of posterior semicircular canal
p ssc	posterior semicircular canal
par for	paraquadrate foramen
par pro	paroccipital process

pin for	pineal foramen
post scar	posterior scar on stapes
pozy	post-zygapophysis
pro for	prootic foramen
przy	pre-zygapophyis
ps	parasphenoid
pt	pterygoid
ptf	post-temporal fossa
rec tym	recessus tympanicus
scap cor_l	left scapulocoracoid
scap cor_r	right scapulocoracoid
scl pla	sclerotic plates
se	sphenethmoid
sg for	supraglenoid foramen
sm scar	small scar on stapes
sr	skull roof
st can	stapedial canal
st gro	groove on stapedial rod
st_l	left stapes
st_r	right stapes
unc pro	uncinate process
unf con	unfinished distal concavity
ven com	ventral component of footplate
vs oss_l	left v-shaped ossification
vs oss_r	right v-shaped ossification

3. RESULTS

Each species scanned and reconstructed is presented as a separate chapter with the following sections:

- A synopsis of the questions that the scanning and reconstruction of the specimen hopes to address.
- The background of the species examined with particular emphasis on the specimen or specimens scanned.
- Details of the reconstruction parameters utilised within the particular scanning and reconstruction.
- A full palaeontological description of all material scanned will be given. This description goes beyond presenting the data needed to address the questions regarding the evolution of the middle ear anatomy that were presented at the end of the previous sections of the introduction. The first figure, or the first two figures for *Lydekkerina* and *Micropholis*, of this section is a colour key to help with interpreting all subsequent figures within that chapter.
- Finally, each chapter will conclude with a section dealing with what new information the scanning and reconstruction of the specimen has provided and how this has helped address the questions posed at the start of the chapter.

3.1. ACANTHOSTEGA

From the phylogenies of Laurin & Reisz (1997) and Ruta et al. (2003a) it is clear that *Acanthostega* is one of the most phylogenetically basal early tetrapods. It is thus critically important to investigate fully all aspects of its middle ear and associated structures. A great deal is already known about this region in *Acanthostega* including details of the stapedial morphology, see Clack (1989). In spite of this previous knowledge there is still an incomplete picture of the middle ear and associated structures in *Acanthostega.*

The scanning and reconstruction of a braincase of *Acanthostega* along with the study of current published literature will help address the following questions that were posed in the introduction:

- How did the tetrapod otic region of the braincase and particularly the fenestra ovalis evolve?
- What was the stapedial function before it was coupled to a tympanic membrane?
- Did early tetrapods have a spiracle and did this get transformed into a middle ear space? If not, what was the function of the paired notches in early tetrapods?

See *Acanthostega* Discussion 3.1.4 and Figure 3.1.4—1 for a synopsis of the morphology revealed from the reconstruction of UMZC T.1300d and how this has helped address the above questions.

3.1.1. BACKGROUND

In 1952, Jarvik assigned two 'imperfect skulls' to the new genus and species *Acanthostega gunnari* in honour of the then late Gunnar Säve-Söderbergh. The most complete of these skulls, the holotype, was collected in 1932 by Säve-Söderbergh from the Remigolepis Series of Gauss Halvø of north-east Greenland (Jarvik, 1952). The other skull was collected in 1947 from the Remigolepis Series of Celsius Bjerg, Ymers Ø also of north-east Greenland (Jarvik, 1952). The Remigolepis Series has been dated by Jarvik (1961) as being within the Famennian of the Upper Devonian (Clack, 1988). Jarvik (1952) placed the genus *Acanthostega* in the new family Acanthostegidae and positioned it within the order Ichthyostegalia, although this latter classification was only provisional (Jarvik, 1952). All *Acanthostega* material has been referred to the single species *Acanthostega gunnari*. Subsequent to the original description by Jarvik there have been numerous additional expeditions to the north-east of Greenland which have collected material of *Acanthostega*. The most notable of these were led by Peter Friend in 1970 and a joint Cambridge University and Geological Museum, Copenhagen expedition in 1987.

The material of *Acanthostega* collected in 1970 was originally described by Clack (1988). Further description of this material along with that collected in 1987 has been undertaken by Clack (1989; 1994; 1998; 2002a; 2003b), Clack & Coates (1993), Coates & Clack (1991) and Coates (1996). Although, there has been some overlap, on the whole Clack has dealt with the cranial material of *Acanthostega* while Coates has dealt with the postcranial material. These descriptions along with the extensive mechanical preparation carried out by Sarah Finney, then at the University Museum of Zoology

Cambridge, reveal the anatomy of *Acanthostega* in far greater detail than any other Devonian tetrapod.

Acanthostega has been included in recent phylogenies carried out by Ruta et al. (2003a) and Laurin & Reisz (1997) which place it as one of the most phylogenetically basal tetrapods. The only real difference between the two phylogenies in relation to *Acanthostega* is that Ruta et al. (2003a) places it in a position more phylogenetically basal than *Ichthyostega*, whilst, Laurin & Reisz (1997) place them in a clade which is itself rooted in the base of the tetrapod phylogeny. *Acanthostega*'s position within early tetrapod phylogeny makes it critically important in investigating and evaluating the character states of the middle ear and associated structures in the phylogenetically most basal tetrapods. The manual preparation and descriptions of *Acanthostega* have greatly informed our knowledge in this area, for example see Clack (1989; 1998) for details of its stapedial and braincase morphology respectively. In fact, prior to scanning and 3D reconstruction the middle ear and associated structures of *Acanthostega* were more completely known than those of any of the other specimens investigated here. During the course of study leading to this thesis a CT scan series of the braincase of one of the *Acanthostega* specimens was made available for study, however, this scan series did not include any stapedial material. Despite the obvious limitations of the scan series in regards to the lack of stapedial information and the previously detailed descriptive work on the braincase carried out using mechanical preparation it was decided to reconstruct the scan series. The critical phylogenetic position of *Acanthostega* makes any additional information on its braincase highly important.

The braincase of *Acanthostega gunnari* specimen UMZC T.1300d (Figure 3.1.1—1) was scanned at the request of Dr. Jenny Clack. This braincase specimen, which has been extensively mechanically prepared, belongs to skull A of UMZC T.1300 from Clack's

original description (1988) of the material collected in 1970. UMZC T.1300 was collected by John Nicholson at site G920 of the upper Britta Dal Formation situated on the south-east slope of Stensiös Bjerg (Clack, 1988) and is thus dated as Famennian of the Upper Devonian. The skull roof of UMZC T.1300d has previously been figured (see text-fig. 2 of Clack (1988)) and after the extensive mechanical preparation the braincase was figured in detail (see figure 1 of Clack (1998)). UMZC T.1300d appears to have been the main source of morphological information used to create the braincase reconstruction of *Acanthostega* presented in figure 8 of Clack (1998).

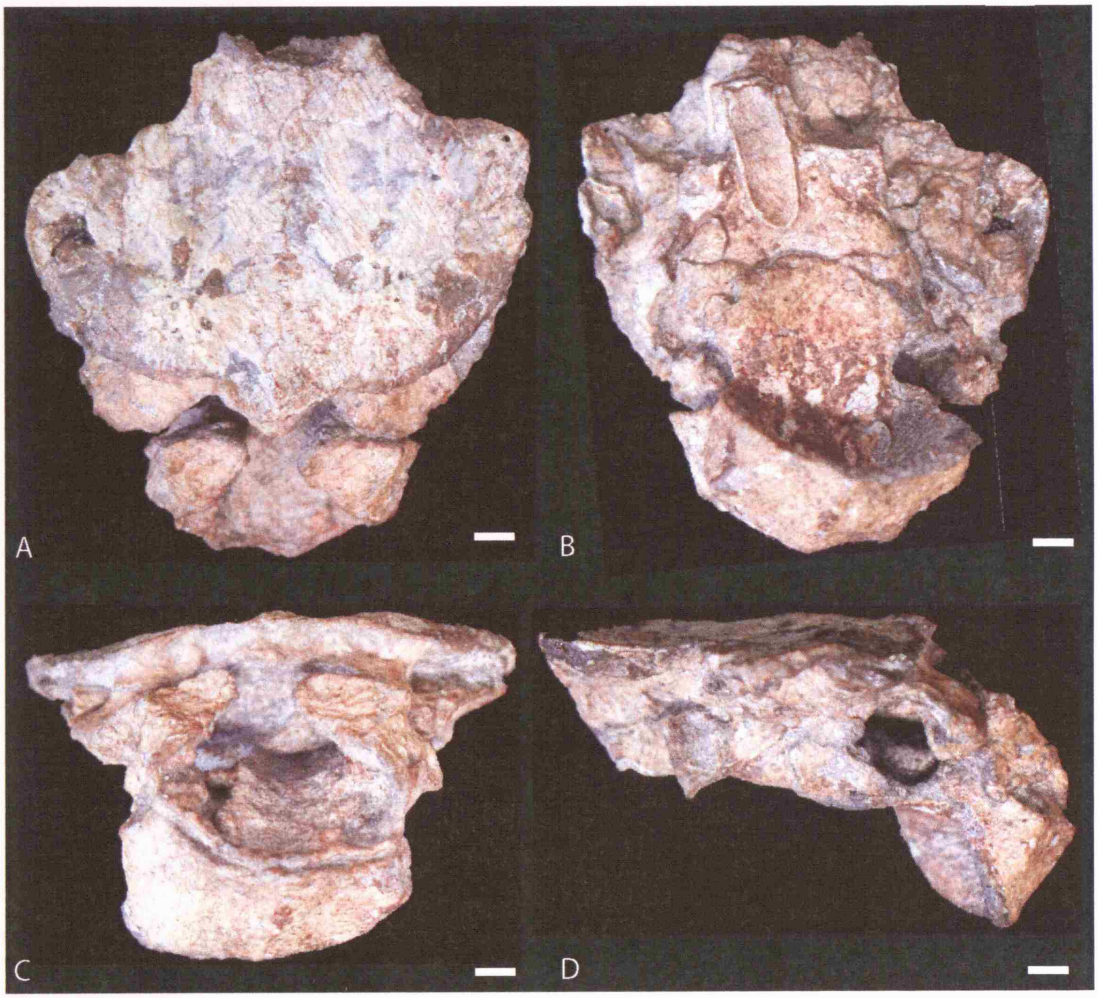

Figure 3.1.1—1 *Acanthostega* specimen UMZC T.1300d. A, dorsal view. B, ventral view. C, posterior view. D, left lateral view. Scale bars = 2mm.

3.1.2. RECONSTRUCTION PARAMETERS

UMZC T.1300d was scanned on the HRXCT system at Penn State. Unfortunately the scan ran from the anterior extent of the specimen to approximately the middle of the exoccipitals and thus excluded the posterior end of the specimen. The scan was produced with 2400 views per rotation with 41 slices being produced per rotation meaning the specimen was rotated 14 times within the x-ray field. This produced a scan series in 16bit resolution (1024 pixels by 1024 pixels) comprising 574 slices each of 0.04397mm thickness (i.e. approximately 23 slices per mm). Each slice has a field of view of 40mm giving a pixel size of 0.03906mm.

The use of all 574 slices, an extremely large dataset, in Mimics created an unstable environment to model the elements. I, therefore, decided to create a Mimics project using every other slice (all odd numbered slices from 1-573) meaning the project contained a stack of 287 slices. This stack was interpreted within Mimics with a contrast set at -686 to -340 to maximise the otherwise quite poor contrast between fossilised material and the matrix. Even after this optimalisation the fossilised material proved problematic to model and thus it was necessary to utilise manual thresholding to model all elements present in the project. The presence of highly x-ray opaque crystalline constituents within the specimen added a further degree of complexity to the modelling process.

All elements created in the Mimics project were imported into Rhino without any alteration of coordinates. However, in order to improve the aesthetic appearance of the model a smoothing transformation over all world coordinates with a factor of 1.5 was utilised.

3.1.3. DESCRIPTION

The reconstruction of *Acanthostega* specimen number UMZC T.1300d (Figure 3.1.3—2 and 3) includes the fused skull roof, otic capsules and dorsal laterosphenoid region (lsr) complex, the ventral braincase region (basisphenoid-parasphenoid complex (bs-ps), possible otic elements and occipital region), part of an intercentrum (int cen) and a previously undescribed element (Figure 3.1.3—4 and 5). All these regions have been described in some detail previously by Clack (1998) and thus only further information discovered from the scanning and reconstruction will be described in detail here.

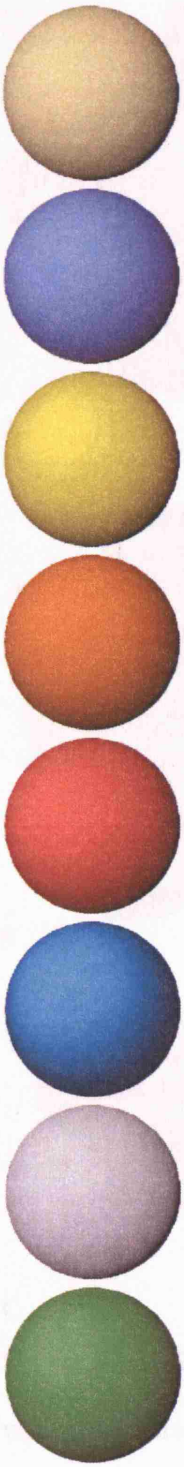

= Base colour for all elements unless stated below

= Skull roof, otic capsules and dorsal laterosphenoid region

= Basisphenoid-parasphenoid complex

= V-shaped ossifications - possible ventral otic elements

= Basioccipital-exoccipital complex

= Possible arcual plate

= Rod like elements within brain cavity

= Intercentrum

Figure 3.1.3—1 Colour key.

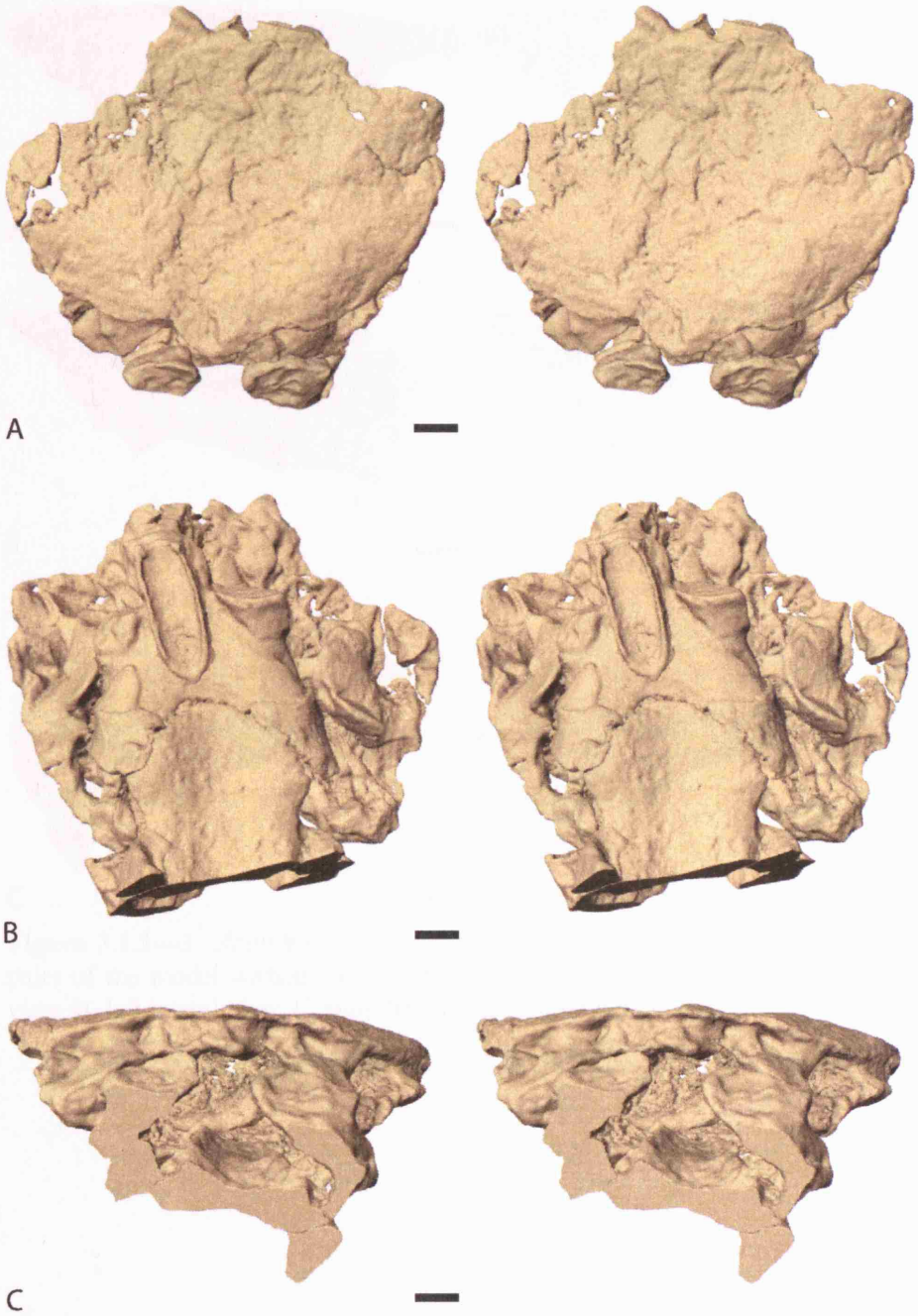

Figure 3.1.3—2 *Acanthostega* specimen UMZC T.1300d. Mono colour stereo pairs of model without correction for translocations or damage. A, dorsal view. B, ventral view. C, posterior view. Scale bars = 2mm.

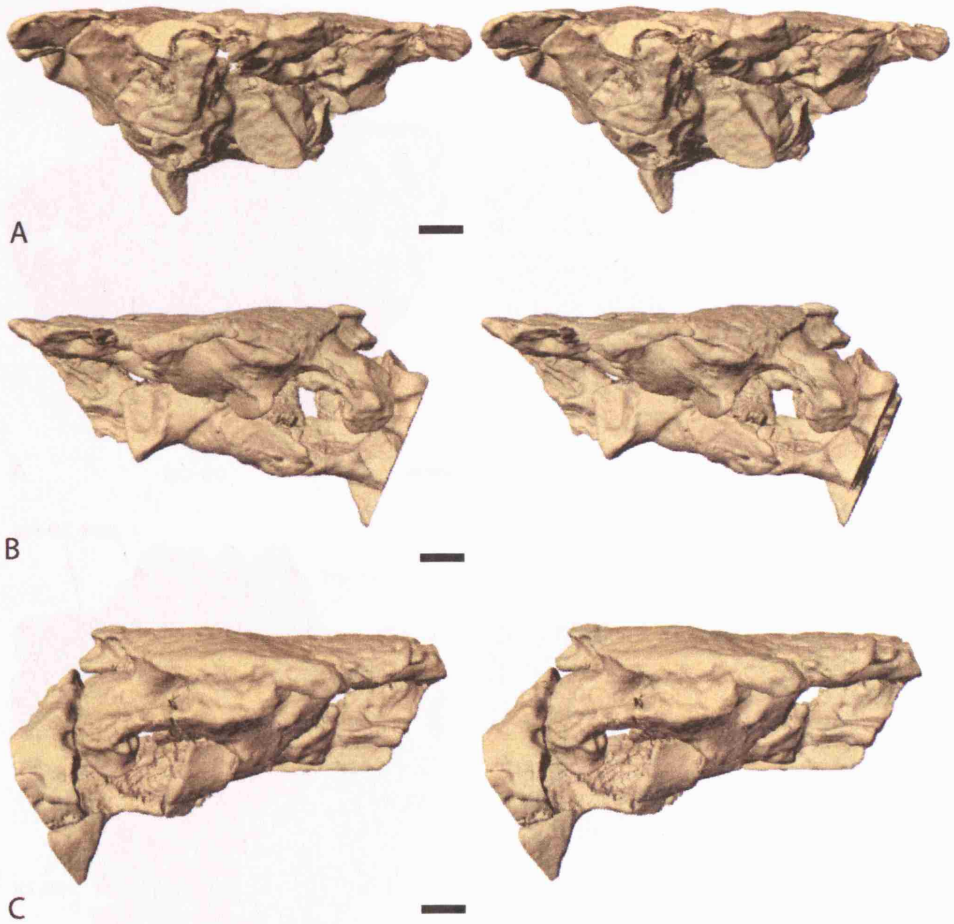

Figure 3.1.3—3 *Acanthostega* specimen UMZC T.1300d. Mono colour stereo pairs of the model without correction for translocations or damage. A, anterior view. B, left lateral view. C, right lateral view. Scale bars = 2mm.

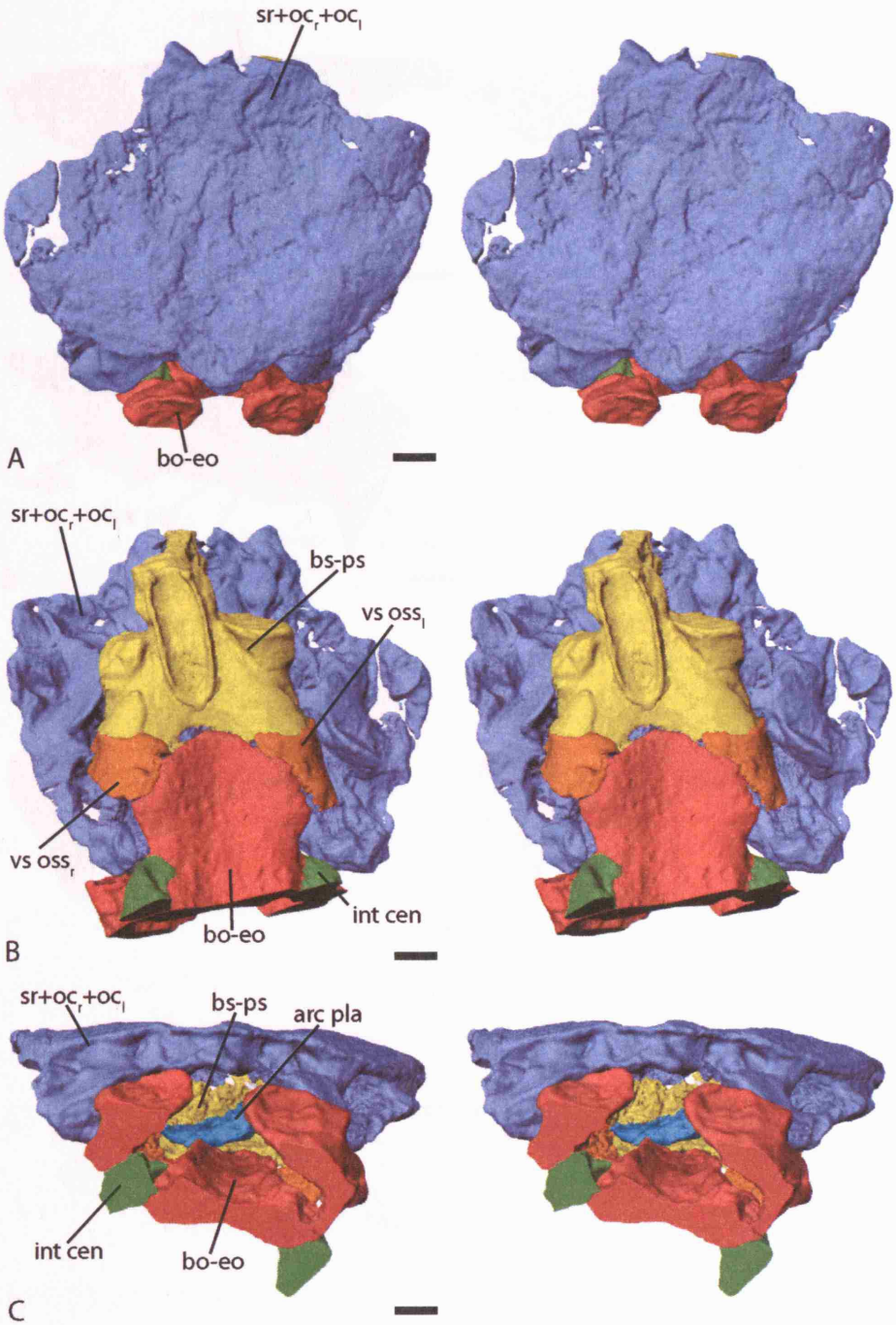

Figure 3.1.3—4 *Acanthostega* specimen UMZC T.1300d. Stereo pairs of the model without correction for translocations or damage. A, dorsal view. B, ventral view. C, posterior view. Scale bars = 2mm.

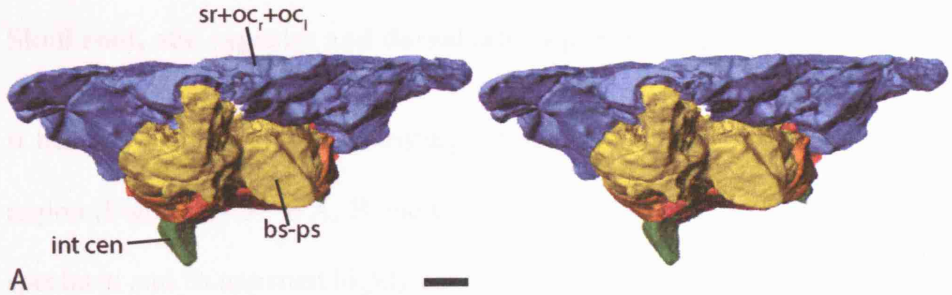

A

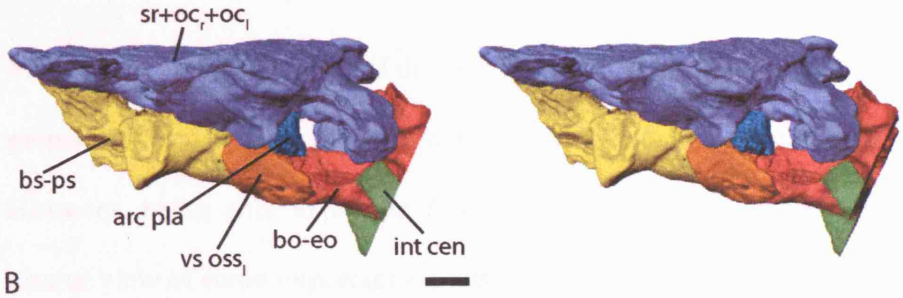

B

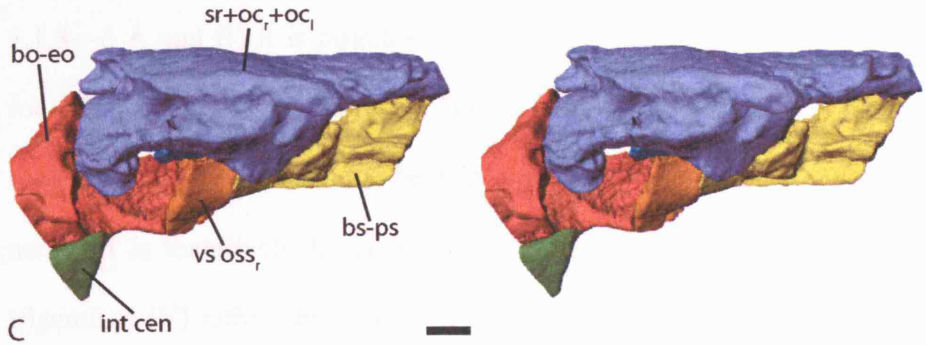

C

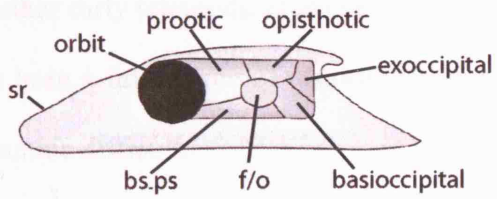

D

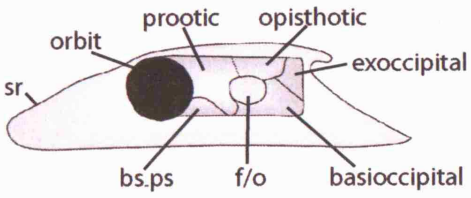

E

Figure 3.1.3—5 A, B and C *Acanthostega* specimen UMZC T.1300d. Stereo pairs of the model without correction for translocations or damage. A, anterior view. B, left lateral view. C, right lateral view. Scale bars = 2mm. D and E, diagrammatic representations of the braincase of *Acanthostega*, anterior to the left. D, with v-shaped ossifications classified as part of the basisphenoid-parasphenoid complex. E, with v-shaped ossifications classified as part of the otic capsules.

Skull roof, otic capsules and dorsal laterosphenoid region

It has not proved possible to distinguish the separate ossifications which make-up this region (Figure 3.1.3—6 A, B and C) because of the scan resolution, the crushing of the specimen and its apparent highly ossified nature.

Most of the external surface of this region has previously been visualised by mechanical preparation and there is little extra information that can be gained from the scan slices. However, being able to isolate this region from the other elements has provided a clearer view of some important aspects. In ventral and offset anteroventral view (Figure 3.1.3—6 A and B) it is possible to see a large foramen on each side of the specimen roughly at the join between the laterosphenoid and the anterior regions of the otic capsule (oc). This foramen has been interpreted as being the exit point of the facial (VII) nerve. It is tentatively interpret as the prootic foramen (pro for) for the exit of the trigeminal (V) rather than facial (VII) nerve from comparison with *Edops* (Romer & Witter, 1942), *Dendrerpeton* (Robinson et al., 2005), *Eryops* (Sawin, 1941) and a range of other early tetrapods. However, it is clear from an offset anteroventral view that there has been a fair degree of distortion which makes accurate interpretation of the various foramina difficult.

Despite the poor resolution it was possible to gain a low resolution endocast from the dorsal braincase (Figure 3.1.3—6 D). The approximate dorsal paths of both the anterior (a scc) and posterior (p scc) semicircular canals can be visualised from this endocast, allowing the first measurement of the anteroposterior extent of the inner ear of *Acanthostega*. The endocast is, however, too unresolved to visualise any other structures. In internal view of the dorsal braincase two rod like elements have been

identified (Figure 3.1.3—6 B), although both have been displaced slightly. Their origin and function are unknown.

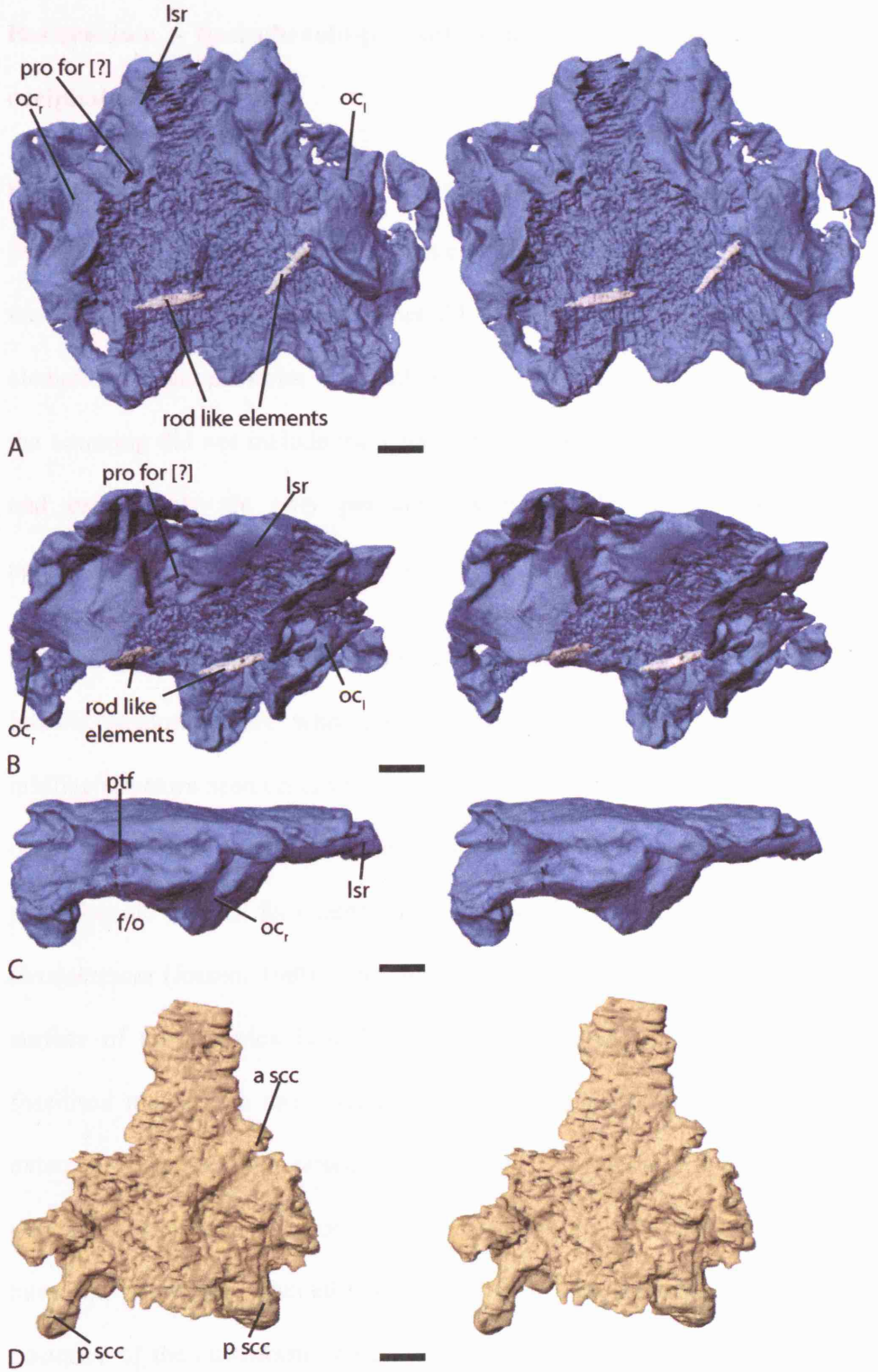

Figure 3.1.3—6 *Acanthostega* specimen UMZC T.1300d. Stereo pairs. A, B and C the skull roof, otic capsules and dorsal laterosphenoid region. A, ventral view. B, offset anteroventral view. C, right lateral view. D, dorsal view of braincase endocast. Scale bars = 2mm.

Basicranium - basisphenoid-parasphenoid complex, possible otic elements and occipital region

For convenience the ventral part of the braincase includes the parasphenoid (ps) even though it is a dermal bone. This region can be distinguished into three distinct elements; the anterior basisphenoid-parasphenoid complex, the central paired possible otic elements and the posterior occipital (Figure 3.1.3—7 and 8). As mentioned previously the scanning did not include the posterior extent of the specimen thus the basioccipital and exoccipitals are only partially present in the scans even though they are approximately complete in UMZC T.1300d.

The basisphenoid-parasphenoid complex (Figure 3.1.3—9 and 10) cannot be divided into its component parts with total accuracy. It would, however, appear that the raised midline structure seen on the ventral surface of the complex is of entirely parasphenoid origin and would therefore correspond exactly to the midline plate-like area of the parasphenoid seen in, for example *Eusthenopteron* (Jarvik, 1954; 1980) and *Powichthys thosteinssoni* (Jessen, 1980). The extent to which the parasphenoid covered the ventral surface of the complex is difficult to assess, although, from the appearance of the fossilised material in cross section it does seem likely that this coverage was more extensive than just the raised midline area. The anterior part of the basisphenoid-parasphenoid complex is not complete as the cultriform process (cul pro) that would have run below the sphenethmoid region (se) is only partially present. Dorsal to the posterior of the cultriform process part of the sphenethmoid is fused to the complex. Posterior to the sphenethmoid ossification and medial to the basipterygoid (art) processes there are paired chambers (ant cham) whose posterior walls are formed by the crista sellaris (cri sel) (Figure 3.1.3—9 B). These chambers are undoubtedly

homologous to those in *Kyrinion*, *Dendrerpeton* (Robinson et al., 2005), *Lydekkerina*, *Micropholis* and a range of other early tetrapods. Clack (1998) described the lateral opening of these chambers as the interorbital foramen and postulated that this opening was for the interorbital vein, the exit of the trigeminal (V) nerve and 'perhaps' the rectus eye muscles. If the large foramen between the otic capsules and the 'laterosphenoid' region is interpreted as the prootic foramen then the trigeminal (V) nerve could not have passed through the opening. There do, however, appear to be clear 'retractor pits' or anterior chambers which have been suggested in other early tetrapods to be the origin of the lateral rectus eye muscles, see for example Sawin (1941) and all other descriptive chapters. The author agree with Clack (1998) that there is some uncertainty as to whether 'retractor' pits or anterior chambers in the basisphenoid-parasphenoid complex are for the insertion of the retractor bulbi or the rectus eye muscles. It does not seem possible to differentiate between these two possibilities because the region is still relatively poorly known in early tetrapods.

Posterior to these anterior chambers the basisphenoid forms the well ossified crista sellaris which would have continued in cartilage and contacted both the 'laterosphenoid' and the anterior of the otic capsules. Above the anterior chambers the crista sellaris forms a midline prong (mid pro) as also seen in *Dendrerpeton* (Robinson et al., 2005). Lateral to the crista sellaris the basisphenoid-parasphenoid complex forms the bi-facetted basipterygoid process as previously described by Clack (1998) and also seen in *Dendrerpeton* (Robinson et al., 2005).

Posterior to both the crista sellaris and the basipterygoid articulations the complex forms rounded ventrolateral wings. A groove runs from the medial margin of each basipterygoid articulation to the posterolateral corner of each wing (Figure 3.1.3—9 A

and 10 C). This could be homologous to one in *Dendrerpeton* (Robinson et al., 2005) which runs medial to the basipterygoid articulation and then passes anteromedially through the parasphenoid in a well defined foramen, however no such foramen is observed in *Acanthostega*. It seems likely that in *Dendrerpeton* (Robinson et al., 2005) this groove is the path of the internal carotid artery (ca gro) and thus this may also be the case in *Acanthostega*, although Clack (1998), with reference to early actinopterygians, also postulates that its path could suggest a spiracular canal.

The posterior margin of the basisphenoid-parasphenoid complex and its relationship to the basioccipital has not been known with total certainty (Figure 3.1.3—7 and 8). Clack (1998) debated whether the anterior or posterior grooves observed on the ventral braincase of UMZC T.1300d delineated the separation between the basisphenoid-parasphenoid complex and the basioccipital. Initially, Clack (1998) interpreted the posterior groove as being the true separation between the basisphenoid-parasphenoid complex and the basioccipital. After being informed by the morphology observed in *Acanthostega* specimen MGUH f.n. 1300a the anterior groove was instead interpreted as delineating this separation. Personal inspection of MGUH f.n. 1300a has convinced me that the posterior limit of the basisphenoid-parasphenoid complex seen on the left hand side corresponds directly to the anterior groove of UMZC T.1300d. This interpretation is reinforced by the position of the groove which runs medial to the basipterygoid articulation to the posterolateral corner of the wing of the complex. The relationship of this groove to the proposed posterior margin of the basisphenoid-parasphenoid complex is nearly identical in both UMZC T.1300d and MGUH f.n. 1300a. I, therefore, concur that the anterior of the two grooves observed in UMZC T.1300d correspond to the posterior margin of the basisphenoid-parasphenoid complex. However, from the scanning and reconstruction of UMZC T.1300d it is quite clear that

the posterior groove also appears to be a real margin between two ossifications and is not a taphonomic artefact. There appears to be a pair of v-shaped ossifications (vs oss) which sit between the basisphenoid-parasphenoid complex and the basioccipital allowing only the possibility of limited contact at the midline. The author is unaware of such an arrangement being previously described in any other tetrapod and so am cautious about any interpretation. It seems most fruitful to compare this morphology to the braincases of osteolepiform fishes. Unfortunately, the braincases of osteolepiforms rarely preserve the sutures between separate ossifications and so the relative contributions of the different ossifications of the braincase are very difficult to interpret. Additionally, this region of the braincase in osteolepiforms is radically different from the condition in early tetrapods. Osteolepiforms, such as *Eusthenopteron* (Jarvik, 1954; 1980) and *Megalichthys* (Romer, 1937), have a large unossified basicranial fenestra below the anterior extension of the notochord. Lateral to this fenestra it is claimed that the otic capsules form a shelf region. It is possible that in a similar manner the v-shaped ossifications which appear to be present in *Acanthostega* may be ventral extensions of the otic capsules (see Figure 3.1.3—5 E).

A more fruitful comparison is made with the braincase of the tristichopterid sarcopterygian *Mandageria fairfaxi* (Johanson & Ahlberg, 1997) (see Figure 3.1.3—13). The braincase reconstruction of *Mandageria fairfaxi* (text-fig.10 of Johanson, Ahlberg & Ritchie (2003)) shows ventral extensions of the braincase which form part of the anterior boundary of the vestibular fontanelle. It was possible for Johanson et al. (2003) to determine that these ventral extensions are of otic capsules rather than basioccipital origin because the basioccipital is unossified in *Mandageria fairfaxi*. The form and position of these ventral extensions in *Mandageria fairfaxi* (see Figure 3.1.3—13) are clearly highly similar to the v-shaped ossifications of UMZC T.1300d. It seems clear

that the most likely solution is that these v-shaped ossifications represent ventral extensions of the anterior region of the otic capsules which have been separated from the rest of the otic capsules by the dorsoventral compression of the specimen. This interpretation is clearly only speculative and, in fact, in many respects the v-shaped ossifications resemble the lateral wings of the parasphenoid described in other early tetrapods such as *Dendrerpeton* (Robinson et al., 2005) and *Kyrinion* 3.2. Additional material or a more detailed scan series of UMZC T.1300d will probably be needed to investigate this further.

Posteriorly the v-shaped ossifications are fused to the basioccipital region of the occipital complex. There is a small apparently unossified chevron shaped space at the midline separating the basisphenoid-parasphenoid complex from the basioccipital (Figure 3.1.3—8). There appears to have been no direct contact osseous between the basisphenoid-parasphenoid complex and the basioccipital, although, this could be a preservational artefact. Posteriorly the basioccipital forms a large but shallow anteroposterior channel which the notochord would have sat above (Figure 3.1.3—11 A and B). This channel narrows significantly towards the anterior extent of the basioccipital.

Lateral to the channel for the notochord the basioccipital forms the dorsal margin for the fenestra ovalis (f/o). The anterior boundary is formed by the v-shaped ossifications described previously within this thesis. As Clack (1998) described, there does not appear to be any contribution of the basisphenoid-parasphenoid complex to the boundary of the fenestra ovalis. The only exception to this would be if the v-shaped ossifications are interpreted as lateral wings of the parasphenoid. The dorsal and posterodorsal margin is formed from the otic capsules while the posteroventral margin

is formed by the exoccipitals which are only partly present in the scan series. As mentioned by Clack (1998) the exoccipitals appear to be fused to the basioccipital but are separated from the otic capsules by a metotic fissure. The large size of this fissure may well, at least in part, represent translocations of the various braincase elements rather than a true reflection of its original size. Behind the exoccipitals small parts of the intercentrum are present in the scan series.

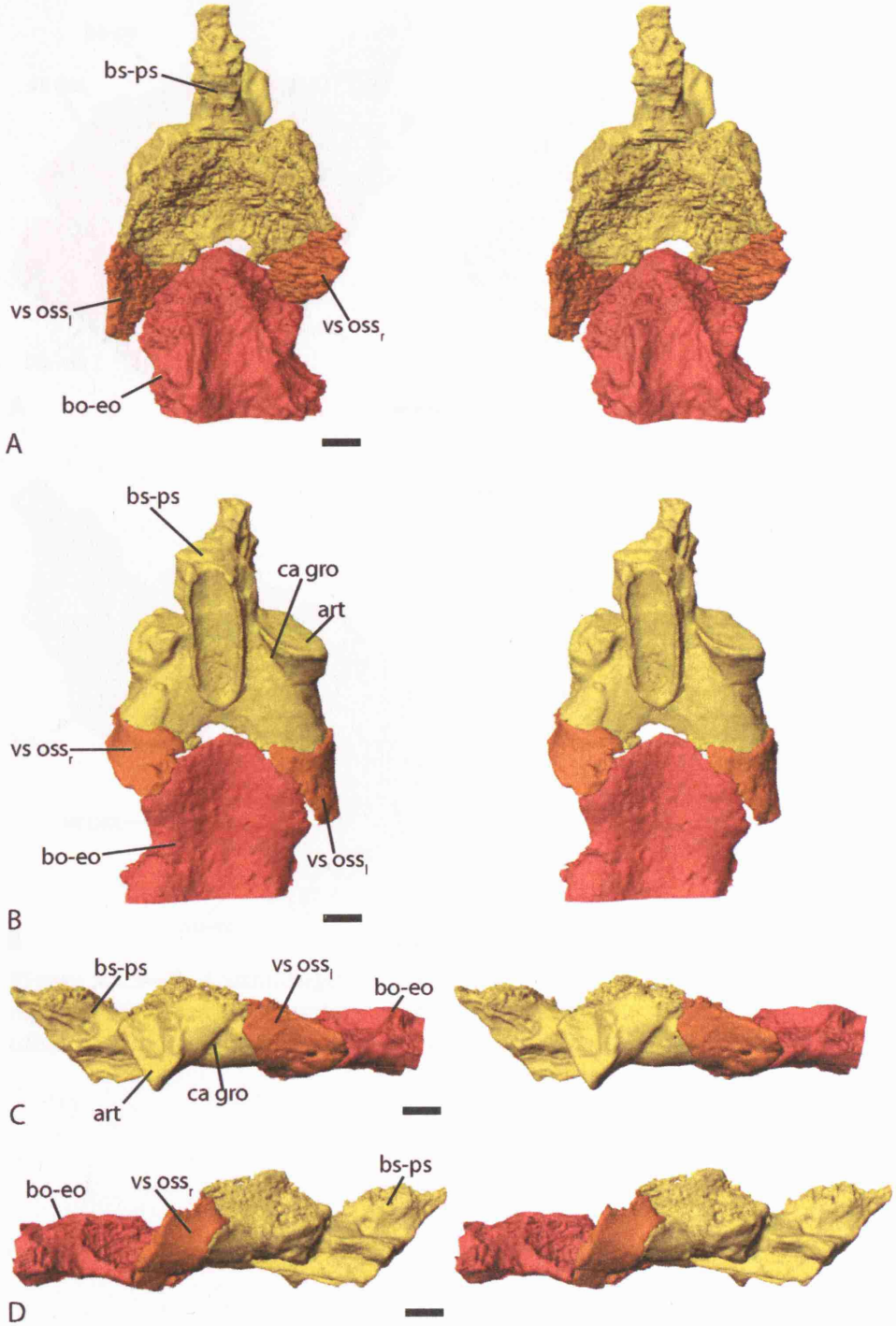

Figure 3.1.3—7 *Acanthostega* specimen UMZC T.1300d. Stereo pairs of the ventral braincase region - basisphenoid-parasphenoid complex, possible otic elements and occipital region. A, dorsal view. B, ventral view. C, left lateral view. D, right lateral view. Scale bars = 2mm.

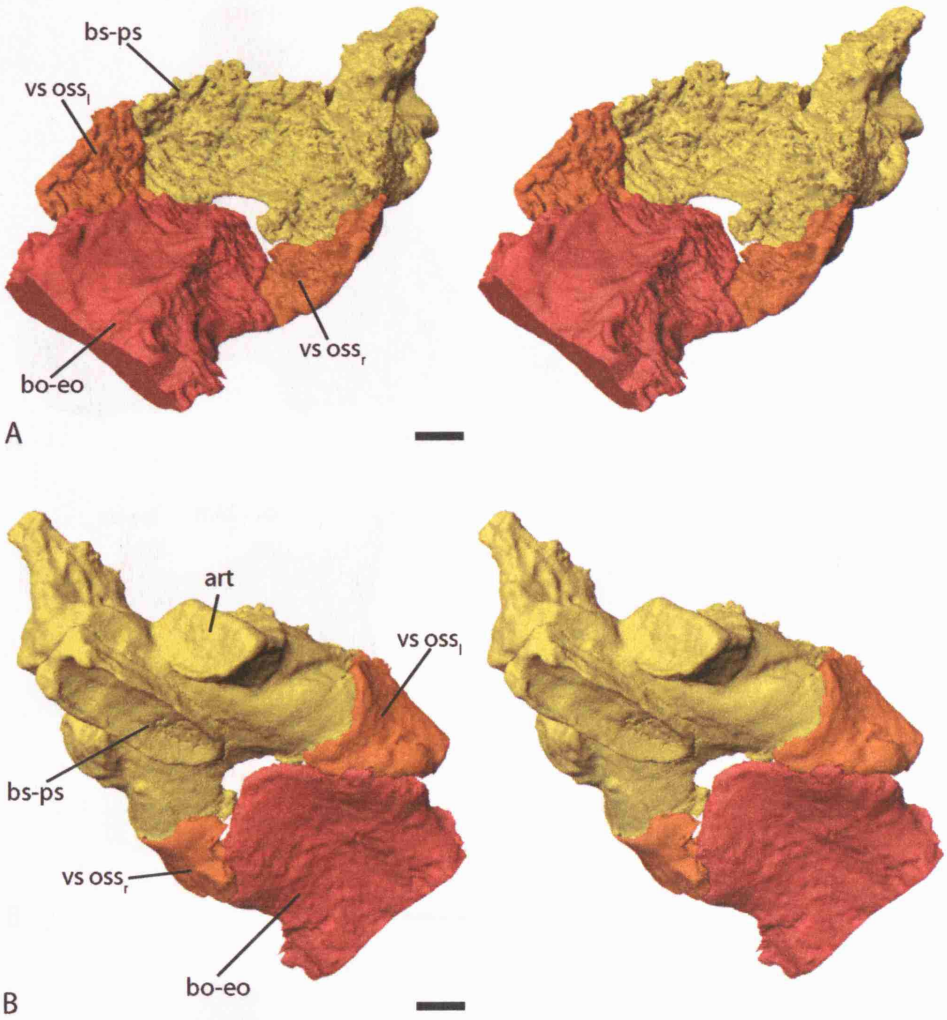

Figure 3.1.3—8 *Acanthostega* specimen UMZC T.1300d. Stereo pairs of the ventral braincase region - basisphenoid-parasphenoid complex, possible otic elements and occipital region. A, offset posterodorsal view. B, offset anteroventral view. Scale bars = 2mm.

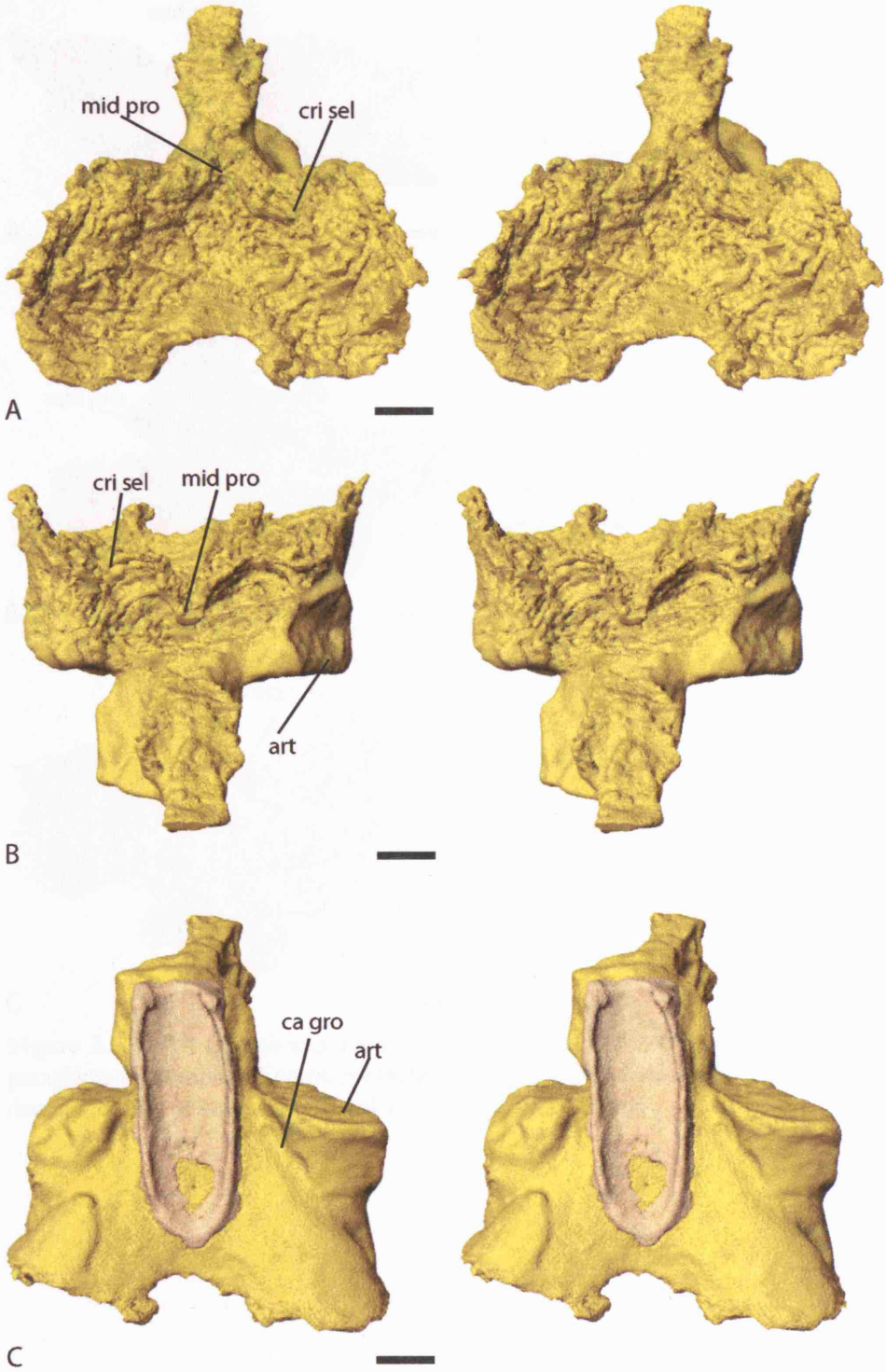

Figure 3.1.3—9 *Acanthostega* specimen UMZC T.1300d. Stereo pairs of the basisphenoid-parasphenoid complex. Central parasphenoid plate in beige. A, posterodorsal view. B, anterodorsal view. C, ventral view. Scale bars = 2mm.

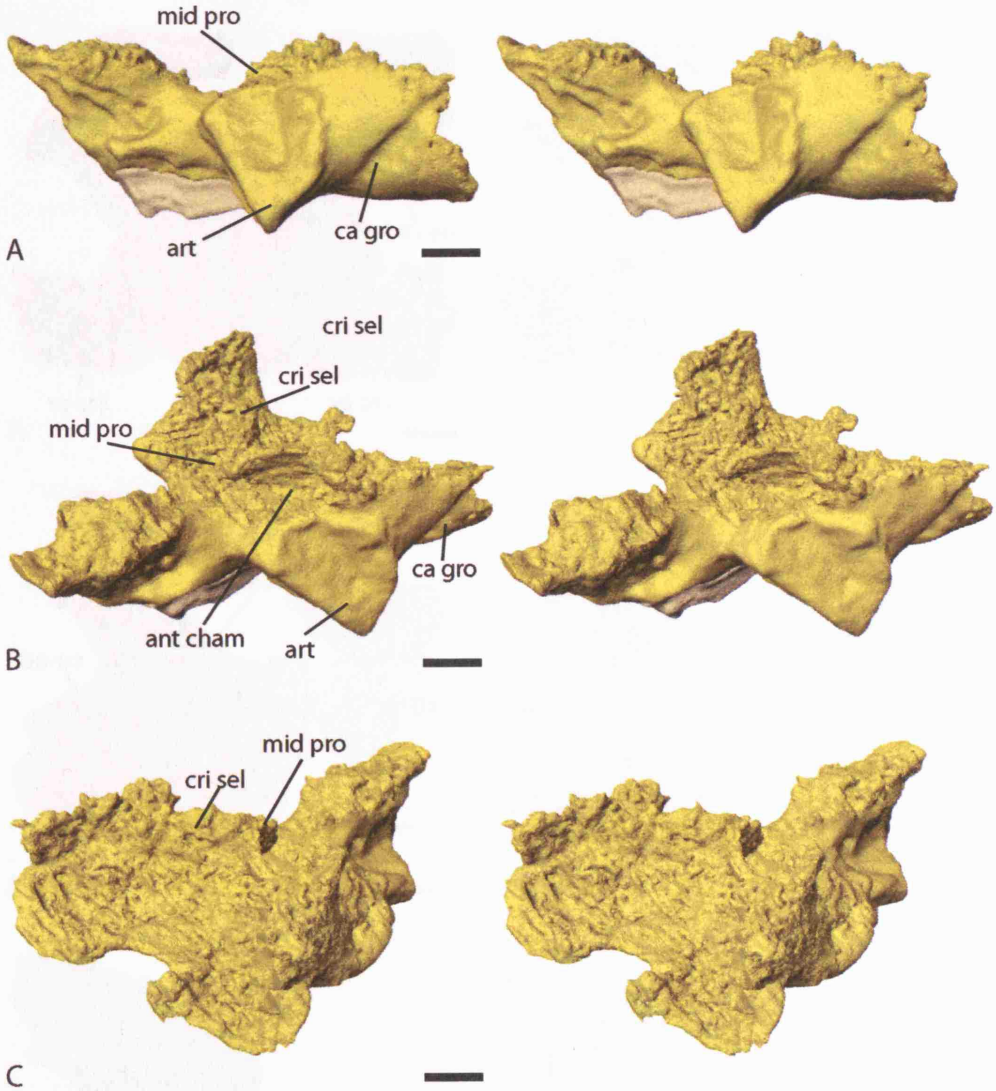

Figure 3.1.3—10 *Acanthostega* specimen UMZC T.1300d. Stereo pairs of the basisphenoid-parasphenoid complex. Central parasphenoid plate in beige. A, left lateral view. B, offset antero-dorsal view. C, offset posterodorsal view. Scale bars = 2mm.

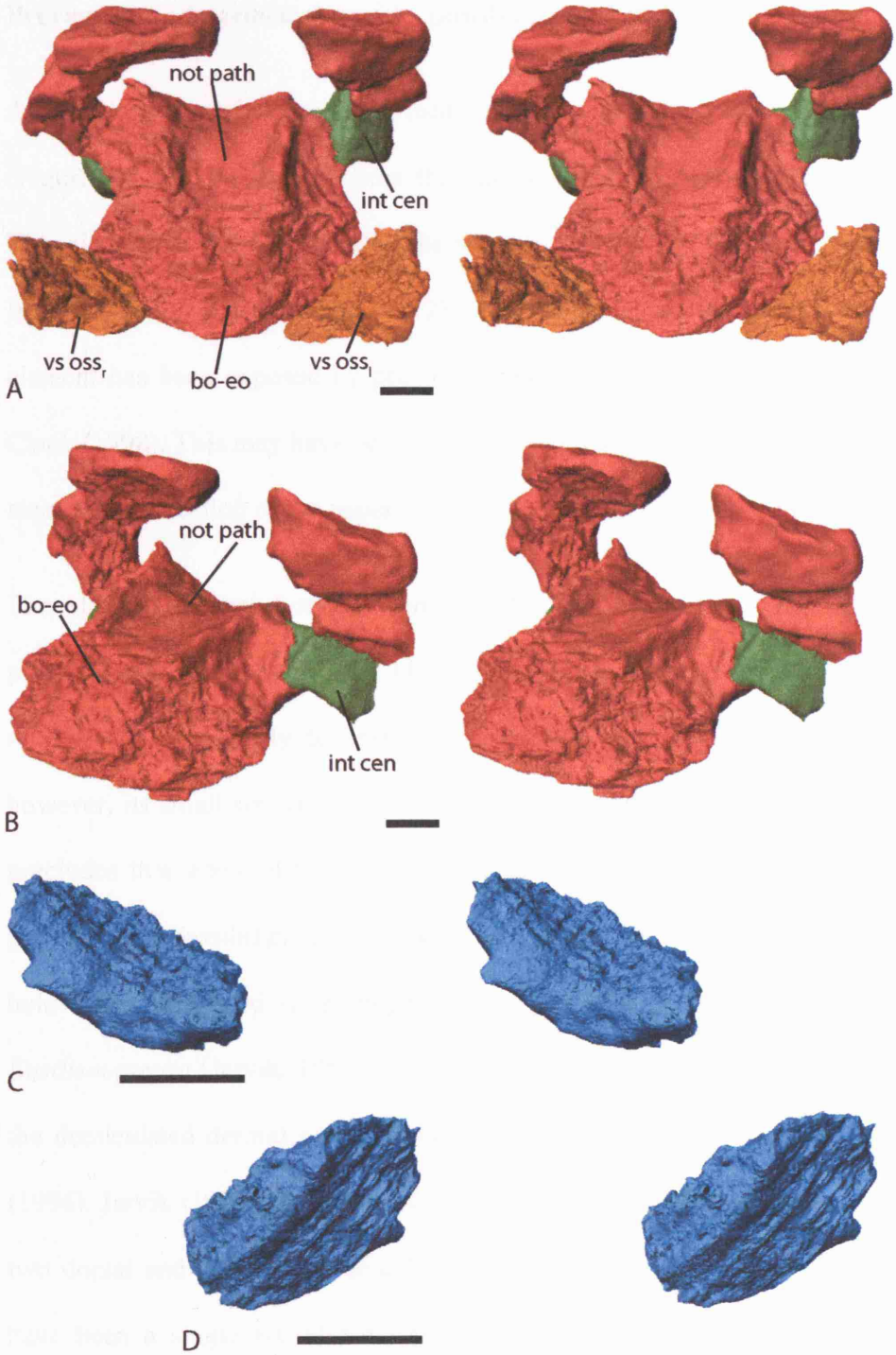

Figure 3.1.3—11 *Acanthostega* specimen UMZC T.1300d. Stereo pairs. A, anterior view of the occipital complex, v-shaped elements and intercentrum section. B, left anterolateral view of the occipital complex and intercentrum section. C and D, possible arcual plate. C, offset posterodorsal view. D, offset anteroventral view. Scale bars = 2mm.

Previously undescribed element – possible arcual plate

An additional, previously undescribed, element within the braincase has been modelled (Figure 3.1.3—11 C and D) from the scanning and reconstruction of UMZC T.1300d. This element is situated dorsal to the anterior extension of the basioccipital, just offset from the midline (Figure 3.1.3—12). It is apparent that the posterior surface of this element has been exposed by previous preparation, although, this was not figured by Clack (1998). This may have been due to extra preparation taking place on the specimen since the publication of the paper.

The element is oval from an approximately dorsal view and crescent shaped in a posterior view (Figure 3.1.3—11 C and D). In many respects its morphology is reminiscent of an early tetrapod pleurocentrum, such as those seen in *Lydekkerina*, however, its small size relative to that of the intercentrum in UMZC T.1300d seems to precludes this interpretation. Its symmetrical shape also seems to preclude it being a proatlas. One possibility is it may be an arcual plate (arc pla). These plates sit above and below the notochord in a range of sarcopterygian fishes, such as, *Latimeria* and *Eusthenopteron* (Jarvik, 1980). These endochondral plates should not be confused with the denticulated dermal paraotic plate of Jarvik (1980) or the parotic plate of Janvier (1996). Jarvik (1980) figures one dorsal and two ventral arcual plates in *Latimeria* and two dorsal and one ventral arcual plates in *Eusthenopteron.* There is also claimed to have been a single arcual plate present in *Ichthyostega* (Jarvik, 1996), in a similar position to the element seen in UMZC T.1300d, although re-examination of this material using traditional methods and CT scanning have failed to show the presence of any arcual plates in *Ichthyostega.* The position and orientation of the element in UMZC T.1300d might be used to suggest that it is a ventral arcual plate, although, it could be a

dorsal arcual plate which fell to its current position when the notochord and surrounding soft tissue rotted away. Apart from possibly *Ichthyostega* the author knows of no other recorded case of an arcual plate present in a tetrapod. This is significant because it shows a character state which links early tetrapods with the osteolepiforms.

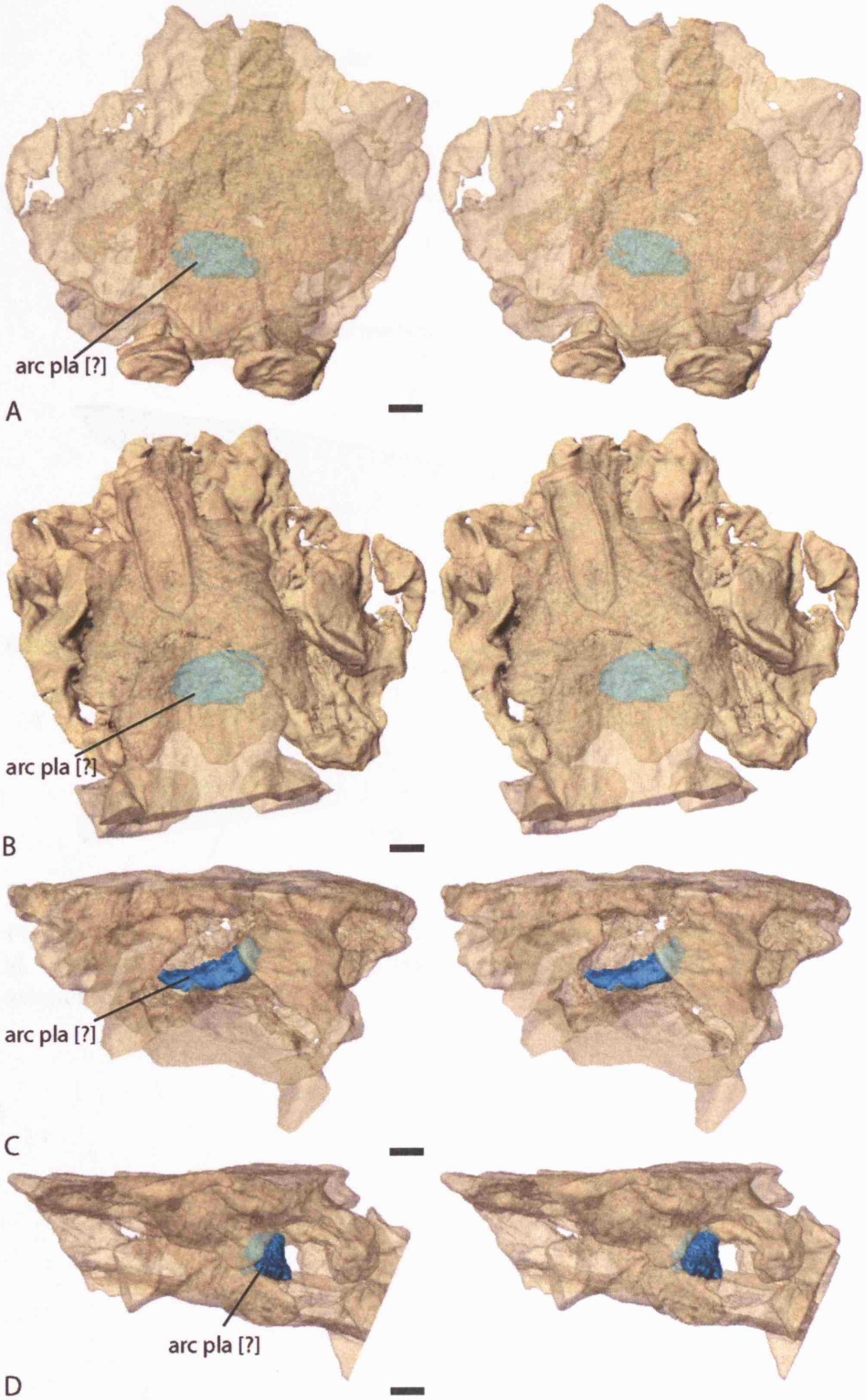

Figure 3.1.3—12 *Acanthostega* specimen UMZC T.1300d. Stereo pairs of the model to show position of possible arcual plate. A, dorsal view with the skull roof, otic capsules and dorsal lateral-osphenoid region semi-transparent. B, ventral view with the ventral braincase region - basisphenoid-parasphenoid complex, possible otic elements and occipital region semi-transparent. C, posterior view with all elements bar the possible arcual plate semi-transparent. D, left lateral view with all elements bar the possible arcual plate semi-transparent. Scale bars = 2mm.

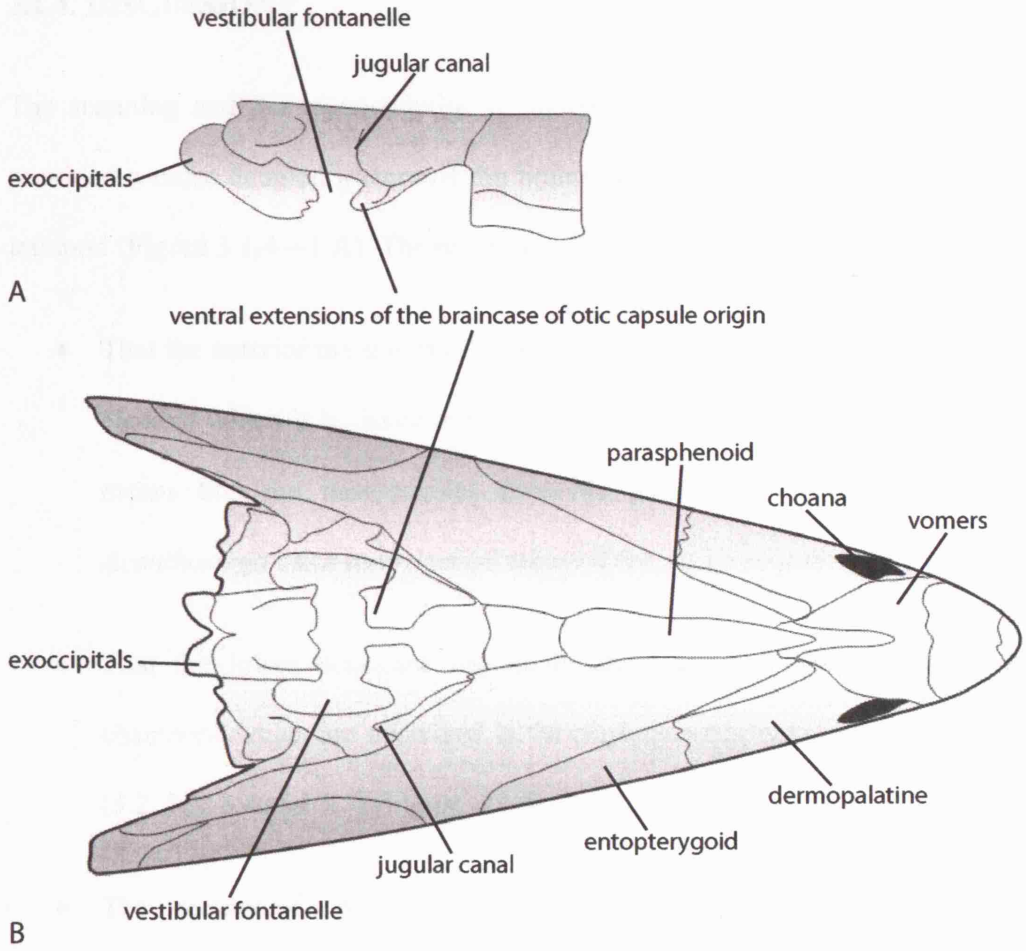

Figure 3.1.3—13 Braincase and palate reconstruction of *Mandageria fairfaxi* (after Johanson et al. (2003). A, braincase from right lateral view. B, braincase and palate from ventral view, anterior to the right.

3.1.4. DISCUSSION

The scanning and 3D reconstruction of *Acanthostega* specimen UMZC T.1300d has provided a more detailed picture of the braincase of this highly important stem-group tetrapod (Figure 3.1.4—1 A). The reconstruction illustrates:

- That the anterior margin of each fenestra ovalis is formed by a v-shaped ossified element which is believed to be of otic capsule origin (Figure 3.1.4—1 B). This means that the basioccipital does not form the anterior margin and that *Acanthostega* has a more typical tetrapod fenestra ovalis margin.

- That the lower braincase has many characteristics, such as paired anterior chambers, which are described in the phylogenetically more advanced tetrapods (3.2, 3.3, 3.4 and 3.5) (Figure 3.1.4—1 C).

- The presence of a previously unidentified ossified element in the middle of the braincase (Figure 3.1.4—1 D).

- The author believes that this ossified element could represent the first reliable identification of an arcual plate in a tetrapod (Figure 3.1.4—1 E).

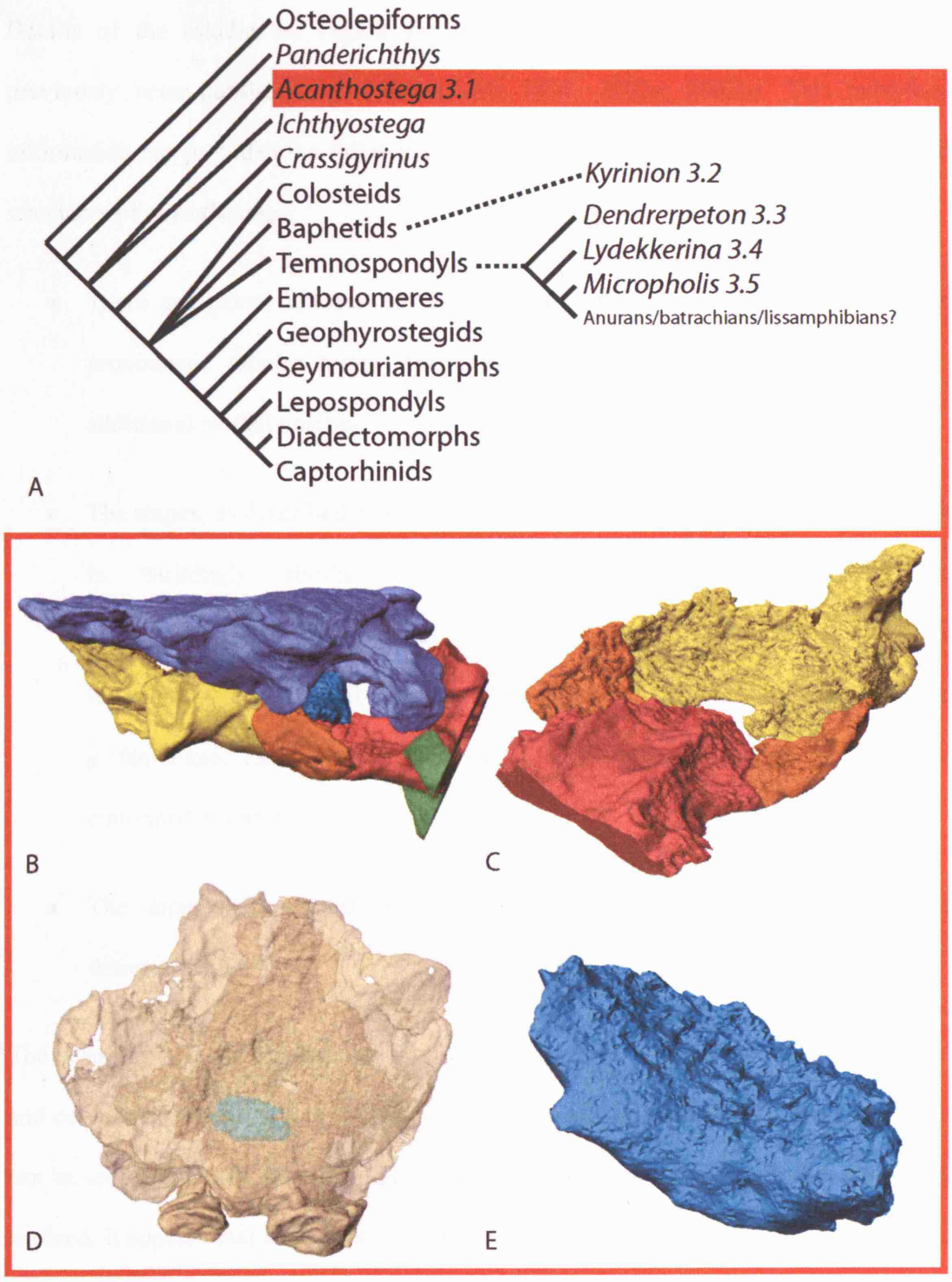
Osteolepiforms
Panderichthys
Acanthostega 3.1
Ichthyostega
Crassigyrinus
Colosteids
Baphetids
Temnospondyls
Embolomeres
Geophyrostegids
Seymouriamorphs
Lepospondyls
Diadectomorphs
Captorhinids
Kyrinion 3.2
Dendrerpeton 3.3
Lydekkerina 3.4
Micropholis 3.5
Anurans/batrachians/lissamphibians?
A
B
C
D
E

Details of the middle ear region and associated structures of *Acanthostega* have previously been published by Clack (1989; 1998; 2002a; 2003b). This published information has provided the following characteristics of the middle ear and associated structures of *Acanthostega*:

- There are paired notches on the posterior margin of the skull lateral to the pronounced tabular horns. The tabulars also form the entire boundary to additional medial notches.

- The stapes, as described by Clack (1989), is a 'massive, expanded stapes' which is 'strikingly similar to those of two unrelated Carboniferous tetrapods...*Greererpeton*...[and]...*Pholiderpeton*'. The stapes has a stout footplate with a stapedial foramen. At its distal end the stapes broadens out into a 'fan-shaped ramus'. It has been suggested that this laminar region may have continued as cartilage (Clack, 1989).

- The stapes sits within an unossified region of the posterolateral braincase, the fenestra ovalis.

The scanning and 3D reconstruction of UMZC T.1300d has provided a more detailed and comprehensive picture of the braincase of *Acanthostega* (Figure 3.1.3—2 and 3). It can be seen that in a number of respects the braincase is more 'fish-like' than previously realised. It appears that there was a single arcual plate dorsal to the anterior extent of the basioccipital. It also seems that the contact between the basisphenoid-parasphenoid complex and the basioccipital was limited by the presence of a pair of v-shaped ossifications. The exact homology of these structures with the braincase elements of osteolepiform fishes and other early tetrapods has been discussed in the description

section of this chapter 3.1.3. These v-shaped elements formed the anterior boundary of each fenestra ovalis (compare Figure 3.1.3—5 D with E) and are important in interpreting the radical changes which occurred from the osteolepiform hyomandibular's bi-facetted articulation with the braincase to the tetrapod stapes positioned in an unossified region of the braincase.

Thanks to the previous published accounts of the middle ear region of *Acanthostega* along with details presented in this chapter and information gained from the other chapters it is believed the following can be stated with confidence:

- *Acanthostega*, as previously stated it does not appear to have possessed a tympanic membrane (Clack, 1989). The posterior notches provide little evidence for any ring shaped support structure or such, as seen in temnospondyls. The morphology of the stapes also appears to preclude the presence of such a structure.

- The stapes has a stout footplate and a broad rather laminar distal end. It seems likely that this distal end may have been finished and possibly even extended in cartilage.

- The footplate of the stapes was situated within an unossified region of the braincase, the fenestra ovalis. It is highly likely that this brought the stapes in contact with the perilymphatic space of the inner ear. The stapes was thus in intimate contact with the inner ear – a condition not seen in osteolepiform fishes.

- It seems highly unlikely that the stapes functioned as a supportive element bracing the braincase against the palatoquadrate as has been suggested for the colosteid *Greererpeton* (Carroll, 1980; Smithson, 1982). As mentioned by Clack

(1988; 1989) the braincase of *Acanthostega* seems quite well connected to the skull roof and therefore the stapes could not have given much useful additional support. The stapes in *Acanthostega* also sits within an unossified region of the braincase which seems a structurally flawed location to expect a bracing strut, although this does appear to be the case in early amniotes (Clack, 2002c; Clack, 2002d; Clack & Allin, 2004). The stapes, although, massive compared to those seen in extant tetrapods, is not excessively robust and in fact its distal end may have continued as a thin cartilaginous lamina. Furthermore, the palatoquadrate shows no evidence for any stapedial contact. This seems to raise doubts about whether the stapes formed a strut between the braincase and the palatoquadrate. This however, clearly does not discount the proposal that the stapes of early tetrapods, such as *Acanthostega*, functioned as part of their ventilation system (Clack, 1992; Clack, 2002d).

- It has been proposed that those early tetrapods which do not have a tympanic membrane but possess temporal notches may have had a persistent spiracle (Carroll in (Panchen, 1985)). The paired posterior notches are proposed to have in some way supported the external openings of the spiracles. If this interpretation is correct then it is most likely that *Acanthostega* also had a persistent spiracle and that this spiracular space would have been in intimate association with the stapes. Undoubtedly, this would have allowed the stapes to pass vibrations from the spiracle to the inner ear. This functional interpretation will be raised in more detail within the discussion section of the *Kyrinion* chapter 3.2.4. This close associated with the proposed spiracular space may well have meant that it functioned as part of the animals ventilation system (Clack,

1992; Clack, 2002d), possibly regulating the inhalation/exhalation though the spiracle.

Owing to the morphology previously described in *Acanthostega* it seems clear that we can say with confidence that the stapes in early tetrapods, before it was coupled to a tympanic membrane, did not universally function as a supportive strut. In fact, as will be elaborated in the discussion section of the *Kyrinion* chapter 3.2.4 the supportive function for the early tetrapod stapes might only be a specialisation of *Greererpeton* or colosteids as a whole. It appears that the primary function of the stapes in most early tetrapods may well have been for hearing even if no tympanic membrane was present. This function may also have been combined with a role in their ventilation system as proposed by Clack (1992; 2002d) although the author does not envisage any contact between the stapes and the palatoquadrate complex. The association of the stapes to the proposed spiracular space may well have conferred hearing advantages in both an aquatic and terrestrial environment, as Clack (1983) suggested for the stapes of *Pholiderpeton.* It is conceivable that the middle ear morphology observed, in *Acanthostega,* is transitional and that development of such a system could lead to the evolution of a tympanic membrane coupled stapes. This will be detailed further in the *Kyrinion* chapter 3.2.4.

3.2. KYRINION

Kyrinion has been classified by Clack (2003a) as a baphetid. In the phylogenetic analyses of Laurin & Reisz (1997) and Ruta et al. (2003a) baphetids, or loxommatids in the case of Laurin & Reisz, are positioned directly below the split between temnospondyls and all other phylogenetically higher early tetrapods. *Kyrinion* and baphetids in general are placed in a critical position in the early tetrapod phylogeny with regards to their middle ear anatomy. No member of the baphetids has a well preserved middle ear and associated structures which have been previously described. Both stapes of *Kyrinion* have been partially exposed by previous preparation (Clack, 2003a) and, therefore, it is a perfect specimen for investigating the middle ear region of phylogenetically advanced stem-group tetrapods very close to the proposed split between the lineages leading to amphibians and amniotes. A more complete understanding of this region in a baphetid will, hopefully, address the following questions:

- What was the stapedial function before it was coupled to a tympanic membrane?
- How did a stapes coupled to a tympanic membrane evolve?
- Did early tetrapods have a spiracle and did this get transformed into a middle ear space? If not, what was the function of the paired notches in early tetrapods?
- Is the proposed spiracular opening in early tetrapods in anyway homologous to the tympanic membrane? If so, is this in all tetrapods?

There was also the possibility that the scanning and reconstruction of *Kyrinion* would help address issues regarding the origin of some of the unique middle ear characteristics

of extant amphibians, such as, the opercular system. However, it seems that baphetids are too phylogenetically basal to be expected to exhibit such specialised morphology.

See *Kyrinion* Discussion 3.2.4 and Figure 3.2.4—1 for a synopsis of the morphology revealed from the reconstruction of NEWHM: 2000.H845 and how this has helped address the above questions.

3.2.1. BACKGROUND

The species name *Kyrinion martilli* Clack, 2003 is assigned to a single specimen NEWHM: 2000.H845 (Figure 3.2.1—1 and 2) which also forms the type species for the genus. NEWHM: 2000.H845 was collected by David Martill in 1993 at Whitley Bay, Tyne and Wear, northeast England (Clack, 2003a). *Kyrinion* proved difficult to date as it was found as an isolated block within Pleistocene clay but was clearly much older than Pleistocene (Clack, 2003a). It is believed that the block was transported to the find locality as part of an ice sheet deposit. However, with knowledge of the surrounding geology and spore analysis carried out by Dr J.E.A. Marshall of Southampton Oceanographic Centre, England it was possible to date *Kyrinion* to the late Langsettian Sub Epoch of the Westphalian (A), Upper Carboniferous (Clack, 2003a).

The specimen consists of a single cranial block with isolated postcranial material. To facilitate the study of the specimen the block has been subdivided by Clack into more manageable sections using a diamond wire saw with a 0.3mm diameter (Clack, 2003a). Furthermore, various aspects of the cranial material have been exposed via manual preparation carried out by Sarah Finney. Clack published the first description of this specimen in 2003 which details all the external and internal cranial anatomy along with some postcranial material which could be observed from the sectioning and manual preparation. From the character states observed, especially the enigmatic triangular shaped orbits, *Kyrinion* has been classified as a baphetid (Clack, 2003a). Although no detailed cladistic analysis has been undertaken which includes *Kyrinion*, there appears to be no reason to question this classification at this time.

Due to *Kyrinion* not being placed in a phylogeny using cladistic analysis the phylogenetic position of baphetids as a whole has to be used as a proxy. The

superfamily Baphetoidea Cope, 1875 has directly replaced Loxommatoidea Romer, 1966 (which was in turn a correction of the superfamily name Loxommoideae Watson, 1929) (Milner & Lindsey, 1998). When Watson erected Loxommoideae in 1929 it included one family, the Loxommidae Watson, 1917 (later to be renamed the Loxommatidae Romer, 1966), which included the four genera – *Loxomma*, *Baphetes*, *Orthosaurus* (later to be renamed *Megalocephalus* as the name was already used elsewhere) and *Spathicephalus*. Apart from name changes this grouping has remained relatively constant.

The interrelationships of *Loxomma*, *Baphetes*, *Megalocephalus* and *Spathicephalus* within the baphetids have not to date been considered in a strict cladistic fashion, although this is now underway (A.C.Milner, Pers.Comm). However, an investigation by Beaumont (1977) split Loxommatoidea into two families; Spathicephalidae containing 'the highly aberrant' *Spathicephalus* and Loxommatidae (now named Baphetidae) containing the remaining genera *Loxomma*, *Baphetes* and *Megalocephalus*. Some cladistic analyses, such as that of Clack (2001), have recently placed *Eucritta melanolimnetes* Clack, 1998 as the sister group to the family Baphetidae. This is also the case with the 'single tree derived from reweighting characters by their consistency index' and the 'strict consensus of 2160 equally parsimonious trees obtained after removal of lower jaw characters' of Ruta et al. (2003a). However, none of these analyses have included *Spathicephalus*. Furthermore, there is uncertainty as to whether *Eucritta* falls within the Baphetoidea or even is its sister group, for example see its conflicting positions within the cladograms of Ruta et al. (2003a). The phylogenetic position of *Kyrinion* within the Baphetoidea is not known.

The phylogenetic position of the baphetids relative to other early tetrapods, proposed by cladistic analyses, has changed frequently. Previously baphetids have been classified as

belonging to the order Temnospondyli within the now defunct subclass Labyrinthodontia, which included all early tetrapods except the lepospondyls (Romer, 1966). However, this arrangement is now generally believed to be due to ancestral character states, such as, the relative arrangement of the parietals, post-parietals, supratemporals and tabulars (Clack, 2003a). Recent cladistic analyses, such as Ruta et al. (2003a) and Laurin & Reisz (1997), have placed the baphetids as the sister group to most other early tetrapods including temnospondyls, lepospondyls and 'anthracosaurs'. In both the aforementioned phylogenies *Acanthostega* and *Ichthyostega* are more basal early tetrapods than the baphetids. The phylogenies differ in their placement of the colosteids, which are placed with in the temnospondyls by Laurin & Reisz (1997) but are classified as more basal than the baphetids by Ruta et al (2003a). In the case of Ruta et al. (2003a) baphetids are the sister group to the crown group tetrapods while in the case of Laurin & Reisz (1997) they are phylogenetically quite basal stem group tetrapods. Many phylogenies, however, have been unable to resolve fully the position of baphetids relative to other early tetrapods, for example see Clack (2001) and Ahlberg & Milner (1994). Although, they do appear to have branched off relatively close to the node separating temnospondyls and 'Anthracosaurs'.

Figure 3.2.1—1 *Kyrinion* specimen NEWHM: 2000.H845 in dorsal view. Scale bar = 10mm.

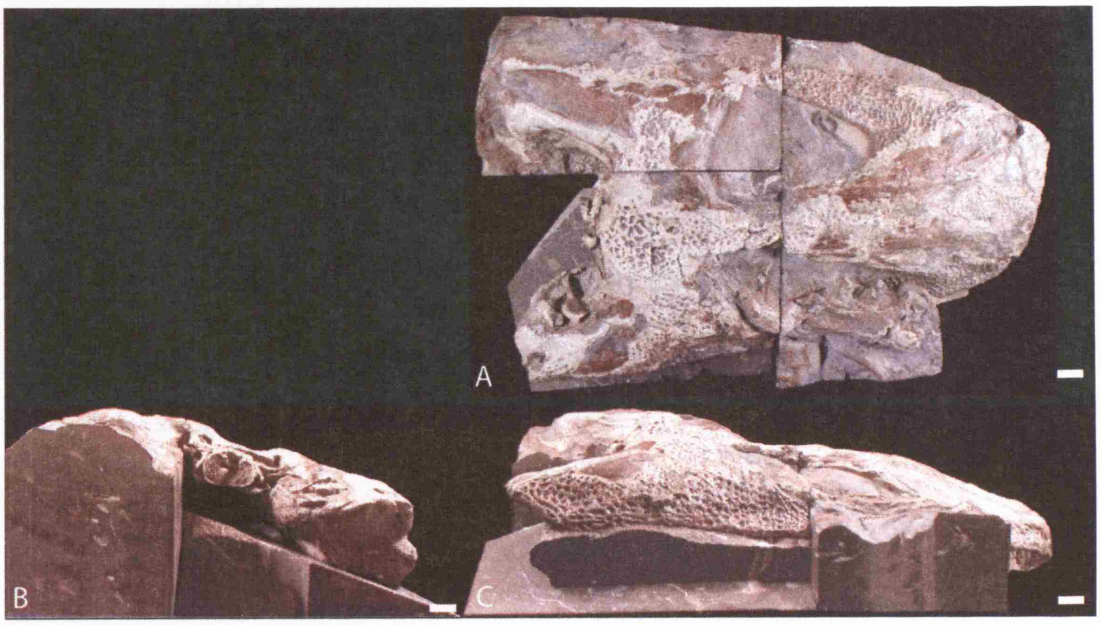

Figure 3.2.1—2 *Kyrinion* specimen NEWHM: 2000.H845.A, dorsal view. B, posterior view. C, right lateral view. Scale bars = 10mm.

3.2.2. RECONSTRUCTION PARAMETERS

Kyrinion specimen number NEWHM: 2000.H845 was scanned on the high energy subsystem scanner at UTCT. An offset rotation (translate-rotate) was utilised to maximise the scan detail. As mentioned previously Clack subdivided this specimen into more manageable sections (Figure 3.2.1—2). Due to cost and time constraints it was decided to scan only one section (Figure 3.2.2—1) which contained the braincase, partial left stapes, right stapes and posterior right palatoquadrate complex. The partially eroded skull roof and cheek of this region were also present in the scanned section.

A sole scan series was produced in 16bit resolution (1024 pixels by 1024 pixels), comprising 251 slices each of 0.375mm thickness (i.e. approximately 2.7 slices per mm). Although, slice thickness was 0.375mm the interslice spacing was set at 0.333mm, meaning that each slice actually overlapped with those on either side by 0.021mm, producing a contiguous rather than continuous slice series.

Unfortunately the scanning of *Kyrinion* proved somewhat problematic as it had to be halted and restarted numerous times. This produced slightly different parameters and TIFF files sizes for certain scan slices. Slices 1-109 (with a field of view of 121mm) have a slightly larger field of view than slices 110-251 (with a field of view of 119.7mm). Slice groups 2-95, 96-109 and 1+110-251 each have very slightly differing TIFF files sizes. Furthermore, the TIFF files in series 96-109 have different specific pixel properties (pixel type, unsigned short; pixel byte swapping, low byte first) relative to those of 1-95 and 110-251 (pixel type, unsigned short; pixel byte swapping, high byte first). These differences cause problems when importing TIFF files into Mimics; slice groups 2-95, 96-109 and 110-251 have had to be reconstructed separately within Mimics and married together in the 3D manipulation package, Rhino3D (Figure 3.2.2—

1). Slice 1 which has a different TIFF file size to slice group 2-95 has been discarded because it does not form a stack and, therefore, cannot be imported into Mimics.

As is the case with many CT scans of Palaeozoic tetrapods the slices of *Kyrinion* have a relatively high amount of noise – making modelling of fossilised material problematic and time consuming. Unusually for CT scans the fossilised material of *Kyrinion* is frequently less x-ray opaque than the matrix (Figure 3.2.2—2), although, in certain areas of the slices the reverse is true. This feature along with the background noise meant that manual thresholding and drawing tools had to be used to model elements within the three different stacks of slices. The noise has also reduced the aesthetics of the elements created in this manner.

Elements modelled from the stack created from slice group 96-109 were imported into Rhino3D with no alteration of coordinates. However, to marry accurately together these elements to those modelled from the stacks created from slice groups 2-95 and 110-251 altered coordinates had to be used. The three coordinates x, y and z correspond approximately to mediolateral, dorsoventral and anteroposterior of the specimen respectively. For elements from the stack created from slice group 2-95 the x value was 0.4mm, the y value remained unchanged and the z value was -34.88mm. For elements from the stack created from slice group 110-251, which contained most of the stapedial and braincase information, the x, y and z values were 0.7mm, 0.3mm and 4.88mm respectively. A smoothing transformation over all world coordinates with a factor of 1.5 was used to improve the appearance of the reconstruction.

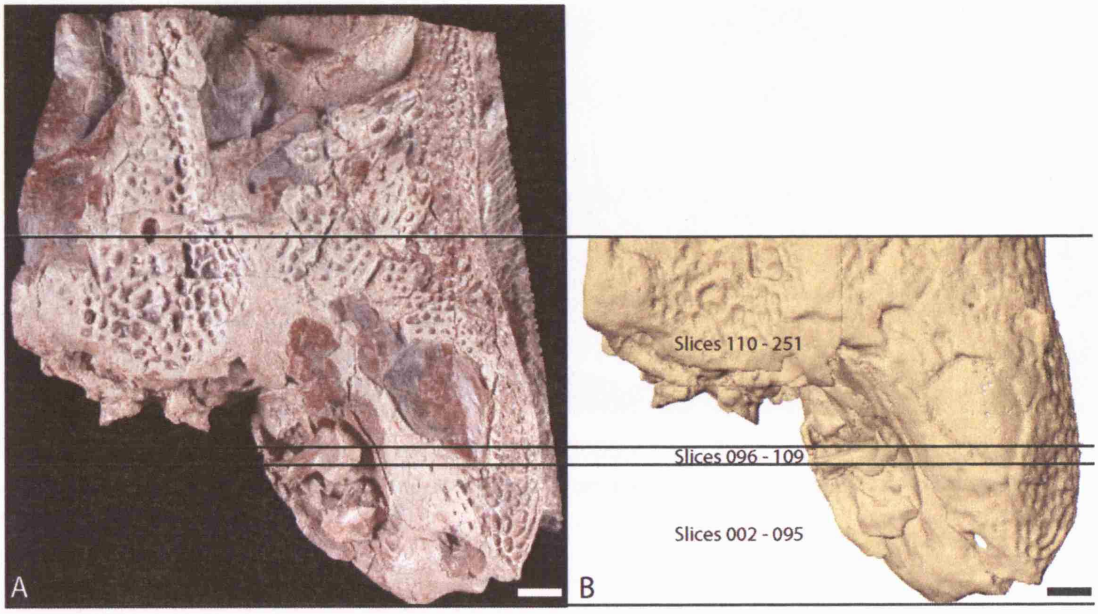

Figure 3.2.2—1 *Kyrinion* specimen NEWHM: 2000.H845. A, dorsal view of section utilised for CT scanning. B, dorsal view of the model to show the relationship of the three sections to the original specimen. Scale bars = 10mm.

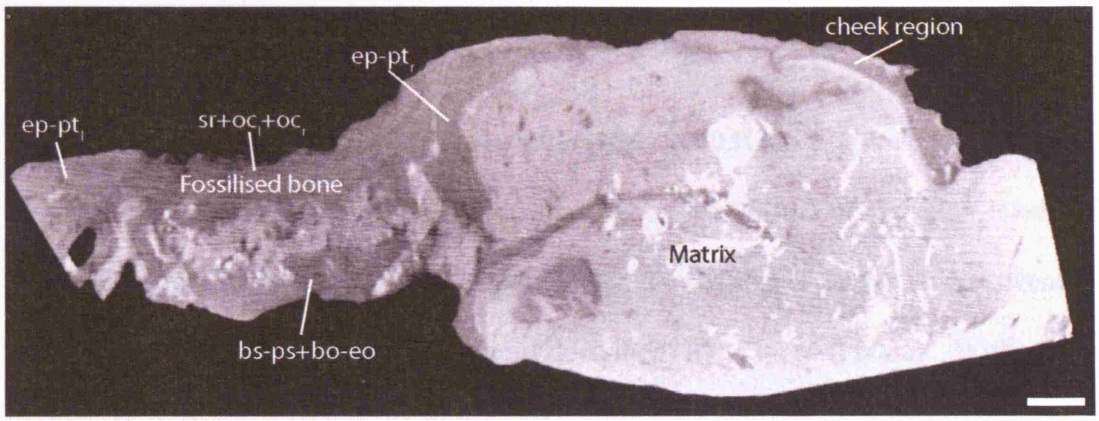

Figure 3.2.2—2 *Kyrinion* specimen NEWHM: 2000.H845. Transverse CT scanning slice to demonstrate the contrast between the fossilised bone and the matrix. Scale bar = 10mm.

3.2.3. DESCRIPTION

The reconstruction of *Kyrinion* specimen NEWHM: 2000.H845 (Figure 3.2.3—2) from CT scan slices also proved problematic due to noise within the slices, high levels of fusion between different ossifications and a larger than expected degree of dorsoventral compression than had previously been described by Clack (2003a). With these limitations in mind it should be noted that unlike the reconstruction of *Dendrerpeton acadianum* 3.3 (Robinson et al., 2005) it has not proved possible to fully discern the separate ossifications in the reconstruction with complete accuracy.

The reconstruction (Figure 3.2.3—3) contains:

- The posterior skull roof (presumably parietals, supratemporals, postparietals and tabulars) strongly fused to the posterior sphenethmoid region (or 'laterosphenoid') and paired otic capsules.
- The right dermal cheek region (presumably squamosal, a part of the jugal and quadratojugal).
- The right palatoquadrate complex (containing epipterygoid, pterygoid and quadrate) and a small section of the left palatoquadrate complex.
- A 'lower braincase and occipital' complex consisting of the parasphenoid, basisphenoid, basioccipital and exoccipitals.
- The near complete right stapes and medial (proximal end) of the left stapes.
- Fragmentary elements including a rib and possible visceral arch material.

The area of the skull which has been scanned is not disarticulated; relationships between elements appear to have been preserved, apart from the near uniform dorsoventral compression.

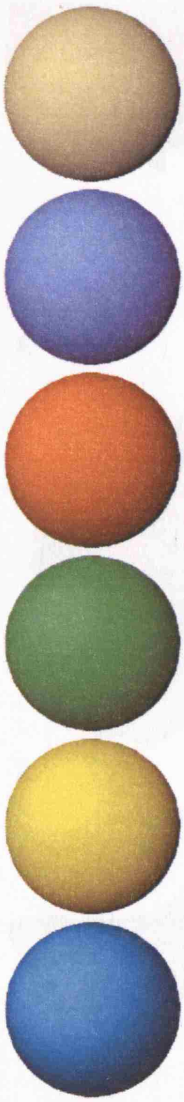

Figure 3.2.3—1 Colour key.

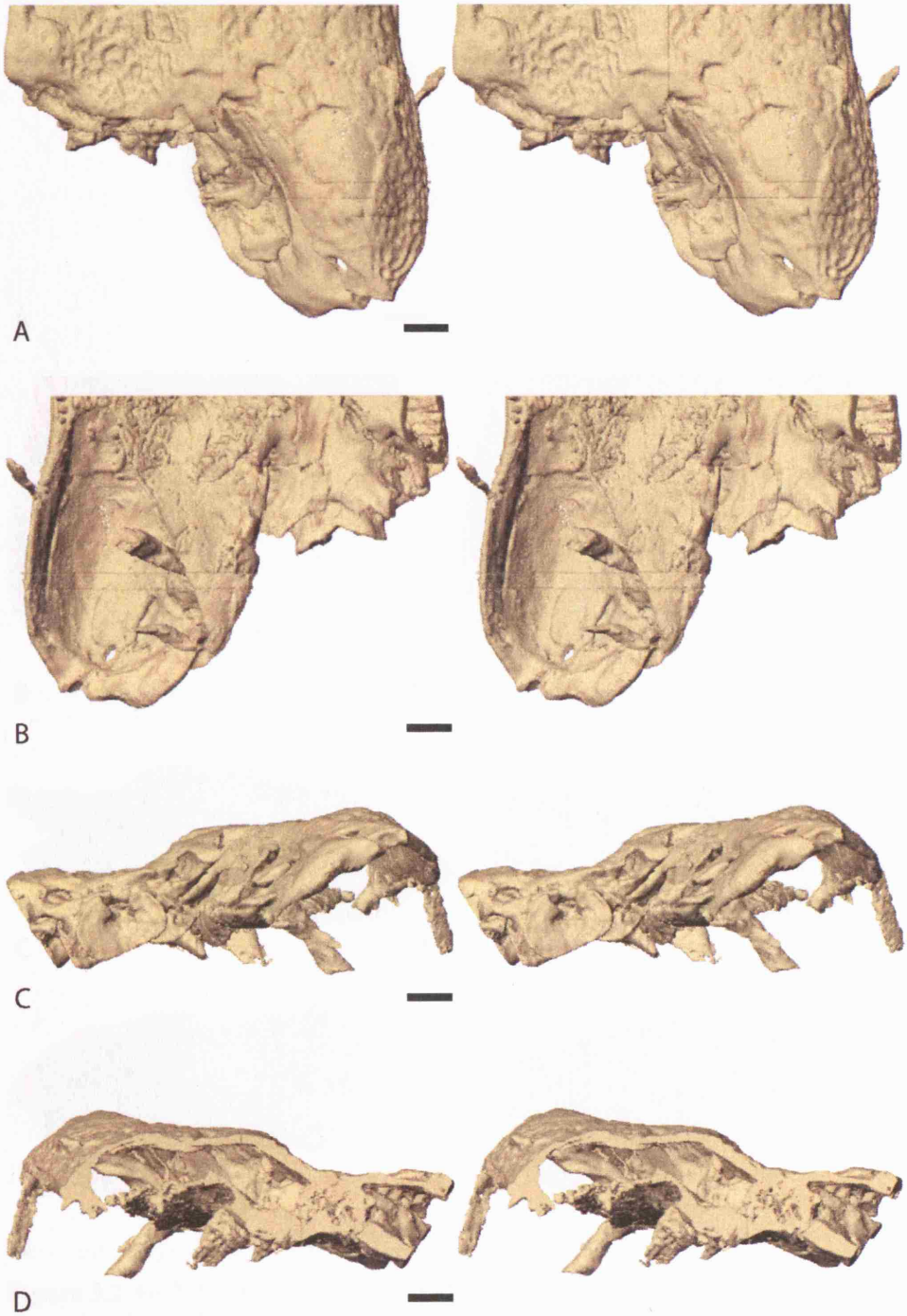

Figure 3.2.3—2 *Kyrinion* specimen NEWHM: 2000.H845. Mono colour stereo pairs of the model without correction for translocations. A, dorsal view. B, ventral view. C, posterior view. D, anterior view. Scale bars = 10mm.

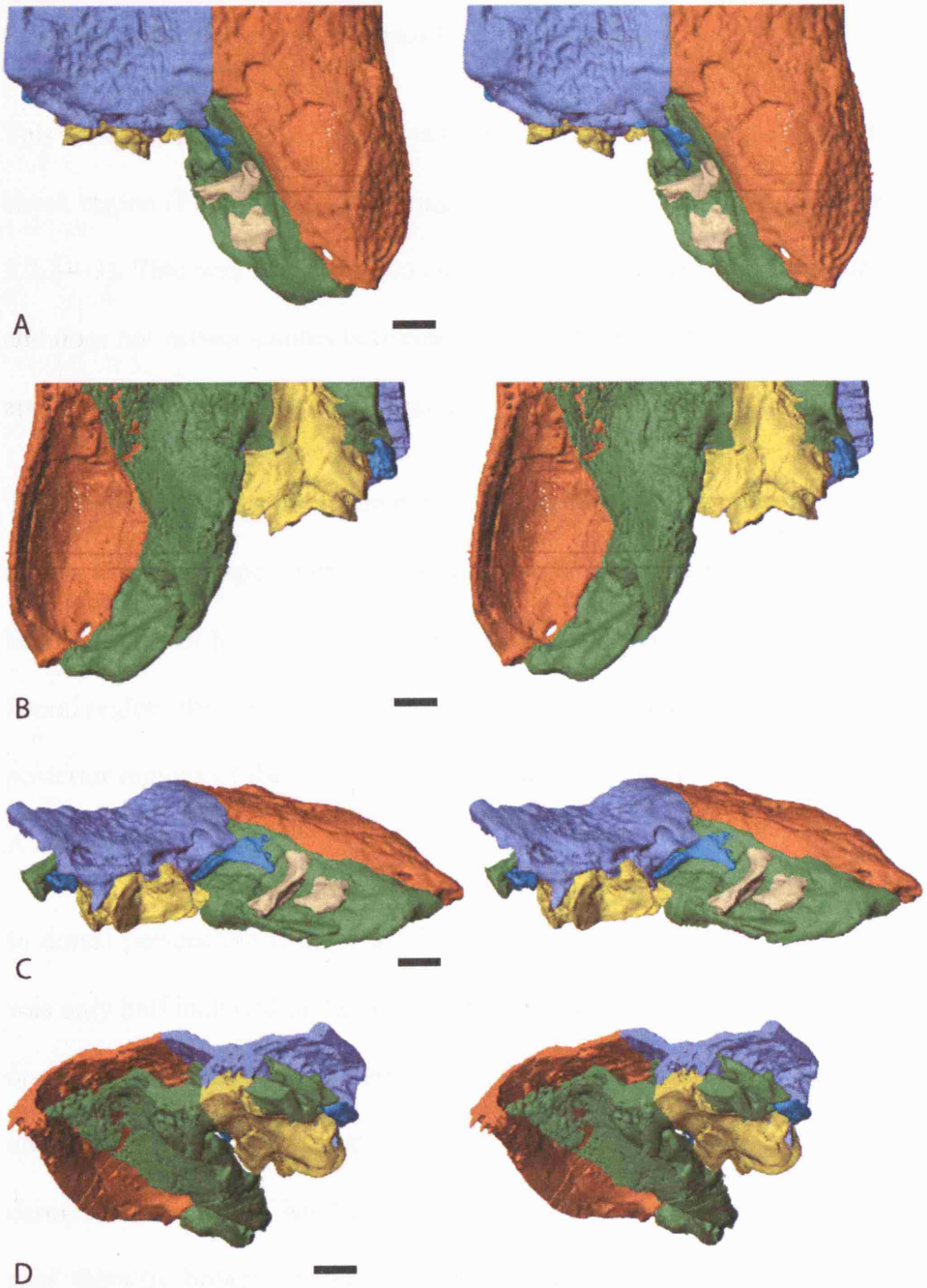

Figure 3.2.3—3 *Kyrinion* specimen NEWHM: 2000.H845. Stereo pairs of the model without correction for translocations. A, dorsal view. B, ventral view. C, offset posterodorsal view. D, offset anteroventral view. Scale bars = 10mm.

Skull roof, posterior sphenethmoid and otic capsules

This complex (Figure 3.2.3—4) has been arbitrarily distinguished from the right dermal cheek region (Figure 3.2.3—7) along a line anterior to the right temporal notch (Figure 3.2.3—3). This was carried out to aid observation of the stapes and surrounding region and does not reflect sutures between the supratemporal and tabular of the skull roof (sr) and the squamosal of the cheek region.

The general form of this complex suggests that the dorsoventral compression that affects the whole specimen has caused a particular distortion. It appears that there has been a degree of bending causing the midline of the complex to dip relative to the more lateral region; this in turn may have caused the ventral extensions of the opisthotics and posterior regions of the sphenethmoid (se) to have splayed out laterally (Figure 3.2.3—4 A and C).

In dorsal perspective (Figure 3.2.2—1) it can be seen that the pineal foramen (pin for) was only half included in the scan series. The characteristic pitted or honeycomb dermal ornamentation that is also present in *Loxomma*, *Baphetes* and *Megalocephalus* is most clearly visualised in the region behind the pineal foramen; lateral to this region the dermal ornamentation has been rather worn away. At the posterior margin of the skull roof there is broken surface leading to paired tabular 'horns'. This region is not complete as the dermal elements have been somewhat eroded or broken off. For this reason one cannot be sure of the extent of the posterior skull roof and whether the tabulars formed distinct horns, as seen in *Acanthostega* and many embolomeres, or simply formed the lateral margin of the posterior extension. In either case it is clear that the tabulars projected posteriorly forming the posteromedial border to the temporal notch.

In anterior view (Figure 3.2.3—4 C) it can seen that the well ossified posterior region of the sphenethmoid or 'laterosphenoid' (lsr) is fully fused to the skull roof. The resolution of the scans has made it difficult to locate the exit points for the various cranial nerves expected in this area. The lateral splaying of the two walls of this region adds weight to the prior postulation that this complex has been deformed by the dorsoventral compression.

From the 3D reconstruction of this region it was not possible to find evidence for separate prootic and opisthotic elements of the otic capsules (oc) and so they are treated as single ossifications. The otic capsules are most clearly observed in the lateral perspective (Figure 3.2.3—4 B) in which the dorsal boundaries of the fenestrae ovales (f/o) are visible. At the anterior margins of the otic capsules there are foramina, visible clearly on the left side, which are believed to be the prootic foramina (pro for) for the exit of the trigeminal (V) nerve. Also on the left side a foramen above the otic capsule running through to the left post-temporal fossa (ptf) is also visible. This foramen (ot for) is undoubtedly the post-temporal foramen in Romer & Witter's description of *Edops* (1942) and the 'spiracular canal' of *Eusthenopteron* (Jarvik, 1980). It seems likely that the vena capitalis dorsalis would have exited the post-temporal fossa through this foramen. This foramen also appears to be present in the baphetids *Loxomma* and *Megalocephalus* (Beaumont, 1977) and is very clearly seen in *Dendrerpeton* (Robinson et al., 2005).

In posterior view (Figure 3.2.3—4 A) the suggested bending deformation of this complex is clearly visible from the depressed midline of the skull roof and the lateral splay of the 'opisthotics'. The robust 'opisthotics' form the paired paroccipital processes (par pro) which are also seen in other baphetids and temnospondyls (for

example *Lydekkerina*). The 'opisthotics' are fully fused with the tabulars, although, it cannot be ascertained whether these fusions are at the distal end of the paroccipital processes or in a more proximal position. In posterior view it is clear that the ventromedial extent of the opisthotics of *Kyrinion* are positioned anterolateral to the occipital condyle (occ cond). It seems likely that this positional relationship is an artefact of the bending of the complex and dorsoventral compression of the specimen. Originally the 'opisthotics' would have contacted and fused with the exoccipitals in a more dorsomedial position. Clack (2003a) states that the 'opisthotics' form 'a continuous structure across the midline with no sutures to delimit ossifications or to mark a supraoccipital component' – no further information can be gleaned for this character state from the reconstruction. The 'opisthotics', along with the postparietals and tabulars frame the paired post-temporal fossae. It is difficult to assess the true size of the post-temporal fossae because of the dorsoventral compression and the eroded posterior margins of the postparietals and tabulars.

The internal aspects of the otic capsules have resisted rigorous attempts to elucidate the appearance of the vestibular apparatus in *Kyrinion* (Figure 3.2.3—5 A). It is believed that the collapse of the otic capsules onto the lower braincase is the main cause of the disrupted situation observed within the capsules. Some measurements of the labyrinths can, however, be gained from frontal CT sections (Figure 3.2.3—5 B).

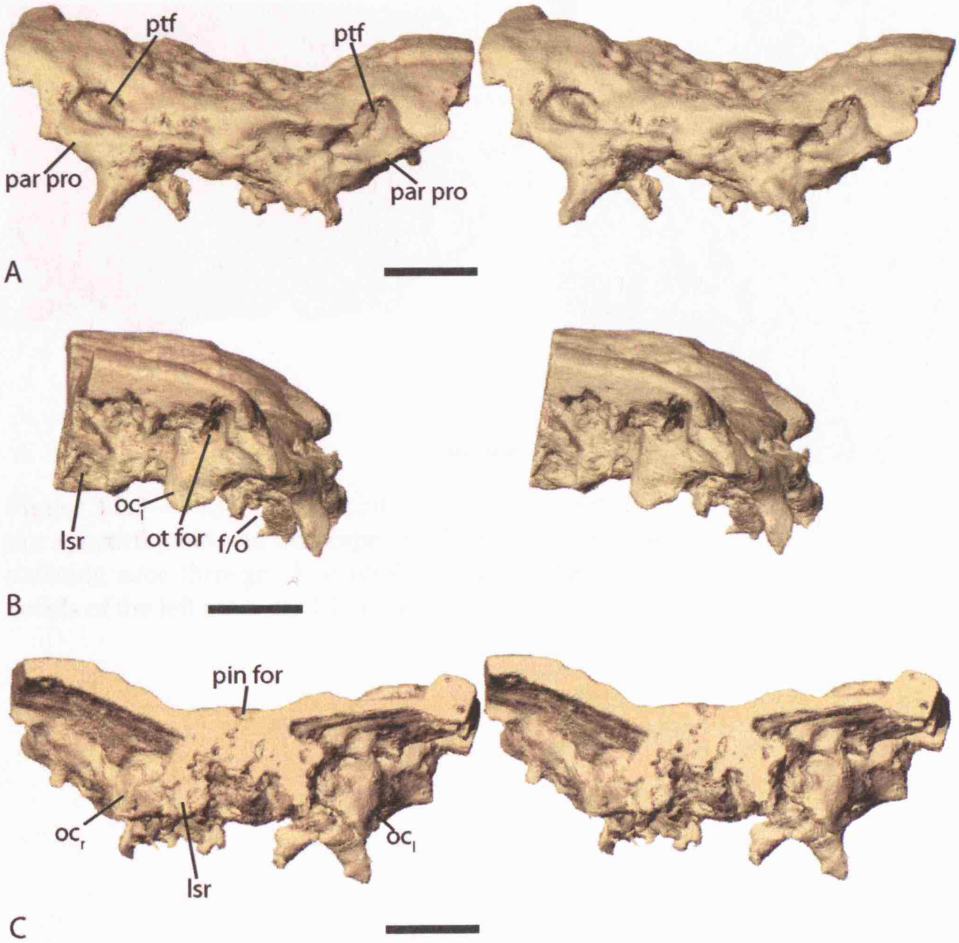

Figure 3.2.3—4 *Kyrinion* specimen NEWHM: 2000.H845. Stereo pairs of the skull roof, posterior sphenethmoid and otic capsules. A, posterior view. B, left lateral view. C, anterior view. Scale bars = 10mm.

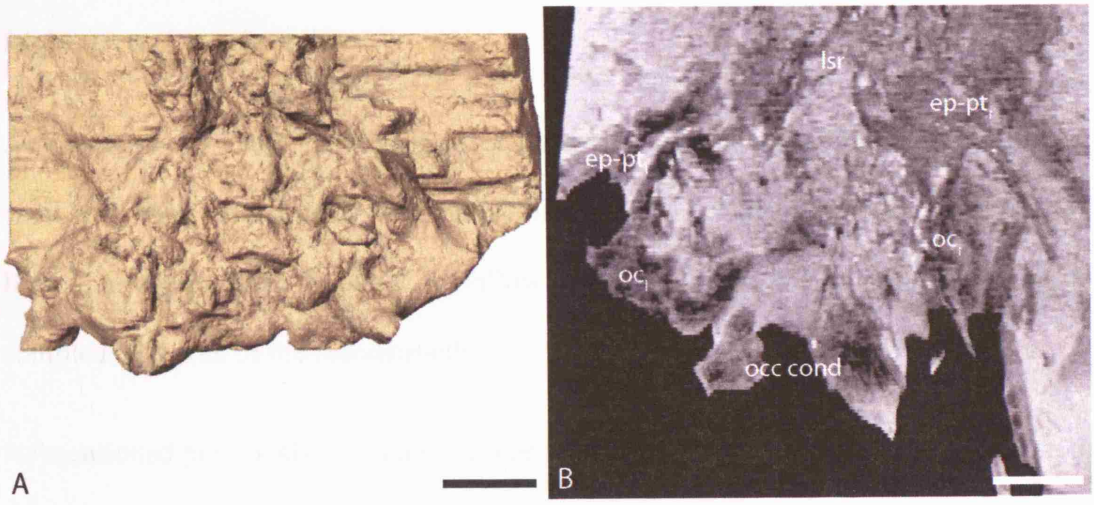

Figure 3.2.3—5 *Kyrinion* specimen NEWHM: 2000.H845. A, ventral view of skull roof, posterior sphenethmoid and otic capsules showing poorly resolved internal structure. B, frontal CT scanning slice through skull roof, posterior sphenethmoid and otic capsules region showing details of the left inner ear labyrinth. Scale bars = 10mm.

Right dermal cheek region

As mentioned by Clack (2003a) many of the dermal elements forming the outside of the skull have been eroded away as is evident in the dermal cheek region (Figure 3.2.3—6). It has, however, been possible to follow the contours of the surface remaining to complete this area of the reconstruction.

As mentioned previously the skull roof has been separated arbitrarily from this region of the reconstruction in front of the right temporal notch in order to aid visualisation. The dermal cheek region has also been separated from the palatoquadrate complex. This was carried out by following the external contours and the appearance of the fossilised bone in the scan slices. It should be noted, however, that it is very difficult to visualise sutures in the slices of *Kyrinion* and, therefore, the division between the dermal cheek region and the palatoquadrate may not be 100% accurate. It appears that the dermal cheek region contained the squamosal, a posterior section of the jugal and the quadratojugal. The honeycomb dermal ornament observed behind the pineal foramen is also present on the dorsal surface of the cheek region (Figure 3.2.3—7), although it is eroded frequently.

A foramen, described by Clack (2003a) as the paraquadrate foramen (par for), is present on the posteromedial boundary of the cheek region, probably near the junction between squamosal, quadratojugal and quadrate (Figure 3.2.3—7). The paraquadrate foramen is found frequently in early tetrapods, for example in *Palaeoherpeton* (labelled 'quadrate foramen' in Panchen's reconstruction of the then *Palaeogyrinus* (1964)) and *Crassigyrinus* (Panchen, 1985). It has been described an unambiguous synapomorphy of the 'Limnarchia', a post-eryopoid clade of temnospondyls, (Yates & Warren, 2000). A paraquadrate foramen is observed in *Eucritta* (Clack, 2001) and is also clearly figured

by Beaumont (1977) in *Megalocephalus* (her figures 8, 11, 12 and 13), although, it appears smaller and less well defined than in *Kyrinion.* In fact, in many respects from the personal observation of *Loxomma* specimen BMNH R.37955 it seems that the 'stapedial groove' of *Loxomma*, *Baphetes* and *Megalocephalus* (Beaumont, 1977) bears many resemblances to the paraquadrate foramen of *Kyrinion.* If these grooves are, in fact, foramina, which could be the case in at least some of the specimens, then they maybe homologous to paraquadrate foramina. The appearance and position of the groove in the cranial reconstruction of *Loxomma* (Beaumont's figure 3 (1977)) is particularly suggestive of this homology.

In ventral view it can be seen that the jugal and quadratojugal form the curved lateral boundary of the large somewhat triangular subtemporal vacuities (Figure 3.2.3—3). The medial boundary of the subtemporal vacuity is formed by the pterygoid (pt) and quadrate with the ectopterygoid forming a small section of the anterior margin.

The only other real feature of note in this complex is the three teeth which appear on the anteromedial boundary of the complex (Figure 3.2.3—7 C). No information of tooth root or crown structure can be gained from the slices.

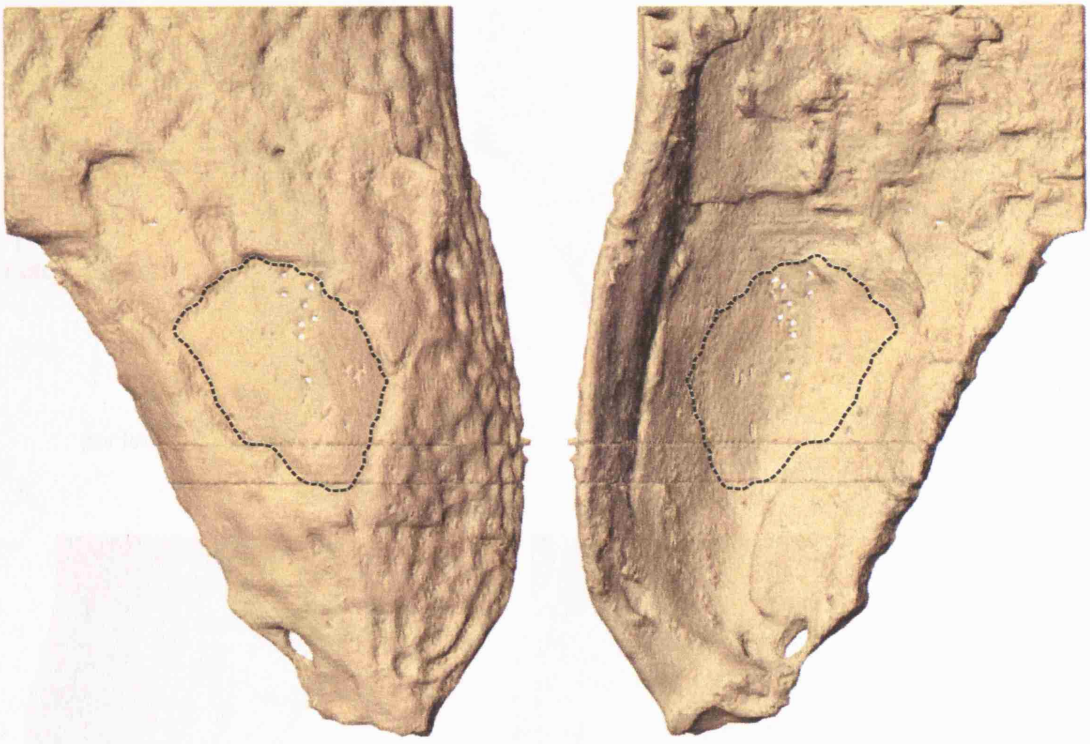

Figure 3.2.3—6 *Kyrinion* specimen NEWHM: 2000.H845. Dermal cheek region with dashed line demarcating area reconstructed from internal mould. A, dorsal view. B, ventral view. Scale bars = 10mm.

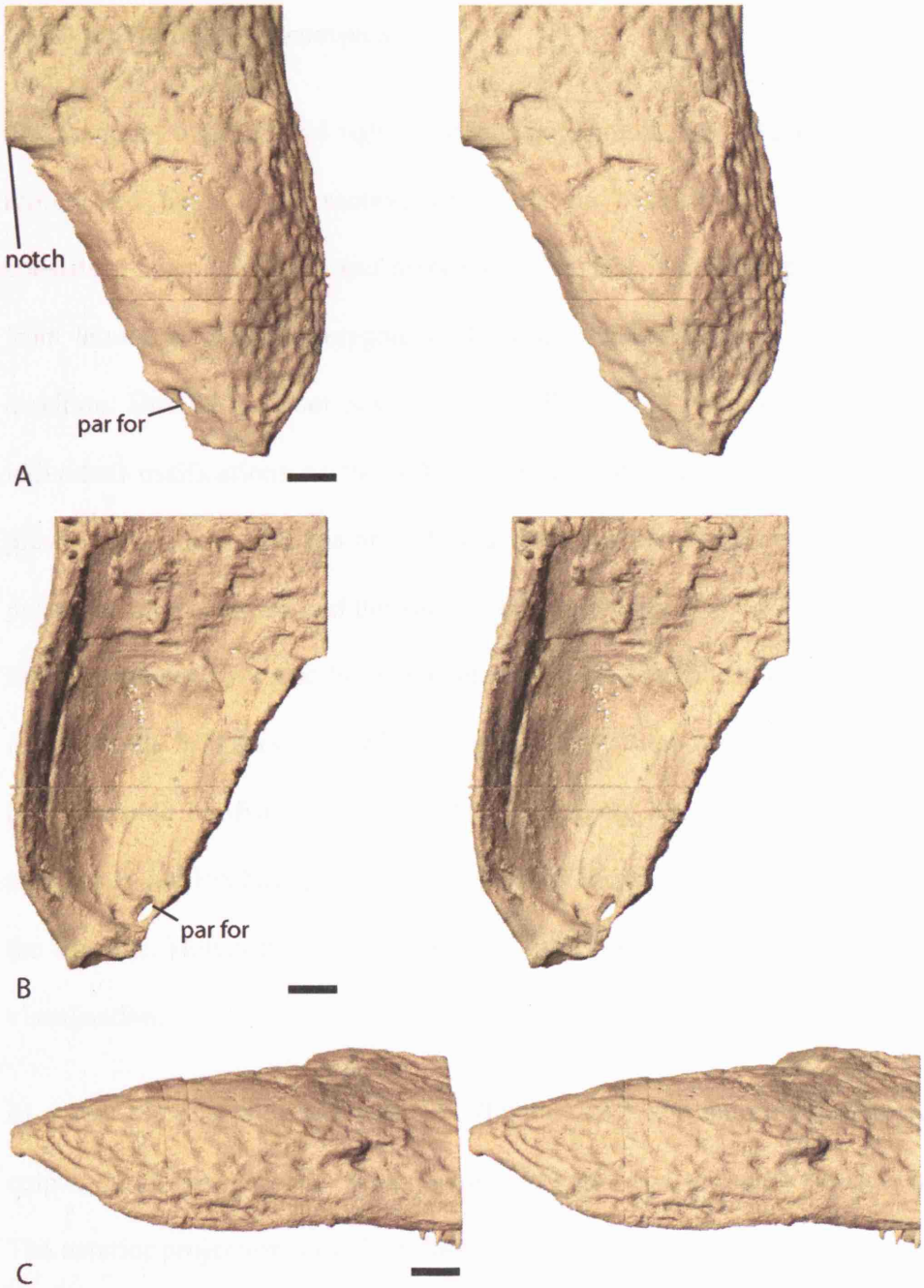

Figure 3.2.3—7 *Kyrinion* specimen NEWHM: 2000.H845. Stereo pairs of the dermal cheek region. A, dorsal view. B, ventral view. C, right lateral view. Scale bars = 10mm.

Right palatoquadrate complex

Fragments of both left and right palatoquadrate complexes are present. The left is only represented by a small section lateral to the basipterygoid articulation (art) and consisting of epipterygoid and pterygoid. The right, which is approximately complete from lateral to the basipterygoid backwards, consists of epipterygoid, pterygoid and quadrate. Due to the poor scan image quality it was not possible to distinguish the individual ossifications of the left and right palatoquadrate complexes. However, as previously mentioned it has proved possible to discern the boundary between the right palatoquadrate complex and the surrounding structures (Figure 3.2.3—8). Both left and right complexes have also been separated from the basisphenoid-parasphenoid complex (bs-ps) at the basipterygoid articulations. Both articulations are highly fused; it has not been possible to distinguish accurately the suture between the right palatoquadrate complexes and the basisphenoid-parasphenoid complex, although, this was possible on the left side. However, it was deemed necessary to divide them to aid description and visualisation.

In dorsal view of the right complex (Figure 3.2.3—9) the anterior projection of the epipterygoid, the quadrate ramus of the pterygoid and the quadrate can be visualised. The anterior projection, or columella cranii, of the epipterygoid, which can also be seen from anterior and medial views, is stout and not rod like. The morphology of the columella cranii is in agreement with the rather limited information on the baphetids described by Beaumont (1977); no information is available on the epipterygoids in *Spathicephalus*. The stout morphology of the columella cranii which does not contact the skull roof is more reminiscent of the morphology seen in embolomeres such as *Pholiderpeton* (Clack, 1987) and stereospondyls temnospondyls such as *Benthosuchus*

(Bystrow & Efremov, 1940; Yates & Warren, 2000) than more basal temnospondyls such as *Edops* (Romer & Witter, 1942), *Dendrerpeton* (Robinson et al., 2005) and *Eryops* (Sawin, 1941).

Posterior to the columella cranii is a large notch. This notch separates the columella cranii from the rest of the palatoquadrate complex (Figure 3.2.3—9). Directly posterior to this notch the palatoquadrate complex contacts and fuses with the anterior region of the otic capsule, which is at least positionally equivalent to the prootic. This process is quite large with a broad area of contact between the anterior otic capsule and the palatoquadrate as appears to have also been the case with *Megalocephalus* (Beaumont's figure 12 (1977)). The author believes that the dorsal otic processes of *Kyrinion*, alternatively termed 'prootic buttresses' or 'otic processes of the epipterygoids', to be homologous to those described in *Edops* (Romer & Witter, 1942) and *Eryops* (Sawin, 1941). Clack (1987) describes a 'paratemporal process' on the epipterygoid in *Pholiderpeton* which it is claimed to have been in contact with the skull roof. The close association of the otic capsules with the skull roof in *Kyrinion* lends support to the idea that the dorsal otic processes are homologous to 'paratemporal processes' and that a unified name, such as, 'dorsal epipterygoid processes' (dep) should be used to reduce confusion. Behind the process the laminar palatoquadrate, presumably composed of pterygoid on its medial and epipterygoid on its lateral surface, passes posterolaterally towards the quadrate. From its appearance in dorsal and medial view (Figure 3.2.3—9 and 10) it is obvious that the palatoquadrate in this region has been distorted by the dorsoventral compression. There is extensive buckling, especially, where it appears that the fragmentary remains have been crushed on to relatively thin palatoquadrate causing it to bend downwards.

Ventrally the palatoquadrates contribute to the medial margin of the subtemporal vacuity. At the posterior margin of the subtemporal margin is the elongate bi-lobed articulatory surface of the quadrate. At the anteromedial edge of the palatoquadrate complex fragment of the model, below the columella cranii, the pterygoid, and probably epipterygoid, fused with the basisphenoid-parasphenoid complex. This fusion, at the basipterygoid articulation was robust removing any movable articulation between the braincase and the palatoquadrate complex. Although, it was not possible to distinguish accurately the suture of the basipterygoid articulation it appears that the pterygoid had migrated across onto the ventral braincase (Figure 3.2.3—8). Posterior to this fusion is a pronounced notch which can be interpreted as the buccal end of the large spiracular tube that leads to the temporal notch.

Although the left palatoquadrate complex is only partially present in the cranial section scanned it provides information which cannot be gleaned from the right complex. The fragment (Figure 3.2.3—10 C) consists mainly of the palatoquadrates contribution to the basipterygoid articulation and the epipterygoids ascending process (asc pro) or columella cranii. The columella cranii has the same stout appearance as has been described for the right side.

It was possible to determine accurately the boundary between the left palatoquadrate and the basisphenoid-parasphenoid complex as the suture between the two complexes was visible on the left but not on the right. From a medial view of the left palatoquadrate complex the rounded cone shape of the basipterygoid socket (art soc) is clearly visible directly below the columella cranii (Figure 3.2.3—10 C). This cone shape appears to be homologous to the 'conical recess' of *Megalocephalus* (Beaumont, 1977).

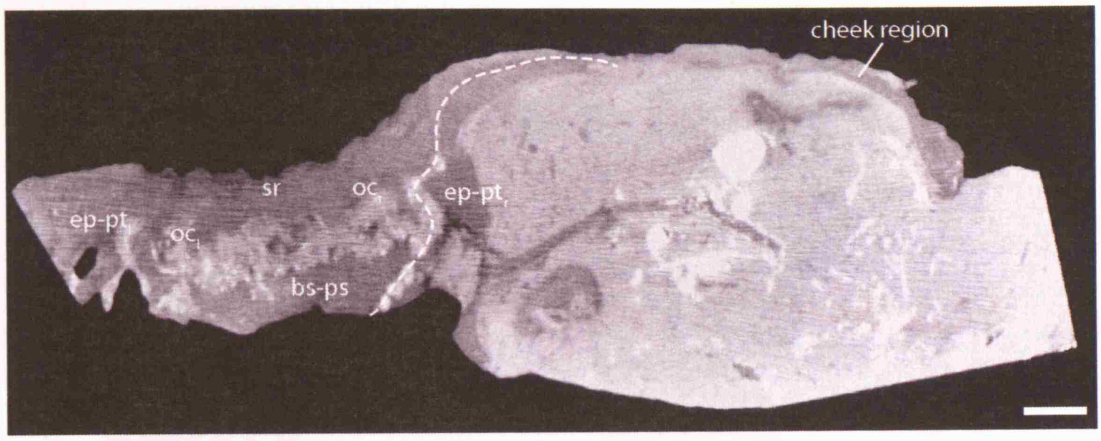

Figure 3.2.3—8 *Kyrinion* specimen NEWHM: 2000.H845. Transverse CT scanning slice with dashed line demarcating the split between the right palatoquadrate complex, the skull roof and the lower braincase. Scale bar = 10mm.

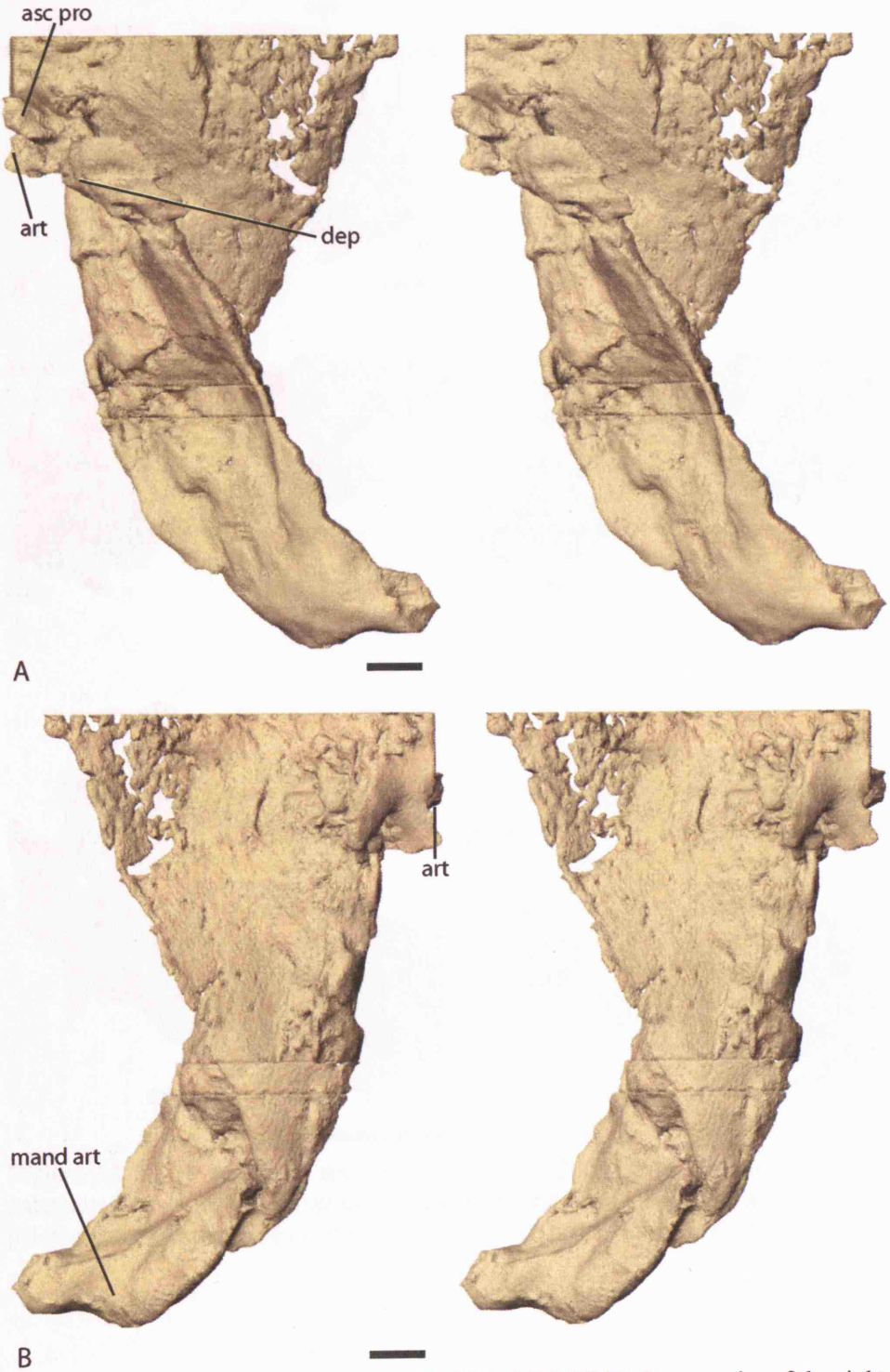

Figure 3.2.3—9 *Kyrinion* specimen NEWHM: 2000.H845. Stereo pairs of the right palatoquadrate complex. A, dorsal view. B, ventral view. Scale bars = 10mm.

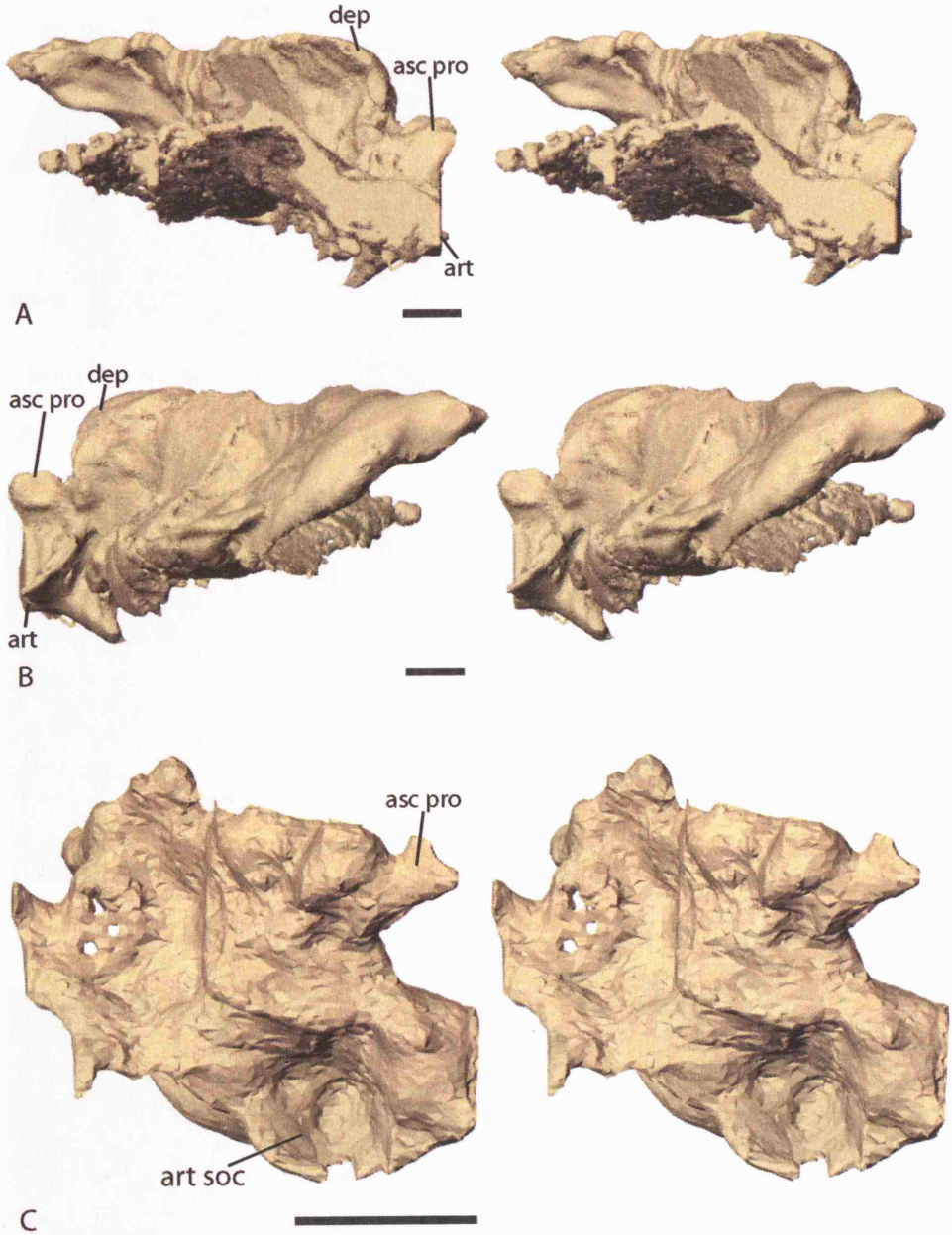

Figure 3.2.3—10 *Kyrinion* specimen NEWHM: 2000.H845. Stereo pairs. A and B, right palatoquadrate complex. A, anterior view. B, posterior view. C, medial view of part of the left palatoquadrate complex showing the basipterygoid articulation. Scale bars = 10mm.

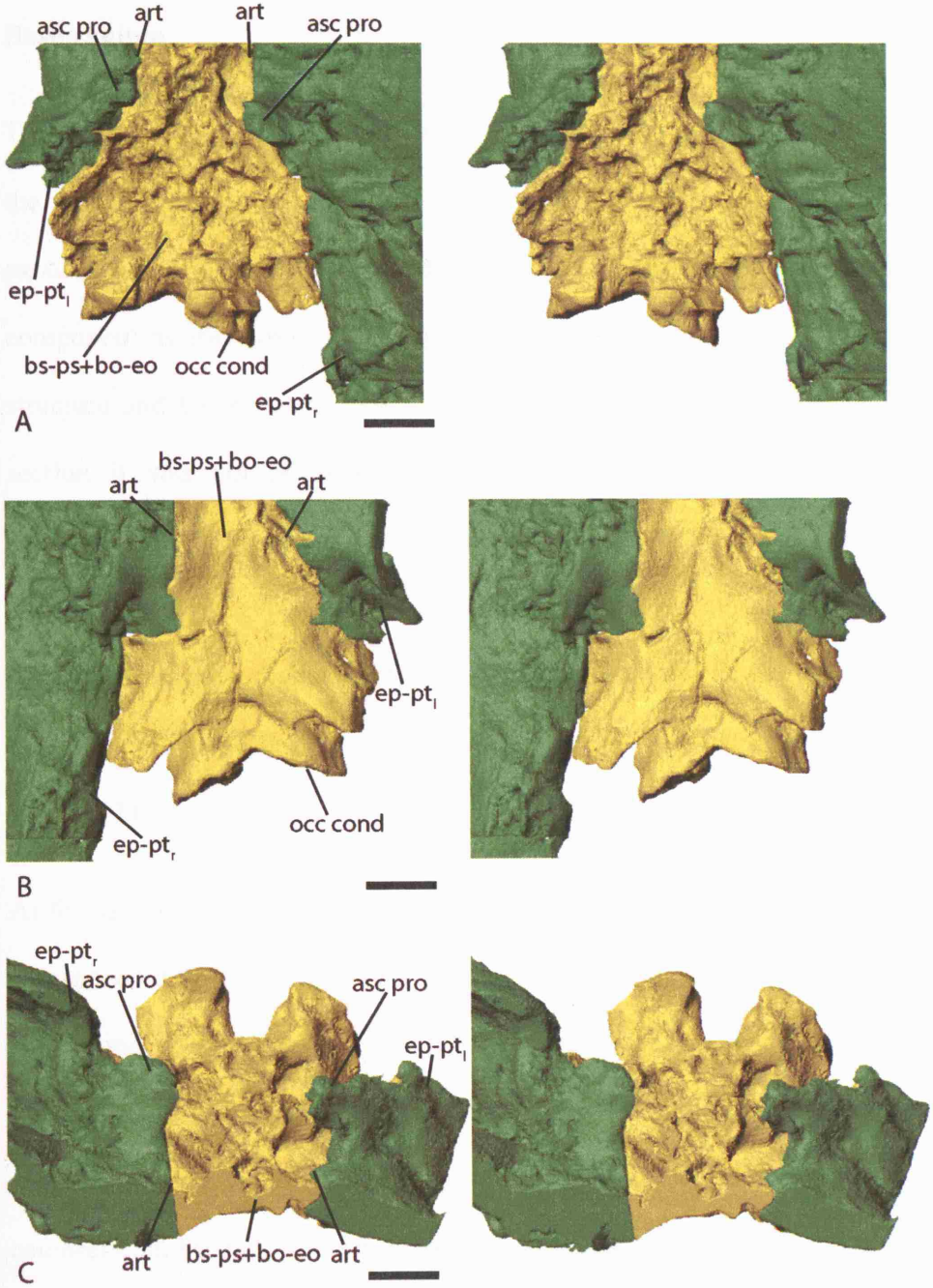

Figure 3.2.3—11 *Kyrinion* specimen NEWHM: 2000.H845. Stereo pairs of the palatoquadrate complexes, lower braincase and occipital complex. A, dorsal view. B, ventral view. C, anterodorsal view. Scale bars = 10mm.

Basicranium

This complex (Figure 3.2.3—12 and 13) extends from the pituitary fossa to the back of the occipital condyle. It consists of the parasphenoid, basisphenoid, basioccipital and exoccipitals all fused together. It has not proved possible to distinguish the individual component ossifications within the reconstruction due to the co-ossified nature of the structure and the noise prevalent throughout the scan. As mentioned in the previous section it was not possible to separate accurately the braincase from the right palatoquadrate complex because the suture could not be followed in the scan series; the chosen boundary has been somewhat arbitrary to aid visualisation (Figure 3.2.3—11). It has, however, proved possible to follow the suture between the left palatoquadrate and the braincase providing an accurate view of the basipterygoid articulation (Figure 3.2.3—11).

At the anterior boundary of the complex the basisphenoid, which is fully fused to the parasphenoid (ps) below, forms paired walls running anteroposteriorly. These walls correspond to the ventral part of the posterior region of the sphenethmoid or 'laterosphenoid'. The dorsal parts of the walls are present in the skull roof and otic capsules section, although, they have been splayed laterally due to the dorsoventral compression. Medial to these walls there is a poorly defined pit which is interpreted as the sella turcica. Paired anterior chambers (ant cham) are present below the walls of the 'laterosphenoid' just in front of the crista sellaris (cri sel) (Figure 3.2.3—13 A). These chambers are clearly visualised from an offset anterolateral orientation. It seems likely that they are the origin site of the lateral rectus eye muscles and may also have contained the exit point for the abducens (VI) nerve, although, this cannot be confirmed in *Kyrinion* because of the lower resolution of the reconstruction. These paired anterior

chambers are also present in the reconstructions of *Acanthostega* and *Dendrerpeton* (Robinson et al., 2005) and have also been described in a wide range of other early tetrapods such as the temnospondyls *Eryops* (Sawin, 1941), the embolomere *Archeria* (Clack & Holmes, 1988) and the seymouriamorph *Seymouria* (White, 1939).

Lateral to the paired anterior chambers the basisphenoid-parasphenoid complex fused to the epipterygoid-pterygoid complex (ep-pt) at the basipterygoid articulation (Figure 3.2.3—11). The contact between these two complexes was extensive allowing, probably, no movement. The dorsoventral compression has caused part of the left basipterygoid articulation to 'peel away' from the braincase producing a fissure in the ventral surface labelled 'y', 'breakage at basipterygoid junction' in Clack's figure 5b (2003a). No material is missing from this fissure as the two sides would form a perfect match if brought back together. It seems that the epipterygoid-pterygoid complex has rotated dorsolaterally relative to its pre-distortion position. The extent of the suture on the ventral surface between the two complexes becomes harder to resolve behind the fissure, although, it seems clear that there was palatoquadrate fusion to the anterior part of the lateral wing of the parasphenoid. With the left palatoquadrate complex removed the internal surface of the articulation can be seen. At its anterior extent the basisphenoid-parasphenoid complex forms a small bi-facetted projection which fitted tightly into the conical recess of the epipterygoid-pterygoid component of the basipterygoid articulation. Posterior to this projection the articulation appears to have been a relatively simple line suture with no interlocking components. Prior to the dorsoventral distortion, this area of contact may have been less extensive.

Behind the 'sella turcica' region lays the dorsum sellae, although this is clearly not fully preserved. As was seen in the reconstruction of *Dendrerpeton* (Robinson et al., 2005) it

is likely that the dorsum sellae of *Kyrinion* was also formed from the basisphenoid with the parasphenoid only contributing to the ventral plate beneath this region. Lateral to the dorsum sellae the basisphenoid formed the paired dorsally projected walls of the crista sellaris which flow posterolaterally into the lateral flanges of the parasphenoid (lat fla). In dorsal view the posterior extent of the basisphenoid within the braincase is visible as a posteriorly projecting midline point which contacts the anterior extent of the basioccipital (Figure 3.2.3—12 A). This posterior projection of the basisphenoid and the anterior extent of the basioccipital separate the floor of the braincase in two equal halves. The anterior extension of the basioccipital is clearly homologous to that seen in *Dendrerpeton* (Robinson et al., 2005) and probably also in *Acanthostega.* It seems likely that this anterior extension lay directly below the notochord in *Kyrinion.* Behind this extension the basioccipital is fully fused to the paired exoccipitals forming the occipital condyle (Figure 3.2.3—12 C). This condyle has been described in detail by Clack (2003a) but the scanning and reconstruction have provided some additional information. It appears that the condyle has not been crushed by the dorsoventral compression, the structure has remained in near perfect condition (witness for example the foramina on the lateral sides of the exoccipitals claimed to be the exit points for the hypoglossal (XII) nerve (Clack, 2003a)). The compression in this region caused the lower and upper parts of the braincase to be forced closer together. This movement of the occipital condyle relative to the otic capsules caused the 'opisthotics' to splay out laterally. This collapse has produced dorsal gaps between the opisthotics and the exoccipitals in the region which Clack (2003a) correctly termed 'lateral otic fissures' (see her figures 6 and 7). The facets for the opisthotics to attach to the exoccipitals can be seen in these gaps within dorsal and lateral views.

In ventral view the parasphenoid's contribution to the lower braincase is most apparent (Figure 3.2.3—12 B). It appears to form the entire exposed buccal surface between the basipterygoid articulations. Posteriorly to this area the parasphenoid sweeps dorsolaterally forming the lateral flanges or lateral wings which are seen in *Loxomma*, *Megalocephalus* and *Baphetes*. Lateral flanges of the parasphenoid appear to be a common feature of the early tetrapod braincase. The right flange of the parasphenoid is approximately complete while the distal section of the left is present in the adjoining section which was not scanned. The left flange also contains a foramen leading through to the cranial cavity (see Figure 3.2.3—12 A, B and D 'foramen'). This foramen has not been documented by Clack and is not present on her figure 6b (Clack, 2003a). This may mean that the foramen was damaged by preparation, a notion supported by the lack of an equivalent foramen on the other side.

Alternatively, the absence of an equivalent foramen on the right side could be due to the scan slice thickness and an inability to visualise such a small structure (the right having not been exposed to manual preparation unlike the left side). The foramen may have been the 'foramen faciale' illustrated by Goodrich (1930) in *Salamandra* for the exit of a branch of the facial (VII) nerve but this is by no means clear.

At its posterior margin the parasphenoid forms the anterior margin of a large chevron shaped groove which is shallow at the midline but opens out laterally into large expanded furrows or pockets between the occipital condyle and the lateral flange . This groove has been described by Clack (2003a) as the 'parasphenoidal tubera' for the attachment of the hypaxial musculature. From its position this large groove appears to be at least functionally equivalent to the 'crista muscularis' described by Damiani

(2001) in mastodonsaurids. Posterior to this groove a relatively large amount of the basioccipital's contribution to the occipital condyle is visible.

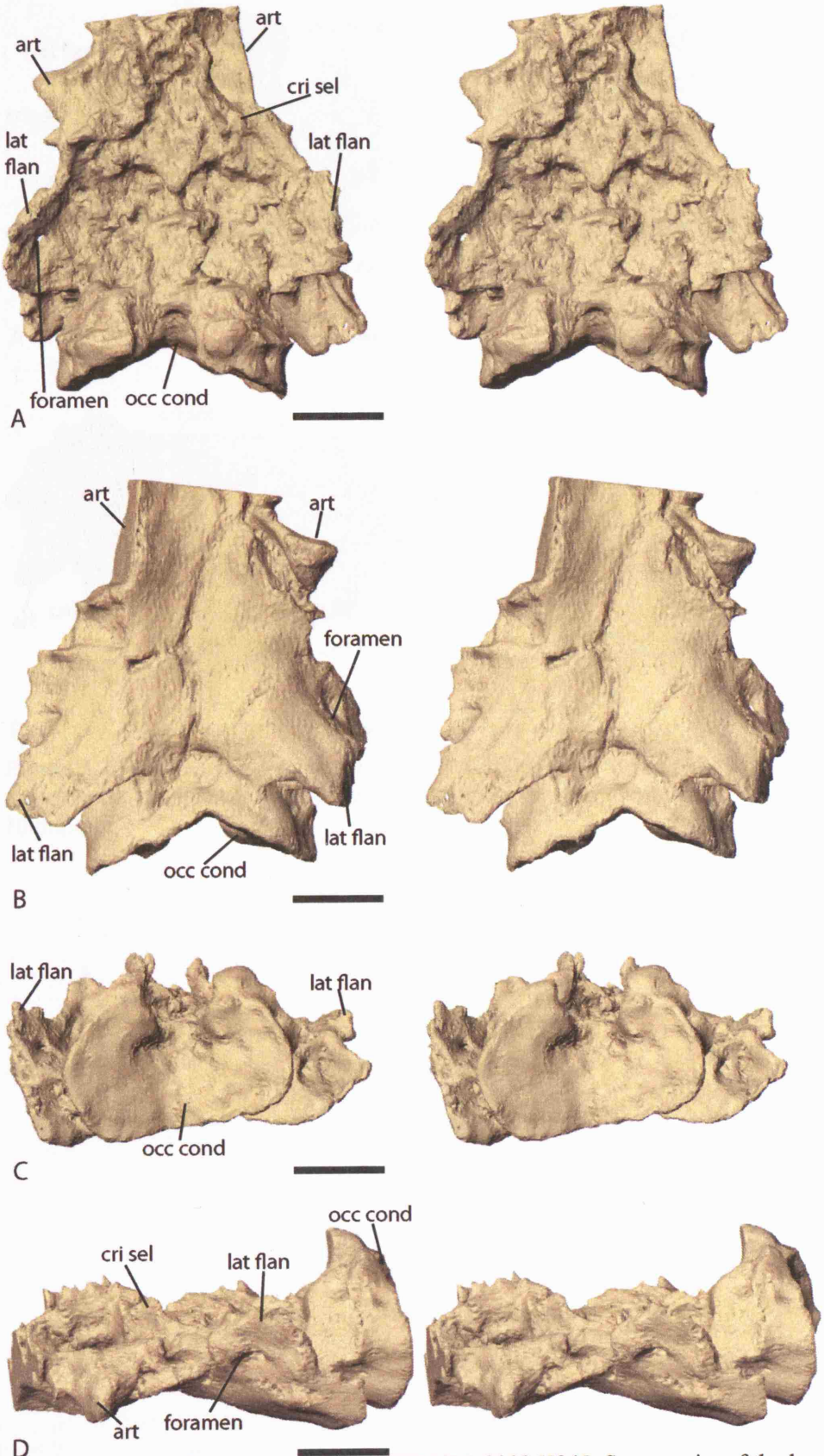

Figure 3.2.3—12 *Kyrinion* specimen NEWHM: 2000.H845. Stereo pairs of the lower braincase and occipital complex. A, dorsal view. B, ventral view. C, posterior view. D, left lateral view. Scale bars = 10mm.

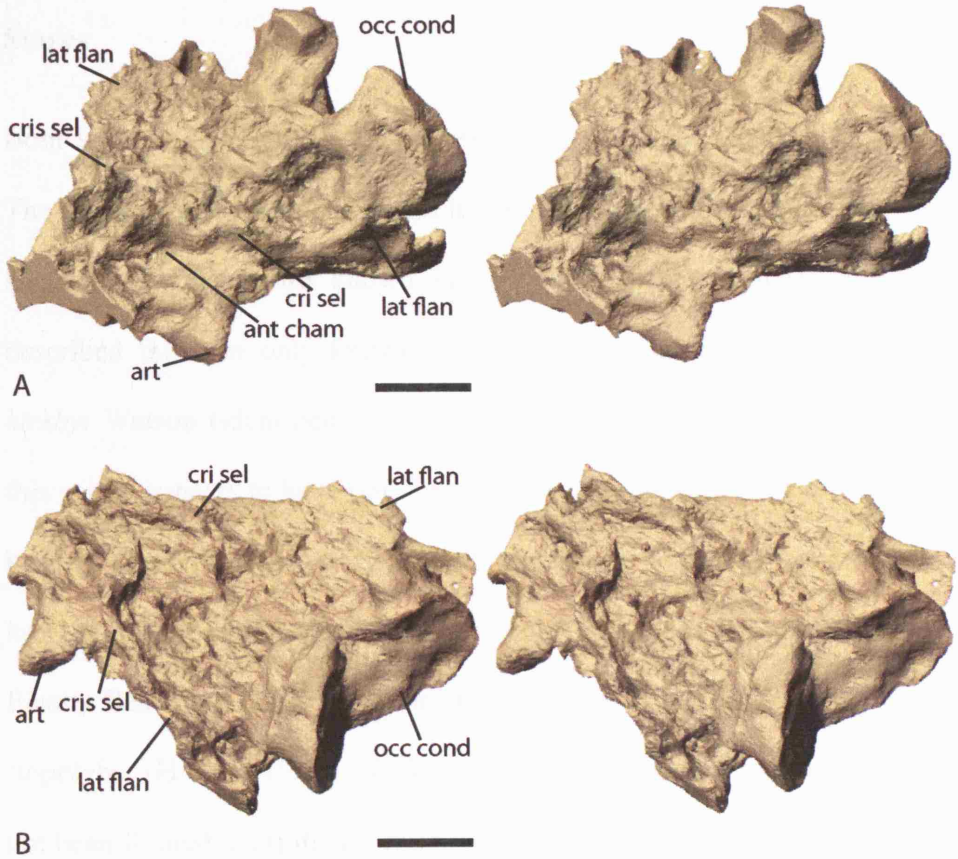

Figure 3.2.3—13 *Kyrinion* specimen NEWHM: 2000.H845. Stereo pairs of the lower braincase and occipital complex. A, offset anterodorsal view. B, offset posterodorsal view. Scale bars = 10mm.

Stapes

Both left and right stapes (st) are present in NEWHM: 2000.H845 (Figure 3.2.3—3). The presence of both stapes makes it unique amongst known baphetids; single stapes or stapedial fragments are known in only three baphetid specimens. Watson (1929) described the then only known 'embolomerous Labyrinthodont' stapes in *Baphetes kirkbyi* Watson (identified as specimen H.M. G15.91 by Beaumont (1977)); although this stapes appears to have only been preserved in negative the essential morphology is known. The right stapes of *Spathicephalus mirus* Watson specimen NMS G 1950.56.5 has also been described and figured *in situ* (Beaumont & Smithson figure 7b (1998)). Finally Beaumont (1977) mentions that a triangular stapedial footplate is present in the 'topotype' (H.M. G.15.21) of *Megalocephalus pachycephalus* Barkas although this has not been figured. Despite information from *Baphetes kirkbyi*, *Spathicephalus mirus* and *Megalocephalus pachycephalus* stapedial morphology of the baphetids has remained very poorly understood. The morphology of *Kyrinion* described by Clack contains the fullest account of baphetid stapedial morphology to date.

As mentioned previously the section of *Kyrinion* that was scanned contained the proximal end of the left stapes and all preserved areas of the right stapes. Both have been partially exposed by manual preparation carried out by Sarah Finney. CT scanning and 3D reconstruction has allowed the detailed visualisation of the morphology of the stapes that could not have been gained from manual preparation alone.

The right stapes is exposed along its dorsoposterior margin. There appears to have been some damage to this region caused by weathering; in other respects the right stapes is complete (Figure 3.2.3—14 and 15). The stapes does not appear to have been greatly distorted by the dorsoventral compression which has affected the whole specimen. This

compression caused the otic capsules to be closer to the lateral flanges of the parasphenoid thus reducing the dorsoventral size of the fenestra ovalis (fenestra vestibuli of Clack). This reduction in the size of the fenestra ovalis may have caused some limited crushing of the proximal end of the stapes, although, none is immediately apparent. The dorsoventral compression is not expected to have affected the distal end of the stapes because it was surrounded by soft tissue or soft sediment infill which would have collapsed in preference to the ossified stapes. This, of course, presumes that crushing occurred relatively soon after its interment and that it was not due to later compaction in the fossilisation process once solid matrix had surrounded the specimen and all its internal spaces.

At its proximal end the right stapes appears to have contacted, but not fused with the lateral flange of the parasphenoid. There is no other evidence that the stapes was in contact with any other ossification, such as, the quadrate ramus of the pterygoid or any other areas of the palatoquadrate complex. In posterior view the contact with the lateral flange of the parasphenoid is most clearly seen (Figure 3.2.3—17). This contact appears to have been articulatory rather than the possibly sutural as suggested by Clack (2003a). The contact takes the form of an elongate anteroposterior hinge which would have limited the movement to the dorsoventral plane rather then possibly allowing anteroposterior rotation. A flattened hinge may actually be a common feature within the specimens examined in this thesis. The anteroposterior elongate nature of the ventral stapedial footplate of *Dendrerpeton* being a clear example.

The right footplate (fp), seen in medial view (Figure 3.2.3—14 D), is elongate with distinct dorsal and ventral components. The ventral component (ven com), which articulated with the lateral flange of the parasphenoid, is concave and open posteriorly.

It is postulated that the dorsal component (dor com) would have contacted the perilymphatic space of the inner ear. The arrangement of the stapedial footplate in *Kyrinion* is reminiscent of the bi-partite footplates seen in a range of temnospondyl stapes such as *Eryops* (Sawin, 1941), *Dendrerpeton* (Robinson et al., 2005) and *Doleserpeton* (Bolt & Lombard, 1985; Lombard & Bolt, 1988). A thin ventral concave articulatory surface and a larger dorsal component can also be seen in the stapes of the embolomere *Pholiderpeton* (Clack, 1983). The open posterior margin of the ventral surface in *Kyrinion* is also reminiscent of the posterior notches seen in temnospondyl stapes. Lateral to the footplate in most early tetrapods the stapes is pierced by a stapedial foramen (see for example *Dendrerpeton* (Robinson et al., 2005)) but no such foramen is seen in either stapes of *Kyrinion*. The lack of a stapedial foramen could be an artefact of the dorsoventral compression which may have crushed this area of the stapes. Alternatively, the lack of a stapedial foramen could represent the true character state for *Kyrinion*. If this is the case it would be quite unique for an early tetrapod stapes as most do possess a stapedial foramen. A noticeable stapedial foramen is present in *Acanthostega* (Clack, 1989), *Ichthyostega* (Clack et al., 2003), *Greererpeton* (Smithson, 1982), *Pholiderpeton* (Clack, 1983), *Captorhinus* (Fox & Bowman, 1966), *Pederpes finneyae* (Clack, 2002b) and most phylogenetically early temnospondyls.

The open posterior margin of the ventral component of the footplate is clearly visible in posterior view (Figure 3.2.3—14 A) as is the dorsal expansion of the stapes which produces the dorsal component of the footplate. The stapes can be seen to project dorsolaterally in posterior and anterior views.

In dorsal and ventral perspective (Figure 3.2.3—15) the stapes tapers from the elongate footplate to a waisted region approximately one third to half the way along the stapes.

The ventral surface of this triangular region is convex and smooth with no discernable landmarks. In contrast the dorsal surface is concave with a roughened surface suggesting the possible paths of the facial (VII) nerve or possible muscular attachments. There appears to be two grooves in this dorsal surface, although, because of resolution problems their true nature cannot be debated with confidence. Posterior to the waisted region the stapes expands anteroposteriorly producing a thin laminar distal end. The overall shape of the stapes in a dorsal perspective is a posteriorly skewed figure of eight. The laminar distal end of the stapes is somewhat eroded at its lateral margin leaving only some fragmentary internal mould. This internal mould has been modelled and added to the stapes. It seems clear that the stapes would have extended even further laterally, although, there is no evidence that it would have contacted the palatoquadrate complex. See Figure 3.2.3—18, 19 and 20 for various views of the right stapes *in situ.*

The proximal end of the left stapes (Figure 3.2.3—16), although clearly not as informative as the right, allows us to test certain aspects of the character states observed in the right. The concave ventral surface for articulation with the lateral flange of the parasphenoid and the larger dorsal surface are visible in medial view as is the open posterior margin of the ventral surface. Also notable is the roughened dorsal surface of the stapes lateral to the elongate footplate. Furthermore, there appear to be twin grooves running posterolaterally on the dorsal surface, as also seen in the right stapes. From the morphology of the proximal end of the left stapes it appears that the character states observed on the right stapes are reliable and not artefacts of poor resolution from the scan data.

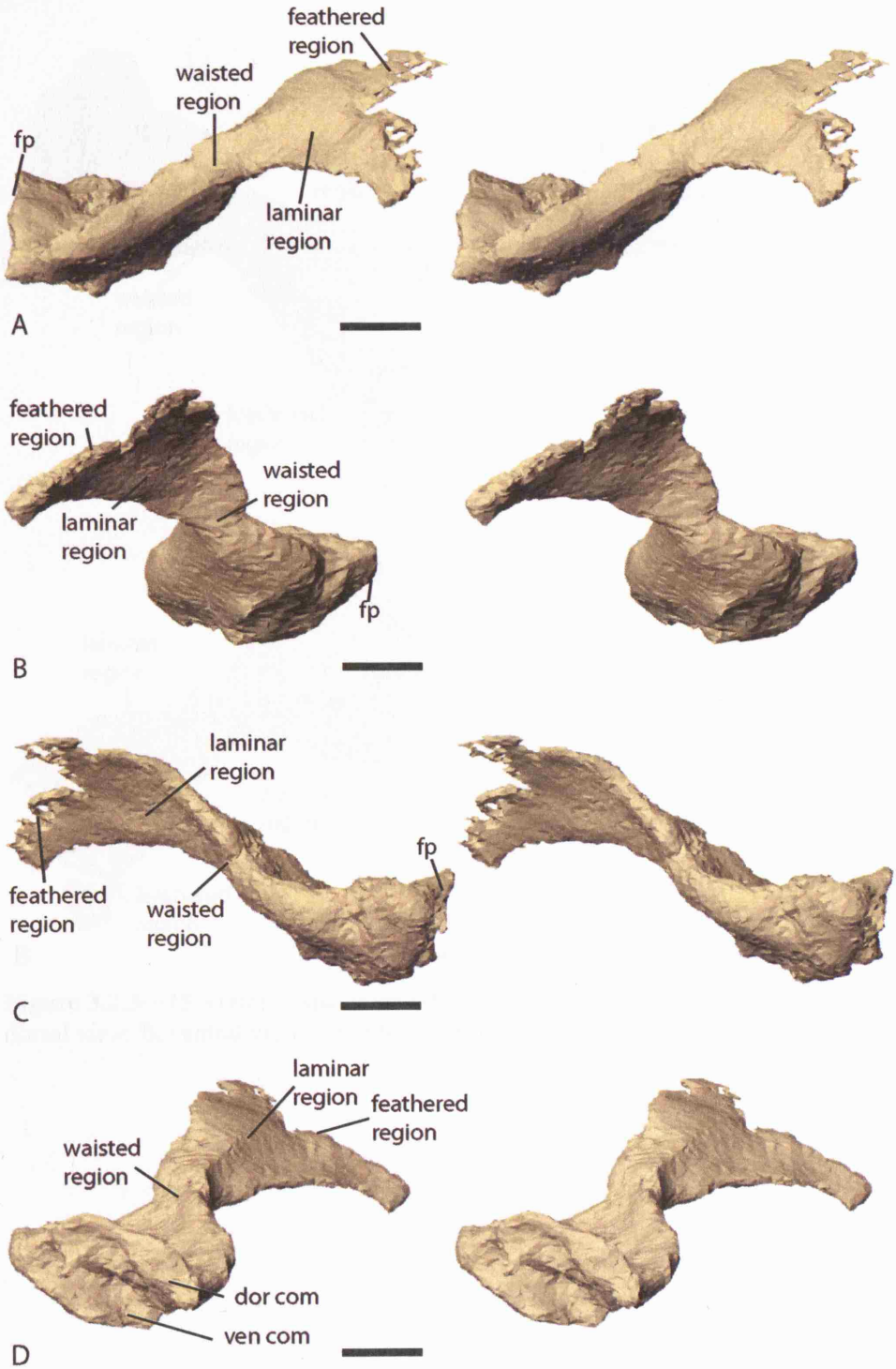

Figure 3.2.3—14 *Kyrinion* specimen NEWHM: 2000.H845. Stereo pairs of the right stapes. A, posterior view. B, lateral view. C, anterior view. D, medial view. Scale bars = 5mm.

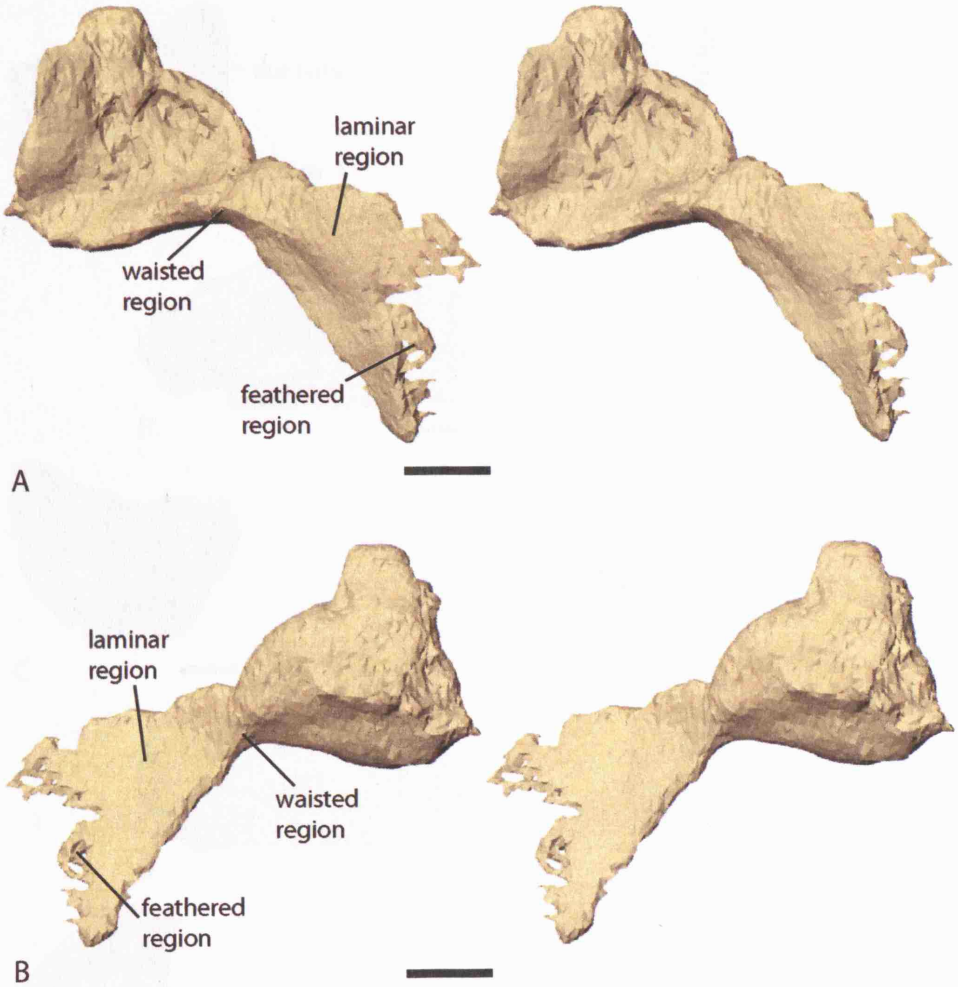

Figure 3.2.3—15 *Kyrinion* specimen NEWHM: 2000.H845. Stereo pairs of the right stapes. A, dorsal view. B, ventral view. Scale bars = 5mm.

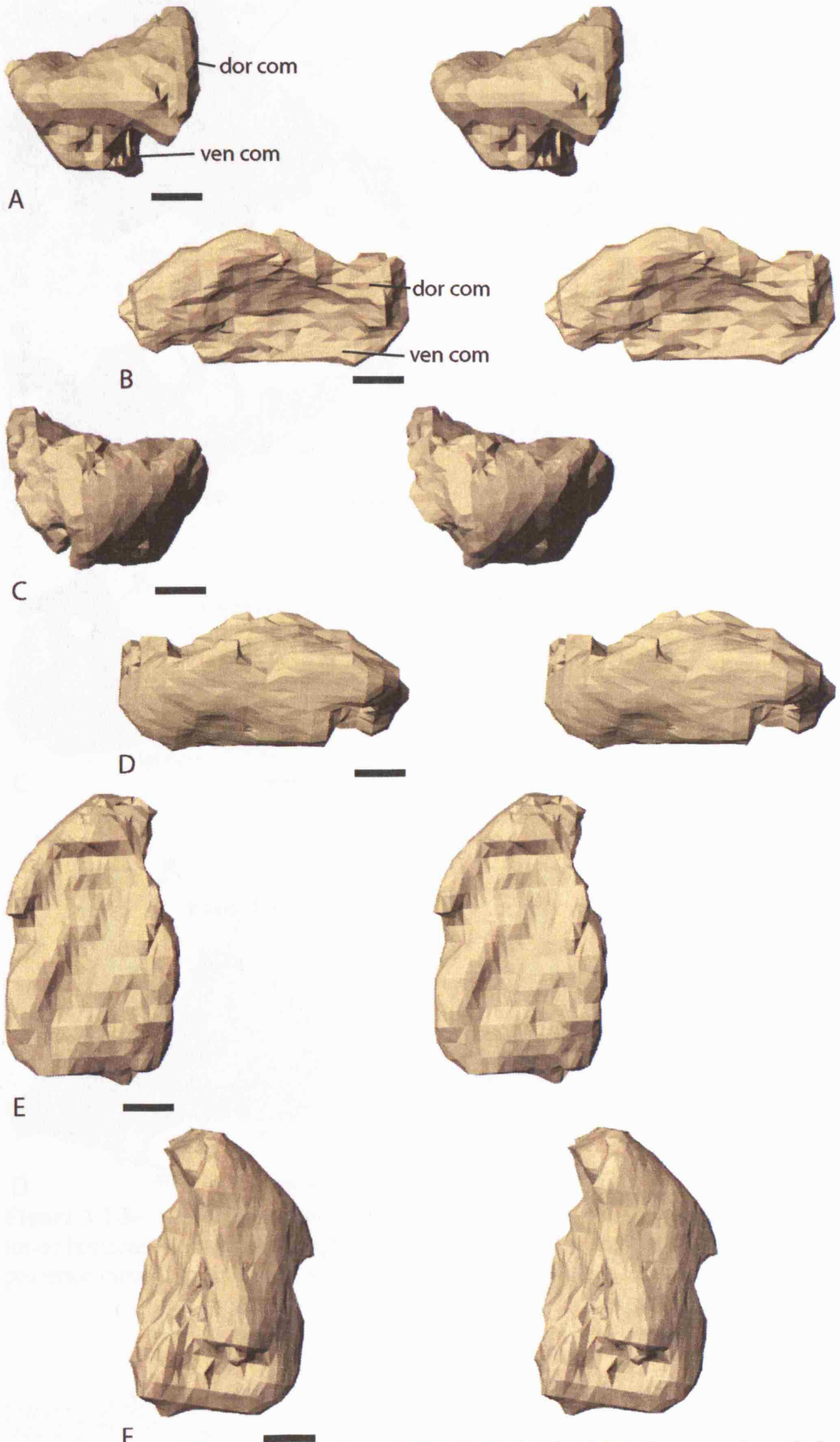

Figure 3.2.3—16 *Kyrinion* specimen NEWHM: 2000.H845. Stereo pairs of the left stapes footplate element. A, posterior view. B, medial view. C, anterior view. D, lateral view. E, dorsal view. F, ventral view. Scale bars = 2mm.

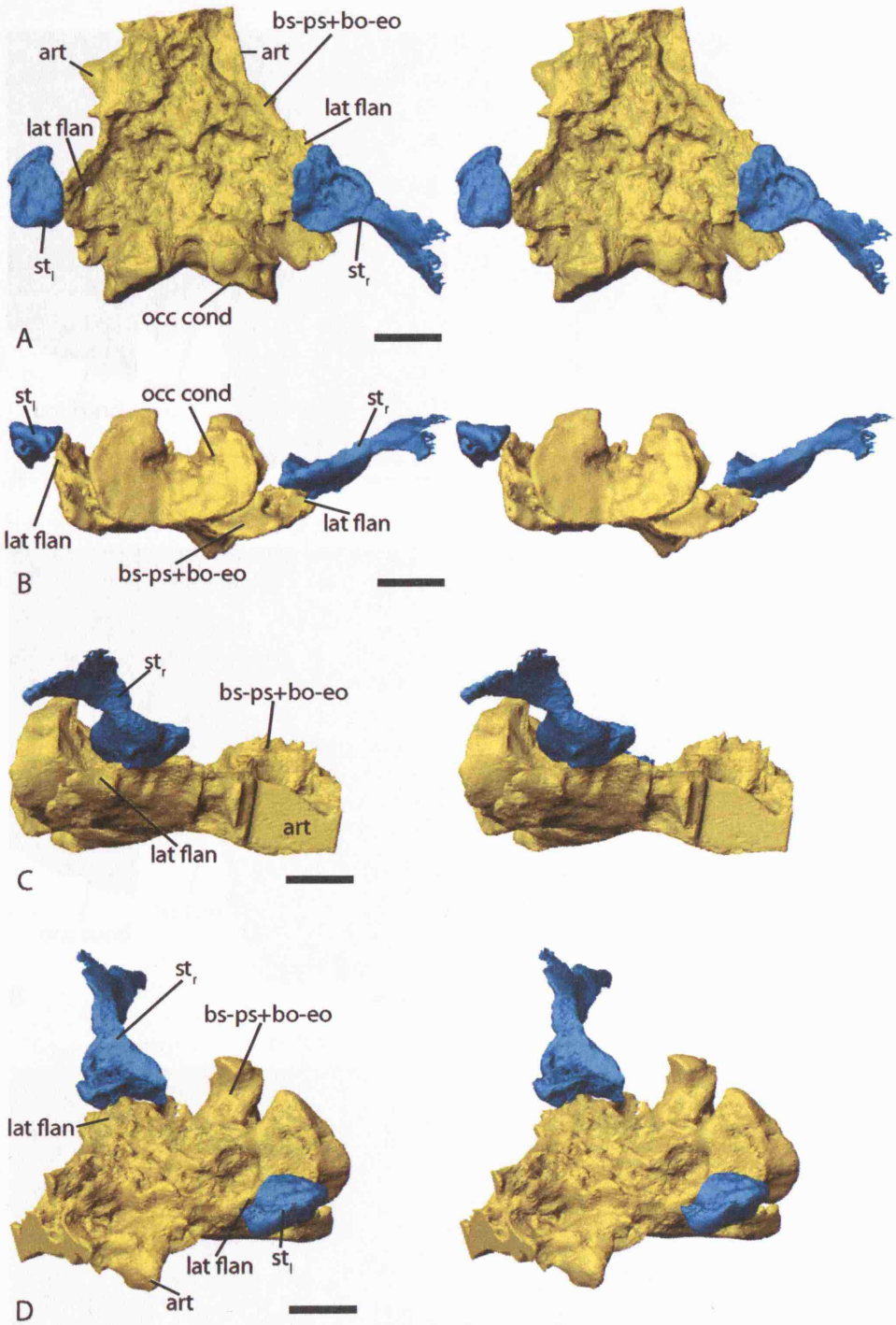

Figure 3.2.3—17 *Kyrinion* specimen NEWHM: 2000.H845. Stereo pairs of the stapes and the lower braincase and occipital region with no correction for any translocations. A, dorsal view. B, posterior view. C, right lateral view. D, left anterolateral view. Scale bars = 10mm.

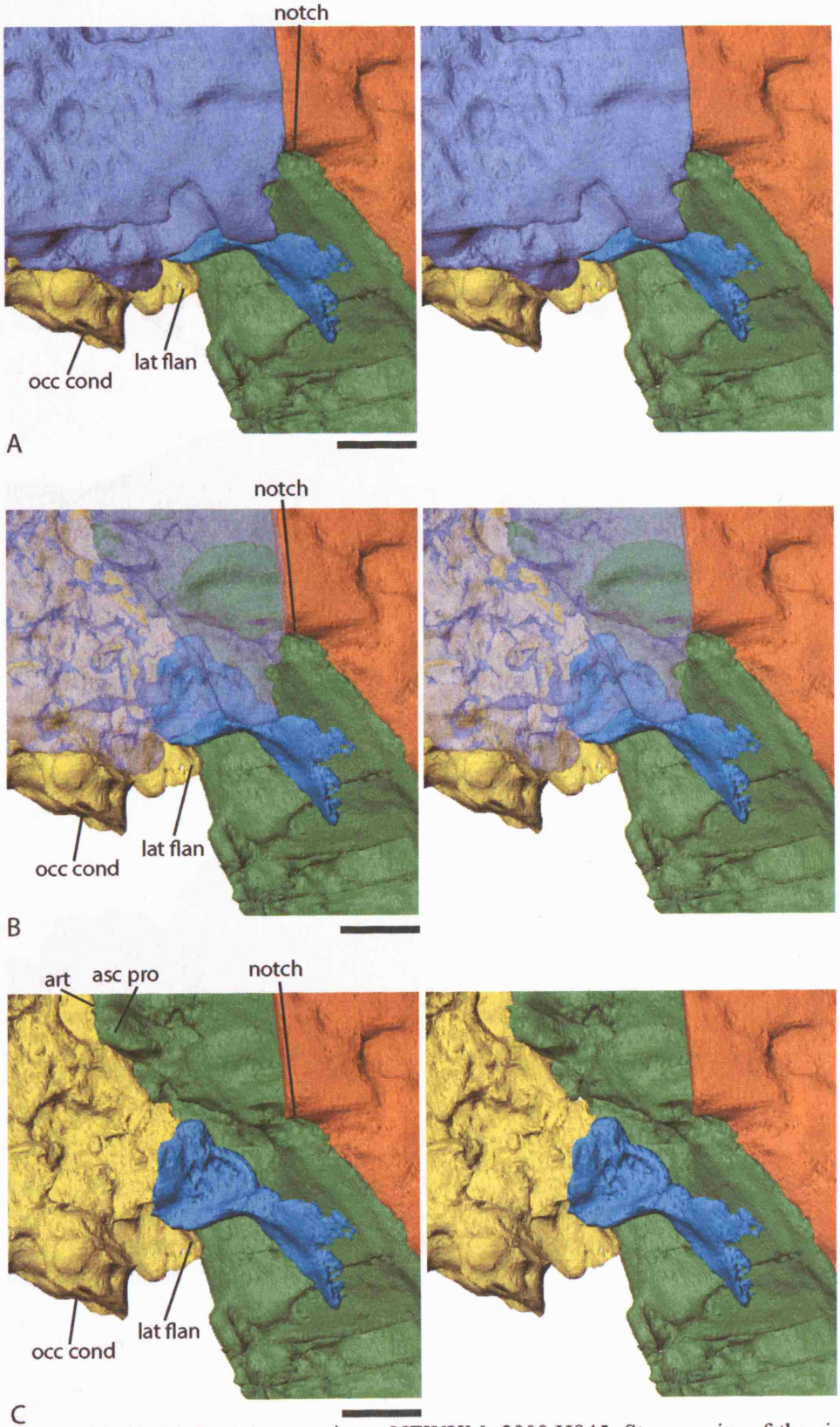

Figure 3.2.3—18 *Kyrinion* specimen NEWHM: 2000.H845. Stereo pairs of the right stapes *in situ*. A, dorsal view. B, dorsal view with skull roof, posterior sphenethmoid and otic capsules semi-transparent. C, dorsal view with skull roof, posterior sphenethmoid and otic capsules removed. Scale bars = 10mm.

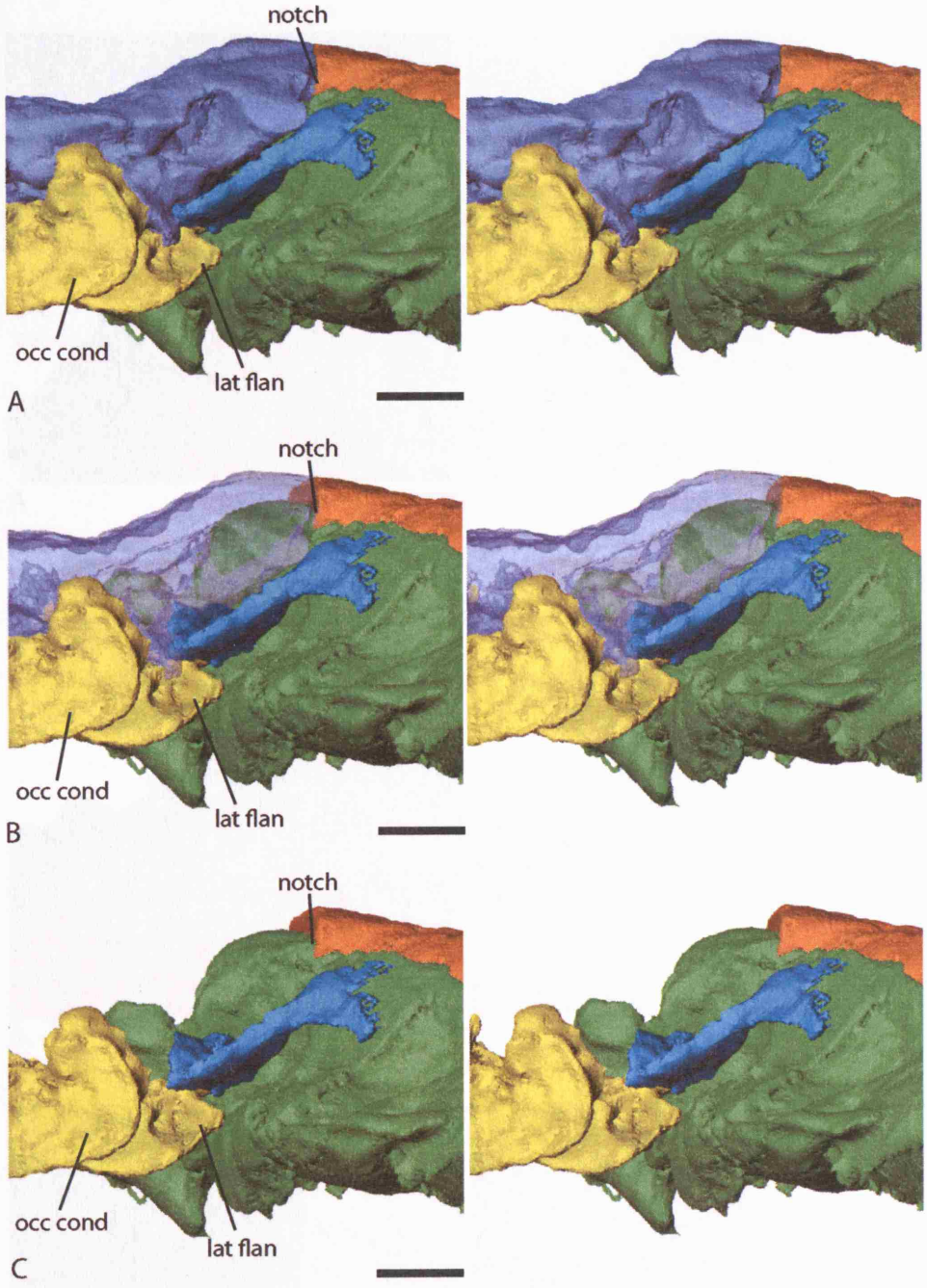

Figure 3.2.3—19 *Kyrinion* specimen NEWHM: 2000.H845. Stereo pairs of the right stapes *in situ*. A, posterior view. B, posterior view with skull roof, posterior sphenethmoid and otic capsules semi-transparent. C, posterior view with skull roof, posterior sphenethmoid and otic capsules removed. Scale bars = 10mm.

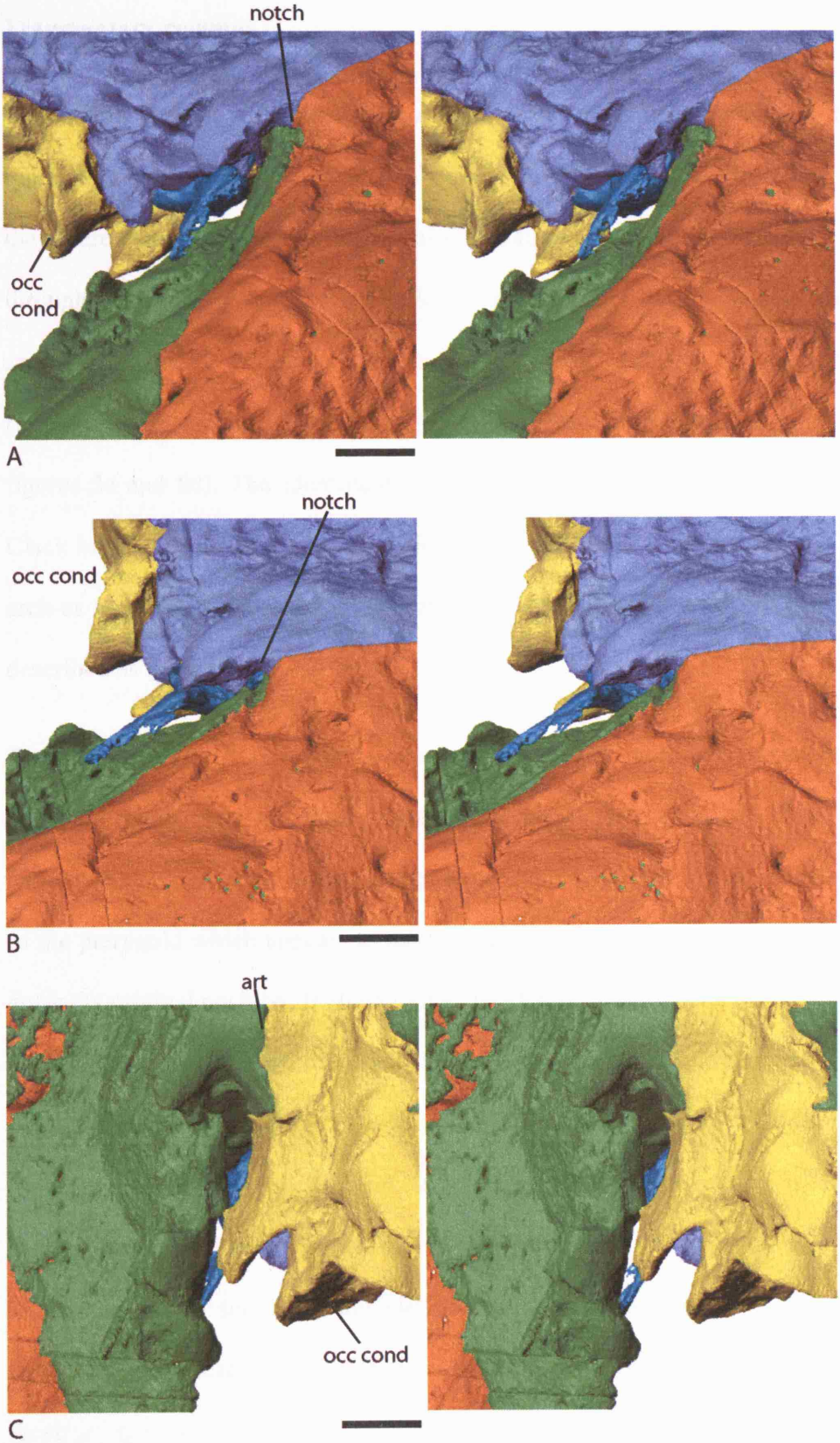

Figure 3.2.3—20 *Kyrinion* specimen NEWHM: 2000.H845. Stereo pairs of the right stapes *in situ*. A, offset posterodorsal view. B, right dorsolateral view. C, ventromedial view. Scale bars = 10mm.

Fragmentary remains

The cranial section of *Kyrinion* that was scanned contains numerous fragmentary remains (Figure 3.2.3—21). Some of these have been described by Clack (2003a) as they were exposed by previous manual preparation whilst others have been found only through the scanning and reconstruction of the specimen. In the section scanned there are three fragments that have been described by Clack (2003a); the proximal end of a rib (her figures 5a and 5b), a ceratohyal (her figures 3a and 8c) and an atlas arch (her figures 3a and 8d). The identification of the rib fragment is not in doubt. In contrast Clack has doubts about the classification of both the other elements; describing the atlas arch as 'probable' and mentioning that she is not 'entirely convinced' that the element described as the ceratohyal is such.

The scanning and 3D reconstruction has provided a more complete picture of the element provisionally described as the (presumably right) ceratohyal (Figure 3.2.3—22 and 23). The element is found posterior to the right stapes resting on the quadrate ramus of the pterygoid which appears to have buckled beneath it. It seems that this element is not in its original position. In dorsal view the element has been fully exposed by manual preparation revealing a paddle like shape with an expanded blade attached to a short rod like section. The expanded area is smooth and undamaged with a well defined concave articulatory facet at its distal end. In contrast the rod like section is damaged and displays an area of broken bone as mentioned by Clack (2003a). In dorsoposterior view it can clearly be seen that the element has a noticeably curved appearance. This curvature is greatest at the distal end of the expanded area leading to the articulatory facet.

With scanning and reconstruction the details of the underside to this element can now be seen. Below the expanded area there is a large groove which appears to be an articulatory surface, although, this cannot be confirmed. Additionally, below the rod like area and part of the expanded area there is a large concave depression which may represent a region of contact or articulation with other elements. The complexity of the under side of this element suggests that it was in contact with numerous other structures whose identification, of course, depends on its classification. The position in which it was found suggests that it was part of either the visceral arches or the anterior vertebral column. The relative lack of information regarding both these possibilities in baphetids renders the identification of the element problematic. In fact the visceral arch morphology is poorly known in all early tetrapods with only *Acanthostega* providing a useful comparison. The element could conceivably belong to either the hyoid arch or the anterior branchial arches. Clack's suggestion of the element being a ceratohyal would mean that it was the largest ventral component in the hyoid arch. The robust construction of this element supports this inference, however, its morphology is very different to that of the ceratohyals described in *Acanthostega* (Coates & Clack, 1991) or *Eusthenopteron* (Jarvik, 1954; 1980). Clack gives no account as to whether the element may represent a complete ceratohyal, a proximal end or a distal end or indeed whether it is from the left or right side. If this element is indeed a ceratohyal then it would appear that the articulatory surface at the distal end of the expanded area would have contacted the hypohyal, however, the laminar appearance of this end shows more similarity with the posterior part of the ceratohyal in *Acanthostega.* The additional concavities on the element's underside and its curved appearance are very different to the ceratohyal morphologies of *Acanthostega* and *Eusthenopteron.*

Alternatively, this element could be a near complete right first hypobranchial. The articulatory surface at the distal end would then have contacted the basibranchial. The concavities on the underside might therefore correspond to areas in close proximity to the hypohyal and the ceratohyal. This arrangement, with the expanded area pointing anterodorsally is in some agreement with the condition seen in *Eusthenopteron* (Jarvik, 1954; 1980). However, it is not possible without further investigation to state with confidence what bone within the visceral arches this element corresponds to, or indeed, whether it belongs to the visceral arches at all.

No additional information has been gained in regards to the 'probable atlas arch' of Clack (2003a) and therefore its identification is not commented on further.

Of the fragmentary elements that have not been previously described by Clack (2003a) two which project ventrally and are in at least superficial contact with the right palatoquadrate complex are of note. The posterior most of these elements is not complete (Figure 3.2.3—24) as it continues into the section ventral to that which has been scanned. This element is rod like with a rather flattened end. Approximately half way along its length, before the rod flattens out, there is a large notch. There is also an additional notch or concavity on one side of the flattened end. It does not seem to be a rib or any part of the vertebral column but an element of the visceral arches. Its flattened appearance and large notch are reminiscent of the reconstructed ceratohyal of *Acanthostega* (Coates & Clack, 1991).

The second element is located lateral to the basipterygoid articulation. Its appearance is a rather fragmentary laminar element which has come into intimate contact with the palatoquadrate complex. This contact is likely to be a preservational artefact rather than a true *in situ* condition. It has not proved possible to identify what this element may be.

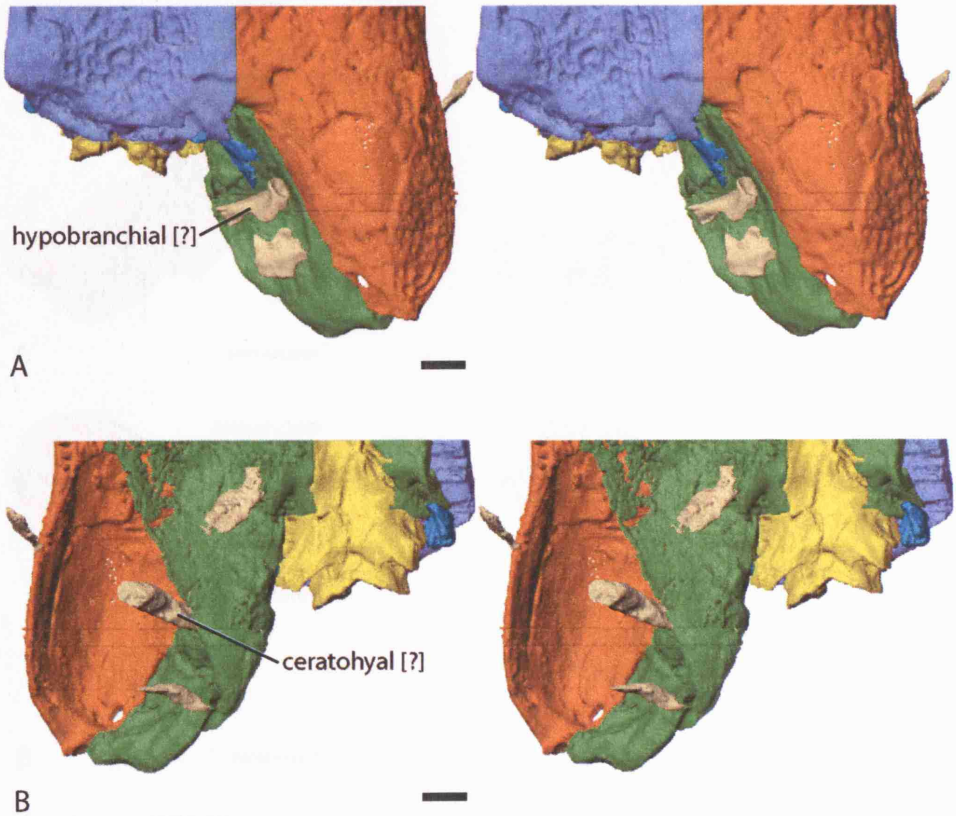

Figure 3.2.3—21 *Kyrinion* specimen NEWHM: 2000.H845. Stereo pairs of the whole model showing the location of fragmentary remains. Fragmentary remains shown in beige. A, dorsal view. B, ventral view. Scale bars = 10mm.

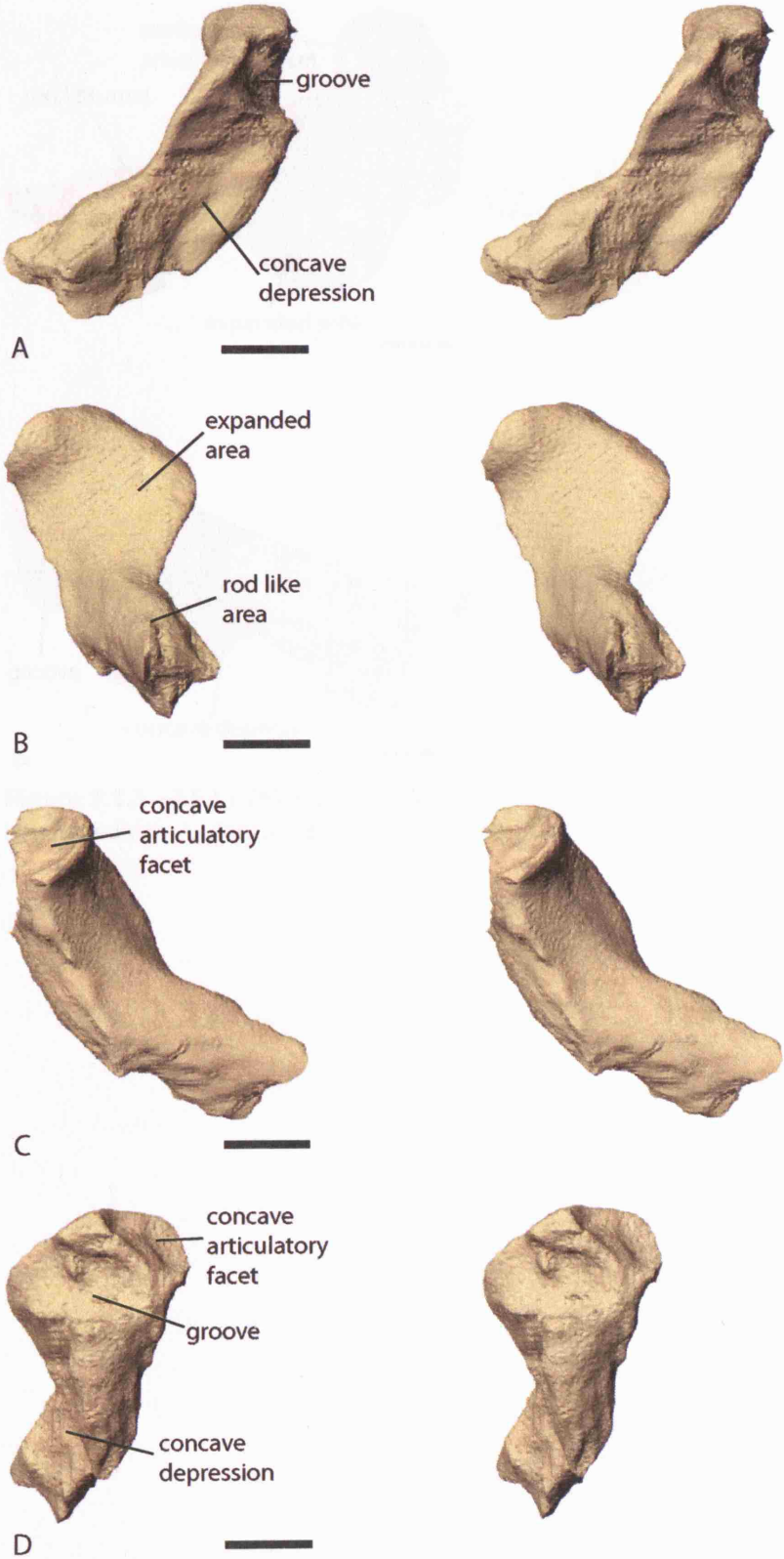

Figure 3.2.3—22 *Kyrinion* specimen NEWHM: 2000.H845. Stereo pairs of possible first right hypobranchial. A, posterior view. B, medial view. C, anterior view. D, lateral view. Scale bars = 5mm.

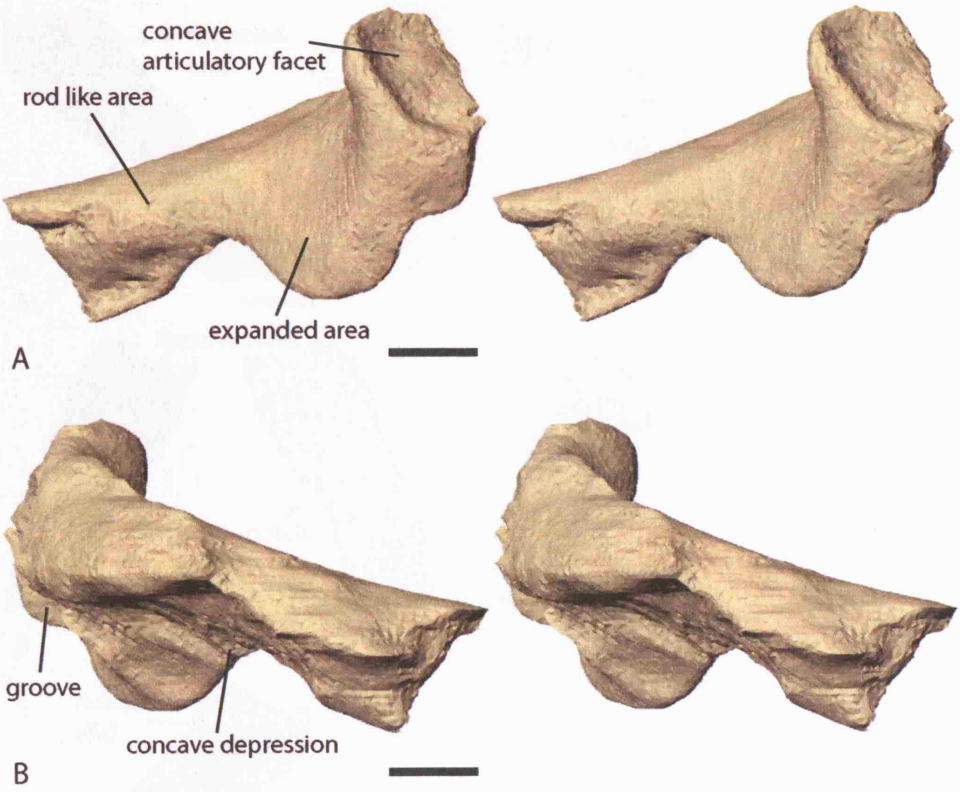

Figure 3.2.3—23 *Kyrinion* specimen NEWHM: 2000.H845. Stereo pairs of possible first right hypobranchial. A, dorsal view. B, ventral view. Scale bars = 5mm.

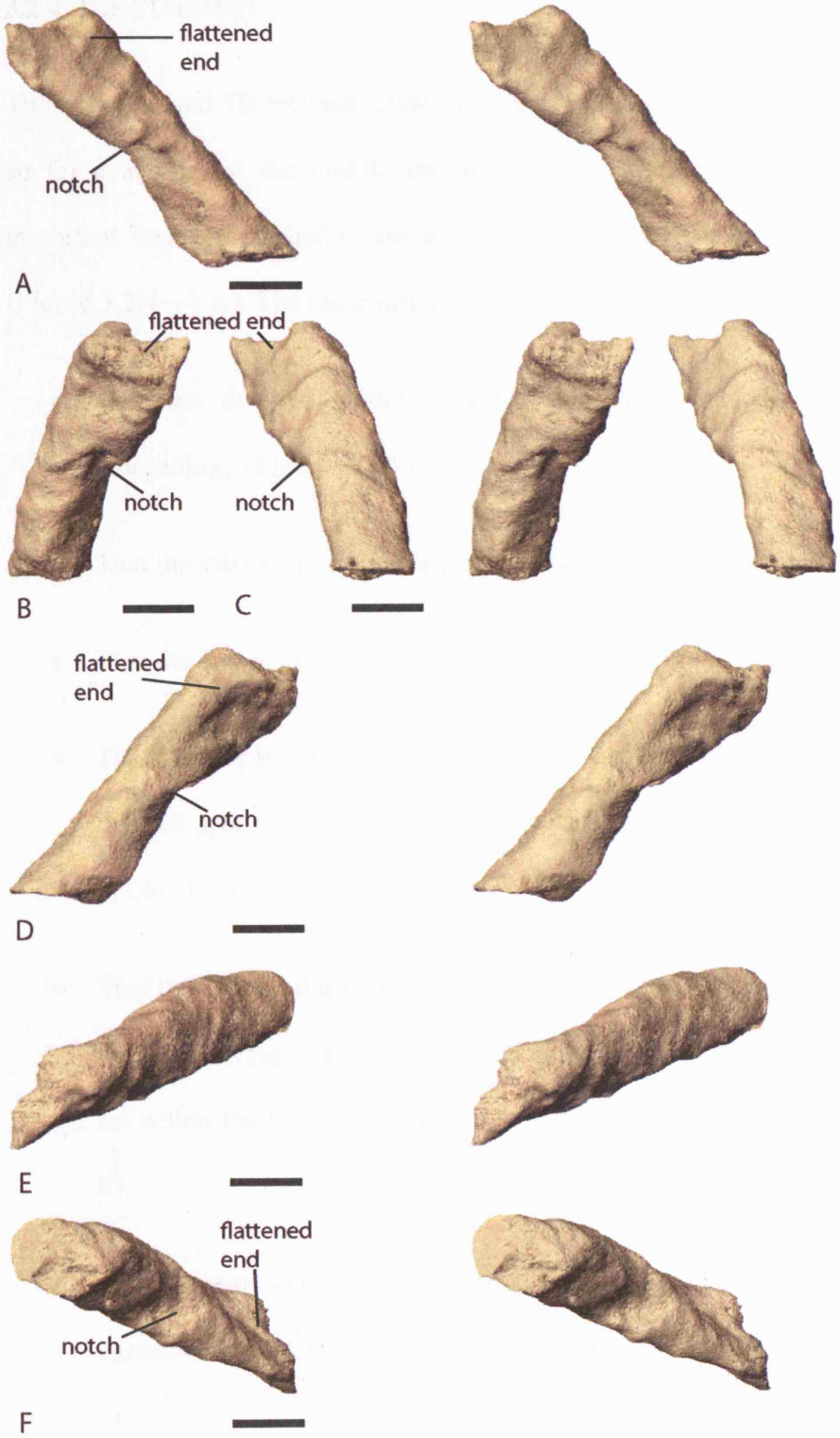

Figure 3.2.3—24 *Kyrinion* specimen NEWHM: 2000.H845. Stereo pairs of possible ceratohyal. A, posterior view. B, medial view. C, lateral view. D, anterior view. E, dorsal view. F, ventral view. Scale bars = 5mm.

3.2.4. DISCUSSION

The scanning and 3D reconstruction of *Kyrinion* provides the most detailed information so far available on the middle ear and associated structure of a baphetid. This is important because baphetids are at a critical position in early tetrapod phylogeny (Figure 3.2.4—1 A). The reconstruction illustrates:

- The first detailed model of a baphetid stapes including all aspects of its morphology (Figure 3.2.4—1).
- That the stapes has a dorsolateral orientation (Figure 3.2.4—1 B).
- That the stapes has a thin laminar distal end (Figure 3.2.4—1 C).
- That the stapes did not contact the palatoquadrate and instead sat above a well defined space between the braincase and the palatoquadrate complex (Figure 3.2.4—1 D).
- That the ventral stapedial footplate component articulated, but did not fuse, with the lateral wing of the parasphenoid (Figure 3.2.4—1 E). The dorsal component sat within the fenestra ovalis and contacted the inner ear space (Figure 3.2.4—1 E).
- There appears to have been no stapedial foramen (Figure 3.2.4—1 B) which is in agreement with Clack's previous description (2003a).

The only previous description of *Kyrinion* (Clack, 2003a) included details of the exposed regions of both stapes along with a discussion of its function relative to the stapes of other early tetrapods. The reconstruction of the right stapes and left stapedial footplate and the surrounding structures in the scan series allows a far more complete picture of the middle ear region to be revealed. This permits a detailed investigation of the functional aspects of the middle ear of *Kyrinion* and early tetrapods in general. The following can be stated with some confidence regarding the middle ear and associated structures of *Kyrinion:*

- As with *Acanthostega* it seems highly unlikely that *Kyrinion* possessed a tympanic membrane. There are no grooves on or around the temporal notches to suggest such a structure (Figure 3.2.3—2). Additionally, there appears to be no evidence for a posterior support for such a structure; there are no unfinished areas which might suggest a cartilaginous posterior strut.

- The stapes has an elongate footplate with two distinct components. This morphology can be seen on both the complete right stapes (Figure 3.2.3—14) and the section of the left which was included in the scan (Figure 3.2.3—16).

- The ventral component of the footplate is anteroposteriorly concave (Figure 3.2.3—14). This concave area contacted, but did not fuse with, the lateral wing of the parasphenoid (Figure 3.2.3—17). The unfused contact between the stapes and the parasphenoid would have allowed a certain degree of movement. This movement would have been limited primarily to the dorsoventral plane by the anteroposterior elongate nature of the articulation. There would have been limited or non-existent anteroposterior rotation or any twisting movement. Thus the stapes had a very controlled and conservative rotation through the

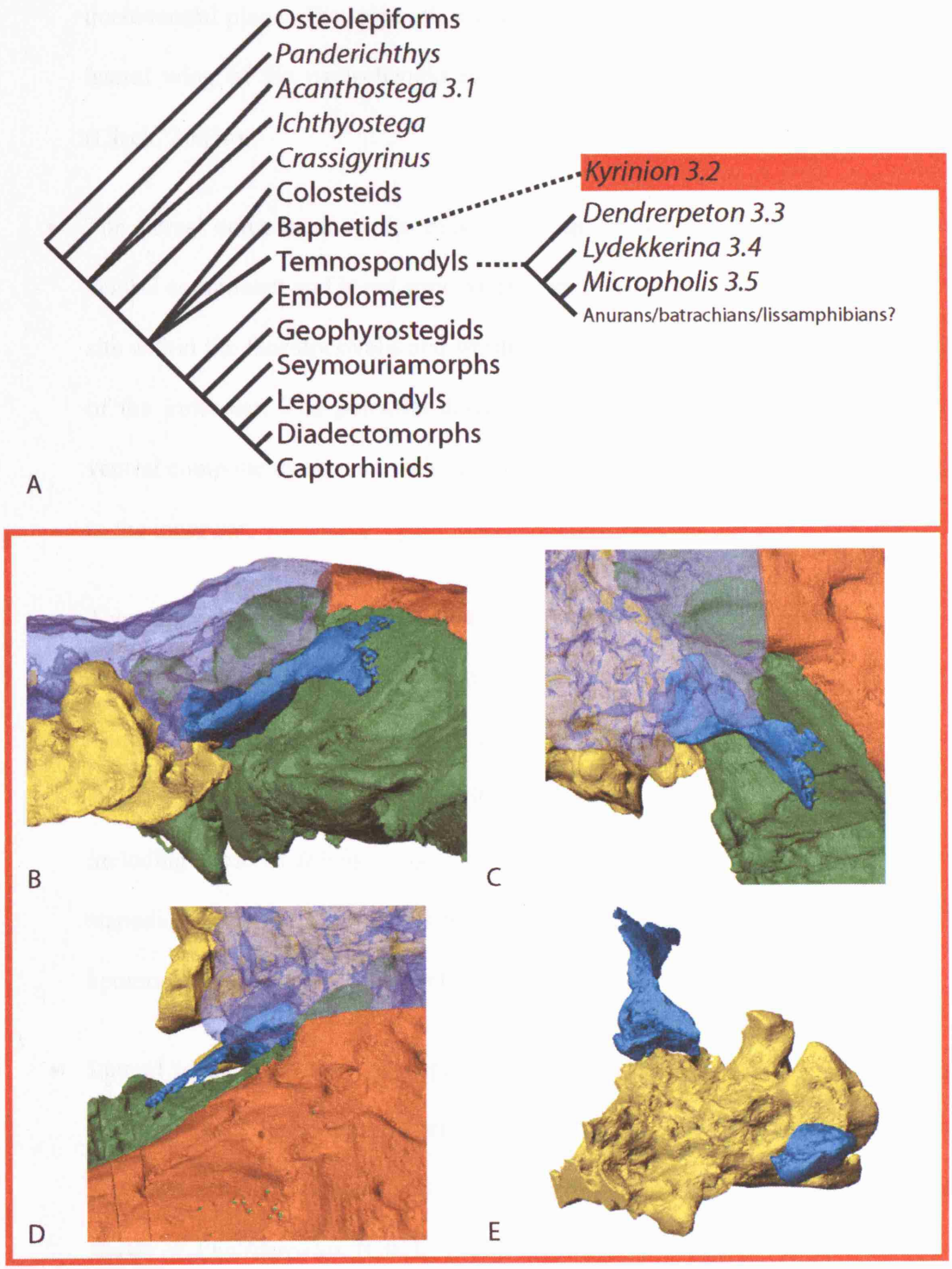

Figure 3.2.4—1 Summary *Kyrinion* figure - specimen NEWHM: 2000.H845. A, basic phylogenetic consensus created from the early tetrapod phylogenies of Ruta et al. (2003) and Laurin & Reisz (1997) with temnospondyl detail from Ruta et al. (2003) and Yates & Warren (2000). B, posterior view of right stapes *in situ* - see figure 3.2.3—19. C, dorsal view of right stapes *in situ* - see figure 3.2.3—18. D, right lateral view of right stapes *in situ* - see figure 3.2.3—20. E, antero-lateral view of lower braincase and stapes - see figure 3.2.3—17. For scale bars see referred to figures.

dorsoventral plane. The stapes thus does not appear to have been sutured to the lateral wing of the parasphenoid as had been previously tentatively proposed (Clack, 2003a).

- The dorsal component of the stapedial footplate is noticeably larger than the ventral component and is not concave (Figure 3.2.3—14). The dorsal component sits within the fenestra ovalis and would have contacted the perilymphatic space of the inner ear. The potential dorsoventral rotation of the stapes around the ventral components contact with the parasphenoid would have passed vibrations to the inner ear.

- The stapes does not appear to have had a stapedial foramen (Figure 3.2.3—14 and 16) which is in agreement with the previous description by Clack (2003a). The author believes the presence of a stapedial foramen is an ancestral character state for tetrapods as the vast majority of the stapes described in early tetrapods, including those of *Ichthyostega* and *Acanthostega*, appear to have possessed a stapedial foramen. Thus the character state observed in *Kyrinion* may be an apomorphy of *Kyrinion* or baphetids as a whole.

- Lateral to the footplate the stapes narrows to a waisted region approximately halfway along its length (Figure 3.2.3—15). This waisted region may well represent a more extreme version of the condition seen in the slightly crushed stapes of *Pholiderpeton* (Clack, 1983). Lateral to this waisted region the stapes expands and forms a thin laminar surface which projects posterolaterally (Figure 3.2.3—15). This laminar surface has an unfinished posterolateral margin which suggests that it may have extended as a thin sheet of cartilage which could have significantly increased its surface area.

- The overall morphology of *Kyrinion*'s stapes (Figure 3.2.3—14 and 15) does not suggest that it has a supportive function bracing the braincase against the palatoquadrate as was suggested by Carroll (1980) and Smithson (1982) for the stapes of the colosteid *Greererpeton.* The stapes of *Kyrinion* appears to have been able to articulate with the parasphenoid, the dorsal component was probably in contact with the inner ear and the dorsolaterally directed distal end has a thin fan-shaped form. The braincase is highly fused to the skull roof and as may have been the case with *Acanthostega* (Clack, 1994) there is no clear evidence on the palatoquadrate complex for any stapedial contact.

- The stapes of *Kyrinion* functioned as a lever system. Such a system has a centre of rotation (the fulcrum, F), a force of resistance (R) and an acting effort force (E) (Figure 3.2.4—2 A, B and C). A type II system has a centre of rotation (the fulcrum) at one end of a lever, an acting effort force at the other end with a force of resistance between. In the case of *Kyrinion*'s stapes the articulation between the ventral component of the footplate and the lateral wing of the parasphenoid represents the fulcrum of the type II lever system (Figure 3.2.4—2 D). The force of resistance is represented by the movement of the dorsal component of the footplate against the perilymphatic fluid of the inner ear. Finally any force acting on the distal end of the stapes would constitute an acting effort force. Thus any force acting on the distal end of the stapes would be significantly further from the fulcrum of the system than the resistance force of the dorsal component's movement of the perilymphatic fluid. The force applied at the distal end of the stapes would be amplified by the system providing increased force at the dorsal footplate component. The stapes confers clear mechanical advantage which could be used to amplify forces elicited by sound waves.

- If one follows Panchen's (1985) proposal that there may have been a persistent spiracle in early tetrapods then it seems logical to assume that this would have been the case in *Kyrinion*. It would seem likely that each spiracle would have begun in the buccal cavity just behind the basipterygoid articulation. Each would have ended in a temporal notch. Running from the buccal cavity to the notch each spiracle would have occupied at least part of the space bounded by the braincase of the medial side and the palatoquadrate complex on the lateral side. As can be seen from the reconstruction, this space in *Kyrinion* is well defined. It is also clear that the stapes of *Kyrinion* would have been intimately associated with this space. The stapes may have lain directly above the proposed spiracular space or it may have been at least partially enveloped by it. As with *Acanthostega* the close association of the stapes to the spiracular region is also suggestive of it having a role in the animals ventilation.

It is proposed that the evidence presented within this chapter, suggests that the middle ear of *Kyrinion* was not involved with the bracing of the braincase against the palatoquadrate complex. It seems difficult to imagine that the stapes of *Kyrinion* did not have a hearing capacity and that this may indeed have been its primary function although it may also have been involved in the animal ventilation system in some way. The stapes does not contact the palatoquadrate complex but instead sits above a space (which is in agreement with the previous description of *Kyrinion* (Clack, 2003a)) which may well have been occupied by a spiracle.

It seems clear that the presence of an open spiracle is the ancestral condition for tetrapods. The two most closely related extant fish groups to tetrapods, the coelacanths and the dipnoans, have closed and specialised spiracles. However, it is clear that the

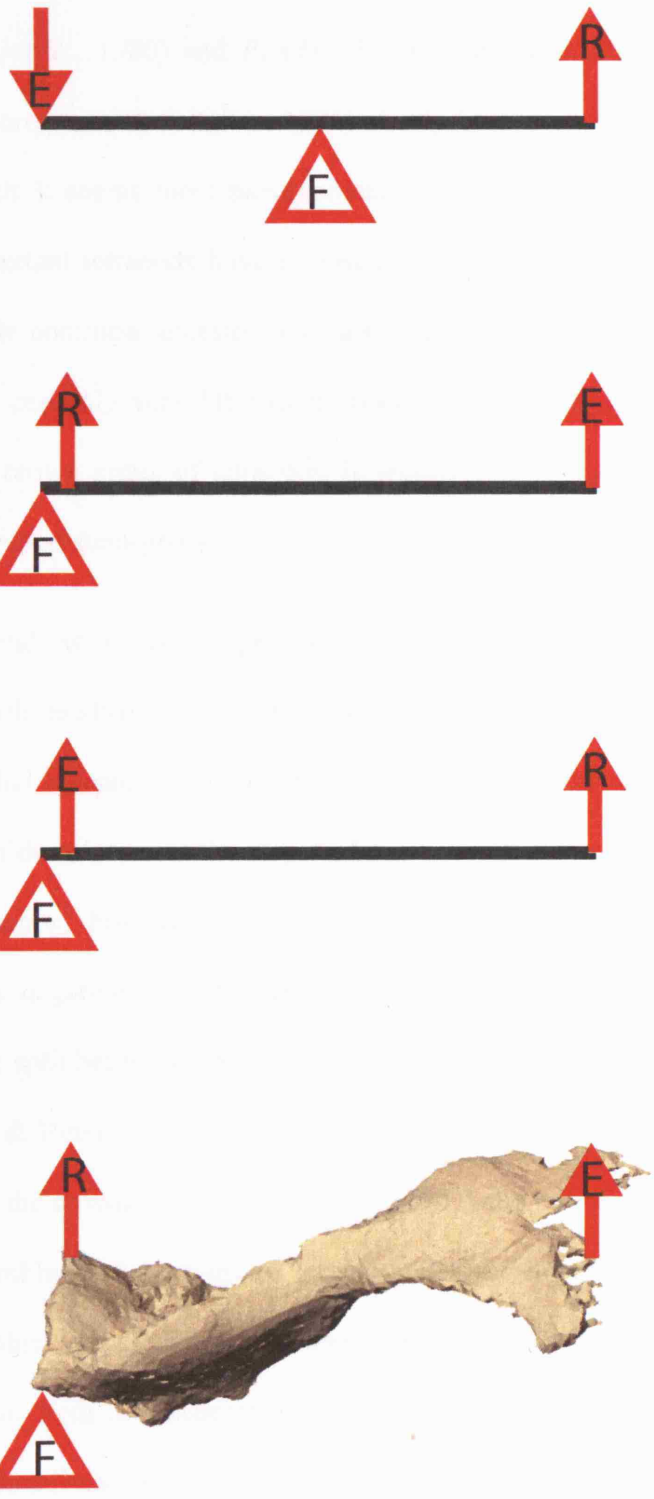

Figure 3.2.4—2 Lever system models. E = effort, R = resistance, F = fulcrum. A, Type I lever system. B, Type II lever system. C, Type III lever system. D, Posterior view of right stapes of *Kyrinion* specimen NEWHM: 2000.H845 demonstrating its type II lever system function.

fossil fish most closely related to tetrapods had open spiracles. Specimens of both *Eusthenopteron* (Jarvik, 1980) and *Panderichthys* (Ahlberg et al., 1996; Brazeau & Ahlberg, 2006; Vorobyeva & Schultze, 1991) clearly have paired openings at the back of the skull which it seems most parsimonious to deduce would have housed open spiracles. As all extant tetrapods have a closed spiracle it also seems most logical to presume that their common ancestor may also have had a closed rather than open spiracle. There is certainly very little fossil evidence to suggest that an open spiracle persisted into the crown group of tetrapods. It, therefore, appears that an open spiracle was lost in the tetrapod stem-group.

Kyrinion, a baphetid, as mentioned previously (3.2.1) has not, itself, been included in any known cladistic analysis. However, it is believed that *Kyrinion's* the middle ear region and stapedial morphology is highly likely to be representative of all baphetids. Certainly the brief description of the stapes of *Baphetes* by Watson (1929) fully agrees with that of *Kyrinion*, however its stapes now appears to have been lost or was described from a negative mould (Clack, 2003a). Baphetids have been positioned directly below the split between temnospondyls and other phylogenetically higher early tetrapods (Laurin & Reisz, 1997; Ruta et al., 2003a). Thus, baphetids appear to be the sister grouping to the crown group of Ruta et al. (2003) and are placed at the top of the paraphyletic assemblage of stem-group tetrapods. As a stem-group tetrapod it is not possible to determine with confidence whether *Kyrinion* would have had open or closed spiracles, although, from the anatomy described above it seems certain that it would have been highly important in its hearing abilities.

If the spiracles of *Kyrinion* were open they may have functioned as 'inhalant foramina' as suggested by Carroll in a presentation to the Society of Vertebrate Palaeontology in

1980 (Panchen, 1985). This means that the stapes of *Kyrinion* would have been in intimate association with an air filled space and also with the inner ear via the dorsal component of the footplate.

In a fully aquatic environment the stapes of *Kyrinion* may have lain mediolateral to an enclosed air filled space. This space would have been linked to the inner ear via the stapes. Thus as was postulated to be the case in *Crassigyrinus scoticus* Watson (Panchen, 1985) *Kyrinion*'s middle ear region could have functioned in an analogous manner to the Weberian apparatus of ostariophysan fishes. In fact, this arrangement of a dorsoventrally mobile stapes in contact with a defined airspace and the perilymphatic space is similar to although not as extreme as, that described in *Ichthyostega* (Clack et al., 2003). In *Ichthyostega* a specialised aquatic hearing function was proposed and a less specialised system could also be present in *Kyrinion* and possibly other early tetrapods such as *Pholiderpeton* or *Acanthostega.*

On land the stapes of *Kyrinion*, despite its large size relative to those of extant tetrapods, would also have functioned as a sound transmitting element. An open spiracle would have been only temporarily open to the external environment when inhaling or exhaling. This would be advantageous to restrict the exposure of the spiracle to the external environment in order to limit evaporative water loss. The closure of the proposed spiracular space would have created a temporary taut soft-tissue structure which would have functioned as a primitive vibratory structure coupled to the stapes. This clearly would not have given *Kyrinion* a hearing system of high acuity, although, it would certainly have been an improvement over not having such a faculty at all. If *Kyrinion* possessed closed spiracles the stapes would have constantly been in contact with a taut soft-tissue structure which would represent a primitive but permanent sound collecting

device. However, clearly these interpretations rest on assumptions of soft-tissue anatomy inferred from the fossilised material.

The presumed presence of a spiracular space in *Kyrinion* and its proposed function as part of a hearing system leads to interesting questions regarding the homology of this to the middle ear space and of the precise spiracular opening to the tympanic membrane. From developmental studies, it is known that in amniotes, although the middle ear cavity may be derived from the spiracular space the tympanic membrane is not positionally homologous to the spiracular opening of fish (Goodrich, 1930). In Goodrich's (1930) own words 'it is no longer supposed that the tympanic membrane represents the wall between the outgrowing endodermal pouch and the ectodermal ingrowth which becomes pierced in the development of an ordinary gill-slit'. Parrington (1958) discussed the question of homology of the fish spiracular opening to the tetrapod tympanic membrane and pointed out that the developmental work which disproves the homology actually only applies to amniotes. These studies do not preclude the possibility that tympanic membrane of anurans could indeed have been derived from the original spiracular opening presumed to be present in early tetrapods such as *Kyrinion.* In fact, the hearing anatomy envisaged for *Kyrinion* could represent a transition between a closed spiracular space and a tympanic membrane. Clearly, the phylogenetic position of *Kyrinion* relative to temnospondyls and the position of anurans to temnospondyls greatly affects the envisaged evolutionary continuity between the middle ear of *Kyrinion* and the tympanic membranes which is generally believed to have been present in some temnospondyls and anurans. The over-riding significance of this will be discussed in a broader context within the overall discussion and conclusions.

The scanning and reconstruction of *Kyrinion* has helped increase our knowledge of all areas of uncertainty raised by the questions in the introduction to this chapter. Certainly in *Kyrinion* and possibly other early tetrapods such as *Pholiderpeton* the stapes does not appear to have functioned as a supportive strut between the palatoquadrate complex and the braincase. The stapes of *Kyrinion* are directed towards the temporal notches, they have a lamina distal end, do not contact the palatoquadrate and there is no evidence for any previous contact. In *Kyrinion* it seems most likely that the stapes had a hearing role and that, in fact, this may have been its primary function. The interpretation of the stapes and middle ear region of *Kyrinion* provides a possible functional elucidation of the origin of a stapes coupled to a tympanic membrane. This interpretation rests on the assumption that the well-defined space between the buccal cavity and the temporal notch would have been occupied by a persistent spiracular space. Developmental work precludes the possibility that the tympanic membranes in amniotes are derived from the spiracular openings, however, this could indeed be the case in anurans.

3.3. DENDRERPETON

Dendrerpeton is a phylogenetically basal temnospondyl and is, therefore, important to the investigation of the evolution of a tympanic membrane coupled to a stapes and the more detailed origin of the particular middle ear morphologies observed in extant amphibians. As previously mentioned temnospondyls are frequently cited in the origin of anurans, batrachians or lissamphibians as a whole. *Dendrerpeton*'s middle ear is very poorly known, although, there have been previous partial descriptions of the stapes (Clack, 1983; Godfrey, Fiorillo & Carroll, 1987) which have suggested that it has a stout morphology similar to that seen in *Pholiderpeton* or *Greererpeton* rather than the typical temnospondyl rod like stapes.

The poorly known nature of the middle ear region of *Dendrerpeton* means that it is impossible to know which questions scanning and reconstruction of this region could address. If it has a transitional middle ear morphology, as has been suggested by previous studies (Clack, 1983; Godfrey et al., 1987), it could shed light on the origin of the typical temnospondyl rod like stapes presumably coupled to a tympanic membrane. If this is the case then the following questions could be addressed:

- What was the stapedial function before it was coupled to a tympanic membrane?
- How did a stapes coupled to a tympanic membrane evolve?
- Did early tetrapods have a spiracle and did this get transformed into a middle ear space? If not, what was the function of the paired notches in early tetrapods?
- Is the proposed spiracular opening in early tetrapods in anyway homologous to the tympanic membrane? If so, is this in all tetrapods?

If, however, it emerges that the previous descriptions of the stapedial morphology in *Dendrerpeton* are in some way inaccurate then the scanning and reconstruction could help address the following questions:

- When did a tympanic membrane coupled to a stapes first evolve in tetrapods and in what group was this?
- When is the first evidence of a muscle connecting the stapes to the shoulder girdle?
- When did the opercular apparatus evolve in tetrapods and in what group was this?
- Did the common ancestor of batrachians, lissamphibians or all tetrapods possess an opercular apparatus?
- When is the first evidence of a muscle connecting the opercular apparatus to the shoulder girdle?

See *Dendrerpeton* Discussion 3.3.4 and Figure 3.3.4—1 for a synopsis of the morphology revealed from the reconstructions and how this has helped address the above sets of questions.

3.3.1. BACKGROUND

Dendrerpeton acadianum was first described by Owen from scattered cranial and postcranial remains of a lower jaw, iliac bone, humerus and vertebrae collected by Dawson and Lyell (Owen, 1853), from the Upper Carboniferous tree stump locality of Joggins, Nova Scotia (Lyell & Dawson, 1853). A second species of *Dendrerpeton* was identified in 1863, *Dendrerpeton oweni* Dawson, from material previously assigned to *Hylonomus lyelli* Dawson (Dawson, 1863). Over the next 140 years many more specimens have been described and attributed to various species of the genus *Dendrerpeton.* To re-evaluate the number of species and the validity of the characters used in their classification Steen (1934) reviewed the amphibian fauna of the Joggins locality, including all recognised *Dendrerpeton* species at that time. In his paper 'Labyrinthodonts from the Joggins Formation' Carroll recognised a single species, *Dendrerpeton acadianum* (1967). More recently, Milner (1980) has reviewed the amphibian fauna from the Upper Carboniferous of Ireland naming a single species of *Dendrerpeton*, *Dendrerpeton rugosum* Huxley, which is described as being closely related to *D.acadianum.* Milner (1996) also revisited the Joggins material and concluded that there are three species of *Dendrerpeton* present at that locality – namely *D.acadianum*, *D.confusum* Milner and *D.helogenes* Steen. Currently, Milner recognises four species of *Dendrerpeton*: three from Nova Scotia, Canada, and one from Ireland.

Along with other well-known genera, such as *Edops* and *Trimerorhachis*, *Dendrerpeton* is considered as one of the basal members of the Temnospondyli (Holmes, 2000). The temnospondyls are the most common of those "early tetrapods" that appear in the mid-Carboniferous after the paucity of Romer's gap. They are present in the fossil record from the Carboniferous until the mid-Cretaceous and undergo two major radiations; one

during the mid to late Carboniferous and a second in the Early Triassic after the Permian extinction event. General consensus places *Dendrerpeton* close to the base of the temnospondyls, however, its exact relationship to other primitive temnospondyls has been the subject of some debate. Current cladistic phylogenies all agree in positioning *Dendrerpeton* between *Edops* and the more derived *Eryops* (Ruta et al., 2003a) (Holmes, Carroll & Reisz, 1998) and (Milner & Sequeira, 1994).

Dendrerpeton is found in two major localities, the Joggins Tree Stump Locality, Nova Scotia, Canada and Jarrow Colliery, Castlecomer, County Kilkenny, Ireland. Both these localities are dated as early Upper Carboniferous (Calder, 1998) and have preserved the 3D structure of the material present such that even moderately sized temnospondyls such as *Dendrerpeton* have remained uncrushed. Unfortunately, a large proportion of early temnospondyl material, such as the Viséan *Balanerpeton* from East Kirkton Quarry, Bathgate, Scotland (Milner & Sequeira, 1994), displays a high degree of dorsoventral compression and severe distortion of internal cranial structures such that only the skull roof and palate can be well characterised. Work on larger temnospondyls such as *Eryops* (Sawin, 1941) and *Edops* (Romer & Witter, 1942) has so far yielded the most complete descriptions of internal cranial anatomy, but some aspects of these reconstructions have attracted critical attention in recent years and until these specimens are thoroughly re-described their reconstructed anatomy has to be viewed with caution. A more recent description of *Trimerorhachis* (Schoch, 1999a), provides a lower resolution of braincase details but is less contentious. However, even in the few temnospondyl specimens with good 3D preservation, the potential for a detailed characterisation of internal structures such as braincase, inner ear and stapes is usually limited by the time-consuming and frequently destructive nature of preparation. For

these reasons the internal cranial structures of *Dendrerpeton* have remained almost wholly unknown.

To investigate the internal cranial anatomy of *Dendrerpeton* and to have a more complete understanding of the hearing abilities of this early temnospondyl two specimens of *Dendrerpeton acadianum* were scanned and reconstructed. The specimens chosen (BMNH R.436 and NSM 987 GF 99.1) differ greatly in their external preservation and also on the quality of the scan data and hence the informative nature of the reconstructions. Two separate specimens of *Dendrerpeton* were scanned because it seemed unlikely that the reconstruction of only one whould provide a full data set. BMNH R.436 was scanned to examine internal cranial anatomy. NSM 987 GF 99.1 was chosen to investigate the external cranial anatomy.

The first reconstruction is based on a specimen of *Dendrerpeton acadianum* (BMNH R.436) at the Natural History Museum, London, which was identified by J.W. Dawson and presented to this museum in 1882 (Figure 3.3.1—1). It was collected from the coal formation in Joggins, Nova Scotia and is dated as Langsettian Sub Epoch of the Westphalian, Carboniferous, not the Duckmantian Sub Epoch as initially claimed (Milner, 1996). BMNH R.436 consists of an incomplete post-orbital cranium and semi-articulated postcranial material. It was first described in a publication by M.C. Steen (1934) in her review 'The Amphibian Fauna from the South Joggins, Nova Scotia' (see her text-figures 2, 5c and 7 for specimen diagrams and her text-figure 3 for a reconstruction of the posterior view of the cranium). The postcranial material of the specimen was more thoroughly described by Carroll (1967) in his review of the 'labyrinthodonts' from Joggins (his text-figures 10, 12e, 13 and 14), but no attempt was made to reconstruct the cranium. Milner (1980) figured the temporal notch and the

posterior section of the cheek in his review of *Dendrerpeton* (his text-figure 4), while the right stapes was reconstructed by Clack (1983) (her figure 11). BMNH R.436 is mentioned in a publication by Milner (1996) in review of the amphibians from the Upper Carboniferous of Joggins, Nova Scotia. The reconstruction BMNH R.436 was present by myself in 2005 (Robinson et al.) and is covered in more detail in this chapter. In all publications BMNH R.436 is classified at *Dendrerpeton acadianum* and there is no evidence to challenge the validity of this classification (A. R. Milner, pers.comm.).

The first documented preparation of BMNH R.436 was undertaken by D.M.S Watson before 1934 and involved splitting the single large block in two (Steen, 1934). One of these contains the cranium that was subsequently freed from the main body of the matrix (Figure 3.3.1—2). Additional parts of the cranium are present in adjoining fragments. Unfortunately, some parts of the cranium such as the occipital condyle were prepared in negative and now only exist as natural moulds.

The second reconstruction is based on a *Dendrerpeton acadianum* specimen (NSM 987 GF 99.1) at the Nova Scotia Museum of Natural History (Figure 3.3.1—3). This specimen was collected on a beach near Coal Mine Point, Joggins by Lin Kebang and Wu Xiao-chun as part of a Redpath Museum field party in 1987 (Holmes et al., 1998). NSM 987 GF 99.1 is dated as Lower Pennsylvanian (Westphalian A), although, due to possible translocation of the specimen from its original bed, this dating cannot be 100% reliable (Holmes et al., 1998). It consists of near complete articulated cranial and postcranial remains in a large sandy siltstone block which has been extensively manually prepared. A description of the prepared specimen was produced by Holmes et al. (1998). No additional description of NSM 987 GF 99.1 has been produced to date.

Figure 3.3.1—1 *Dendrerpeton* specimen BMNH R.436 in dorsal view. Dashed line demarcating main cranial block. Scale bar = 10mm.

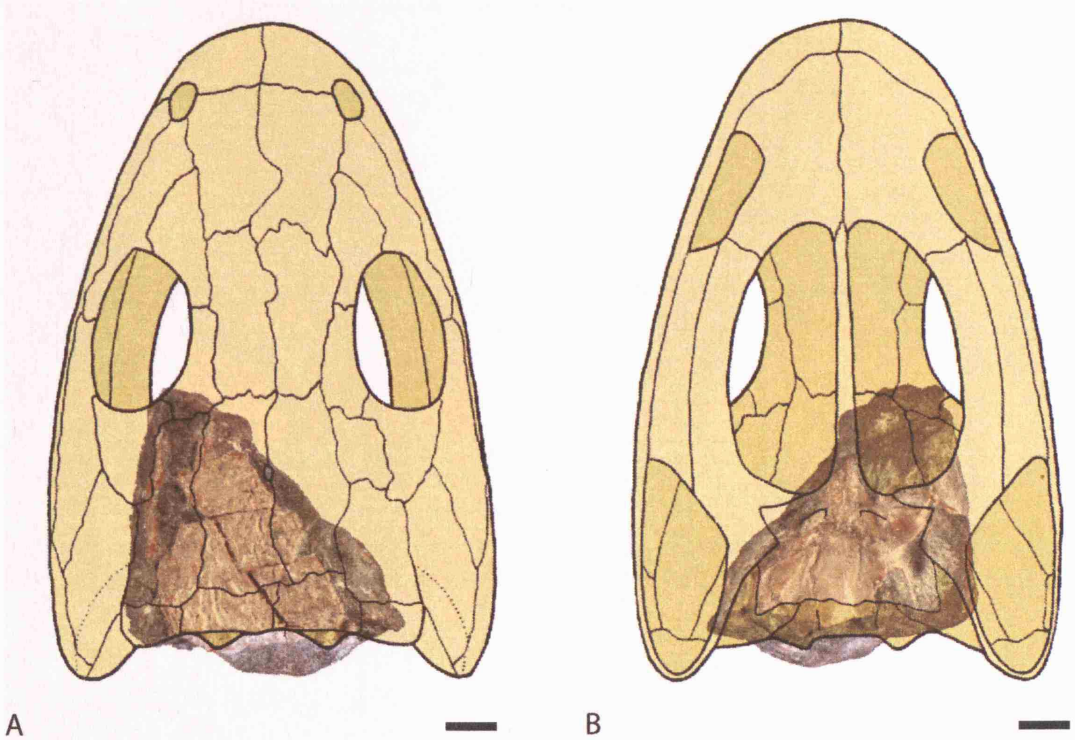

Figure 3.3.1—2 Main cranial block of BMNH R.436 placed in approximate position of a full cranial representation of *Dendrerpeton* (after Carroll, 1967) for orientation and appreciation of the incomplete nature of the specimen. A, dorsal view. B, ventral view. Scale bars = 5mm.

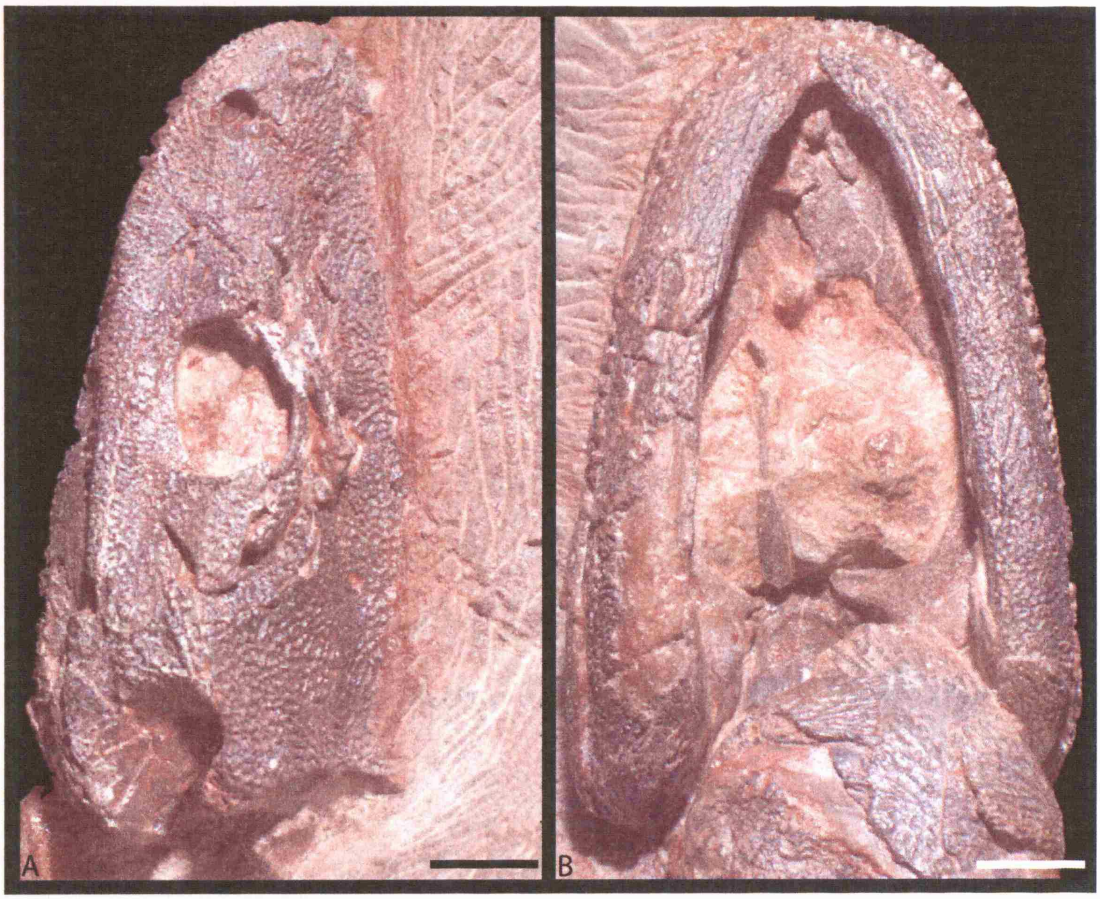

Figure 3.3.1—3 *Dendrerpeton* specimen NSM 987 GF 99.1. A, dorsal view. B, ventral view. Scale bars = 10mm.

3.3.2. RECONSTRUCTION PARAMETERS

The present study focuses on improving our understanding of the internal cranial structure of *Dendrerpeton*. For this purpose the cranial regions of BMNH R.436 and NSM 987 GF 99.1 were scanned and reconstructed.

First reconstruction - BMNH R.436

BMNH R.436 was scanned with the ultra-high resolution subsystem at UTCT. Initially, it was decided to scan only the single block containing the most significant regions of the cranium (Figure 3.3.1—1 and 2). After reviewing the material in more detail it was decided to produce a second scan series that included adjoining fragments to permit a reconstruction of all cranial remains.

Scan series one, of the single block, was produced with 1000 views per rotation and 4 samples per view. This means that each slice was produced from a sinogram containing 1000 views with each view being a combination of four samples to improve image quality. 25 slices were produced with each rotation of the specimen meaning that the single cranial block was rotated 20 times within the x-ray field. This produced a scan series of 16bit resolution (1024 pixels by 1024 pixels), comprising 912 slices each of 0.0319mm thickness (i.e. approximately 31 slices per mm). In order to render it more manageable, this very large data set was reduced to 8bit resolution (512 pixels by 512 pixels) and every other slice was taken – giving a data set of 456 slices each of 0.0319mm thickness and an inter-slice thickness of 0.0319mm (approximately 16 slices per mm). Scan series two, which included adjoining fragments, was produced with 1000 views per rotation and 4 samples per view as with scan series one. 27 slices were produced with each rotation of the fragments meaning that they were rotated 23 times

within the x-ray field. This produced a scan series of 16bit resolution (1024 pixels by 1024 pixels), with 621 slices each of 0.0604mm thickness (i.e. approximately 17 slices per mm). This data set was utilised in 16bit resolution but only slices providing data on the cranial structures were included, thus yielding 403 slices.

The stacks produced from each of the two scan series were reconstructed within Mimics. The quality of the preservation allowed initial rapid production of elements with a universal threshold. However, for increased resolution manual thresholding and other features within Mimics, such as the manual erase tool and region growth features, were used to produce the final elements which were then exported as binary STL files. The elements from the stack created from scan series one were imported into Rhino3D. Elements created from the stack from scan series two were imported into the same Rhino3D file and their position and orientation manually adjusted to marry them to the elements from scan series one.

It was possible to use the scan series to reconstruct areas of BMNH R.436 that are no longer present. It proved possible to model the internal surfaces of absent bones, such as the pterygoid, by tracing the surface contours through the scan series and producing reconstructions. In areas where bone has been lost but the internal moulds have been preserved on both sides, such as the occipital condyle, it was possibe to model the air spaces and reconstruct the bone from them; this is known as the airfill technique. Furthermore, by using a reverse threshold and fill technique the inner ear spaces inside the otic capsules were modelled within Mimics and exported in the usual way.

Second reconstruction – NSM 987 GF 99.1

The sole scan series of NSM 987 GF 99.1 was produced on the high energy subsystem scanner at UTCT. The posterior region of the cranium was included in the scan series

along with certain aspects of the postcranial material. As with *Kyrinion* an offset rotation (translate-rotate) was used to increase the scan detail. This produced a scan series in 16bit resolution (1024 pixels by 1024 pixels) consisting of 162 slices each of 0.333mm thickness (i.e. 3 slices per mm).

3.3.3. DESCRIPTION

The scanning of BMNH R.436 and NSM 987 GF 99.1 has provided information on the cranial anatomy of *Dendrerpeton*. From visual inspection BMNH R.436 is a rather poor specimen compared to the exquisitely preserved and articulated NSM 987 GF 99.1. The converse is the case with the results of the scanning and reconstruction of these two specimens. BMNH R.436 provides a detailed insight into the internal cranial anatomy of *Dendrerpeton* including a perfectly preserved stapes. In contrast the large single block of NSM 987 GF 99.1 necessitated the use of the high energy subsystem rather than ultra-high resolution subsystem scanner at UTCT. The use of the high energy subsystem scanner and the large size of the block compared to the size of the cranium caused the scan slices to be poorly resolved, compared to those of BMNH R.436, which greatly reduced the information gained. The 3D reconstructions of *Dendrerpeton* will be described separately; BMNH R.436 first followed by NSM 987 GF 99.1.

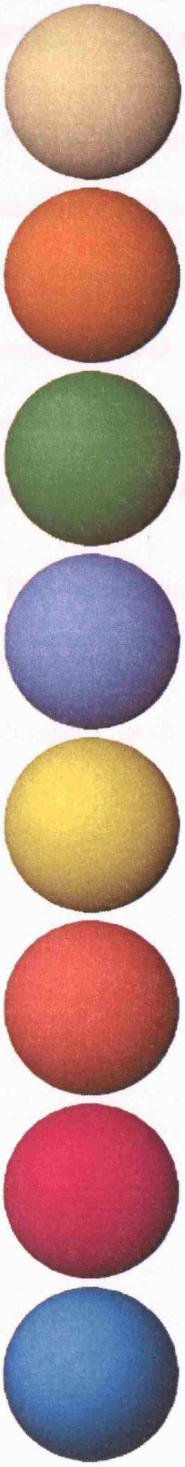

= Base colour for all elements unless stated below

= Skull roof

= Epipterygoid-pterygoid complexes

= Otic capsules

= Basisphenoid-parasphenoid complex

= Basioccipital-exoccipital complex plus airfill

= Mandibles

= Stapes

Figure 3.3.3—1 Colour key.

FIRST RECONSTRUCTION – BMNH R.436

The reconstruction of BMNH R.436 presents a detailed picture of the braincase anatomy and hearing apparatus of an early temnospondyl. The braincase reconstruction is limited to the area posterior to the pituitary fossa as this specimen lacks the sphenethmoid region (Figure 3.3.3—2). The preserved parts of the braincase are essentially undistorted and complete, except for some external damage caused by the previous mechanical preparation.

The reconstruction comprises the parasphenoid-basisphenoid complex, the left epipterygoid-pterygoid complex, otic capsules with inner ear labyrinths, occipital complex, both stapes and the posterior skull roof (Figure 3.3.3—3).

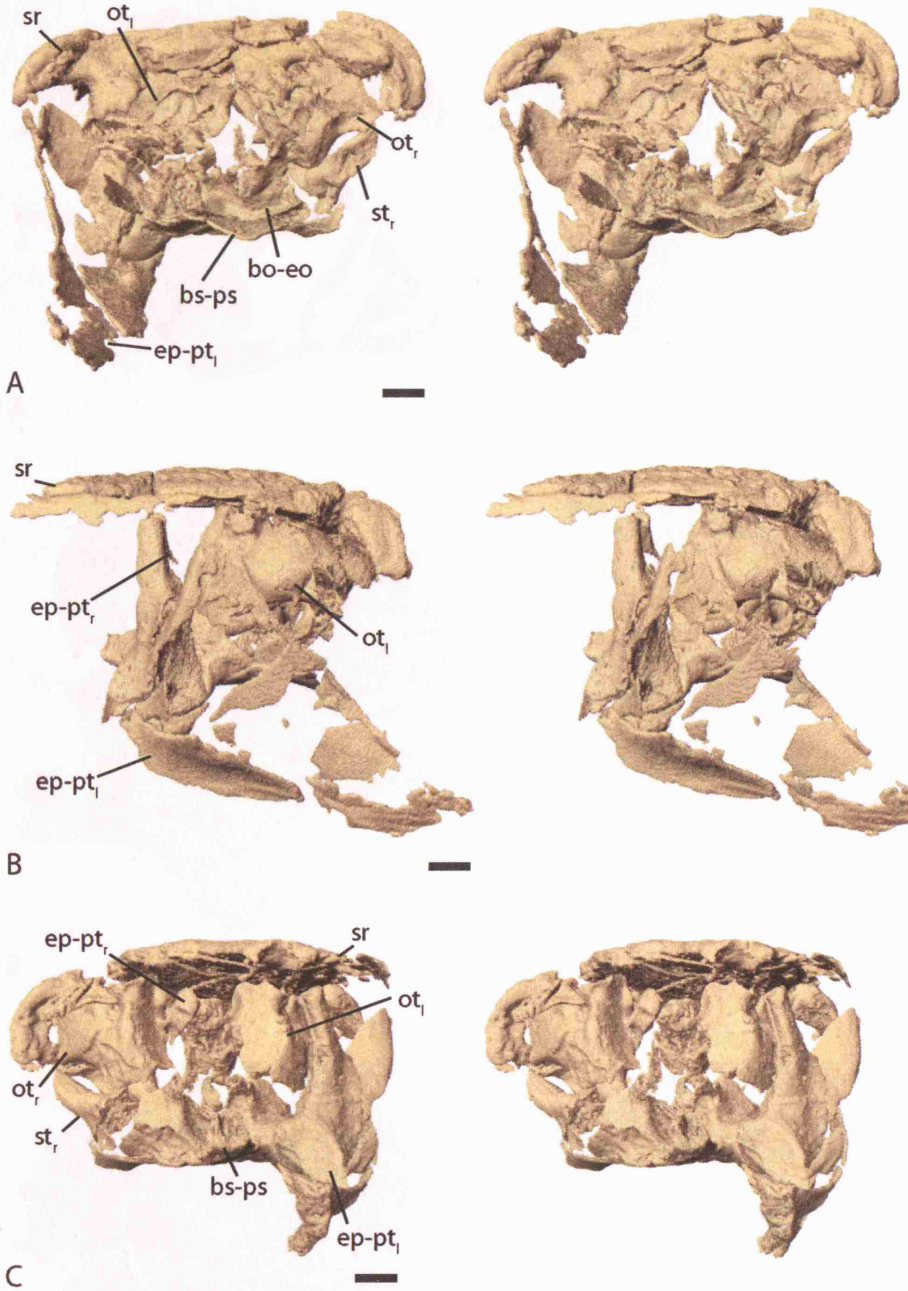

Figure 3.3.3—2 *Dendrerpeton* specimen BMNH R.436. Mono colour stereo pairs of model without correction for translocations or damage. A, posterior view. B, left lateral view. C, anterior view. Scale bars = 2mm.

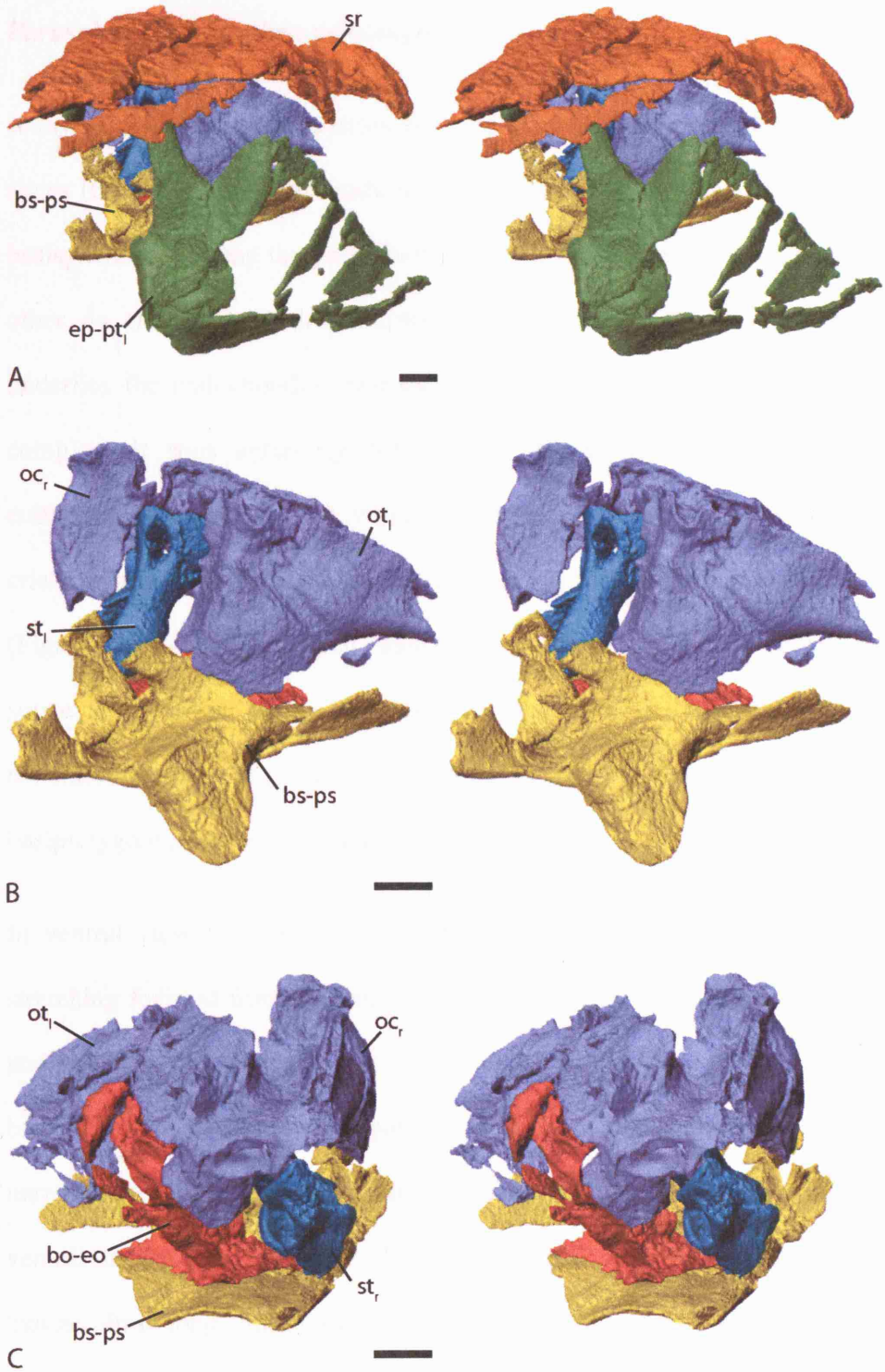

Figure 3.3.3—3 *Dendrerpeton* specimen BMNH R.436. Stereo pairs of model without correction for translocations or damage. A, left anterolateral view. B, left anterolateral view with skull roof and left epipterygoid-pterygoid complex removed. C, right posterolateral view. Scale bars = 2mm.

Parasphenoid-basisphenoid complex

X-ray optical density differences between dermal and endochondral bones in the scan slices (Figure 3.3.3—4 A) made it possible to subdivide this complex (bs-ps) into the basisphenoid (bs) and the parasphenoid (ps). These bones are completely fused to each other on the level of the basipterygoid processes (art). The dermal parasphenoid underlies the endochondral basisphenoid and forms the broad posterior plate of the complex. It runs anteriorly between the basipterygoid articulations to form the cultriform process (cul pro), while the basisphenoid produces the dorsal extension or crista sellaris (cri sel) of the complex as well as the basipterygoid facets. The complex (Figure 3.3.3—5) has been damaged by preparation and separation from the surrounding matrix; parts of the posterior parasphenoid that underlie the basioccipital, the anterior section of the cultriform process, anterior to the pituitary fossa, and the right basipterygoid process are absent.

In ventral view (Figure 3.3.3—5 C) the broad posterior plate of the parasphenoid, stretching forward from its transverse, but somewhat, undulating posterior margin that underlies the basioccipital, narrows to a waist before slightly widening to the base of the basipterygoid processes. The parasphenoid then passes between the processes and narrows abruptly. Its anterior part is broken off just below the sella turcica. On its ventral surface there is a series of 4 small foramina, followed by a larger pair of grooves that are 4mm long. Another groove passes forward around the posteromesial margin of the basipterygoid process and then turns about 80° medially before piercing the parasphenoid through a countersunk foramen and entering the cranial cavity between the walls of the sella turcica. This is the path of the internal carotid artery (ca gro) (Figure 3.3.3—6). Posteriorly, the parasphenoid has large thin lateral flanges (lat fla),

which it is believed to be homologous to the 'cristae ventrolaterales' of *Greererpeton* (Smithson, 1982), that project dorsolaterally, and its smooth dorsal surface is covered medially by the anterior extension of the basioccipital. The lateral flanges do not appear to have been in direct contact with any other braincase element, though it is difficult to be certain as the basioccipital has unfinished lateral margins and, evidently, would have continued as cartilage. Anterior to this broad posterior surface of parasphenoid the basisphenoid forms the crista sellaris, which is developed into a pair of strong dorsal processes with unfinished ends. These would have had a cartilaginous contact to the anterior margin of the otic capsules (oc). The unfinished internal surface of the crista sellaris would clearly have been completed in cartilage and carries the exit points of abducens (VI) nerve and the pretrematic/palatine branch of the facial (VII) nerve. A single ossified prong (mid pro) projecting anteriorly along the midline of the crista sellaris is all that remains of the dorsum sellae (Figure 3.3.3—5 A). As depicted in the reconstructions of *Eryops* (Sawin, 1941) and *Edops* (Romer & Witter, 1942) this ossified prong is all that remains of a thin cartilaginous sheet that reached forward to the sella turcica and pituitary fossa region.

In anterior perspective it is possible to observe a pair of chambers (ant cham) below the dorsum sellae region, ventral to the midline prong of the basisphenoid. These chambers are homologous to the chambers seen in *Eryops* (Sawin, 1941), *Kamacops* (Schoch, 1999b) and *Tersomius* (Carroll, 1964) and are the presumed sites for the origin of the lateral rectus eye muscles. The chambers are also seen in the reconstructions of *Acanthostega*, *Kyrinion* and *Lydekkerina*. Furthermore, unlike Holmes (1989) and Clack & Holmes (1988), the author believes these chambers are homologous to the 'retractor pit' seen in *Archeria*, *Seymouria*, *Eocaptorhinus*, and reptiles. It, therefore, seems that the presence of anterior chambers or 'retractor pits' is an ancestral feature of

early tetrapods and thus cannot be a synapomorphy of a certain subgroup of early tetrapods as has been previously suggested (Clack & Holmes, 1988; Holmes, 1989). Such chambers in the crista sellaris are not documented in *Edops* (Romer & Witter, 1942) or *Trimerorhachis* (Schoch, 1999a). There is a single foramen at the back of each chamber that opens into the brain cavity and probably served as the exit point of the abducens (VI) nerve (Figure 3.3.3—5 A). Lateral to these chambers there are countersunk foramina on either side (Figure 3.3.3—5 A and B) which communicate with the brain cavity through a long canal that may be the path of the pretrematic/palatine branch of the facial (VII) nerve, which in *Salamandra* exits the braincase ventral to the large exit point of the trigeminal and anterior to the foramen faciale (Goodrich, 1930).

The basisphenoid half of the basipterygoid joint is clearly bi-faceted with dorso-lateral and anterior surfaces of equal size and shape (Figure 3.3.3—5 A and C). The surfaces of the facets are unfinished and would have been completed in cartilage. It is clear that there was no suture between the braincase and the palatoquadrate complex but a somewhat moveable cartilaginous articulation. In *Dendrerpeton* the parasphenoid does not contribute to the basipterygoid joint.

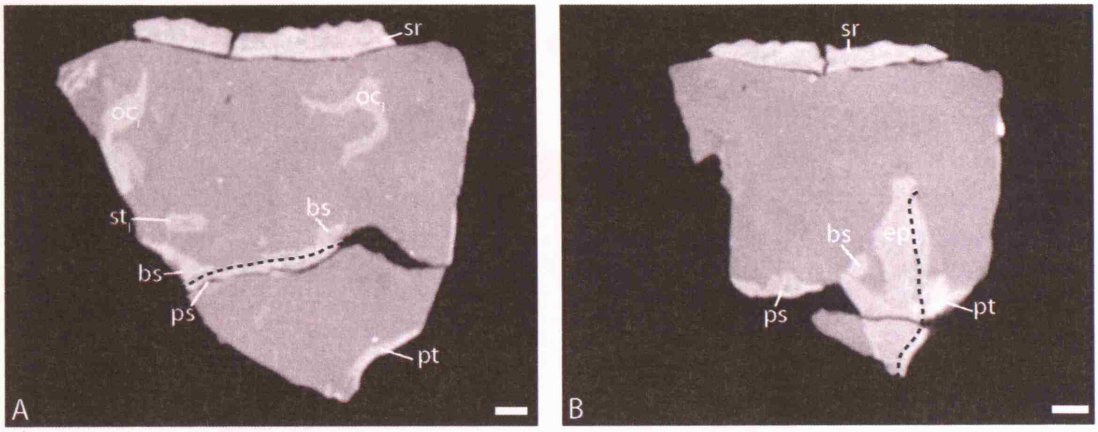

Figure 3.3.3—4 *Dendrerpeton* specimen BMNH R.436. Transverse CT scanning slices in anterior view. A, dashed line demarcating the separation of the dermal parasphenoid from the endochondral basisphenoid. B, dashed lined demarcating the separation of the dermal pterygoid from the endochondral epipterygoid. Scale bars = 2mm.

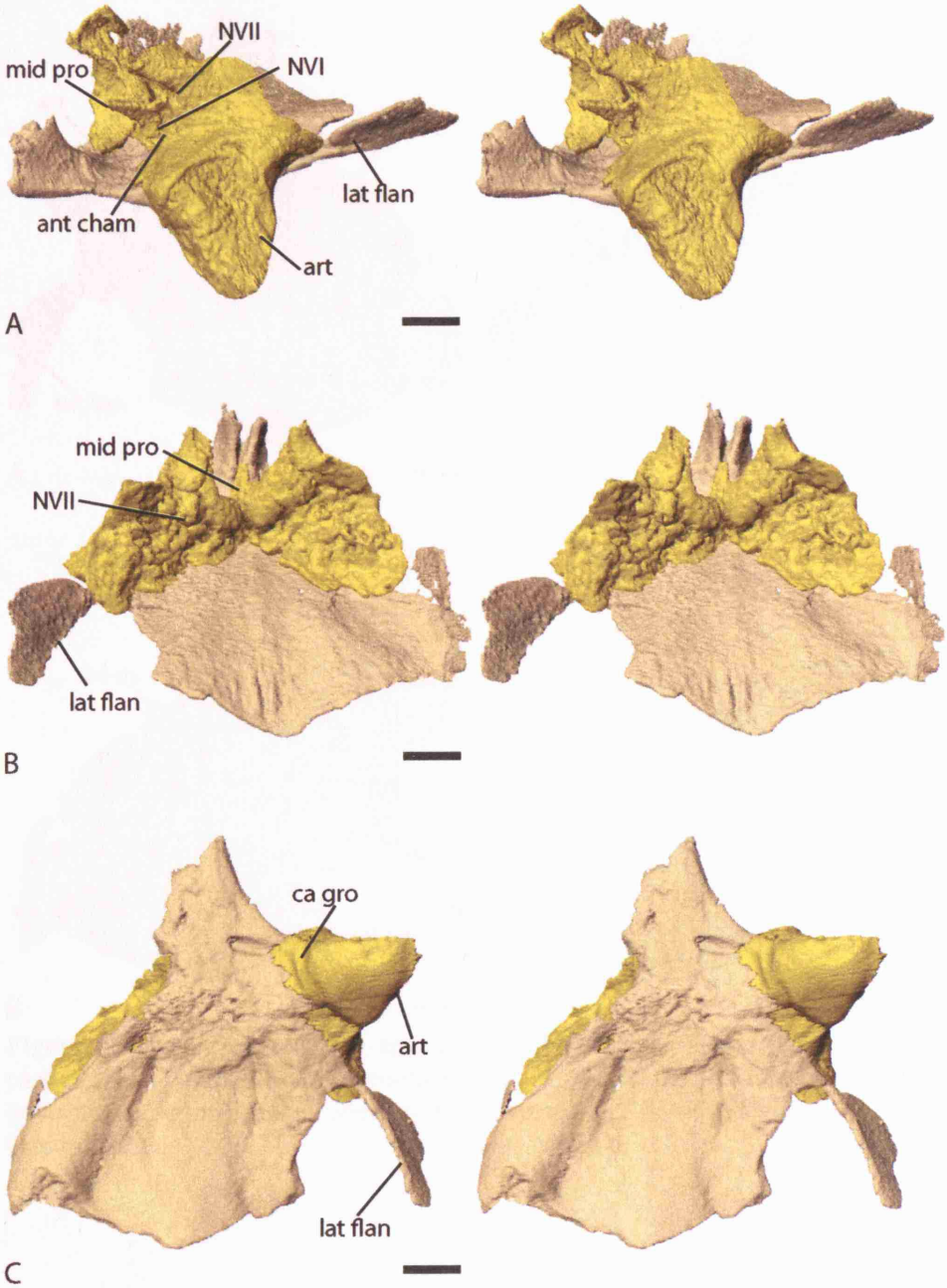

Figure 3.3.3—5 *Dendrerpeton* specimen BMNH R.436. Stereo pairs of the basisphenoid-parasphenoid complex with the parasphenoid in beige. A, left anterolateral view. B, posterodorsal view. C, ventral view. Scale bars = 2mm.

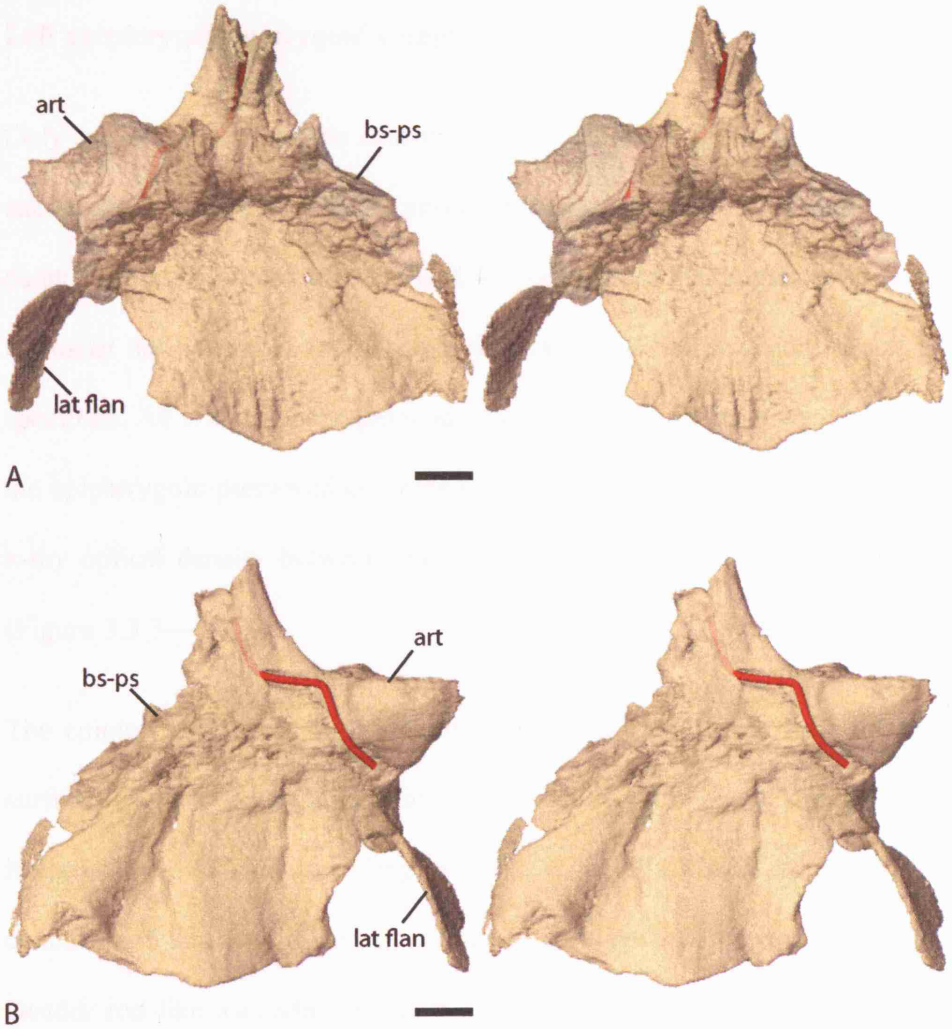

Figure 3.3.3—6 *Dendrerpeton* specimen BMNH R.436. Stereo pairs of the basisphenoid-parasphenoid complex with a reconstruction of part of the left internal carotid artery in red. Basisphenoid-parasphenoid complex semi-transparent. A, dorsal view. B, ventral view. Scale bars = 2mm.

Left epipterygoid-pterygoid complex

Only the left palatoquadrate complex (Figure 3.3.3—7 and 8) is present in the specimen, except for a fragment of the ascending process (asc pro) of the right epipterygoid. The palatoquadrate complex of BMNH R.436 consists of the epipterygoid (ep) and quadrate ramus of the pterygoid (pt); the palatine ramus of the pterygoid is not present in this specimen. As with the parasphenoid-basisphenoid complex it was possible to subdivide the epipterygoid-pterygoid complex (ep-pt) into its components based on differences in x-ray optical density between endochondral epipterygoid and dermal pterygoid bones (Figure 3.3.3—4 B).

The epipterygoid bears all of the anterior and the majority of the dorsolateral contact surfaces of the basipterygoid articulation (Figure 3.3.3—8 A). Dorsal to this articulation it forms the rod-like ascending process, columella cranii, which has an unfinished concave end that would have continued in cartilage and reached the skull roof (sr). The slender rod-like ascending process of the epipterygoid, seen in *Dendrerpeton*, *Edops* (Romer & Witter, 1942) and *Eryops* (Sawin, 1941) is ancestral for temnospondyls (Yates & Warren, 2000). On the anterior face of this process there is a distinct oval scar of unfinished bone (ep mus sca). Although, there is no homologous scar described in other early tetrapods, it is possible that it is the attachment of the homologue of a protractor/levator palatoquadrate/bulbi. This ancient muscle and its homologues are present primitively in bony fish and tetrapods (Lakjer, 1926; Lubosch, 1938; Luther, 1914) and are involved in palatoquadrate and/or eye movement. The ossified part of the epipterygoid fuses with the pterygoid along a dorsoventral suture. Along the anterior margin of this suture the epipterygoid protrudes laterally to the pterygoid (ep lip) (Figure 3.3.3—8 C), which suggests the presence of an unpreserved cartilaginous

extension of the epipterygoid. This extension of the original epipterygoid would have continued posteriorly covering the pterygoid laterally and contacting the quadrate as a thin sheet. There is no evidence for a dorsal otic process of the epipterygoid to contact the otic capsule, which is seen in *Edops* (Romer & Witter, 1942) and *Eryops* (Sawin, 1941).

The left pterygoid is partially exposed on its lateral side with large parts of the bone absent; the surface contours of the remaining internal mould have been used to reconstruct this missing bone (Figure 3.3.3—7).

The laminar triangular form of the pterygoid can be visualised from the internal mould and bone reconstruction (Figure 3.3.3—8). The posterior corner of this right angle triangle would have contacted the quadrate, whilst dorsally the hypotenuse would have contacted the squamosal, the actual contact probably being affected by a narrow strip of cartilaginous epipterygoid. At its anteroventral corner the pterygoid fuses to the epipterygoid and forms a small part of the dorsolateral surface of the palatoquadrate contribution to the basipterygoid articulation. Lateral to the fusion with the epipterygoid the pterygoid curves laterally and then posteriorly to form a large concavity which is obviously homologous to the 'excavatio tympanica' (ex tym) of the temnospondyls *Benthosuchus* (Bystrow & Efremov, 1940) and *Edops* (Romer & Witter, 1942) and other non-temnospondyl tetrapods such as *Greererpeton* (Smithson, 1982). Bystrow stated this 'served as the anterior wall of [the] tympanical cavity'. This feature is also seen in *Lydekkerina*. Posterior to this cavity the pterygoid is featureless with no evidence of muscle attachments or otic processes.

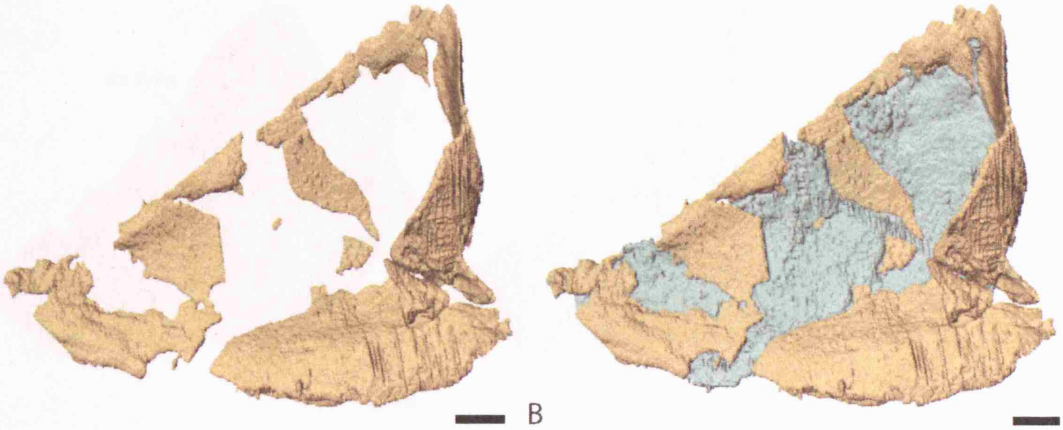

Figure 3.3.3—7 *Dendrerpeton* specimen BMNH R.436. Medial view of the left pterygoid. A, remaining fossilised bone. B, remaining fossilised bone with internal mould in light green. Scale bars = 2mm.

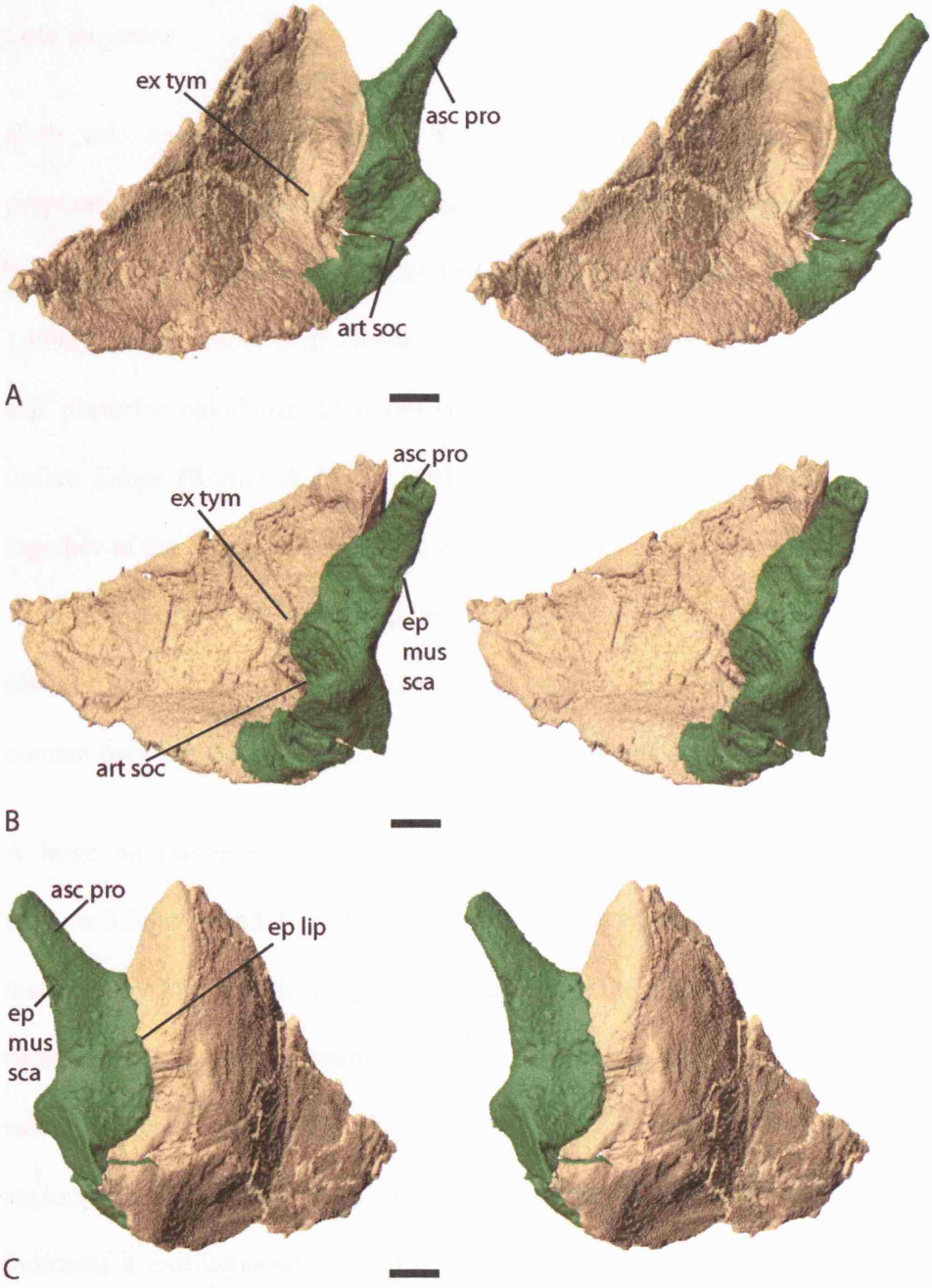

Figure 3.3.3—8 *Dendrerpeton* specimen BMNH R.436. Stereo pairs of the left epipterygoid-pterygoid complex. Pterygoid in beige. A, posteromedial view. B, anteromedial view. C, anterolateral view. Scale bars = 2mm.

Otic capsules

Both otic capsules are present in BMNH R.436, although, they have posterior preparation damage and the right capsule displays a small degree of distortion (Figure 3.3.3—9, 10, 11 and 12). As has been noted in other basal temnospondyls (Schoch, 1999a) the otic capsule of *Dendrerpeton* cannot be subdivided into an anterior prootic and posterior opisthotic. In a similar fashion to *Trimerorhachis* (Schoch, 1999a), but unlike *Edops* (Romer & Witter, 1942), the otic capsules in *Dendrerpeton* do not fuse together at the dorsal midline. The capsules suture to the occipital complex posteriorly. Anteroventrally, they are separated from the basisphenoid and parasphenoid by a distinct gap which it is assumed would have been bridged via cartilage; providing contact between the otic capsules and the lower braincase.

A large post-temporal fossa (ptf) reaches anteriorly over the dorsal capsule surface (Figure 3.3.3—9 and 11). It is bordered laterally by a dorsal ridge of the capsule and medially by the capsule proper. Halfway along the floor of both post-temporal fossae there is a small circular opening that may have been filled with cartilage. The floor of each post-temporal fossa is also unfinished in *Lydekkerina.* The dorsal ridge and the region anterior to this post-temporal fossa has a concave unfinished surface that indicates a cartilaginous contact to the skull roof. The posteromesial part of the otic capsule, by contrast, has a well-ossified dorsal surface, but this has an unusual rugose texture and was, evidently, also separated from the skull roof by a substantial cartilage pad. The anterior part of the dorsal ridge harbours an anterolateral notch (Figure 3.3.3—9 and 11). This is interpreted as a remnant of a foramen whose dorsal cartilaginous margin has been lost and that is homologous to the 'post-temporal foramen' of *Edops* (Romer & Witter, 1942), the corresponding foramen in *Eryops* (Sawin, 1941) and that

observed in *Kyrinion* and *Lydekkerina*. This foramen (ot for) seems likely to have contained a vein, possibly the vena capitis dorsalis, that served the muscles housed in the post-temporal fossa and ran ventrally into the jugular vein as indicated by a shallow indentation ventral to the notch. A similar foramen is illustrated by Jarvik as the 'spiracular canal' in his figure 86A (1980) of *Eusthenopteron*.

The lateral surface of the otic capsule is dominated by a protrusion (Figure 3.3.3—9 B and 11 B), the crista parotica, which contains the horizontal semicircular canal (h scc). The ossified dorsal margin of the fenestra ovalis (f/o) lies ventromedial to the crista parotica. The otic capsule curves medially below the crista parotica forming a domed roof below the post-temporal fossa which then curves ventrally to form the dorsal margin of the fenestra ovalis. Experimental positioning of the stapes (st) relative to the otic capsule indicates that the curvature of the otic capsule below the crista parotica served to accommodate the dorsolaterally directed shaft of the stapes. There is a small notch in the dorsal margin of each fenestra ovalis on both sides of the specimen that suggests a foramen of unknown function.

The fenestra ovalis, which can also be seen in lateral view, of *Dendrerpeton* clearly would have had cartilaginous ventral, anterior and posterior margins. As with many early tetrapods the exact size of the fenestrae ovales cannot be determined, nor can the presumed cartilaginous component of the stapedial footplate (fp). It was not possible to figure accurately the cartilaginous components of the footplate and margin of the fenestra ovalis, although, this has been attempted previously in the reconstructions of *Edops* (Romer & Witter, 1942) and *Eryops* (Sawin, 1941). Therefore, it is not possible to determine the exact relative contributions of occipital and otic components to the fenestra ovalis margin. The otic capsule and parasphenoid form most of the margin and

that the exoccipital was probably also involved. The basioccipital contribution is unknown, but if it existed it could only have amounted to a small section of the posteroventral margin, similar to that in *Trimerorhachis* (Schoch, 1999a) and *Edops* (Romer & Witter, 1942).

Anterior to the crista parotica in lateral view a pronounced rounded groove (jug gro) (Figure 3.3.3—9 B, C and 12 B, C) extends from anterodorsal to posteroventral, and sends a branch vertically to the aforementioned notch in the dorsal ridge. This appears to mark the path of the internal jugular vein, which is joined by a vein exiting from the post-temporal fossa as described in *Eryops* (Sawin, 1941). The course of this path seems to be homologous to the canal that is postulated to have contained the jugular vein beneath the lateral commissure in osteolepiforms.

In dorsal view the anterior surface of the capsule curves sharply medially and slightly posteriorly towards the midline. The medial margin of this anterior surface contains a shallow notch that is believed to be the (anatomically) posterior margin of the prootic foramen (pro for) with a presumed cartilaginous anterior rim. The prootic foramen serves as the exit point of the trigeminal nerve but not the vena cerebralis medialis as suggested by Sawin (1941) in *Eryops*. The vena cerebralis medialis is claimed to exit with cranial nerve VII and join the vena cerebralis lateralis outside the cranial cavity (Goodrich, 1930).

The bony labyrinths of the inner ear can be visualized from internal views of the otic capsules (Figure 3.3.3—10 and 12) and from an internal mould of the right side (Figure 3.3.3—13). The areas occupied by the three semicircular canals and their associated ampullae are all clearly visible. Within the right otic capsule the space occupied by the horizontal semicircular canal has remained intact, whereas the dorsal paths of the

anterior (a scc) and posterior (p scc) semicircular canals as well as the superior sinus were unossified and cannot be fully reconstructed. The left otic capsule has more extensive damage to its horizontal and posterior canals due to the previous mechanical preparation.

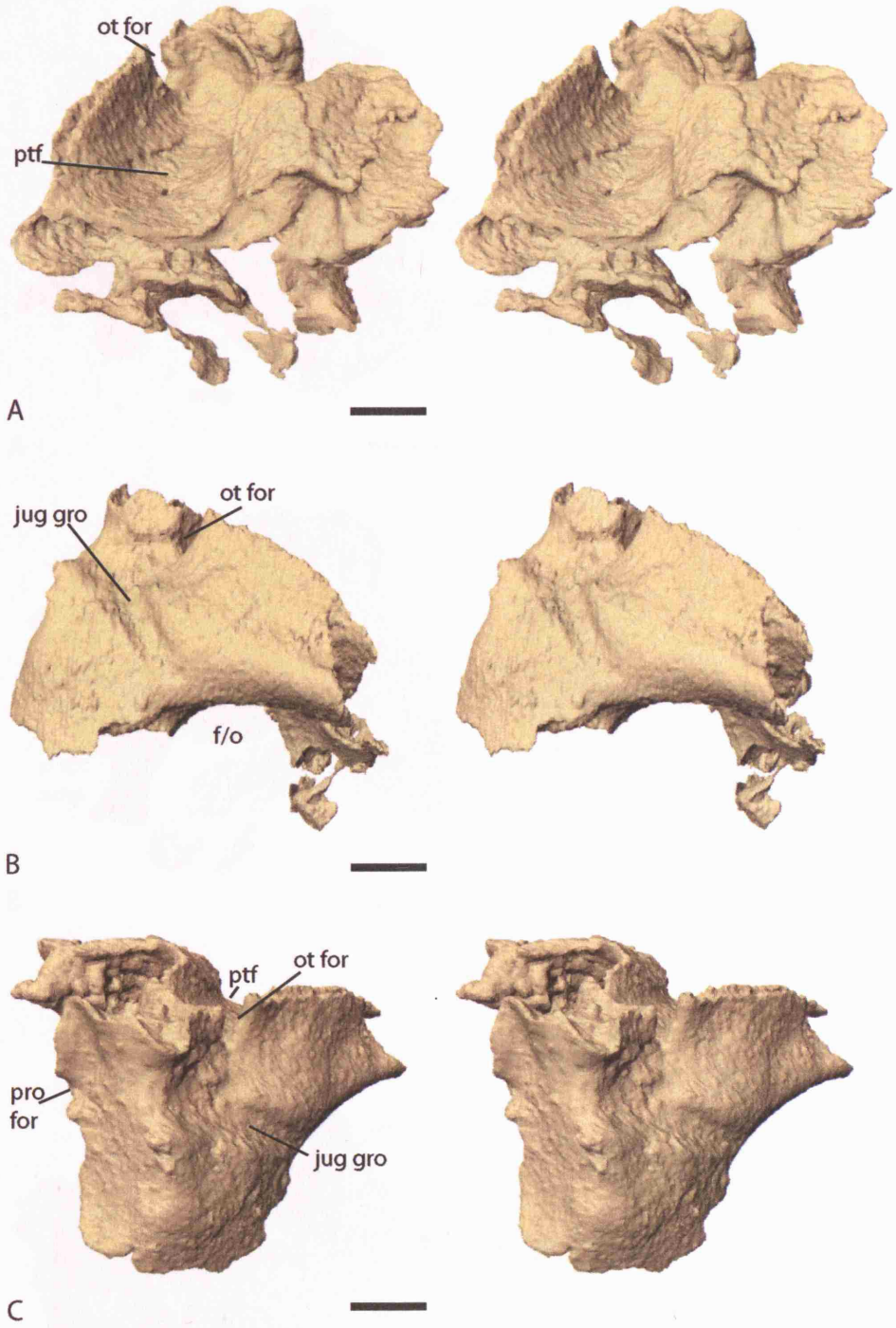

Figure 3.3.3—9 *Dendrerpeton* specimen BMNH R.436. Stereo pairs of the left otic capsule. A, posterodorsal view. B, lateral view. C, anterior view. Scale bars = 2mm.

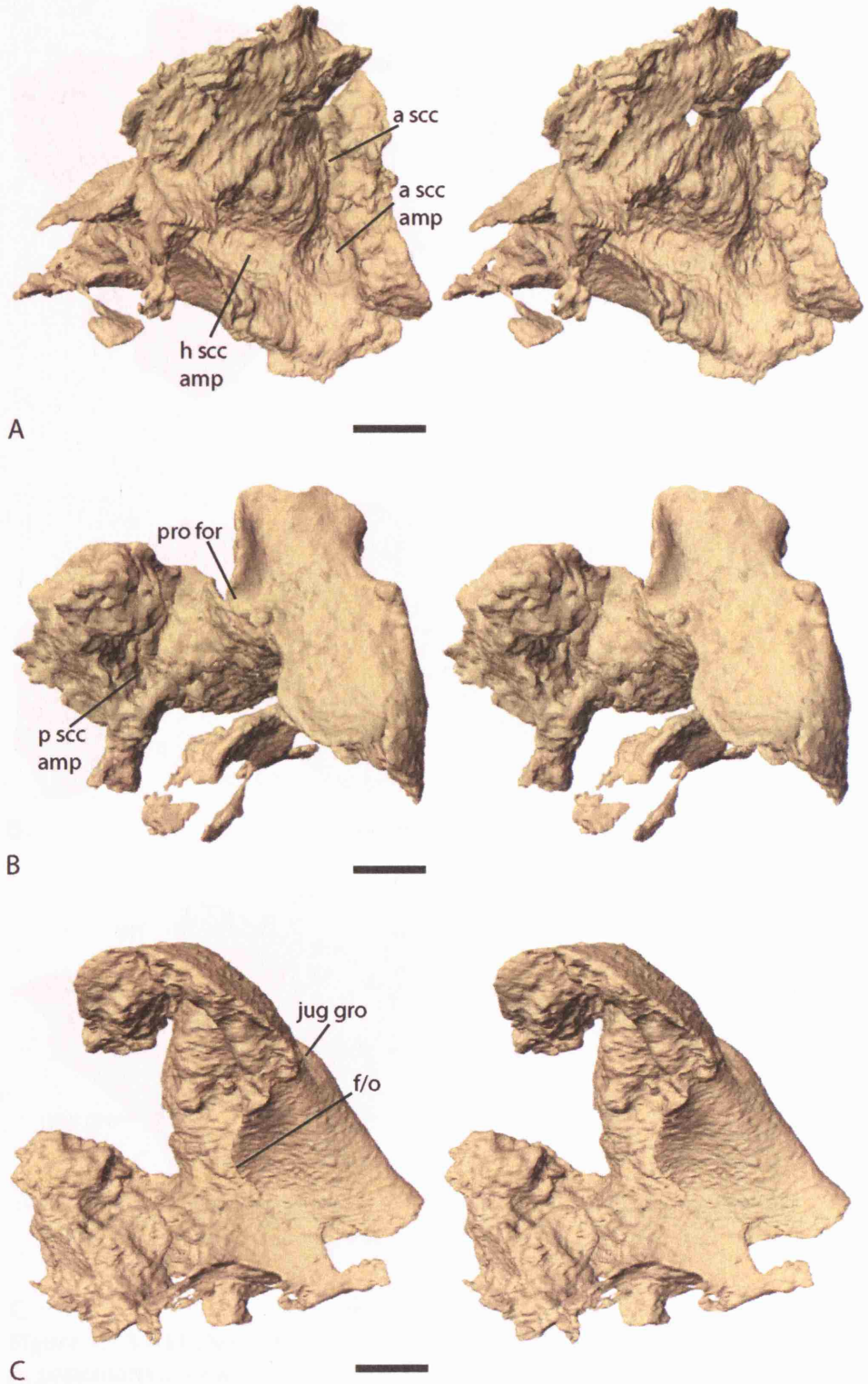

Figure 3.3.3—10 *Dendrerpeton* specimen BMNH R.436. Stereo pairs of the left otic capsule. A, posteromedial view. B, anteromedial view. C, ventral view. Scale bars = 2mm.

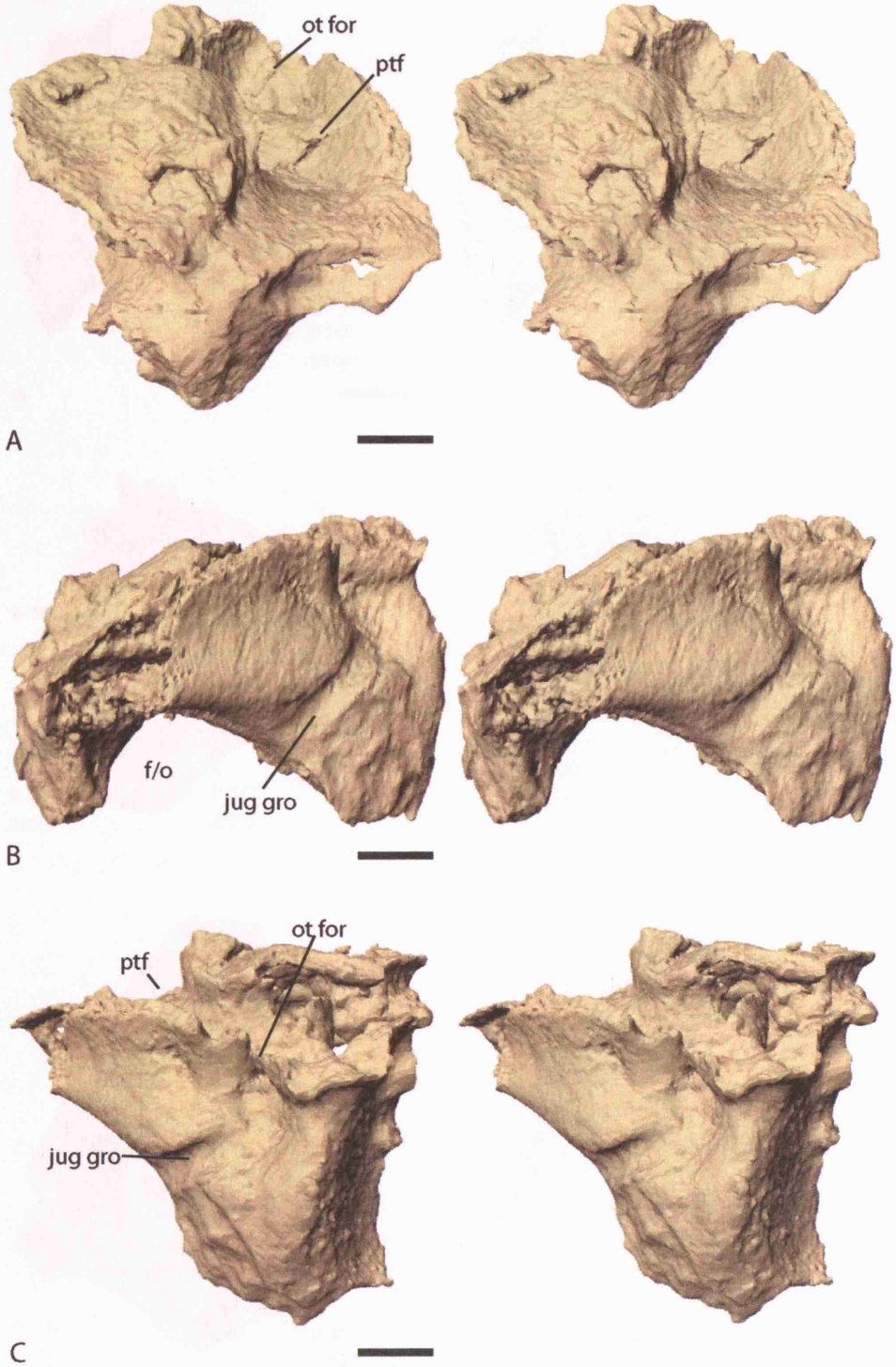

Figure 3.3.3—11 *Dendrerpeton* specimen BMNH R.436. Stereo pairs of the right otic capsule. A, posterodorsal view. B, lateral view. C, anterior view. Scale bars = 2mm.

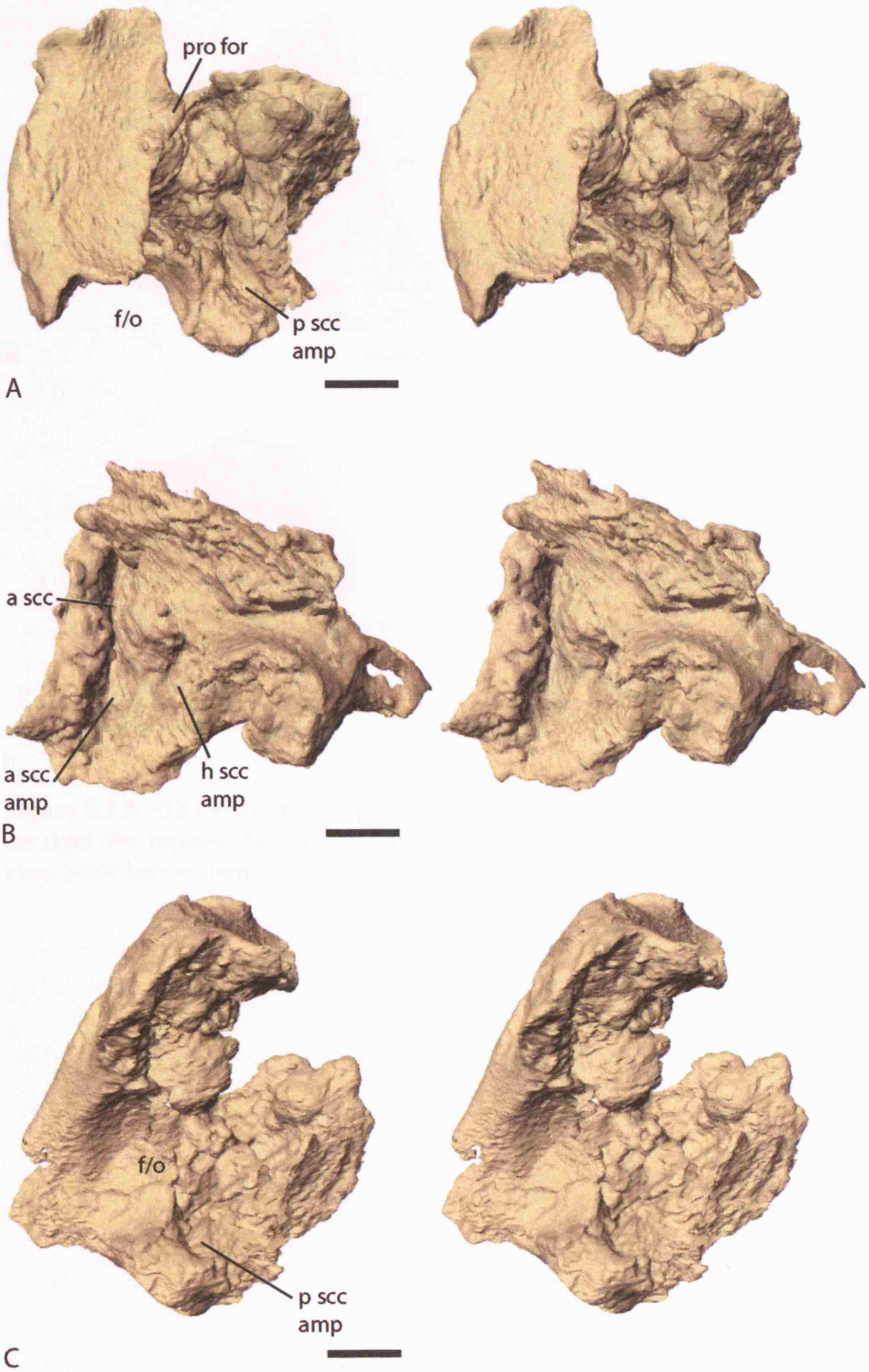

Figure 3.3.3—12 *Dendrerpeton* specimen BMNH R.436. Stereo pairs of the right otic capsule. A, anteromedial view. B, posteromedial view. C, ventral view. Scale bars = 2mm.

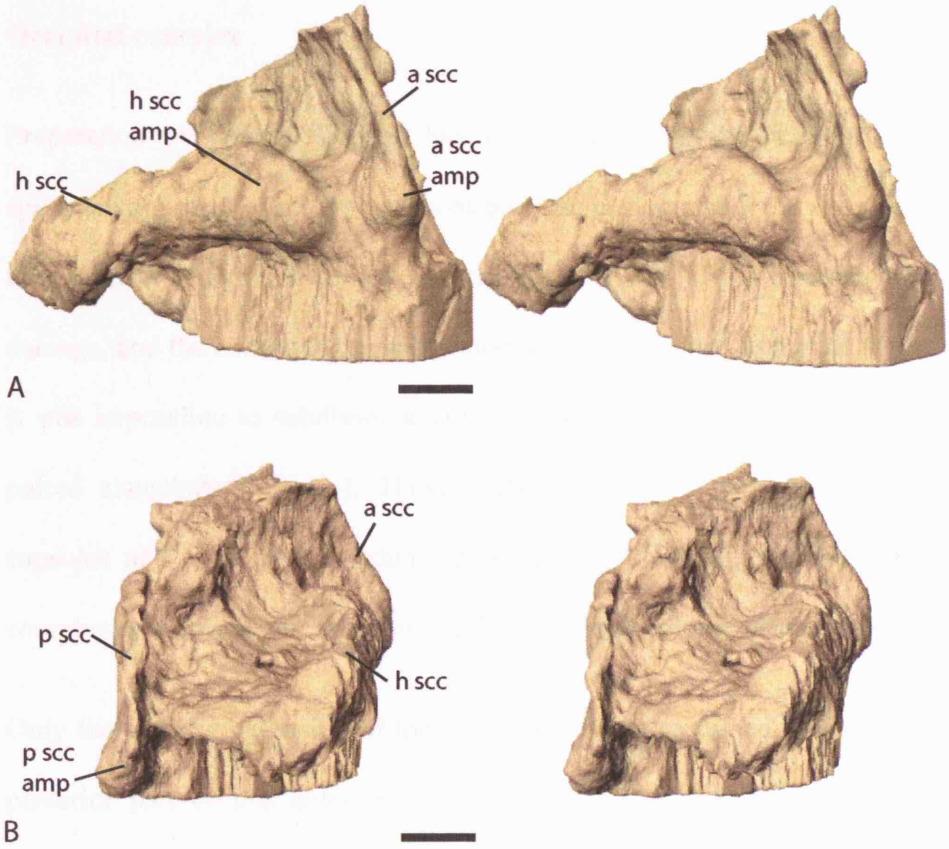

Figure 3.3.3—13 *Dendrerpeton* specimen BMNH R.436. Stereo pairs of the internal mould of the right otic capsule showing the inner ear structures. A, anterolateral view. B, posterolateral view. Scale bars = 2mm.

Occipital complex

Preparation by D.M.S. Watson has greatly damaged the occipital complex of this specimen and destroyed large parts of both the basioccipital and exoccipitals, as well as the posterior margin of the left otic capsule and part of the parasphenoid. Due to this damage, and the consequent need to model these structures as airfills (Figure 3.3.3—14), it was impossible to subdivide accurately the occipital complex into basioccipital and paired exoccipitals (bo-eo). Those parts of the exoccipitals that suture to the otic capsules and the anterior extension of the basioccipital, are the only parts of this complex that are present as preserved bone in the specimen (Figure 3.3.3—15).

Only the anterior extension of the basioccipital has remained entirely undamaged. The posterior part of this anterior extension is fused at the ventral midline whereas its anterior half has remained as an unfused paired structure that reaches forward and contacts the basisphenoid. The midline split between the paired structures of the basioccipital is the pit for the anterior most part of the notochord, as seen in *Lydekkerina*. Lateral to the notochordal pit (not pit) the raised finished surfaces of the basioccipital slope anteriorly. Each one carries a large rounded notch with a lateral lip extension (Figure 3.3.3—15 B and C). The unfinished nature of this lip suggests that it was continued in cartilage and may have housed cranial nerve VIII as it passed to the otic region. Further, anterior to this notch the raised right hand surface of the basioccipital terminates, whereas the left side continues anteriorly and contacts the basisphenoid. Lateral to these raised medial surfaces the anterior extension of the basioccipital exhibits an unfinished dorsal surface. This unfinished surface, the incomplete nature of the raised anterior extension and the lack of a corresponding ossification on the right side suggests a large cartilaginous component that would have

joined the raised extension to support the hindbrain. The parasphenoid underlies the basioccipital across this entire anterior extension.

Further information on the occipital complex was gained by using an airfill technique to model areas removed by preparation. The specimen had previously been split transversely, creating part and counter-part of the occipital region. The anterior face of this split which contains most of the occipital and otic structures has been prepared mechanically, however, bone was removed in preference to matrix. Its counterpart predominantly preserves the imprint of the condyle and posterior margin of the otic capsule, although, there are fragments of the fossilised occipital material still present (Figure 3.3.3—15 A). By placing the part and counter-part together for the second scan series and by modelling the air-spaces between the parts it was possible to reconstruct for the first time the 'lost' bones (Figure 3.3.3—14). The horseshoe shape of the occipital condyle (occ cond) became apparent in a posterior view of this reconstruction (Figure 3.3.3—15 A). This shape is reminiscent of the primitive temnospondyl condition, seen for example in *Edops* (Romer & Witter, 1942) and *Trimerorhachis* (Schoch, 1999a). However, the slightly bi-facetted *Dendrerpeton* condyle with its thin ventral basioccipital component and paired dorsal exoccipital pads is more derived than the condition observed in *Edops*. Nevertheless, the form bears more resemblance to the primitive condition than the strap-shaped, bi-facetted condyle of *Eryops* (Sawin, 1941), *Kamacops* (Schoch, 1999b) and stereospondyls such as *Lydekkerina* (Parrington, 1947). The form of the foramen magnum (fm) can be seen above the condyle.

The rest of the airfill reconstruction appears to show parasphenoid, exoccipital and posterior margin of the otic capsule, however, exact boundaries cannot be resolved and only estimates are shown in Figure 3.3.3—14 B.

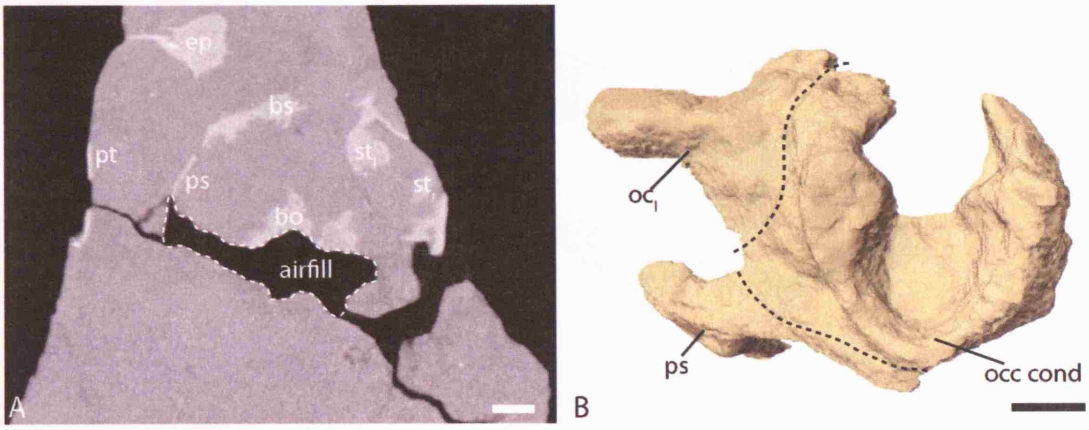

Figure 3.3.3—14 *Dendrerpeton* specimen BMNH R.436. A, frontal CT scanning slice with dashed line demarcating the airfill area. B, posterior view of the airfill model with dashed lines demarcating the approximate contributions by the different ossifications. Scale bars = 2mm.

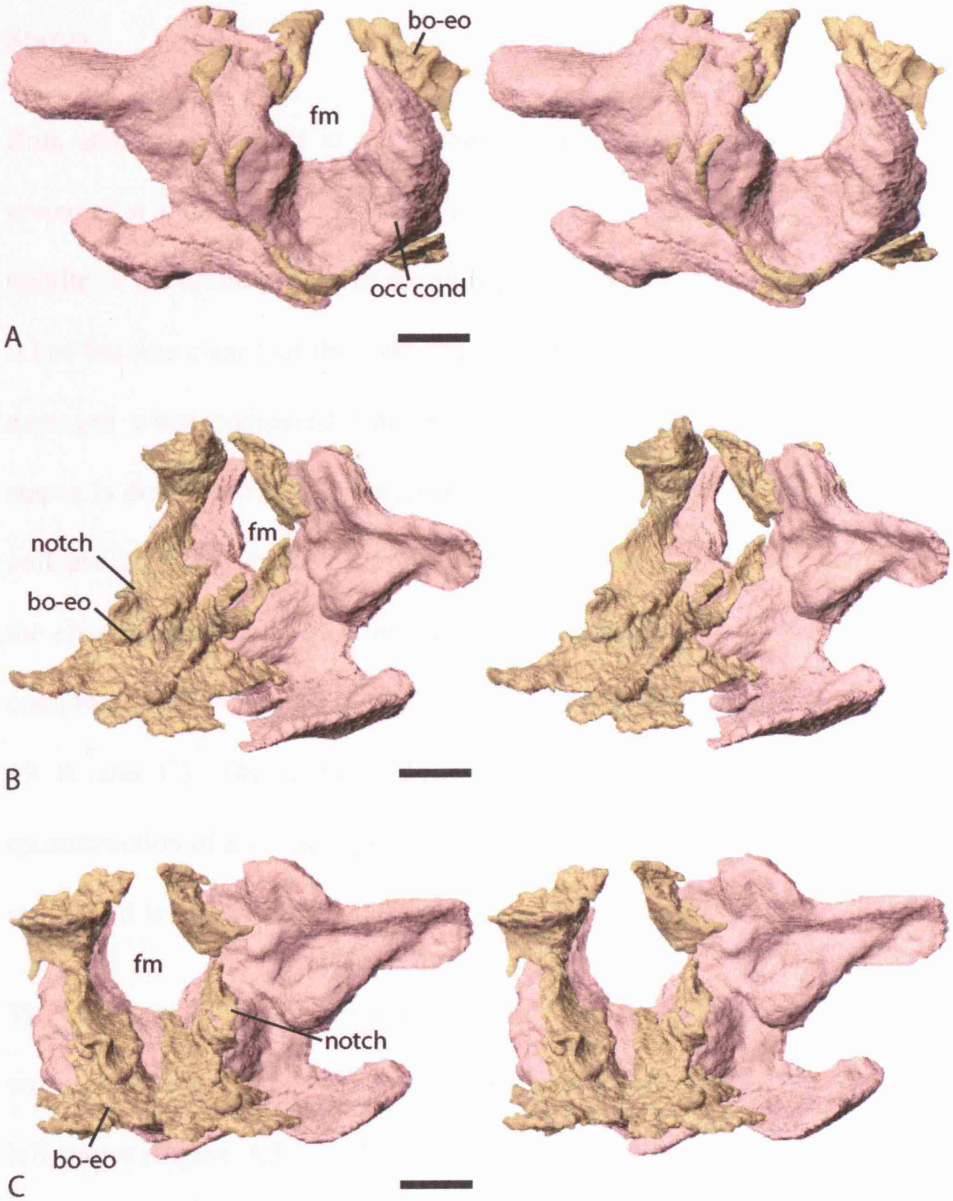

Figure 3.3.3—15 *Dendrerpeton* specimen BMNH R.436. Stereo pairs of the basioccipital-exoccipital complex and airfill model. Airfill model in light pink. A, posterior view. B, left anterolateral view. C, anterior view. Scale bars = 2mm.

Stapes

Both stapes are present in the specimen, the right having been exposed by previous preparation and described by Clack (1983). The undamaged left stapes was found in the middle of the braincase above the parasphenoid and the basioccipital (Figure 3.3.3—16). It has become clear that the right stapes (Figure 3.3.3—19 and 20) is both distorted and damaged when compared with the left stapes (Figure 3.3.3—17 and 18). The right stapes is dorsoventrally compressed along its whole length, causing the dorsal part to collapse on the ventral part with an anterior skew. As seen from a medial perspective the characteristic bipartite temnospondyl footplate is still discernible. The dorsoventral compression is evidenced by the collapse of the stapedial canal (st can) (Figure 3.3.3—19 A and C). The distal end of the stapes is also missing. Thus the previous reconstruction of a *Dendrerpeton* stapes by Clack (1983) is based on a poorly preserved stapes and is superseded by the present data.

The stapes of *Dendrerpeton* consists of a footplate and stapedial shaft, and appears to correspond to the pars media or columella of extant amphibians. The footplate of the left stapes (Figure 3.3.3—17 D) has a large dorsal component (dor com) and a smaller concave ventral component (ven com). Both parts of the footplate have an unfinished surface which suggests an internal cartilaginous extension, possibly equivalent to a pars interna. The footplate is almost entirely surrounded by a raised lip except for a small posteroventral region. The ventral part of the footplate is triangular, being most broad at its anterior and coming to a point at the posterior extension of its flat ventral surface. The dorsal part protrudes above the ventral and has a small concavity at its most dorsal extent. The dorsal part would have contacted the perilymphatic space while the ventral

part would have articulated with the lateral flange of the parasphenoid, both via the internal cartilaginous extension.

The stapedial canal which runs horizontally, lateral to the division of the footplate, separates the shaft of the stapes into two branches (Figure 3.3.3—17 A and C). The dorsal branch is approximately twice the diameter of the ventral one. Lateral to the stapedial canal there is a large horseshoe-shaped scar on the posterior surface of the shaft (Figure 3.3.3—17 A) with apices pointing medially towards the footplate. This scar is clearly not an artefact as the left stapes is in a near perfect state of preservation and there is evidence of an equivalent scar on the right stapes (post scar) (Figure 3.3.3—19 A, although, the extensive damage to this stapes renders a firm interpretation difficult). The detailed appearance of this scar suggests that it is a muscle attachment. One would expect to see a more pronounced unfinished surface of the spongy interior bone as seen on the footplate if this scar was for a cartilaginous process, although, it cannot be entirely discounted. It may be homologous to the posterior concavity on the stapes of *Doleserpeton annectens* Bolt (Bolt & Lombard, 1985; Lombard & Bolt, 1988) and/or the posterior rugosity on the stapes of *Trimerorhachis* (Lombard & Bolt, 1988) and *Pholiderpeton* (Clack, 1983). The scar could also be equivalent to the small process seen in this position on the stapes of *Lydekkerina* specimen UMZC T.206 and *Sclerocephalus* (Schoch, 2002). Extending distally from this scar a small groove (st gro) diminishes near the end of the stapes. This groove appears to be homologous to that present in exactly the same place on the stapes of *Doleserpeton annectens*. There is an additional small scar (sm scar) above the anterior opening of the stapedial canal which again is clearly not an artefact.

Distally, the shaft of the stapes curves forwards and exhibits a gentle anterior twist (Figure 3.3.3—18). Its distal part is somewhat flattened and spatulate but narrows at the tip to a small but well-defined unfinished area (unf con) that may have harboured the cartilaginous plug of the extrastapes or pars externa. This extrastapes would have extended dorsally and laterally, but its precise size and shape are, of course, unknown.

Neither stapes is preserved *in situ*. The dorsal margin of the fenestra ovalis on the otic capsule and the lateral flanges of the parasphenoid have been used as landmarks in an attempt to reconstruct the original position of the stapes. The stapes is placed in a dorsolateral orientation similar to that seen in *Eryops* (Sawin, 1941) and *Edops* (Romer & Witter, 1942).

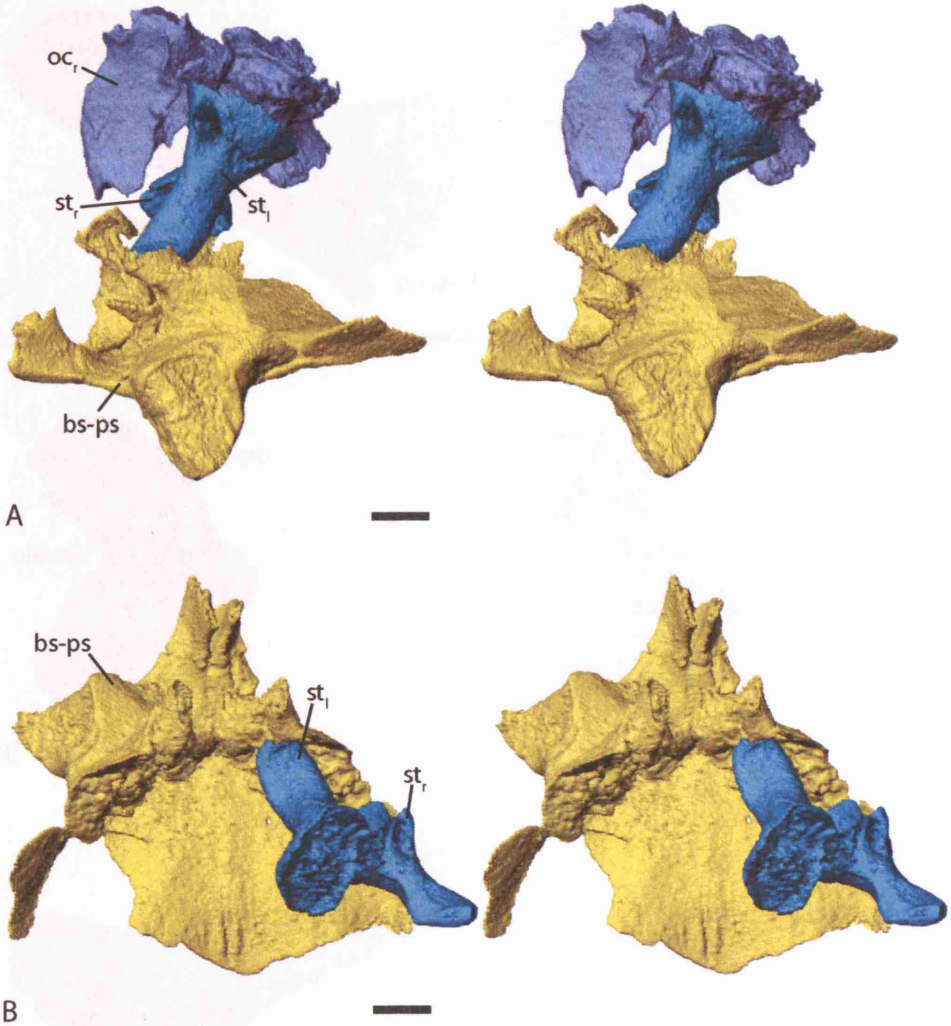

Figure 3.3.3—16 *Dendrerpeton* specimen BMNH R.436. Stereo pairs showing both stapes *in situ*. A, left anterolateral view of the basisphenoid-parasphenoid complex, the right otic capsule and both stapes. B, dorsal view of the basisphenoid-parasphenoid complex and both stapes. Scale bars = 2mm.

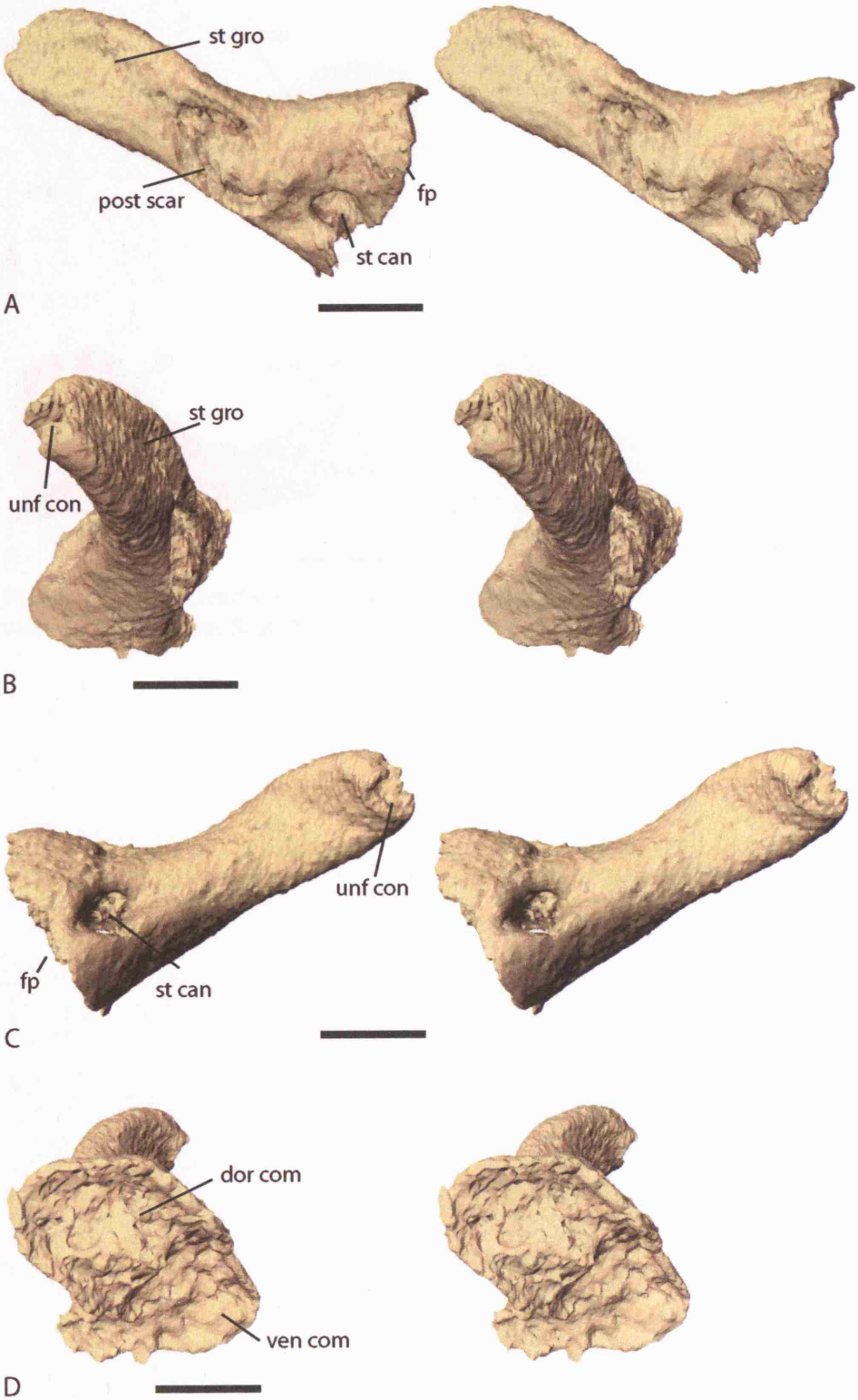

Figure 3.3.3—17 *Dendrerpeton* specimen BMNH R.436. Stereo pairs of the left stapes. A, posterior view. B, lateral view. C, anterior view. D, medial view. Scale bars = 2mm.

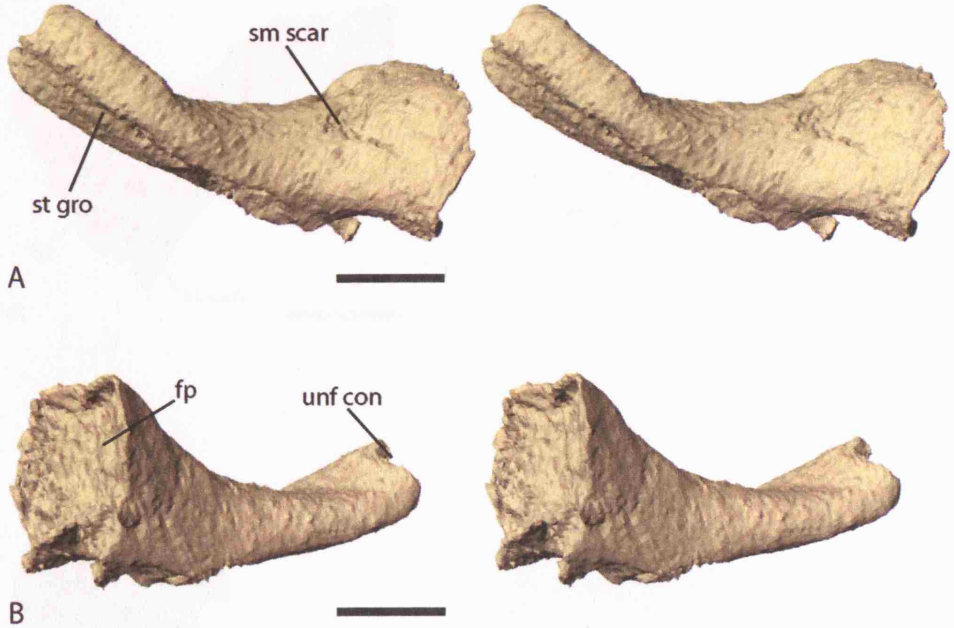

Figure 3.3.3—18 *Dendrerpeton* specimen BMNH R.436. Stereo pairs of the left stapes. A, dorsal view. B, ventral view. Scale bars = 2mm.

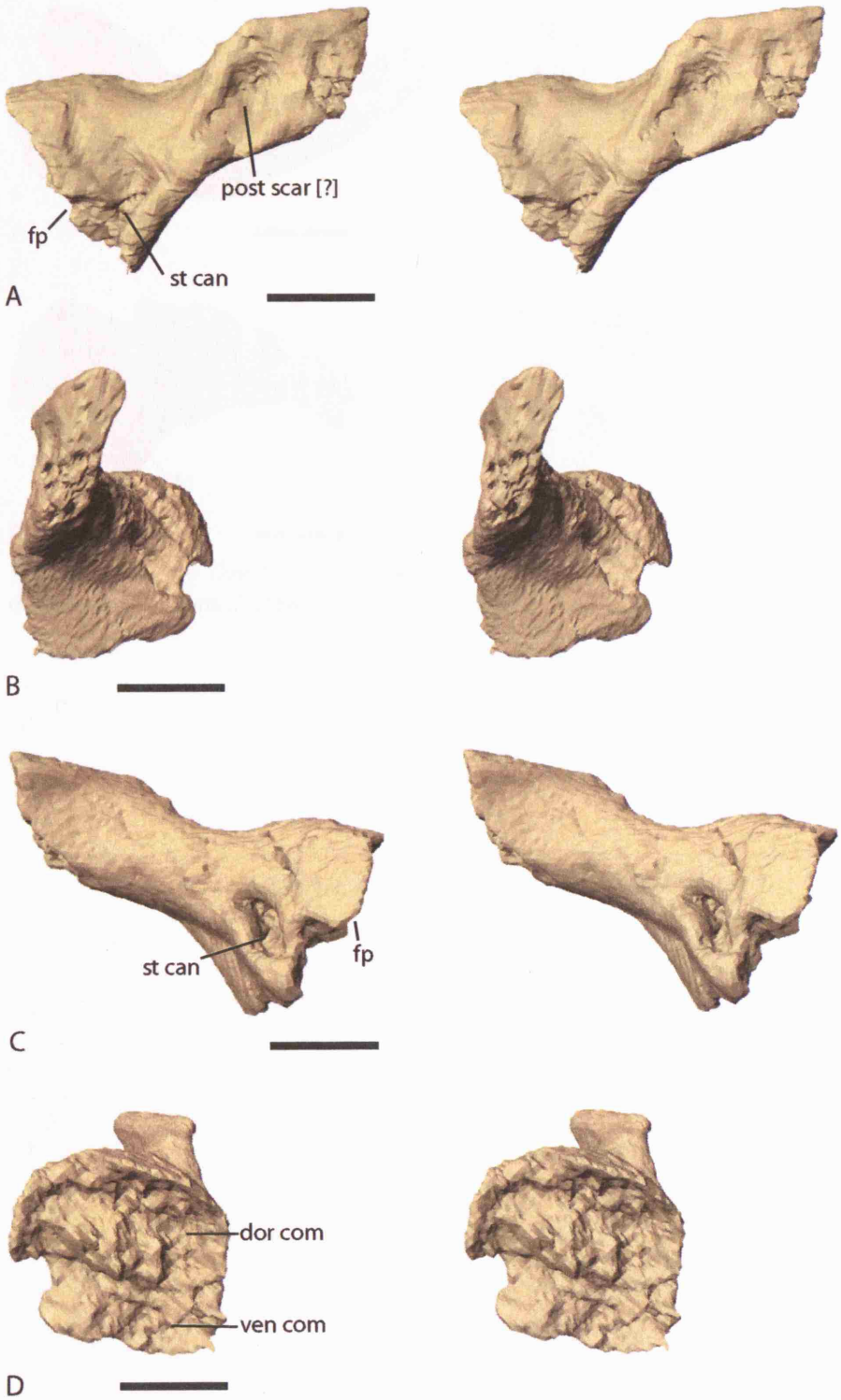

Figure 3.3.3—19 *Dendrerpeton* specimen BMNH R.436. Stereo pairs of the right stapes. A, posterior view. B, lateral view. C, anterior view. D, medial view. Scale bars = 2mm.

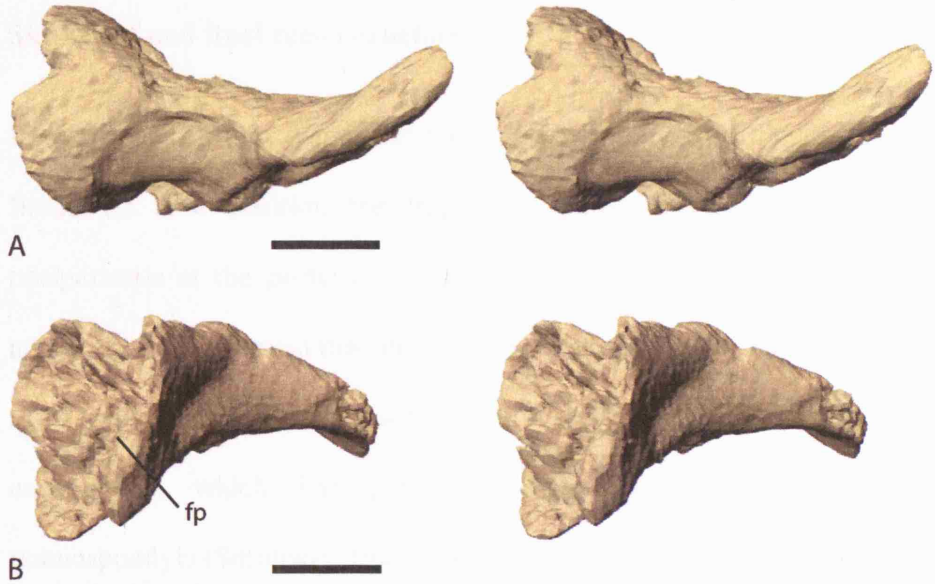

Figure 3.3.3—20 *Dendrerpeton* specimen BMNH R.436. Stereo pairs of the right stapes. A, dorsal view. B, ventral view. Scale bars = 2mm.

Skull roof and final reconstruction

It was impossible to demarcate the individual sutures of the fragmentary skull roof. Based on their position the fragments appear to consist of paired tabulars and postparietals at the posterior margin, with paired parietals and supratemporals more anteriorly. It is observed that the braincase is shifted to the right hand side relative to the skull roof. The postparietals send down ventral extensions posteriorly that contact the exoccipitals, which has previously been suggested as a synapomorphy of temnospondyls (Smithson, 1982). The ventral surface of the skull roof is separated from the otic capsules by a substantial gap that is, evidently, natural and must have been filled with cartilage. However, there is no direct evidence on the skull roof for such cartilaginous contacts with the otic capsules or epipterygoids.

It seems likely that BMNH R.436 came to rest with its cranium lying on its right hand side at death or soon after. With a certain degree of decomposition of the soft tissue, including cartilage, the internal cranial elements moved with gravity to the right hand side. This explains the lateral shift of the braincase relative to the skull roof and the movement of the basioccipital to the right hand side. Furthermore, this accounts for the translocation of the left stapes to its current position within the braincase, having passed through the enlarged decomposed fenestra ovalis. Fortunately, this displacement protected the left stapes from damage and rendered it the best preserved temnospondyl stapes known to date.

The skull of the specimen has been reconstructed with all the preserved elements in their presumed life positions (Figure 3.3.3—21, 22 and 23). As can be seen, the braincase of *Dendrerpeton* contains a melange of characters shared with basal temnospondyls such as *Edops* and more derived temnospondyls such as *Eryops*. The

form of the fenestra ovalis, the occipital condyle and palatoquadrate complex are more similar to the *Edops* condition. By contrast, the otic capsules and the basisphenoid-parasphenoid complex in *Dendrerpeton* resemble more those of *Eryops*. A more detailed phylogenetic comparison is limited by the lack of information on the internal cranial structures of other early temnospondyls. However, the observed character combination is clearly consistent with the currently favoured phylogenetic position of *Dendrerpeton*. This final reconstruction also demonstrates the stapes in its correct dorsolateral orientation, extending towards the temporal notch and having no contact with the palatoquadrate complex (Figure 3.3.3—22 and 23).

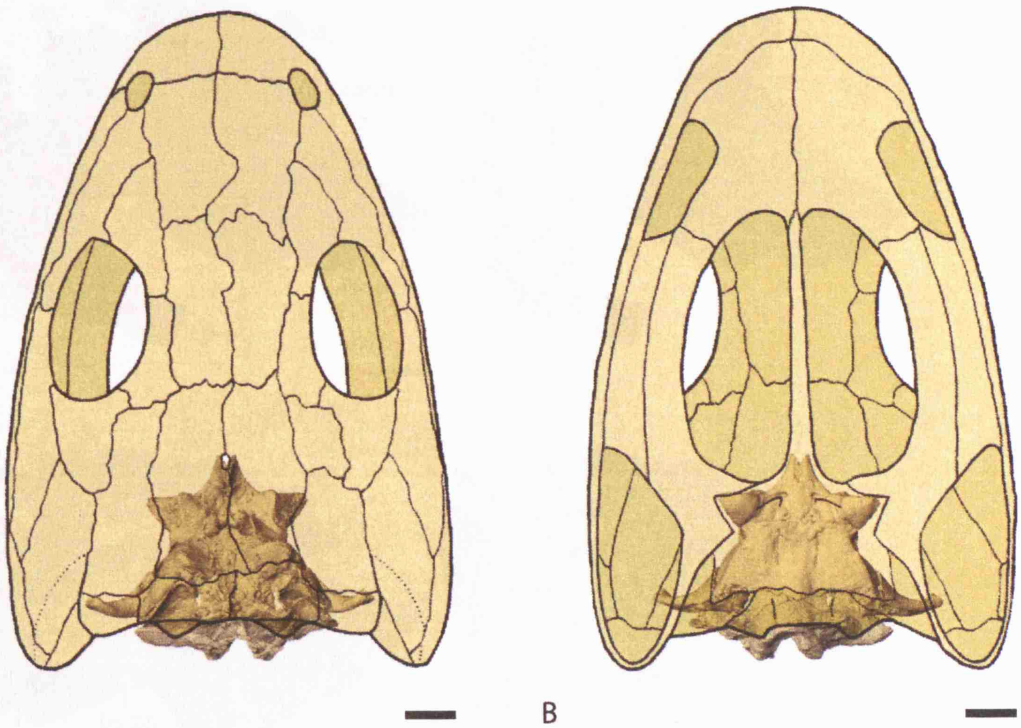

Figure 3.3.3—21 Final reconstruction of the braincase and associated elements of BMNH R.436 in approximate position in a full cranial reconstruction of *Dendrerpeton* (after Carroll, 1967) for orientation purposes. A, dorsal view. B, ventral view. Scale bars = 5mm.

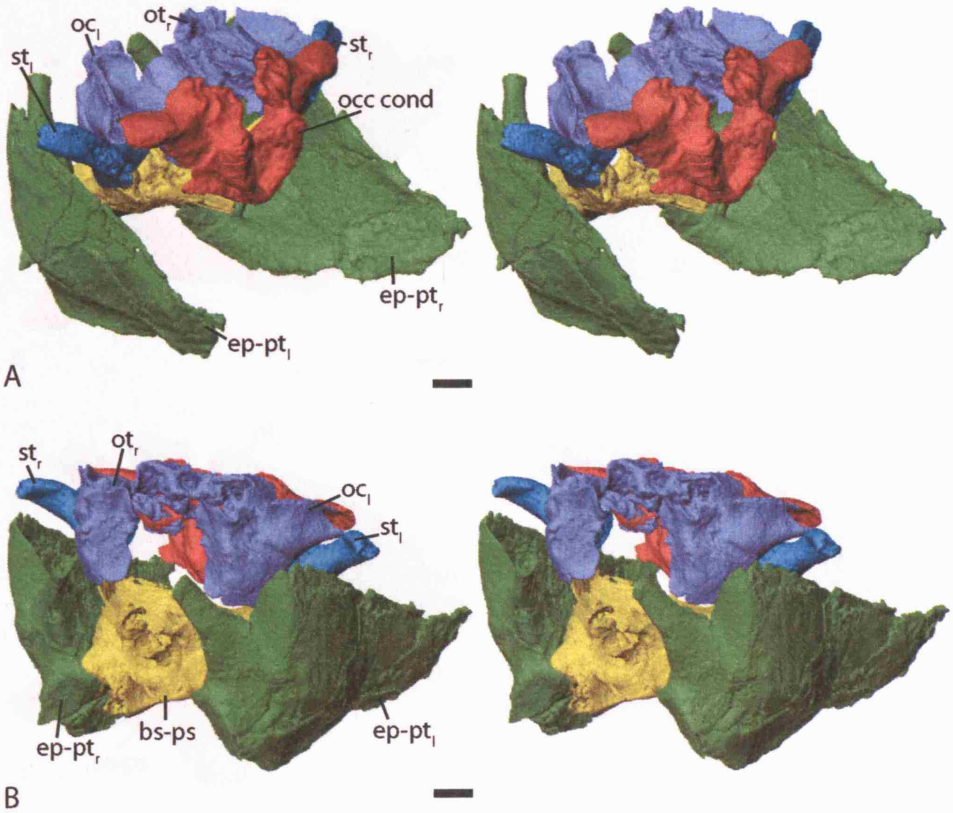

Figure 3.3.3—22 *Dendrerpeton* specimen BMNH R.436. Stereo pairs of the final reconstruction including both epipterygoid-pterygoid complexes. A, left posterolateral view. B, left anterolateral view. Scale bars = 2mm.

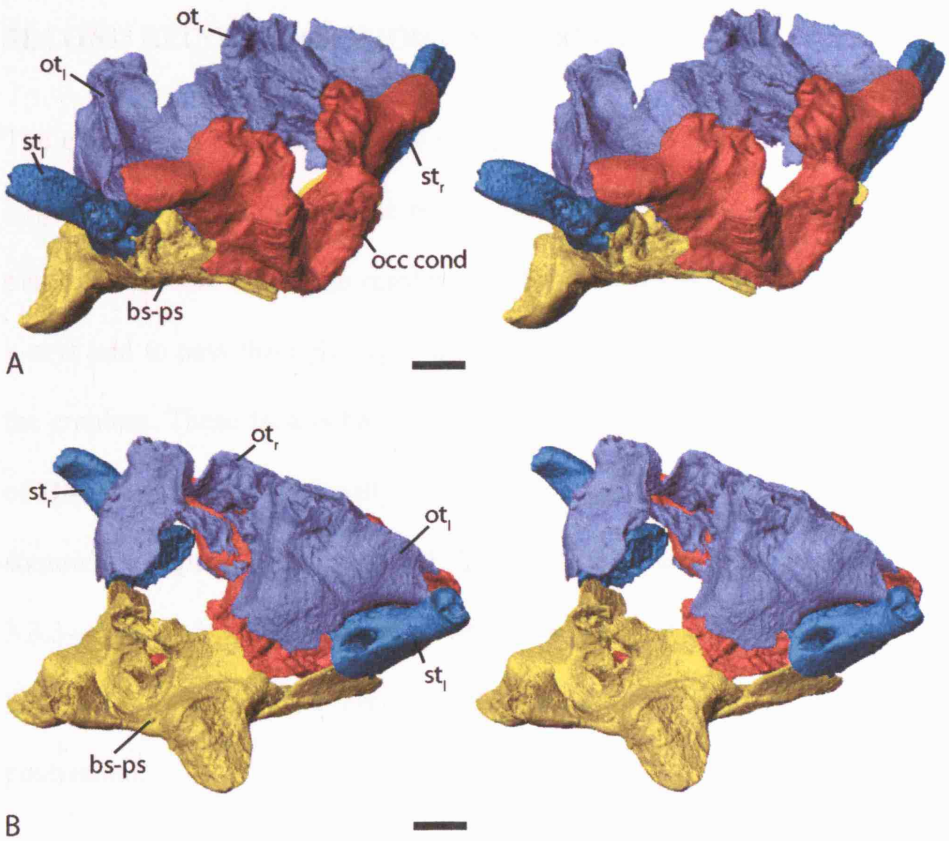

Figure 3.3.3—23 *Dendrerpeton* specimen BMNH R.436. Stereo pairs of the final reconstruction excluding both epipterygoid-pterygoid complexes. A, left posterolateral view. B, left anterolateral view. Scale bars = 2mm.

SECOND RECONSTRUCTION – NSM 987 GF 99.1

The cranium of NSM 987 GF 99.1 (Figure 3.3.1—3) has not been separated from the large block which contains the rest of the specimen. This means that it could not be placed within the ultra-high resolution subsystem scanner at UTCT. Due to its size the x-rays had to pass through large amounts of matrix and a metal support, in addition, to the cranium. These factors have contributed to relatively poor results compared to those of BMNH R.436. Additionally, it seems that the internal cranial structures have been somewhat displaced and distorted. The reconstruction of NSM 987 GF 99.1 (Figure 3.3.3—24 and 25) runs from the orbits to the back of the skull and includes aspects of the pectoral girdle. The cranial material will be described first followed by the postcranial.

CRANIAL

The cranial reconstruction (Figure 3.3.3—26 A and B) consists of the dermal skull roof and cheek region from the orbits backwards, aspects of the palatoquadrate complexes, the sphenethmoid, both otic capsules, the left stapes and the occipital complex. There are also numerous sclerotic plates (scl pla) from the right orbit and the posterior regions of the mandibles.

Skull roof, cheek region and palatoquadrate complexes

The skull roof has a certain degree of damage posteromedial to the left orbit which can be seen in Holmes et al.'s figure 3a (1998). Apart from this damage, the skull roof with its stereotypical ornament is essentially complete and undistorted. Of most interest are the large temporal notches (Figure 3.3.3—26 A), which reach from quadrate to tabular and have smoothed, unornamented surfaces. The morphology of the notches will be

considered along with the stapedial function and hearing abilities of *Dendrerpeton* in the discussion.

Both palatoquadrate complexes are present but are poorly resolved in the scans and reconstruction. Details of the complexes are, however, clearly shown in the description of BMNH R.436. The only additional information shown in NSM 987 GF 99.1 is the palatine branch of the left pterygoid. One point of note is that the palatoquadrates of NSM 987 GF 99.1 appear be far less vertical than those of BMNH R.436, although this could be a taphonomic effect.

Sphenethmoid

A small fragment of the sphenethmoid region (se) medial to the palatal vacuities is preserved (Figure 3.3.3—26 B). This poorly resolved structure has been slightly laterally displaced. It was approximately horseshoe shaped in cross section with a medial ventral ridge, presumably parasphenoid. Remarkably no more detail of the parasphenoid is seen in the scans of NSM 987 GF 99.1 even though visual inspection of the specimen clearly demonstrates its presence.

Otic capsules

Both otic capsules are present in this reconstruction. Along with the occipital region and the left stapes the otic capsules appear to have been swept posteriorly during the deposition of the specimen. This movement would also have caused the sclerotic plates to assume the position in which they have been found. Although both otic capsules are present neither is in anyway as well preserved or as informative as those of BMNH R.436. Their general form, however, can clearly be homologised with the capsules in the first *Dendrerpeton* reconstruction. A point of note, however, is that the size of the

otic capsules, in relation to the skull roof, appear to relatively larger in BMNH R.436 than those of NSM 987 GF 99.1. Due to the incomplete nature of the skull roof of BMNH R.436, and the otic capsules of NSM 987 GF 99.1, any difference should not be overly interpreted at this stage.

Left stapes

Only the proximal end of the left stapes of NSM 987 GF 99.1 could be modelled from the scan series due to its poor resolution. Although, no additional details on stapedial morphology can be gained from this reconstruction the stapedial foramen and the posterior notch in the footplate can clearly be observed.

Occipital complex

Resolution becomes increasingly poor towards the posterior region of the scan series because the specimen block gets progressively larger causing greatly increased levels of noise. Only the anterior extensions of the basioccipital can be roughly modelled in this region of the specimen.

Mandibles

The posterior regions of both mandibles (mand) are present in the second reconstruction of *Dendrerpeton* (Figure 3.3.3—26 C, D and E for details of the right mandible). The previous description by Holmes et al. (1998) gives a full account of the morphology. The only extra information gained from the scanning and 3D reconstruction is the shape of the mandibular articulatory surface (mand art) and fossa (mand foss) which is viewed in a dorsal perspective.

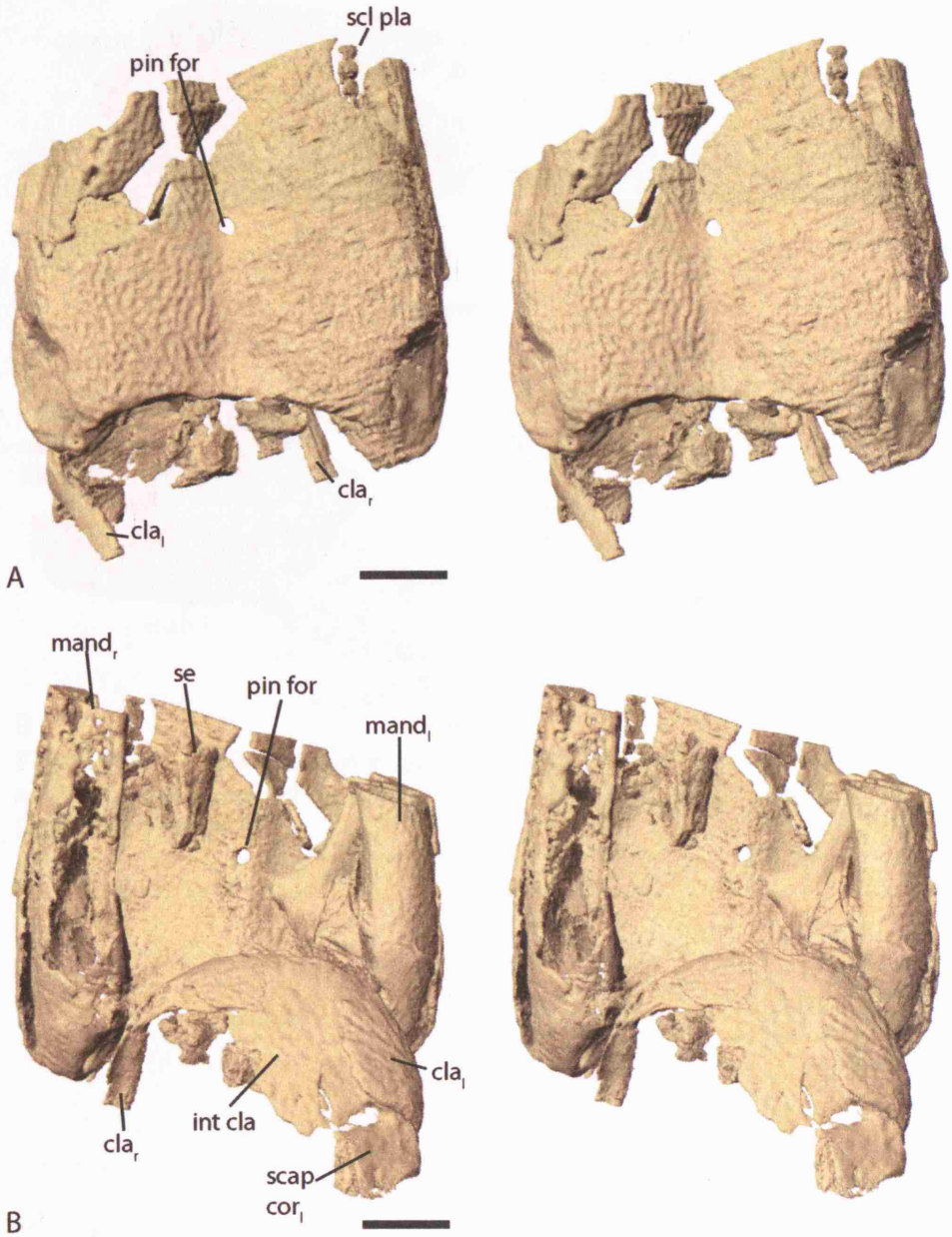

Figure 3.3.3—24 *Dendrerpeton* specimen NSM 987 GF 99.1. Mono colour stereo pairs of the model without correction for translocations or damage. A, dorsal view. B, ventral view. Scale bars = 10mm.

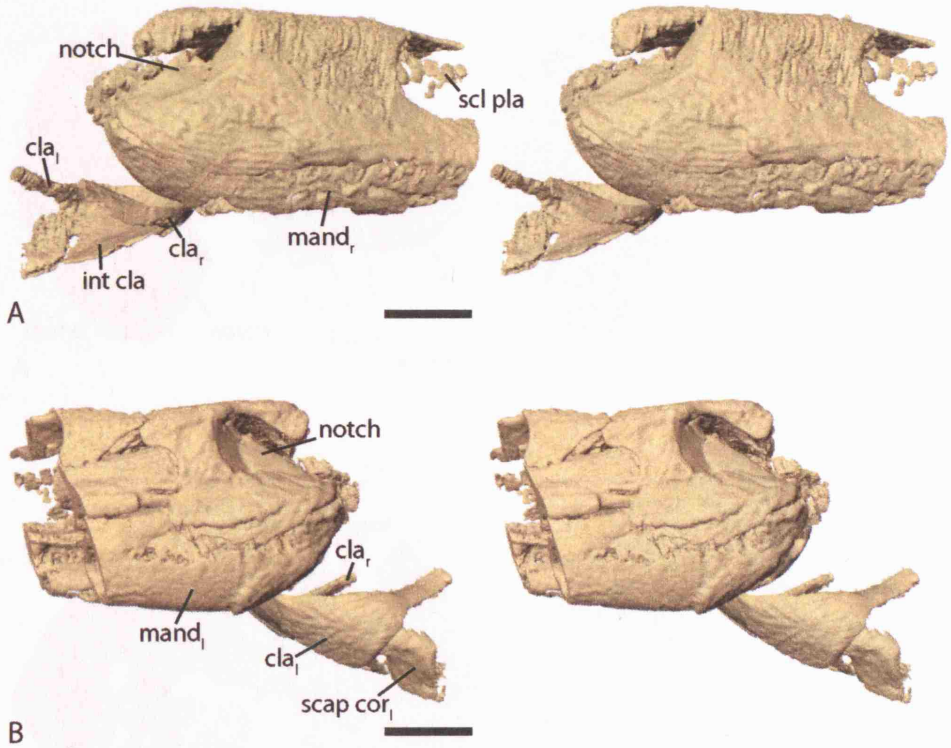

Figure 3.3.3—25 *Dendrerpeton* specimen NSM 987 GF 99.1. Mono colour stereo pairs of the model without correction for translocations or damage. A, right lateral view. B, left lateral view. Scale bars = 10mm.

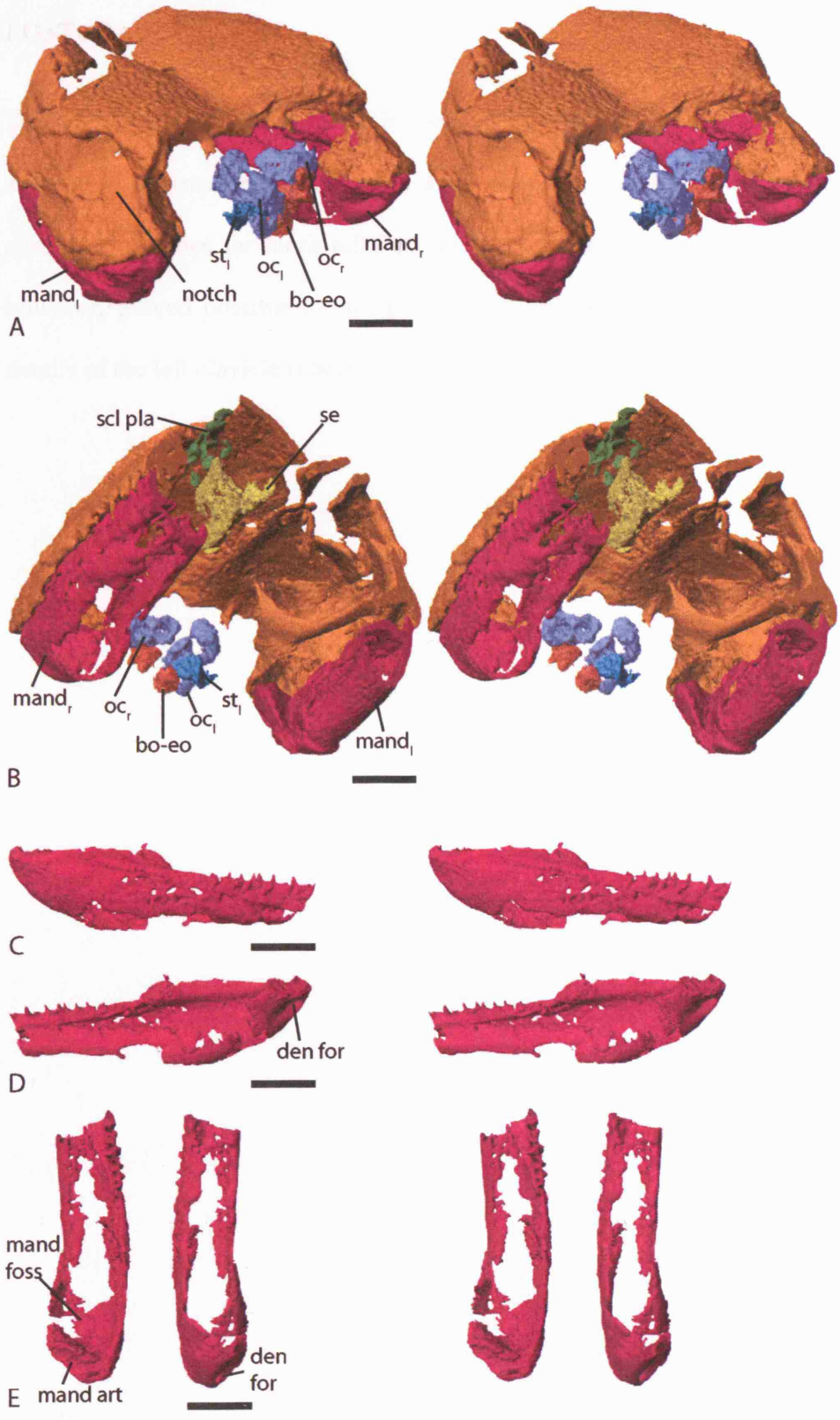

Figure 3.3.3—26 *Dendrerpeton* specimen NSM 987 GF 99.1. Stereo pairs. A and B, cranium. A, offset posterodorsal view. B, offset anteroventral view. C, D and E, right mandible. C, right lateral view. D, medial view. E, dorsal and ventral views. Scale bars = 10mm.

POSTCRANIA

Due to the increased noise levels in the posterior region of the scan series only certain aspects of the pectoral girdle have been resolved. In fact visual inspection of the specimen provides far more information (pers.obs. and Holmes et al. (1998)). It has, however, proved possible to isolate the clavicles (cla_l and cla_r) (Figure 3.3.3—27 for details of the left clavicle (cla_l)).

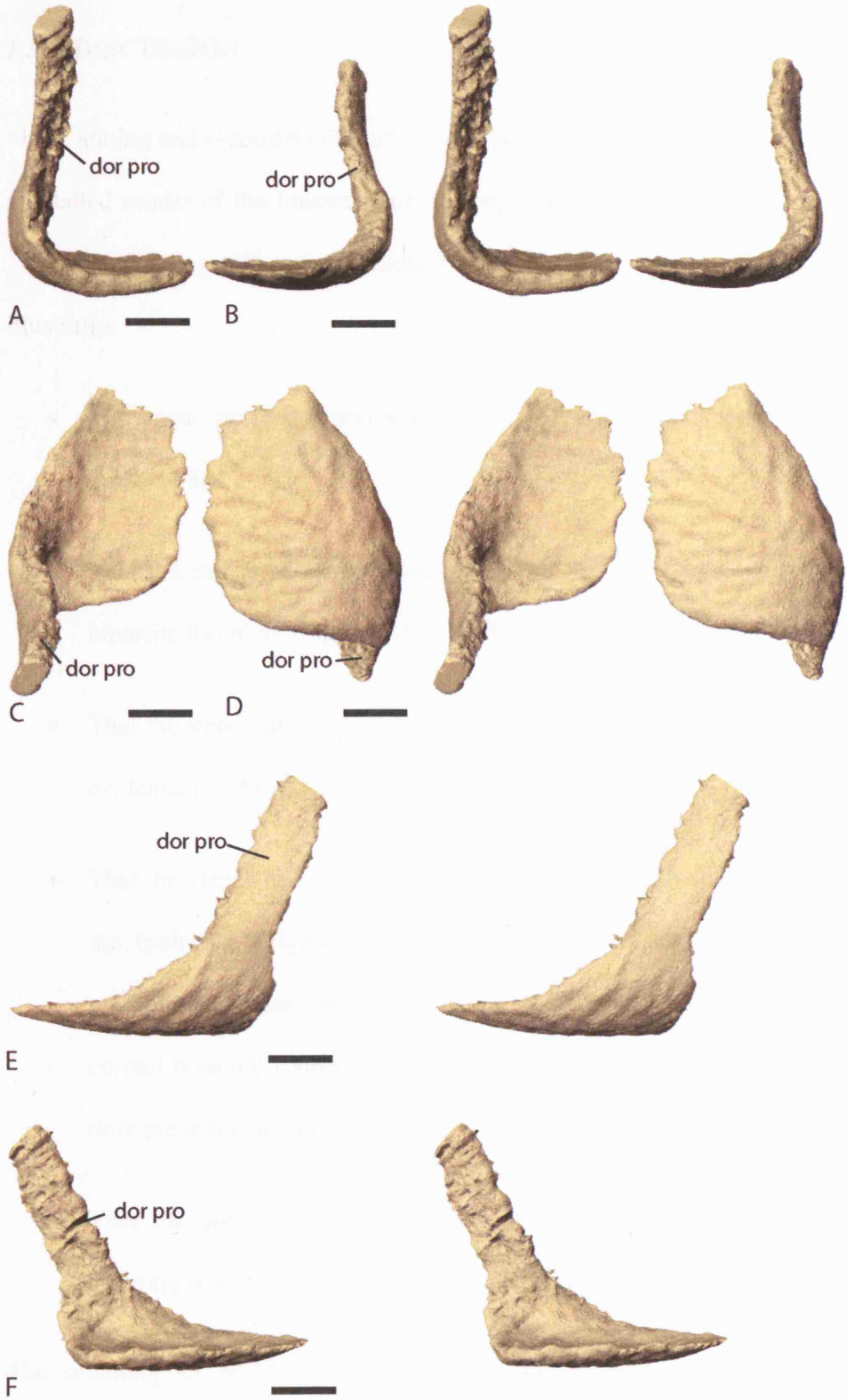

Figure 3.3.3—27 *Dendrerpeton* specimen NSM 987 GF 99.1. Stereo pairs of left clavicle. A, posterior view. B, anterior view. C, dorsal view. D, ventral view. E, left lateral view. F, medial view. Scale bars = 5mm.

3.3.4. DISCUSSION

The scanning and reconstruction of *Dendrerpeton* specimen BMNH R.436 has provided a detailed model of the braincase of this phylogenetically basal temnospondyl (Figure 3.3.4—1 A) along with a high resolution model of the left stapes. The reconstruction illustrates:

- The most perfectly preserved stapes of any temnospondyl known (Figure 3.3.4—1 B).
- That the stapes of *Dendrerpeton* was rod like and had a typical temnospondyl bipartite footplate (Figure 3.3.4—1 B and C).
- That the stapedial footplate contains a posterior notch which provides supportive evidence for the presence of an operculum (Figure 3.3.4—1 C).
- That the stapes had a scar on its posterior surface which does not point towards the braincase (Figure 3.3.4—1 D). Its position and morphology suggests a possible muscular connection to the shoulder girdle. If this interpretation is correct it would represent the earliest such evidence for such a system which is only present in extant anurans.
- That the preserved dorsal margins of the fenestrae ovales have allowed the accurate reorientation of the translocated stapes (Figure 3.3.4—1 E).

The scanning of NSM 987 GF 99.1 did not provide any additional information regarding the middle ear of *Dendrerpeton* but clearly demonstrates that large well defined temporal notches were present.

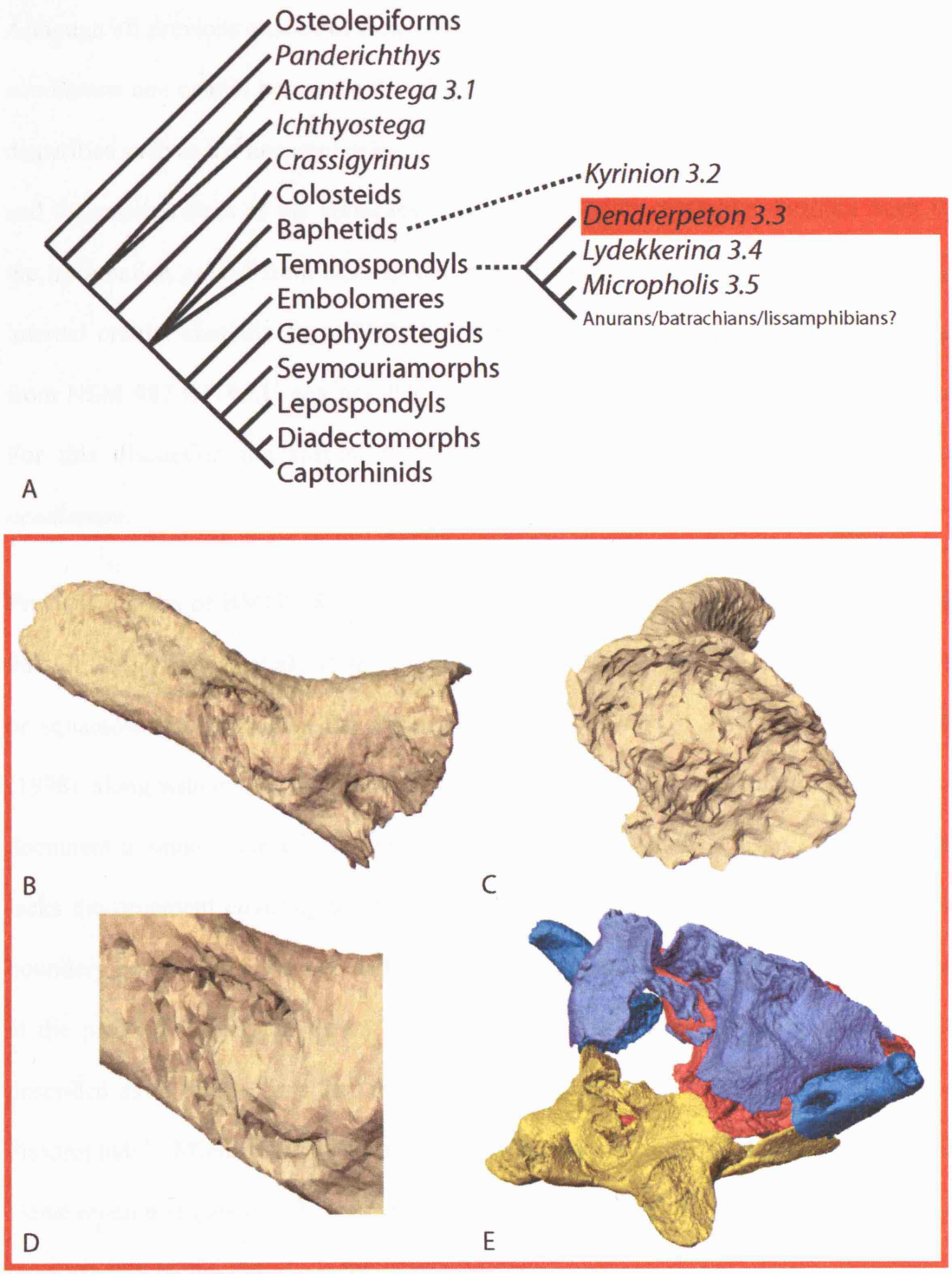

Figure 3.3.4—1 Summary *Dendrerpeton* figure - specimen BMNH R.436. A, basic phylogenetic consensus created from the early tetrapod phylogenies of Ruta et al. (2003) and Laurin & Reisz (1997) with temnospondyl detail from Ruta et al. (2003) and Yates & Warren (2000). B, posterior view of left stapes - see figure 3.3.3—17. C, footplate of left stapes - see figure 3.3.3—17. D, close up view of posterior scar on left stapes - see figure 3.3.3—17. E, anterolateral view of brain-case and stapes in reconstructed position - see figure 3.3.3—23. For scale bars see referred to figures.

Although all previous studies of these specimens have described them as *Dendrerpeton acadianum* one cannot be certain that they belong to the same species. There are a few disparities such as the apparent orientational difference of the palatoquadrate complexes and the relative sizes of the braincase to the overall skulls. However, because most of the information gained from each specimen is not comparable to the other (i.e. mainly internal cranial anatomy from BMNH R.436 whilst mainly external cranial anatomy from NSM 987 GF 99.1) any possible variation has to be taken with extreme caution. For this discussion the specimens as both treated as belonging to *Dendrerpeton acadianum.*

Previous studies of BMNH R.436 and other *Dendrerpeton* specimens, especially NSM 987 GF 99.1 (Holmes et al., 1998), show that *Dendrerpeton* possesses temporal notches or squamosal embayments. The description of NSM 987 GF 99.1 by Holmes et al. (1998), along with my personal observation of this specimen means that it is possible to document a smooth surface that extends anteriorly and ventrally from the notch and lacks the ornament covering the cheek and skull roof. A curved ridge runs along the boundary between this smooth surface and the ornamented skull. There is a protrusion at the posterior (quadrate) extent of this smooth surface which Holmes et al. (1998) described as 'a modest swelling that may be homologous to the dorsal process of the dissorophids'. Milner (1980) also mentions a similar process on the quadrate of *Dendrerpeton rugosum* in his review. This quadrate process and the curved ridge have been used by Holmes et al. (1998) to propose that *Dendrerpeton* may have possessed 'a frog-like tympanic ring'.

The morphology of the notch clearly suggests the presence of a tympanic ear, however, conclusive proof for a tympanic hearing system requires detailed information on the

middle ear. Before scanning and reconstructing BMNH R.436 its exposed right stapes, described by Clack (1983), was then the only reliably identified stapes of *Dendrerpeton* available for detailed analysis and interpretation. This stapes was compared most readily with that of *Pholiderpeton* (Clack, 1983) and not to the rod like stapes in other temnospondyls such as *Lydekkerina.* Holmes (2000) described the right stapes of BMNH R.436 as being large and 'hyomandibula-like'. Additionally, Godfrey et al. (1987) tentatively described a large ossified element medial to the quadrate ramus of the pterygoid in NSM 978 GF 53.1 as a stapes. Thus prior to the scanning and 3D reconstruction of BMNH R.436, *Dendrerpeton* was claimed to have a robust stapedial morphology, as also described in other early tetrapods such as, *Pholiderpeton* and *Acanthostega.* This morphology seems unlikely to have been coupled to a tympanic membrane.

Clearly there was an inconsistency between the external cranial anatomy, which strongly suggested the presence of a tympanic membrane, and the described stapedial morphology, whose form seemed incompatible with a tympanum coupled function. This inconsistency meant that studying the middle ear anatomy of *Dendrerpeton* was important in elucidating the hearing abilities of phylogenetically basal temnospondyls. Therefore, it was difficult to predict which of the questions posed in the introduction could be addressed by scanning and reconstructing the middle ear region. If the stapes was indeed most comparable to that of other early tetrapods such as *Pholiderpeton* rather than the rod like stapes expected of temnospondyls then *Dendrerpeton* could address questions regarding the transition from a possible supporting stapes to a stapes coupled to a tympanic membrane. Alternatively, if the previously described stapedial morphology was proved to be influenced by taphonomic distortion and/or misidentification then *Dendrerpeton* could help address questions regarding the origin

of a stapes coupled to a tympanic membrane. It could also help investigate the origin of numerous middle ear specialisations of extant amphibians.

The detailed figures of the middle ear and associated structures of *Dendrerpeton*, produced by the scanning and reconstruction of BMNH R.436 and NSM 987 GF 99.1, allow me to state with confidence the following:

- The paired notches on the posterior margin of the skull roof in *Dendrerpeton* (Figure 3.3.3—24 and 25) would have supported an approximately round tympanic membrane. These notches should therefore be termed 'otic notches' rather than 'temporal notches' or 'squamosal embayments'. There is no evidence, whatsoever, for an ossified element in the notch region as described by Laurin (2005) in the temnospondyl *Iberospondylus schultzei.*

- Each notch has a smooth internal surface which does not have the surrounding dermal ornament which covers the skull roof (Figure 3.3.3—24 and 25). This could reflect an out pocketing of the air filled middle ear space which would have contacted the medial surface of the tympanic membrane, as seen in extant anurans (Wever, 1985).

- A cartilaginous dorsal extension of the quadrate would have provided the posterior support for the tympanic membrane. The curved ridge forming the margin of the notch in NSM 987 GF 99.1 (Figure 3.3.3—25) provides evidence for a tympanic annulus which would have rested against this curved ridge.

- It now appears that the previous descriptions of the stapedial morphology of *Dendrerpeton* (Clack, 1983; Godfrey et al., 1987; Holmes, 2000) have indeed been influenced by taphonomic distortion and/or misidentification. It can be

seen that its right partially exposed stapes is distorted and incomplete (Figure 3.3.3—19 and 20) compared with the complete and undistorted left stapes of BMNH R.436 (Figure 3.3.3—17 and 18). Additionally, the element tentatively identified as a stapes in NSM 978 GF 53.1 may actually represent a branchial or possibly vertebral element. The willingness of Godfrey et al. (1987) to identify this element as a stapes seems likely to be due to the prior description of the right stapes of BMNH R.436 (Clack, 1983) rather than any specific anatomical features present on the element.

- The stapes of *Dendrerpeton* was not like those described in *Pholiderpeton* and *Greererpeton*; it was not robust or hyomandibula-like. In fact, from the rod like left stapes of BMNH R.436 (Figure 3.3.3—17 and 18) it can be seen that in many respects the stapes is that of a typical temnospondyl.

- The stapes has a bi-partite footplate (Figure 3.3.3—17) as also seen in a range of temnospondyls (such as *Lydekkerina*, *Doleserpeton* (Bolt & Lombard, 1985; Lombard & Bolt, 1988) and *Micropholis*) and also *Kyrinion*. The unfinished appearance and raised margin of the footplate suggests that it would have been finished in cartilage. This cartilaginous component can be thought of as at least functionally equivalent to the pars interna present in extant anurans.

- The ventral component of the footplate has a rather triangular form which is anteroposteriorly elongate (Figure 3.3.3—17), although not to the same extent as seen in *Kyrinion*. There is no positional information available for the left stapes of BMNH R.436. However, from comparison with other temnospondyls and also the right stapes it seems clear that this ventral component would have contacted, but not fused with the, lateral wing of the parasphenoid.

- The dorsal component of the footplate is far larger than the ventral (Figure 3.3.3—17) as is also the case in *Dendrerpeton*, *Lydekkerina* and *Micropholis*. This component would have contacted the perilymphatic space of the inner ear via cartilage as envisaged would also have been the case with most early tetrapods, such as *Acanthostega* and *Kyrinion*.

- In the posteroventral margin of the footplate there is a distinct notch (Figure 3.3.3—17) which has been described in a range of temnospondyls and previously homologised to a notch in the posteroventral footplate margin of extant anurans (Bolt & Lombard, 1985). This notch in extant anurans articulates with the opercular element within the fenestra ovalis (Bolt & Lombard, 1985) and may, therefore, be evidence for an operculum in *Dendrerpeton*.

- Lateral to the footplate there is a stapedial foramen which runs anteroposteriorly (Figure 3.3.3—17).

- On the posterior surface of the stapes, lateral to the stapedial foramen, there is a pronounced horseshoe shaped scar (Figure 3.3.3—17). This seems likely to represent a muscle scar rather than evidence for a cartilaginous process. The function of this scar in *Dendrerpeton* cannot be determined with certainty, but its posterior and somewhat lateral orientation renders a connection with the otic capsule unlikely (and thus discounts a stapedius muscular connection). Its orientation rather suggests a muscular connection to the shoulder girdle comparable to the columellaris muscle (Wever, 1979; Wever, 1985) or a branch of the levator scapulae superior muscle (Hetherington, 1987; Hetherington & Lombard, 1983) of anurans. If this is the correct interpretation, then

Dendrerpeton possesses the earliest known example of a muscular connection between stapes and shoulder girdle as seen in extant lissamphibians.

- At the distal end of the stapes there is an unfinished concavity (Figure 3.3.3—17) which is also observed in *Lydekkerina*. It is believed, from comparison with extant anurans, that this is for a distal cartilaginous extension to the stapes. This cartilaginous extension to the stapes may be homologous to the extrastapes or pars externa of extant anurans which connects the stapes to the tympanic membrane (there is no direct connection).

- The orientation of the stapes can be estimated from the right stapes of BMNH R.436 and the relative position of the braincase and palatoquadrate complexes. Each stapes had a dorsolateral orientation reaching towards an otic notch (Figure 3.3.3—22 and 23). The ventral footplate contacted, but did not fuse with, the lateral wing of the parasphenoid while the dorsal component would have contacted the perilymphatic space of the inner ear. The stapes does not contact the palatoquadrate but sits within a well defined space between the braincase and the palatoquadrate complex. This space represents the middle ear cavity.

- The stapes was coupled to a tympanic membrane via a cartilaginous extension or extrastapes. The stapes did not have a supportive function; there can be little doubt that it was adapted for transmitting airborne sound.

Before reviewing the questions which the scanning and reconstruction of *Dendrerpeton* may address it is interesting to compare its stapes with that of another modestly sized temnospondyl, *Doleserpeton annectens*. Comparison to such modestly sized rather than large examples is advantageous because early large temnospondyls lack allometric

scaling of the stapes relative to the rest of the skull. Their stapes can become quite massive (see *Eryops* (Sawin, 1941)) and would certainly have had different sound transmission properties. The stapes of the far more derived *Doleserpeton annectens,* a dissorophoid temnospondyl, has a well characterised morphology (Bolt & Lombard, 1985; Lombard & Bolt, 1988).

The left stapes of *Dendrerpeton* is approximately 9mm long compared to the left stapes of *Doleserpeton* depicted by Lombard & Bolt (1988) which is approximately 1.6mm long. The ratio of skull width to stapedial length for *Dendrerpeton* is approximately 4.3:1 while for *Doleserpeton* the ratio is approximately 5:1 (based on the 'composite drawing of skull of *Doleserpeton*' (Bolt, 1969)). Therefore, although the two stapes differ greatly in length, the ratio of skull width to stapedial length are comparable.

The stapes of both *Dendrerpeton* and *Doleserpeton* share many characters with those of other temnospondyls, including the anteroposteriorly directed stapedial foramen and the bipartite footplate with a flat ventral margin. Beyond these similarities, the two stapes share a marked concavity or scar on their posterior surface, lateral to the stapedial foramen (a rugose surface is seen in a similar position in *Trimerorhachis* (Lombard & Bolt, 1988)). The presence of similar posterior scars on the stapes of *Doleserpeton* and *Trimerorhachis* could, possibly, indicate the presence of a muscular connection to the shoulder girdle as postulated above in *Dendrerpeton.* The presence of a small groove running from this scar to the distal end of the stapes is also shared by *Dendrerpeton* and *Doleserpeton,* although the significance of this groove is uncertain.

Despite the numerous similarities between the two stapes there are noticeable differences in the size and form of the stapedial footplate. In *Doleserpeton* its ventral component is not triangular in shape as in *Dendrerpeton,* and is only comprised of a flat

ventral margin (Bolt & Lombard, 1985; Lombard & Bolt, 1988). Although, the posterior extension of the flat ventral margin in *Dendrerpeton* is clearly homologous to that of *Doleserpeton,* it is narrower. The dorsal part of the footplate of *Dendrerpeton* is concave, like that of *Doleserpeton*, but has a more unfinished surface that suggests a larger cartilaginous component.

It is interesting to compare the dorsolateral stapedial orientation seen in *Dendrerpeton*, *Edops* (Romer & Witter, 1942), and *Eryops* (Sawin, 1941) with the more lateral orientation suggested for the stapes of *Doleserpeton* (Bolt & Lombard, 1985; Lombard & Bolt, 1988) and *Micropholis*. The dorsolateral flange of the parasphenoid and the dorsal fenestra ovalis margin in the otic capsule determine the orientation of the stapedial footplate surface in *Dendrerpeton.* While the stapedial footplate surface in *Doleserpeton* runs vertically, that of *Dendrerpeton* is oriented at an approximate 45° angle. The similar morphology of the two stapes suggests that *Doleserpeton* had a more dorsally directed stapes than previously assumed or more likely that the orientation of the fenestra ovalis is different (vertical instead of angled at 45°). If the orientation seen in *Dendrerpeton* and other early temnospondyls is the ancestral condition for temnospondyls then the different orientation seen in *Doleserpeton* necessitates different braincase morphology. This presumed remodelling of the braincase would involve lateral expansion of the perilymphatic space under the inner-ear labyrinths, possibly, producing a lateral chamber of the perilymphatic space as seen in lissamphibians (Wever, 1985). Alternatively, the vertical orientation of the fenestra ovalis could have been produced by a medial contraction of the ventral margin. Clearly further investigation of this area is needed.

The above synopsis of middle ear anatomy and function demonstrates that *Dendrerpeton* has provided evidence for addressing questions posed within the neontological section of the introduction rather than those within the palaeontological section. *Dendrerpeton*, a phylogenetically basal temnospondyl from the early Late Carboniferous, possessed an ear adapted to the perception of airborne sound. It is one of the earliest tetrapods which can be stated reliably to have possessed a tympanic membrane and thus demonstrates that phylogenetically basal temnospondyls are likely to have been the first tetrapod group to have had such a system.

The detailed anatomy of the middle ear region revealed from the scanning and reconstruction of BMNH R.436 suggests that numerous character states observed in extant lissamphibians may have been present in temnospondyls. The posterior scar observed on the left stapes is plausible osteological evidence for the presence of a columellaris muscle (or branch of the levator scapulae superior) connecting the stapes to the shoulder girdle in temnospondyls. The presence of a similar scar on the stapes of both *Doleserpeton* and *Trimerorhachis* adds weight to this conclusion. Furthermore, the presence of a distinct notch in the posteroventral margin of the stapedial footplate in *Dendrerpeton* is, possibly, evidence for the presence of an opercular apparatus in this phylogenetically basal temnospondyl. It should be noted, however, that both these structures cannot be conclusively proved to be present in *Dendrerpeton* because this would require soft-tissue preservation (in extant anurans even the operculum is rarely ossified) which, of course, is not present in any *Dendrerpeton* specimen.

3.4. LYDEKKERINA

Lydekkerina is a stereospondyl temnospondyl. It is generally claimed that *Lydekkerina* along with many higher temnospondyls possessed a rod like stapes coupled to a tympanic membrane. The stapes of *Lydekkerina* has been figured on many previous occasions (see for example Watson (1919), Broili & Schröder (1937) and Parrington (1948)), although, there are many aspects of uncertainty regarding its true form. A detailed investigation into the middle ear and associated structures of *Lydekkerina* using CT scanning and 3D reconstruction will facilitate a more complete understanding of the stapedial morphology of this historically important specimen and also help address the following questions which were raised in the introduction:

- When did a tympanic membrane coupled to a stapes first evolve in tetrapods and in what group was this?
- When is the first evidence of a muscle connecting the stapes to the shoulder girdle?
- When did the opercular apparatus evolve in tetrapods and in what group was this?
- Did the common ancestor of batrachians, lissamphibians or all tetrapods possess an opercular apparatus?
- When is the first evidence of a muscle connecting the opercular apparatus to the shoulder girdle?

Although it has never been suggested that stereospondyls gave rise to all or some of the extant amphibian groups the anatomy of *Lydekkerina* can be used to inform us of the

character states of higher temnospondyls in general that need clarification. It should also be noted that *Lydekkerina*, as a stereospondyl, is a small number of nodes closer to the dissorophoid temnospondyls than *Dendrerpeton* (Robinson et al., 2005). As dissorophoids are frequently implicated in the origin of some, or all, of the extant amphibian orders (see for example Ruta et al. (2003a)) it might be expected that *Lydekkerina* will possess some additional characteristics with the extant amphibians. Thus it was decided to scan and reconstruct a specimen of *Lydekkerina* to investigate the hearing abilities of higher temnospondyls and to explore the possibility that middle ear characteristics, such as the opercular system, may have been present in temnospondyls. Such observations will greatly help in assessing the relationship between the hearing anatomy of temnospondyls and anurans, batrachians or lissamphibians as a whole.

See *Lydekkerina* Discussion 3.4.4 and Figure 3.4.4—1 for a synopsis of the morphology revealed from the reconstruction of UMZC T.242 and how this has helped address the above questions.

3.4.1. BACKGROUND

In 1889 Lydekker assigned specimens BMNH R.506-508 from the Karoo system of the Orange Free State to the new species *Bothriceps huxleyi* Lydekker, 1889. The type specimen for this new species was BMNH R.507 (Lydekker, 1889). A broader description of *Bothriceps huxleyi* (including BMNH R.506-508 and BMNH R.504-505) was published the following year (Lydekker, 1890) including a dorsal figure of the type specimen. The lower jaw of *Bothriceps huxleyi* was subsequently described by Watson (1912) based on specimens BMNH R.504-508.

In 1915 Broom examined four skulls of *Bothriceps huxleyi* at the then British Museum of Natural History, however it is unclear which of the previously mentioned BMNH specimens these were. He also examined some specimens at the Bloemfontein Museum and questioned the positioning of *Bothriceps huxleyi* in the same genus as *Bothriceps australis* Huxley, 1859 (Broom, 1915). He renamed the specimens previously called *Bothriceps huxleyi* as *Lydekkerina huxleyi* in honour of the recently deceased Lydekker (Broom, 1915). This publication also featured the first diagrammatic representation of the skull roof suture pattern in *Lydekkerina huxleyi*. Broom (1930) subsequently described two additional species *Lydekkerina dutoiti* Broom, 1930 and *Lydekkerina putterilli* Broom, 1930. The first detailed description of *Lydekkerina huxleyi* was undertaken by Watson (1919) based on the seven skulls at the then BMNH (one skull in each of BMNH R.505-508 and three skulls in BMNH R.504). Broili and Schröder's (1937) description added more detail including information on the atlas-axis complex. Parrington (1948) described two additional specimens of *Lydekkerina huxleyi* along with a specimen labelled *Lydekkerina*, sp. indet. which was figured with an unusual stapedial morphology along with details of the cervical vertebrae. Subsequently two

additional species, *Lydekkerina kitchingi* Broom, 1950 and *Lydekkerina panchetensis* Tripathi, 1969, were added to the genus. A recent review of the composition of the Lydekkerinidae, (Shishkin, Rubidge & Kitching, 1996), stated that a maximum of two species are present in the genus *Lydekkerina*; *Lydekkerina huxleyi* and *Lydekkerina panchetensis*, *Lydekkerina dutoiti* having been renamed *Broomulus dutoiti* by Romer, 1947 and *Lydekkerina putterilli* and *Lydekkerina kitchingi* being referred to as 'non-lydekkerinid taxa formerly assigned to Lydekkerinidae' (Shishkin et al., 1996).

The genus *Lydekkerina* is part of the family Lydekkerinidae which according to Shishkin et al. (1996) also contains the 'principal' genera *Eolydekkerina*, *Broomulus*, *Chomatobatrachus* and *Luzocephalus*. The genera *Limnoiketes* Parrington, 1948 and *Putterillia* Broom, 1930 are claimed by Shishkin et al. (1996) to be specimens of *Lydekkerina*.

Lydekkerinidae is in turn part of the stereospondyls, a group of temnospondyls which stretched from the Permian to the Cretaceous. Stereospondyli includes the mastodonsaurids/capitosaurids and the trematosaurids which together are the sister group to the more basal rhinosuchids (Damiani, 2001; Pawley & Warren, 2005; Yates & Warren, 2000). The position of Lydekkerinidae within the Stereospondyli changes frequently. *Lydekkerina* has been placed within the capitosaurs (Yates & Warren, 2000), as part of a polytomy derived from the rhinosuchids (Milner, 1990) and as the sister group to the clade containing mastodonsaurids/capitosaurids and the trematosaurids with rhinosuchids being more basal (Pawley & Warren, 2005). It does, however, appear that the genus *Lydekkerina* is a phylogenetically relatively basal stereospondyl. It should be noted at this stage that stereospondyls are not defined by the presence of

stereospondylus vertebrae – many groups including *Lydekkerina* have rhachitomous vertebrae with separate intercentra and paired pleurocentra.

It was decided to scan and reconstruct a specimen of *Lydekkerina huxleyi* in order to have a greater understanding of the hearing structures of this well known temnospondyl which is generally accepted to have had the ability to hear airborne sounds. The scanning and reconstruction will also provide information on the internal cranial anatomy of *Lydekkerina* and details of the postcranial morphology which despite recent work (Pawley & Warren, 2005) is still not fully characterised.

Lydekkerina huxleyi specimen UMZC T.242 (Figure 3.4.1—1 A and B) was chosen for this study because it has been partly but not fully prepared and has little or no distortion. Additionally, UMZC T.242 has an articulated series of cervical vertebrae and most of the pectoral girdle. The specimen was collected by Parrington in 1964 from Harrismith, South Africa (Lystrosaurus zone, Early Triassic). It forms part of the F. R. Parrington Collection at the University Museum of Zoology Cambridge. To the author's knowledge this specimen has never been figured or described in any previous publication.

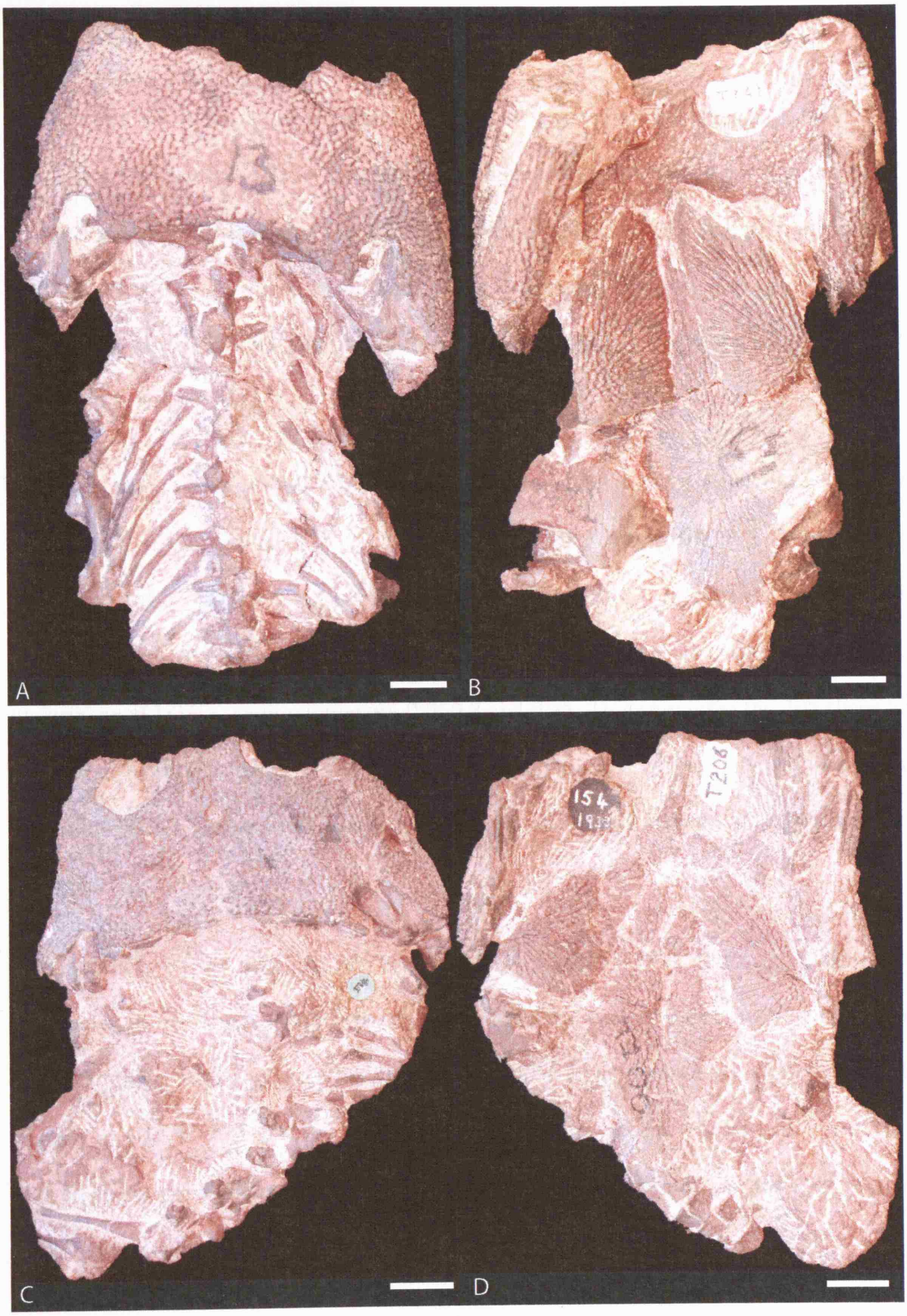

Figure 3.4.1—1 A and B, *Lydekkerina* specimen UMZC T.242. A, dorsal view. B, ventral view. C and D, *Lydekkerina* specimen UMZC T.206. C, dorsal view. D, ventral view. Scale bars = 10mm.

3.4.2. RECONSTRUCTION PARAMETERS

Lydekkerina specimen number UMZC T.242 was scanned on the ultra-high resolution subsystem scanner at UTCT. The scan was produced with 1000 views per rotation and 2 samples per view. This means that each slice was produced from a sinogram containing 1000 views with each being a combination of two samples to improve image quality. 15 slices were produced with each rotation of the specimen meaning that it was rotated 47 times within the x-ray field.

A single scan series of the whole specimen (cranial and postcranial material) was produced in 16bit resolution (512 pixels by 512 pixels), comprising 705 slices each of 0.15388mm thickness (i.e. approximately 6.5 slices per mm). In order to improve the slice image quality the scan data was processed with a beam hardening algorithm, undertaken at UTCT, with parameters 0.0, 0.8 and 0.25. This converted the 705 slices to 16bit with resolution 1024 pixels by 1024 pixels. The field of view for all slices was 73.61mm giving a pixel size of 0.072mm for the slices with resolution 1024 pixels by 1024 pixels.

The large size of the data set, 705 slices at 1024 pixels by 1024 pixels, prohibited the processing in one stack within Mimics. To resolve the issue the data set was split into two contiguous stacks. The 395 anterior most slices which contain all cranial material present in UMZC T.242 were imported into Mimics to model cranial structures. The 485 posterior most slices, including 175 slices containing some of the posterior region of the skull, were imported into Mimics to model the postcranial material.

Both stacks were interpreted within Mimics with the contrast set at -1014 to 3071 for maximum visualisation of the fossilised material relative to the matrix. Although the

fossilised material of UMZC T.242 was on the whole lighter in colour than the matrix in the CT slices there was significant noise which prevented the rapid modelling of the fossilised material using the general thresholding tool. Therefore, manual thresholding and drawing tools were utilised within Mimics to select accurately fossilised material and exclude matrix from the final model.

Elements modelled from the stack created from the posterior most 485 slices were imported into Rhino3D with no alteration of coordinates. In order to marry accurately these elements with those from the stack, created from the anterior most 395 slices, altered coordinates had to be used. The three coordinates x, y and z correspond approximately to mediolateral, dorsoventral and anteroposterior of the specimen respectively. For elements from the stack created from the anterior 395 slices the x and y values were zero and the z value was 47.70mm. This created a very large Rhino3D file, therefore, for more stable processing separate Rhino3D files for cranial and postcranial elements were also created. A smoothing transformation over all world coordinates with a factor of 1.5 was used to improve the appearance of the reconstruction whilst not removing any important details.

3.4.3. DESCRIPTION

The scanning and 3D reconstruction of UMZC T.242 (Figure 3.4.3—3 and 4) has revealed details of both the cranial and postcranial skeleton. The cranial elements will be described first followed by the postcrania.

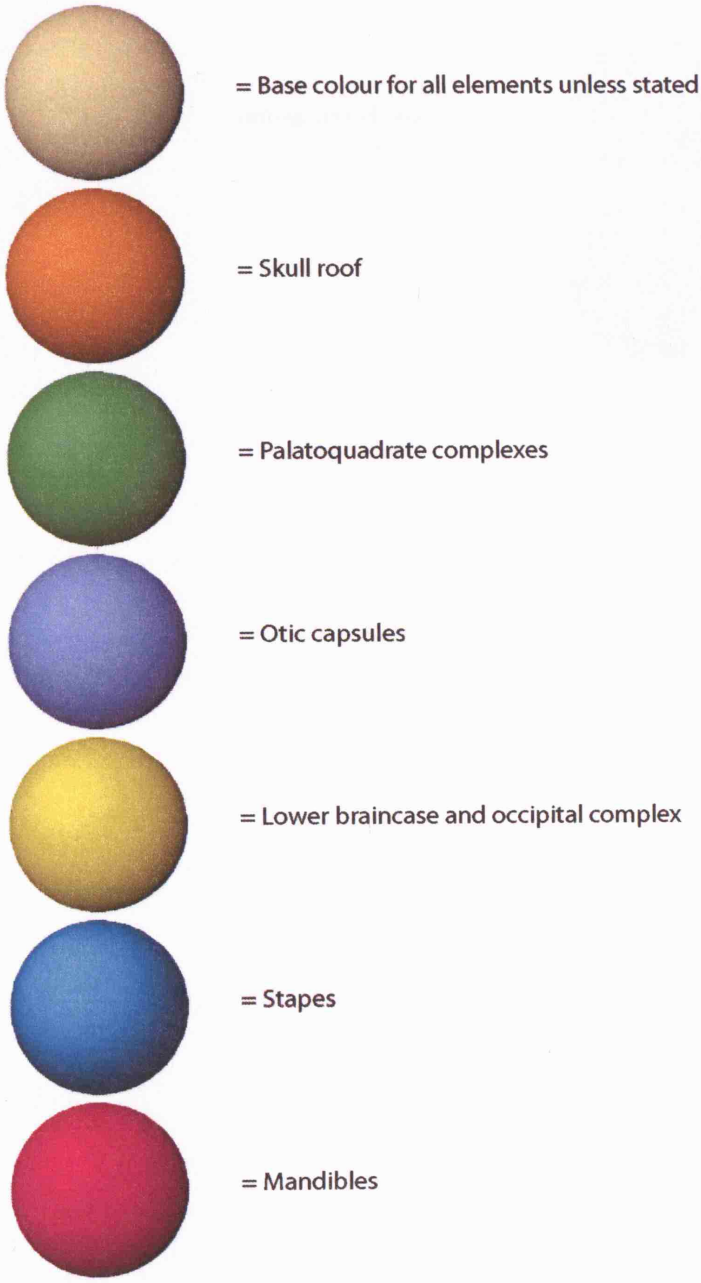

Figure 3.4.3—1 Colour key – cranial.

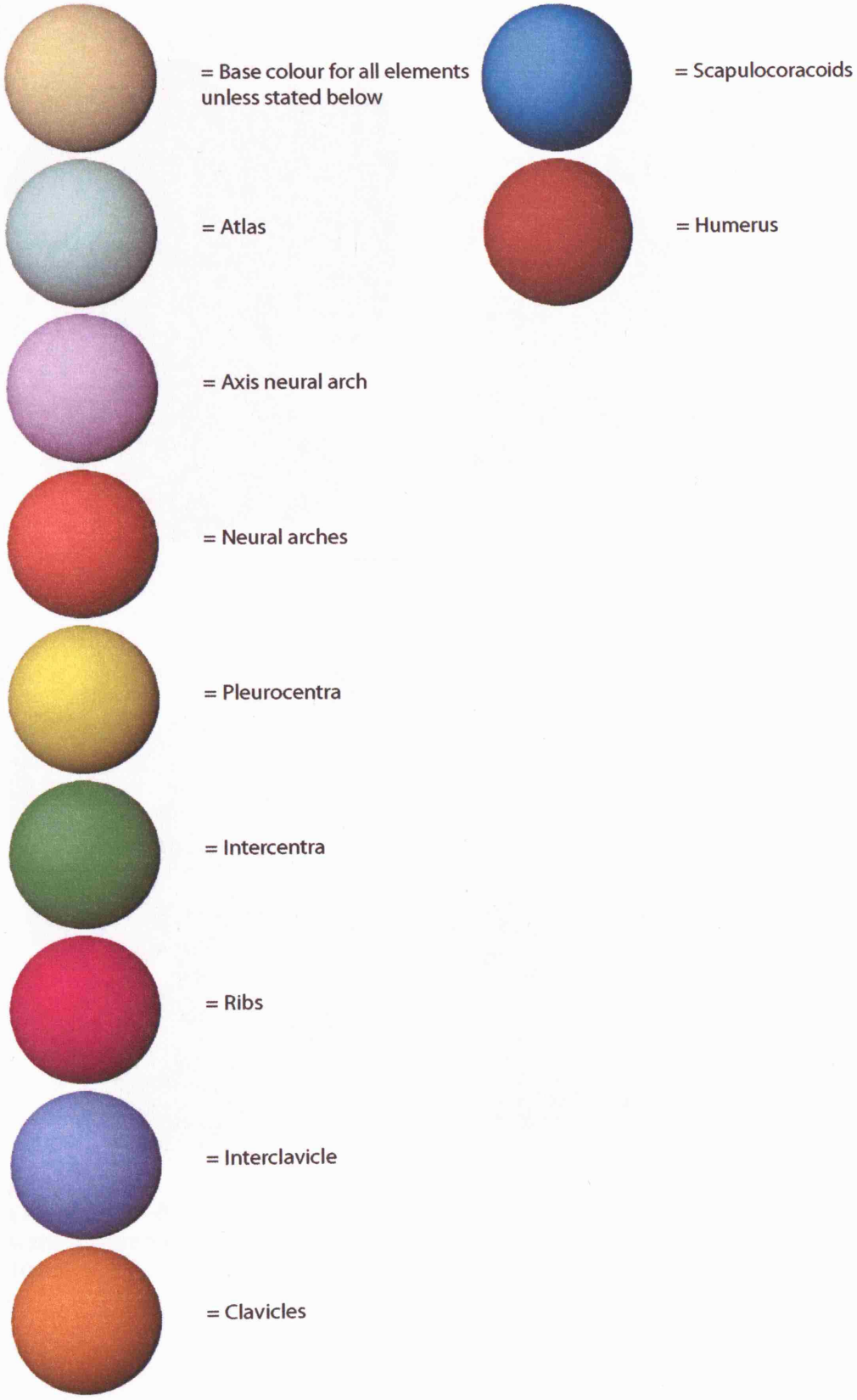

Figure 3.4.3—2 Colour key – postcranial.

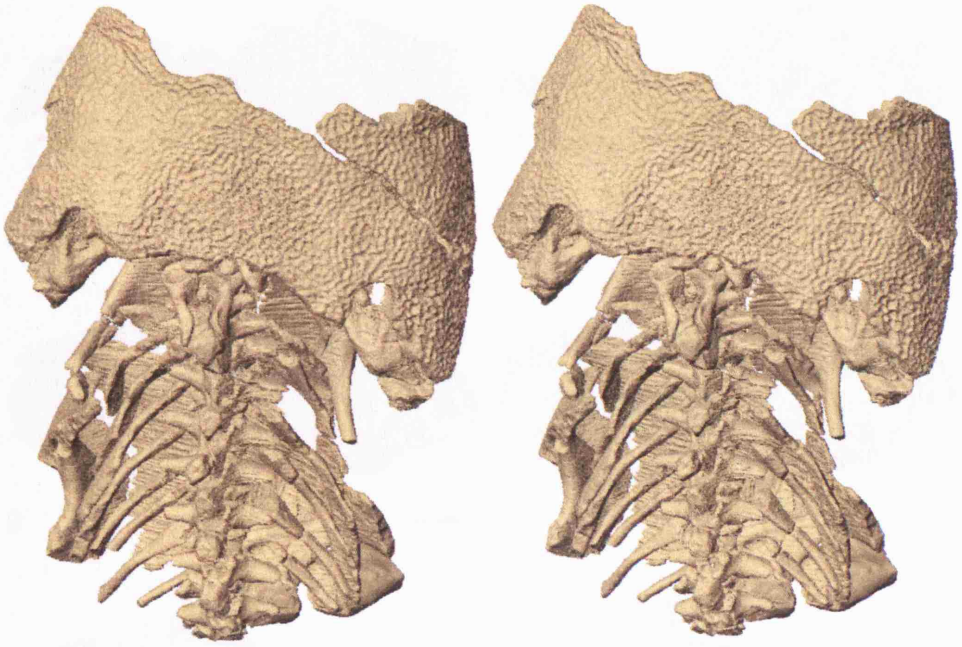

A

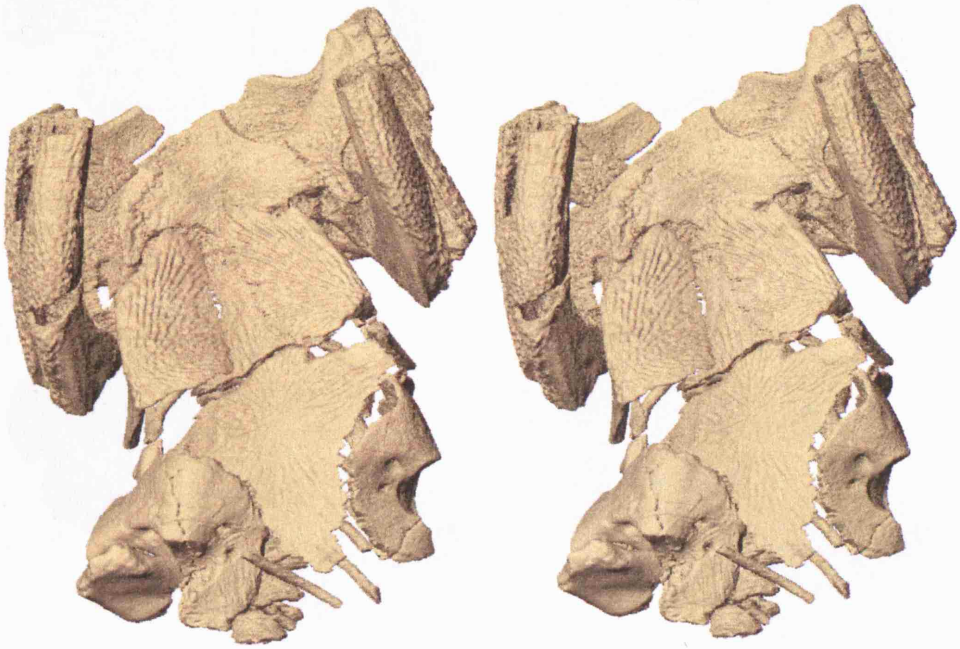

B

Figure 3.4.3—3 *Lydekkerina* specimen UMZC T.242. Mono colour stereo pairs of the model without correction for translocations or damage. A, dorsal view. B, ventral view. Scale bars = 10mm.

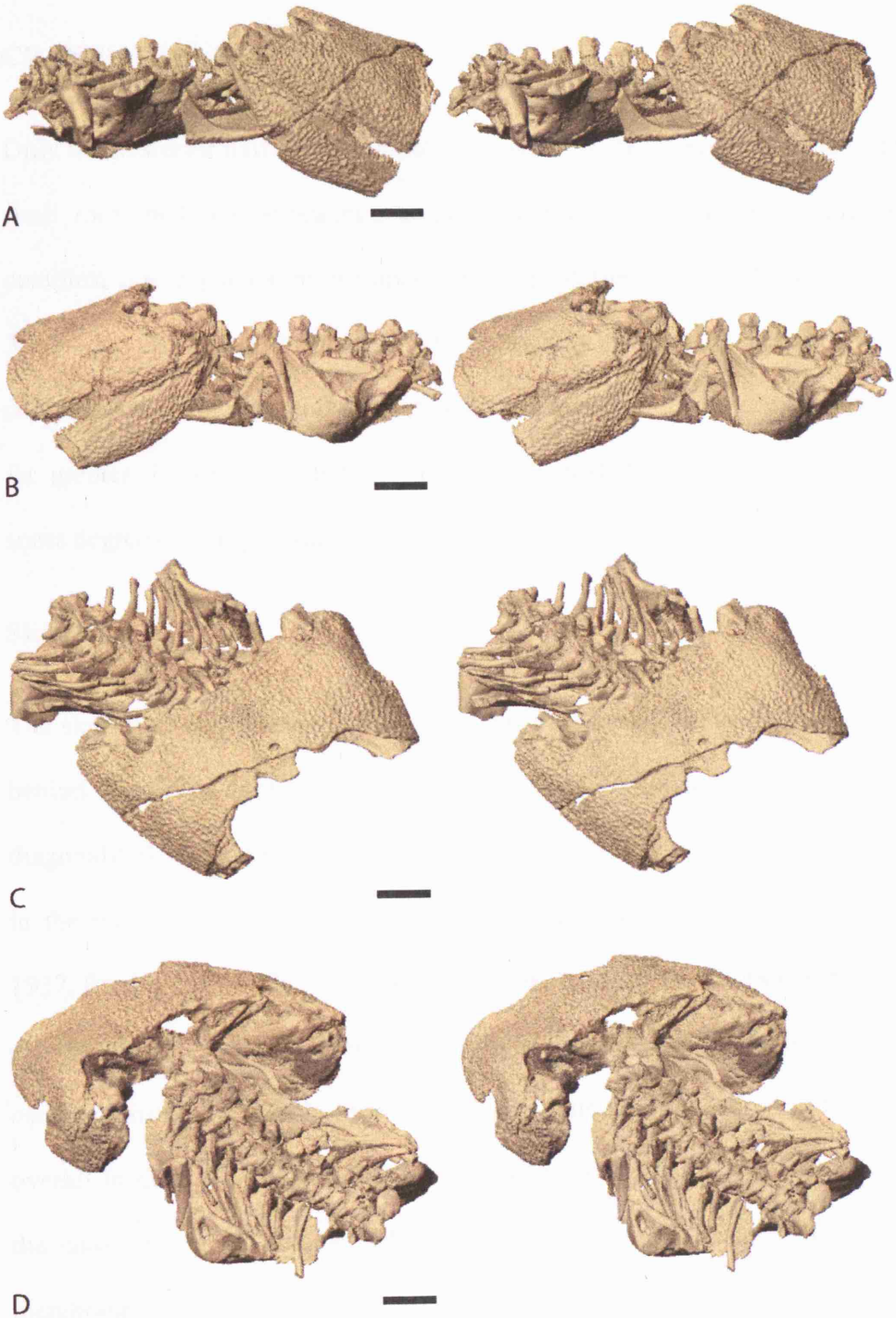

Figure 3.4.3—4 *Lydekkerina* specimen UMZC T.242. Mono colour stereo pairs of the model without correction for translocations or damage. A, right lateral view. B, left lateral view. C, offset anterodorsal view. D, offset posterolateral view. Scale bars = 10mm.

CRANIUM

Only the posterior half of the cranium of UMZC T.242 is present, which consists of the skull roof, both palatoquadrate complexes, the fused lower braincase and occipital complex, otic capsules, both stapes and the posterior regions of the mandibles (Figure 3.4.3—5). The whole skull appears to be entirely undistorted without any dorsoventral compression. Although, the skull is slightly larger than the holotype (BMNH R.507) its far greater dorsoventral dimensions suggests that the holotype may have undergone some degree of compression.

Skull roof

The skull roof (sr) (Figure 3.4.3—5 A and D) is nearly complete and undamaged from behind the orbits (or) and pineal foramen (pin for) apart from a crack which runs diagonally from the midline to the right posterior corner. The external surface is covered in the typical ornament which has been documented previously (Broili & Schröder, 1937; Parrington, 1948; Shishkin et al., 1996; Watson, 1919). As has been the case with all the skulls scanned it has not proved possible to distinguish the component ossifications of the roof because the sutures cannot be visualised in the CT scans. The overall form of the skull roof is as described for other specimens of *Lydekkerina* with the paired posterior notches which are generally accepted to have housed tympanic membranes. The ventral extensions of the postparietals for contact with the exoccipitals can be seen in posterior view. For a more detailed description of the skull roof, complete with suture patterns, see Broili & Schröder figure 1 (1937), Parrington figure 1 (1948) and Shishkin et al. figure 7 (1996).

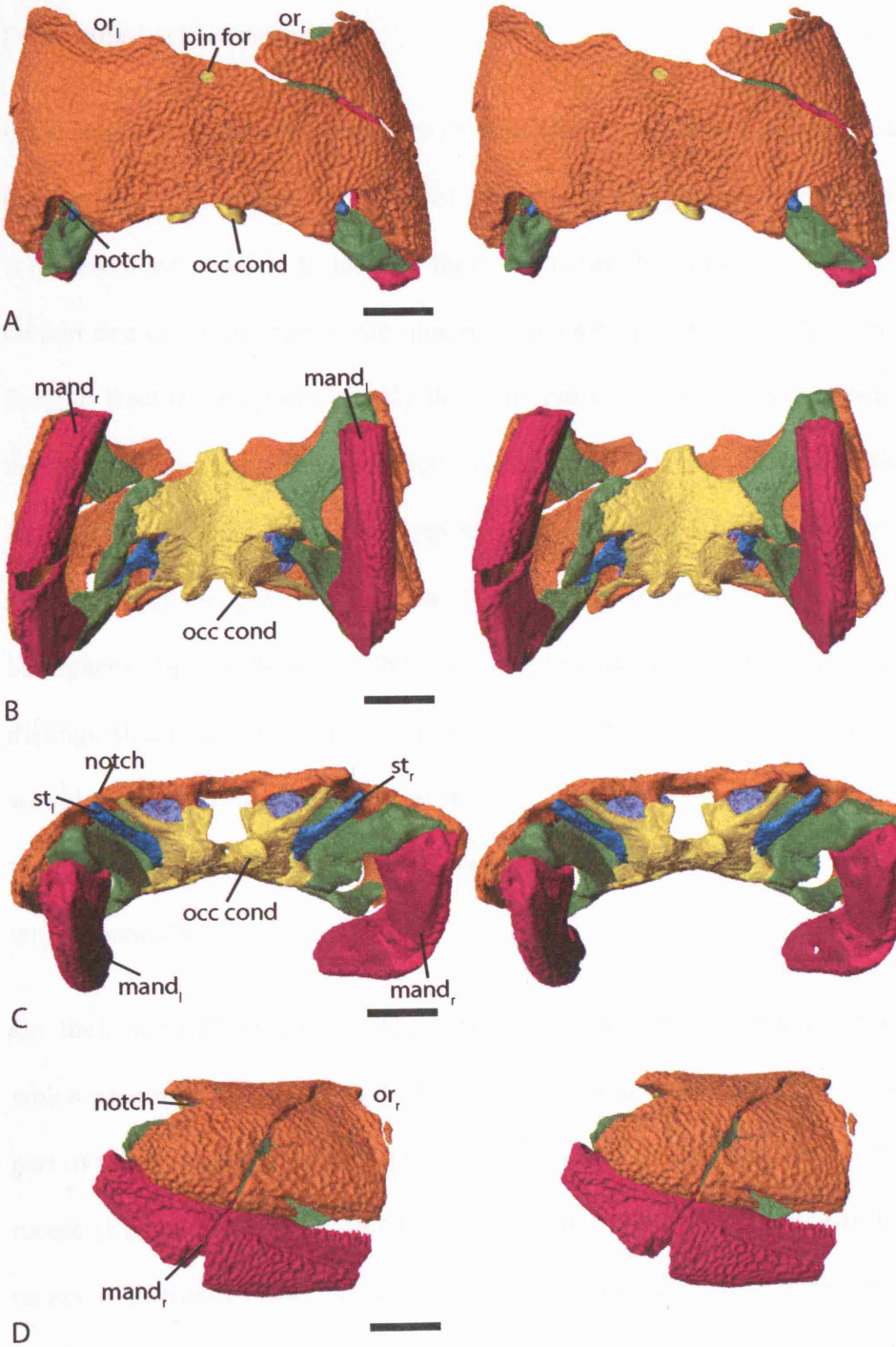

Figure 3.4.3—5 *Lydekkerina* specimen UMZC T.242. Stereo pairs of the cranial model without correction for translocations and damage. A, dorsal view. B, ventral view. C, posterior view. D, left lateral view. Scale bars = 10mm.

Palatoquadrate complexes

Both palatoquadrate complexes are present (Figure 3.4.3—6) and essentially complete (Figure 3.4.3—7 and 8). They consist of epipterygoid, pterygoid and quadrate, although it has not been possible to identify their exact contribution to the complex. Both have a certain degree of damage to the quadrate ramus of the pterygoid (pt) which has caused them to fracture in approximately the same place; it has proved possible to correct this damage by computer manipulation within Rhino3D. The right complex also has a fracture in front of the basipterygoid articulation (art) caused by the cranial crack mentioned in the previous section. Both complexes (ep-pt) were fully fused to the basisphenoid-parasphenoid at the basipterygoid articulation, although it was possible to distinguish this articulation in what appears to be the true place (Figure 3.4.3—6). There would have been no movement at this articulation. A fused basipterygoid articulation without movement is a character state which is present in most, if not all, higher temnospondyls.

On their ventral surface the palatoquadrates are covered in a shagreen of denticles which pass seamlessly across the basipterygoid articulation and fully covers the anterior part of the parasphenoid (ps). In medial view it can be seen that there is a conical shaped recess (Figure 3.4.3—7 F and 8 F) above the basipterygoid articulation. This conical recess is formed by the basisphenoid-parasphenoid complex (bs-ps) ventrally and the palatoquadrate complex dorsally and is most probably homologous to that described in *Benthosuchus* (Bystrow & Efremov, 1940), although this appears to have been formed entirely from palatoquadrate. Above this conical recess one would expect to see the ascending process (asc pro) or columella cranii of the epipterygoid. However, no evidence for a columella cranii can be seen in UMZC T.242 (Figure 3.4.3—7 and 8) as

it would appear that the epipterygoid remained cartilaginous in *Lydekkerina* and thus is not preserved. A columella cranii seems to have been present in all early tetrapods and is clearly figured by Bystrow & Efremov (1940) in *Benthosuchus.*

The palatoquadrate forms the quadrate ramus of the pterygoid posterior to the basipterygoid articulation. As mentioned previously both right and left quadrate rami of the pterygoid have been fractured but their triangular outline can be seen clearly. At the anterior margin of this triangular outline the pterygoid forms a curved wall which is clearly homologous to the excavatio tympanica (ex tym) originally termed by Bystrow & Efremov (1940) for the equivalent structure in *Benthosuchus* but is also seen in other temnospondyls such as *Edops* (Romer & Witter, 1942) and *Dendrerpeton* (Robinson et al., 2005). The excavatio tympanica formed the anterior boundary of the middle ear cavity.

In addition, the posterior margin of the middle ear cavity may have been formed by the pronounced fold of the quadrate ramus of the pterygoid (Figure 3.4.3—7 A, C, F and 8 A, C, F). This fold runs dorsoposteriorly from behind the basipterygoid articulation towards the quadrate before sweeping dorsoanteriorly and becoming confluent with the posterolateral margin of the temporal notch. A similar fold in the quadrate ramus of the pterygoid has been described as the 'otic flange' in *Rhineceps*, *Uranocentrodon* and *Wetlugasaurus* by Watson (1962). Watson called the space enclosed anteriorly by this 'otic flange' as the 'stapedial groove'. This stapedial groove seems likely to have contained a middle ear cavity which stretched from behind the basipterygoid articulation to the temporal notch.

A crest in the quadrate ramus of the pterygoid has previously been described in *Lydekkerina* by Shishkin et al. (1996) as the 'oblique crest of pterygoid (=crista obliqua

pterygoidei)'. It is believed that this structure is equivalent to the fold seen in UMZC T.242 and that both are homologous to the 'otic flange' of Watson (1962). Furthermore, it is hypothesised that this fold in *Lydekkerina* is likely to be homologous to the 'crista obliqua' of *Benthosuchus* (Bystrow & Efremov, 1940) and the 'oblique ridge of pterygoid' (Damiani, 2001). Although the morphology of this structure is quite varied it seems reasonable to assume that it always functioned as the posterior margin of the middle ear space. The term crista obliqua (cri obl) seems most appropriate as it appears to be the first reference to this structure.

Posterior to the crista obliqua the quadrate forms the jaw articulation which has an elongate bi-lobed form.

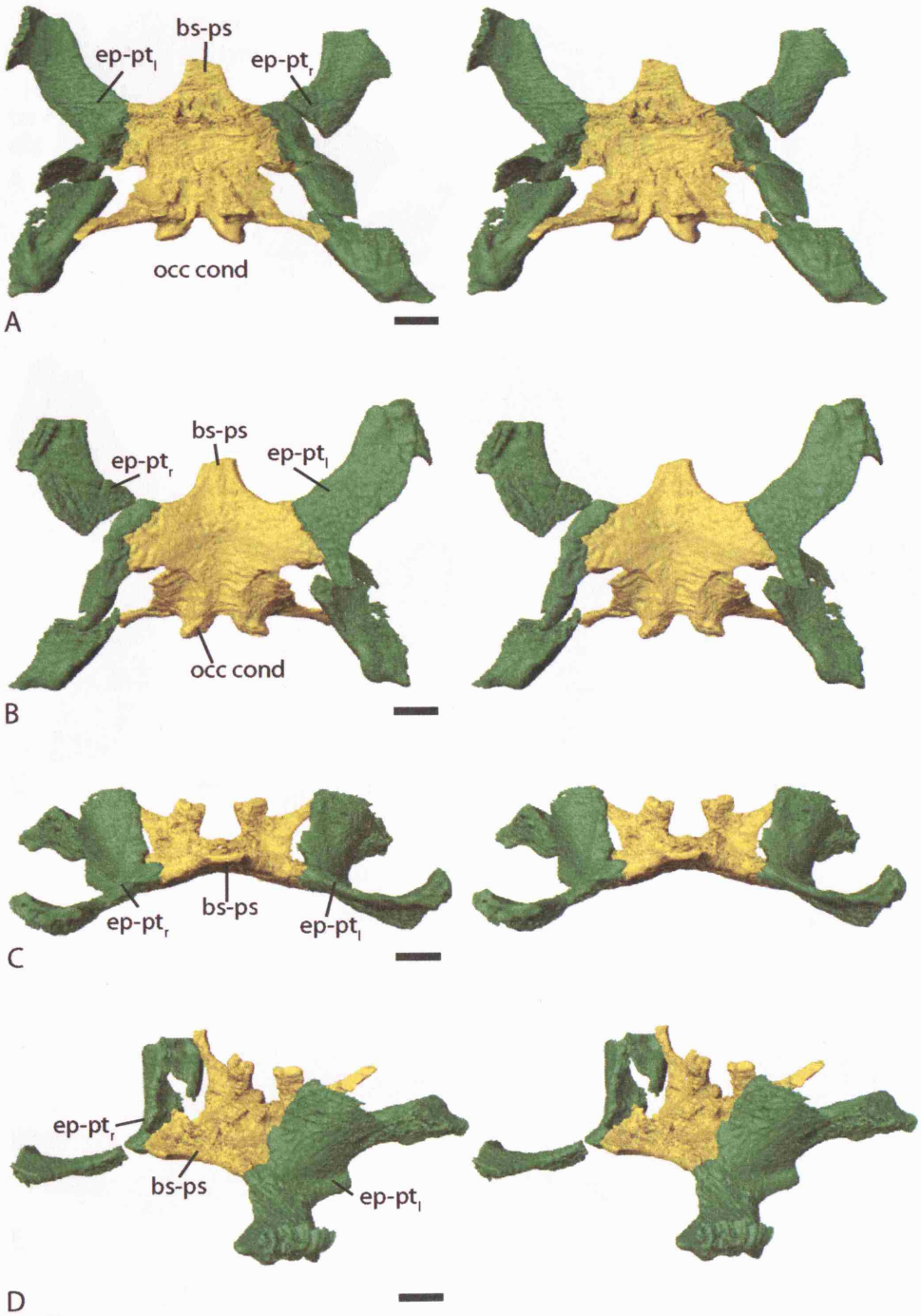

Figure 3.4.3—6 *Lydekkerina* specimen UMZC T.242. Stereo pairs of the palatoquadrate complexes and lower braincase and occipital complex. A, dorsal view. B, ventral view. C, anterior view. D, left anterior lateral view. Scale bars = 5mm.

Figure 3.4.3—7 *Lydekkerina* specimen UMZC T.242. Stereo pairs of the left palatoquadrate complex with correction for translocation and damage. A, posterior view. B, anterior view. C, dorsal view. D, ventral view. E, left lateral view. F, medial view. Scale bars = 2mm.

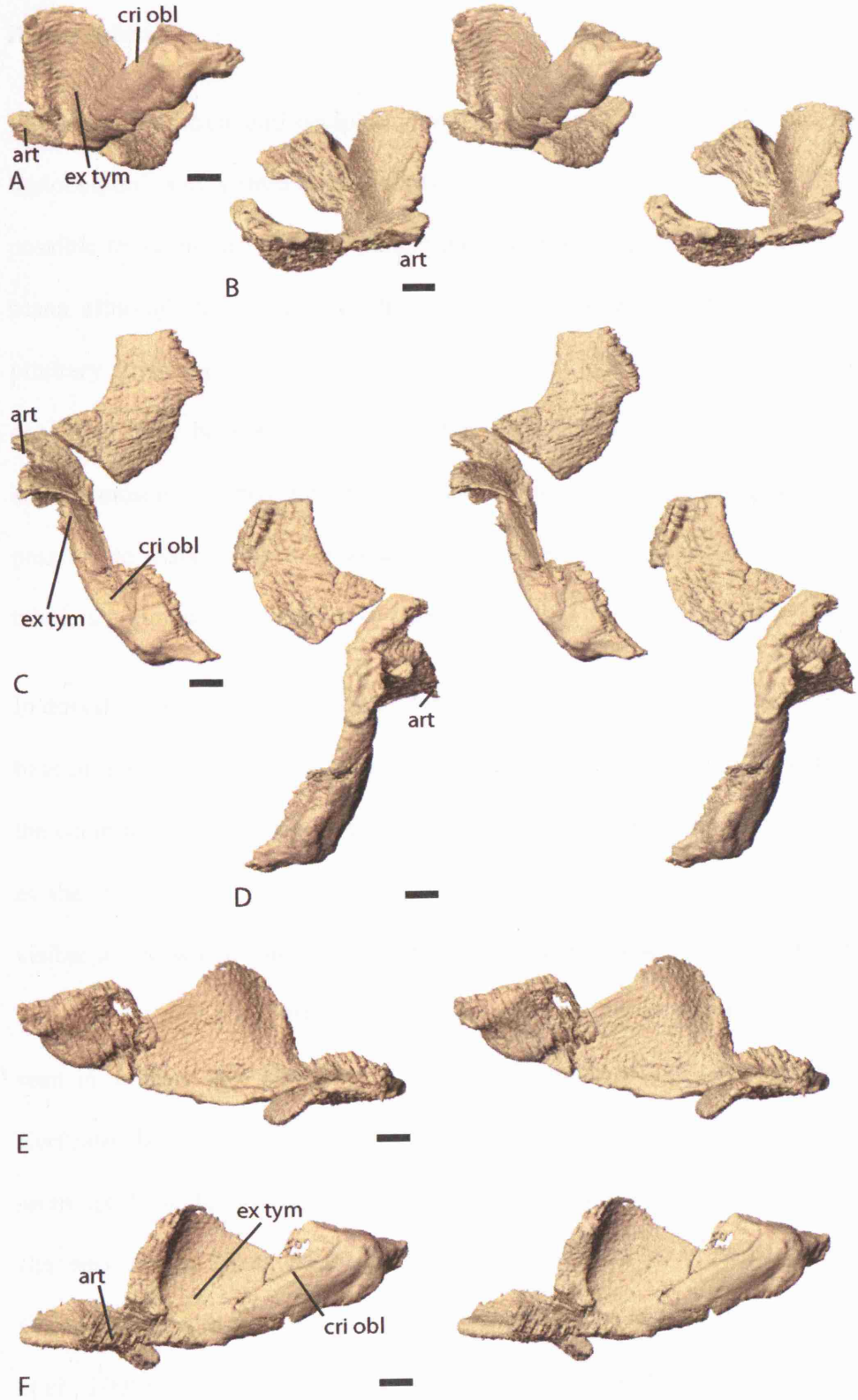

Figure 3.4.3—8 *Lydekkerina* specimen UMZC T.242. Stereo pairs of the right palatoquadrate complex with correction for translocation and damage. A, posterior view. B, anterior view. C, dorsal view. D, ventral view. E, left lateral view. F, medial view. Scale bars = 2mm.

Basicranium

The lower braincase and occipital complex consists of the basisphenoid, parasphenoid, basioccipital and paired exoccipitals (Figure 3.4.3—9 and 10). It has not proved possible to distinguish the component parts of this complex, due to the resolution of the scans, although their relative contributions can be estimated. The complex runs from the pituitary fossa region to the back of the occipital condyle (occ cond). There does not appear to have been any damage to the complex, however, poor scanning resolution and/or unossified areas have reduced the detail and extent of the model. It has proved possible to discern the boundaries between the complex, the palatoquadrates and the tabulars although high degrees of fusion mean that these may not be 100% accurate.

In dorsal view (Figure 3.4.3—9 C) the general form of the complex can be seen with the base of the cultriform process (cul pro) merging into the basipterygoid articulations with the occipital condyle most posterior. The anterior region of the complex is not complete as the posterior region of the sphenethmoid (se) (laterosphenoid region (lsr)) is not visible in the scans. The apparent lack of an ossified laterosphenoid region is also seen in *Dendrerpeton* (Robinson et al., 2005). Paired anterior chambers (ant cham) can be seen in anterior and lateral views. These chambers are also present in *Acanthostega*, *Kyrinion*, *Dendrerpeton* (Robinson et al., 2005) and many other early tetrapods and seem likely to be the origin site of the lateral rectus eye muscles. There are paired channels linking the anterior chambers to the cranial cavity presumably for the abducens (VI) nerve as with the foramina at the back of the chambers in *Dendrerpeton* (Robinson et al., 2005). Dorsomedial to the paired anterior chambers there is a midline prong (mid pro), presumably basisphenoid, which projects anteriorly and is all that remains of the dorsum sellae (Figure 3.4.3—9 B). This midline prong is homologous to that seen in

Dendrerpeton (Robinson et al., 2005). Behind the anterior chambers the basipterygoid forms a small dorsal wall, the crista sellaris (cri sel). The author believes that this wall would have continued in cartilage to contact the anteroventral margins of the otic capsules (oc) and merged with the laterosphenoid region.

Lateral to the crista sellaris the basisphenoid-parasphenoid complex fuses with the palatoquadrate complexes (Figure 3.4.3—6). This anteroposteriorly elongate fusion produces a basipterygoid articulation with no possibility of movement. Behind the articulation the lower braincase (still presumably basisphenoid-parasphenoid) contacts medially to produce distinct notches (rec tym) before widening again posterodorsally to form a laminar expansion which seamlessly flows into the occipital condyle and paroccipital processes (par pro) (Figure 3.4.3—9). On both sides of UMZC T.242 the notches behind the basipterygoid articulations enclose spaces (Figure 3.4.3—9 and 10) which stretch up to the posterior margin of the stapes (st) and are bordered dorsally by the otic capsules and posteriorly by the exoccipitals. The spaces open medially into the cranial cavity. It is not clear to what extent the space would have been reduced by cartilage but it seems likely that this would not have been in anyway complete. These notches have previously been figured in all *Lydekkerina* descriptions in which the palatal surface has been shown (see for example Watson's figure 5 (1919), Parrington's figure 1b (1948), and Shishkin et al.'s figure 7b (1996)). Similar notches are present in Bystrow & Efremov's (1940) figures 10b and 11c of *Benthosuchus*, and in Warren's (1980) figures 3, 4 and 6 of *Parotosuchus*. Shishkin et al. state that this notch was first described by Warren in *Parotosuchus*, however, it seems clear that Bystrow & Efremov's (1940) description of a similar notch between the exoccipital and parasphenoid as the 'recessus tympanicus' was the first description. Warren did not think that the notch of *Parotosuchus* was homologous to that of *Lydekkerina*, however,

Shishkin et al. (1996) claim this to be the case. It seems likely that the notches seen in UMZC T.242, other *Lydekkerina* specimens, *Parotosuchus* and *Benthosuchus* are equivalent to each other. It, therefore, seems appropriate to term the notch in all these specimens 'recessus tympanicus'.

While Warren (1980) did not comment on the function of this notch in *Parotosuchus*, Shishkin et al. (1996) stated that the notch may have been a 'ventral remnant of the embryonic fissura metotica [metotic fissure]'. Shishkin et al. (1996) stated that, because a notch did not seem to be present on the right side of *Lydekkerina* specimen BP/1/5082B, the notches had a 'non-functional (rudimentary) nature'. Alternatively, the close relationship of the notch to the fenestra ovalis (f/o), the stapes, the presumed tympanic cavity and the cranial cavity, suggests that it may have a role in the hearing function (Figures 3.4.4—17, 18 and 19). The possible exact functions of the 'recessus tympanicus' will be described along with the discussion of the hearing of *Lydekkerina*.

Medial to the notches described previously the parasphenoid plate stretches posteriorly to contact the exoccipitals and basioccipital. Above this dermal laminar plate the endochondral basioccipital, and possibly exoccipitals, forms the anterior extension which has also been described in *Dendrerpeton* (Robinson et al., 2005). This anterior extension is bilaterally symmetrical with raised platforms either side of a deep channel, just as with *Dendrerpeton* (Robinson et al., 2005). The raised platforms are a shallow u-shape in cross section and appear to have notches on their lateral surface as also described in *Dendrerpeton* (Robinson et al., 2005), although, they are not as clear in UMZC T.242. Unlike *Dendrerpeton* (Robinson et al., 2005) the raised platforms are joined at the midline for part of their length producing a bridge over the deep channel. The deep channel is the notochordal pit (not pit). The reduced diameter notochord

would have passed through the hole between the pads of the atlas and then into the notochordal pit between the anterior extensions.

In posterior view the occipital complex can be observed (Figure 3.4.3—9 A). As has been previously shown (see for example Watson's (1919) figure 4 and Shishkin et al.'s (1996) figure 7c) the condyle is bi-facetted as is the case with higher temnospondyls (post-eryopoid). It is presumed in this thesis that the facets are made from the exoccipitals, although, there may be a small basioccipital component ventrally.

Dorsally the exoccipitals contact both the postparietals and the tabulars lateral to the foramen magnum (fm). Unfortunately it was not possible to demarcate the boundary between the exoccipitals and the skull roof with 100% certainty. It does, however, seem likely that the exoccipitals did fuse with the tabulars along the posterior surface of the paroccipital processes and that the 'opisthotic' was not exposed posteriorly as was depicted by Watson (1919) in his figure 4. At the medial end of each paroccipital process there is a foramen which seems likely to be the exit points for the vagus (X) nerve.

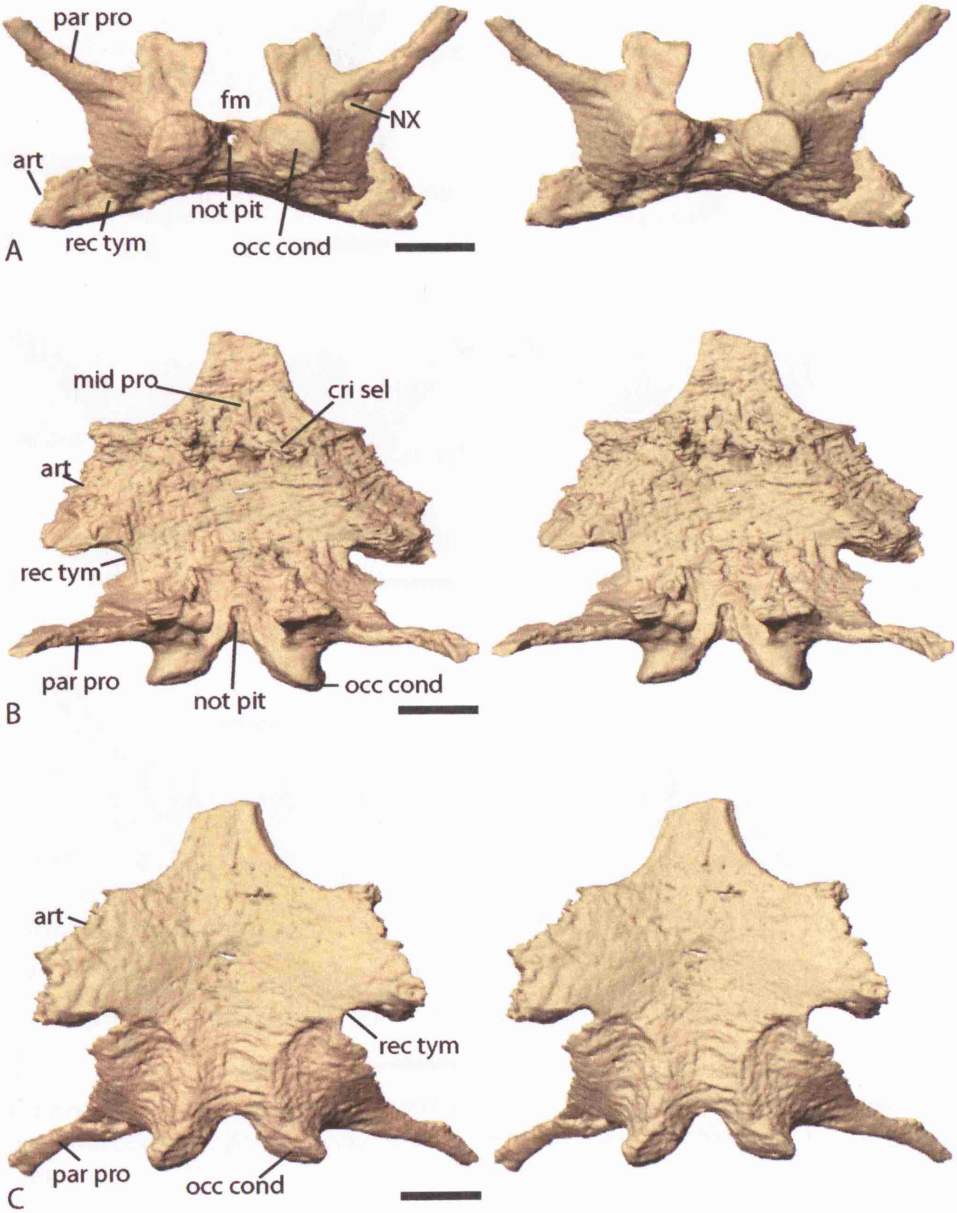

Figure 3.4.3—9 *Lydekkerina* specimen UMZC T.242. Stereo pairs of the lower braincase and occipital complex. A, posterior view. B, dorsal view. C, ventral view. Scale bars = 5mm.

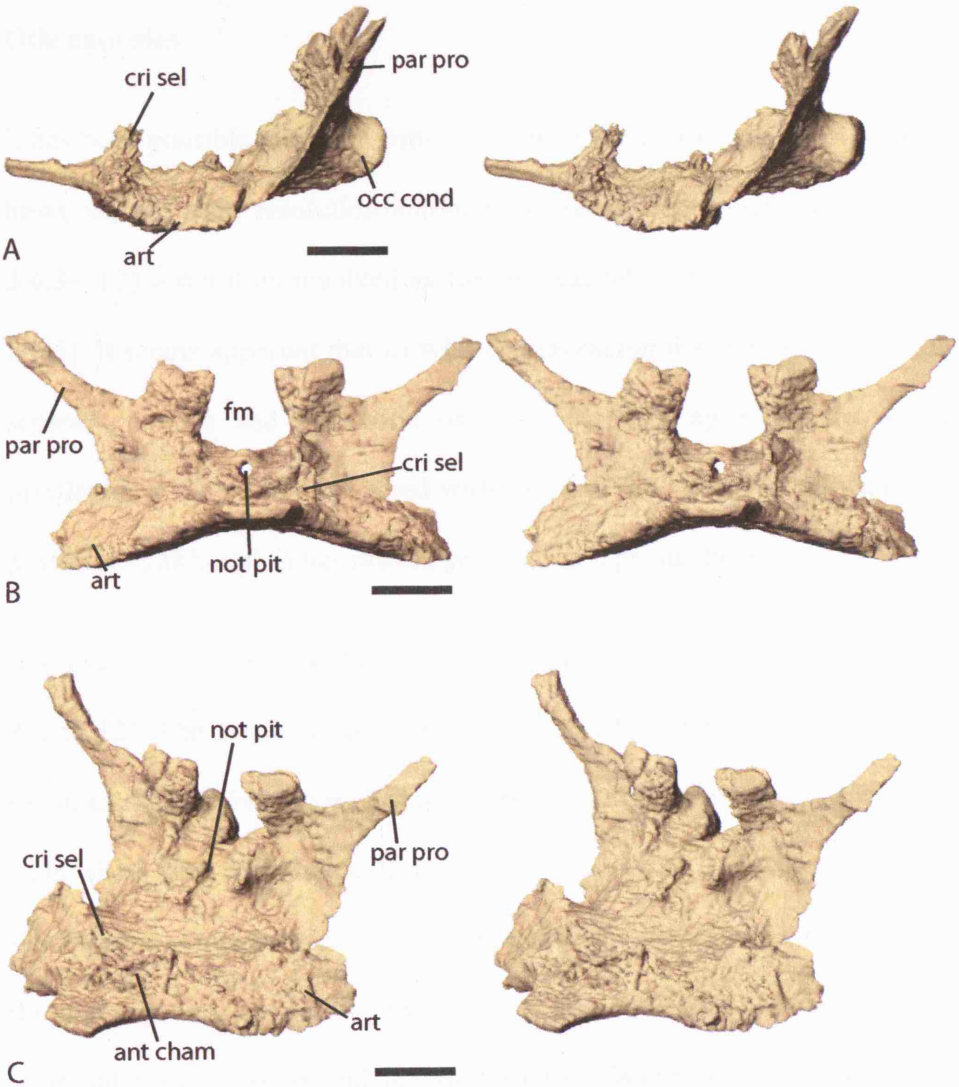

Figure 3.4.3—10 *Lydekkerina* specimen UMZC T.242. Stereo pairs of the lower braincase and occipital complex. A, left lateral view. B, anterior view. C, offset anterodorsal view. Scale bars = 5mm.

Otic capsules

It has been possible to model both otic capsules within UMZC T.242 (Figure 3.4.3—11), however, the scan resolution and/or poor ossification means that the models (Figure 3.4.3—12) are not as resolved as the otic capsules of *Dendrerpeton* (Robinson et al., 2005). It seems apparent that as with *Dendrerpeton* the otic capsules are not formed by separate prootic and opisthotic ossifications; they appear to be formed by single ossifications. Both capsules fused with the skull roof anterodorsally and the exoccipitals posteriorly, although it has proved possible to separate them.

In dorsal view the incomplete nature of the otic capsules can be seen (Figure 3.4.3—11 A and 12). The features can, however, be clearly interpreted with reference to the otic capsules of *Dendrerpeton* (Robinson et al., 2005). Anteriorly the capsules form large pads which fuse with the skull roof; in *Dendrerpeton* (Robinson et al., 2005) these pads would have contacted the skull roof via cartilage. In a similar manner to *Dendrerpeton* the otic capsules of *Lydekkerina* form the lateral, ventral and medial walls of the post-temporal fossa (ptf) behind the anterior pad. Within the anterior region of the wall, lateral to the post-temporal fossa, there is a foramen which passes to the lateral surface of the capsule (Figure 3.4.3—12 A and B). This foramen (ot for) is homologous to the notch seen in *Dendrerpeton* (Robinson et al., 2005), the 'post-temporal foramen' of *Edops* (Romer & Witter, 1942) and the corresponding foramen see in *Eryops* (Sawin, 1941). This foramen is described in *Baphetes kirkbyi* Watson, 1929 as the 'entry point of the vena capitis dorsalis' (Beaumont, 1977). As mentioned in the *Dendrerpeton* description (Robinson et al., 2005) a similarly located foramen is figured in *Eusthenopteron* (Jarvik, 1980). The capsule ventral and medial to the post-temporal fossa is poorly preserved and suggests that it was cartilaginous. The lack of a thick

ossified floor to the post-temporal fossa is in agreement with the condition seen in *Dendrerpeton* where there is also a small unossified region or foramen.

The overall general form of the capsules from ventral and anterior views is also in agreement with those of *Dendrerpeton* (Robinson et al., 2005). On both capsules it is possible to observe grooves that pass from the anterior boundaries posteroventrally towards the fenestrae ovales. This groove may represent the path of the jugular vein (jug gro) as was hypothesised to be the case in *Dendrerpeton* (Robinson et al., 2005). On the left capsule this groove passes below the 'post-temporal fenestra', and therefore the jugular vein may have given off the vena capitis dorsalis at this point. The dorsal boundaries of both fenestrae ovales are present although both are incomplete.

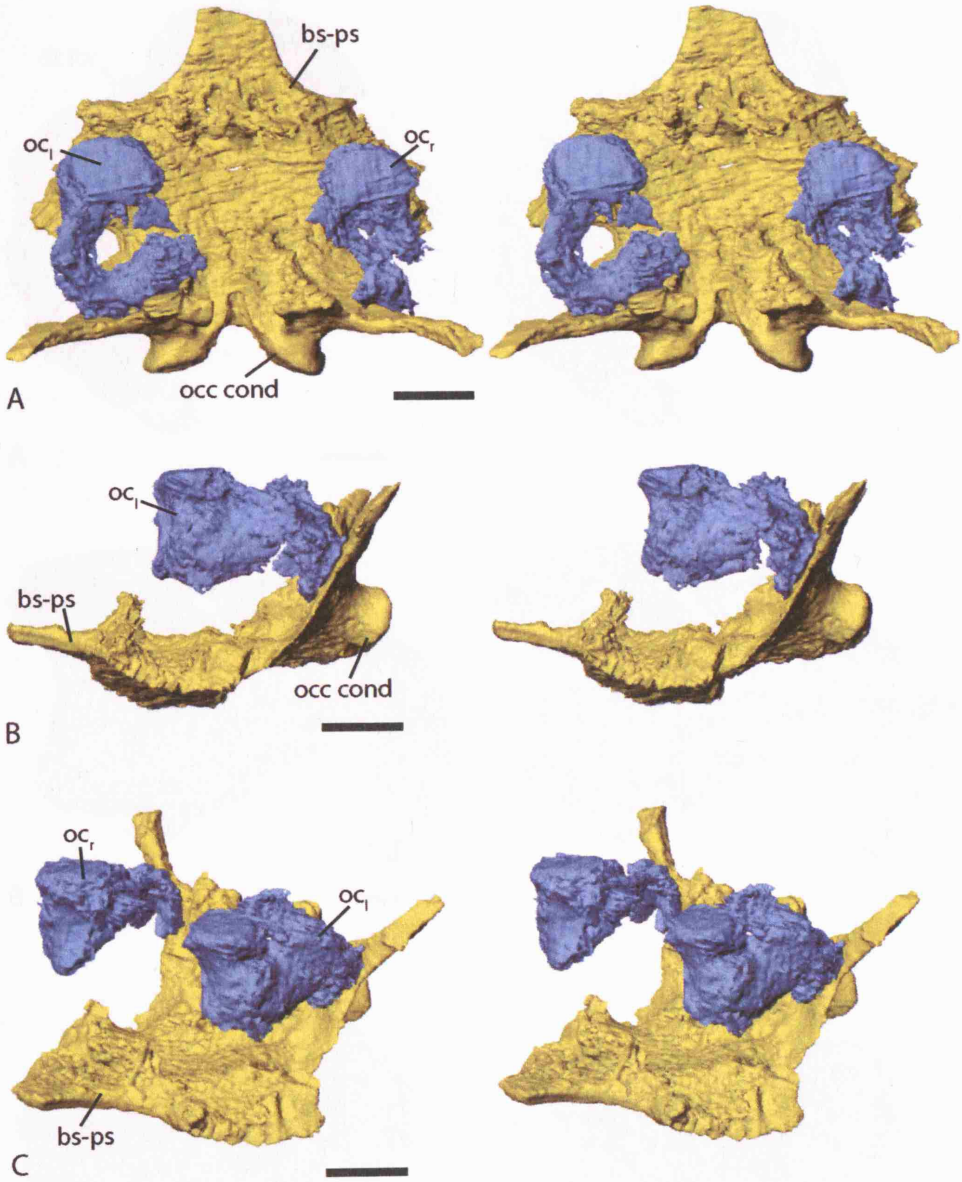

Figure 3.4.3—11 *Lydekkerina* specimen UMZC T.242. Stereo pairs of the otic capsules and lower braincase and occipital complex. A, dorsal view. B, left lateral view. C, offset anterodorsal view. Scale bars = 5mm.

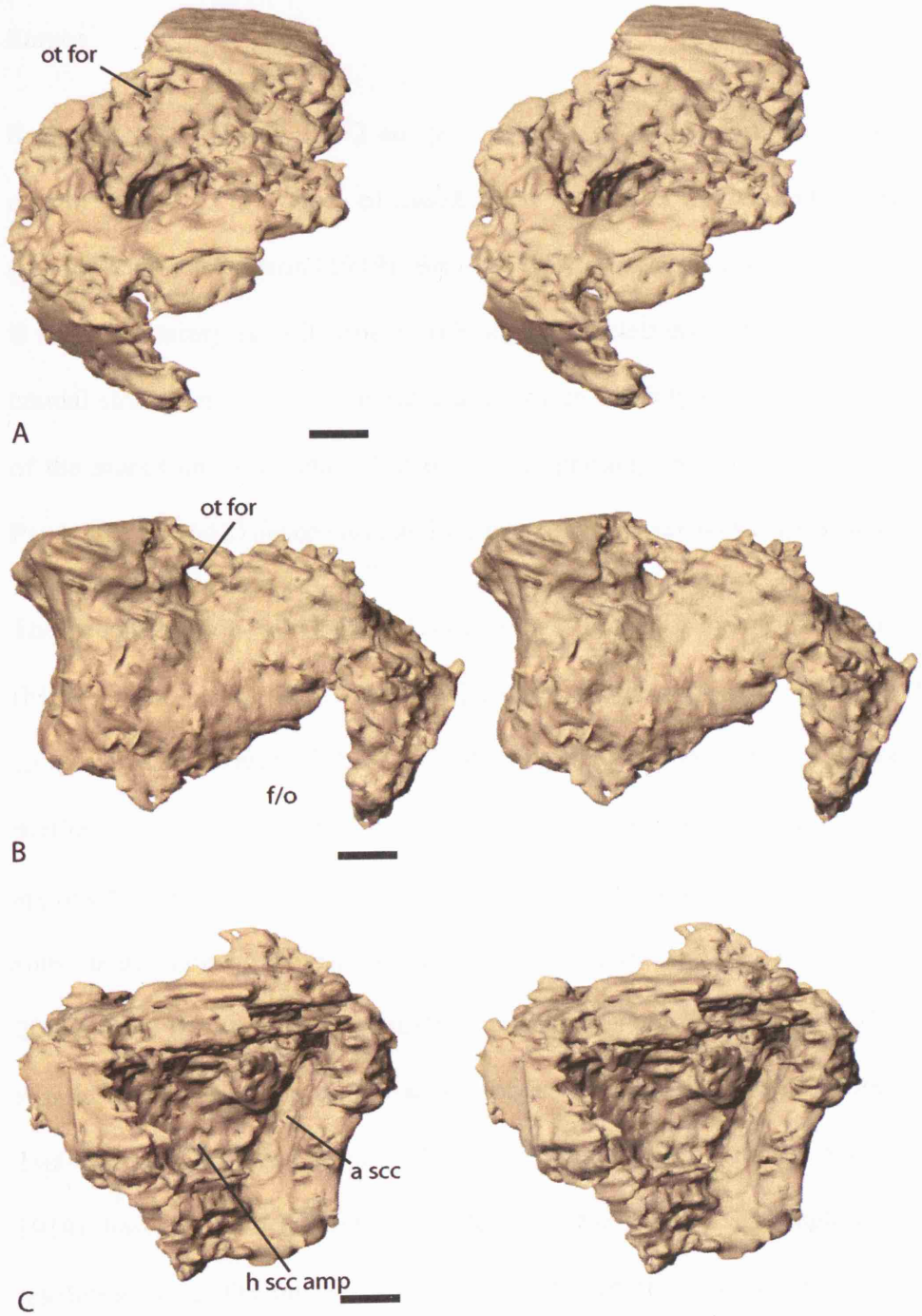

Figure 3.4.3—12 *Lydekkerina* specimen UMZC T.242. Stereo pairs of the right otic capsule. A, posterodorsal view. B, anterolateral view. C, posteromedial view. Scale bars = 2mm.

Stapes

Both stapes of UMZC T.242 are present and are in their original location. Although certain aspects of the stapes of *Lydekkerina* have been figured and/or described before (see for example Watson (1919), Broili & Schröder (1937) and Parrington (1948)) there is still uncertainty as to its true morphology and relationship to the surrounding internal cranial structures. The most notable areas of uncertainty surround the proximal contact of the stapes and the detailed stapedial morphology including suggested processes in Parrington's (1948) description and figuring of *Lydekkerina* sp. specimen UMZC T.206.

The reconstruction of UMZC T.242 shows that *Lydekkerina* has a rod like stapes (Figure 3.4.3—13, 14, 15 and 16) which projects postero-dorsolaterally into the temporal notch (Figure 3.4.3—17, 18 and 19). The footplate (fp) of the stapes is bi-partite with anteroventral (ven com) and posterodorsal surfaces (dor com) of approximate equal size (Figure 3.4.3—16 A). The surfaces are not separated as seen in some large stereospondyls, such as, *Mastodonsaurus giganteus* Jaeger, 1828 (Schoch, 2000). Only the anteroventral surface has any contact with the ossified internal cranial structures. Lateral to the footplate a stapedial foramen has been described frequently in *Lydekkerina* (Broili & Schröder, 1937; Parrington, 1948; Shishkin et al., 1996; Watson, 1919), however, this feature is not clear in UMZC T.242, although, this is probably a resolution issue. On the posterior surface of each stapes it is possible to see a groove running from near the proximal end to the distal end. This groove is homologous to that on the stapes of *Dendrerpeton* (Robinson et al., 2005). At the distal end of each stapes there is an unfinished concavity (unf con) which provides evidence for a cartilaginous extrastapes or pars externa as with *Dendrerpeton.*

The reconstructed stapes of UMZC T.242 do not appear to possess any of the processes described by Parrington (1948) in UMZC T.206 (Figure 3.4.1—1 C and D). The reduced resolution in the scanning of UMZC T.242 means that certain processes described in UMZC T.206 could be present but have not been resolved. In order to investigate this further UMZC T.206 was re-examined (Figure 3.4.3—20).

In comparison to UMZC T.242 it seems clear that the cranium of UMZC T.206 has been somewhat dorsoventrally compressed. There is a notable fracture in the skull anterior to the right temporal notch. Furthermore, this compression appears to have changed the position of the right stapes, as described by Parrington (1948), from postero-dorsolateral, as seen in UMZC T.242, to a posterolateral orientation. The footplate is thus artificially close to the skull roof and the whole stapes has been rotated anteriorly. This movement of the stapes does not appear to have actually caused any distortion.

The small stapedial foramen in Parrington's (1948) figures 3b and 3c is correctly identified. By comparison with the stapes of other temnospondyls, such as, *Dendrerpeton* (Robinson et al., 2005) and *Eryops* (Sawin, 1941) the stapedial foramen in UMZC T.206 would have run originally more anteroposteriorly than dorsoventral orientation of the foramen in the specimen today. This reorientation of the stapes in UMZC T.206 allows the reinterpretation of the 'antero-dorsal process' and 'antero-ventral process' (av pro) as the anterior and posterior corners of the ventral part of the footplate (Figure 3.4.3—20). The prominence of the posterior corner of the ventral part of the footplate demonstrates that *Lydekkerina* had a clear notch in the posterior margin of the footplate as described in *Dendrerpeton* (Robinson et al., 2005) and other temnospondyls. The 'process for extension to quadrate' is on the posterior surface of the

stapes in UMZC T.206 approximately one third of the way along the stapes from the footplate. A process in the same position and of similar morphology has been described in *Sclerocephalus haeuseri* Goldfuss, 1847 (Schoch, 2002) and possibly also *Edops* (Romer & Witter, 1942). The position of this process in UMZC T.206 and *Sclerocephalus* is similar to the scar seen on the posterior surface of the stapes in *Dendrerpeton* (Robinson et al., 2005).

It is possible to build up a complete picture of the stapedial morphology in *Lydekkerina* from the combined study of both stapes in UMZC T.242 and the right stapes in UMZC T.206. The stapes was rod like with a small stapedial foramen and directed postero-dorsolaterally into the temporal notch. The footplate was bi-partite with a notch directed posteriorly. The ventral part of the footplate articulated with the parasphenoid (Figure 3.4.3—18); there was no contact with any other ossified cranial element. Each stapes was enclosed within a space created by the excavatio tympanica and crista obliqua of the palatoquadrate and capped by the temporal notch (Figure 3.4.3—17 and 19). Functional interpretation and further details of the stapes and the surrounding structures will follow in the discussion chapter.

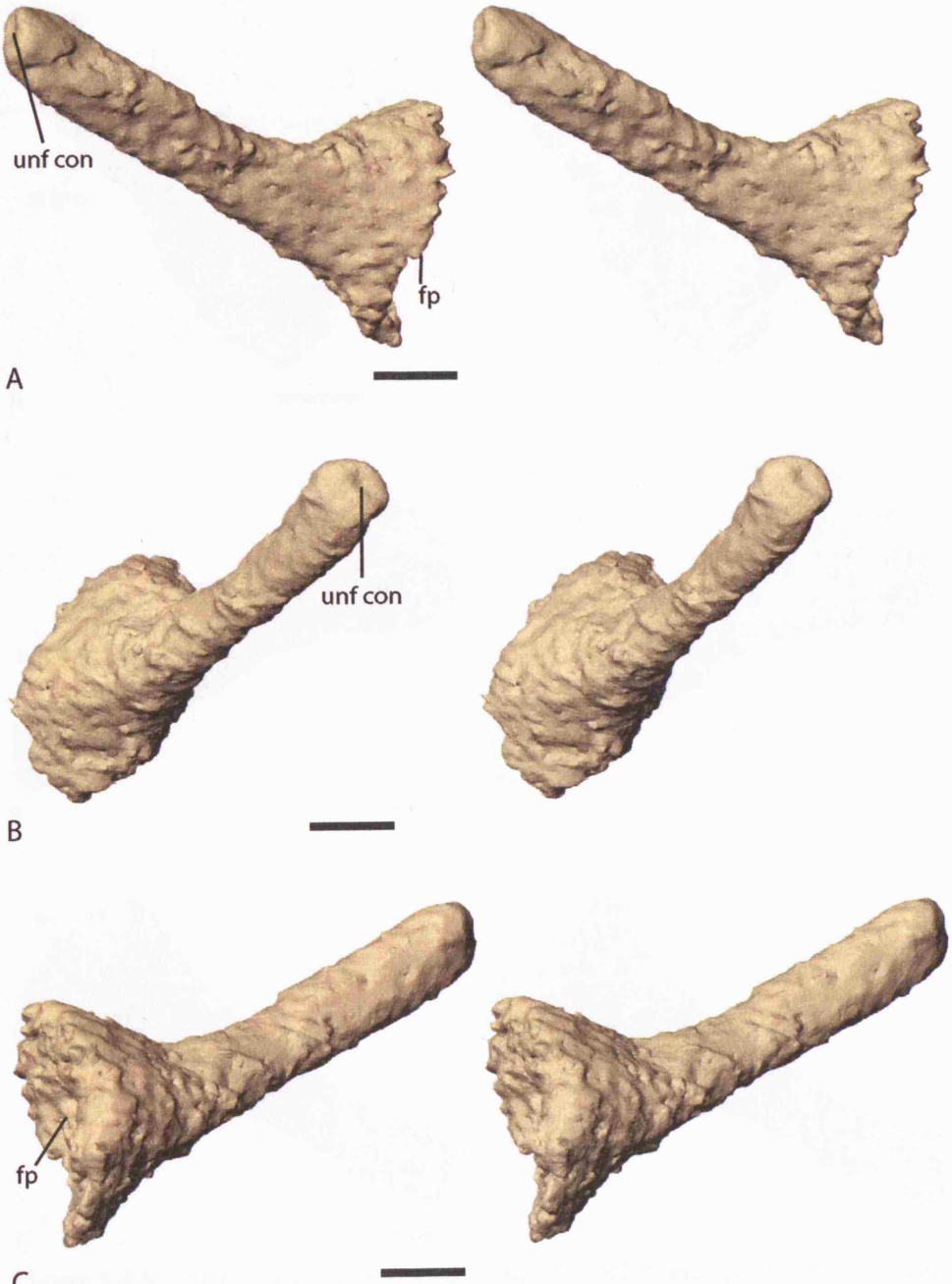

Figure 3.4.3—13 *Lydekkerina* specimen UMZC T.242. Stereo pairs of the left stapes. A, posterior view. B, left lateral view. C, anterior view. Scale bars = 2mm.

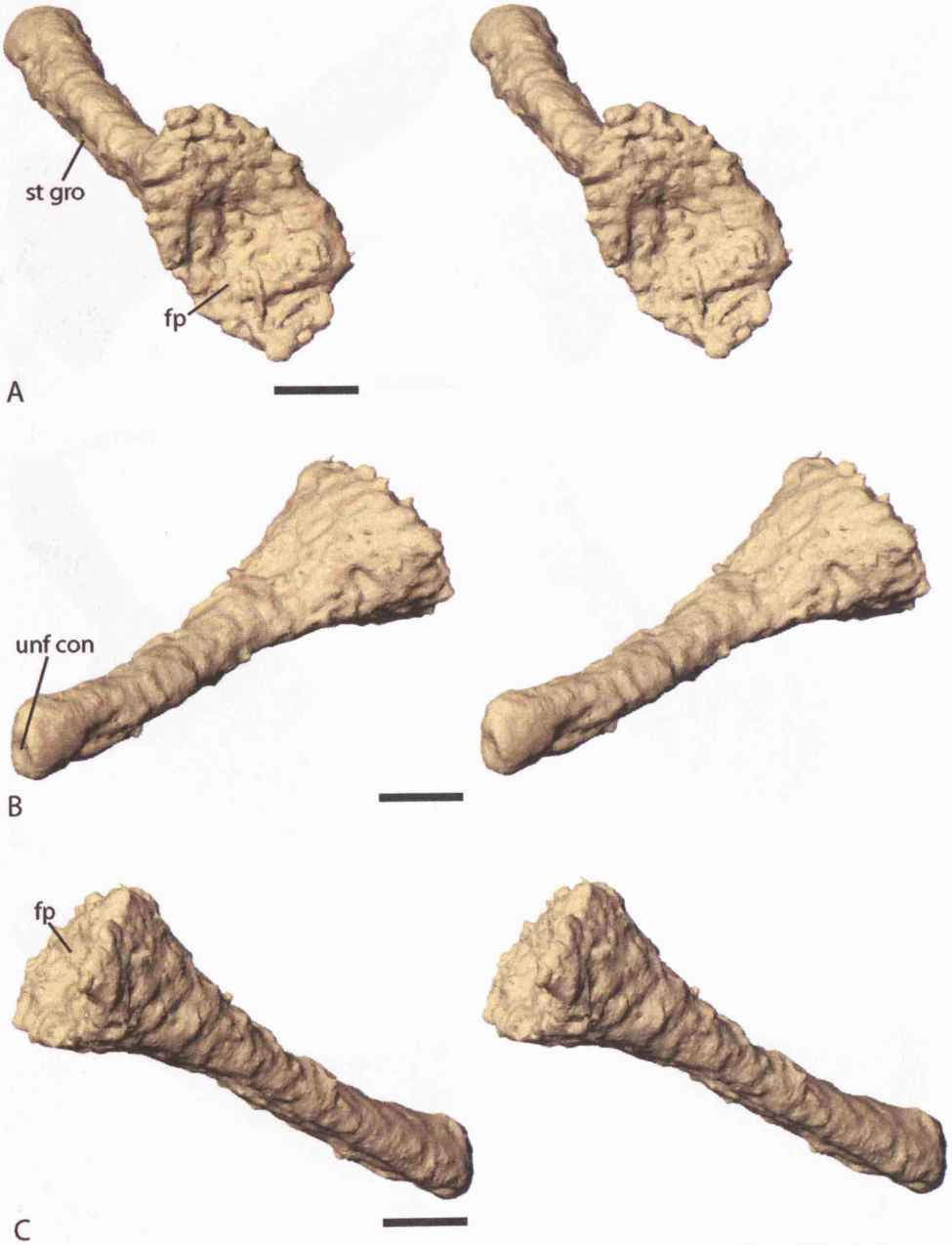

Figure 3.4.3—14 *Lydekkerina* specimen UMZC T.242. Stereo pairs of the left stapes. A, medial view. B, dorsal view. C, ventral view. Scale bars = 2mm.

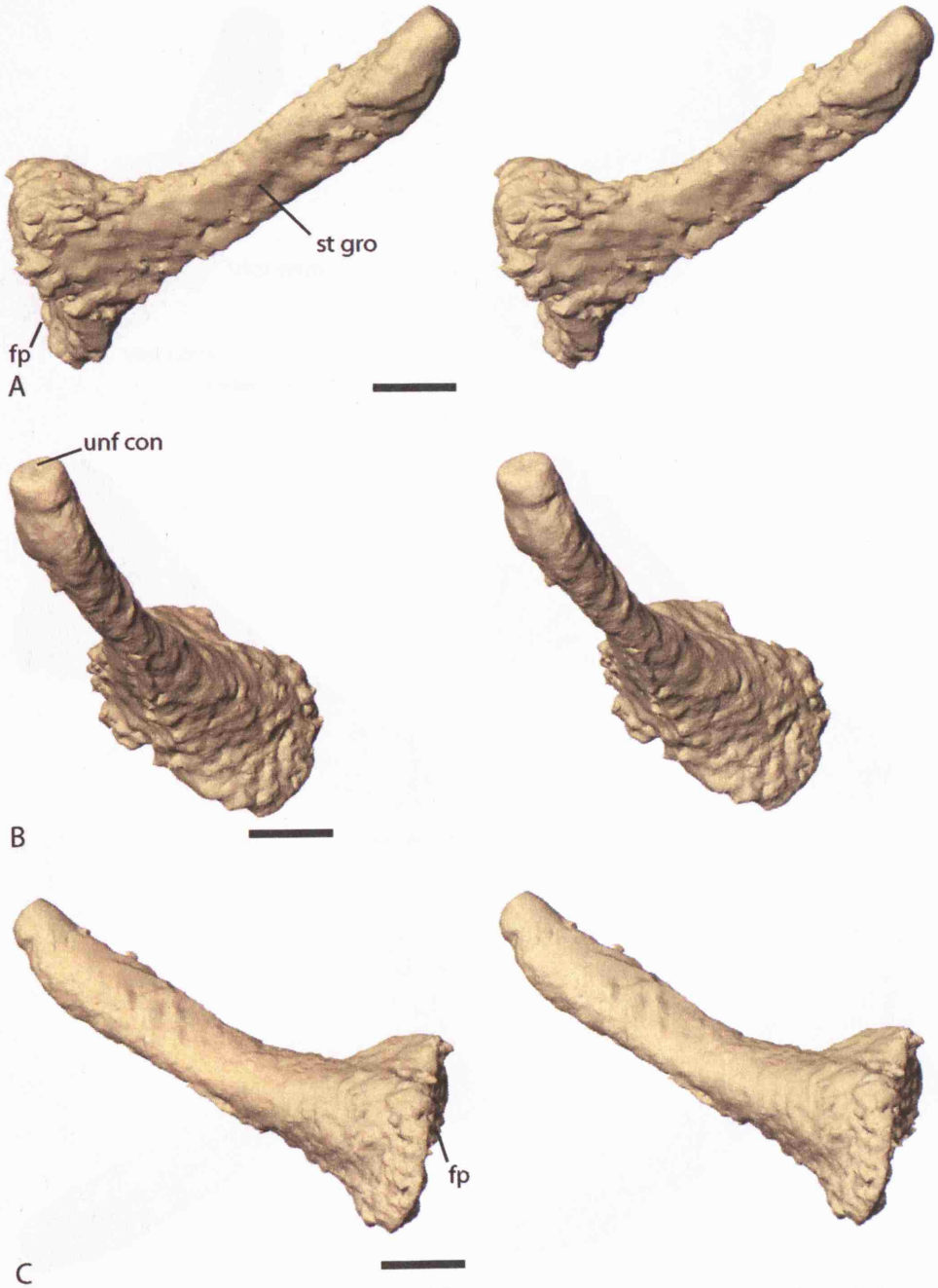

Figure 3.4.3—15 *Lydekkerina* specimen UMZC T.242. Stereo pairs of the right stapes. A, posterior view. B, right lateral view. C, anterior view. Scale bars = 2mm.

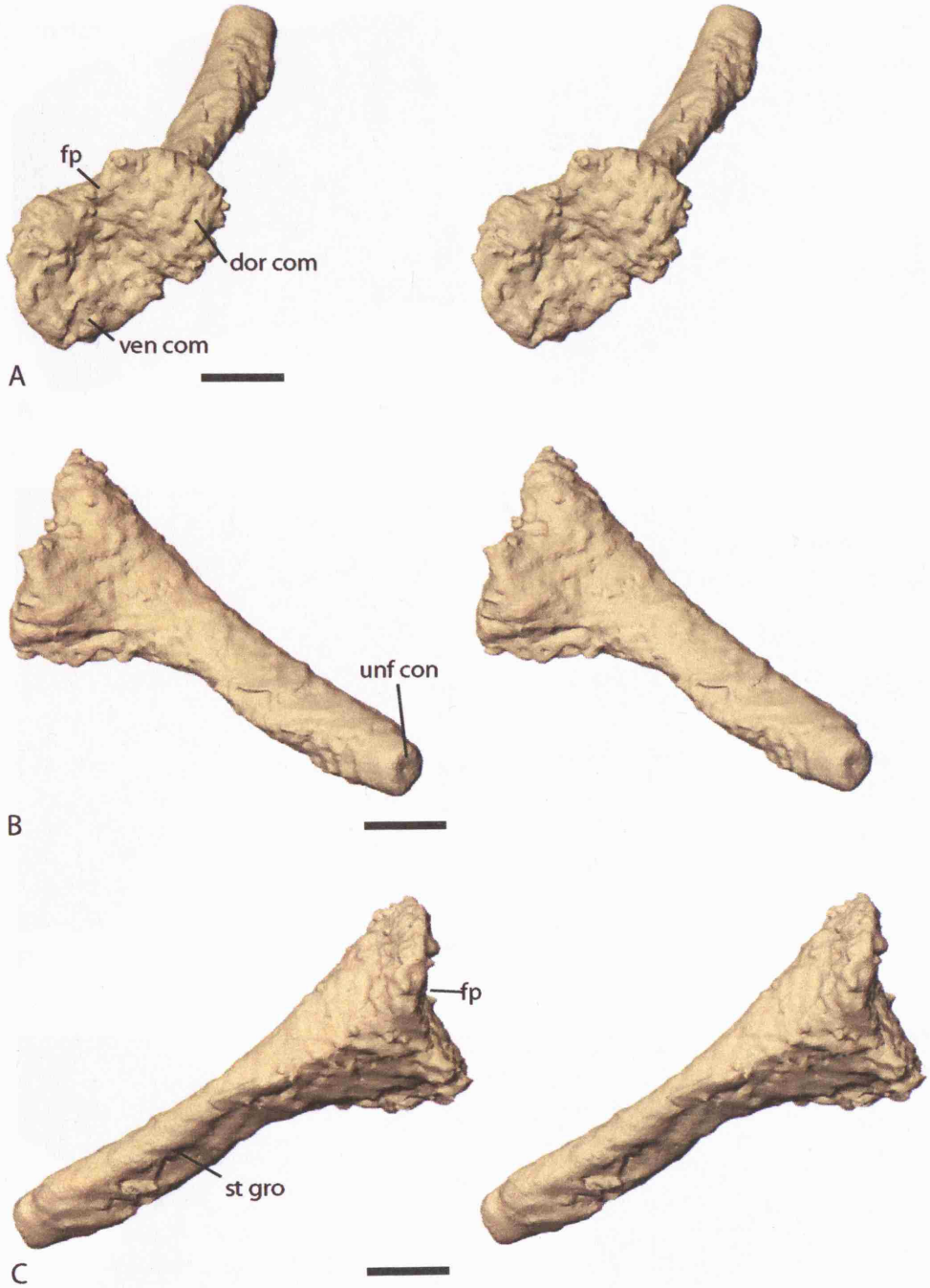

Figure 3.4.3—16 *Lydekkerina* specimen UMZC T.242. Stereo pairs of the right stapes. A, medial view. B, dorsal view. C, ventral view. Scale bars = 2mm.

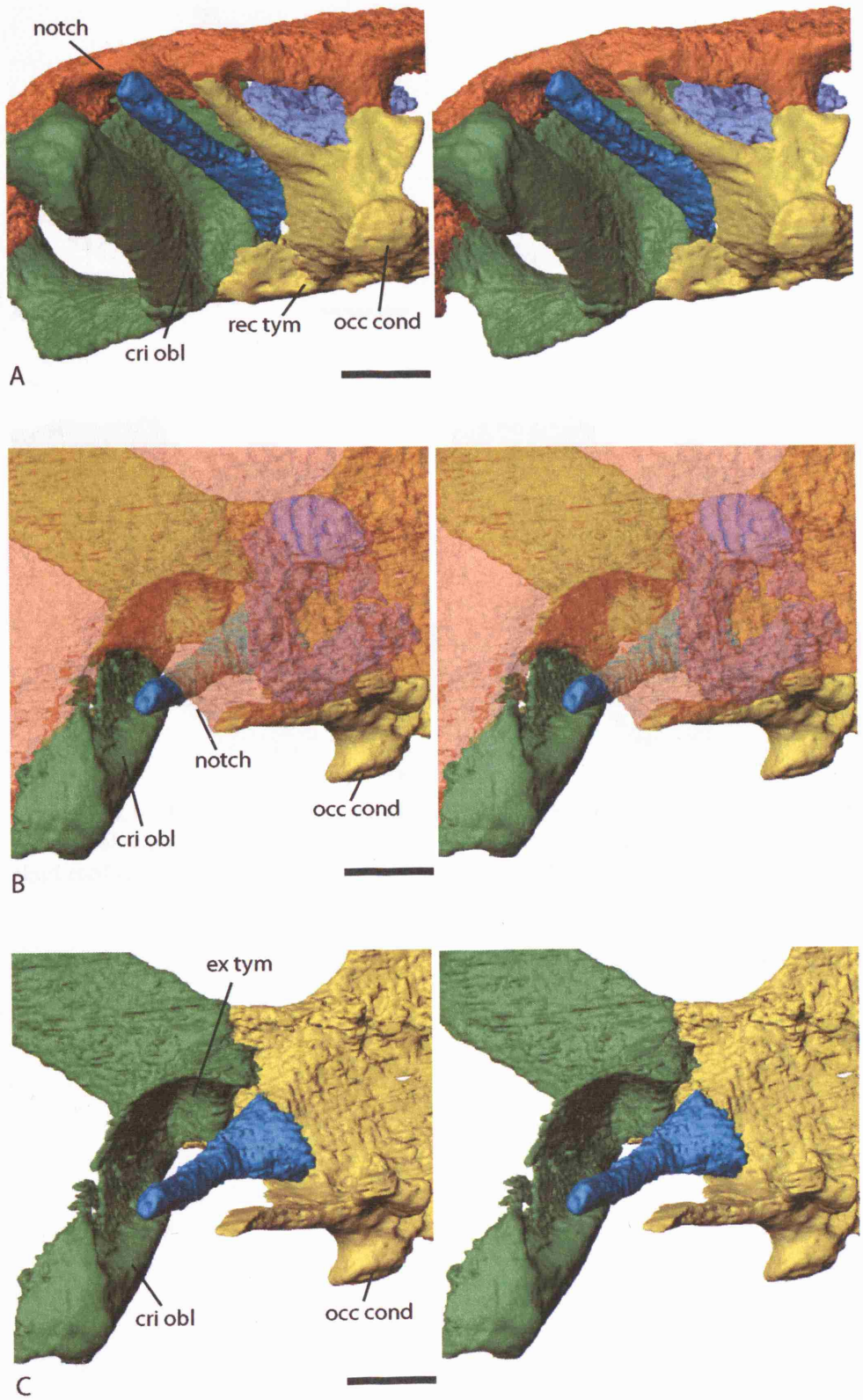

Figure 3.4.3—17 *Lydekkerina* specimen UMZC T.242. Stereo pairs of the left stapes *in situ*. A, posterior view. B, dorsal view with skull roof semi-transparent. C, dorsal view with skull roof and left otic capsule removed. Scale bars = 5mm.

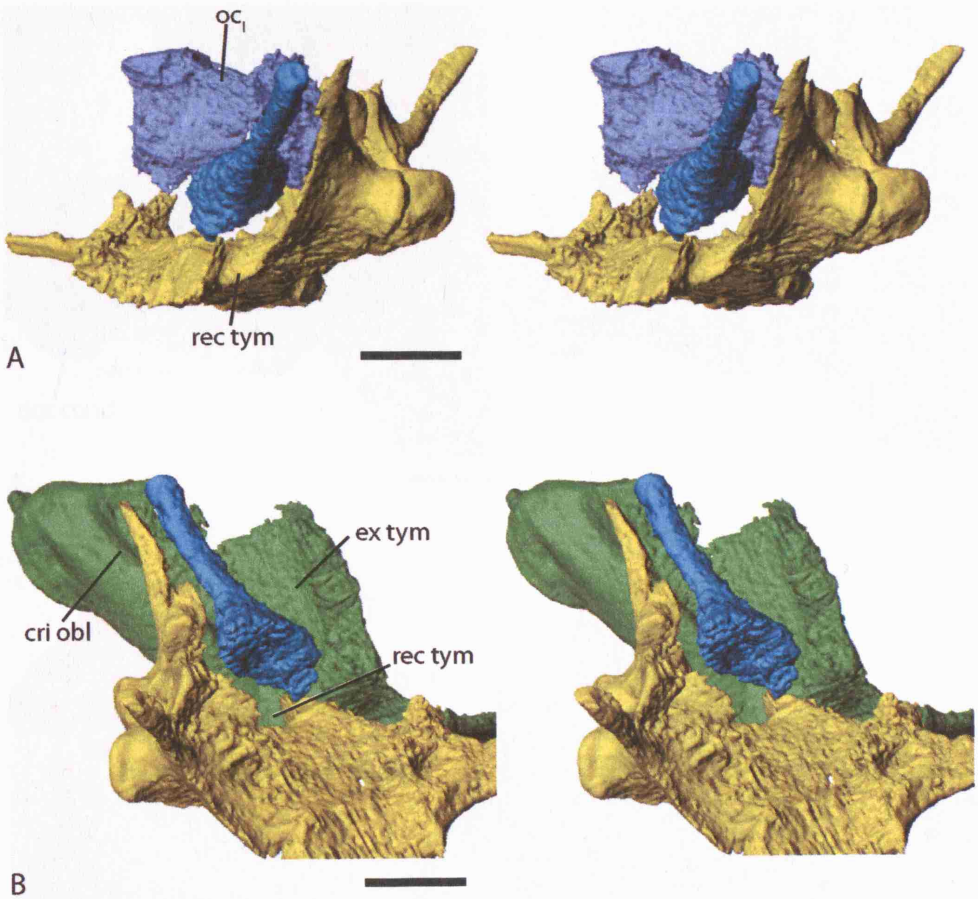

Figure 3.4.3—18 *Lydekkerina* specimen UMZC T.242. Stereo pairs of the left stapes *in situ*. A, left lateral view with skull roof and palatoquadrate complexes removed. B, medial view with skull roof and otic capsules removed. Scale bars = 5mm.

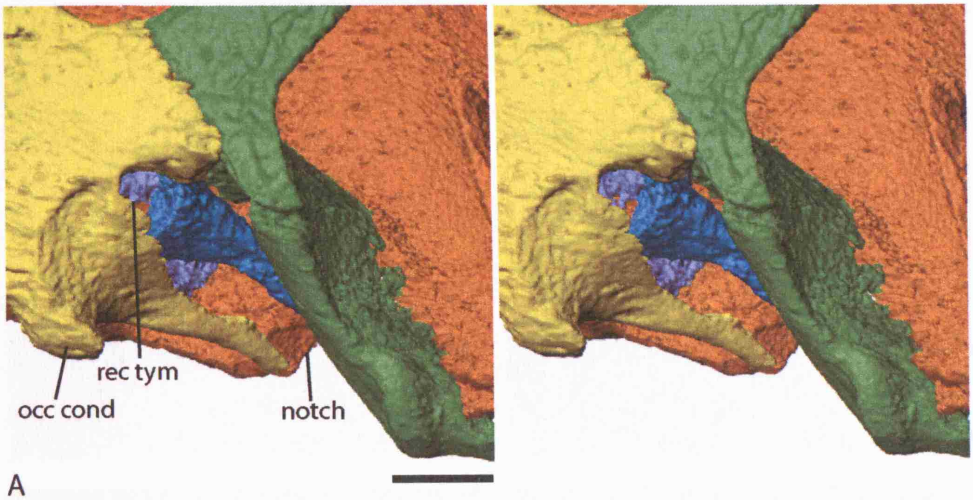

A

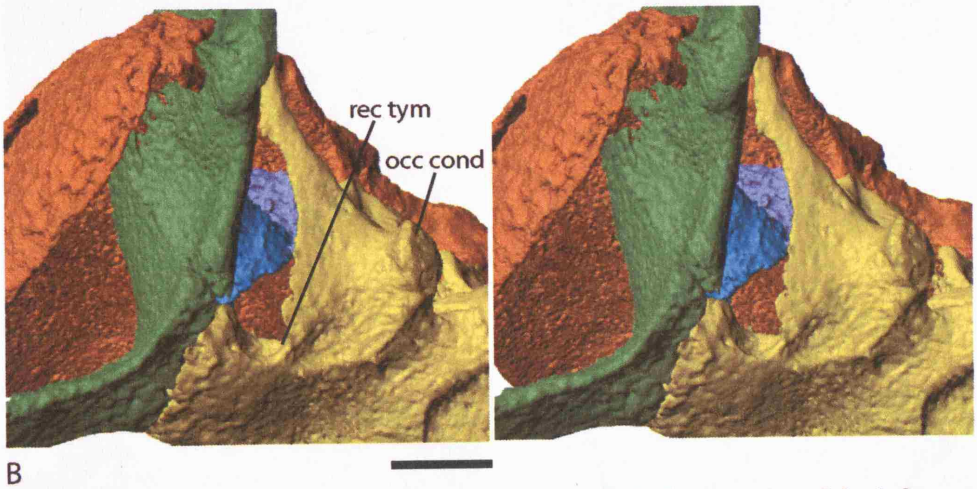

B

Figure 3.4.3—19 *Lydekkerina* specimen UMZC T.242. Stereo pairs of the left stapes *in situ*. A, offset ventral view with mandibles removed. B, left ventrolateral view with mandibles removed. Scale bars = 5mm.

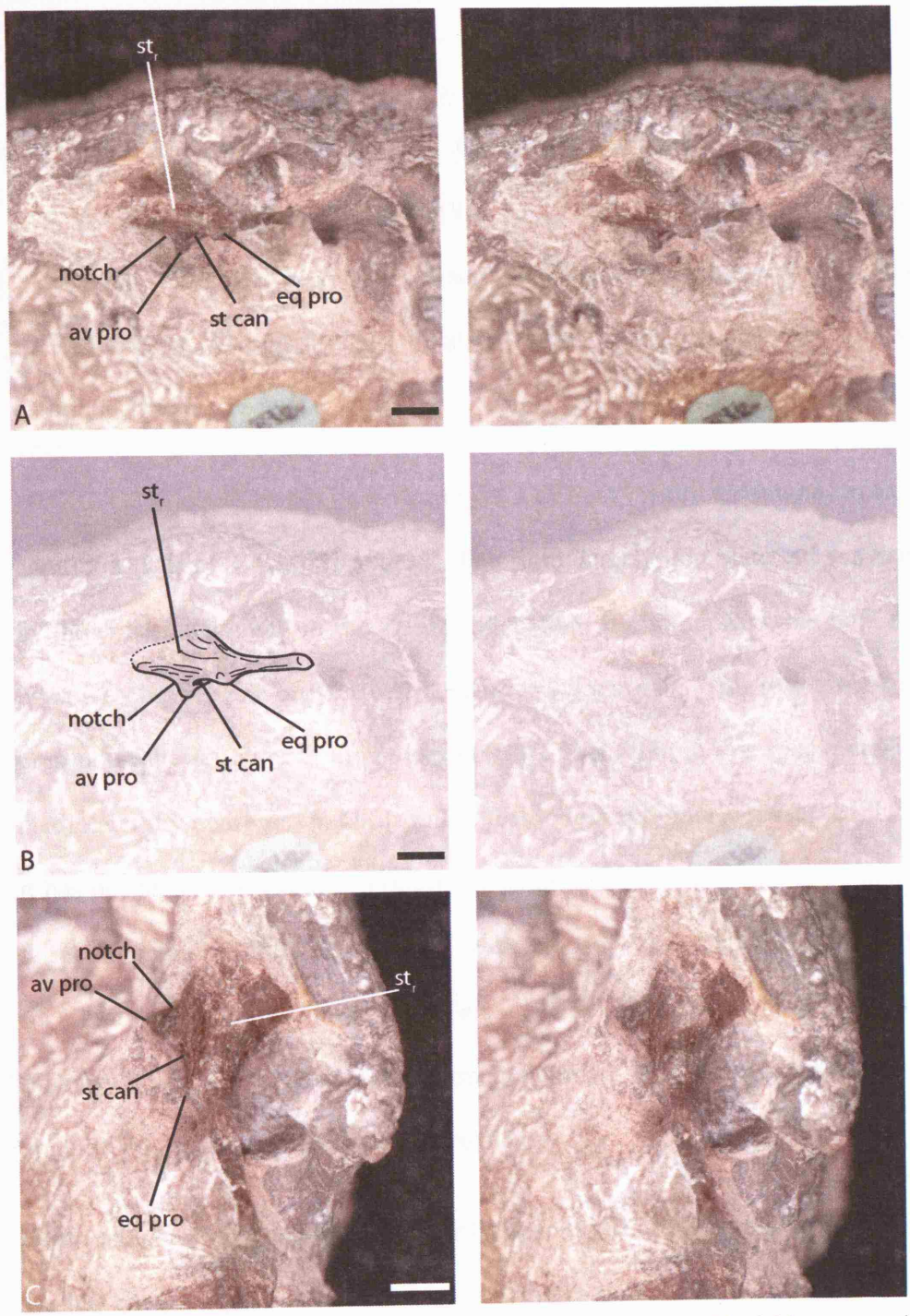

Figure 3.4.3—20 Photographic stereo pairs of the right stapes of *Lydekkerina* specimen UMZC T.206 *in situ*. A, posterior view. B, posterior view with interpretive line drawing showing main stapedial features. C, posterior view with dorsal to the right. Scale bars = 2mm.

Mandibles

Very little has been published on the mandibles of *Lydekkerina* since their first description in the then *Bothriceps* (Watson, 1912). The rather poor outline drawing produced in 1912 was altered by the addition of a postsplenial (postsphenial of Watson, 1919) bone by Watson in 1914 (Watson, 1919). Parrington (1948) only very briefly mentioned the lower jaws.

UMZC T.242 contains the posterior regions of both mandibles (mand) in an undistorted condition (Figure 3.4.3—21 and 22). The right is more complete but has been damaged by the crack mentioned in the skull roof section. It also appears that both retroarticular processes have been broken off at some previous date. The retroarticular process is present on the left side of the holotype (BMNH R.507); in this specimen the process is mediolaterally compressed but is rather featureless and poorly preserved. Unfortunately, it has not proved possible to visualise separate sutures within the mandibles. However, it seems apparent from comparison with closely related specimens described in the literature (for example *Rhineceps* (Watson, 1962), *Uranocentrodon* (Broom, 1930) and *Eryops* (Sawin, 1941)) that both fragments consist of articular, prearticular, surangular, angular, postsplenial, dentary and coronoid.

Teeth are present on both mandibular fragments with four on the left and approximately twelve on the right. In lateral view dermal ornament is present on the surangular, angular and postsplenial. No details of the lateral line system figured by Parrington (1948) in his figure 2 can be made out in UMZC T.242. In dorsal perspective the large ovoid mandibular fossa (mand foss) and the articular surface (mand art) of the jaw joint can be seen.

On the medial surface of each mandible an inframeckelian fossa (im foss) is present below the anterior part of the mandibular fossa. It is not known which ossifications form the boundaries of these fossae. At the posterior extent of each mandible, below the articular surface, there is an elongate depression containing a foramen. This foramen (the 'dental foramen' (den for)) and depression have been figured in *Rhineceps* (Watson, 1962) and *Eryops* (Sawin, 1941).

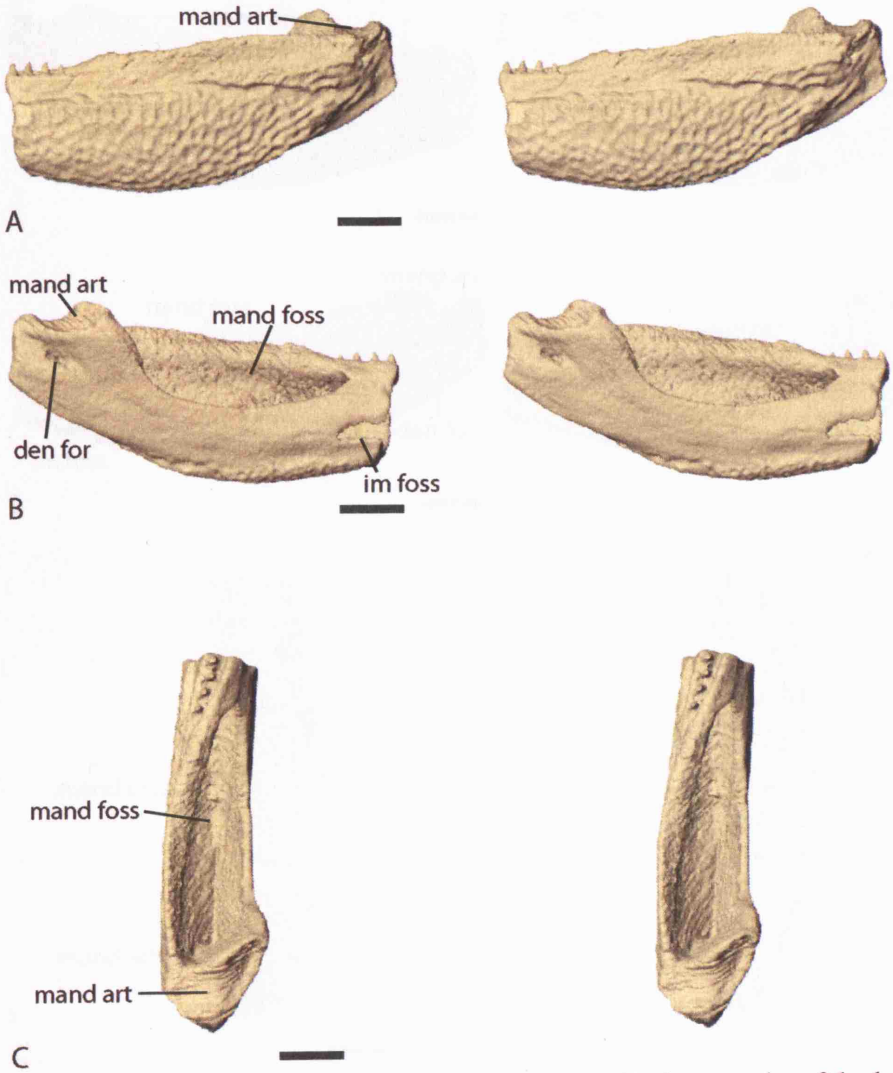

Figure 3.4.3—21 *Lydekkerina* specimen UMZC T.242. Stereo pairs of the left mandible. A, left lateral view. B, medial view. C, dorsal view. Scale bars = 5mm.

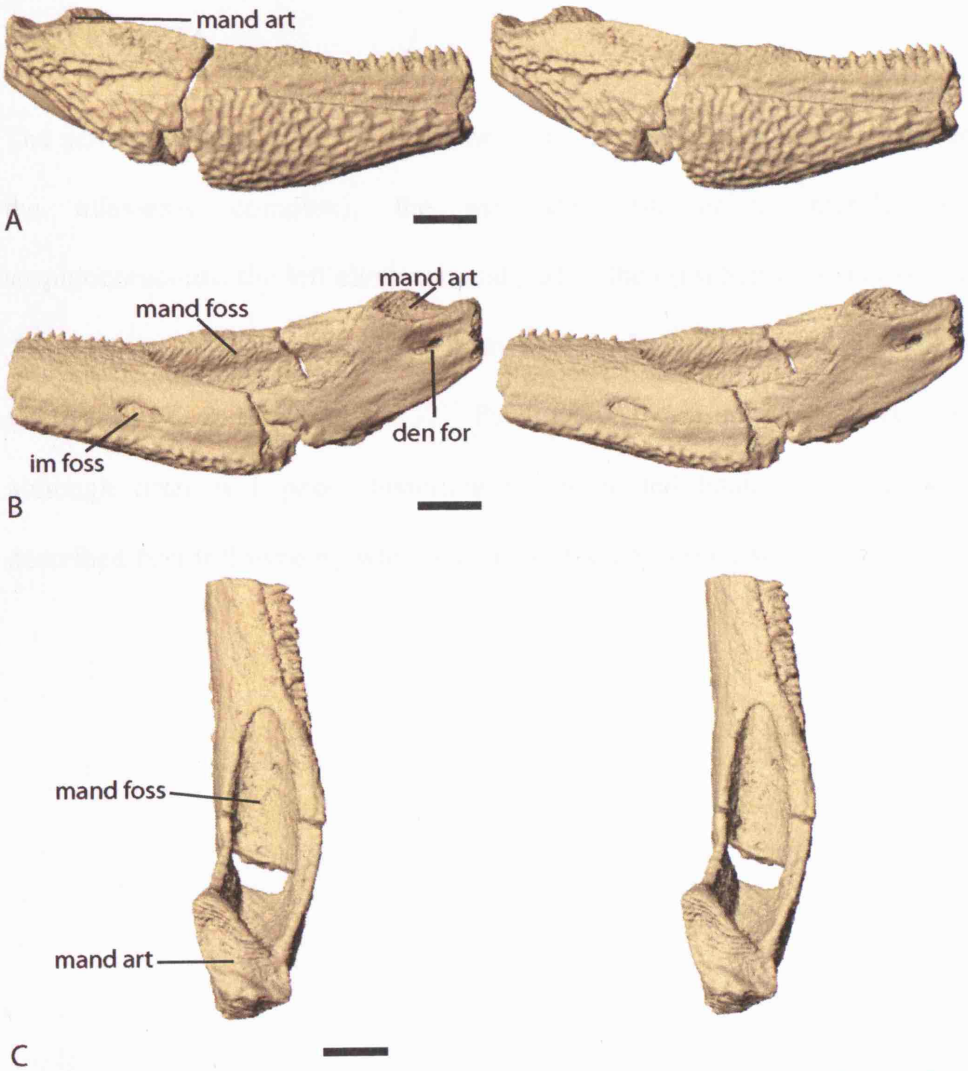

Figure 3.4.3—22 *Lydekkerina* specimen UMZC T.242. Stereo pairs of the right mandible. A, right lateral view. B, medial view. C, dorsal view. Scale bars = 5mm.

POSTCRANIA

The postcranial of UMZC T.242 consists of the ten most anterior vertebrae (including the atlas-axis complex), the associated rib pairs, interclavicle, clavicles, scapulocoracoids, the left cleithrum and part of the right humerus (hum) (Figure 3.4.3—23 and 24). All these areas have been described previously (for example see Watson (1919), Broili & Schröder (1937), Parrington (1948) and Pawley & Warren (2005), although, often with poor illustration and/or limited detail. The axial skeleton will be described first followed by what remains of the appendicular skeleton.

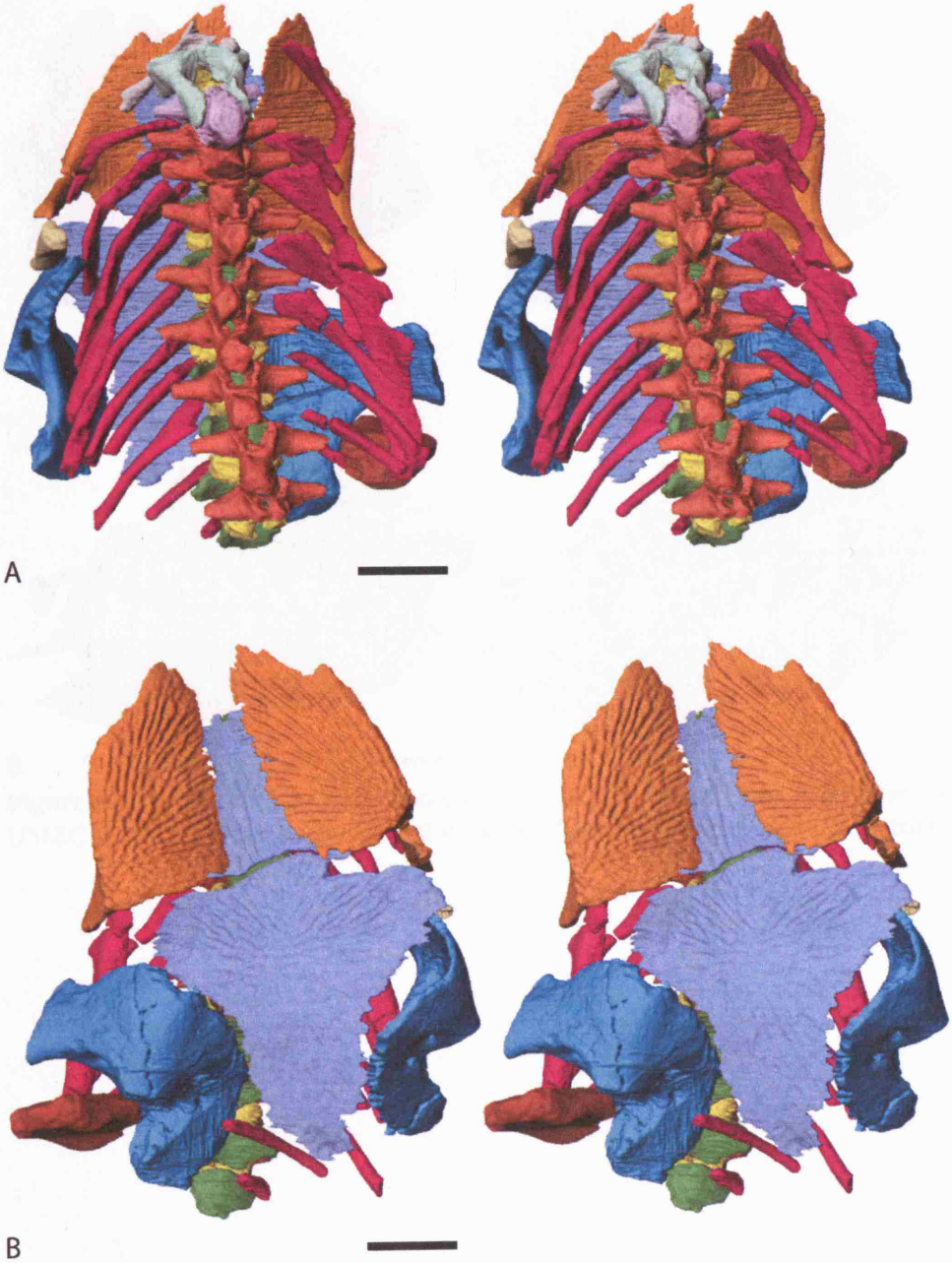

Figure 3.4.3—23 *Lydekkerina* specimen UMZC T.242. Stereo pairs of the postcranial model of UMZC T.242. A, dorsal view. B, ventral view. Scale bars = 10mm.

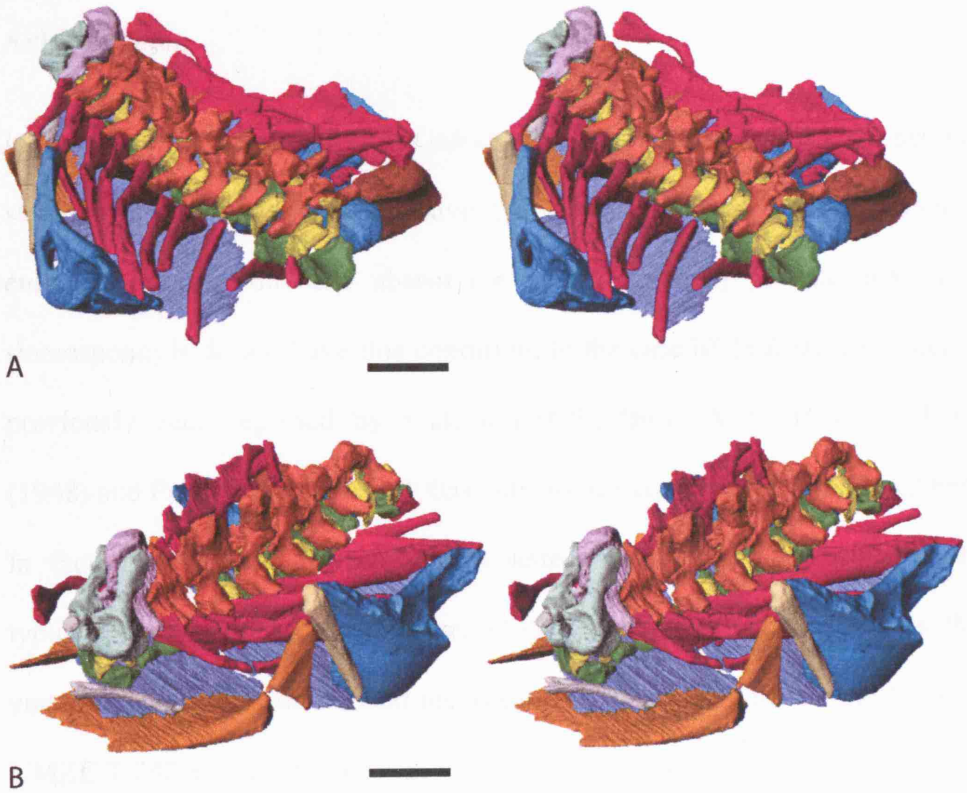

Figure 3.4.3—24 *Lydekkerina* specimen UMZC T.242. Stereo pairs of the postcranial model of UMZC T.242. A, offset posterodorsal view. B, offset anterodorsal view. Scale bars = 10mm.

Axial skeleton

In most recent classifications *Lydekkerina* has been classified as belonging to the stereospondyls yet it does not have the stereospondylus vertebral condition with an enlarged intercentrum and absent (or highly reduced) pleurocentra. In fact, many stereospondyls do not have this condition. In the case of *Lydekkerina* pleurocentra have previously been reported by Watson (1919), Broili & Schröder (1937), Parrington (1948) and Pawley & Warren (2005), although, frequently they are described as reduced. In fact, Pawley and Warren (2005) state that 'the vertebrae [of Lydekkerina] are typically neorhachitomous (Romer, 1947), in that the intercentrum is the dominant vertebral element, with reduced pleurocentra'. The information collected from scanning UMZC T.242 appears to disagree with this statement (Figure 3.4.3—25 and 26).

The anterior most part of the axial skeleton of UMZC T.242 is the atlas (Figure 3.4.3—27 and 28 A and B), a single ossified element which consisted of the first neural arch fully fused to its corresponding intercentrum. There appears to have been no proatlantal arch, (paired unfused proatlas neural arches as seen in early tetrapods such as *Greererpeton* (Godfrey, 1989) and *Eryops* (Moulton, 1974)). Unlike the only previous description of the atlas (Broili & Schröder, 1937) there does not appear to have been a separate intercentrum as it appears to have been incorporated into the atlas element. The full incorporation of the intercentrum into the atlas complex is described by Romer (1947) as occurring in 'later temnospondyls'; certainly in the description of the postcranial of phylogenetically earlier temnospondyl *Eryops* (Moulton, 1974) the atlas has a separate intercentrum which did not fuse with the neural arches. In anterior view the form of the atlas of *Lydekkerina* is most clearly visualised. The neural spines of the atlantal arch do not fuse at the midline but instead clasp, but in no way unite, with the

fused neural spines of the axis. These paddle shaped spines contract lateral to the neural tube and then expand into crescent shaped concave pads which fuse at their ventral margin. This ventral fusion represents part of the intercentrum which also contribute to the ventral part of the paired pads. Medial to the pads is an oval hole, which is open dorsally, for the reduced notochord to pass through to the notochordal pit within the basioccipital. In posterior view the articulatory surfaces for contact with the neural spine of the axis are visible on the medial surface of the spines. Furthermore, it seems likely that there was contact with both the axis neural arch and intercentrum (int cen) more ventrally. Behind the pads of the atlas it can be seen that the notochordal tube narrowed rapidly from the large diameter of the axis tube to the small oval hole mentioned previously. There are no ribs associated with the atlas as is the standard condition.

There has been a small degree of disturbance in the axis and third vertebra region in the otherwise fully articulated cervical vertebrae series; the left pleurocentrum from the third vertebra appears to have been translocated forwards causing the left pleurocentrum of the axis vertebra to be slightly displaced (Figure 3.4.3—27). Nevertheless, the composition and orientation of all elements in the axis can be reconstructed with some confidence. The axis (Figure 3.4.3—27 and 28 C and D) consists, like all other vertebrae in UMZC T.242 (except the atlas), of a fused neural arch, paired pleurocentra and an intercentrum. The most prominent difference between the axis and the more posterior vertebrae is the anteriorly expanded neural arch which has contact surfaces for the unfused spines of the atlas. The condition is very similar to that depicted in *Eryops* (Moulton, 1974). Lateral to the spine the neural arch forms the diapophysis for articulation with the tuberculum process of the first ribs. In posterior view the area of the post-zygapophysis (pozy) are visible, although, not clearly defined. In contrast on the ventromedial surface of the neural arch the large contact surface for the pleurocentra

are present. From the fact that no pleurocentra is found directly attached to the neural arch in any of the vertebrae it would appear that this contact was cartilaginous.

The pleurocentra of the axis are crescent shaped with a large contact surface in their anterior faces for the presumed cartilaginous contact with the neural arch. Their internal surface is curved to lie against the notochord, while the posterior margin is approximately straight in lateral view. The intercentrum of the axis has a curved, rather poorly defined, crescent shape. There is no evidence for parapophysis, for the articulation with the capitulum of the first ribs, on the dorsolateral margins of the intercentrum.

The third to the tenth vertebrae have roughly the same form and orientation (Figure 3.4.3—25 and 26). They all consist of fused neural arches, paired pleurocentra and intercentrum. The intercentrum from the eleventh vertebra is also present. The neural arches are very similar to that of the axis, minus the anterior extension of the spine for contact with the neural spines of the atlas. All spines have been damaged and it is difficult to see the full extent of their dorsal extension, although, the sixth vertebra gives a reasonable guideline (Figure 3.4.3—29, 30 and 31). In lateral view it is apparent that each neural arch has a derived form with a neural spine displaced posteriorly relative to the transverse processes and diapophysis (dia). The neural spines sit above the post-zygapophysis and the transverse processes sit below the pre-zygapophysis (przy). This condition is 'common to Mesozoic temnospondyls' (Warren & Snell, 1991) and contrasts with the more ancestral condition seen in *Eryops* (Moulton, 1974).

The pleurocentra and intercentra are approximately uniform throughout the series and vary little from those described for the axis. As with the axis it is clear that the pleurocentra had a far more dominant role in the vertebral column than suggested by

material examined by Pawley and Warren (2005). They do not appear to be 'very thin' (Watson, 1919) and are over half as wide anteroposteriorly as the intercentra. From the size of the pleurocentra in UMZC T.242 it would appear that *Lydekkerina* has a fully rhachitomous vertebral condition without reduced pleurocentra of so called 'neorhachitomous' temnospondyls. In fact, the pleurocentra of UMZC T.242 make a larger contribution to the cervical vertebrae than appears to have been the case with the stereotypical rhachitomous temnospondyl *Eryops* (Moulton, 1974) – this is in direct contrast with the situation described by Pawley & Warren (2005). As with the axis the pleurocentra have well defined anterior surfaces for contact, probably via cartilage, to the neural arches.

The intercentra are approximately oval in dorsal view and a shallow crescent shape in anterior view. In lateral view they are roughly triangular shaped with a concave ventral surface. The composite reconstruction presented by Pawley & Warren (2005) in their text-figure 5d-f are quite different with a far more horseshoe shaped intercentrum in anterior view. There also does not appear to be any evidence for parapophyses on the posterolateral margins of any of the intercentra, although this could represent a limitation of the scanning resolution rather than a true characteristic as they have been noted in *Lydekkerina* on numerous occasions and can be seen on the intercentra of UMZC T.206 pers.obs and Parrington (1948). The intercentra are not paired and divided along the midline as described by Parrington (1948). This may be a developmental difference or as Parrington mentions the intercentra may have been broken in their preservation.

The ribs associated with the axis and the following eight cervical vertebrae are nearly all present (Figure 3.4.3—32) and do not appear to have been distorted, although, their

positions have clearly changed for there is no contact with the vertebral column. All have dorsoventrally elongate proximal ends with near separate tuberculum and capitulum surfaces producing a flattened 'figure of eight' articulatory surface (Figure 3.4.3—32 E). The ribs all narrow from their proximal ends until they have a rod like appearance with approximately circular cross sections – producing triangular heads. Apart from these consistent features the ribs vary in character from anterior to posterior. The ribs associated with the axis have a noticeable posterior bend lateral to the head in posterior view. This bend is present to a progressively lesser extent in the ribs associated with the third to seventh vertebrae. The ribs associated with the third to seventh vertebrae become flattened and paddle shaped distal to their rod like areas. This dorsoventral expansion of the ribs produces distinct uncinate processes (unc pro) on their dorsal margin, which can be observed clearly in the ribs associated with the fourth and fifth vertebrae on the left side. The remains of the more posterior ribs seem to have an overall more rod shaped appearance.

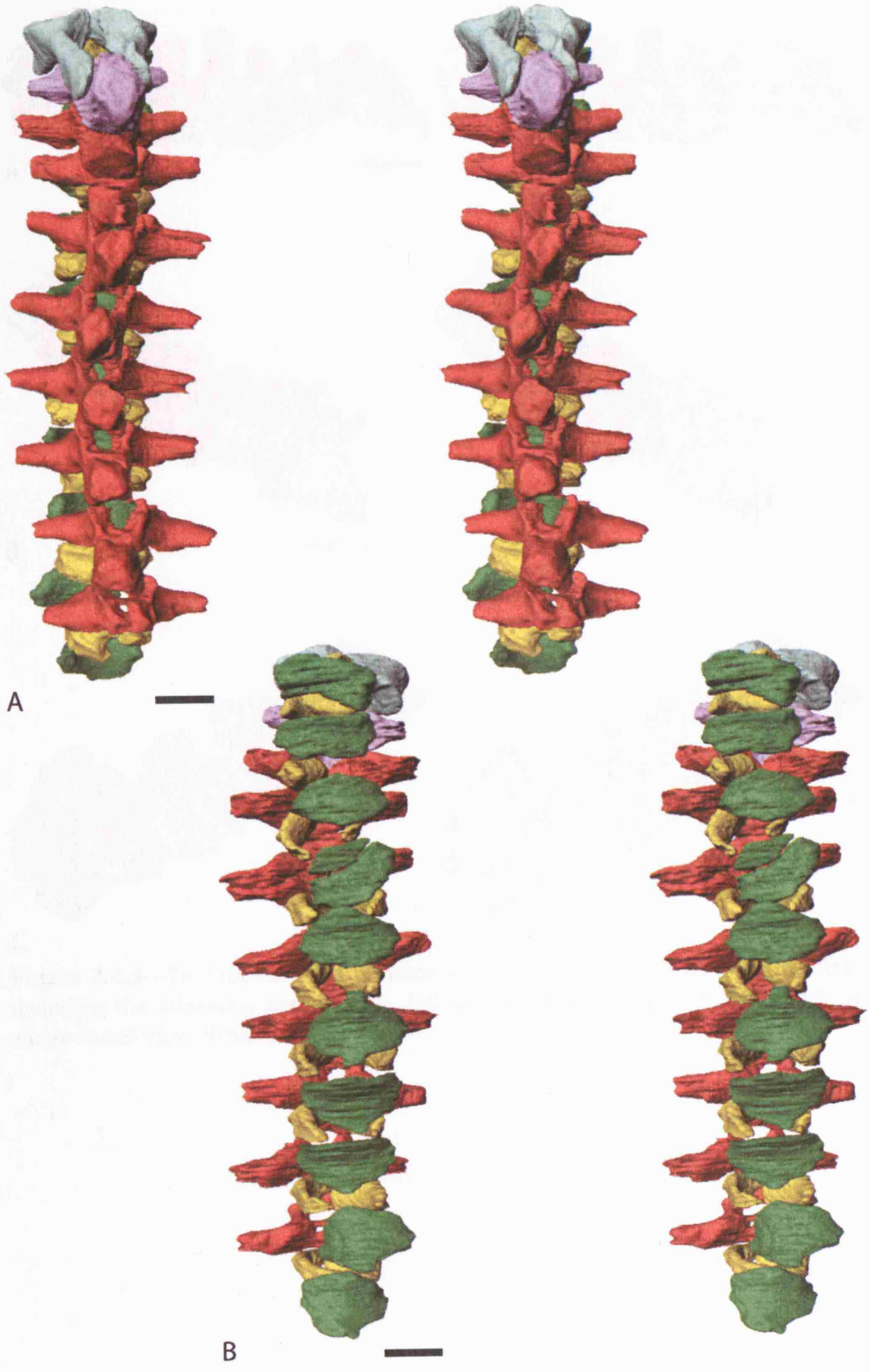

Figure 3.4.3—25 *Lydekkerina* specimen UMZC T.242. Stereo pairs of the first 10 vertebrae including the atlas-axis complex. A, dorsal view. B, ventral view. Scale bars = 5mm.

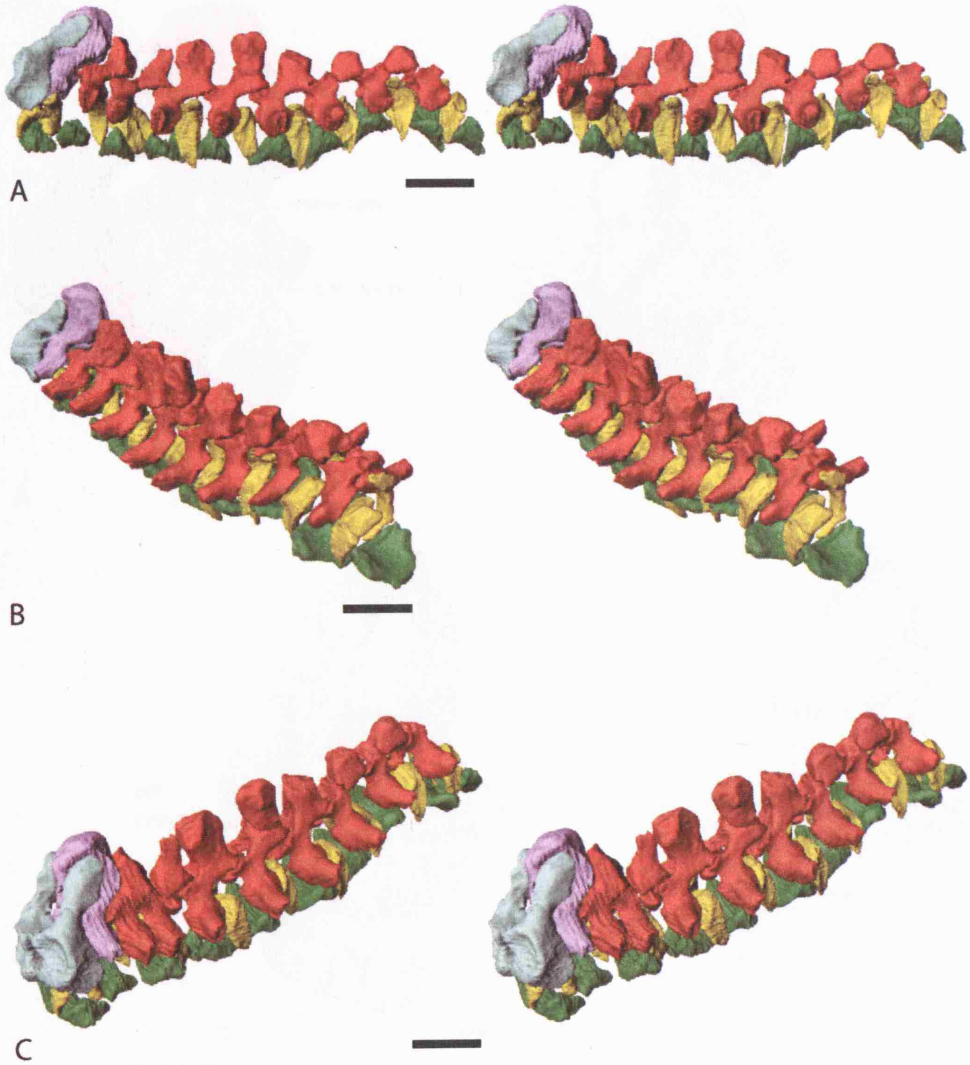

Figure 3.4.3—26 *Lydekkerina* specimen UMZC T.242. Stereo pairs of the first 10 vertebrae including the atlas-axis complex. A, left lateral view. B, offset posterodorsal view. C, offset anterodorsal view. Scale bars = 10mm.

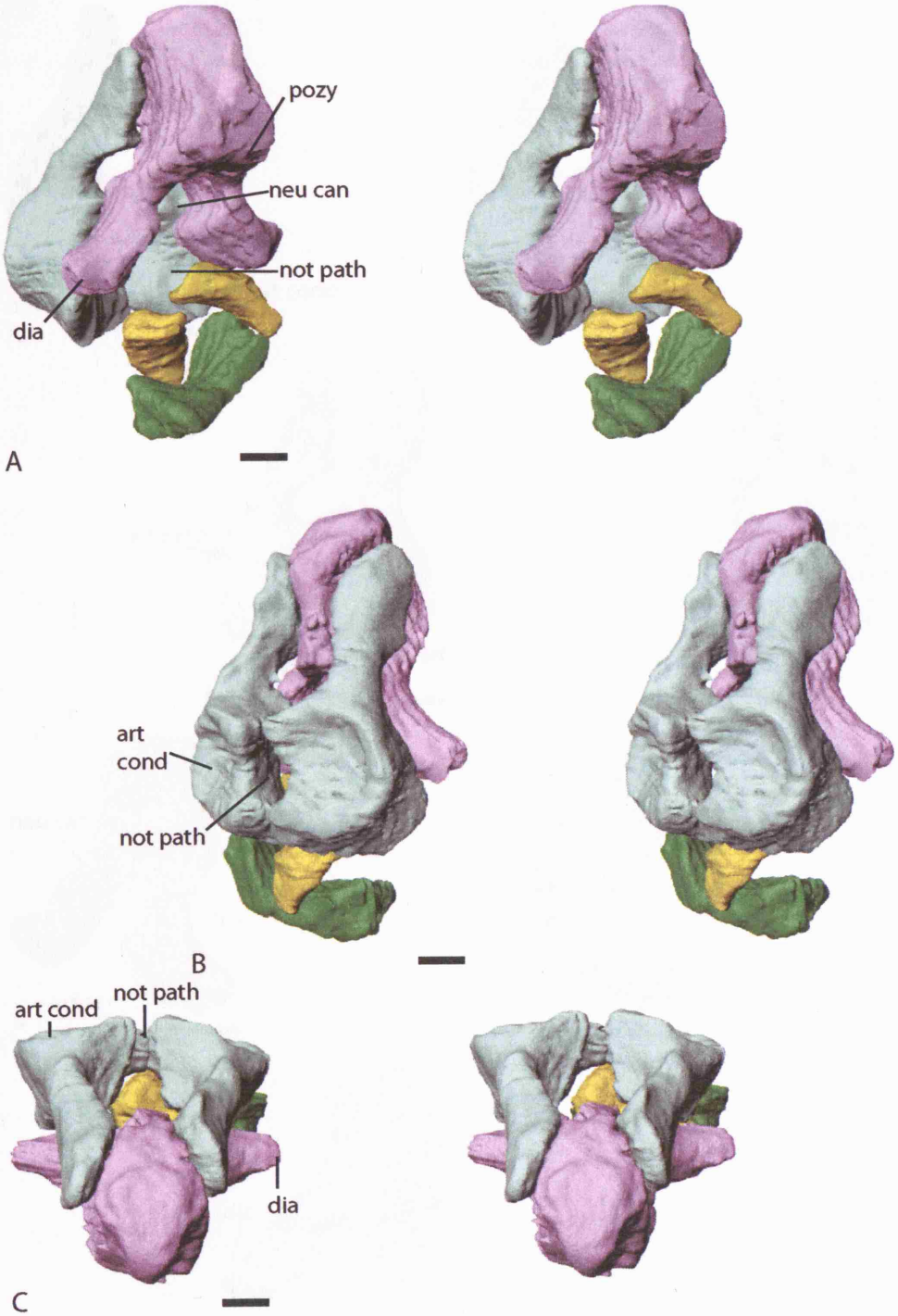

Figure 3.4.3—27 *Lydekkerina* specimen UMZC T.242. Stereo pairs of the atlas-axis complex. A, left posterolateral view. B, left anterolateral view. C, dorsal view. Scale bars = 2mm.

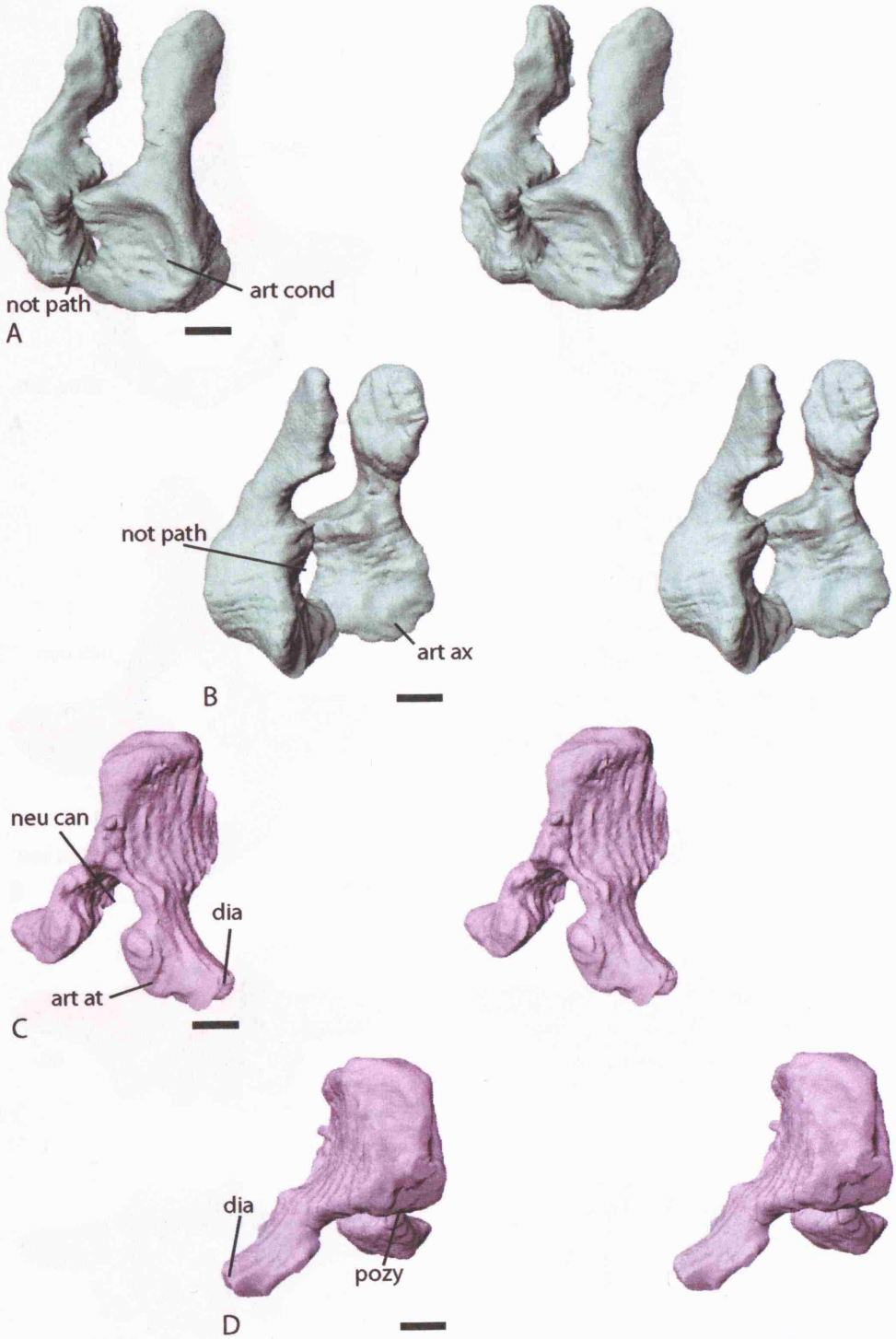

Figure 3.4.3—28 *Lydekkerina* specimen UMZC T.242. Stereo pairs. A, atlas in left anterolateral view. B, atlas in left posterolateral view. C, neural arch of the axis in left anterolateral view. D, neural arch of the axis in left posterolateral view. Scale bars = 2mm.

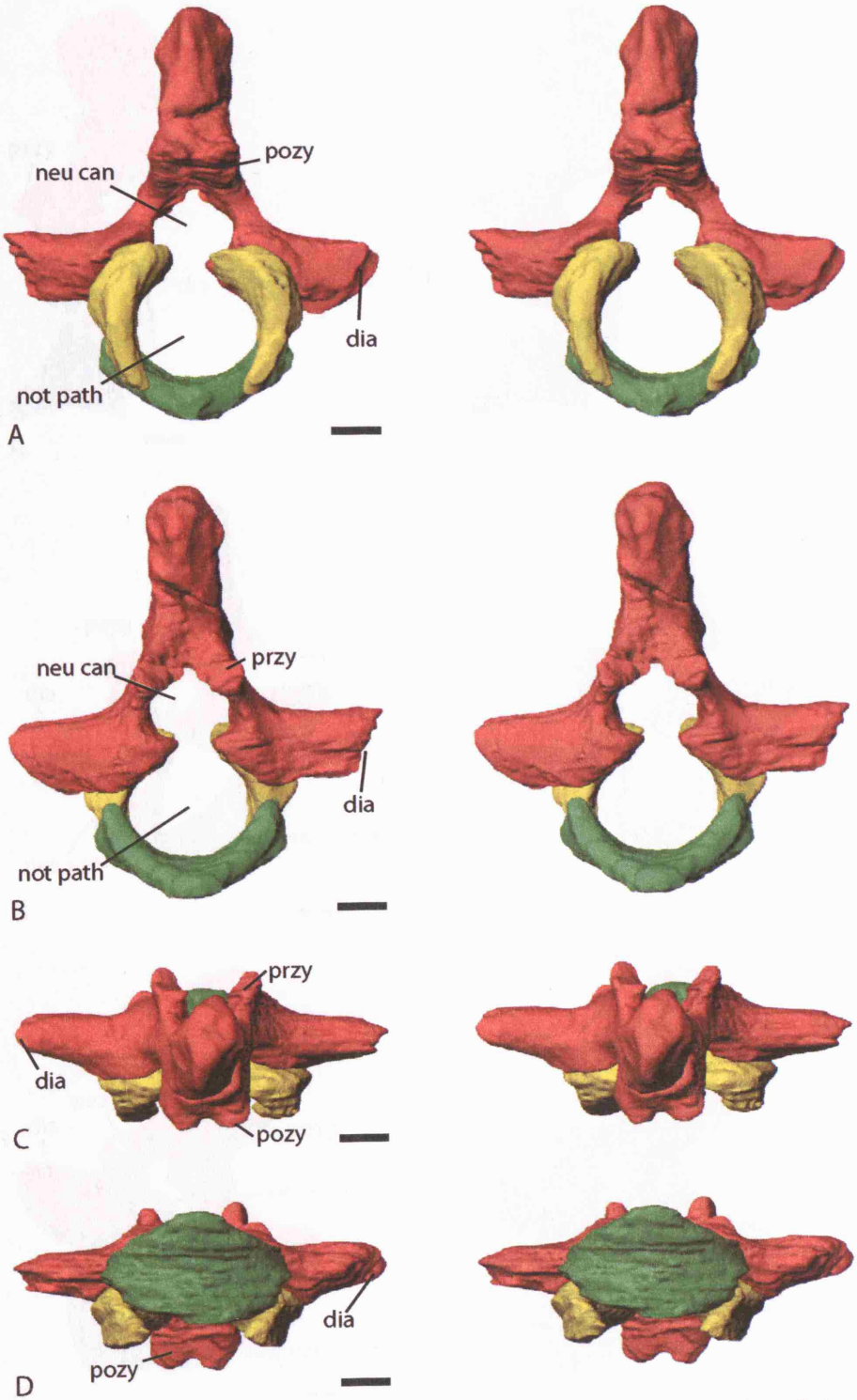

Figure 3.4.3—29 *Lydekkerina* specimen UMZC T.242. Stereo pairs of the 6th vertebra with correction for slight translocations. A, posterior view. B, anterior view. C, dorsal view. D, ventral view. Scale bars = 2mm.

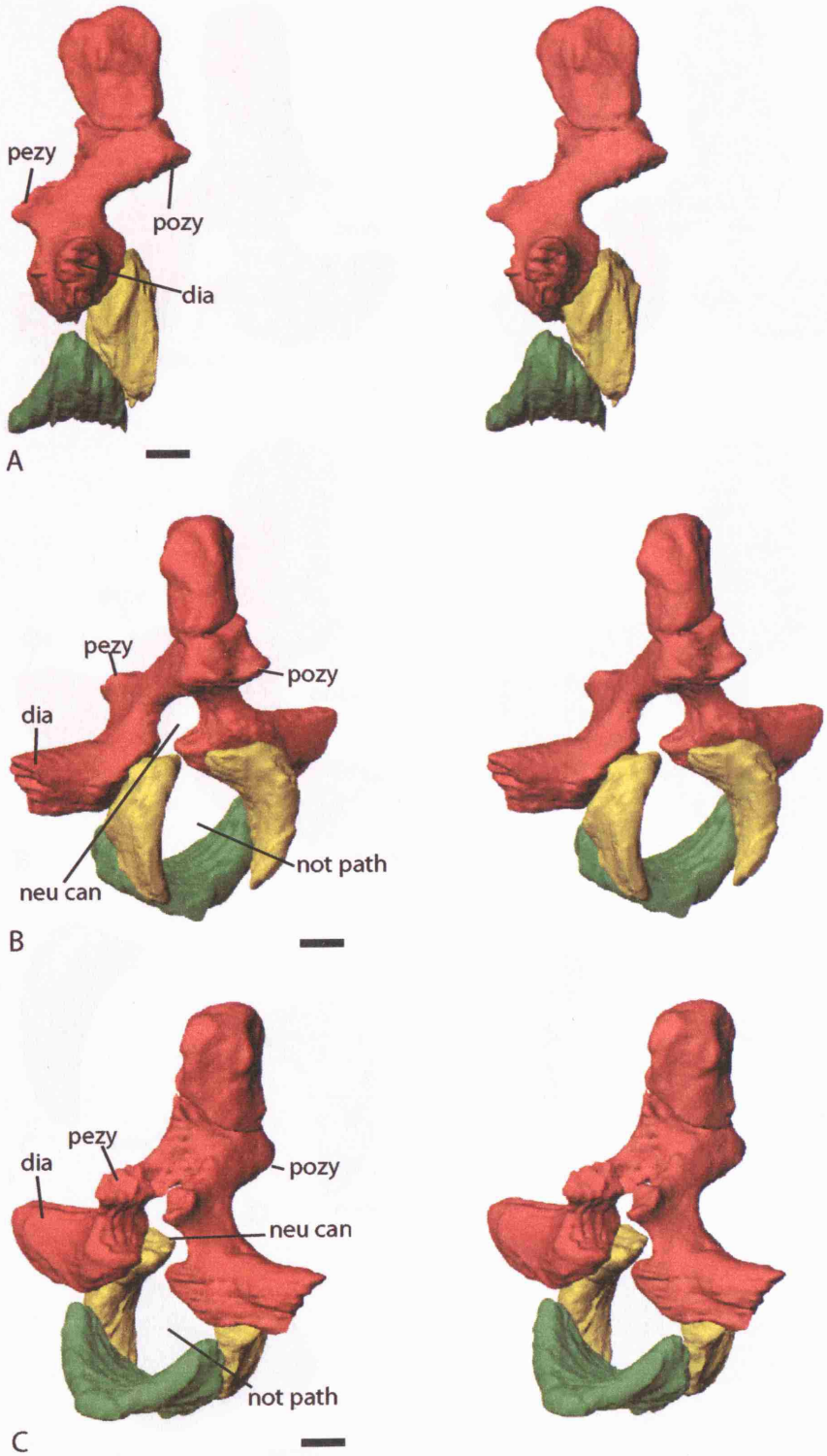

Figure 3.4.3—30 *Lydekkerina* specimen UMZC T.242. Stereo pairs of the 6th vertebra with correction for slight translocations. A, left lateral view. B, left posterolateral view. C, left antero-lateral view. Scale bars = 2mm.

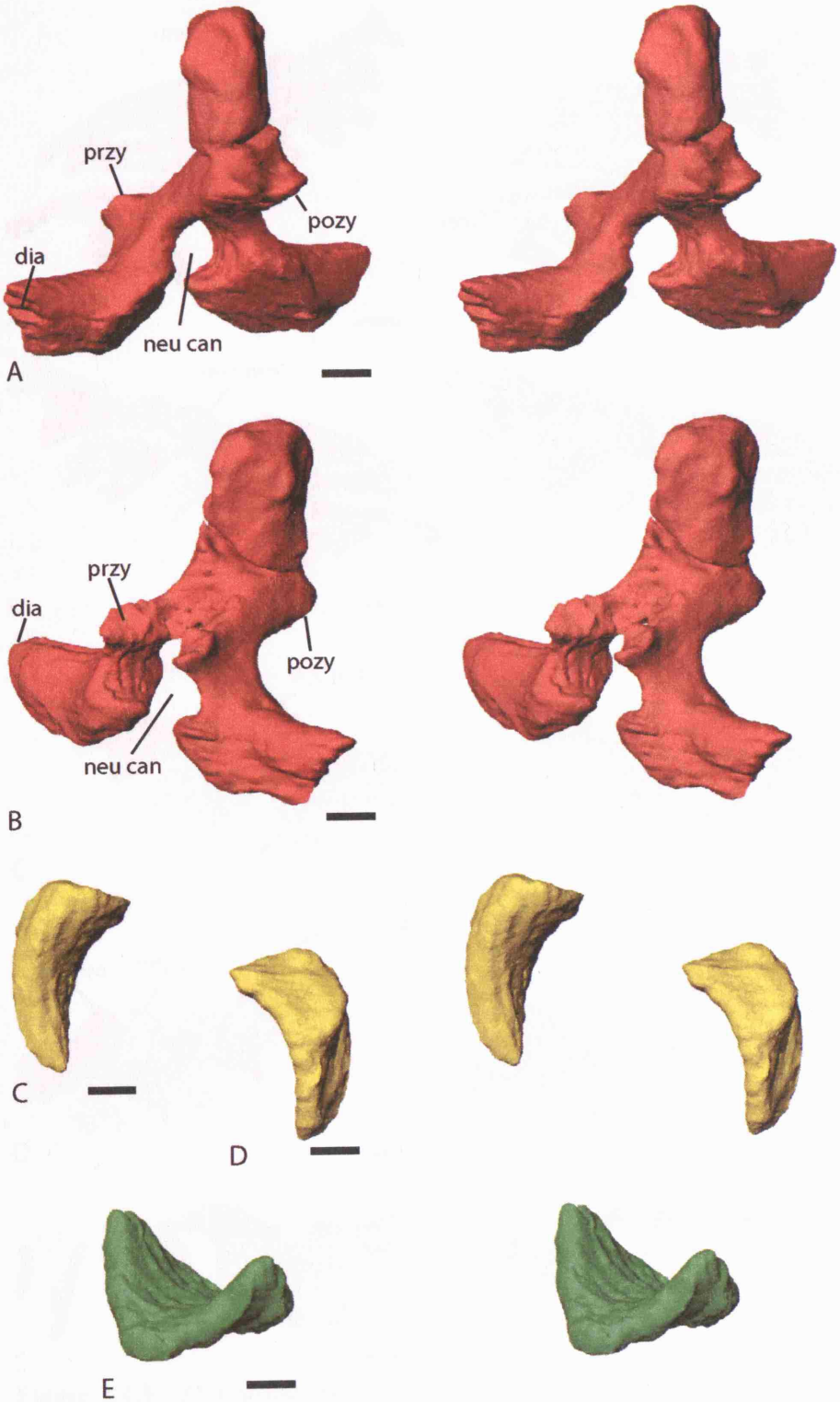

Figure 3.4.3—31 *Lydekkerina* specimen UMZC T.242. Stereo pairs. A, neural arch of the 6th vertebra in left posterolateral view. B, neural arch of the 6th vertebra in left anterolateral view. C, left pleurocentra of the 6th vertebra in posterior view. D, left pleurocentrum of the 6th vertebra in anterior view. E, intercentrum of the 6th vertebra in left anterolateral view. Scale bars = 2mm.

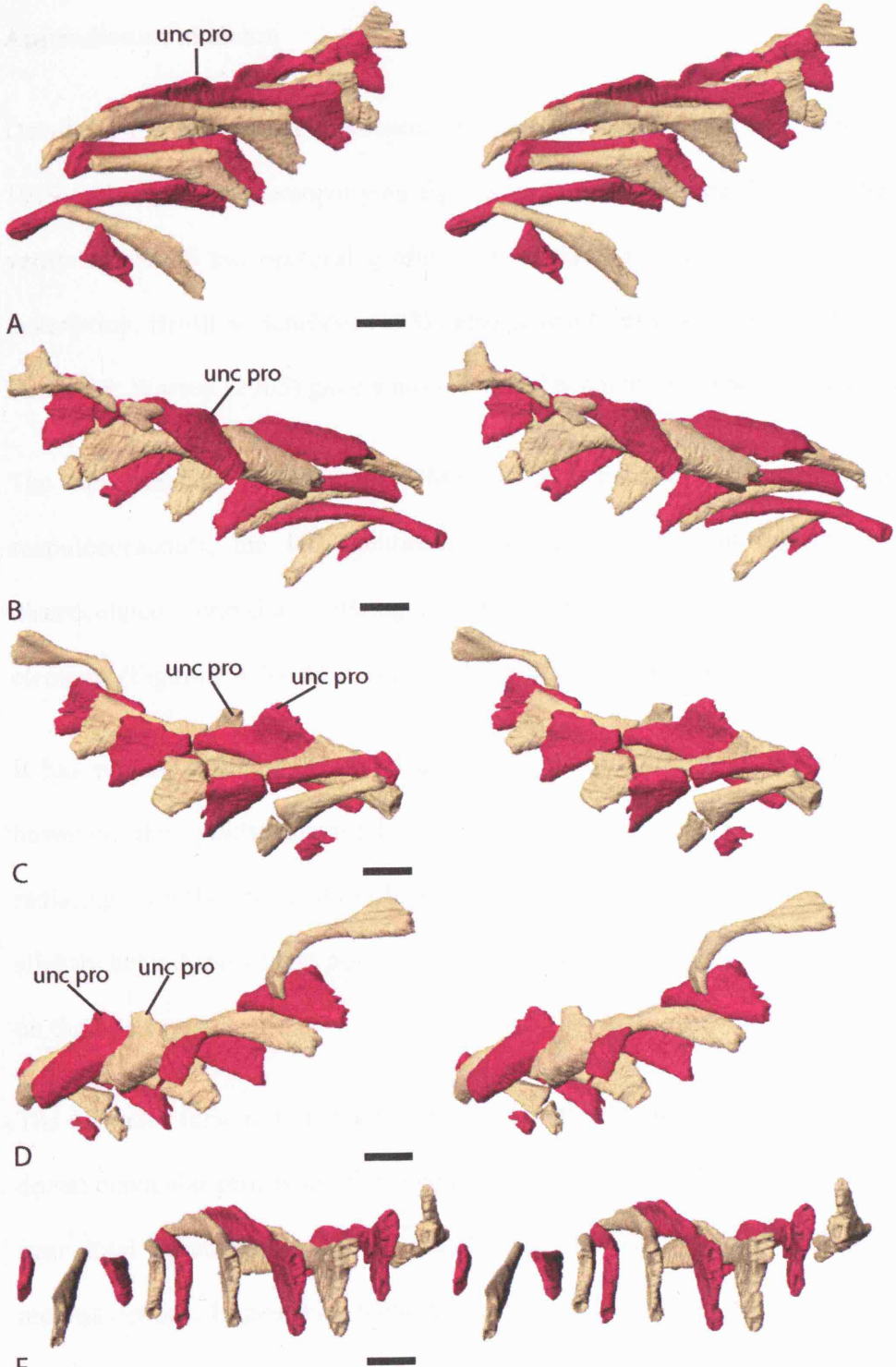

Figure 3.4.3—32 *Lydekkerina* specimen UMZC T.242. Stereo pairs. A, left cervical ribs in posteromedial view. B, left cervical ribs in left anterolateral view. C, right cervical ribs in posteromedial view. D, right cervical ribs in right anterolateral view. E, left cervical ribs in medial view showing the 'figure of eight' articulatory surfaces. Odd numbered ribs in beige to aid visualisation. Scale bars = 5mm.

Appendicular skeleton

Details of the appendicular skeleton of *Lydekkerina* were first described by Watson in 1919, although, the accompanying figures were rather limited. Broom (1930) figured a ventral view of the pectoral girdle of *Lydekkerina*, however, there was little extra description. Broili & Schröder (1937) also gave a brief description of the pectoral girdle. Pawley & Warren (2005) gave a more detailed account of the pectoral girdle.

The appendicular skeleton of UMZC T.242 consists of interclavicle, clavicles, scapulocoracoids, the left cleithrum and part of the right humerus in a slightly disarticulated condition, although, there is no actual distortion of the individual elements (Figure 3.4.3—33 A and B). All elements have some degree of damage.

It has proved difficult to model accurately the margin of the interclavicle (int cla), however, the typical diamond shape is clear (Figure 3.4.3—33 C). The rugosity radiating from the centre of ossification is also visible. This centre of ossification is only slightly behind the widest point of the interclavicle. There are no other features of note on the intercentrum.

The clavicles (cla_l and cla_r) are essentially complete apart from the distal extent of the dorsal clavicular processes (dor pro) (Figure 3.4.3—34 and 35). Their morphology is in near total agreement with that of Pawley & Warren (2005) in their composite reconstructions. In posterior view it can be seen that dorsal clavicular processes are at right angles to the ventral surface of the clavicle. The left cleithrum (cle_l) (Figure 3.4.3—33 D and E) also conforms to the description of Pawley &Warren (2005).

The remaining parts of the pectoral girdle are the paired endochondral scapulocoracoids (scap cor) (Figure 3.4.3—36 and 37). Both have a certain degree of damage to the

dorsal scapula blade with the posterior margin of the left dorsal scapula blade being completely lost. The right scapulocoracoid, however, demonstrates the broad dorsal scapula blade previously figured in *Lydekkerina* (Pawley & Warren, 2005). In lateral and posterior views the enclosed supraglenoid foramen (sg for) and the glenoid fossa (gle foss) are visible and conform to previous description Pawley & Warren (2005). In ventral view the coracoid foramen (cor for), the glenoid foramen (gle for), infraglenoid recess (ig rec) and ridge (ig rid) can also be seen medial to the glenoid fossa.

Unfortunately, it has not proved possible to find any scarring on the pectoral girdle which would suggest muscular connections to the middle ear region, as seen in extant anurans and urodeles. It is not believed, however, that this in any way precludes the possibility of such attachments, as there are also no muscle scars for the large muscle groups which would have attached to the pectoral girdle, such as the levator scapulae. The muscles may never have made noticeable scars on the pectoral girdle or they may not have been prominent enough to have been preserved and visualised.

The only additional appendicular element present in UMZC T.242 is the proximal end of the right humerus (Figure 3.4.3—23 and 24).

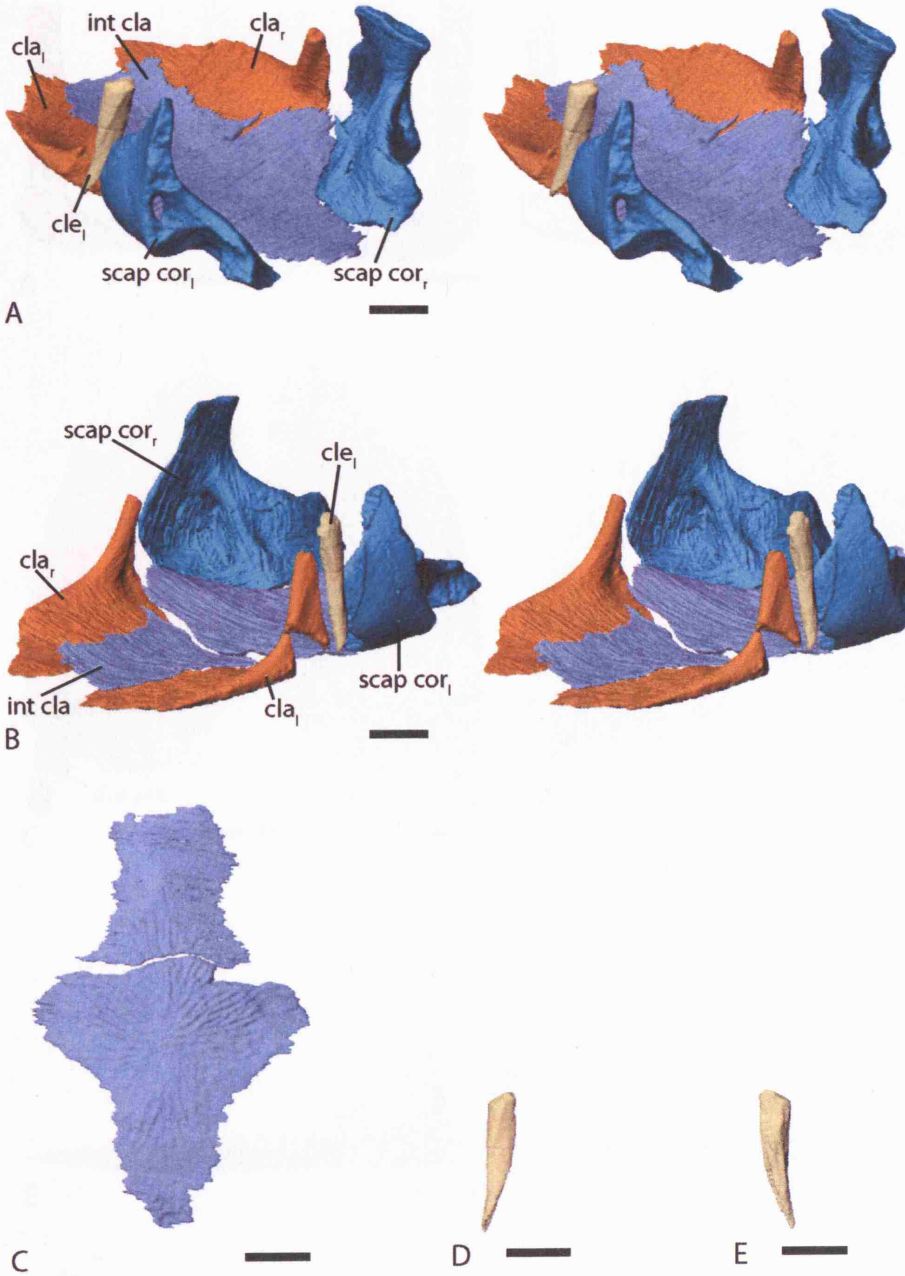

Figure 3.4.3—33 *Lydekkerina* specimen UMZC T.242. A and B, stereo pairs of the pectoral girdle with correction for translocations. A, offset posterodorsal view. B, offset anterodorsal view. C, interclavicle in ventral view. D and E, left cleithrum. D, left lateral view. E, medial view. Scale bars = 10mm.

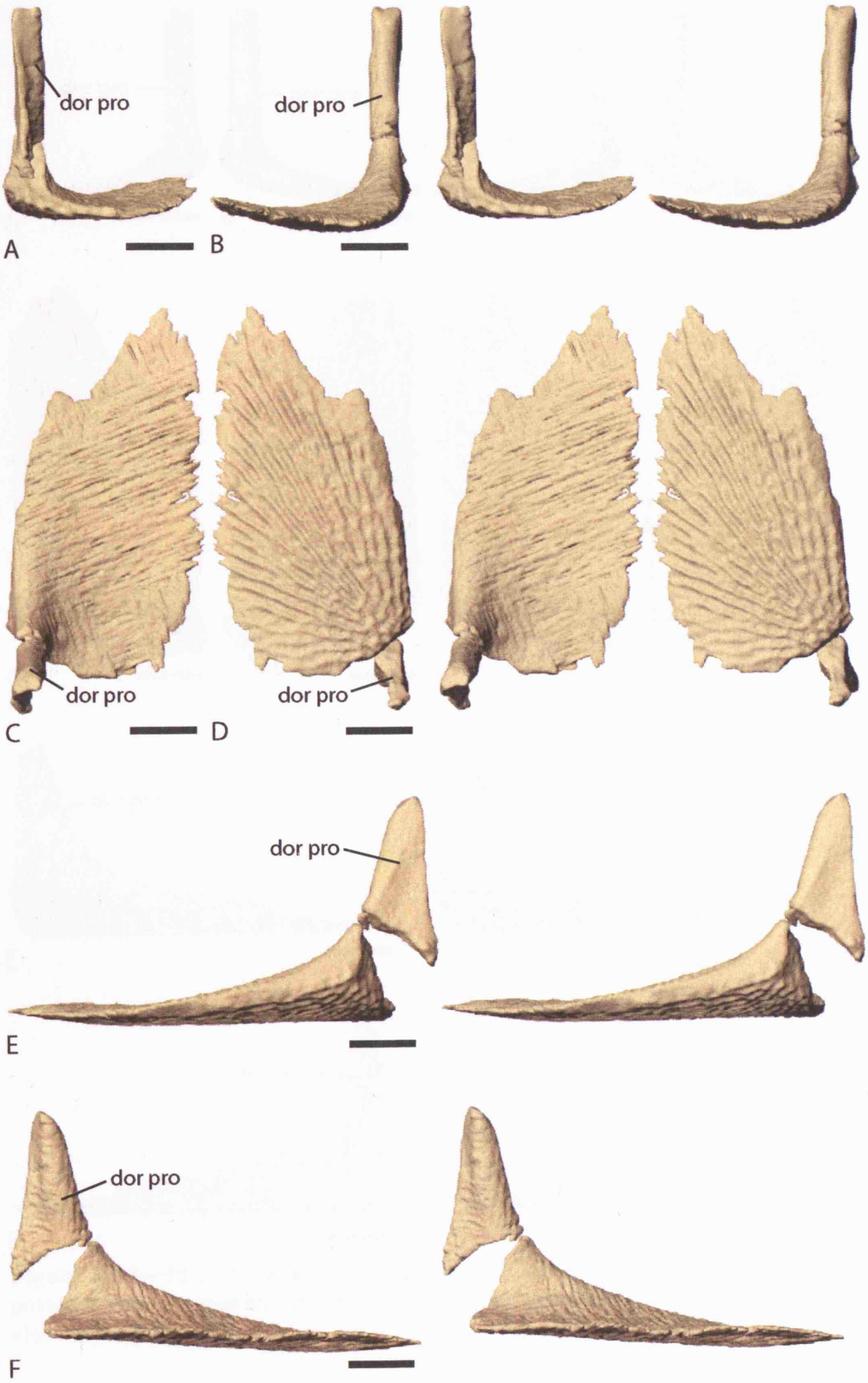

Figure 3.4.3—34 *Lydekkerina* specimen UMZC T.242. Stereo pairs of the left clavicle. A, posterior view. B, anterior view. C, dorsal view. D, ventral view. E, left lateral view. F, medial view. Scale bars = 5mm.

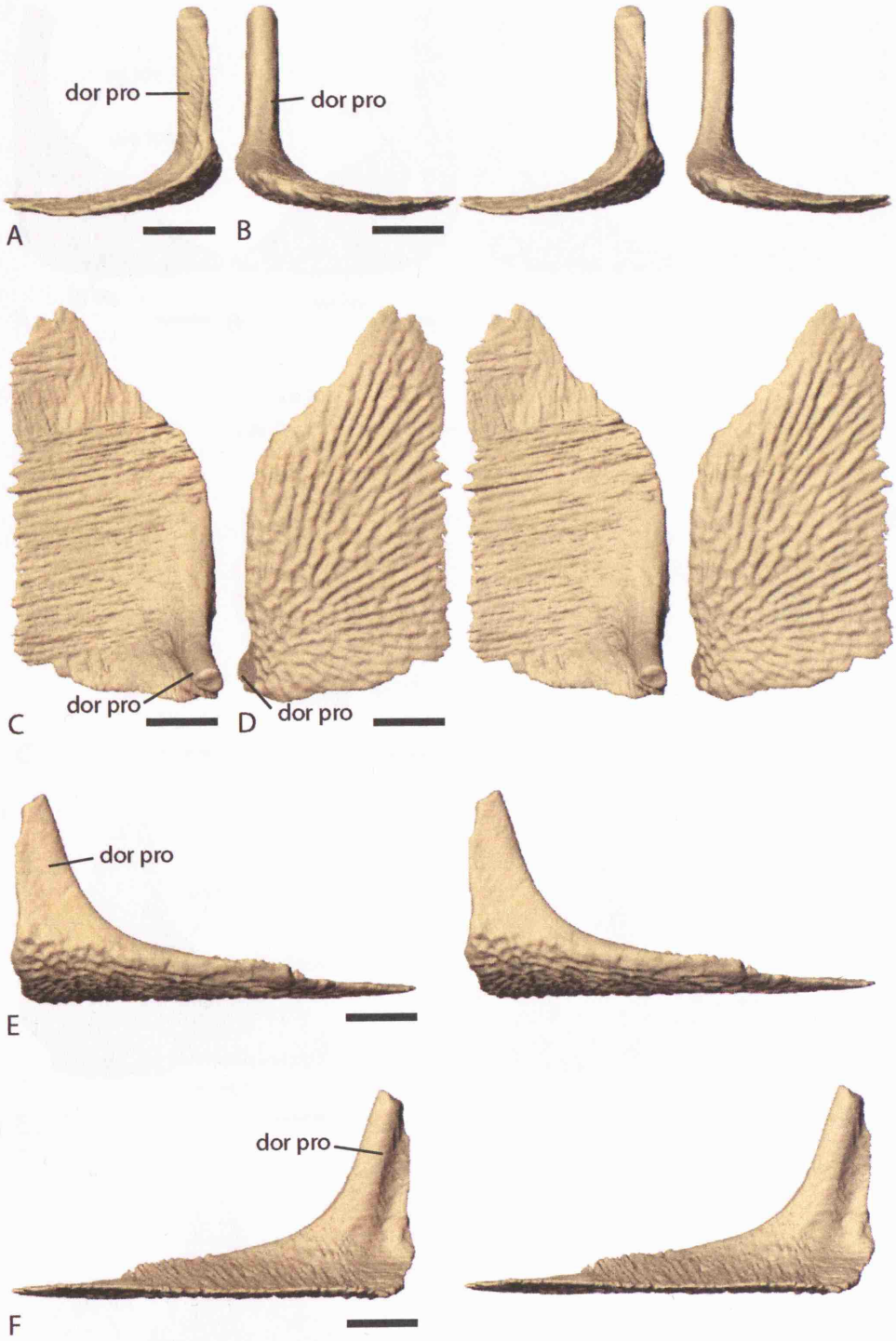

Figure 3.4.3—35 *Lydekkerina* specimen UMZC T.242. Stereo pairs of the right clavicle. A, posterior view. B, anterior view. C, dorsal view. D, ventral view. E, right lateral view. F, medial view. Scale bars = 5mm.

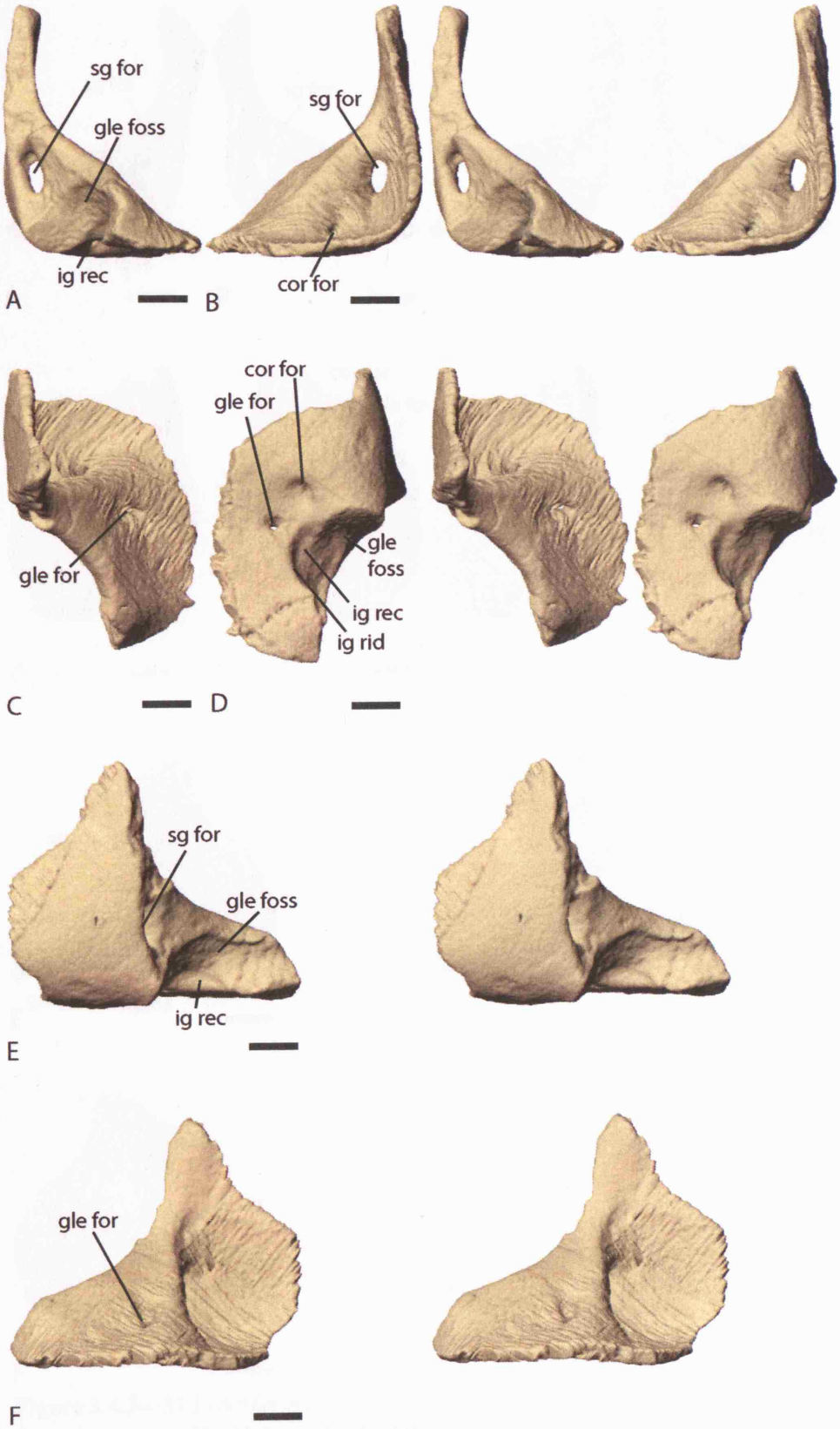

Figure 3.4.3—36 *Lydekkerina* specimen UMZC T.242. Stereo pairs of the left scapulocoracoid. A, posterior view. B, anterior view. C, dorsal view. D, ventral view. E, left lateral view. F, medial view. Scale bars = 5mm.

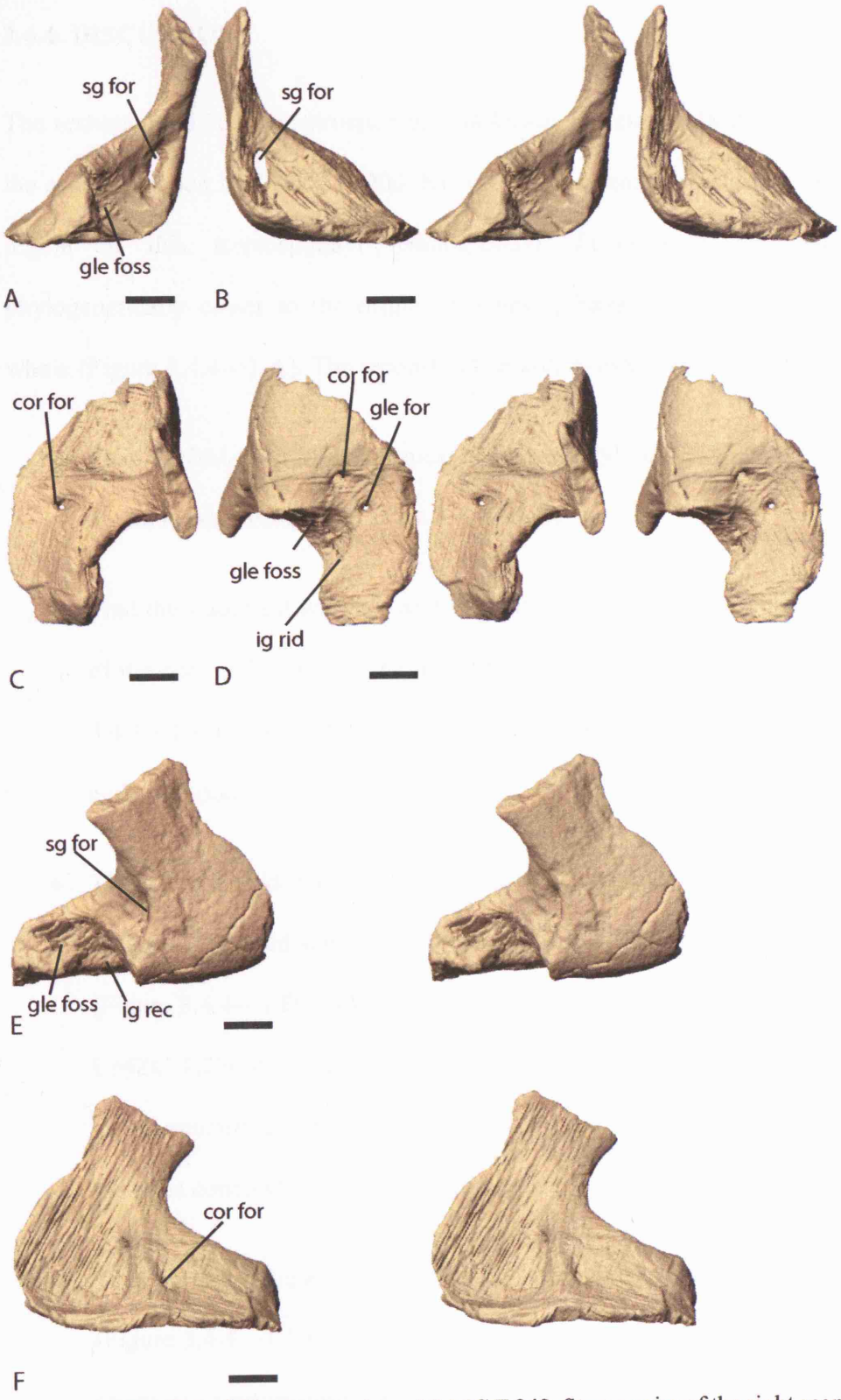

Figure 3.4.3—37 *Lydekkerina* specimen UMZC T.242. Stereo pairs of the right scapulocoracoid. A, posterior view. B, anterior view. C, dorsal view. D, ventral view. E, right lateral view. F, medial view. Scale bars = 5mm.

3.4.4. DISCUSSION

The scanning and 3D reconstruction of *Lydekkerina* specimen UMZC T.242, along with the re-examination of UMZC T.206, has provided a detailed picture of the middle ear region of this stereospondyl temnospondyl. *Lydekkerina* is believed to be phylogenetically closer to the origin of anurans, batrachians or lissamphibians as a whole (Figure 3.4.4—1 A). The reconstruction and re-examination illustrates:

- That *Lydekkerina* had a typical temnospondyl rod like stapes which had a dorsolateral orientation (Figure 3.4.4—1 B).

- That the stapes sat within a well defined space bounded by the otic capsule, part of the occipital complex, the palatoquadrate complex and the skull roof (Figure 3.4.4—1 C). This is the most detailed picture of the middle ear space of any early tetrapod.

- That there is evidence for the presence of an opercular apparatus. There is a well defined unossified space behind the footplate of the stapes in the fenestra ovalis (Figure 3.4.4—1 D). Additionally from the re-examination of the right stapes of UMZC T.206 it appears that there is a posterior notch in the footplate which in extant anurans articulated with the operculum. These lines of evidence provided the most conclusive proof that temnospondyls possessed opercular apparatuses.

- That the right stapes of UMZC T.206 is rod like and had a posterior process (Figure 3.4.4—1 E) which may be homologous to the scar observed on the left stapes of *Dendrerpeton* specimen BMNH R.436 (3.3).

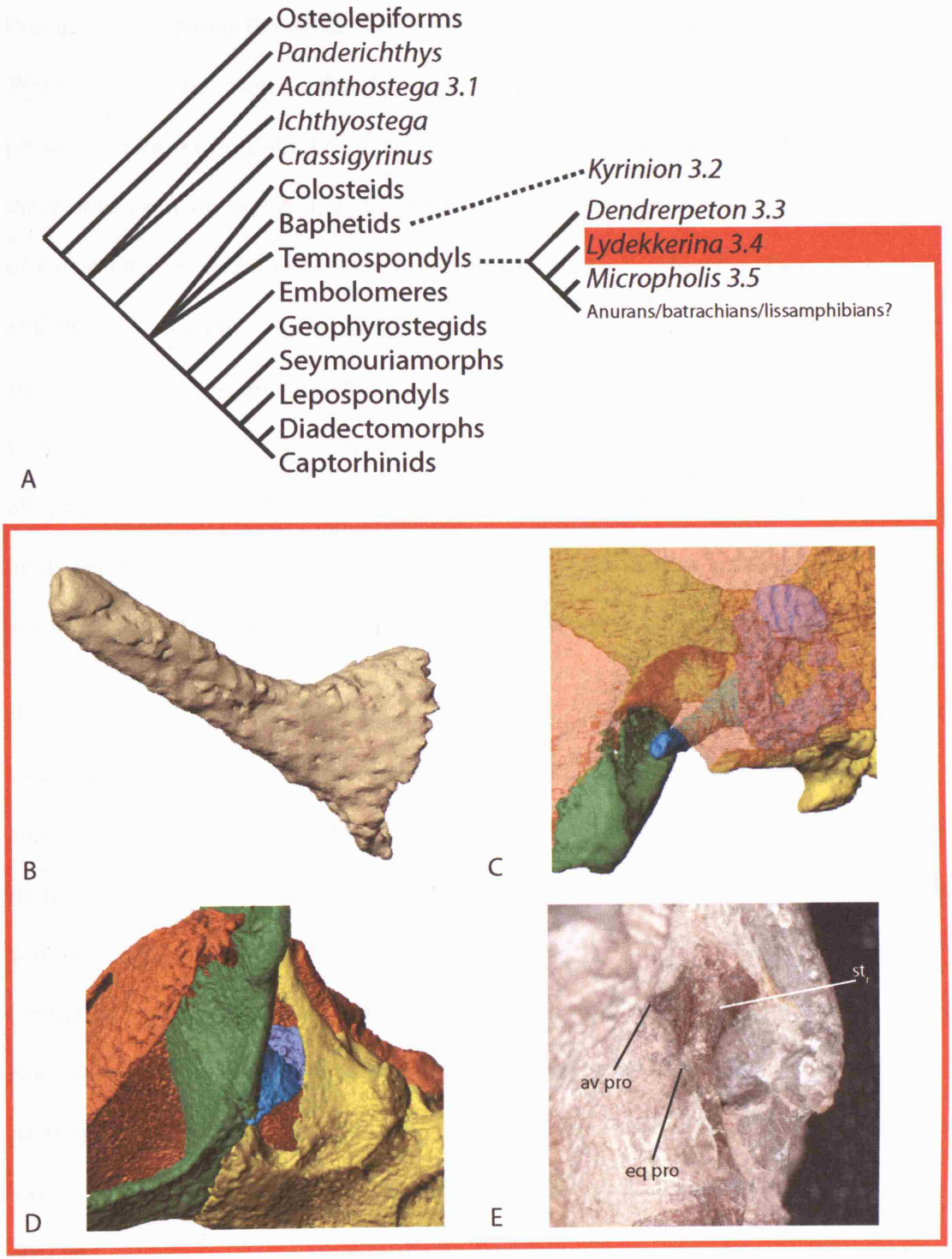

Figure 3.4.4—1 Summary *Lydekkerina* figure - specimen UMZC T.242. A, basic phylogenetic consensus created from the early tetrapod phylogenies of Ruta et al. (2003) and Laurin & Reisz (1997) with temnospondyl detail from Ruta et al. (2003) and Yates & Warren (2000). B, posterior view of left stapes - see figure 3.4.3—13. C, dorsal view of left stapes *in situ* - see figure 3.4.3-17. D, posterolateral view of left stapes *in situ* - see figure 3.4.3—19. E, posterior view of right stapes of UMZC T.206 *in situ* - see figure 3.4.3—20. For scale bars see referred to figures.

Previous descriptions (Broili & Schröder, 1937; Parrington, 1948; Shishkin et al., 1996; Watson, 1919) demonstrate that *Lydekkerina* has well defined temporal notches in the posterior margin of the skull roof and rod like stapes which point towards the middle of these notches. This morphology has been interpreted as clear evidence for the presence of an ear adapted to the perception of airborne sound in *Lydekkerina* (Parrington, 1949) and thus the notches are frequently termed 'otic notches' and are envisaged to have supported tympanic membranes coupled to a stapes. There has been very little controversy regarding this functional interpretation of *Lydekkerina's* middle ear, although a recent conference abstract by Laurin (2005) has suggested 'that the widely held idea that many temnospondyls possessed a tympanum is unlikely'. It is unclear whether Laurin (2005) includes *Lydekkerina* in this rather extreme assertion.

In spite of the accepted functional interpretation of the middle ear of *Lydekkerina* (barring the possible exception of Laurin) there are still many aspects of its middle ear anatomy that are not fully known. There is inconsistency between the rod like stapedial morphology generally depicted for *Lydekkerina* and the apparently more robust and complex stapes of *Lydekkerina* sp. specimen UMZC T.206 described by Parrington (1948) (see his figure 3 B and C). There is also uncertainty regarding the relationship of each stapes to the surrounding structures such as the braincase, fenestrae ovales and palatoquadrate complexes. Furthermore, it is unclear whether *Lydekkerina* possesses any of the specialisations of the Lissamphibian middle ear mentioned in the introduction chapter.

The following can be stated with some confidence regarding the middle ear and hearing abilities of *Lydekkerina* based on the reconstructed model of UMZC T.242, the re-examination of UMZC T.206 and previously published descriptions:

- *Lydekkerina* has paired notches at the posterior margin of the skull roof (Figure 3.4.3—5) which should be termed otic notches. These otic notches would have supported round tympanic membranes. There is no evidence for an ossified element or 'bony septum' in the otic notches, as described in *Iberospondylus schultzei* (Laurin, 2005), of any *Lydekkerina* specimen thus far described.

- Both stapes of UMZC T.242 have a rod like appearance and bi-partite footplates (Figure 3.4.3—13, 14, 15 and 16). The ventral component of the footplate articulated, but did not fuse, with the braincase. It is believed that the dorsal component of the footplate would have sat within the fenestra ovalis and passed vibrations on to the perilymphatic space of the inner ear. The stapes thus appear to conform to the typical temnospondyl condition which was observed clearly in *Dendrerpeton* (Robinson et al., 2005). Due to the relatively poor resolution of the scan series and subsequent lower model detail, additional stapedial characteristics had to be gained from the visual re-examination of UMZC T.206.

- From the re-examination of the right stapes of UMZC T.206 (Figure 3.4.3—20) it is apparent that it had a far more rod like appearance than would seem to be the case from Parrington's (1948) figure 3. The processes described by Parrington on the right stapes have also been reinterpreted. The 'antero-dorsal process' is the anteroventral corner of the footplate while the 'antero-ventral process' is the posteroventral corner. The clear view of the posterior footplate margin shows that *Lydekkerina* has a notch in the posterior margin above the 'antero-ventral process' (see Parrington (1948) figure 3B and Figure 3.4.3—20). As with *Dendrerpeton* (Robinson et al., 2005) this notch is probably homologous to the notch observed in the stapes of extant anurans (Bolt &

Lombard, 1985) and which may suggest the presence of an operculum in the fenestra ovalis of *Lydekkerina.*

- The re-examination of UMZC T.206's right stapes (Figure 3.4.3—20) also allows a reappraisal of the 'process for extension to quadrate' described by Parrington (1948) (see also Figure 3.4.3—20). It seems highly unlikely that this process would have been extended in cartilage and contacted the quadrate as envisaged and figured by Parrington (his figure 4A (Parrington, 1958)). Not only would this entail an incredibly long cartilaginous extension but also an extremely convoluted route curving around the crista obliqua (Figure 3.4.3—7 and 8), which was interestingly not figured in Parrington's figure 4A (1958). The exact function of this process is unknown, although it is positioned in approximately the same place as the posterior scar on the stapes of *Dendrerpeton* (Robinson et al., 2005) specimen BMNH R.436 and *Doleserpeton* (Bolt & Lombard, 1985; Lombard & Bolt, 1988). It would seem most parsimonious to assume that all share the same function.

- The distal end of the stapes has a small unfinished concavity (Figure 3.4.3—13, 14, 15 and 16) which could be evidence for a short cartilaginous extension. As with *Dendrerpeton* (Robinson et al., 2005) this could be at least functionally homologous to the extrastapes or pars externa of extant anurans.

- *Lydekkerina* has a well defined unossified region of the braincase running from the posterior margin of the stapes to the 'recessus tympanicus' (Figure 3.4.3—9 and 10). It has previously been suggested that this may simply represent a 'ventral remnant of the embryonic fissura metotica' with a 'non-functional (rudimentary) nature' (Shishkin et al., 1996). However, its close association with

the stapes and supposed middle ear space suggests a possible functional role. It may represent a pressure release system or, possibly, further evidence to support the presence of an opercular apparatus in *Lydekkerina*; the operculum in extant anurans and urodeles sits in an unossified space posterior to the stapedial footplate.

- The stapes of *Lydekkerina* (from the scanning and reconstruction of UMZC T.242) can be seen to articulate, but not fuse, with the lower braincase (presumably parasphenoid) and points towards the middle of the otic notch (Figure 3.4.3—17, 18 and 19). The stapes sits within a well defined space occupied by the middle ear cavity and filled with air. This space runs from behind the basipterygoid articulation to the otic notch and is bound anteriorly by the excavatio tympanica and posteriorly by the crista obliqua. Therefore, it is clear that *Lydekkerina* had a relatively well isolated middle ear cavity.

It is believed that *Lydekkerina* possessed an ear adapted to the perception of airborne sound. It would seem most parsimonious to assume that *Lydekkerina* and *Dendrerpeton* share a common ancestor which would have possessed an ear adapted to the perception of airborne sound, although rigorous proof of this would require optimalisation of the relevant characters onto a recent and trusted phylogeny of temnospondyls. Additionally acoustic experiments could be used to investigate the hearing properties of an ear as envisaged in *Lydekkerina*.

The reconstruction of UMZC T.242 and the re-examination of the right stapes of UMZC T.206 have shown numerous characters of the middle ear of *Lydekkerina* which provide evidence, although not conclusive proof, for the presence of structures now only seen in extant anurans and urodeles. As mentioned above there is a process on the

posterior surface of the stapes which would have had the same function as the scar seen on the stapes of *Dendrerpeton* (Robinson et al., 2005) and *Doleserpeton* (Bolt & Lombard, 1985; Lombard & Bolt, 1988). This may thus represent evidence for a muscular connection between the stapes and the shoulder girdle as seen in extant anurans. The presence of a notch in the posterior margin of the stapedial footplate and the clearly defined unossified space contiguous to the fenestra ovalis are osteological pointers towards the presence of an opercular apparatus in *Lydekkerina*. Extrapolation from this inference can lead to the possible conclusion that a muscular connection between the opercular apparatus and the shoulder girdle also existed, although there is no direct evidence to support this inference.

3.5. MICROPHOLIS

Micropholis is a dissorophoid temnospondyl. The phylogenetic analyses of Laurin & Reisz (1997) and Ruta et al. (2003a) class dissorophoid temnospondyls as 'higher' temnospondyls. The phylogeny of Ruta et al. (2003a) proposes that a monophyletic Lissamphibia is nested within the dissorophoid temnospondyls and are thus potentially crucially important in assessing the character states of the middle ear region and associated structures in the common ancestor of the lissamphibians. Knowledge of the middle ear and associated structures will help address the following questions:

- Did the common ancestor of anurans, urodeles and caecilians have a tympanic membrane coupled to a stapes?
- When is the first evidence of a muscle connecting the stapes to the shoulder girdle?
- When did the opercular apparatus evolve in tetrapods and in what group was this?
- Did the common ancestor of batrachians, lissamphibians or all tetrapods possess an opercular apparatus?
- When is the first evidence of a muscle connecting the opercular apparatus to the shoulder girdle?

See *Micropholis* Discussion 3.5.4 and Figure 3.5.4—1 for a synopsis of the morphology revealed from the reconstruction of BMNH R.436 and how this has helped address the above questions.

3.5.1. BACKGROUND

At the end of 1850 C. W. Stow collected a skull of 'a little undescribed reptile' along with 'a nearly perfect skeleton of a small reptile', some other reptile remains and the skull of a small '*Dicnodon*' in South Africa (Stow, 1858a; Stow, 1858b). The details of this collection were presented to the Geological Society of London on the evening of November 17th 1858 (Huxley, 1859; Stow, 1858a; Stow, 1858b). Huxley subsequently described the little reptilian skull, including numerous figures, and erected the species name *Micropholis stowii* in honour of Stow in a paper presented to the aforementioned society on March 23rd 1859. This specimen, BMNH R. 4382, the holotype for *Micropholis*, is now in the Natural History Museum's collection having resided in the Geological Society's collection until 1911.

In 1876 Owen described and named an additional skull as *Petrophryne granulata* but mentioned that with some additional character clarification 'the genus *Petrophryne* must sink into a synonym of *Micropholis*'. This specimen, BMNH R.510, the holotype for *Petrophryne*, (Figure 3.5.1—1 A and B), was collected and presented to the then British Museum of Natural History by W. Guybon Atherstone (Owen, 1876). Zittel subsequently examined BMNH R.510 and concluded that '*Petrophryne* Owen... Aus Triasandstein vom Tafelberg im Capland scheint nicht von *Micropholis* verschieden zu sein...' ['*Petrophryne* Owen... From the Triassic sandstone of Tafelberg, Cape of Good Hope does not seem to be different to *Micropholis*...'] (Zittel, 1888). Lydekker (1890) agreed with Zittel that *Petrophryne* was a junior synonym of *Micropholis*. Lydekker (1890) differentiated *Micropholis stowii* (his *Micropholis stowei*) from *Micropholis granulata* on the basis that the latter is smaller than the former. In fact, the skull of the holotype of *Micropholis granulata* is larger than that of the holotype of *Micropholis*

stowii. In contrast, Watson (1913) did not differentiate *Micropholis granulata* from *Micropholis stowii* (his *Micropholis stowi*) and figured the holotype of *Micropholis granulata* (BMNH R.510) and the only other specimen previously classified as such (BMNH R.510a) as *Micropholis stowii*. Subsequent descriptions by Broili & Schröder (1937) and Boy (1985) follow Watson in using the single species *Micropholis stowii* and also follow his incorrect spelling *Micropholis stowi*.

Micropholis stowii is a relatively small temnospondyl which has not been placed in any of the recent cladistic phylogenies such as Ruta et al. (2003a) and Laurin & Reisz (1997). In Milner (1990) Micropholidae (containing *Micropholis*) was placed on a trichotomy with Dissorophidae and a clade containing Branchiosauridae, Peliontidae and Lissamphibia. Watson (1919) classified Micropholis as belonging to the order Labyrinthodontia, the grade Rhachitomi and the family Micropholidae, a new family containing only *Micropholis*. Romer (1966) and Carroll (1988) place *Micropholis* in the order Temnospondyli, the superfamily Eryopoidea and the family Dissorophoidae. In 1969 Bolt created the new superfamily Dissorophoidea which contained dissorophoids, trematopsids and doleserpetontids. Boy (1972) added Micromelerpetontidae, Branchiosauridae and *Micropholis* to the Dissorophoidea. Boy (1972; 1985) stated that *Micropholis* was one of the most phylogenetically basal and primitive members of the Dissorophoidea. Daly (1994) proposed a new family, the Amphibamidae, to fit within the Dissorophoidea. This family contained *Eoscopus*, *Amphibamus*, *Doleserpeton*, *Tersomius* and *Micropholis*. Thus Dissorophoidea consisted of the families Trematopidae, Micromelerpetontidae, Amphibamidae (containing *Micropholis*), Dissorophidae and Branchiosauridae. The phylogeny presented by Milner (1990) and Holmes (2000) followed this classification. Warren & Hutchinson (1990) added the

genus *Lapillopsis* to the infrequently used family Micropholidae. Micropholidae currently contains only *Micropholis stowii* and *Lapillopsis nana*.

The proposed phylogenetic position of *Micropholis* at the base of the Dissorophoidae means that its middle ear anatomy and associated structures are of great interest. Although, there have been numerous descriptions of the external cranial and postcranial anatomy of *Micropholis* the braincase and middle ear region are incredibly poorly known. The braincase has not been described previously and there is only a very brief and limited prior description of its stapedial morphology (Boy, 1985). It was therefore decided to scan and reconstruct two specimens of *Micropholis stowii* from the Natural History Museum's collections. The first of these specimens was BMNH R.510 (Figure 3.5.1—1 A and B), Owen's holotype for '*Petrophryne granulata*'. As previously mentioned this specimen was discovered and given to the then British Museum of Natural History by W. Guybon Atherstone (Owen, 1876). BMNH R.510 has been figured and described by Owen (1876), Zittel (1888) and Watson (1913). The second specimen scanned was BMNH R.4384 (Figure 3.5.1—1 C and D) which was presented to the British Museum of Natural History in 1911 by the Geological Society, London along with BMNH R.4382 (Huxley's holotype of *Micropholis stowii*) and BMNH R.4383. Specimens BMNH R.510, R.510a and R.4382-4 are the five mentioned by Watson (1913) in his description of *Micropholis stowii*. Despite this, the author is unaware of any direct description or published figure of BMNH R.4384. According to Watson (1913) all specimens of *Micropholis stowii* at the then British Museum of Natural History, except Huxley's holotype (BMNH R.4382), are from the '*Procolophon* zone of Donnybrook, Upper Zwartkei, District Queenstown' which is dated as Induan of the Early Triassic (Lucas, 1998).

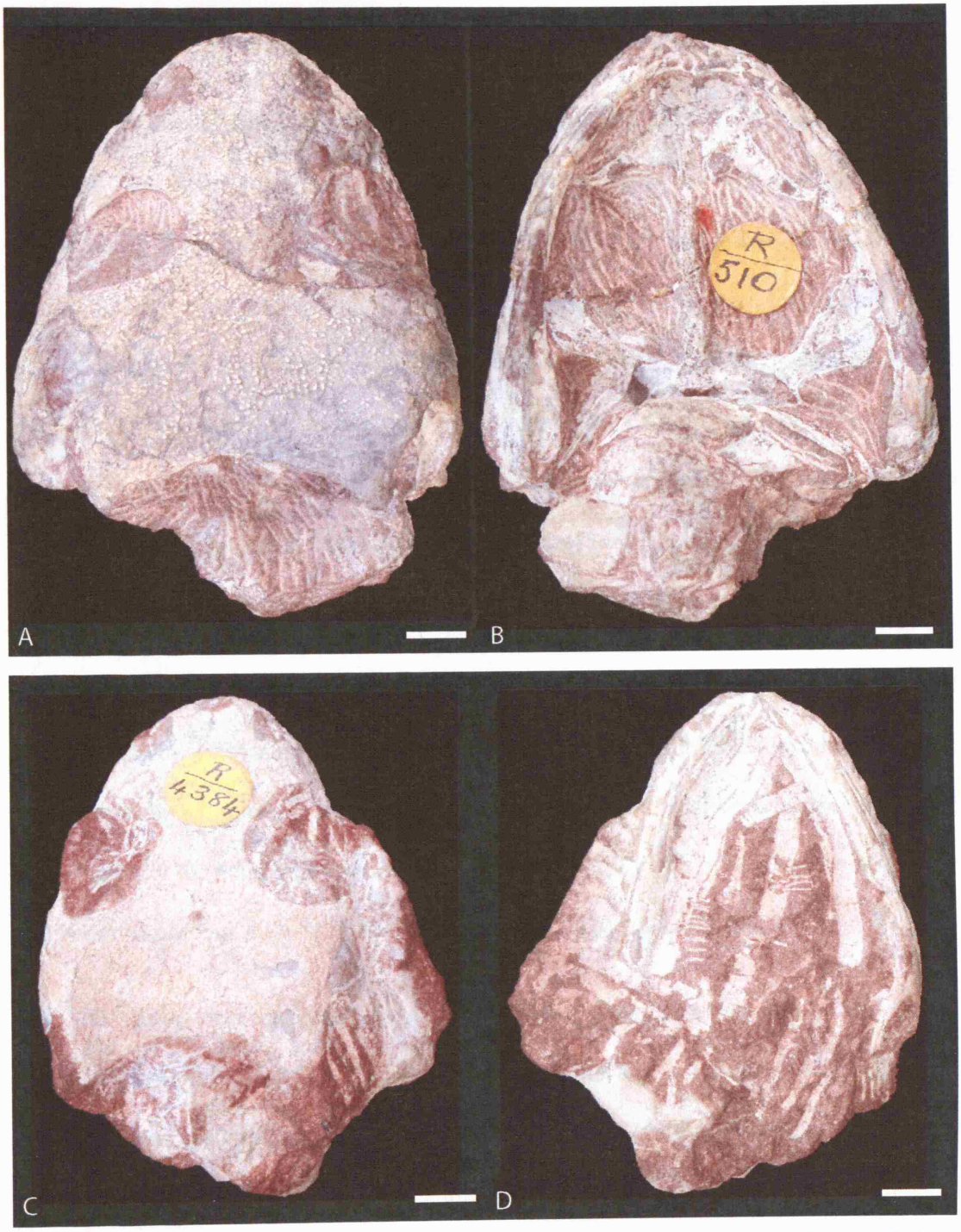

Figure 3.5.1—1 A and B, *Micropholis* specimen BMNH R.510. A, dorsal view. B, ventral view. C and D, *Micropholis* specimen BMNH R.4384. C, dorsal view. D, ventral view. Scale bars = 5mm.

3.5.2. RECONSTRUCTION PARAMETERS

Micropholis stowii specimens BMNH R.510 and BMNH R.4383 were scanned on the ultra-high resolution subsystem scanner at UTCT. To reduce the time and hence cost of the scanning it was decided to scan both specimens in the same scan series; with the ventral surface of each skull facing each other. The scan was produced with 2000 views per rotation and 3 samples per view. This means that each slice was produced from a sinogram containing 2000 views with each view being a combination of three samples to improve the image quality. The scan series was produced with 15 slices per rotation meaning that the specimens were rotated 24 times within the x-ray field.

A single scan series for both of the specimens was produced from the orbits to the posterior extent of the specimens. This scan series was produced in 16bit resolution (1024 pixels by 1024 pixels), comprising 360 slices each of 0.08928mm thickness (i.e. approximately 11 slices per mm). In order to increase the slice image contrast and overall quality the scan data was reconstructed (at UTCT) with a 'drift-removal' process and beam-hardening algorithm with coefficients of 0.0, 0.8 and 0.15.

The 360 slices were imported into Mimics in the usual manner. Due to the limited number of masks available in Mimics versions 7 and 8 it was decided to interpret the two specimens in different Mimics projects. Furthermore the postcranial material of BMNH R.510 was modelled in a separate Mimics project and then married together with the cranial material in Rhino3D. In all Mimics projects dealing with *Micropholis* the contrast was set to 660-2478 to maximise the grey scale differentiation between the fossilised material and the matrix. Within the Mimics project dealing with the cranial reconstruction of BMNH R.510 it was possible to model areas of the skull roof where only the external mould remained using a narrow ranged grey scale threshold. This

technique was also used to model the area of plaster reconstruction which was discovered due to the scanning and reconstruction of BMNH R.510. The scan slices of cranium of BMNH R.510 had far greater grey scale differentiation between the fossilised material and the matrix than for the cranium of BMNH R.4384. It proved possible to gain far more information from BMNH R.510 than from BMNH R.4384, therefore, it was decided to concentrate solely on the former specimen. The 3D reconstruction of *Micropholis* is thus based on the cranial and postcranial Mimics projects of BMNH R.510. All elements from these two projects were exported from Mimics as binary STL files and imported into Rhino3D without any alteration of coordinates. To improve the aesthetic appearance of the model a smoothing transformation over all world coordinates with a factor of 1.0 was used.

3.5.3. DESCRIPTION

BMNH R.510 (Figure 3.5.1—1 A and B) was scanned from midway between the orbits to the posterior extent of the specimen. The reconstruction (Figure 3.5.3—3) consists of all cranial and postcranial material in this region of the specimen excluding the mandibles which proved too fragmentary to model.

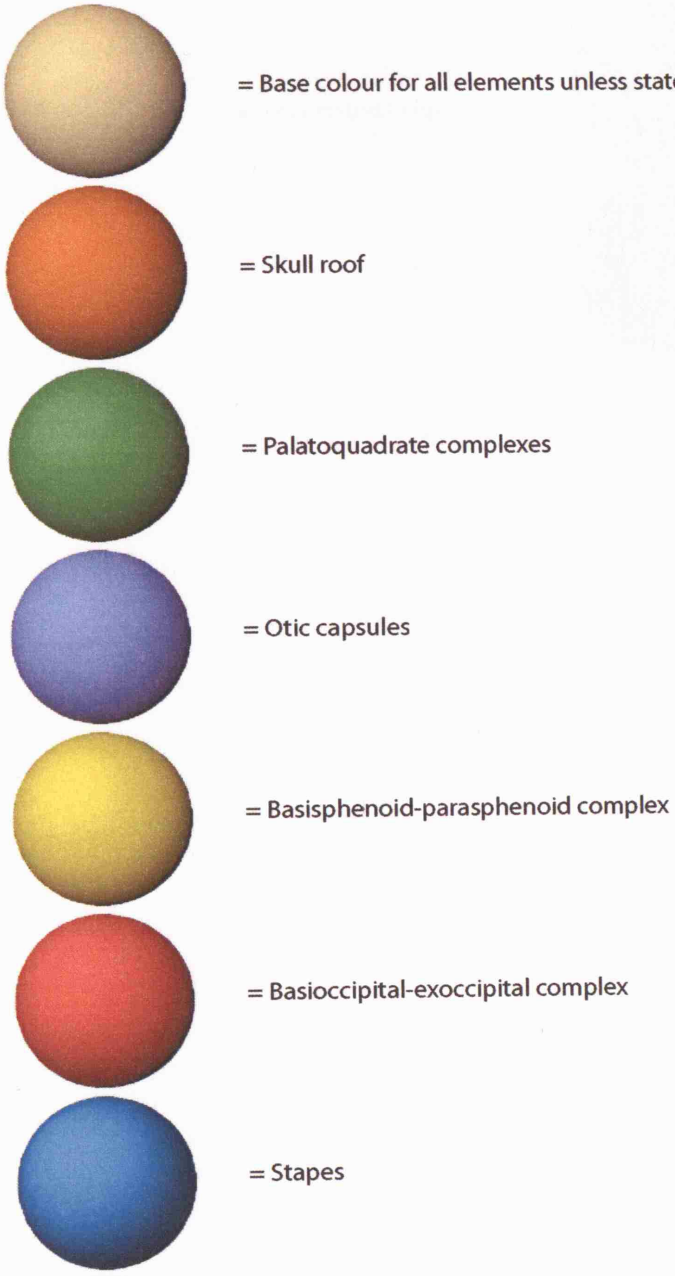

Figure 3.5.3—1 Colour key – cranial.

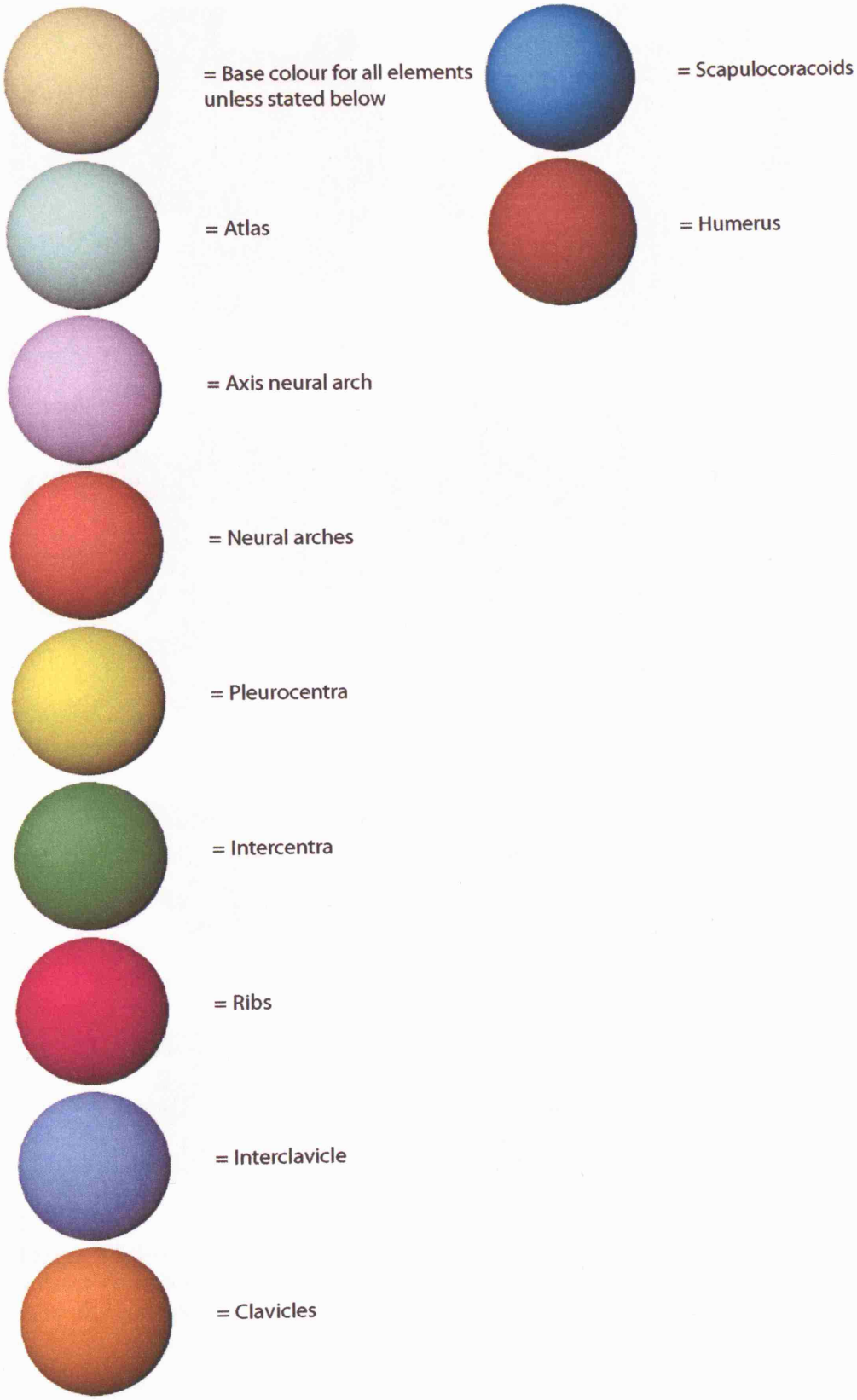

Figure 3.5.3—2 Colour key – postcranial.

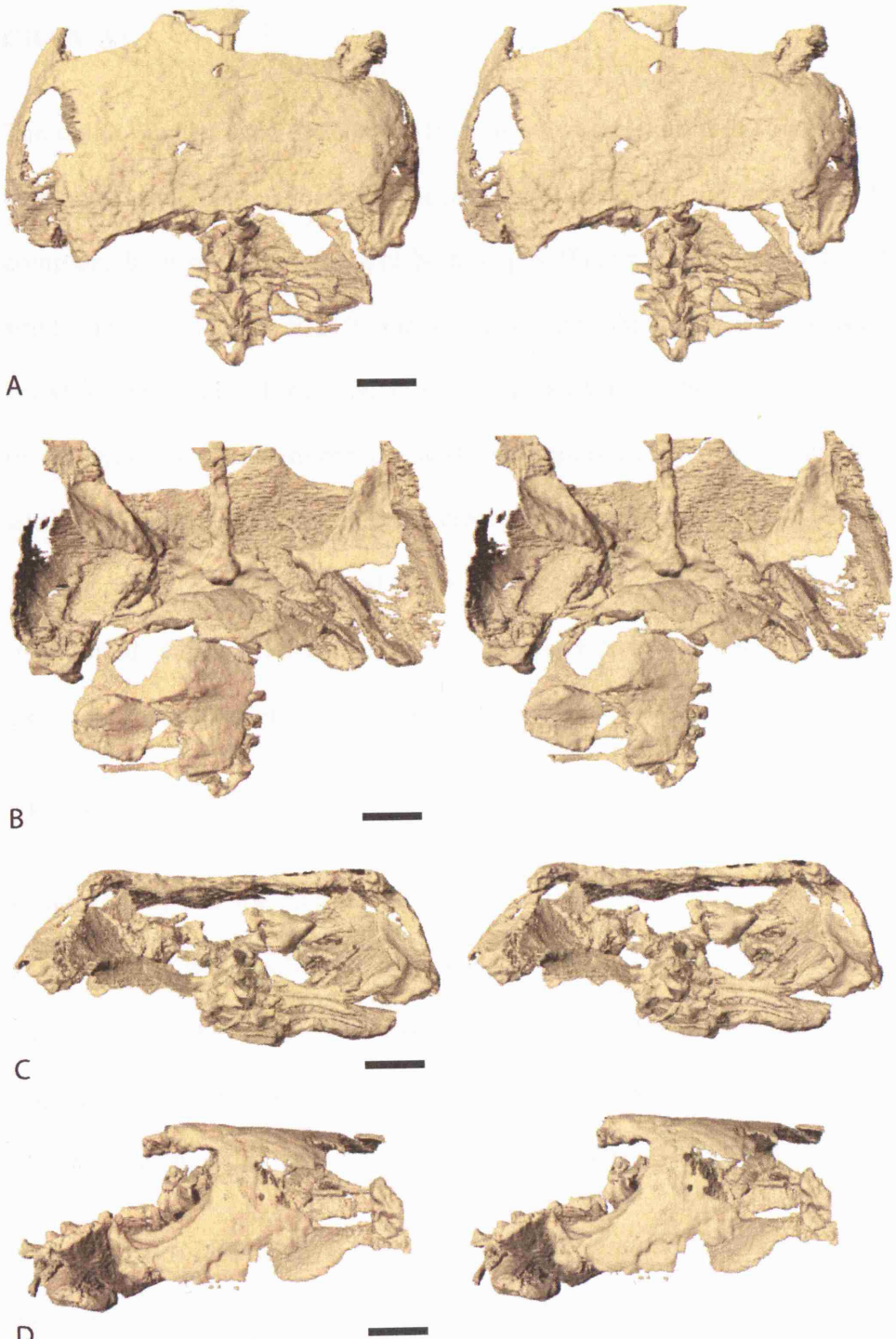

Figure 3.5.3—3 *Micropholis* specimen BMNH R.510. Mono colour stereo pairs of the model without correction for translocations or damage. A, dorsal view. B, ventral view. C, posterior view. D, right lateral view. Scale bars = 5mm.

CRANIAL

The cranial material of BMNH R.510 consists of the skull roof (Figure 3.5.3—4), both palatoquadrate complexes, the basisphenoid-parasphenoid complex, the occipital complex, both otic capsules and both stapes (Figure 3.5.3—5 and 6). The relatively small size of BMNH R.510, the required slice thickness and the lack of contrast between the fossilised material and the matrix have combined to reduce the resolution of the scan slices and hence the aesthetic appearance of the model. A great deal of additional information regarding the cranial anatomy of *Micropholis* has, however, been gleaned from the scanning and 3D reconstruction. All elements within the model are undistorted, although, there has been a certain amount of translocation which has, for example, caused the braincase to be slightly disarticulated.

Skull roof

Owen (1876) was the first to figure the skull roof (sr) of BMNH R.510, although, the suture pattern was not figured until Watson (1913). The subsequent figures of the skull roof suture pattern by Broili & Schröder (1937) and Boy (1985) do not differ significantly from that of Watson. As with all scans it has not been possible to differentiate the skull roof suture pattern in the reconstruction of *Micropholis*.

The skull roof of BMNH R.510 is not complete and appears to have been damaged by previous preparation (Figure 3.5.3—4 A and C). The dermal bone is no longer present behind the right orbit and anterior to the left notch, although the internal mould remains. Additionally, the right tabular horn appears to have been broken off in the course of previous preparation to the right otic region and has at some stage been replaced with a plaster replica. It has proved possible to model both the internal moulds and the

replicated right tabular horn to gain a more complete model of the skull roof and cheek region (Figure 3.5.3—4 B and D). The large posterior notch can be visualised from this model. The right notch, which is approximately complete, has a large curved concave surface which runs from the tabular horn to the quadrate (Figure 3.5.3—4 D, 5 C, D and 6 A). The quadrate has a noticeable dorsal extension similar, although, more pronounced to that seen in *Dendrerpeton* (Robinson et al., 2005) specimen NSM 987 GF 99.1 and *Doleserpeton* (Bolt, 1969). This dorsal extension is possible evidence for a cartilaginous extension from the quadrate which might have linked up with the tabular horn. Visual inspection illustrates that the internal concave surface of the notch does not have the ornamented appearance of the rest of the skull roof. This character state is similar to that seen in *Dendrerpeton* specimen NSM 987 GF 99.1 and may be indicative of a middle ear cavity reaching towards the outer surface of the notch.

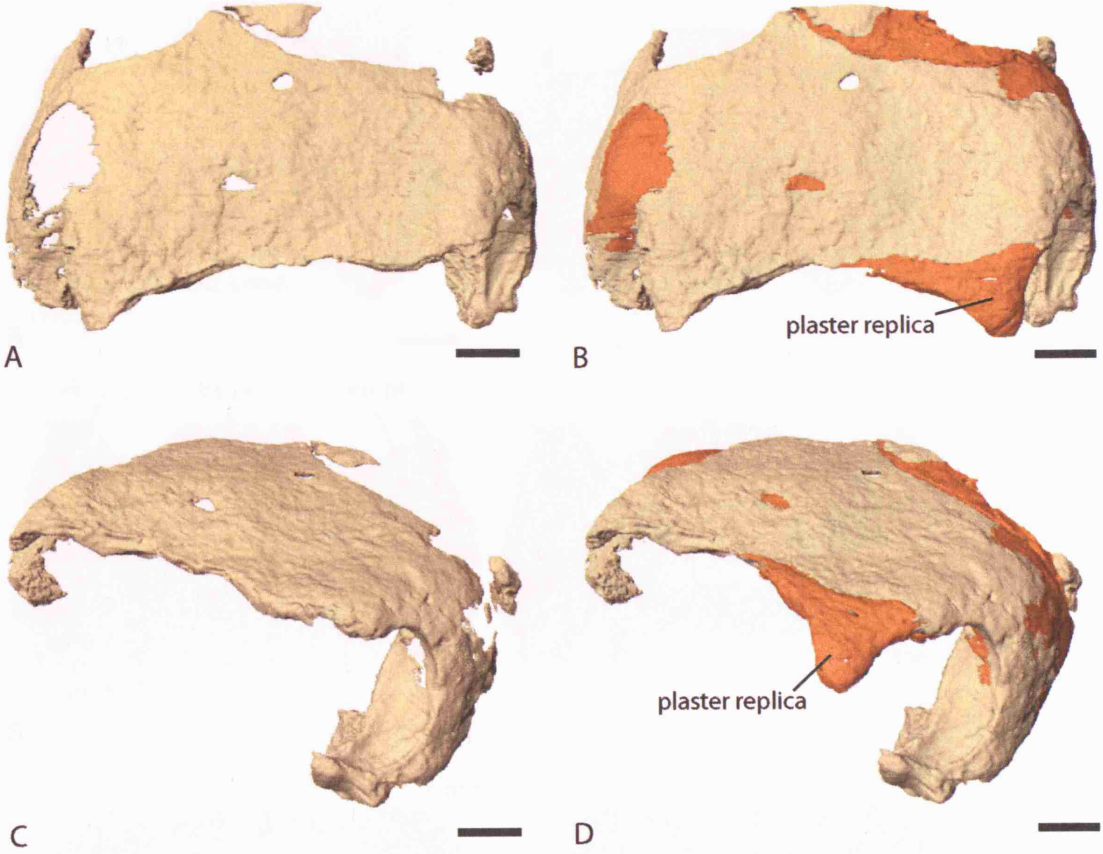

Figure 3.5.3—4 *Micropholis* specimen BMNH R.510. A and B, dorsal view of skull roof. C and D, offset posterodorsal view of skull roof. In B and D the areas modelled from internal mould and repaired region are shown in orange. Scale bars = 5mm.

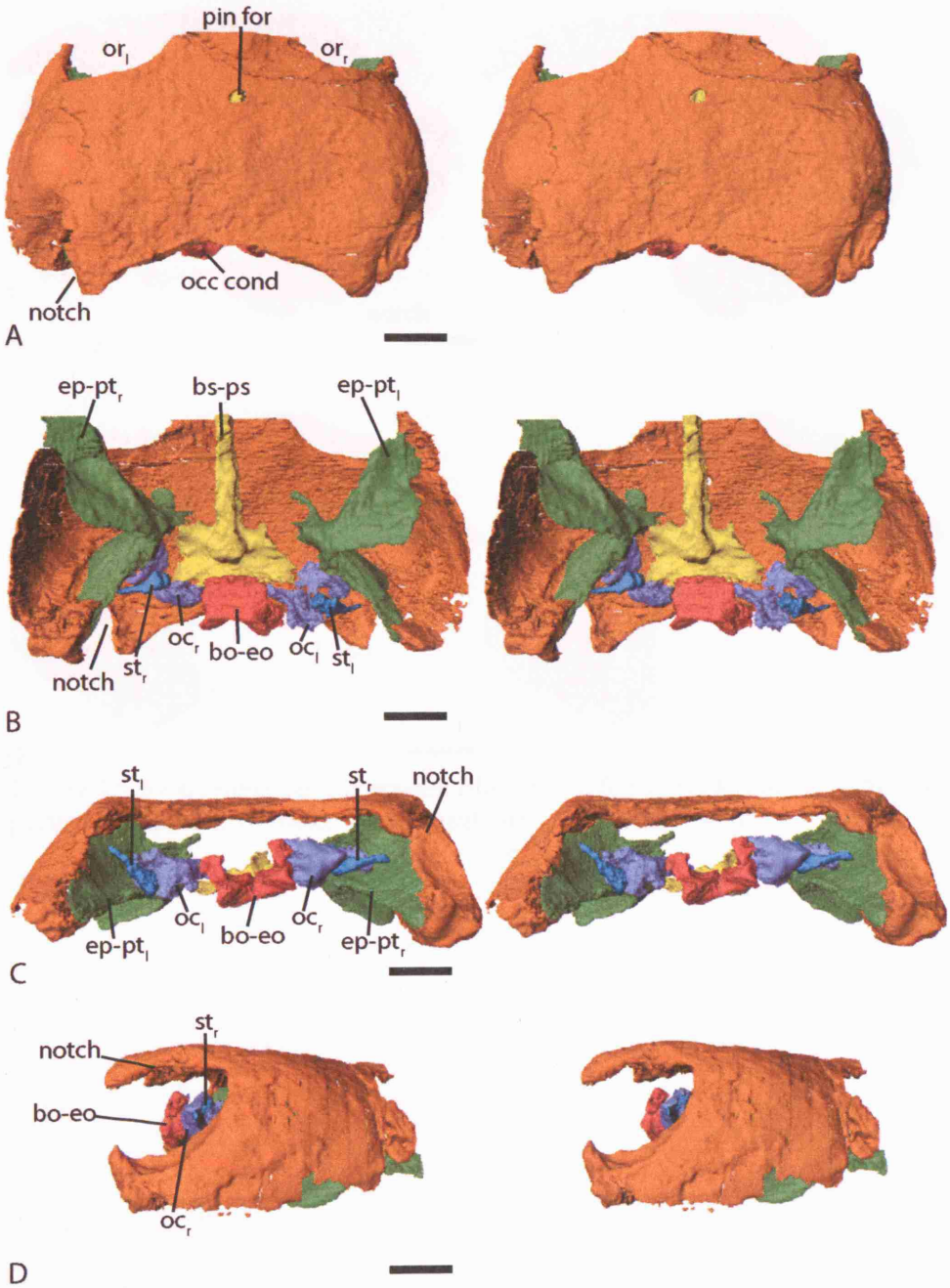

Figure 3.5.3—5 *Micropholis* specimen BMNH R.510. Stereo pairs of the cranial model. A, dorsal view. B, ventral view. C, posterior view. D, right lateral view. Scale bars = 5mm.

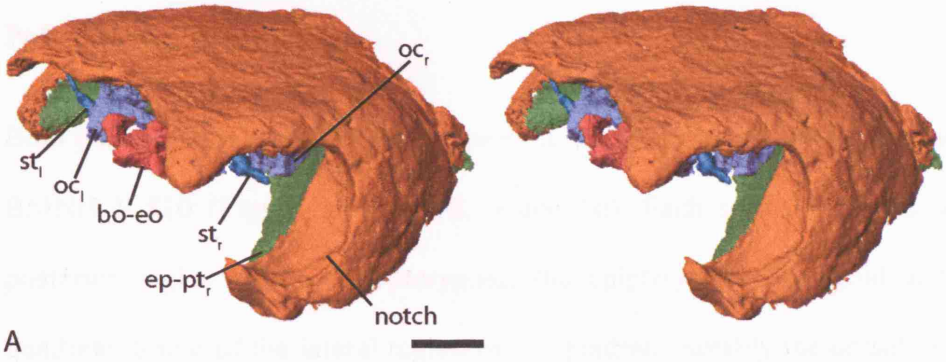

A

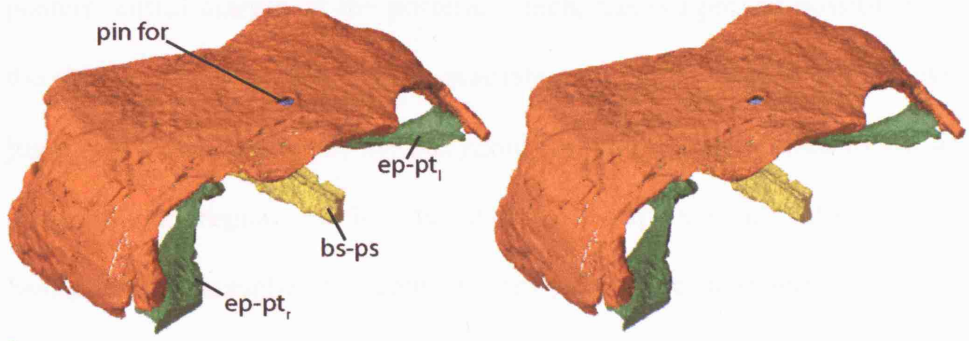

B

Figure 3.5.3—6 *Micropholis* specimen BMNH R.510. Stereo pairs of the cranial model. A, offset posterodorsal view. B, offset anterodorsal view. Scale bars = 5mm.

Palatoquadrate complexes

Both palatoquadrate complexes are present, approximately complete and undistorted in BMNH R.510 (Figure 3.5.3—7, 8, 9 and 10). Each seems likely to consist of the posterior region of the ectopterygoid, the epipterygoid, pterygoid and part of the quadrate. Some of the lateral region of the quadrate, notably the dorsal extension at the posteroventral margin of the posterior notch, has not proved possible to separate from the skull roof model. Each palatoquadrate complex is fused at the ectopterygoid to the jugal region. Furthermore, the pterygoid (pt) and quadrate fused to the squamosal and quadratojugal region. Each palatoquadrate complex would also have contacted the basisphenoid-parasphenoid complex (bs-ps) at the basipterygoid articulation (art), although, this region is not preserved in BMNH R.510 which suggests that it was cartilaginous.

The morphology of both the palatoquadrate complexes is essentially identical apart from the ascending process (asc pro) or columella cranii of each epipterygoid. Anteriorly the presumed ectopterygoid flows into the pterygoid. The pterygoid forms a broad ventrolaterally directed curved flange on its posterior margin. This flange can also be seen to a lesser extent in the reconstructed palatal morphology of *Doleserpeton* (Bolt, 1969). Medial to this broad flange the palatoquadrate narrows towards the basipterygoid articulation. As previously mentioned the region of attachment to the basisphenoid-parasphenoid is not fully preserved and may have been cartilaginous. Dorsoposterior to the basipterygoid articulation the palatoquadrate expands to form the lamina quadrate ramus of the pterygoid and the ascending process or columella cranii of the epipterygoid.

Directly above the basipterygoid articulation the left palatoquadrate complex has an anterodorsally directed rod shaped ascending process of the epipterygoid which

presumably would have continued in cartilage (Figure 3.5.3—7 and 8). In contrast the ascending process of the epipterygoid of the right palatoquadrate complex has a more amorphous form (Figure 3.5.3—9 and 10). The right side most likely represents a damaged area or possibly an ossified element which has been translocated within the specimen; it could indeed represent part of the basipterygoid articulation. Posterior to the ascending process the quadrate ramus of the pterygoid expands both posterolaterally and dorsolaterally. Anteriorly the quadrate ramus of the pterygoid forms a broad concavity which is clearly homologous to the excavatio tympanica (ex tym) described by Bystrow & Efremov (1940) in *Benthosuchus* and also seen in *Dendrerpeton* (Robinson et al., 2005) and *Lydekkerina*. This concavity probably represents the anterior margin of the middle ear cavity. Posteriorly this fan-shaped lamina fuses seamlessly along its entire length with the inner margin of the large posterior notch. There is no evidence of a ridge or crista obliqua (cri obl) on the quadrate ramus of the pterygoid in *Micropholis*. If, however, it is assumed that the crista obliqua of *Lydekkerina* functioned as the posteroventral margin of a middle ear space It is believed that the curved ventral margin of the quadrate ramus of the pterygoid performed this function in *Micropholis*. This leads me to conclude that the crista obliqua is at least functionally equivalent to the curved ventral margin of the quadrate ramus of the pterygoid in *Micropholis* and possibly also in *Dendrerpeton* (Robinson et al., 2005). *Lydekkerina* would have needed a crista obliqua rather than simply using a curved ventral margin of the palatoquadrate complex because the notch and proposed middle ear region are relatively much smaller than those of either *Micropholis* or *Dendrerpeton* (Robinson et al., 2005). The relatively small size of the proposed middle ear region of *Lydekkerina* means that the posterior margin of the middle ear space does not reach

anywhere near the posteroventral extent of the suspensorium and a ridge part way along the pterygoid ramus, the crista obliqua, is used instead.

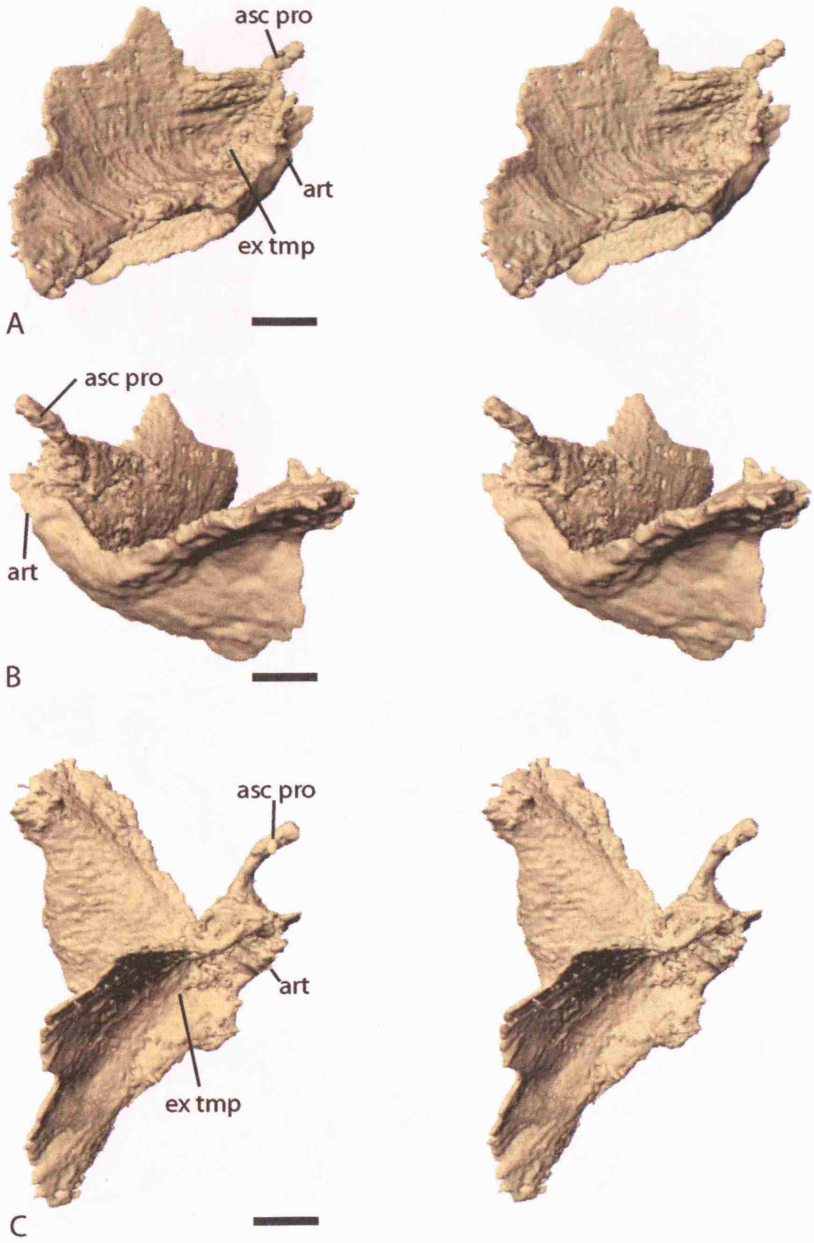

Figure 3.5.3—7 *Micropholis* specimen BMNH R.510. Stereo pairs of the left palatoquadrate complex. A, posterior view. B, anterior view. C, dorsal view. Scale bars = 2mm.

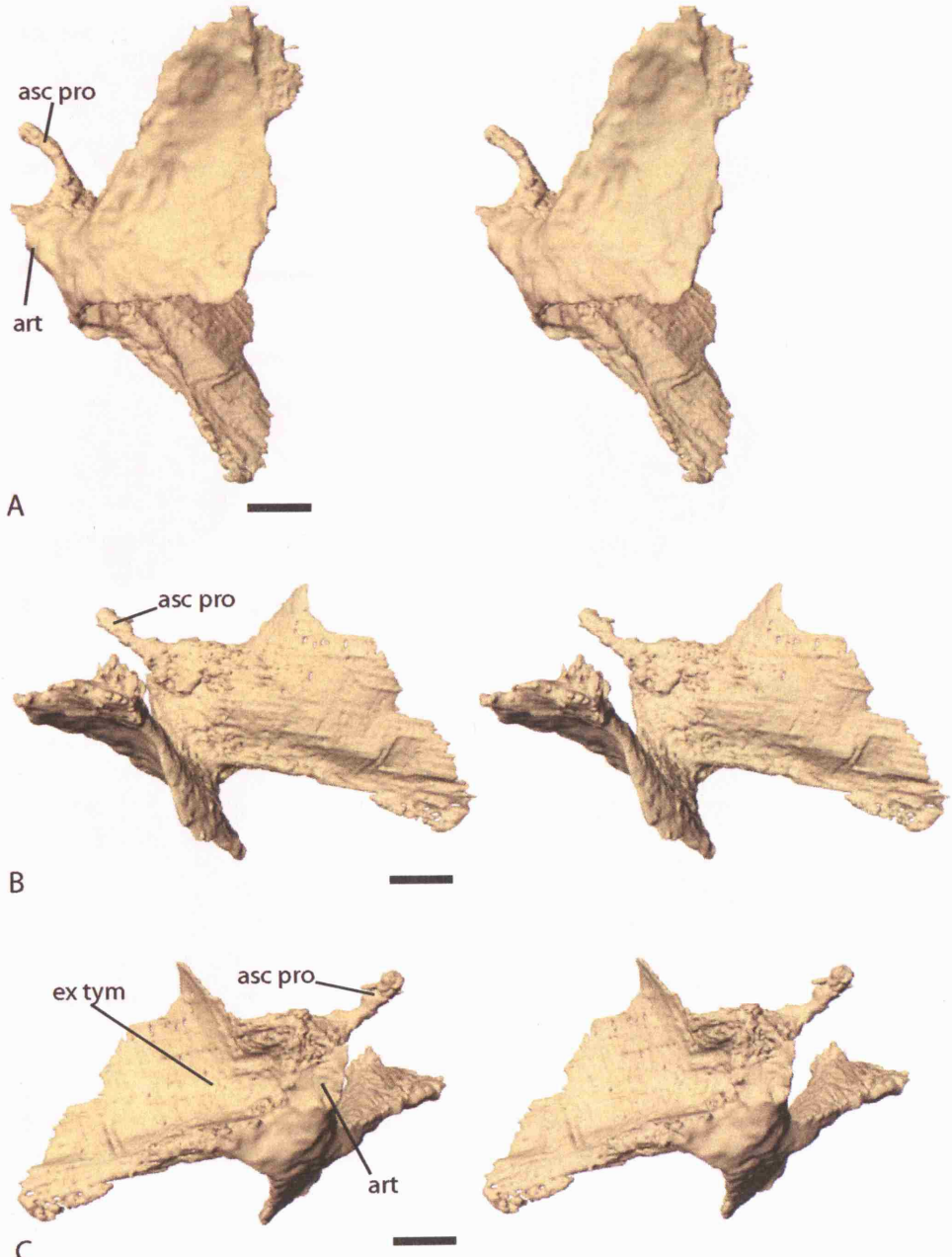

Figure 3.5.3—8 *Micropholis* specimen BMNH R.510. Stereo pairs of the left palatoquadrate complex. A, ventral view. B, left lateral view. C, medial view. Scale bars = 2mm.

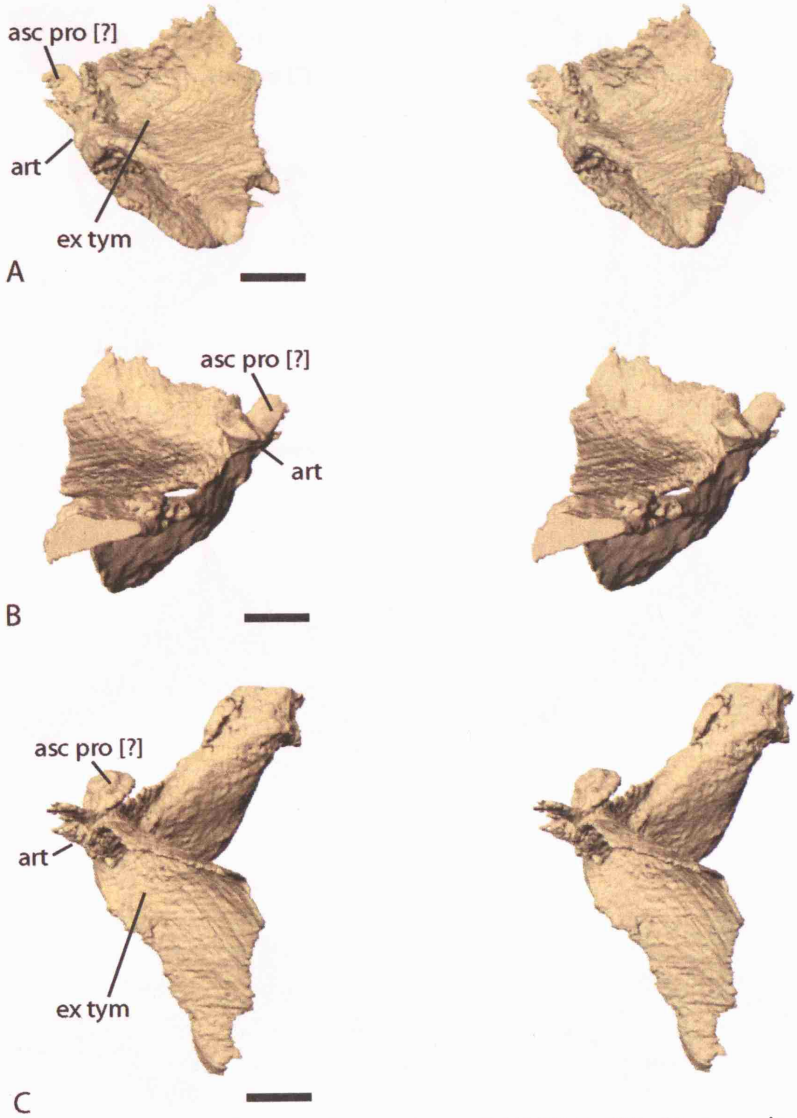

Figure 3.5.3—9 *Micropholis* specimen BMNH R.510. Stereo pairs of the right palatoquadrate complex. A, posterior view. B, anterior view. C, dorsal view. Scale bars = 2mm.

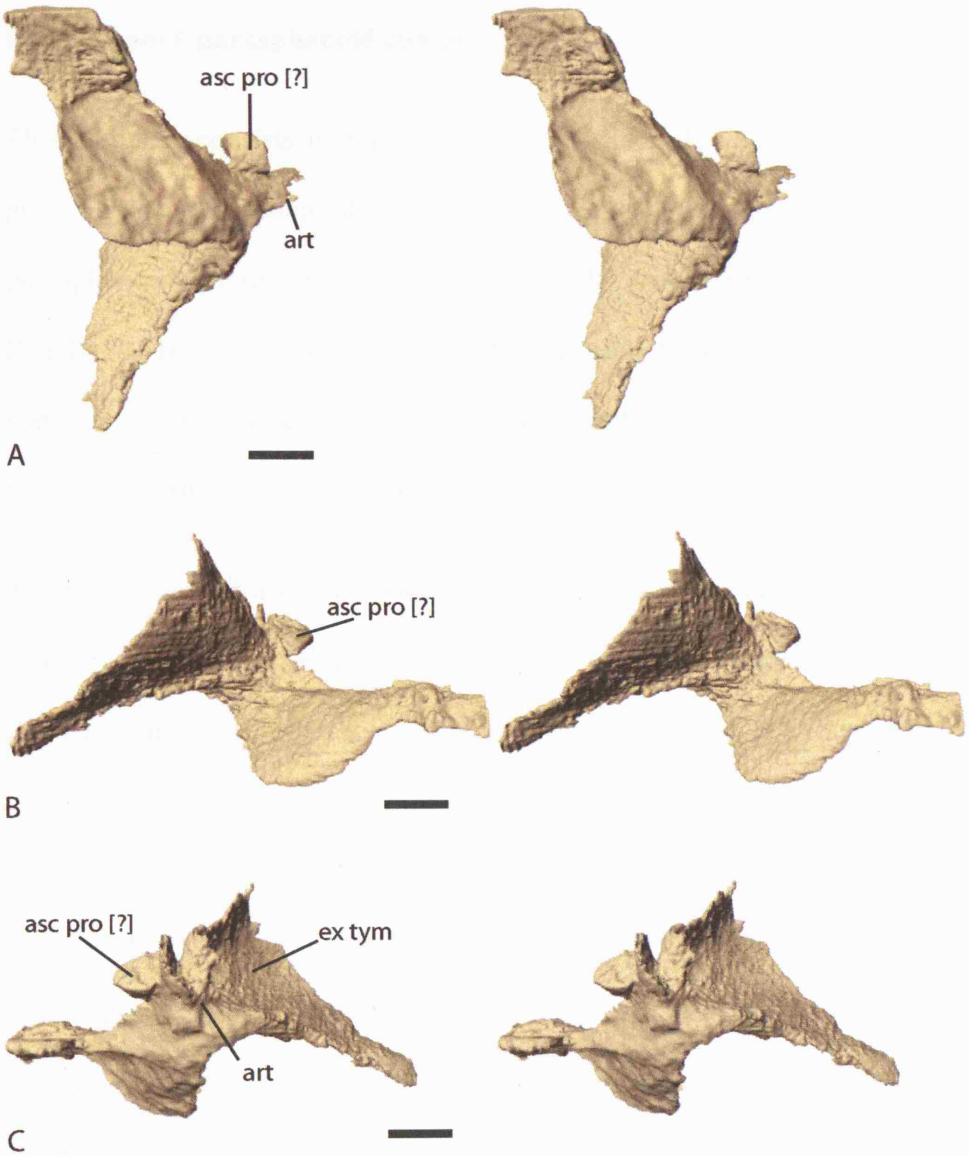

Figure 3.5.3—10 *Micropholis* specimen BMNH R.510. Stereo pairs of the right palatoquadrate complex. A, ventral view. B, right lateral view. C, medial view. Scale bars = 2mm.

Basisphenoid-parasphenoid complex

This complex consists of the posterior sphenethmoid (se) and cultriform process (cul pro) of the parasphenoid, the basisphenoid and the posterior expansion of the parasphenoid (Figure 3.5.3—11 and 12 A, B). Anteriorly the complex continues in BMNH R.510, although not visualised in the scan, to contact the vomers. Laterally, the complex would have contacted the palatoquadrate complexes whilst posteriorly it fuses with the anterior extension of the basioccipital.

The sphenethmoid and cultriform process are well preserved, although there is a crack caused by previously undocumented damage. In lateral perspective (Figure 3.5.3—11 E and F) it can be seen that this region is set ventrally relative to the posterior part of the complex. This ventral ossification of the sphenethmoid and cultriform process terminates bulbously between the basipterygoid articulations. Directly above this bulbous area there are paired shallow concavities (Figure 3.5.3—12 A) which are homologous to those seen in *Acanthostega*, *Kyrinion*, *Dendrerpeton* (Robinson et al., 2005), *Lydekkerina* and other early tetrapods, see Clack & Holmes (1988). These shallow cavities maybe the attachment site of the lateral rectus eye muscles. Posterior to these cavities the basisphenoid forms the crista sellaris (cri sel) which would have continued in cartilage and fused with the otic capsules (oc). The basipterygoid articulations are positioned laterally to the crista sellaris, although, as mentioned previously there appears to have been only a cartilaginous contact between the braincase and the palatoquadrate complexes.

Behind the crista sellaris the parasphenoid (ps) expands to form a lamina area. Its surface is rather incomplete and has proved difficult to model within the scan slices. The thin nature of this lamina area and the background noise of the scan series has

caused it to be only partially reconstructed. Being dermal bone the parasphenoid could not of course have been continued in cartilage. It seems likely that the lamina surface would have continued posterolaterally on each side to form the ventral surface of the fenestra ovalis (f/o) with which the stapes (st) would have articulated. At its posteromedial margin the parasphenoid fuses with the anterior extension of the basioccipital. It may well form a thin ventral surface below part of this anterior extension, although, this could not be differentiated within the scan slices.

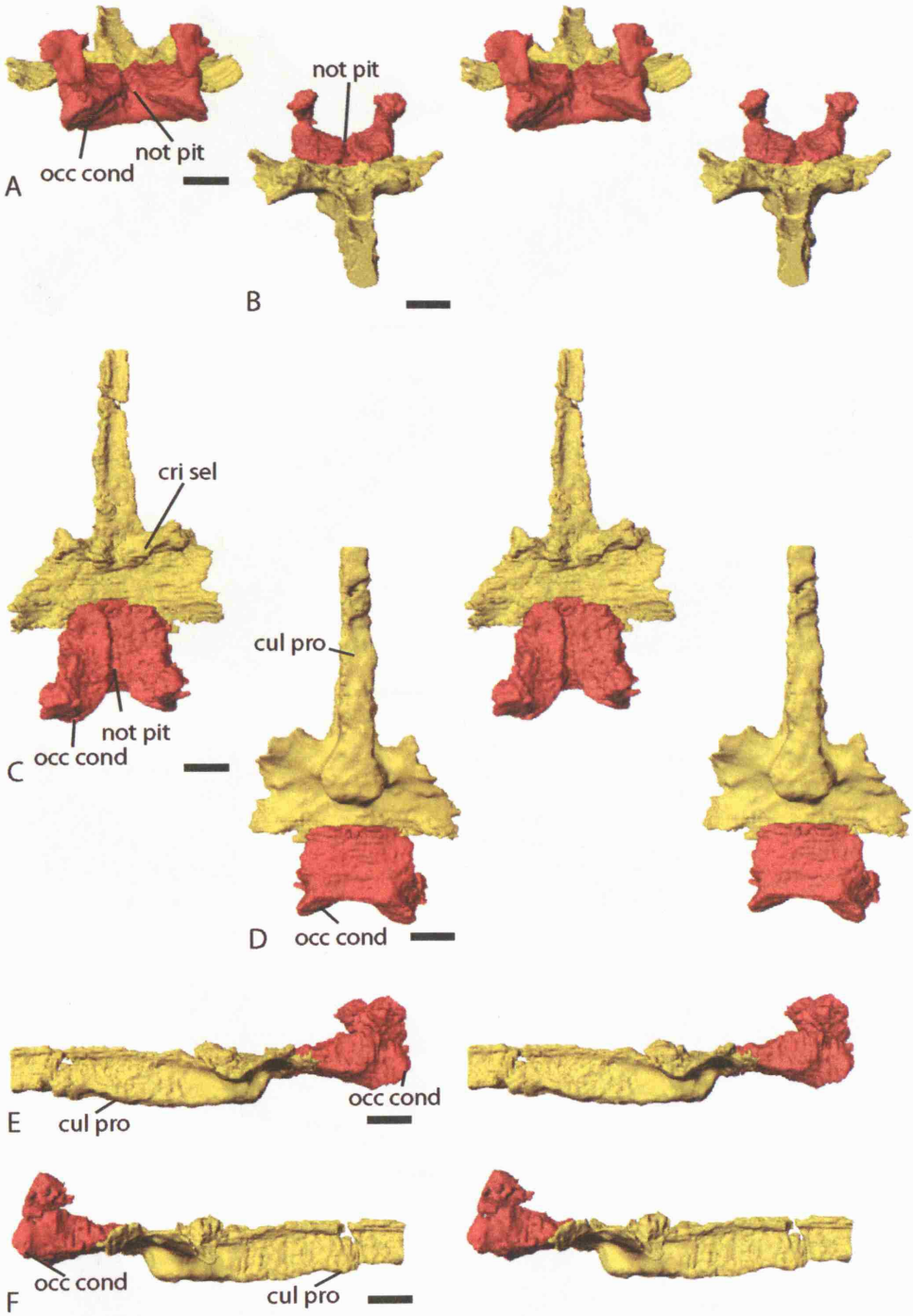

Figure 3.5.3—11 *Micropholis* specimen BMNH R.510. Stereo pairs of the basisphenoid-parasphenoid complex and the occipital complex. A, posterior view. B, anterior view. C, dorsal view. D, ventral view. E, left lateral view. F, right lateral view. Scale bars = 2mm.

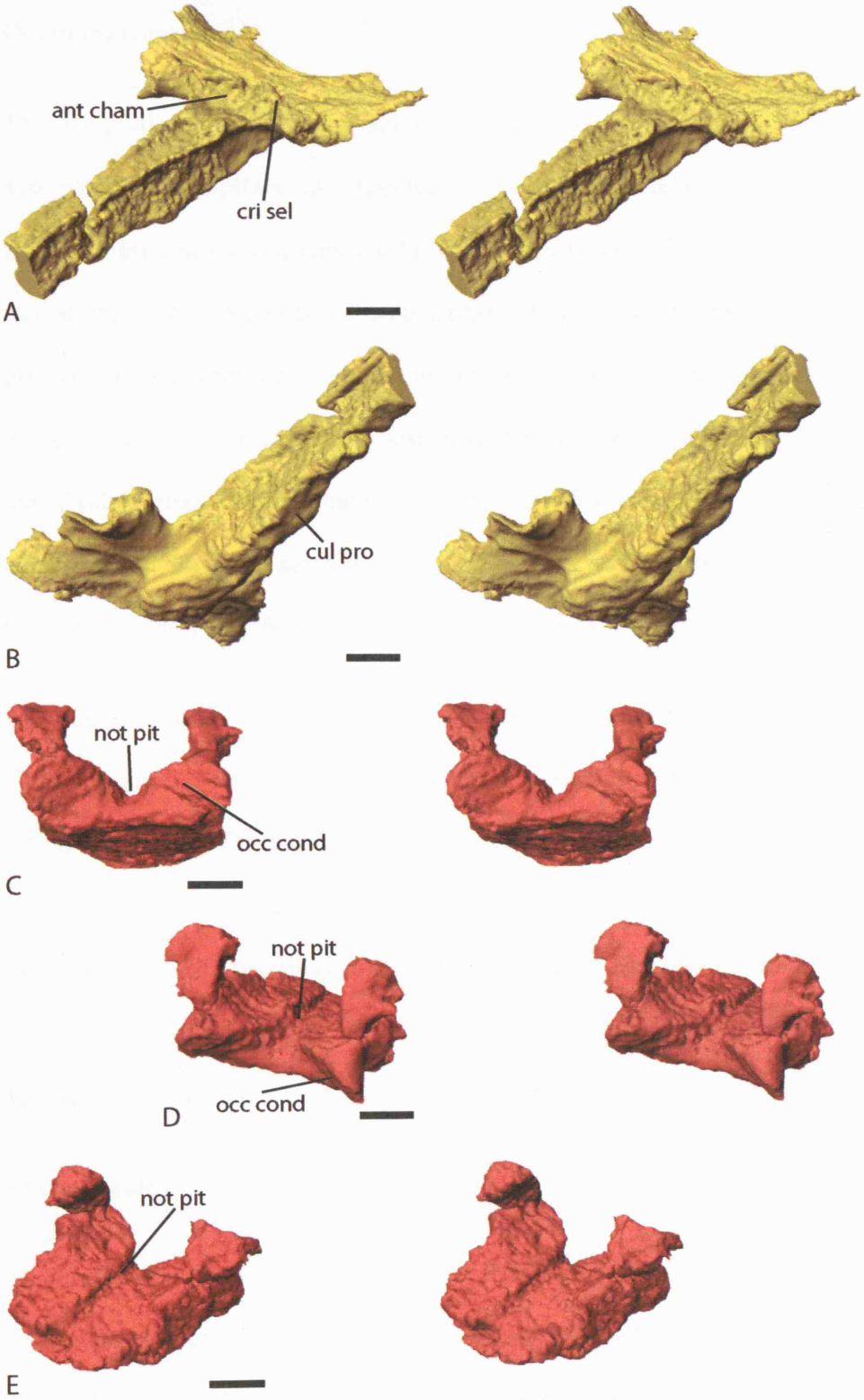

Figure 3.5.3—12 *Micropholis* specimen BMNH R.510. Stereo pairs. A and B, basisphenoid-parasphenoid complex. A, offset anterodorsal view. B, offset anteroventral view. C, D and E, occipital complex. C, posterior view. D, offset posterodorsal view. E, offset anterodorsal view. Scale bars = 2mm.

Occipital complex

The occipital complex (Figure 3.5.3—11 and 12 C, D, E) consists of the basioccipital and paired exoccipitals, as expected there is no evidence of a supraoccipital. The basioccipital and exoccipitals are fused together (bo-eo). The anterior extension of the basioccipital, which contacts the parasphenoid, has a paired appearance with a midline groove running from the occipital condyle (occ cond) to its anterior extent. This groove is the notochordal pit (not pit) as also described in *Dendrerpeton* (Robinson et al., 2005) and *Lydekkerina*. The appearance of this anterior extension is also similar to that suggested by the serial sectioning of *Tersomius* (Carroll, 1964). The paired portions of the anterior extension flow back to form the occipital condyle.

The occipital condyle (Figure 3.5.3—12 C and D) has the typical bi-facetted appearance of post-eryopoid temnospondyls and looks especially similar to that of *Doleserpeton* (Bolt, 1969) and *Tersomius* (Carroll, 1964). It is not possible to delineate the exact contributions the basioccipital and exoccipitals make to the occipital condyle. Dorsolateral to the occipital condyle the exoccipital extends towards both the posterior region of the otic capsules and the skull roof, although, this arrangement is not fully known due to the disturbance which has occurred.

Otic capsules

Both otic capsules are present in BMNH R.510 (Figure 3.5.3—13 and 14). They appear to have been slightly translocated and are not in contact with the occipital complex. It is likely that they would have been in contact with both the occipital complex and the basisphenoid-parasphenoid complex. Furthermore, both the otic capsules and the

occipital complex would have contacted the skull roof via cartilaginous extensions as envisaged in *Dendrerpeton* (Robinson et al., 2005).

Unlike all the other otic capsules described in this thesis those of *Micropholis* are both preserved as separate anterior and posterior sections. The left and right anterior sections are approximately mirror images of each other. The same is also the case with the posterior sections. This could lead to the belief that this separation is not caused by the breaking of a single ossification. The separate parts could, therefore, be due to weakness at a suture between anterior and posterior ossifications. Alternatively, the separate parts could be caused by an unossified cartilaginous region which, of course, has not been preserved. This character state of well ossified but unfused anterior and posterior sections of the otic capsules is also shared with *Doleserpeton* (Bolt, 1969), although, this does not appear to be the case in *Tersomius* (Carroll, 1964). It seems logical, therefore, to call the anterior section a prootic and the posterior section an opisthotic.

Each prootic section (Figure 3.5.3—13 A, B and 14 C, D) has been slightly translocated and now lies on its side on the palatoquadrate complex behind the ascending process of the epipterygoid. In anterolateral view (Figure 3.5.3—13 A and 14 B) it is, however, possible to see a foramen (pro for) on the dorsal margin of the left prootic and a notch in an equivalent position on the right prootic. Although, not well defined it seems clear that these are homologous to the post-temporal foramen described in *Edops* (Romer & Witter, 1942) and also observed in *Dendrerpeton* (Robinson et al., 2005) and *Lydekkerina.* It seems likely that the foramen/notch (ot for) in *Micropholis* would have lead through to the post-temporal fossa (ptf), although, this area is poorly preserved and presumably had an entirely cartilaginous floor.

It is possible to observe the ossified housing for the anterior region of the semicircular canals from an internal view of each prootic (Figure 3.5.3—13 B and 14 B). On the medial side the ossified path of the anterior semicircular canal (a scc) is present running dorsoventral. At the ventral extent of this path, in the right prootic, the ossified shell that housed the anterior ampulla (a scc amp) is preserved. Lateral to the anterior semicircular canal in both prootics there is also an ossified shell that housed the ampulla of the horizontal semicircular canal (h scc amp).

The opisthotics (Figure 3.5.3—13 C, D and 14 C, D) also preserve parts of the posterior ossified housing of the semicircular canals, although, the left is most complete and hence easier to interpret. An internal view of the left opisthotic allows the path that housed the posterior semicircular canal (p scc) and its associated ampulla (p scc amp) to be visualised. Whilst, laterally the posterior end of the horizontal semicircular canal path is preserved. This path is not fully preserved in the prootic and opisthotic, which suggests that the two parts of the otic capsule were joined together via a cartilaginous area. This area would have housed the horizontal semicircular canal, produced the dorsal and anterior margin of the fenestra ovalis and the ventral floor of the post-temporal fossa.

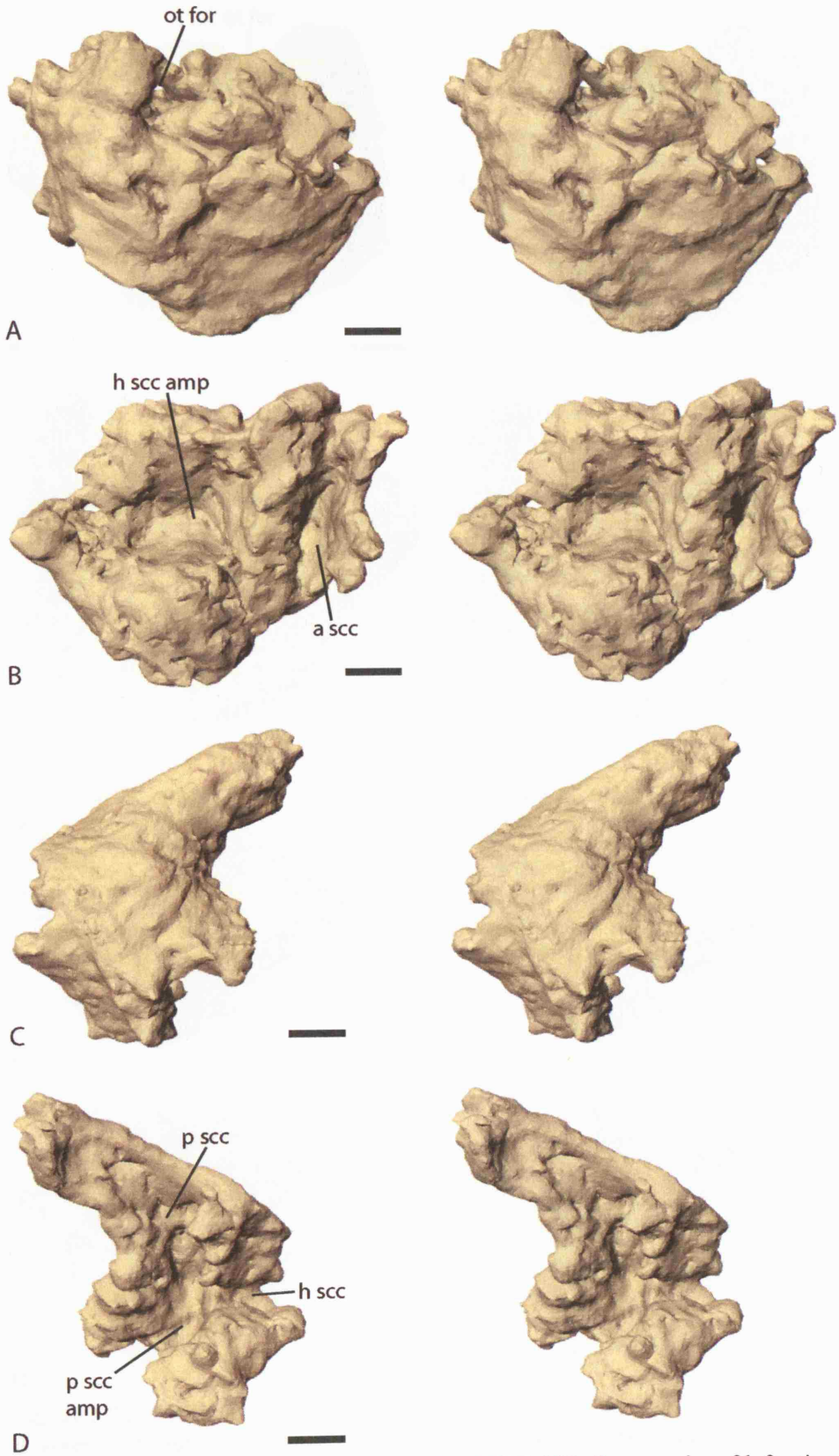

Figure 3.5.3—13 *Micropholis* specimen BMNH R.510. Stereo pairs of left otic capsule. A and B, anterior section or prootic. A, left anterolateral view. B, posteromedial view. C and D, posterior section or opisthotic. C, left posterolateral view. D, anteromedial view. Scale bars = 1mm.

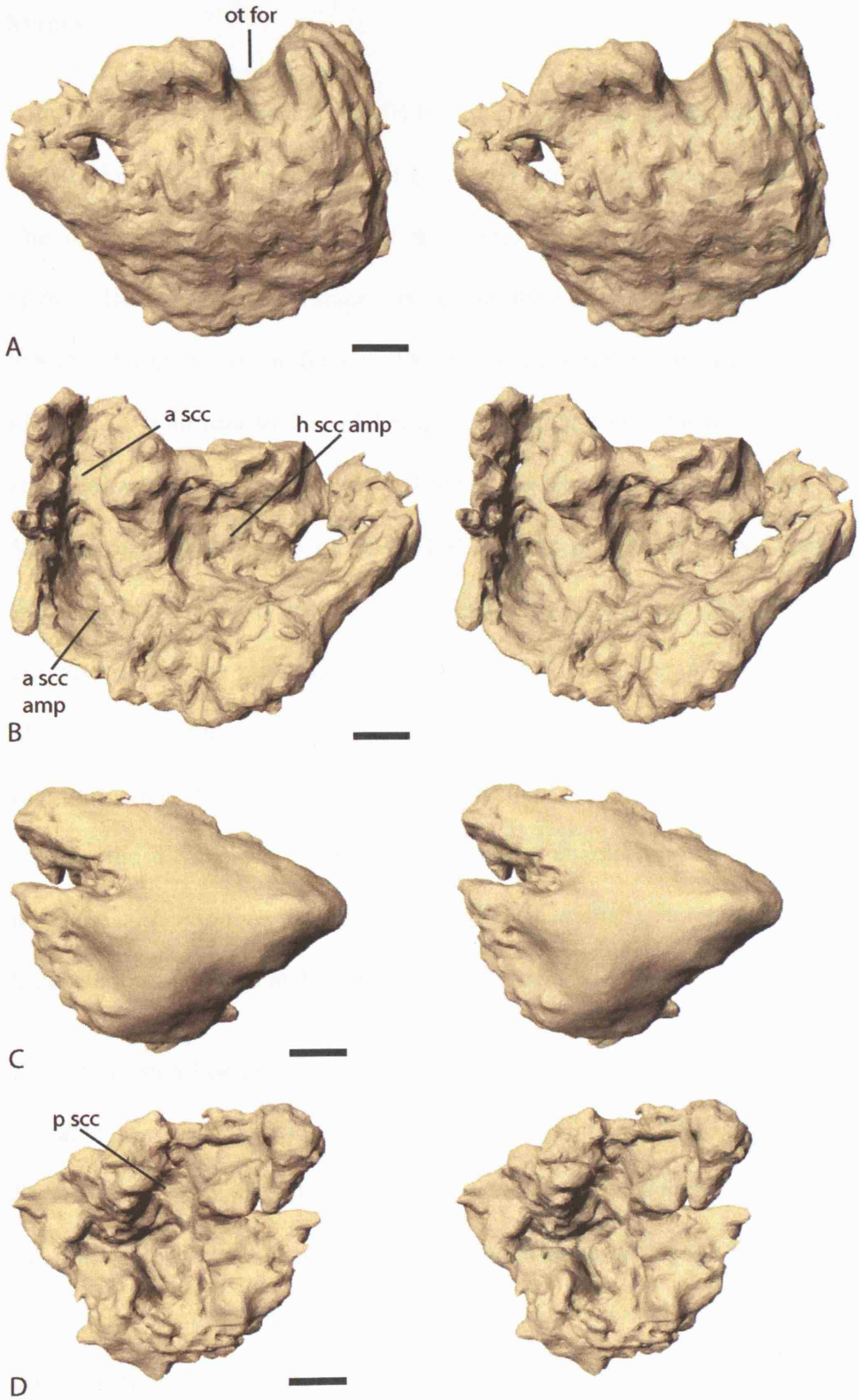

Figure 3.5.3—14 *Micropholis* specimen BMNH R.510. Stereo pairs of right otic capsule. A and B, anterior section or prootic. A, right anterolateral view. B, posteromedial view. C and D, posterior section or opisthotic. C, right posterolateral view. D, anteromedial view. Scale bars = 1mm.

Stapes

Although the right stapes of BMNH R.510 has been exposed by previous undocumented preparation its morphology cannot be clearly ascertained from visual inspection alone. The only previous description of the stapes of *Micropholis* was that given by Boy (1985). He described the stapes as 'er ist ähnlich wie bei *Eryops* lang und schlank; jedoch ist das Foramen für den Durchtritt der Arteria stapedialis (orbitalis) deutlich kleiner' [it is similar to that of *Eryops* i.e. long and thin; however the foramen for the stapedial artery is clearly smaller]. There is no other known description of the stapes of *Micropholis*. Both stapes of BMNH R.510 are present and have been reconstructed from the scan slices (Figure 3.5.3—15 and 16). The stapes of *Micropholis* cannot be characterised in as much detail as was possible with *Dendrerpeton* (Robinson et al., 2005). Due to the small size of *Micropholis's* stapes, the background noise and the required slice thickness prevented a detailed modelling of their surface structure. Despite these factors it has proved possible to characterise the overall morphology of the stapes. *Micropholis* has many typical characteristics of a temnospondyl stapes with a bipartite footplate (fp) and a relatively thin rod.

Due to the small degree of translocation within the posterior region of the skull it is not possible to know accurately the orientation of the stapes. The orientation given in Figure 3.5.3—15 and 16 is based on the position of the stapes within BMNH R.510 and the position of the posterior notches. The bipartite footplate can be observed in a medial view. The ventral component (ven com) is positioned ventrolateral to the dorsal component (dor com). This ventral part is anteroposteriorly elongate, although, clearly it is not as dorsoventrally compressed as that of *Doleserpeton* (Lombard & Bolt, 1988). The ventral part would have articulated with the parasphenoid. The dorsal part is far

more rounded and piston shaped and presumably would have contacted the perilymphatic space of the inner ear. There is a noticeable groove separating the ventral and dorsal parts of the footplate, although, no stapedial foramen can be observed. The lack of such a foramen is probably due to the limited resolution of the scan slices rather than demonstrating its true character state.

Lateral to the footplate the stapes forms a progressively narrowing rod. This rod has a slight anterior twist as also observed in *Dendrerpeton* (Robinson et al., 2005). The rod appears to be featureless without any apparent scars or unfinished areas, although, even if they were present it would probably not have been possible to ascertain their existence from the scans. It is thus impossible to verify the presence or otherwise of a posterior scar or process on the stapes. There is also no direct evidence for an unfinished distal concavity and a presumed cartilaginous extension to the stapes. The possible presence of such an extension, the relative size of the stapes to the posterior notches and their proposed function will be elaborated on in the discussion section.

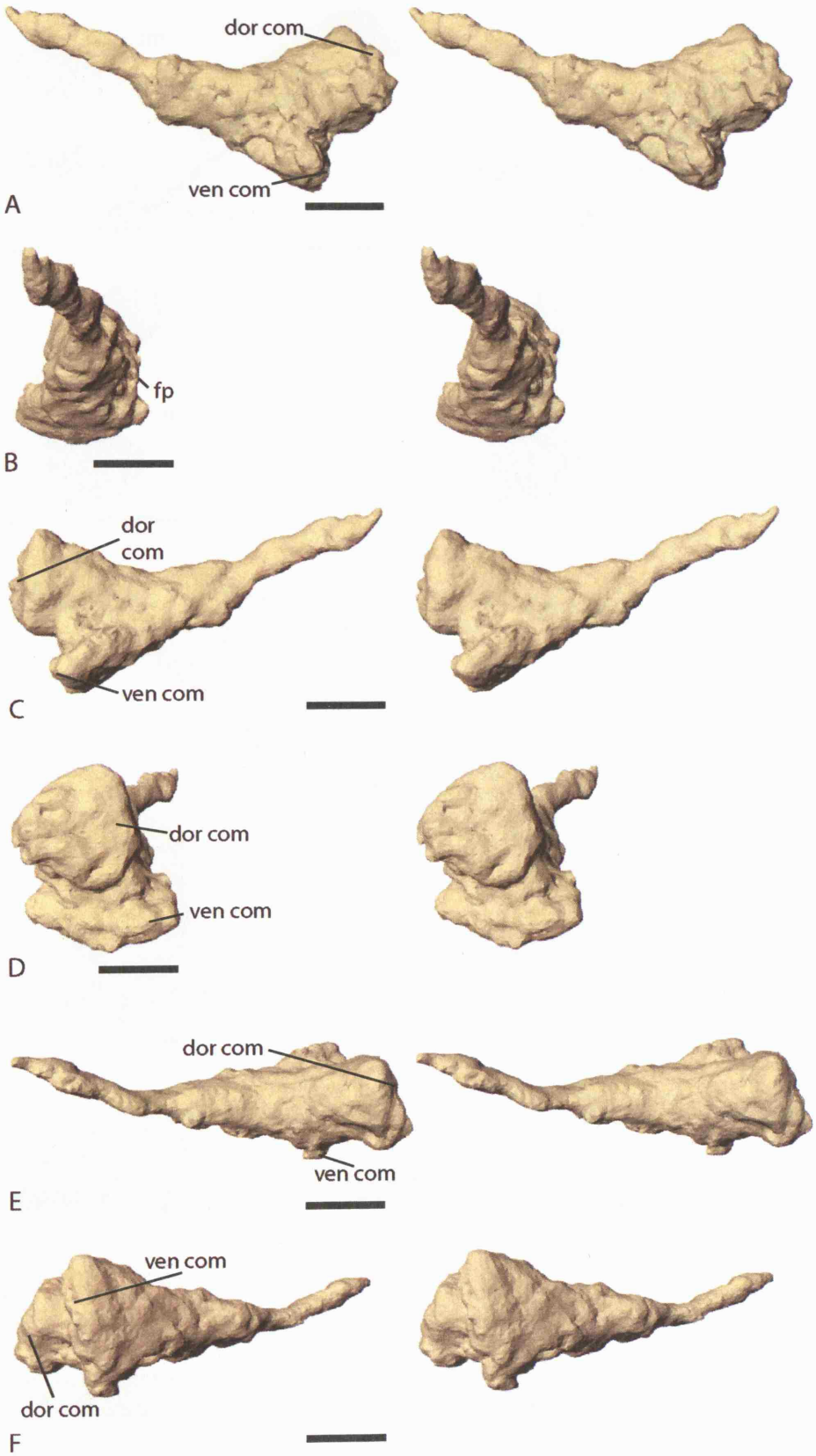

Figure 3.5.3—15 *Micropholis* specimen BMNH R.510. Stereo pairs of the left stapes. A, posterior view. B, left lateral view. C, anterior view. D, medial view. E, dorsal view. F, ventral view. Scale bars = 1mm.

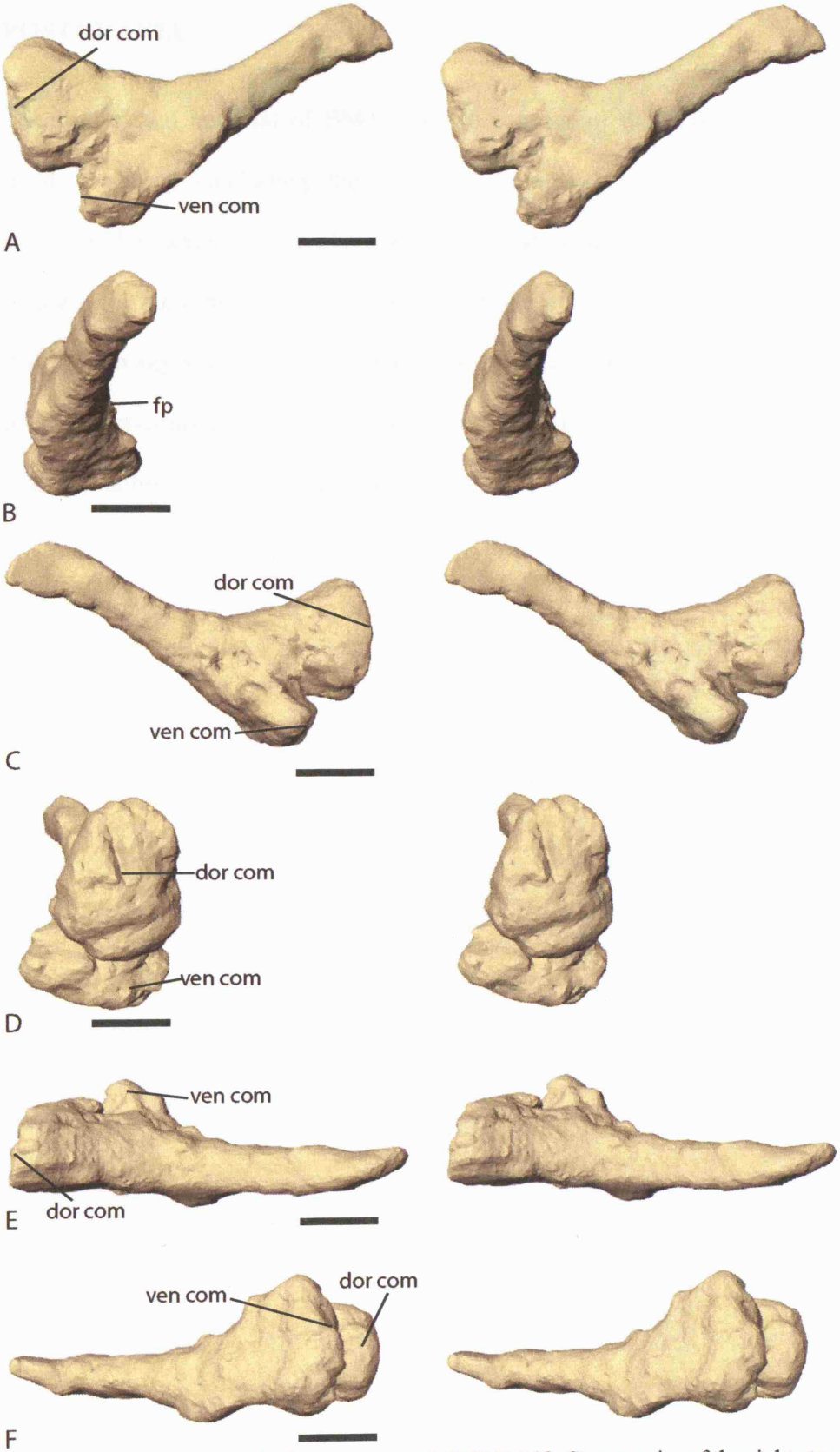

Figure 3.5.3—16 *Micropholis* specimen BMNH R.510. Stereo pairs of the right stapes. A, posterior view. B, right lateral view. C, anterior view. D, medial view. E, dorsal view. F, ventral view. Scale bars = 1mm.

POSTCRANIA

The postcranial material of BMNH R.510 consists of the axial skeleton (six anterior most vertebrae (including the atlas-axis complex) and four right ribs) and the appendicular skeleton (interclavicle, both clavicles, the right scapulocoracoid and part of the right humerus) (Figure 3.5.3—17). None of these elements appear to have been distorted in any way, although, their relative positions have been altered. Certain aspects of the post-cranium of *Micropholis* have been described before by Watson (1913), Broili & Schröder (1937) and Boy (1985).

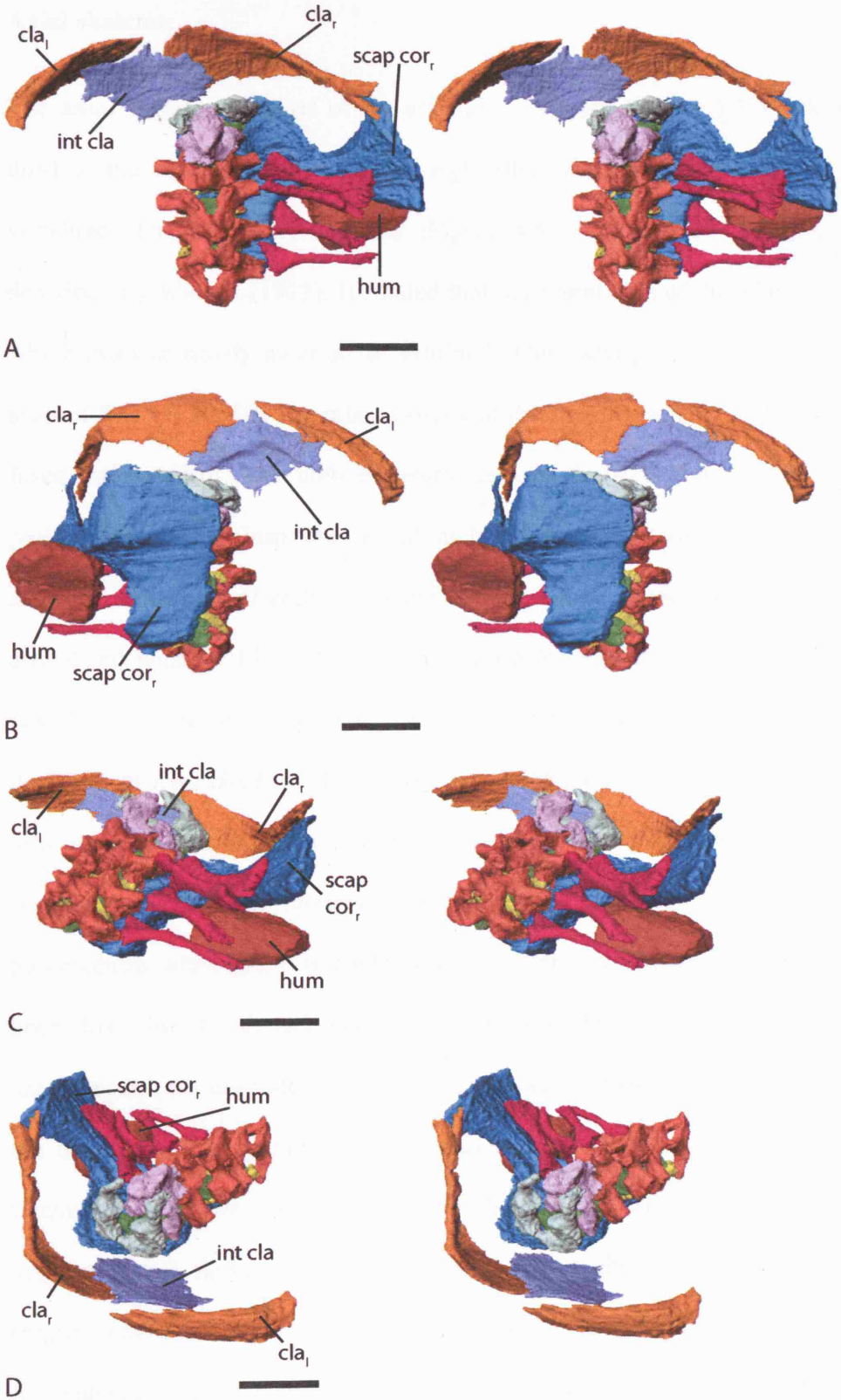

Figure 3.5.3—17 *Micropholis* specimen BMNH R.510. Stereo pairs of the postcranial model. A, dorsal view. B, ventral view. C, right posterolateral view. D, left anterolateral view. Scale bars = 5mm.

Axial skeleton

The axial skeleton consists of the atlas-axis complex (Figure 3.5.3—18 and 19), the third to the sixth vertebrae and the right ribs associated with the third to the sixth vertebrae. The atlas-axis complex (Figure 3.5.3—20 and 21) has previously been described by Watson (1913). He stated that the neural arch of the atlas 'is in two pieces which meet or nearly meet at the midline'. This description is in agreement with the atlas of BMNH R.510. The atlas consists of the first neural arch along with a ventrally fused intercentrum. The unfused neural arch of the atlas form paddle shaped dorsal projections which clasp the neural arch of the axis posteriorly. Ventral to these projections the neural arch forms expanded crescent shaped pads which would have articulated with the bi-facetted occipital condyle. Between these pads the path for the notochord can be seen. The pads fuse below the notochordal path in a similar manner to that seen in *Lydekkerina.* This fusion represents the incorporation of the intercentrum into the atlas. The axis consists of a fused neural arch plus a ventral intercentrum (int cen)which have been fused together. There is no evidence for a set of paired pleurocentra, although, this could well represent a resolution issue or they may have been lost due to disturbance in this region. The neural spine of the axis is anteroposteriorly expanded, relative to the more posterior arches, for articulation with the dorsal pads of the atlas. The neural arch of the axis does not appear to have transverse processes with diapophyses (dia) for the articulation with a rib pair. In support of this finding the ribs that are found on the right of the vertebral column (Figure 3.5.3—17) seem to be associated with the third to the sixth vertebrae. There is no evidence of a more anterior rib, although again this could be due to the previously mentioned disturbance. Posteriorly the neural arch of the axis has post-zygaphophyses (pozy) for contact with the third neural arch (Figure 3.5.3—18 A). It can clearly be seen

in ventral view that the intercentrum of the axis articulated anteriorly with the ventral margin of the atlas. It would also appear that this intercentrum contacted that of the third vertebra posteriorly.

The morphology of the third to sixth vertebrae is quite uniform (Figure 3.5.3—18 and 19). The only exception is the lack of any visible pleurocentra associated with the third vertebrae, although it cannot be confirmed whether this is due to the disturbance or it is a true characteristic of *Micropholis*. The fifth vertebra will be used as an example for all those present in BMNH R.510 (Figure 3.5.3—22, 23 and 24). The neural spine of the fifth neural arch is directly above the post-zygapophyses while the pre-zygapophyses (przy) are above the main body of the neural arch. This produces a neural arch which in lateral view is not dissimilar to that of *Lydekkerina*, although, clearly *Micropholis* has a much shorter neural spine. The diapophyses (dia) for articulation with the tubercular of the ribs are ventrolateral to the pre-zygapophyses. In anterior and posterior view it can be seen that *Micropholis* has relatively wide neural arches which enclose a large neural tube.

The intercentrum associated with the fifth vertebra is approximately oval in dorsal and a shallow crescent shape in anterior view. No articulation surface for the capitulum of a rib can be visualised, although, this is probably a scan resolution issue as they have been described in *Micropholis* previously by Watson (1913). The pleurocentra associated with the fifth vertebra are relatively large (Figure 3.5.3—24 C and D). They are elongate crescent shaped slivers of bone which nearly meet at the ventral midline of the notochordal tube as also described in *Tersomius*, *Eoscopus* and *Amphibamus* (Daly, 1994). On the anterior surface of each pleurocentra there is a flat area which would have

contacted the posterior of the neural arch, probably via cartilage as suggested in *Lydekkerina.*

The four ribs on the right of the vertebral column (Figure 3.5.3—17) all differ greatly from the trunk rib figured by Broili & Schröder (1937). Each of the ribs has a single proximal head for articulation with the diapophysis of the neural arch and parapophysis of the intercentrum. The head appears to be a combination of the tuberculum dorsally and the capitulum ventrally. The heads of the ribs are similar to those previously described in *Lydekkerina.* In contrast to the ribs of *Lydekkerina*, the ribs of *Micropholis* do not appear to possess uncinate processes nor are their distal ends flattened and paddle shaped.

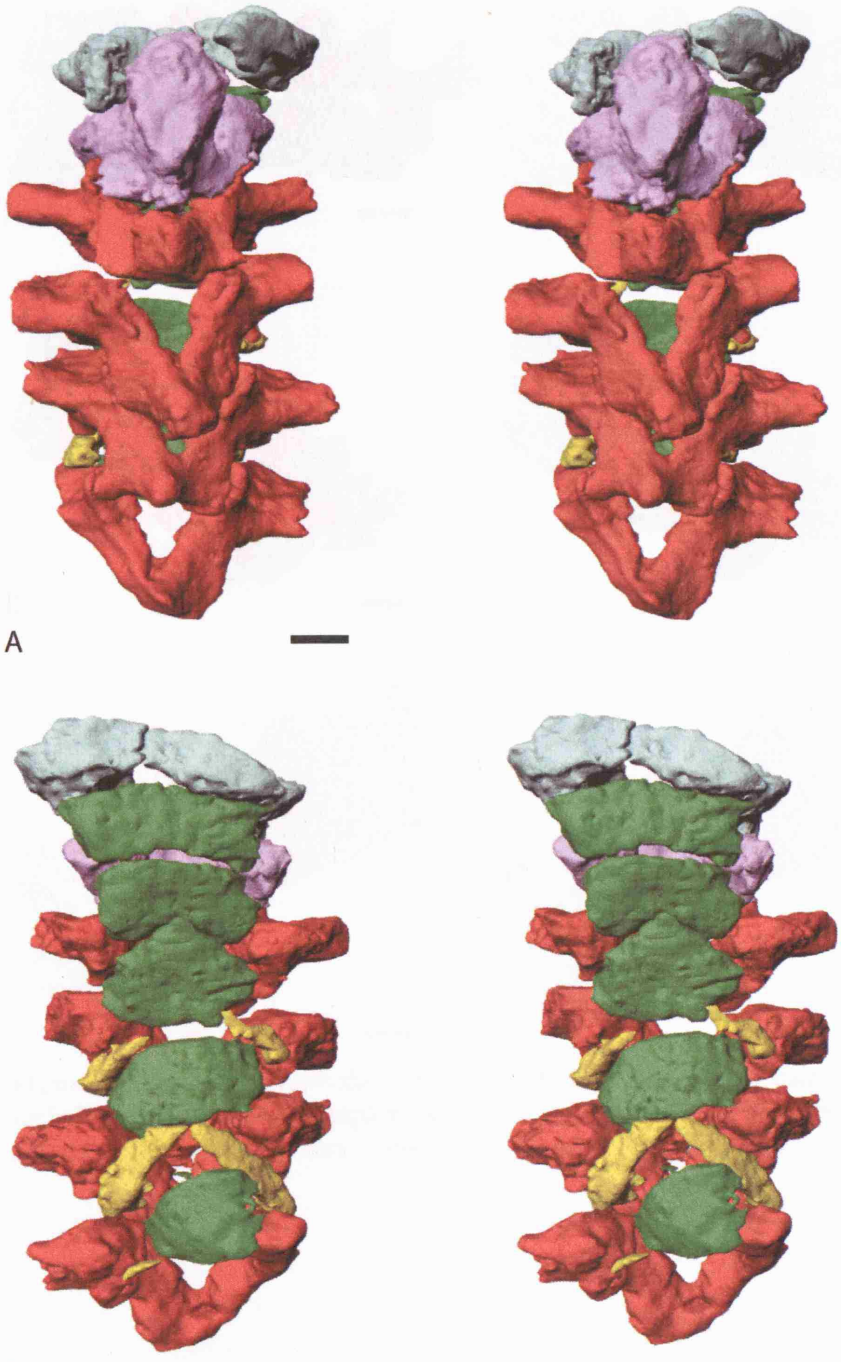

Figure 3.5.3—18 *Micropholis* specimen BMNH R.510. Stereo pairs of the first 6 vertebrae including the atlas-axis complex. A, dorsal view. B, ventral view. Scale bars = 1mm.

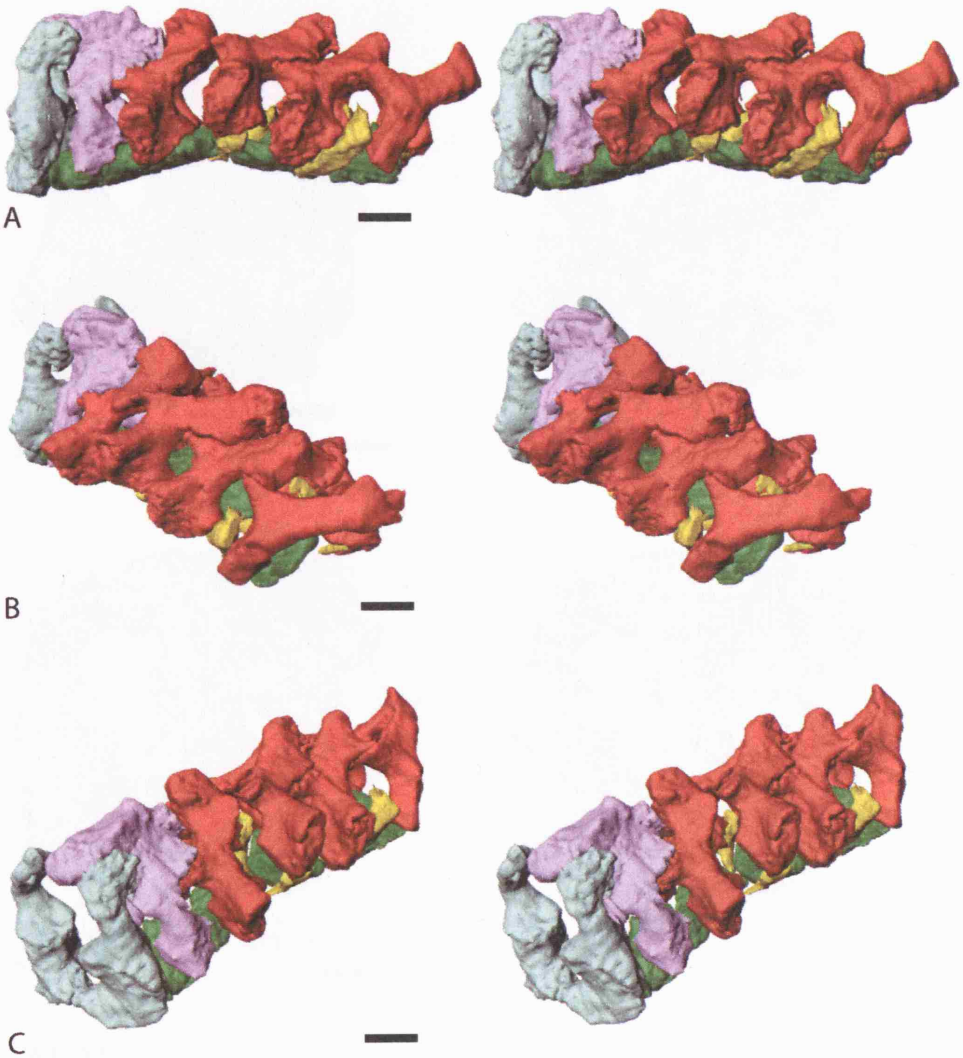

Figure 3.5.3—19 *Micropholis* specimen BMNH R.510. Stereo pairs of the first 6 vertebrae including the atlas-axis complex. A, left lateral view. B, offset posterodorsal view. C, offset anterodorsal view. Scale bars = 1mm.

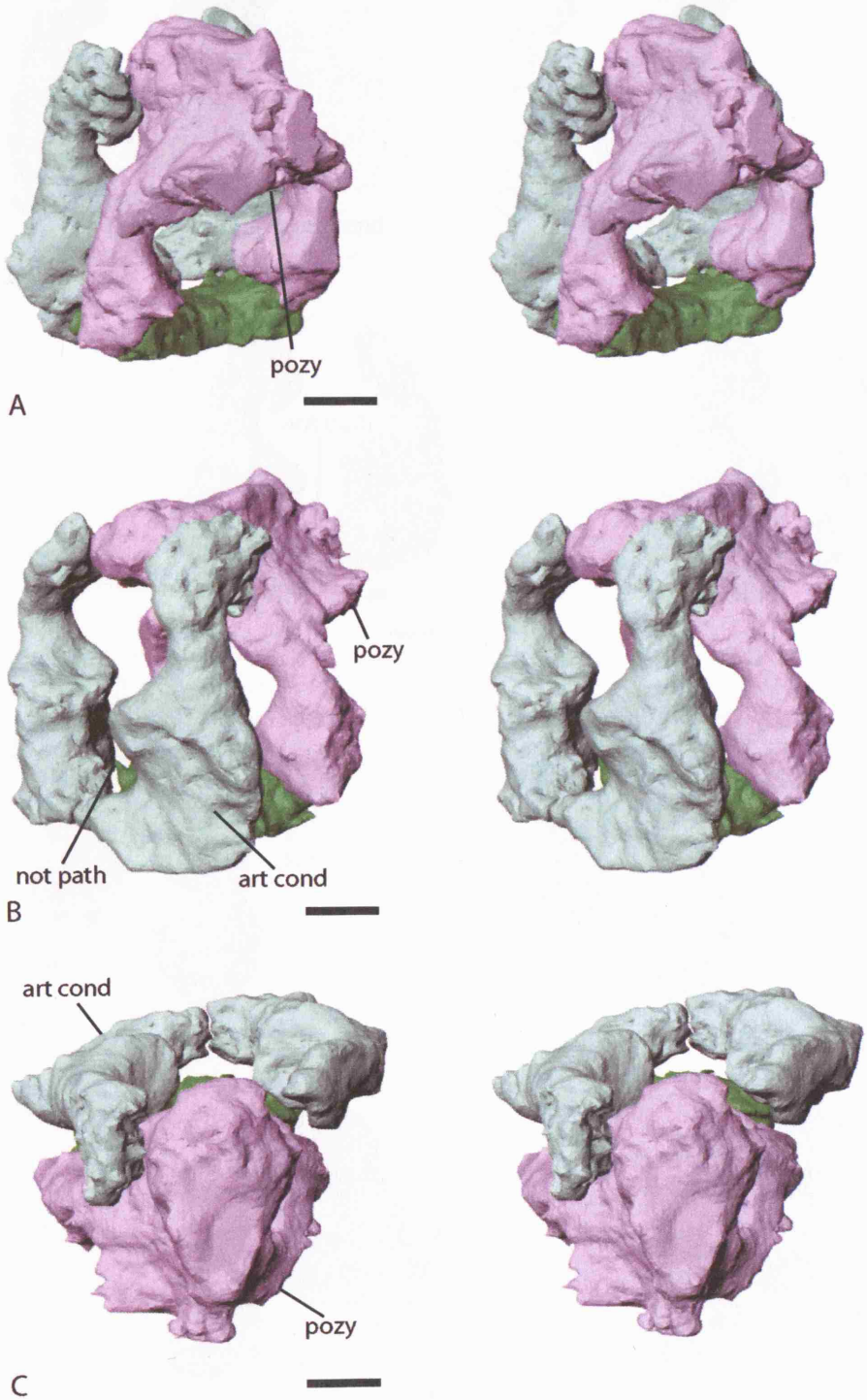

Figure 3.5.3—20 *Micropholis* specimen BMNH R.510. Stereo pairs of the atlas-axis complex. A, left posterolateral view. B, left anterolateral view. C, dorsal view. Scale bars = 1mm.

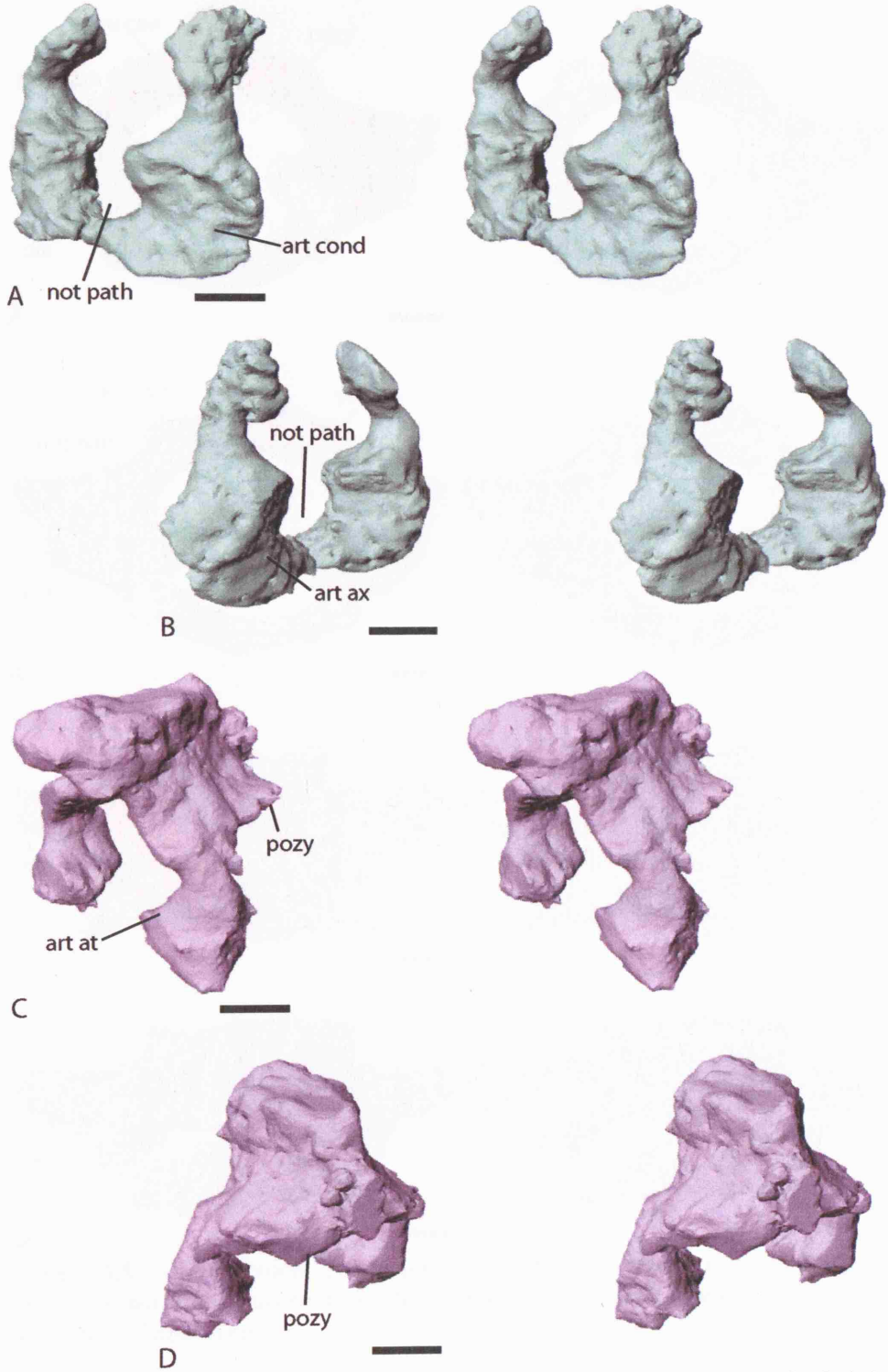

Figure 3.5.3—21 *Micropholis* specimen BMNH R.510. Stereo pairs. A, atlas in left anterolateral view. B, atlas in left posterolateral view. C, axis neural arch in left anterolateral view. D, axis neural arch in left posterolateral view. Scale bars = 1mm.

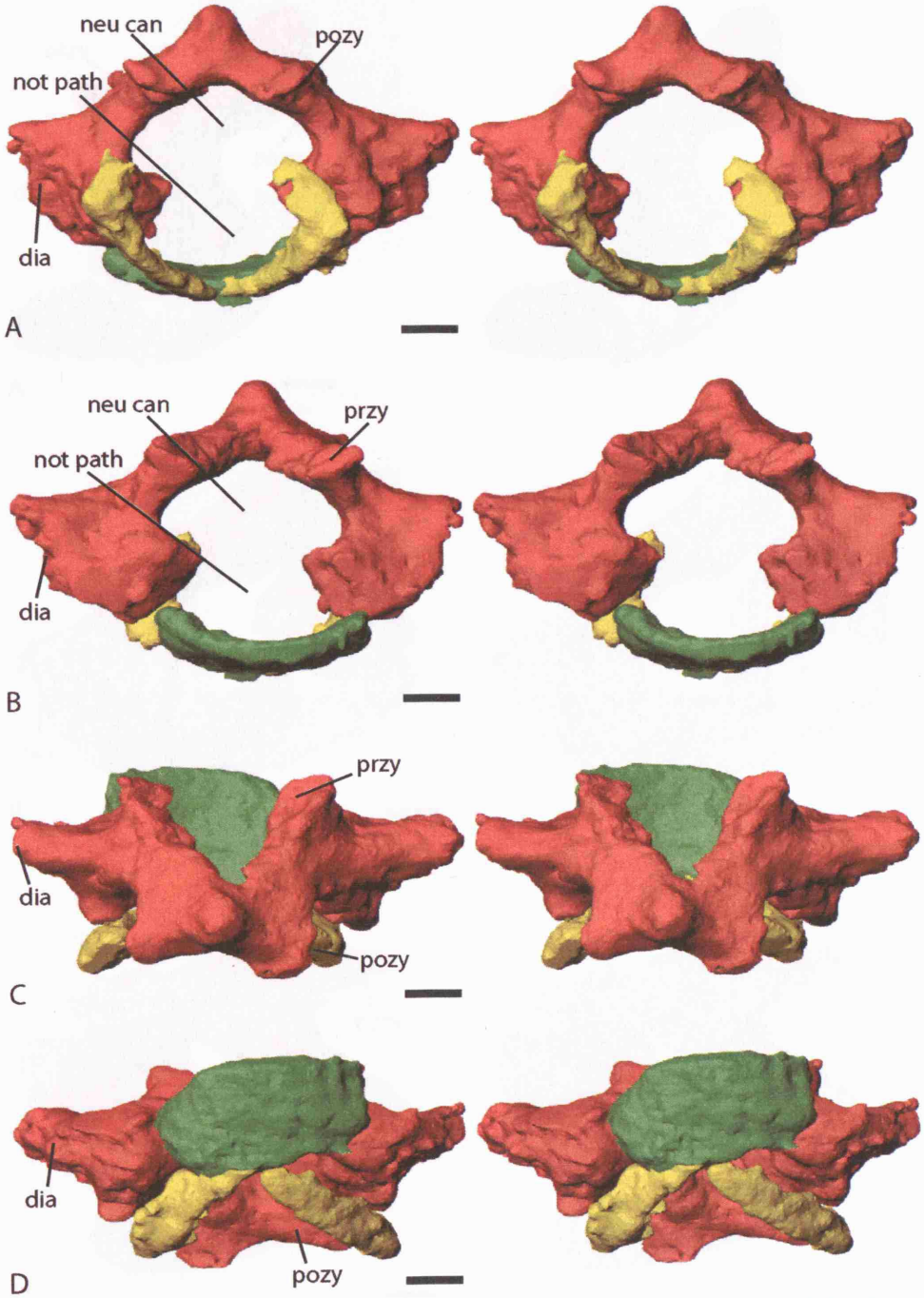

Figure 3.5.3—22 *Micropholis* specimen BMNH R.510. Stereo pairs of the 5th vertebra with correction for slight translocations. A, posterior view. B, anterior view. C, dorsal view. D, ventral view. Scale bars = 1mm.

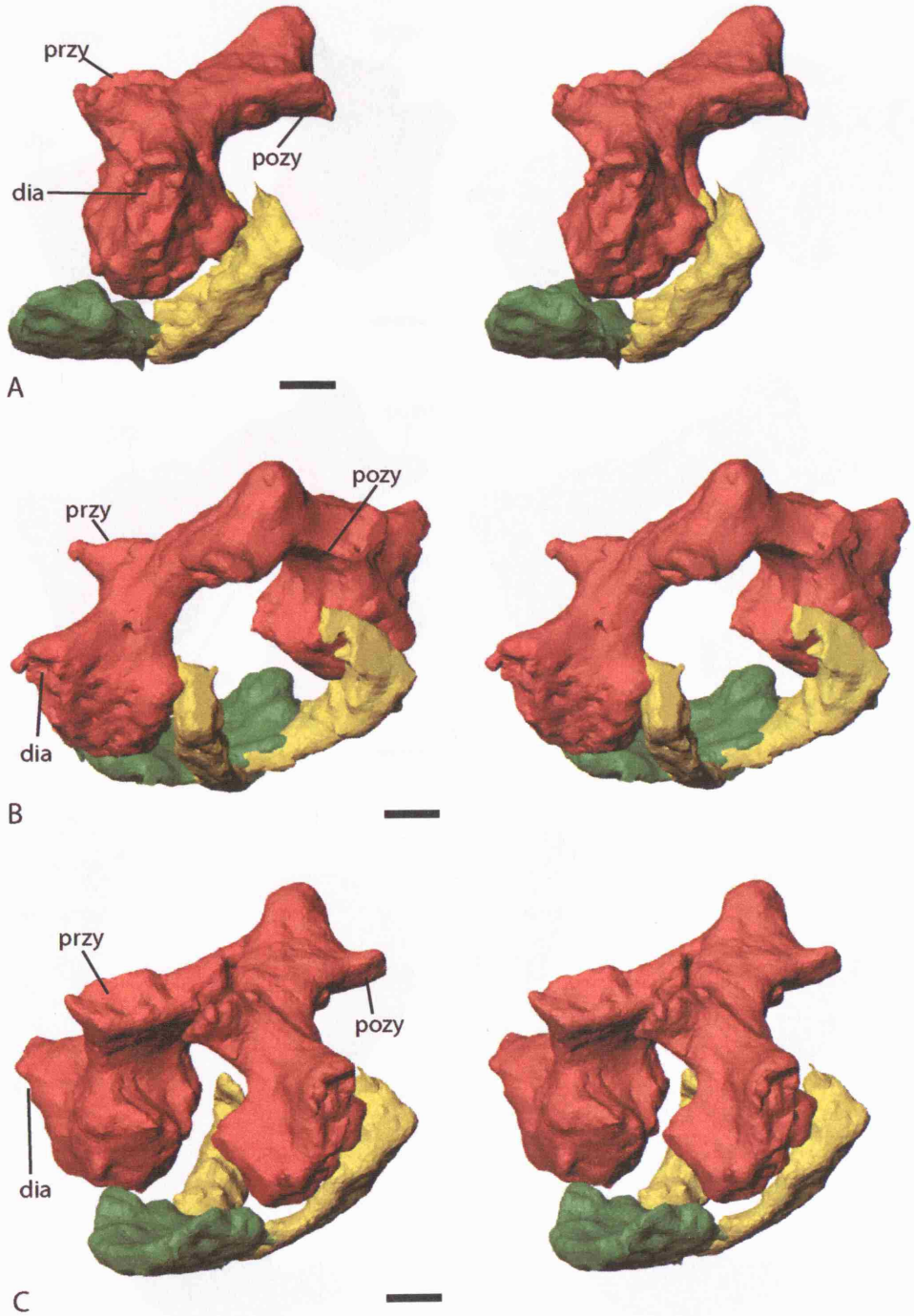

Figure 3.5.3—23 *Micropholis* specimen BMNH R.510. Stereo pairs of the 5th vertebra with correction for slight translocations. A, lateral view. B, left posterolateral view. C, left anterolateral view. Scale bars = 1mm.

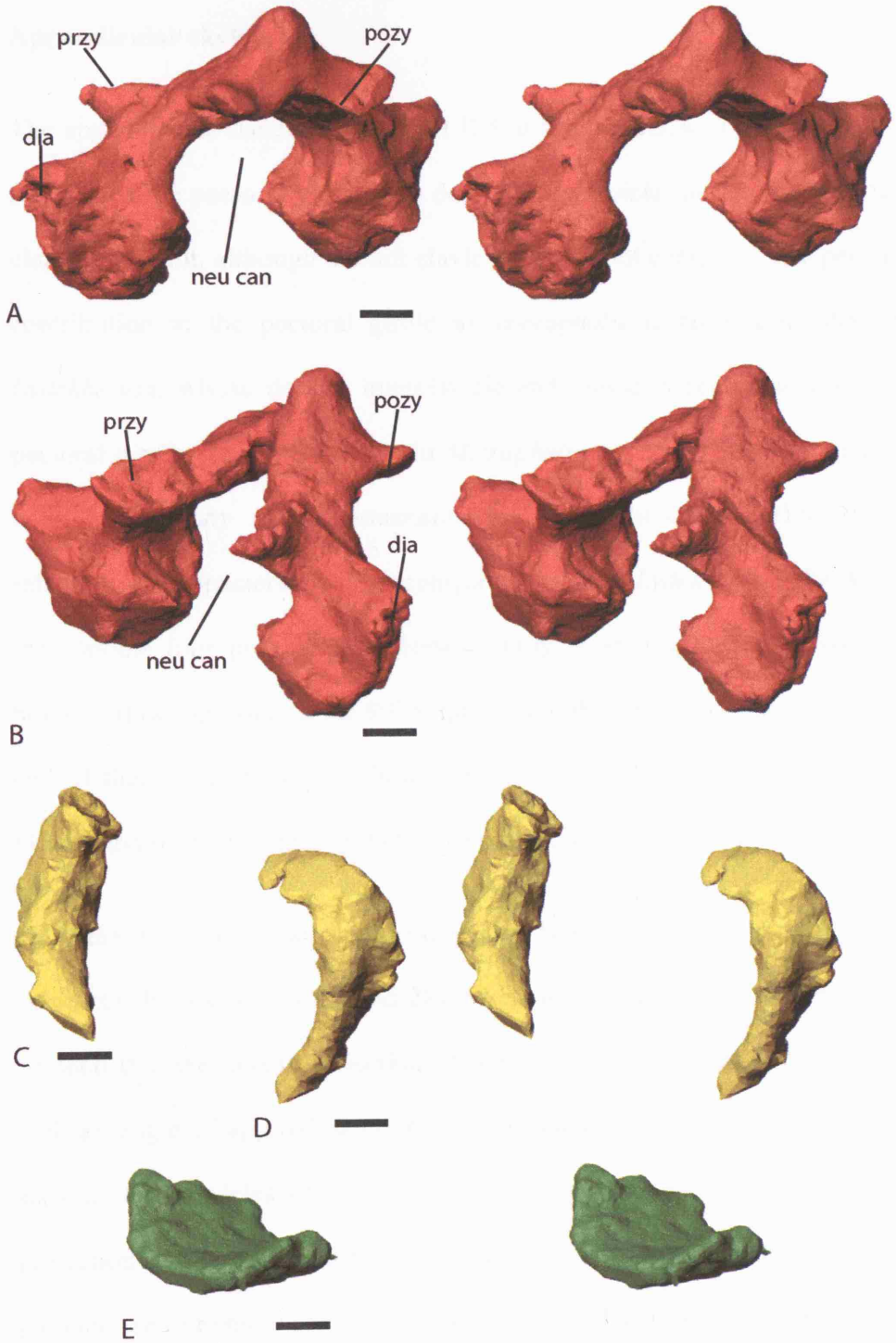

Figure 3.5.3—24 *Micropholis* specimen BMNH R.510. Stereo pairs. A and B, neural arch of the 5th vertebra. A, left posterolateral view. B, left anterolateral view. C and D, left pleurocentrum of the 5th vertebra. C, posterior view. D, anterior view. E, intercentrum of the 5th vertebra in left anterolateral view. Scale bars = 1mm.

Appendicular skeleton

The appendicular skeleton of BMNH R.510 (Figure 3.5.3—17) consists of only partial remains of the pectoral girdle. The dermal interclavicle (int cla) and clavicles (cla_l and cla_r) are present, although the left clavicle (cla_l) is not complete. The percentage dermal contribution to the pectoral girdle in *Micropholis* is far smaller than that seen in *Lydekkerina*, whose dermal interclavicle and clavicles represent a large part of the pectoral girdle. The interclavicle in *Micropholis* is a small flattened hexagonal shaped bone lacking any visible ornamentation. The right clavicle (Figure 3.5.3—25) is relatively anteroposteriorly short compared to that of *Lydekkerina*. The dorsal process of the clavicle (dor pro) projects dorsolaterally at an angle of approximately 65° from horizontal (as opposed to the 90° angle seen in the clavicles of *Lydekkerina*). The distal end of this dorsal projection bifurcates. It is possible that the posterior branch of the bifurcation represents the right cleithrum (cle_r) which has fused to the right clavicle.

Only the right scapulocoracoid (scap cor) is present, although, it is undistorted and complete (Figure 3.5.3—26 and 28). From an anterior and posterior perspective it can be seen that the dorsal projection of the scapulocoracoid projects dorsolaterally, also with an angle of approximately 65°, rather than dorsally or even slightly dorsomedial seen in the clavicles of other temnospondyls (Warren & Snell, 1991). The dorsal projection is anteroposteriorly broad with a characteristic thin anterior projection which produces an extremely recurved anterior margin. The posterior margin is comparatively straight and is inclined at an angle of 55° from the horizontal in lateral view. The projection has a mildly corrugated form which produces a shallow w-shape in cross-section. At the base of the dorsal process a large supraglenoid foramen (gle for) is present which in *Micropholis* appears uniquely to be divided into dorsal and ventral

parts. The glenoid fossa (glen foss) is positioned posteriorly to the dorsal pillar. Additionally, the scapulocoracoid has coracoid (cor for) and glenoid foramina which pass from the medial surface to the ventral side. Of these two foramina only the exit point of the coracoid foramen can be visualised on the ventral surface, although, both can clearly be seen on the medial surface of the scapulocoracoid. This observation is concordant with Watson (1913) when he stated that he could not identify a glenoid foramen on the scapulocoracoid as he was only able to investigate its ventral surface. As with *Lydekkerina* no muscle scars have been visualised on the pectoral girdle of *Micropholis*. As there are no scars from large muscles, such as the levator scapulae, it is not believed that this precludes the presence of muscular connections between the middle ear region and the pectoral girdle.

Finally, the relatively flat proximal end of the right humerus (hum) is also present (Figure 3.5.3—17). No additional information from that given by Watson (1913) can be gained from the humerus of BMNH R.510.

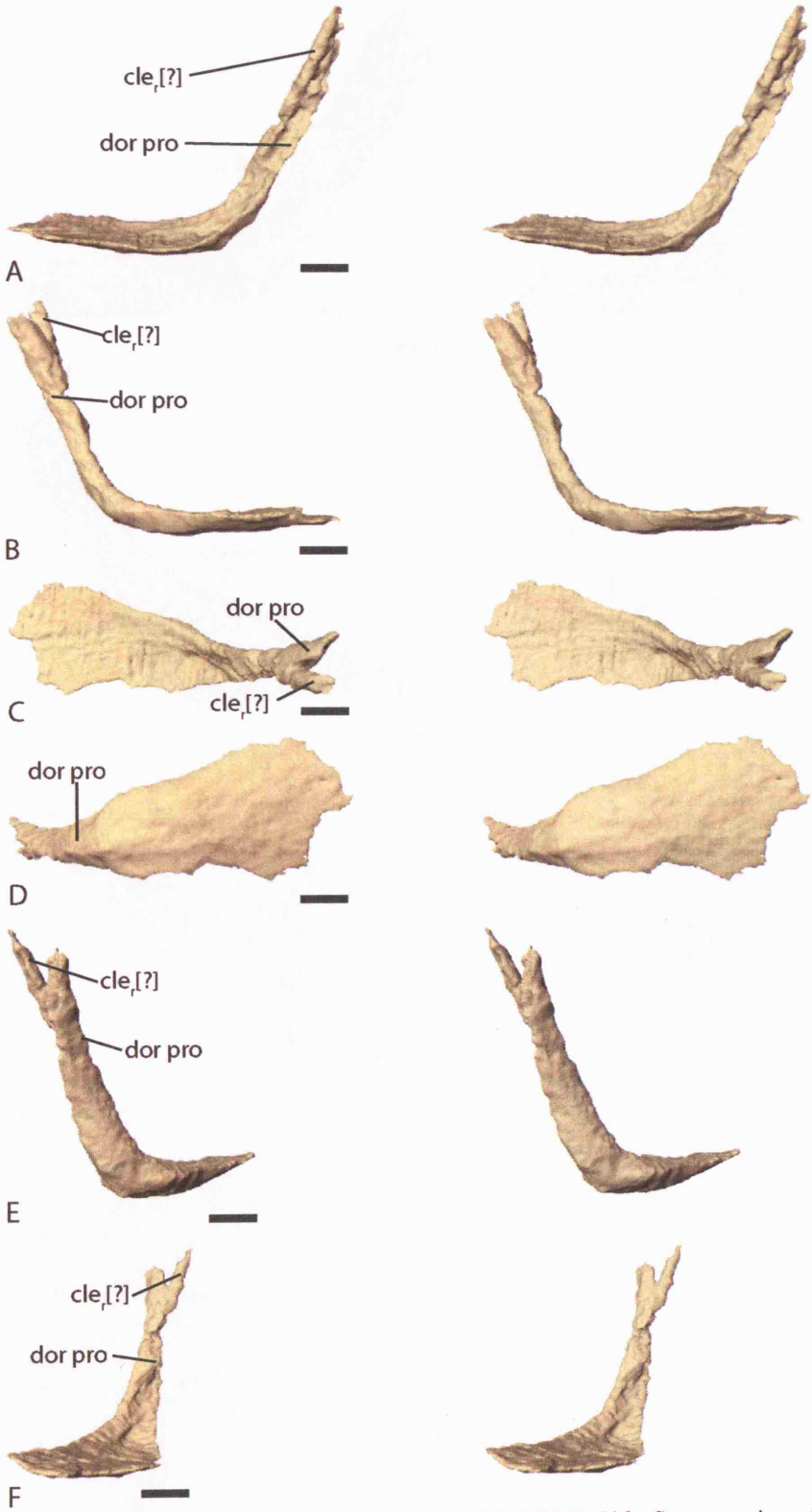

Figure 3.5.3—25 *Micropholis* specimen BMNH R.510. Stereo pairs of the right clavicle. A, posterior view. B, anterior view. C, dorsal view. D, ventral view. E, right lateral view. F, medial view. Scale bars = 2mm.

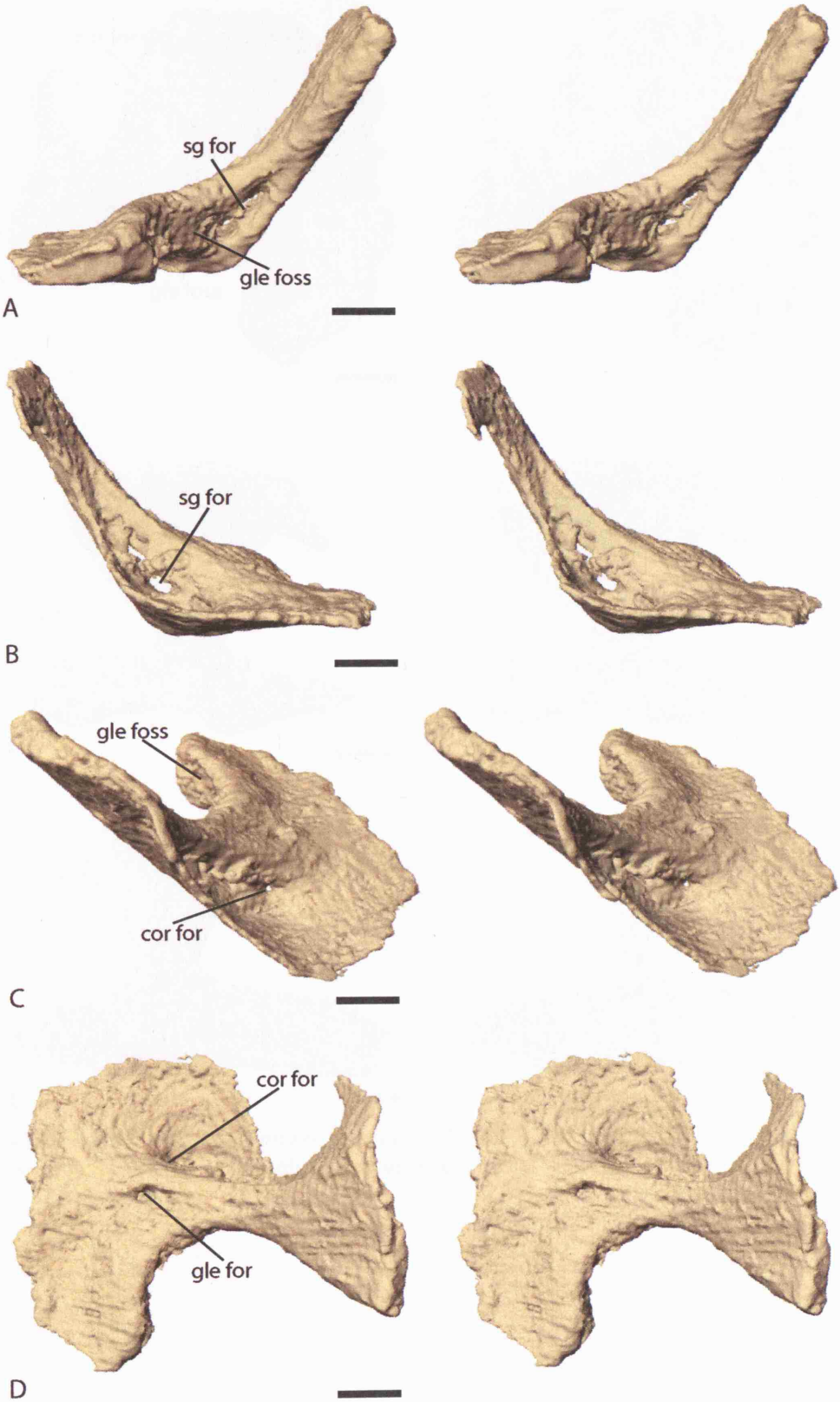

Figure 3.5.3—26 *Micropholis* specimen BMNH R.510. Stereo pairs of the right scapulocoracoid. A, posterior view. B, anterior view. C, offset anterodorsal view. D, dorsal view. Scale bars = 2mm.

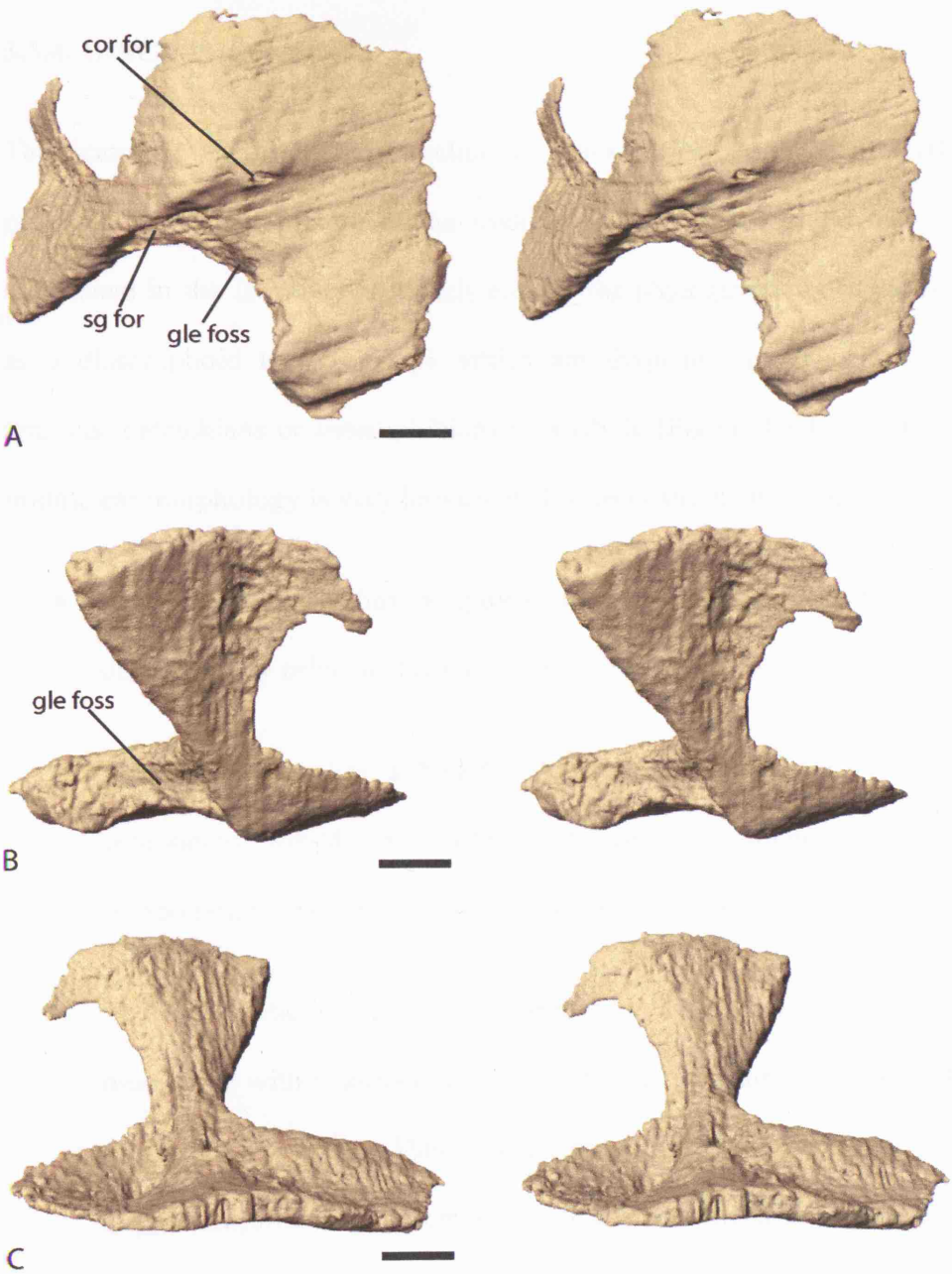

Figure 3.5.3—27 *Micropholis* specimen BMNH R.510. Stereo pairs of the right scapulocoracoid. A, ventral view. B, right lateral view. C, medial view. Scale bars = 2mm.

3.5.4. DISCUSSION

The scanning and 3D reconstruction of *Micropholis* specimen BMNH R.510 has provided a detailed picture of the middle ear of a dissorophoid temnospondyl. As mentioned in the introduction to this chapter the phylogenetic position of *Micropholis* as a dissorophoid temnospondyl, which are frequently implicated in the origin of anurans, batrachians or lissamphibians as a whole (Figure 3.5.4—1 A), means that its middle ear morphology is very important. The reconstruction illustrates:

- That *Micropholis* has a typical rod like temnospondyl stapes which is dorsolaterally orientated (Figure 3.5.4—1 B).

- That the stapes has a bipartite footplate (Figure 3.5.4—1 C). The ventral component would have articulated with the braincase while the dorsal component would have contacted the inner ear space.

- That each otic notch is very large and would have supported a tympanic membrane with a surface area vastly bigger than that of the stapedial footplate (Figure 3.5.4—1 D). This allowed me to conclude that *Micropholis* had the largest amplification potential of all the specimens examined as part of this thesis.

- That each ossified distal end of the stapes points towards but in no way reaches the otic notch (Figure 3.5.4—1 E). It is envisaged that large cartilaginous extrastapes were present which would have bridged the gaps between the tympanic membranes and the ossified distal end of the stapes.

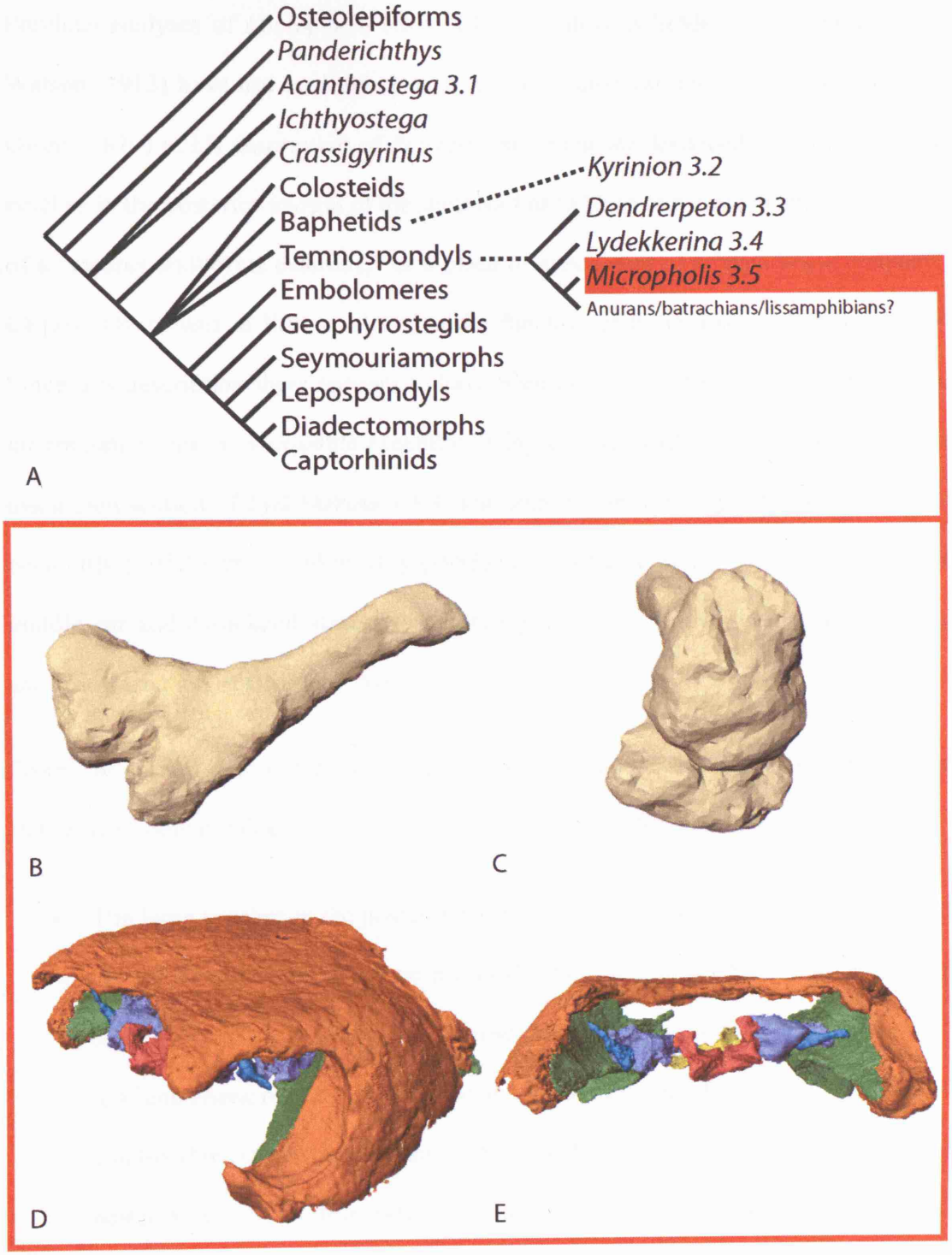

Figure 3.5.4—1 Summary *Micropholis* figure - specimen BMNH R.510. A, basic phylogenetic consensus created from the early tetrapod phylogenies of Ruta et al. (2003) and Laurin & Reisz (1997) with temnospondyl detail from Ruta et al. (2003) and Yates & Warren (2000). B, posterior view of right stapes - see figure 3.5.3—16. C, footplate of right stapes - see figure 3.5.3—16. D, posterolateral view of skull showing otic notch - see figure 3.5.3—6. E, posterior view of skull showing otic notches and stapes - see figure 3.5.3—5. For scale bars see referred to figures.

Previous analyses of *Micropholis* (Boy, 1985; Broili & Schröder, 1937; Owen, 1876; Watson, 1913) have not considered in detail the middle ear and associated structures. Owen (1876) in his description of *Petrophryne granulata* described each of the paired notches in the posterior margin of the skull roof as 'a large semicircular space indicative of a "meatus auditorius externus," or a place of attachment of a "membrane tympani". Clearly, Owen was in little doubt as to the function of these notches in *Micropholis*. Since this description there appears to have been no disagreement with this functional interpretation, the only possible exception being of Laurin (2005) as mentioned in the discussion section of *Lydekkerina* 3.4.4. The stapedial morphology of *Micropholis* had been only partially described by Boy (1985) (see his figure 4A). No other details of the middle ear and associated structures of *Micropholis* were known before the scanning and reconstruction of BMNH R.510.

From the cranial reconstruction presented in this chapter, that the following can be stated with some confidence regarding the middle ear of *Micropholis*:

- The large notches in the posterolateral margin of the skull roof (Figure 3.5.3—5 and 6) should be termed 'otic notches'. The otic notches have smooth internal surfaces which lack the slightly rugose ornament present on the rest of the skull roof and cheek region. The anterior and ventral margin of the notch is formed by a noticeable ridge which separates the smooth area from the cheek region. At the posterior extent of this ridge the quadrate forms an obvious curved dorsal projection. The ridge and the dorsal projection, which it is envisaged to have continued in cartilage and contacted the tabular, would have supported a relatively large and rounded tympanic membrane.

- The stapes of *Micropholis* are small and rod like with a bi-partite footplate (Figure 3.5.3—15 and 16). They thus conform to the expected stapedial morphology of temnospondyls as, also, seen in *Dendrerpeton* (Robinson et al., 2005) and *Lydekkerina*. The dorsal component of the footplate would have contacted the perilymphatic space of the inner ear while the ventral component would have articulated with the braincase, although, this relationship cannot be verified from the scanning and reconstruction of BMNH R.510 because the braincase is not complete. It seems clear that the stapes of *Micropholis* is very similar to that of *Doleserpeton* (Bolt & Lombard, 1985; Lombard & Bolt, 1988) although the dorsal and ventral stapedial footplate components of *Micropholis* are definitely more separate than those of *Doleserpeton* (Bolt & Lombard, 1985; Lombard & Bolt, 1988).

- The small size of the stapes combined with the slice thickness and noise in the scans means it was not possible to verify the presence of muscle scars and/or extra processes on the stapes of *Micropholis* (Figure 3.5.3—15 and 16). It is suggested that a rescanning of *Micropholis* could be undertaken with the stapes perpendicular to the slice orientation to increase the stapedial detail gained. However, a posterior process/scar is likely to be present on the stapes. A posterior notch in the footplate margin is also expected to be present, as also seen in *Dendrerpeton* (Robinson et al., 2005), *Lydekkerina*, *Doleserpeton* (Bolt & Lombard, 1985; Lombard & Bolt, 1988) and other temnospondyls. A detailed scan series with slices perpendicular to the axis of the stapes could be used in the future to elucidate the presence of such features.

- The relationship of both the stapes to the otic notches in BMNH R.510 (Figure 3.5.3—5 C & D) demonstrates that there must have been a large cartilaginous extension coupling the distal end of the stapes to the presumed tympanic membrane. This could be, at least, functionally equivalent to the pars externa or extrastapes of extant anurans. The envisaged size of this cartilaginous extension relative to the size of the stapes is far larger than that proposed in either *Dendrerpeton* (Robinson et al., 2005) or *Lydekkerina.*

- The expected middle ear cavities would have run from behind the basipterygoid articulations to the smooth region of the otic notches. The excavatio tympanica of the palatoquadrate complexes (Figure 3.5.3—7, 8, 9 and 10) form the anterior and ventrolateral extent of the space available for the middle ear cavity.

- Unfortunately it has not been possible to model the fenestra ovalis region of the braincase of *Micropholis* because this region may not have been ossified, preserved or visualised in the scan series. Due to the lack of data from this region of *Micropholis* and the unossified nature of the operculum of modern anurans it has not been possible to investigate the presence or absence of an opercular system in *Micropholis.*

The bullet points above show that *Micropholis* had a stapes coupled to a tympanic membrane via a large cartilaginous extension. It would seem likely that the common ancestor of *Micropholis, Lydekkerina* and *Dendrerpeton* would have possessed such a system and that any differences observed are simply later adaptations.

One notable area of difference between the ear anatomy of *Micropholis* and *Lydekkerina* is in the ratio of the area of the tympanic membrane to the area of stapedial

contact with the inner ear. This will be investigated further within the overall discussion and conclusions chapter, 4.

4. OVERALL DISCUSSION AND CONCLUSIONS

In the introductory chapter numerous questions where raised regarding the origin and evolution of the tetrapod middle ear, with particular emphasis on the specialisations observed in extant amphibians. The combination of HRXCT scanning and advanced 3D reconstruction techniques has allowed a thorough investigation into these questions. The techniques have allowed the detailed re-examination and subsequent high resolution modelling of specimens which have been described previously, without damaging them in any way (Figure 4.1.1—1). The techniques have proved especially adept at visualising the internal cranial anatomy, which had proved problematic to examine with traditional methods. Five species of early tetrapod have been studied as part of this thesis utilising these techniques. As mentioned within the introduction the species where chosen for their suitability to help address the numerous questions raised in the introduction.

The questions framed during the introduction fall into two categories, neontological and palaeontological.

4.1.1. NEONTOLOGICAL QUESTIONS:

- When did a tympanic membrane coupled to a stapes first evolve in tetrapods and in what group was this?

It is believed that the investigations of *Dendrerpeton* (Robinson et al., 2005), *Lydekkerina* and *Micropholis* demonstrate that each of these particular temnospondyls possessed tympanic membranes. It appears to be unlikely that each of these species evolved such a system independently (Figure 4.1.1—1). Therefore,

it seems parsimonious to conclude that their common ancestor would have possessed such a feature and that it occurred very close to the phylogenetic base of temnospondyls. This is in agreement with most previous literature discussing the hearing abilities of temnospondyls, although, Laurin (2005) and Laurin & Soler-Gijon (2006) state 'the widely held idea that many temnospondyls possessed a tympanum is unlikely'. Laurin & Soler-Gijon (2006) argue that the stapes found in most temnospondyls are two massive to have been coupled to a tympanic membrane. They also propose that the rounded temporal notches observed in small to medium sized temnospondyls are not suggestive of tympanic membrane supporting structures but are rather only the result of the relative small skull size of these early tetrapods. The author however believes that the stapedial and temporal notch regions of the temnospondyls described as part of this thesis are highly suggestive of a tympanic ear. Furthermore one does not believe a highly gracile stapes, as seen for example in modern anurans, is necessary for the presence of a tympanic membrane in temnospondyls. Certainly the tympanic ears envisaged in *Dendrerpeton*, *Lydekkerina* and *Micropholis* would not have been of as high fidelity as those in extant Neobatrachia but they would have been functional nevertheless.

It certainly appears that temnospondyls would have been one of the first tetrapod groups to have evolved a tympanic membrane coupled to a stapes (Figure 4.1.1—1). If *Kyrinion* had a closed spiracle it may represent an earlier 'tympanum like' structure. However, as mentioned previously, within the discussion section of the *Kyrinion* results chapter 3.2.4, it is not possible to conclusively elucidate this character state in *Kyrinion*. It, therefore, appears prudent to conclude that temnospondyls were the first tetrapod group in which convincing proof for a tympanic membrane coupled to a stapes is observed, as was previously stated by

Clack (1992; 2002d) and Clack & Allin (2004). The author does not know of any evidence to suggest that an earlier tetrapod specimen would have had a tympanic ear.

- Did the common ancestor of anurans, urodeles and caecilians have a tympanic membrane coupled to a stapes?

Questions regarding the middle ear character states of the common ancestor of the anurans, urodeles and caecilians rest heavily on the monophyly of the lissamphibians and on how they are related to the various early tetrapod groups. Molecular phylogenetic studies, summarised in the introduction chapter, show that the extant amphibians form a monophyletic grouping with respect to amniotes. However, as mentioned by Laurin (2002), the acceptance of a monophyletic Lissamphibia does not preclude the possibility that the different extant amphibian orders are related to different early tetrapod groups as long as this grouping is also monophyletic with respect to amniotes. The phylogenies of Laurin & Reisz (1997) and Ruta et al. (2003a) agree on the fundamental intrarelationships of early tetrapods with the exception of the placement of Lissamphibia and Amniota. A dual origin of lissamphibians within the early tetrapods, with anurans and urodeles most related to temnospondyls and caecilians to lepospondyls (as suggested by Anderson (2001) and Carroll & Currie (1975)), does not fit with the current phylogenetic consensus of the early tetrapods and the molecular evidence of lissamphibian monophyly. Such a dual origin would cause the Lissamphibia to be a polyphyletic assemblage and for caecilians to be more closely related to amniotes than to anurans and urodeles.

The phylogeny of Laurin & Reisz (1997) states that a monophyletic Lissamphibia had its origins within the lepospondyls. As mentioned within the introduction

lepospondyls, with the possible exception of *Adelospondylus watsoni*, do not possess temporal notches. There is very limited stapedial information for lepospondyls, although, it seems apparent that they were not rod like and were directed towards the quadrate rather than coupled to a tympanic membrane. Therefore, if lissamphibians evolved from lepospondyls then the common ancestor would not have possessed a tympanic membrane coupled to a stapes. With this scenario anurans would have independently evolved such a system. There do however appear to be numerous similarities between the middle ear region of microsaurs (Carroll et al., 1998; Carroll & Gaskill, 1978) (part of the lepospondyls), caecilians and especially urodeles. All three groups can be described as having stapes with button shaped footplates and short, broad rods. In all groups this short rod frequently contacts the palatoquadrate complex. Furthermore there is evidence to suggest that microsaurs could have possessed some kind of opercular apparatus (Carroll et al., 1998; Carroll & Gaskill, 1978)thus giving a character state which could link the middle ear of microsaurs with that of urodeles and anurans. The middle ear anatomy of caecilians and urodeles certainly is highly suggestive of a close phylogenetic link between them and microsaurs, however it should be noted that the anatomy in both extant groups could be a result of loss of a more advanced condition due to close association with the substrate of an aquatic lifestyle.

In contrast to Laurin & Reisz (1997) the phylogeny of Ruta et al. (2003) places the origin of the monophyletic Lissamphibia within the temnospondyls. As mentioned above it is believed that there is clear and unequivocal evidence that temnospondyls possessed tympanic membranes coupled to stapes. Thus, if the Lissamphibia evolved from temnospondyls then their common ancestor would have possessed tympanic membranes coupled to stapes as envisaged in *Dendrerpeton* (Robinson et

al., 2005), *Lydekkerina* and *Micropholis*. This would mean that there is evolutionary continuity between the middle ear of temnospondyls and that of extant anurans and, therefore, one fewer envisaged independent origins of an ear adapted to the perception of airborne sound than appears to be the case for the phylogeny of Laurin & Reisz (1997). Both urodeles and caecilians would have lost stapes coupled to tympanic membranes if a monophyletic Lissamphibia evolved from within the temnospondyls.

The numerous similarities between the middle ears of extant anurans and temnospondyls seems to demonstrate that they have evolutionary continuity. Furthermore, taking into account the molecular studies showing lissamphibian monophyly and the current early tetrapod phylogenies, it seems likely that urodeles and caecilians also evolved from temnospondyls and must have lost tympanic membranes. However, this rests fundamentally on the phylogeny of early tetrapods which has changed many times previously and cannot be accepted without caution. Furthermore, in many respects the middle ear regions of caecilians and especially urodeles share many character states with the microsaurs middle ear (Carroll et al., 1998; Carroll & Gaskill, 1978).

- Is the tympanic membrane observed in anurans in any way homologous to that seen in other tetrapod groups?

Based on the detailed study of *Dendrerpeton* (Robinson et al., 2005), *Lydekkerina* and *Micropholis* it is believed that the tympanic membrane of anurans is homologous to those envisaged to have been present in temnospondyls. As mentioned above it is unclear whether *Kyrinion* possessed a closed or open spiracle. If a closed spiracle closely associated with a stapes was present in *Kyrinion* then

there may be evolutionary continuity between it and the tympanic membrane of temnospondyls and hence anurans. This, however, clearly depends on the phylogenetic position of baphetids relative to temnospondyls.

As will be discussed further below it is not believed that the tympanic membrane observed in anurans is in any way homologous to those of amniotes.

- When is the first evidence of a muscle connecting the stapes to the shoulder girdle?

As mentioned within the introduction, anurans are unique amongst extant tetrapods in the presence of a muscular connection between the posterior surface of the stapes and the shoulder girdle. This muscular connection has been termed the columellaris muscle (Wever, 1979; Wever, 1985) or alternatively a branch of the levator scapulae superior (Hetherington, 1987; Hetherington & Lombard, 1983). There is no evidence to suggest that either extant urodeles or caecilians have such a muscular connection.

The scanning and 3D reconstruction of *Dendrerpeton* (Robinson et al., 2005) provides clear evidence for a scar on the stapes. As was seen in results chapter 3.3 it was possible to reorient the stapes of *Dendrerpeton* proving that the scar was on the posterior surface of the stapes. It is postulated that this scar could represent a columellaris muscle scar. This would then represent osteological evidence for a soft-tissue characteristic which would directly link temnospondyls and extant anurans. Furthermore, re-examination of *Lydekkerina* specimen UMZC T.206 has revealed evidence for a homologous scar or process on its stapes. If these interpretations are correct they will represent the earliest evidence of a muscle connecting the stapes to

the shoulder girdle and, also, support the close relationship between anurans and temnospondyls.

- When did the opercular apparatus evolve in tetrapods and in what group was this?

Anurans and urodeles, as mentioned within the introduction, possess an additional element with the fenestra ovalis, the opercular apparatus. This is rarely ossified and consists of a cartilaginous disc which sits in the fenestra ovalis behind the stapedial footplate, if one is present. It is in no way homologous to the operculum in the cheek region of fish. Caecilians do not appear to possess a secondary element within the fenestra ovalis, with the possible exception of *Ichthyophis glutinosus* (Peter, 1898). Due to the unossified nature of the opercular apparatus, fossilised evidence for its presence can be only inferred by looking for the space in which it would have sat within the fenestra ovalis or evidence for opercular contact on the stapes. Inferences based on enlarged fenestra ovalis have to be made with caution because this region of the braincase is frequently poorly preserved and/or ossified.

It seems clear that the examination of *Dendrerpeton* (Robinson et al., 2005) and *Lydekkerina* has provided numerous strands of evidence which indicate the plausible presence of an additional element in the fenestra ovalis, posterior to the stapedial footplate. There is a clearly defined unossified space behind the stapes in *Lydekkerina*, and this was probably also the case in *Dendrerpeton*. Furthermore, there is evidence on the posterior margin of the stapes of both *Dendrerpeton* (Robinson et al., 2005) and *Lydekkerina* which suggest a contact with an opercular element. If these interpretations are correct then it would appear that temnospondyls,

such as the phylogenetically basal *Dendrerpeton* and the stereospondyls *Lydekkerina*, possessed opercular apparatuses in each fenestra ovalis.

Descriptions of microsaurs (Carroll et al., 1998; Carroll & Gaskill, 1978) provide some evidence to suggest that an opercular apparatus may also have been present in microsaurs. Most microsaurs otic regions have an unossified region posteroventral to the fenestra ovalis (such as *Batropetes fritschia*, *Pantylus cordatus*, *Pelodosotis elongatum* and *Cardiocephalus sternbergi*) (Carroll et al., 1998; Carroll & Gaskill, 1978). Furthermore there is an additional ossified element within this region in *Pantylus cordatus* (and possibly other microsaurs such as *Micraroter erythrogeios*, *Rhynchonkos stovalli* and *Euryodus primus*) (Carroll et al., 1998; Carroll & Gaskill, 1978). This would be the earliest known occurrence of a system which is now only seen in extant anurans and urodeles.

From the evidence presented within the thesis and that already published it appears that there is possible evidence for the presence of opercular systems in temnospondyls and microsaurs. The possibility that they are independent origins of similar structures or whether they may share a common origin. This clearly needs further investigation as it raises interesting questions regarding the possible widespread presence of an opercular system in early tetrapods.

- Did the common ancestor of batrachians, lissamphibians or all tetrapods possess an opercular apparatus?

As was the case with questions regarding the presence or absence of a tympanic membrane coupled to a stapes in the common ancestor of lissamphibians, this issue depends on their phylogenetic position relative to the different early tetrapod groups. As was explained above the author believes that, from the molecular studies which

support the monophyly of the Lissamphibia and the current early tetrapod phylogeny, all extant amphibians arose from within temnospondyls. This evolutionary scenario would, therefore, indicate that the common ancestor of the lissamphibians possessed an opercular apparatus. Of course this highly depends on the interpretation of the evidence described above.

- When is the first evidence of a muscle connecting the opercular apparatus to the shoulder girdle?

It has not been possible to find any direct evidence for a muscular connection between the opercular apparatus and the shoulder girdle in spite of the detailed scanning and reconstruction of the species described. However, any evidence supporting an opercular apparatus in temnospondyls can probably be taken as evidence for such a muscular connection. As far as the author is aware all opercular apparatuses present in extant amphibians have muscular connectivity with the shoulder girdle (Monath, 1965; Wever, 1979; Wever, 1985).

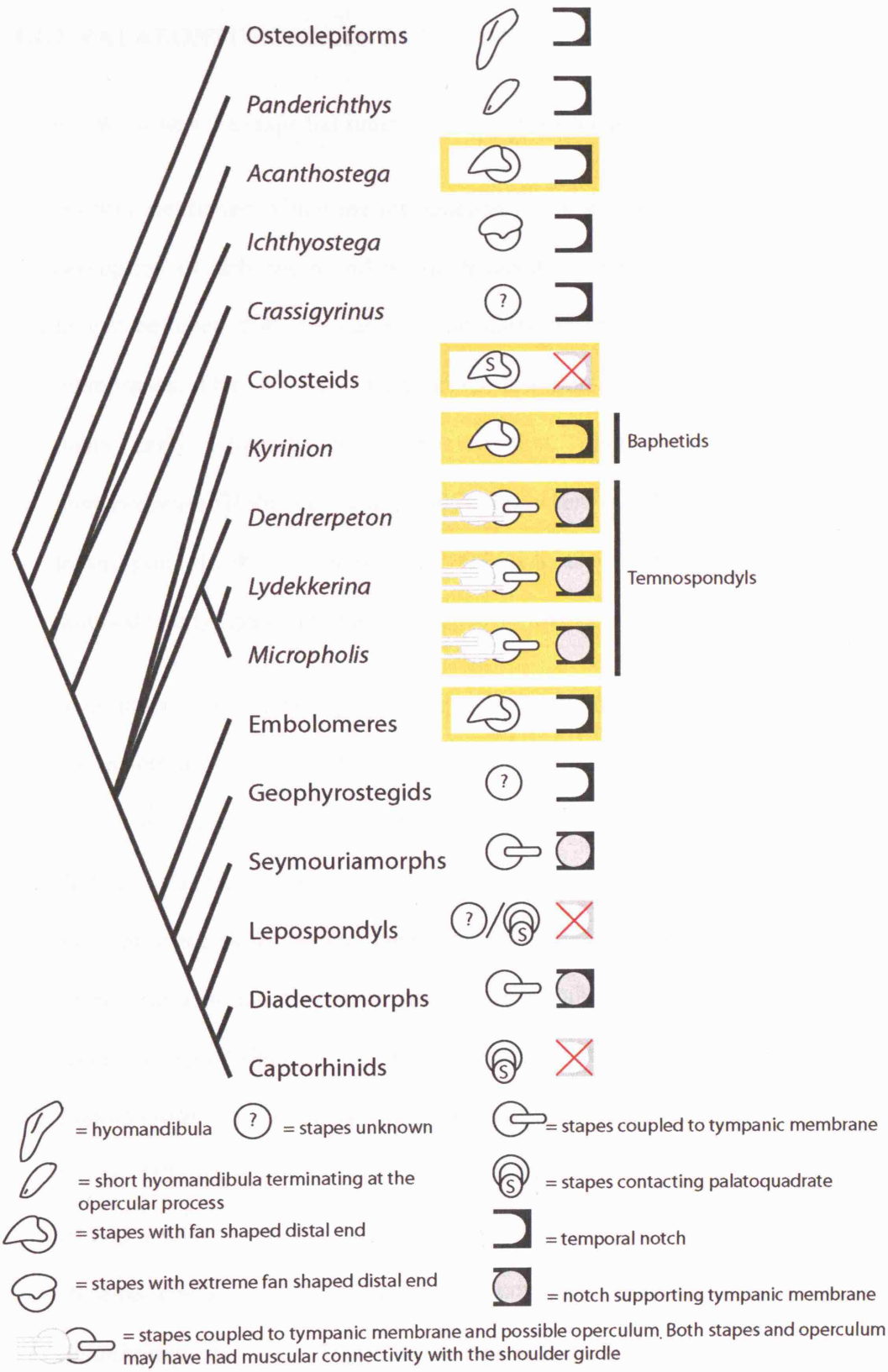

Figure 4.1.1—1 Consensus phylogeny of early tetrapods (see introduction chapter for details) showing middle ear character states. Boxed specimens have had their middle ear function revised within this thesis. Highlighted specimens have had their middle ears morphology and function extensively characterised within this thesis.

4.1.2. PALAEONTOLOGICAL QUESTIONS:

- What was the stapedial function before it was coupled to a tympanic membrane?

As was mentioned within the introduction multiple origins of an ear adapted to the perception of airborne sound within tetrapods is now generally accepted. It is no longer believed that the stapes of all early tetrapods were coupled to tympanic membranes. This of course leads to the questions regarding stapedial function in many early tetrapods. It is believed that, from the evidence observed in *Dendrerpeton* (Robinson et al., 2005), *Lydekkerina*, *Micropholis* and many other temnospondyls, that it is most parsimonious to assume that the presence of a stapes coupled to a tympanic membrane is the primitive condition for temnospondyls.

In contrast to temnospondyls the author believes that the stapedial function of stem-group tetrapods is far more contentious, because their stapedial morphologies are more varied and the middle ear space less well defined. Carroll (1980) suggested that the stapes, or hyomandibula, of *Greererpeton* functioned as a supportive element in the skull, bracing the braincase against the palatoquadrate complexes. A supportive function for the stapes of stem-group tetrapods appears to have been widely accepted since its original proposal. Although other early tetrapods, such as *Pholiderpeton* and *Acanthostega*, share similar stapedial morphology to that which Carroll (1980) used to suggest a supportive function the author is reluctant to accept this as a widespread function. The author believes there is no direct evidence for stapedial contact with the palatoquadrate complexes in either of the examinations of *Acanthostega* and *Pholiderpeton*. Additionally, in neither species does there appear to be any conclusive proof for the need for additional support of the braincases. It is believed that a supportive strut would not be placed within a fenestra ovalis, in close

association with the inner ear region because this would place a structural element in intimate association with a delicate and highly sensitive region. However it should be noted that this does appear to be the case in early amniotes (Clack, 2002c; Clack, 2002d). Strong forces acting on an envisaged stapedial strut would seem to be passed direct to the inner ear rather than bracing the braincase. Further analysis of the forces acting through the stapes in both early tetrapods and early amniotes would help to elucidate this important aspect of stapedial function.

A detailed view of an additional, probable, stem-group tetrapod middle ear has been visualised with the scanning and 3D reconstruction of *Kyrinion*. The stapes does not appear to have had a supportive function; there is no evidence for stapedial contact with the palatoquadrate complex. Furthermore, as was described in detail within the *Kyrinion* discussion chapter 3.2.4, the stapes, which is directed dorsolaterally towards the temporal notch, sat above a spiracular space. I believe that the stapes of *Kyrinion* had a primitive hearing function. It is also possible to directly compare the stapedial morphology of *Kyrinion* to that of *Pholiderpeton*, *Greererpeton* and *Acanthostega*. All have a robust footplate which narrows somewhat to a waisted region before expanding to form a more laminar distal end. The similarity of the stapes of *Kyrinion* to those of the aforementioned stem-group tetrapods raises the interesting possibility that the stapedial support hypothesis could in the future be supplanted by a basic hearing function, although clearly further research in this area is needed.

Clack (1992) also proposed that the stapes of early tetrapods, such *Acanthostega* and *Pholiderpeton*, may have functioned as part of their ventilation system. The author believes that the evidence gained from the study of *Kyrinion* does not in anyway

discount this functional interpretation. It is not envisaged that the stapes of *Kyrinion*, or even those of *Acanthostega* or *Pholiderpeton*, would have contacted the palatoquadrate complexes in anyway but their intimate association of the presumed spiracular space could well have conferred an important role in regulating the inhalation/exhalation through the spiracle. The precise nature of this function is, however, not known at this time and clearly further work is needed.

- How did a stapes coupled to a tympanic membrane evolve?

The middle ear region of *Kyrinion* is one of the most detailed models we have for an early tetrapod. However, because soft-tissue is not preserved, it has not proved possible to ascertain whether it would have had an open or closed spiracle. Notwithstanding this uncertainty I believe that *Kyrinion* demonstrates a functional transition to the tympanic membrane coupled to a rod like stapes of temnospondyls. In the discussion section of the *Kyrinion* chapter 3.2.4 it can be seen that the stapes can function as a type II lever system (Figure 3.2.4—2) as also present in temnospondyls and extant anurans. The stapes sits above and behind, but is in close association with, the spiracular or middle ear space. I believe that this condition could have been quite widespread in stem-group tetrapods. Thus, a closing of the spiracle in *Kyrinion* or *Kyrinion*-like tetrapod would create a very crude airborne hearing system with a robust but rather lamina stapes coupled to a primitive tympanum like structure and in close association with an air filled middle ear space. Elaboration of this hypothesised condition, with a more gracile stapes becoming enveloped by the middle ear space and a more developed tympanic membrane, would clearly produce a temnospondyl-like condition which I have described in *Dendrerpeton* (Robinson et al., 2005), *Lydekkerina* and *Micropholis*. The proposed

anatomy of the middle ear region of *Kyrinion* actually has many similarities to that envisaged for *Ichthyostega* (Clack et al., 2003). Both are suspected of having a stapes with a laminar distal end which sit above an air filled spiracle. In both cases it is envisaged that this positioning of the stapes allows vibrations to pass from this air filled space towards the inner ear via the stapes. In a similar manner to *Kyrinion* it might be expected that the stapes of *Ichthyostega* acted as a type II lever system. It should however be noted that the middle ear anatomy of *Ichthyostega* appears to be an extreme specialisation of a system similar to that seen in *Kyrinion* and it has not been observed in any other early tetrapod to date.

- How did the proposed ear, adapted to the perception of airborne sound, change once already evolved? Can an increase in amplification potential be detected in phylogenetically more advanced early tetrapods?

The investigation of *Dendrerpeton* (Robinson et al., 2005), *Lydekkerina* and *Micropholis* demonstrates to me that many temnospondyls possess ears adapted to the perception of airborne sound. It has been possible to accurately quantify many aspects of the middle ears of *Kyrinion*, *Dendrerpeton*, *Lydekkerina* and *Micropholis* (Figure 4.1.2—1). This detailed quantification was only made possible by the scanning and 3D reconstruction techniques utilised as part of this thesis. Even without quantification it is clear that, in comparison to *Dendrerpeton* (Robinson et al., 2005), *Micropholis* and *Lydekkerina* have a far more defined middle ear space with the crista obliqua forming an ossified posterior wall to the space. This would have allowed the middle ear airspace to be more isolated from external vibrations other than those coming from the tympanic membrane, via the stapes. Another area of change involved the increased gracile nature of both *Micropholis's* and

Lydekkerina's stapes compared to that of *Dendrerpeton* (Robinson et al., 2005). This gracile nature in *Lydekkerina* is manifested as a relatively long and thin stapes which reaches very close towards the expected tympanic membrane. In contrast it appears that *Micropholis* has achieved a gracile stapes by means of a large cartilaginous extension or extrastapes. The distal end of the ossified portion points towards, but in no way reaches, the envisaged tympanic membrane. A more gracile stapes in both *Micropholis* and *Lydekkerina* would have allowed an improved transmission of vibrations over a broader frequency range.

Another notable area of difference between the ear anatomy of *Micropholis* and *Lydekkerina* is in the ratio of the area of the tympanic membrane to the area of stapedial contact with the inner ear. This area ratio corresponds to one aspect of the amplification potential of the middle ear, the other being the type II lever system present in *Kyrinion* (Figure 3.2.4—2) and all temnospondyls described within this thesis. The area of a round tympanic membrane can be estimated from the size of the otic notch. The area of stapedial contact with the perilymphatic space of the inner ear can be estimated from the area of the dorsal component of the stapedial footplate. The reconstruction of *Lydekkerina* specimen UMZC T.242 allows me to estimate that the round tympanic membrane would have had an area of 30mm^2 (from a radius of 3.1mm) whilst the dorsal component of the right stapedial footplate is estimated to have had an area of 8.0mm^2 (Figure 4.1.2—1). From the reconstruction of *Micropholis* specimen BMNH R.510 a round tympanic membrane is estimated to have had an area of 58mm^2 (from a radius of 4.3mm) whilst the dorsal component of the right stapedial footplate is estimated to have an area of 2.5mm^2 (Figure 4.1.2—1). Thus the ratio of tympanic membrane area to stapedial contact with the inner ear area is approximately 4:1 for *Lydekkerina* and 23:1 for

Micropholis (Figure 4.1.2—1). Due to area reduction there is clearly a large difference between the amplification potential of the middle ear regions of *Lydekkerina* and *Micropholis*. From this investigation it is clear that *Micropholis* had a far larger area amplification than *Lydekkerina*. However no phylogenetic inferences can be made from this because it is not possible to identify direct ancestors within the fossil record.

- Did early tetrapods have a spiracle and did this get transformed into a middle ear space? If not, what was the function of the paired notches in early tetrapods?

As was reviewed within the discussion section of the *Kyrinion* chapter 3.2.4 I believe that the possession of an open spiracle is the ancestral condition for tetrapods. Although both dipnoans and coelacanths, the phylogenetically closest extant fish groups to tetrapods, have closed spiracles it seems likely that both *Eusthenopteron* and *Panderichthys* had open spiracles and the temporal notches of many early tetrapods may have supported such a structure.

The envisaged position of an open spiracle in *Eusthenopteron*, *Panderichthys* and stem-group tetrapods is in the same place as the envisaged middle ear space of temnospondyls. In all cases it is presumed that the space is connected to the buccal cavity behind the basipterygoid articulation and then passes dorsolaterally between the palatoquadrate and the braincase. Both spaces are believed to end in temporal/otic notches. I believe that there is thus solid evidence to support the homology between the spiracular space and the proposed middle ear space of temnospondyls. This may also mean that the middle ear space of anurans is also homologous to the spiracular space.

- Is the proposed spiracular opening in early tetrapods in anyway homologous to the tympanic membrane? If so, is this in all tetrapods?

As mentioned above I believe that the middle ear space of temnospondyls to be homologous to the spiracular space envisaged to be present in stem-group tetrapods. This, of course, raises questions regarding the initial closing of the spiracular space, presumably in stem-group tetrapods, and whether this is in anyway homologous to the tympanic membrane. As mentioned in the discussion section of the *Kyrinion* chapter 3.2.4, developmental work seems to preclude the possibility that the tympanic membrane of amniotes is derived from a simple closure of the spiracle. However, as far as I am aware there is no such developmental data that precludes the possibility that the tympanic membrane of anurans is derived from simply a closure of the spiracular space. Certainly the osteological evidence seen in *Kyrinion* and the temnospondyls scanned and 3D reconstructed appear to support this evolutionary scenario. So it is possible to homologise the tympanic membranes of temnospondyls (and possibly anurans) to the spiracular openings in early tetrapods, but, this does not appear to be the case with amniotes.

- How did the tetrapod otic region of the braincase and particularly the fenestra ovalis evolve?

I believe the braincases of *Acanthostega*, *Kyrinion*, *Dendrerpeton* (Robinson et al., 2005), *Lydekkerina* and *Micropholis*, along with previously published literature, demonstrate the conservative nature of braincase's otic region in early tetrapods. In all early tetrapods the otic region is of basically the same form, consisting of paired otic capsules each containing a fenestra ovalis. This conservatism is in sharp contrast to the numerous changes observed in the adjacent middle ear space and

stapes. The investigation of *Acanthostega* shows that this phylogenetically basal stem-group tetrapod had a morphology quite similar to that of *Kyrinion* and the more derived temnospondyls. It now seems clear that the anterior margin of *Acanthostega's* fenestra ovalis is produced by the otic capsules, and possibly basisphenoid, without a major contribution by the basioccipital. It has also clear that other features, such as post temporal foramen, are widely observed in early tetrapod otic regions.

One notable feature is the apparent lack of separate prootic and opisthotic components in all the early tetrapods examined with the possible exception of *Micropholis*. It is, however, unclear whether the separate ossifications observed in *Micropholis* should be termed prootic and opisthotic as they appear to be distantly related to those of amniotes. It seems that separate anterior and posterior ossifications of the otic capsules evolved numerous times in tetrapod phylogeny.

	Stapes Volume (mm^3)	Overall Stapes Surface Area (mm^2)	Ratio of Overall Surface Area to Volume	Stapes Length (mm)	Stapedial Footplate Area (mm^2)	Estimated Tympanic Membrane Area (mm^2)	Ratio of Tympanic Membrane to Footplate Area
Kyrinion	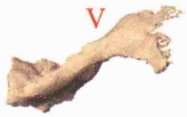 397mm^3	 727mm^2	 ~2:1	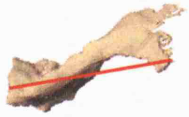 27.4mm	 31.5mm^2	N/A	N/A
Dendrerpeton	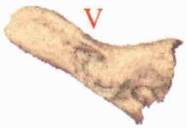 40.3mm^3	 127mm^2	 ~3:1	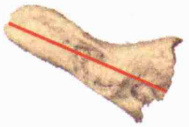 8.90mm	 8.55mm^2	N/A	N/A
Lydekkerina	 119mm^3	 228mm^2	 ~2:1	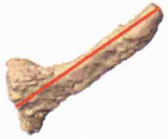 14.8mm	 8.01mm^2	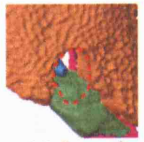 30.3mm^2	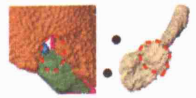 ~4:1
Micropholis	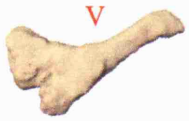 5.39mm^3	 24.3mm^2	 ~4.5:1	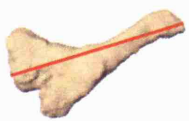 5.10mm	 2.52mm^2	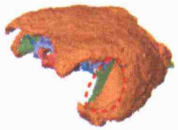 58.8mm^2	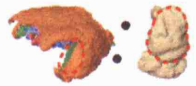 ~23:1

Figure 4.1.2—1 Table summarising the middle ear dimensions of *Kyrinion*, *Dendrerpeton* (BMNH R.436), *Lydekkerina* (UMZC T.242) and *Micropholis* (BMNH R.510). Volumes and surface areas calculated in Mimics and Rhino3D. Tympanic membrane estimates were only possible in *Lydekkerina* and *Micropholis*.

4.1.3. CONCLUSIONS

From the evidence presented in the results chapters 3.1-3.5, and summarised above, I believe that it is possible to illuminate the evolutionary history behind the middle ear region of tetrapods. This information can be combined with other published sources in a general overview of the sequence of character state changes, both osteological and soft tissue, in the evolution of the middle ear and associated structures in early tetrapods.

The re-described material of *Panderichthys* (Brazeau & Ahlberg, 2006) confirms that it is highly likely that the ancestral condition for tetrapods is the possession of paired open spiracles running from the buccal cavity to the back of the head. *Panderichthys* does not appear to have had any adaptations for the perception of airborne sounds. It is apparent that *Panderichthys* did not have fenestrae ovales and therefore its hyomandibula was not in contact with the inner ear space. However, the ossified component of the hyomandibula has been reduced compared to those seen in *Eusthenopteron.* Its ossified distal end terminates at the opercular process rather than continuing ventrally towards the quadrate and contacting the palatoquadrate complex.

In contrast to *Panderichthys* all stem-group tetrapods (using Ruta et al. (2003) as a basis for this term) are believed to have possessed fenestrae ovales and a stapes whose footplates sat within. There must have been an evolutionary advantage in reorganising the otic region and allowing intimate contact between each stapes and the inner ear. Certainly, this would have permitted vibrations to pass easily from the stapes to the inner ear.

I believe that a spiracular space was present in stem-group tetrapods, although, there is no direct soft-tissue evidence. As I mentioned previously it is not possible to determine

whether this space would have been open or closed. It is plausible that it would have been open in phylogenetically basal stem-group tetrapods, such as *Acanthostega*, but closed in the more derived *Kyrinion*. In both case the stapes would have been in close association with this space but probably not fully enveloped by it. From *Kyrinion*, probably the best known middle ear region of any stem-group tetrapod, it appears that the stapes was positioned posterodorsal to this space.

The stapes of stem-group tetrapods, with the exception of *Ichthyostega*, can be generalised as shorter, broader and less strut like than the hyomandibula of osteolepiform fish, such as *Eusthenopteron*. As I mentioned previously, it has been proposed that this stapedial morphology could indicate a supportive function, with each bracing the braincase against the palatoquadrate complexes (Carroll, 1980). However, I do not believe this to be the stapedial function of *Kyrinion* or most other stem-group tetrapods. I see no evidence for stapedial contact with the palatoquadrate complexes in any of the examinations of *Acanthostega*, *Kyrinion* and *Pholiderpeton*. In addition, although it seems clear that the skull of early tetrapods lacked autostyly (Clack, 1992) the authors personal opinion is that there is little conclusive evidence to suggest that a supportive strut between the braincase and the palatoquadrate complexes would have given useful additional support. Any poorly developed struts linking the inner ears with the palatoquadrate complexes, would probably havebeen of rather limited utility. The only stem-group tetrapod which may have had a supportive stapes is *Greererpeton*. It was not possible to independently inspect any *Greererpeton* specimen to check for evidence of stapedial contact with the palatoquadrate complexes, clearly this is an area for future examination. I also suggest that it would be prudent to investigate the functionality of a supportive stapes within the cranium of *Greererpeton* using CT scanning, 3D reconstruction and finite element analysis (FEA).

I believe that the stapes of *Kyrinion*, and probably most other stem-group tetrapods, was closely associated with both the inner ear and a spiracular space. It seems likely that the stapes would have had a primitive hearing function and acted as a type II lever system (Figure 3.2.4—2). This could have been its primary function although it may also have been involved in regulating the spiracular space in some unknown manner, meaning that it would have been involved in the ventilation system of the animals as proposed by Clack (1992).

Based on my investigations of *Dendrerpeton* (Robinson et al., 2005), *Lydekkerina* and *Micropholis* along with previously published literature I propose that the ancestral condition for temnospondyls is the presence of stapes coupled to tympanic membranes. I envisage that this condition would have evolved gradually from a stapes, not dissimilar to that of *Kyrinion*, coupled to a closed spiracle. It seems that the temnospondyl middle ear bears numerous possible soft-tissue synapomorphies with extant anurans, including evidence for an opercular apparatus and muscular connections to the shoulder girdle.

Future research will concentrate on relating the morphology and functional interpretations described within this thesis to the basal amniote middle ear condition. I have found no evidence to support a primitive connection between the stapes and the palatoquadrate (Figure 4.1.1—1). Therefore, it appears that the condition observed in proposed early amniotes, such as captorhinids (Figure 4.1.1—1), whereby the stapes connects the braincase to the palatoquadrate complex, is a derived, rather than retained primitive, condition. In extant tetrapods with such a condition it is generally assumed that this is due to a close association with the substrate, such as, with a burrowing lifestyle, however the functional and evolutionary history of the early amniote middle

ear is unclear. I believe this warrants further investigation, using CT scanning and 3D reconstruction as employed with *Acanthostega*, *Kyrinion*, *Dendrerpeton* (Robinson et al., 2005), *Lydekkerina* and *Micropholis*. The use of CT scanning and 3D reconstruction will allow the detailed investigation of the internal cranial anatomy of early amniotes without damaging the specimens in any way. The models produced from such a technique, as clearly demonstrated within this thesis, will allow unparalleled visualisation of all aspects of the middle ear region preserved within the specimen. Such visualisation will permit the detailed mapping of middle ear character states, including soft-tissue anatomy, onto the early amniote phylogeny as is now becoming possible in early tetrapods.

5. ACKNOWLEDGEMENTS

The research contained within this thesis could not have been achieved without my supervisors, Dr. Georgy Koentges and Dr. Per Ahlberg and the funding provided by the Biotechnology and Biological Sciences Research Council (BBSRC).

I am grateful to both my supervisors for imparting in me a small part of their vast morphological knowledge. I would like to thank Georgy for his commitment to the project and for providing suggestions which improved the clarity and structure of this thesis. I would like to thank Per for providing endless enthusiasm and encouragement for all things palaeontological.

The project depended upon access to many important specimens. I would especially like to thank Dr. Jenny Clack for providing access to *Acanthostega*, *Kyrinion* and *Lydekkerina*. 3D reconstruction of these specimens relied on the excellent scanning provided by Dr. Richard Ketcham and Dr. Matthew Colbert at University of Texas at Austin. I am also grateful to Dr. Angela Milner for providing support throughout my time at the Natural History Museum, London.

I would finally like to thank my parents and friends for providing support and help whenever it was needed.

Random is great, ☺.

6. REFERENCES

Ahlberg PE, Clack JA, and Lukševičs E. 1996. Rapid braincase evolution between *Panderichthys* and the earliest tetrapods. *Nature* **381:** 61-64.

Ahlberg PE, and Milner AR. 1994. The origin and early diversification of tetrapods. *Nature* **368:** 507-514.

Anderson JS. 2001. The phylogenetic trunk: maximal inclusion of taxa with missing data in an analysis of the Lepospondyli (Vertebrata, Tetrapoda). *Systematic Biology* **50:** 170-193.

Anderson JS. 2002. Use of well-known names in phylogenetic nomenclature: a reply to Laurin. *Systematic Biology* **51:** 822-827.

Báez AM, and Basso NG. 1996. The earliest known frogs of the Jurassic of South America: review and cladistic appraisal of their relationships. *Münchner Geowissenschaftliche Abhandlungen, Reihe A. Geologie und Paläontologie* **30.**

Beaumont EH. 1977. Cranial morphology of the Loxommatidae (Amphibia: Labyrinthodontia). *Philosophical Transactions of the Royal Society of London. Series B* **280:** 29-101.

Beaumont EH, and Smithson TR. 1998. The cranial morphology and relationships of the aberrant Carboniferous amphibian *Spathicephalus mirus* Watson. *Zoological Journal of the Linnean Society, London* **122:** 187-209.

Berman DS, Henrici AC, Sumida SS, and Martens T. 2000. Redescription of *Seymouria sanjuanensis* (Seymouriamorpha) from the Lower Permian of Germany based on complete, mature specimens with a discussion on paleoecology of the Bromacker locality assemblage. *Journal of Vertebrate Paleontology* **20:** 253-268.

Berman DS, Reisz RR, and Eberth DA. 1987. *Seymouria sanjuanensis* (Amphibia, Batrachosauria) from the Lower Permian Cutler Formation of north-central New Mexico and the occurence of sexual dimorphism in that genus questioned. *Canadian Journal of Earth Sciences* **24:** 1769-1784.

Berman DS, and Sumida SS. 1990. A new species of *Limnoscelis* (Amphibia, Diadectomorpha) from the Late Pennsylvanian Sangre de Cristo formation of central Colorado. *Annals of Carnegie Museum* **59:** 303-341.

Bolt JR. 1969. Lissamphibian origins: possible protolissamphibian from the Lower Permian of Oklahoma. *Science* **166:** 888-891.

Bolt JR, and Lombard RE. 1985. Evolution of the amphibian tympanic ear and the origin of frogs. *Biological Journal of the Linnean Society, London* **24:** 83-99.

Boy JA. 1972. Die Branchiosaurier (Amphibia) des saarpfälzischen Rotliegenden (Perm, SW-Deutschland). *Abhandlungen des Hessischen Landesamtes für Bodenforschung* **65:** 1-137.

Boy JA. 1985. *Micropholis* the last surviving dissorophoid (Amphibia, Temnospondyli); Lower Triassic. *Neues Jahrbuch für Geologie and Paläontologie, Monatshefte*: 29-45.

Boy JA, and Bandel K. 1973. *Bruktererpeton fiebigi* N. Gen. N. Sp. (Amphibia: Gephyrostegida) der erste tetrapode aus dem Rheinisch-Westfälischen Karbon (Namur B; W.-Deutschland). *Palaeontographica Abteilung A* **145:** 39-77.

Brazeau MD, and Ahlberg PE. 2006. Tetrapod-like middle ear architecture in a Devonian fish. *Nature* **439:** 318-321.

Broili F, and Schröder J. 1937. Beobachtungen an wirbeltieren der karrooformation. *Sitzungsberichte der bayerischen akademie der wissenschaften, mathematisch-naturwissenshaftliche abteilung*: 19-57.

Broom R. 1915. On the Triassic stegocephalians, *Brachyops*, *Bothriceps* and *Lydekkerina*, gen. nov. *Proceedings of the Zoological Society, London*: 363-368.

Broom R. 1930. Notes on some labyrinthodonts on the Transvaal Museum. *Annals of the Transvaal Museum* **14:** 1-10.

Bystrow AP, and Efremov JA. 1940. *Benthosuchus sushkini* - a labyrinthodont from the Eotriassic of Sharzhenga River. *Trudy Paleozoologicheskogo Instituta Akademia Nauk SSSR* **10:** 1-152.

Calder JH. 1998. The Carboniferous evolution of Nova Scotia. In: Blundell DJ and Scott AC, eds. *Lyell: the Past is the Key to the Present. Geological Society Special Publication No.143.* London: The Geological Society. 261-302.

Cannatella DC, and Trueb L. 1988. Evolution of pipoid frogs: intergeneric relationships of the aquatic frog family Pipidae (Anura). *Zoological Journal of the Linnean Society, London* **94:** 1-38.

Carroll RL. 1964. Early evolution of the dissorophid amphibians. *Bulletin of the Museum of Comparative Zoology, Harvard* **131:** 163-250.

Carroll RL. 1967. Labyrinthodonts from the Joggins Formation. *Journal of Paleontology* **41:** 111-142.

Carroll RL. 1969. A middle Pennsylvanian captorhinomorph, and the interrelationships of primitive reptiles. *Journal of Paleontology* **43:** 151-170.

Carroll RL. 1970. The ancestry of reptiles. *Philosophical Transactions of the Royal Society of London. Series B* **257:** 267-308.

Carroll RL. 1980. The hyomandibular as a supporting element in the skull of primitive tetrapods. In: Panchen AL, ed. *The Terrestrial Environment and the Origin of Land Vertebrates*. London: Academic Press. 293-317.

Carroll RL. 1988. *Vertebrate Paleontology & Evolution.* New York: W.H. Freeman & Company.

Carroll RL, Bossy KA, Milner AC, Andrews SM, and Wellstead CF. 1998. *Lepospondyli.* München: Verlag Dr. Friedrich Pfeil.

Carroll RL, and Currie PJ. 1975. Microsaurs as possible apodan ancestors. *Zoological Journal of the Linnean Society, London* **57:** 229-247.

Carroll RL, and Gaskill P. 1978. The order Microsauria. *Memoirs of the American Philosophical Society* **126:** 1-211.

Clack JA. 1983. The stapes of the Coal Measures embolomere *Pholiderpeton scutigerum* Huxley (Amphibian: Anthracosauria) and otic evolution in the early tetrapods. *Zoological Journal of the Linnean Society, London* **79:** 121-148.

Clack JA. 1987. *Pholiderpeton scutigerum* Huxley, an amphibian from the Yorkshire coal measures. *Philosophical Transactions of the Royal Society of London. Series B* **318:** 1-107.

Clack JA. 1988. New material of the early tetrapod *Acanthostega* from the Upper Devonian of east Greenland. *Palaeontology* **31:** 699-724.

Clack JA. 1989. Discovery of the earliest-known tetrapod stapes. *Nature* **342:** 425-427.

Clack JA. 1992. The stapes of *Acanthostega gunnari* and the role of the stapes in early tetrapods. In: Webster DB, Fay RR and Popper AN, eds. *The Evolutionary Biology of Hearing.* New York: Springer-Verlag.

Clack JA. 1994. *Acanthostega gunnari*, a Devonian tetrapod from Greenland; the snout, palate and ventral parts of the braincase, with a discussion of their significance. *Meddelelser om Grønland, Geoscience* **31:** 1-24.

Clack JA. 1997. The evolution of tetrapod ears and the fossil record. *Brain, Behavior and Evolution* **50:** 198-212.

Clack JA. 1998. The neurocranium of *Acanthostega gunnari* Jarvik and the evolution of the otic region in tetrapods. *Zoological Journal of the Linnean Society, London* **122:** 61-97.

Clack JA. 2001. *Eucritta melanolimnetes* from the Early Carboniferous of Scotland, a stem tetrapod showing a mosaic of characteristics. *Transactions of the Royal Society of Edinburgh: Earth Sciences* **92:** 75-95.

Clack JA. 2002a. The dermal skull roof of *Acanthostega gunnari*, an early tetrapod from the Late Devonian. *Transactions of the Royal Society of Edinburgh: Earth Sciences* **93:** 17-33.

Clack JA. 2002b. An early tetrapod from 'Romer's Gap'. *Nature* **418:** 72-76.

Clack JA. 2002c. *Gaining Ground, The Origin and Evolution of Tetrapods.* Bloomington: Indiana University Press.

Clack JA. 2002d. Patterns and processes in the early evolution of the tetrapod ear. *Journal of Neurobiology* **53:** 251-264.

Clack JA. 2003a. A new baphetid (stem tetrapod) from the Upper Carboniferous of Tyne and Wear, U.K., and the evolution of the tetrapod occiput. *Canadian Journal of Earth Sciences* **40:** 483-498.

Clack JA. 2003b. A revised reconstruction of the dermal skull roof of *Acanthostega gunnari*, an early tetrapod from the Late Devonian. *Transactions of the Royal Society of Edinburgh: Earth Sciences* **93:** 163-165.

Clack JA, Ahlberg PE, Finney SM, Dominguez Alonso P, Robinson J, and Ketcham RA. 2003. A uniquely specialized ear in a very early Tetrapod. *Nature* **425:** 65-69.

Clack JA, and Allin E. 2004. The evolution of single- and multiple- ossicle ears in fishes and tetrapods. In: Manley GA, Popper A and Fay RR, eds. *Evolution of the Vertebrate Auditory System.* New York: Springer-Verlag.

Clack JA, and Coates MI. 1993. *Acanthostega gunnari*: our present connection. In Hoch E and Brantsen AK, eds. Deciphering the natural world and the role of collections and museums. The Geological Museum, Copenhagen University.

Clack JA, and Holmes RB. 1988. The braincase of the anthracosaur *Archeria crassidisca* with comments on the interrelationships of primitive tetrapods. *Palaeontology* **31:** 85-107.

Clarke BT. 1987. A description of the skeletal morphology of *Barbourula* (Anura: Discoglossidae), with comments on its relationships. *Journal of Natural History* **21:** 879-891.

Coates MI. 1996. The Devonian tetrapod *Acanthostega gunnari* Jarvik: postcranial anatomy, basal tetrapod relationships and patterns of skeletal evolution. *Transactions of the Royal Society of Edinburgh: Earth Sciences* **87:** 363-421.

Coates MI, and Clack JA. 1991. Fish-like gills and breathing in the earliest known tetrapod. *Nature* **352:** 234-236.

Conroy GC, and Vannier MW. 1984. Noninvasive three-dimensional computer imaging of matrix-filled fossil by high-resolution computed tomography. *Science* **226:** 456-458.

Daly E. 1994. The Amphibamidae (Amphibia: Temnospondyli), with a description of a new genus from the Upper Pennsylvanian of Kansas. *Miscellaneous Publication University Of Kansas Museum Of Natural History* **85:** 1-59.

Damiani RJ. 2001. A systematic revision and phylogenetic analysis of Triassic mastodonsaurids (Temnospondyli: Stereospondyli). *Zoological Journal of the Linnean Society, London* **133:** 379-482.

Dawson JW. 1863. Notice of a new species of *Dendrerpeton,* and of the dermal coverings of certain Carboniferous Reptiles. *Quarterly Journal of the Geological Society, London* **19:** 469-473.

DeVilliers CGS. 1934. Studies of the cranial anatomy of *Ascaphus truei* Stejneger, the American "Liopelmid". *Bulletin of the Museum of Comparative Zoology, Harvard* **77:** 1-38.

Duellman WE, and Trueb L. 1986. *Biology of Amphibians.* New York: McGraw-Hill Book Company.

Eaton TH. 1939. The crossopterygian hyomandibular and the tetrapod stapes. *Journal of the Washington Academy of Sciences* **29:** 109-117.

Estes R. 1981. *Gymnophiona, Caudata.* Stuttgart: Gustav Fischer Verlag.

Evans SE, and Milner AR. 1996. A metamorphosed salamander from the early Cretaceous of Las Hoyas, Spain. *Philosophical Transactions of the Royal Society of London. Series B* **351:** 627-646.

Feller AE, and Hedges SB. 1998. Molecular evidence for the early history of living amphibians. *Molecular Phylogenetics and Evolution* **9:** 509-516.

Fouquette MJ. 2004. Synopsis of recent amphibians to genus. *http://lifesciences.asu.edu/bio474/jfouquette/Amphibia%2004%20final.pdf.*

Fourie S. 1974. The Cranial anatomy of *Thrinaxodon liorhinus. Annals of the South African Museum* **65:** 337-400.

Fox RC, and Bowman MC. 1966. Osteology and relationships of *Captorhinus aguti* (Cope) (Reptilia: Captorhinomorpha). *The University of Kansas Paleontology Contributions* **11:** 1-79.

Frost DR. 1985. *Amphibian Species of the World: A Taxonomic and Geographical Reference.* Lawrence: Allen Press, Inc. and The Association of Systematic Collections.

Gaupp E. 1898. Ontogenese und Phylogenese des schalleitenden Apparates bei den Wirbeltieren. *Ergebniss der Anatomie und Entwicklungsgeschichte* **8:** 990-1149.

Gaupp E. 1913. Die Reichertsche Theorie (Hammer-, Ambos- und Kieferfrage). *Archiv für Anatomie und Physiologie Abteilung Anatomie und Entwicklungsgeschichte* **Supplement-Band:** 1-416.

Godfrey SJ. 1989. The postcranial skeletal anatomy of the Carboniferous tetrapod *Greererpeton burkemorani* Romer, 1969. *Philosophical Transactions of the Royal Society of London. Series B* **323:** 75-133.

Godfrey SJ, Fiorillo AR, and Carroll RL. 1987. A newly discovered skull of the temnospondyl amphibian *Dendrerpeton acadianum* Owen. *Canadian Journal of Earth Sciences* **24:** 796-805.

Goodrich ES. 1930. *Studies on the Structure and Development of Vertebrates.* London: MacMillan and Co. Ltd.

Hay JM, Ruvinsky I, Hedges SB, and Maxson LR. 1995. Phylogenetic relationships of amphibian families inferred from DNA sequences of mitochondrial 12S and 16S ribosomal RNA genes. *Molecular Biology and Evolution* **12:** 928-937.

Heaton MJ. 1979. Cranial anatomy of primitive captorhinid reptiles from the late Pennsylvanian and Early Permian Oklahoma and Texas. *Oklahoma Geological Survey, Bulletin* **127:** 1–84.

Hedges SB, and Maxson LR. 1993. A molecular perspective on lissamphibian phylogeny. *Herpetological Monographs* **7:** 27-42.

Hetherington TE. 1987. Timing of development of the middle ear of Anura (Amphibia). *Zoomorphology* **1106:** 289-300.

Hetherington TE, and Lombard RE. 1983. Electromyography of the opercularis muscle of *Rana catesbeiana:* An amphibian tonic muscle. *Journal of Morphology* **175:** 17-26.

Holmes RB. 1984. The Carboniferous amphibian *Proterogyrinus scheelei* Romer, and the early evolution of tetrapods. *Philosophical Transactions of the Royal Society of London. Series B* **306:** 431-524.

Holmes RB. 1989. The skull and axial skeleton of the Lower Permian Anthracosaurid amphibian *Archeria crassidisca* Cope. *Palaeontographica Abteilung A* **207:** 161-206.

Holmes RB. 2000. Palaeozoic Temnospondyls. In: Heatwole H and Carroll RL, eds. *Amphibian Biology: Palaeontology - The Evolutionary History of Amphibians.* Chipping Norton: Surrey Beatty and Sons. 1081-1120.

Holmes RB, Carroll RL, and Reisz RR. 1998. The first articulated skeleton of *Dendrerpeton acadianum* (Temnospondyli, Dendrerpetontidae) from the Lower Pennsylvanian locality of Joggins, Nova Scotia, and a review of its relationships. *Journal of Vertebrate Paleontology* **18:** 64-79.

Hook RW. 1983. *Colosteus scutellatus* (Newberry), a primitive temnospondyl amphibian from the Middle Pennsylvanian of Linton, Ohio. *American Museum Novitates* **2770:** 1–41.

Huxley TH. 1859. On some amphibian and reptilian remains from South Africa and Australia. *Quarterly Journal of the Geological Society, London* **15:** 642-649.

Ivachnenko MF. 1978. Urodelans from the Triassic and Jurassic of Soviet Central Asia. *Paleontology Journal* **3:** 362-368.

Janvier P. 1996. *Early Vertebrates*. Oxford: Clarendon Press.

Jarvik E. 1952. On the fish-like tail in the ichthyostegid stegocephalians with descriptions of a new stegocephalian and a new crossopterygian from the Upper Devonian of East Greenland. *Meddelelser om Grønland* **114:** 1-90.

Jarvik E. 1954. On the visceral skeleton in *Eusthenopteron* with a discussion of the parasphenoid and palatoquadrate in fishes. *Kungliga Svenska Vetenskapsakademiens Handlingar* **(4) 5:** 1-104.

Jarvik E. 1961. Devonian Vertebrates. In: Raasch GO, ed. *Geology of the Arctic*. Toronto: University of Toronto Press. 197-204.

Jarvik E. 1980. *Basic Structure and Evolution of Vertebrates*. London: Academic Press.

Jarvik E. 1996. The Devonian tetrapod *Ichthyostega*. *Fossils and Strata* **40:** 1-213.

Jenkins FA, and Walsh DM. 1993. An Early Jurassic caecilian with limbs. *Nature* **365:** 246-250.

Jessen HL. 1980. Lower Devonian porolepiformes from the Canadian Arctic with special reference to *Powichthys thorsteinssoni* Jessen. *Palaeontographica Abteilung A* **167:** 180-214.

Johanson Z, and Ahlberg PE. 1997. A new tristichopterid (Osteolepiformes: Sarcopterygii) from the Mandagery Sandstone (Late Devonian, Famennian) near Canowindra, NSW, Australia. *Transactions of the Royal Society of Edinburgh: Earth Sciences* **88:** 39-68.

Johanson Z, Ahlberg PE, and Ritchie A. 2003. The braincase and palate of the tetrapodomorph sarcopterygian *Mandageria fairfaxi*: morphological variability near the fish-tetrapod transition. *Palaeontology* **46:** 271-293.

Ketcham RA, and Carlson WD. 2001. Acquisition, optimization and interpretation of X-ray computed tomography imagery: applications to the geosciences. *Computers & Geosciences* **27:** 381-400.

Kingsbury BF, and Reed HD. 1909. The columella auris in Amphibia. *Journal of Morphology* **20:** 549-628.

Klembara J. 1997. The cranial anatomy of *Discosauriscus* Kuhn, a seymouriamorph tetrapod from the Lower Permian of the Boskovice Furrow (Czech Republic). *Philosophical Transactions of the Royal Society of London. Series B* **352:** 257-302.

Lakjer T. 1926. *Studien über die Trigeminus-Versorgte Kaumuskulatur der Sauropsiden.* Copenhagen: C. A. Reitzel.

Larson A, and Dimmick WW. 1993. Phylogenetic relationships of the salamander families: an analysis of congruence among morphological and molecular characters. *Herpetological Monographs* **7:** 77-93.

Lathrop A. 1997. Taxonomic review of the Megaphryid frogs (Anura: Pelobatoidea). *Asiatic Herpetological Research* **7:** 68-79.

Laurin M. 1995. Comparative cranial anatomy of *Seymouria sanjuanensis* (Tetrapoda: Batrachosauria) from the lower Permian of Utah and new Mexico. *PaleoBios* **16:** 1–8.

Laurin M. 1996. A redescription of the cranial anatomy of *Seymouria baylorensis*, the best known Seymouriamorph (Vertebrata: Seymouriamorpha). *PaleoBios* **17:** 1–16.

Laurin M. 1998. The importance of global parsimony and historical bias in understanding tetrapod evolution. Part I-systematics, middle ear evolution, and jaw suspension. *Annales des Sciences Naturelles* **19:** 1-42.

Laurin M. 2002. Tetrapod phylogeny, amphibian origins, and the definition of the name Tetrapoda. *Systematic Biology* **51:** 364-369.

Laurin M. 2005. The otic region of the Carboniferous temnospondyl *Iberospondylus schultzei*, the middle ear of temnospondyls, and the evolution of hearing in early tetrapods *Fifth World Conference of Herpetology.* Stellenbosch, South Africa. 67-68.

Laurin M, and Reisz RR. 1997. A new perspective on the tetrapod phylogeny. In: Sumida SS and Martin KLM, eds. *Amniote Origins: Completing the Transition to Land.* San Diego: Academic Press. 9-59.

Laurin M, and Soler-Gijon R. 2006. The oldest known Stegocephalian (Sarcopterygii: Temnospondyli) from Spain. *Journal of Vertebrate Paleontology* **26:** 284-299.

Lombard RE, and Bolt JR. 1979. Evolution of the tetrapod ear: an analysis and reinterpretation. *Biological Journal of the Linnean Society, London* **11:** 19-76.

Lombard RE, and Bolt JR. 1988. Evolution of the stapes in the Paleozoic tetrapods. In: Fritzsch B, Ryan MJ, Wilczynski W, Hetherington TE and Walkowiak W, eds. *The Evolution of the Amphibian Auditory System.* New York: John Wiley and Sons. 37-67.

Lombard RE, and Bolt JR. 1995. A new primitive tetrapod, *Whatcheeria deltae*, from the Lower Carboniferous of Iowa. *Palaeontology* **38:** 471-494.

Lubosch W. 1938. Muskeln des Kopfes: Viscerale Muskulatur, C. Amphibien und Sauropsiden. In: Bolk B, Göppert E, Kallius E and Lubosch W, eds. *Handbuch der vergleichenden Anatomie der Wirbeltiere, Band 5.* Berlin: Urban & Schwarzenberg. 1025-1064.

Lucas SG. 1998. Global Triassic tetrapod biostratigraphy and biochronology. *Palaeogeography, Palaeoclimatology, Palaeoecology* **143:** 347-384.

Luther A. 1914. Über die vom N. trigeminus versorgte Muskulatur der Amphibien mit einem vergleichenden Ausblick über den Adductor mandibulae der Gnathostomen, und einem Beitrag zum Verständnis der Organisation der Anurenlarven. *Acta Societatis Scientiarum Fennicae* **44:** 1-151.

Lydekker R. 1889. Note on the occurrence of a species of *Bothriceps* in the Karoo system of South Africa. *Annals and Magazine of Natural History. Series 6* **4:** 475-476.

Lydekker R. 1890. *Catalogue of the Fossil Reptilia and Amphibia. Part IV.* London: Taylor and Francis.

Lyell C, and Dawson JW. 1853. On the remains of a reptile (*Dendrerpeton acadianum*, Wyman and Owen) and of a Land Shell discovered in the interior of an erect fossil tree in the Coal Measure of Nova Scotia. *Quarterly Journal of the Geological Society, London* **9:** 58-63.

Maglia AM. 1998. Phylogenetic relationships of extant Pelobatoid frogs (Anura: Pelobatoidea): Evidence from adult morphology. *Scientific Papers, Natural History Museum, The University of Kansas* **10:** 1-19.

Maree WA. 1945. Contributions to the cranial morphology of the European anuran *Alytes obstetricans* (Laurenti). *Annale van die Universiteit van Stellenbosch* **23:** 43-63.

Mason MJ, and Narins PM. 2002a. Vibrometric studies of the middle ear of the bullfrog *Rana catesbeiana* I. The extrastapes. *Journal of Experimental Zoology* **205:** 3153-3165.

Mason MJ, and Narins PM. 2002b. Vibrometric studies of the middle ear of the bullfrog *Rana catesbeiana* II. The operculum. *Journal of Experimental Zoology* **205:** 3167-3176.

Meyer A, and Zardoya R. 2003. Recent advances in the (molecular) phylogeny of vertebrates. *Annual Review of Ecology, Evolution, and Systematics* **34:** 311-338.

Milner AC, and Lindsey W. 1998. Postcranial remains of *Baphetes* and their bearing on the relationships of the Baphetidae (=Loxommatidae). *Zoological Journal of the Linnean Society, London* **122:** 211-235.

Milner AR. 1980. The temnospondyl amphibian *Dendrerpeton* from the Upper Carboniferous of Ireland. *Palaeontology* **23:** 125-141.

Milner AR. 1990. The radiation of temnospondyl amphibians. In: Taylor PD and Larwood GP, eds. *Major Evolutionary Radiations*. Oxford: Clarendon Press. 321-349.

Milner AR. 1996. A revision of the temnospondyl amphibians from the Upper Carboniferous of Joggins, Nova Scotia. *Special Papers in Palaeontology* **52:** 81-103.

Milner AR, and Sequeira SEK. 1994. The temnospondyl amphibians from the Visean of East Kirkton, West Lothian, Scotland. *Transactions of the Royal Society of Edinburgh: Earth Sciences* **84:** 331-361.

Monath T. 1965. The opercular apparatus of salamanders. *Journal of Morphology* **116:** 149-170.

Moulton JM. 1974. A description of the vertebral column of *Eryops* based on the notes and drawings of A. S. Romer. *Breviora* **428:** 1-44.

Noble GK. 1931. *The Biology of the Amphibia.* New York: McGraw-Hill Book Company, Inc.

Nussbaum RA, and Wilkinson M. 1989. On the classification and phylogeny of caecilians (Amphibia: Gymnophiona), a critical review. *Herpetological Monographs* **3:** 1-42.

Owen R. 1853. Notes on the above-described fossil remains. *Quarterly Journal of the Geological Society, London* **9:** 66-67.

Owen R. 1876. *Descriptive and Illustrated Catalogue of the Fossil Reptilia of South Africa in the Collection of the British Museum.*

Panchen AL. 1964. The cranial anatomy of two coal measure Anthracosaurs. *Philosophical Transactions of the Royal Society of London. Series B* **247:** 593-636.

Panchen AL. 1977. On *Anthracosaurus russelli* Huxley (Amphibia: Labyrinthodontia) and the family Anthracosauridae. *Philosophical Transactions of the Royal Society of London. Series B* **279:** 447-512.

Panchen AL. 1985. On the amphibian *Crassigyrinus scoticus* Watson from the Carboniferous of Scotland. *Philosophical Transactions of the Royal Society of London. Series B* **309:** 505-568.

Parker WK. 1881. On the structure and development of the skull in the Batrachia, part III. *Philosophical Transactions of the Royal Society of London* **172.**

Parrington FR. 1947. Labyrinthodonts from South Africa. *Proceedings of the Zoological Society, London* **118:** 426-445.

Parrington FR. 1948. Labyrinthodonts from South Africa. *Proceedings of the Zoological Society, London* **118:** 426-445.

Parrington FR. 1949. Remarks on a theory of the evolution of the tetrapod middle ear. *Journal of Laryngology and Otology* **63:** 580-595.

Parrington FR. 1958. The problem of the classification of reptiles. *Journal of the Linnean Society London, Zoology* **44:** 99-115.

Pawley K, and Warren AA. 2005. A terrestrial stereospondyl from the Lower Triassic of South Africa: the postcranial skeleton of *Lydekkerina huxleyi* (Amphibia: Temnospondyl). *Palaeontology* **48:** 281-298.

Peabody FE. 1952. *Petrolacosaurus kansensis* Lane, a Pennsylvanian reptile from Kansas. *The University of Kansas Paleontological Contributions Vertebrata* **1:** 1-41.

Peter K. 1898. Die Entwicklung und funktionelle Gestaltung des Schädels von Ichthyophis glutinosus. *Morphologisches Jahrbuch* **25:** 555-628.

Pusey HK. 1943. On the head of the Liopelmid frog, *Ascaphus truei*. I. The chondrocranium, jaws, arches, and muscles of a partly-grown Larva. *The Quarterly Journal of Microscopical Sciences* **84:** 105-185.

Rage J-C, and Rocek Z. 1989. Redescription of *Triadobatrachus massinoti* (Piveteau, 1936) an anuran amphibian from the Early Triassic. *Palaeontographica Abteilung A* **206:** 1-16.

Ramachandran GN, and Lakshminarayanan AV. 1971. Three-dimensional reconstruction from radiographs and electron micrographs: application of convolutions instead of Fourier transforms. *Proceedings of the National Academy of Sciences, USA* **68:** 2236-2240.

Ramaswami LS. 1943. The discoglossid skull. *Proceedings of the Indian Academy of Sciences* **16:** 10-24.

Reisz RR. 1977. *Petrolacosaurus*, the oldest known diapsid reptile. *Science* **196:** 1091-1093.

Rich TH, Hopson JA, Musser AM, Flannery TF, and Vickers-Rich P. 2005. Independent origins of middle ear bones in monotremes and therians. *Science* **307:** 910-914.

Robinson J, Ahlberg PE, and Koentges G. 2005. The braincase and middle ear region of *Dendrerpeton acadianum* (Tetrapoda: Temnospondyli). *Zoological Journal of the Linnean Society, London* **143:** 577-597.

Rocek Z. 1981. Cranial anatomy of frogs of the family Pelobatidae Stannius, 1856, with outlines of their phylogeny and systematics. *Acta Universitatis Carolinae - Biologica*: 1-164.

Romer AS. 1937. The braincase of the Carboniferous crossopterygian *Megalichthys nitidus*. *Bulletin of the Museum of Comparative Zoology, Harvard* **82:** 1-73.

Romer AS. 1946. The primitive reptile *Limnoscelis* Restudied. *American Journal of Science* **244:** 149-188.

Romer AS. 1947. Review of the Labyrinthodontia. *Bulletin of the Museum of Comparative Zoology, Harvard* **99:** 1-368.

Romer AS. 1966. *Vertebrate Paleontology*. Chicago & London: The University of Chicago Press.

Romer AS, and Witter RV. 1942. *Edops,* a primitive rhachitomous amphibian from the Texas red beds. *Journal of Geology* **50:** 925-960.

Ruta M, Coates MI, and Quicke DLJ. 2003a. Early tetrapod relationships revisited. *Biological Reviews* **78:** 251-345.

Ruta M, Jeffery JE, and Coates MI. 2003b. A supertree of early tetrapods. *Proceedings of the Royal Society of London. Series B* **270:** 2507-2516.

San Mauro D, Vences M, Alcobendas M, Zardoya R, and Meyer A. 2005. Initial diversification of living amphibians predated the breakup of Pangaea. *American Naturalist* **165:** 590-599.

Sawin HJ. 1941. The cranial anatomy of *Eryops megacephalus*. *Bulletin of the Museum of Comparative Zoology, Harvard* **88:** 407-463.

Schoch RR. 1999a. Studies on the braincase of early tetrapods: structure, morphological diversity, and phylogeny - 1. *Trimerorhachis* and other primitive temnospondyls. *Neues Jahrbuch für Geologie and Paläontologie, Abhandlungen* **213:** 233-259.

Schoch RR. 1999b. Studies on the braincase of early tetrapods: structure, morphological diversity, and phylogeny - 2. Dissorophoids, eryopids, and stereospondyls. *Neues Jahrbuch für Geologie and Paläontologie, Abhandlungen* **213:** 289-312.

Schoch RR. 2000. The stapes of *Mastodonsaurus giganteus* (Jaeger 1828) - structure, articulation, ontogeny, and functional implications. *Neues Jahrbuch für Geologie and Paläontologie, Abhandlungen* **215:** 177-200.

Schoch RR. 2002. The stapes and middle ear of the Permo-Carboniferous tetrapod *Sclerocephalus. Neues Jahrbuch für Geologie and Paläontologie, Monatshefte*: 671-680.

Shishkin MA, Rubidge BS, and Kitching JW. 1996. A new lydekkerinid (Amphibia, Temnospondyli) from the lower Triassic. *Philosophical Transactions of the Royal Society of London. Series B* **351:** 1635-1659.

Slabbert GK. 1945. Contributions to the cranial morphology of the European anuran *Bombina varieggata* (Linné). *Annale van die Universiteit van Stellenbosch* **23:** 67-89.

Slabbert GK, and Maree WA. 1945. The cranial morphology of the Discoglossidae and its bearing upon the phylogeny of the primitive Anura. *Annale van die Universiteit van Stellenbosch* **23:** 91-97.

Smithson TR. 1982. The cranial morphology of *Greererpeton burkemorani* (Amphibia: Temnospondyli). *Zoological Journal of the Linnean Society, London* **76:** 29-90.

Sollas WJ. 1901. The investigation of fossil remains by serial sections. *Report of the British Association for the Advancement of Science*: 643.

Sollas WJ. 1920. On the structure of *Lysorophus*, as exposed by serial sections. *Philosophical Transactions of the Royal Society of London. Series B* **209:** 481-526.

Sollas WJ, and Sollas IBJ. 1903. An account of the Devonian fish, *Palaeospondylus gunni*, Traquair. *Philosophical Transactions of the Royal Society of London. Series B* **196:** 267-294.

Steen MC. 1934. The amphibian fauna from the South Joggins, Nova Scotia. *Proceedings of the Zoological Society, London* **1934:** 465-504.

Stephenson EM. 1951a. The anatomy of the head of the New Zealand frog, *Leiopelma*. *Transactions of the Zoological Society, London* **27:** 255-305.

Stephenson NG. 1951b. On the development of the chondrocranium and visceral arches of *Leiopelma archeyi*. *Transactions of the Zoological Society, London* **27:** 203-254.

Stow CW. 1858a. On some fossils from South Africa. *Abstracts of the Proceedings of the Geological Society of London* **21:** 77.

Stow CW. 1858b. On some fossils from South Africa. *Quarterly Journal of the Geological Society, London* **14:** 193-195.

Taylor EH, and Noble GK. 1924. A new genus of discoglossid frogs from the Philippine Islands. *American Museum Novitates* **121:** 1-4.

Trueb L, and Cannatella DC. 1982. The cranial osteology and hyolaryngeal apparatus of *Rhinophrynus dorsalis* (Anura: Rhinophrynidae) with comparisons to recent pipid frogs. *Journal of Morphology* **171:** 11-40.

Trueb L, and Cloutier R. 1991. A phylogenetic investigation of the inter- and intrarelationships of the lissamphibia (Amphibia: Temnospondyli). In: Schultze H-P and Trueb L, eds. *Origins of the Higher Groups of Tetrapods: Controversy and Consensus.* Ithaca: Cornell University Press. 223-313.

Tumarkin A. 1948. On the evolution of the auditory perilymphatic system. *Journal of Laryngology and Otology* **62:** 691-701.

Tumarkin A. 1949. On the evolution of the auditory conducting apparatus. Parts I and II. *Journal of Laryngology and Otology* **63:** 119-216.

Tumarkin A. 1968. Evolution of the auditory conducting apparatus in terrestrial vertebrates. In: de Reuck A and Knight J, eds. *Hearing Mechanisms in Vertebrates.* London: J & A Churchill. 18-37.

Vorobyeva EI, and Schultze H-P. 1991. Description and systematics of panderichthyid fishes with comments on their relationship to tetrapods. In: Schultze H-P and Trueb L, eds. *Origins of the Higher Groups of Tetrapods: Controversy and Consensus.* Ithaca: Cornell University Press.

Warren AA. 1980. *Parotosuchus* from the Early Triassic of Queensland and Western Australia. *Alcheringa* **4:** 25-36.

Warren AA, and Hutchinson MN. 1990. *Lapillopsis*, a new genus of temnospondyl amphibians from the Early Triassic of Queensland. *Alcheringa* **14:** 149-158.

Warren AA, and Snell N. 1991. The postcranial skeleton of Mesozoic temnospondyl amphibians: a review. *Alcheringa* **15:** 43-64.

Watson DMS. 1912. On some reptilian lower jaws. *Annals and Magazine of Natural History. Series 8* **10:** 574-587.

Watson DMS. 1913. *Micropholis stowi*, Huxley, a temnospondylous amphibian from South Africa. *Geological magazine* **10:** 340-346.

Watson DMS. 1919. The structure, evolution and origin of the Amphibia. - The "Orders" Rachitomi and Stereospondyli. *Philosophical Transactions of the Royal Society of London. Series B* **209:** 1-73.

Watson DMS. 1929. The Carboniferous Amphibia of Scotland. *Palaeontologia Hungarica* **1:** 221-252.

Watson DMS. 1962. The evolution of the labyrinthodonts. *Philosophical Transactions of the Royal Society of London. Series B* **245:** 219-265.

Wellstead CF. 1991. Taxonomic revision of the Lysorophia, Permo-Carboniferous lepospondyl amphibians. *Bulletin of the American Museum of Natural History* **209:** 1-90.

Westoll TS. 1943. The hyomandibular of *Eusthenopteron* and the tetrapod middle ear. *Proceedings of the Royal Society of London. Series B* **131:** 393-414.

Wever EG. 1978. *The Reptile Ear: Its Structure and Function.* Princeton: Princeton University Press.

Wever EG. 1979. Middle ear muscles of the frog. *Proceedings of the National Academy of Sciences, USA* **76:** 3031-3033.

Wever EG. 1985. *The Amphibian Ear.* Princeton: Princeton University Press.

White TE. 1939. Osteology of *Seymouria baylorensis* Broili. *Bulletin of the Museum of Comparative Zoology, Harvard* **85:** 325-410.

Yates AM, and Warren AA. 2000. The phylogeny of the 'higher' temnospondyls (Vertebrata: Choanata) and its implications of the monophyly and origins of the Stereospondyli. *Zoological Journal of the Linnean Society, London* **128:** 77-121.

Zardoya R, and Meyer A. 2001. On the origin of and phylogenetic relationships among living amphibians. *Proceedings of the National Academy of Sciences, USA* **98:** 7380-7383.

Zittel KA. 1888. *Handbuch der Palaeontologie, Palaeozoologie 3 Vertebrata.* Munich and Leipzig.